Analysis of the F-bracket
determination of the effective with of the wall plate

Welmer, L.

Award date:
2016

TU/e

Master thesis Structural Design

Analysis of the F-bracket

Determination of the effective width of the wall plate

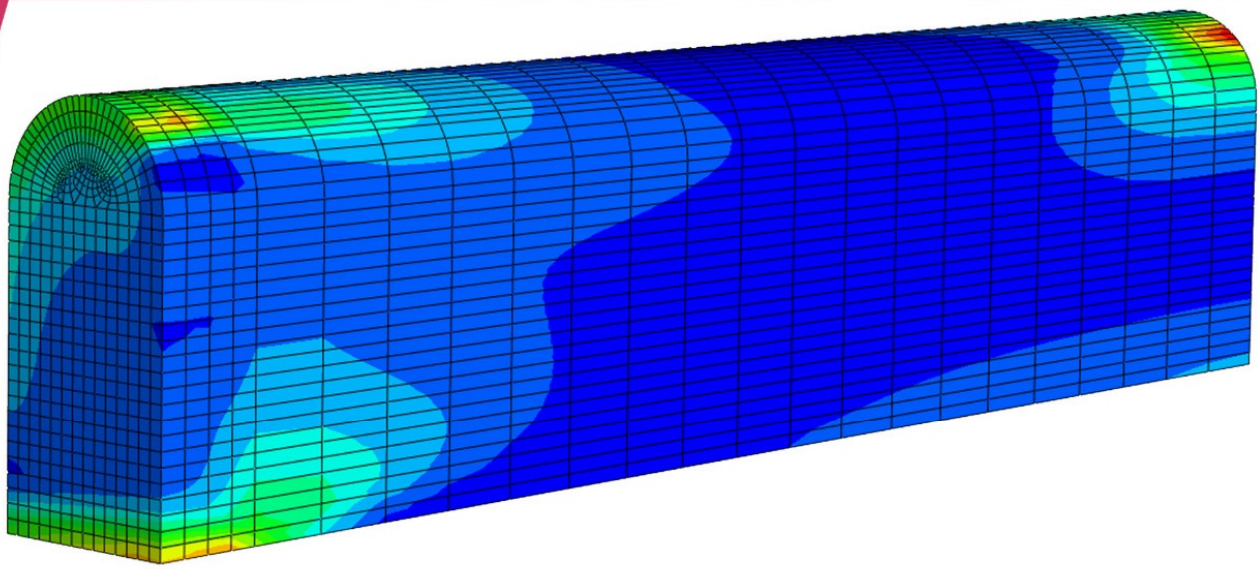

L. Welmer

04-08-2016 / 0651309 / Architecture, Building and Planning

Technical University of Eindhoven

Prof. dr. ir. A.J.M. Jorissen

dr. ir. A.J.M. Leijten

Prof. ir. S.N.M. Wijte

M. Timmer

University of Technology Eindhoven

Department of the Built Environment
P.O. box 513
5600 MB
Eindhoven, The Netherlands
A: Groene Loper 6
T: +31 (0)40 247 4311
E: secretariaat.b@bwk.tue.nl

Master
Architecture, Building and Planning

Unit
Structural Design

Student
L. (Laurens) Welmer
0651309 / s080688
T: +31 6 18 91 61 53
E: l.welmer@student.tue.nl / laurenswelmer@gmail.com

Supervisors
Prof. dr. ir. A.J.M. (André) Jorissen
dr. ir. A.J.M (Ad) Leijten
Prof. ir. S.N.M. (Simon) Wijte
M. (Mark) Timmer

Script number
A-2016.148

Summary

Roofs can be divided into two types of roofs. There are flat roofs and pitched roofs. The construction of a pitched roof often consists of rafters, girders, or a combination of both. Rafters are wooden beams spanning from ridge to eaves, whereas girders bridge the lateral distance from building wall to building wall. A rafter transfers the forces to the floor. The transition from the roof to the floor is called the connection detail. An example of such a connection detail is the use of a wooden wall plate in combination with steel F-brackets. When the assembly of the detail takes place, first, it is necessary to determine the proper position of the brackets, after which the brackets are fastened to the floor with expansion dowels. Subsequently, the correct depth of the wall plate in the brackets is determined, filling up the space underneath the wall plate at the location of the brackets by shims or wedges. In some cases, the entire space underneath the wall plate is filled with either PUR or shrink mortar. Thereafter, the complete roof element is brought into position, wherein the rafters are fixed to the wall plate by means of a coach screw. The rafters are not able to transfer the axial forces to the wall plate directly. Instead, the axial forces are transferred to the supporting panel, after which it passes them on to the supporting batten, which is in direct contact with the wall plate. However, the shear forces are transferred directly from the rafters to the wall plate. The wall plate, supporting batten and supporting panel are continuous elements, in contrast to the brackets and the rafters. The mutual distance between brackets or rafters is called the center-to-center distance of the element. The course of the forces can be simplified as a local load, which gradually spreads over a certain distance, after which it yields back to a local force. The concentration of the forces in the brackets causes problems for the wall plate. Although the wall plate is a continuous element, it is only able to transfer the forces over a certain distance near the brackets. This distance is called the effective width of the wall plate. The literature is limited to assumptions about the size of the effective width, while design calculations in practice omit the effective width entirely. Instead, the full length between the brackets is taken as the effective width, which is an incorrect assumption, as well as unsafe. The main research question is to determine the resistance of the wall plate. The sub-questions consist of the determination of the effective width of the wall plate, as well as the determination of the effects on the effective width of the wall plate caused by various variables. One can think of the different center-to-center distances of the brackets, variation in roof inclination and the difference depths of adding. By means of a literature study and analytical research two formulas are established for determining the resistance of the wall plate. The resistance of the wall plate is expressed in terms of maximum allowable stresses. The maximum compressive stresses are a summation of compressive stresses and bending stresses, while the maximum tensile stresses only consist of bending stresses. The bending stresses are a result of an internal bending moment, which arises by the translation of the composed horizontal force at the top of the wall plate to the flanges of the bracket halfway and at the bottom of the wall plate. Both the analytical research as well as the numerical research yield a determination for the eccentricity of the internal bending moment. Results from the experimental research give an overview of the stress flow by measuring the strains in the supporting batten. Subsequently, this is validated by a three-dimensional numerical model. Results from both researches congregate to an assumption for the effective width of the wall plate. In addition, it appears that the roof inclination and the depth of the adding have no influence on the effective width, in contrast to the center-to-center distance of the brackets, which indeed have an influence on the effective width.

Samenvatting

Daken kunnen onderverdeeld worden in twee type daken. Zo zijn er platte daken en hellende daken. De constructie van een hellend dak bestaat vaak uit sporen, gordingen of een combinatie ervan. Sporen zijn houten balken die van nok tot dakgoot lopen, terwijl gordingen de zijwaartse afstand van bouwmuur tot bouwmuur overbruggen. Een sporenkap draagt zijn krachten af aan de vloer. De overgang van het dak naar de vloer wordt het verbindingsdetail genoemd. Een voorbeeld van zo'n verbindingsdetail is het gebruik van een houten muurplaat in combinatie met stalen F-beugels. Bij de assemblage van het detail worden eerst de juiste posities van de beugels bepaald, waarna de beugels met spreidpluggen aan de vloer bevestigd worden. Hierna bepaalt men de juiste hoogte van de muurplaat in de beugels, waarbij ter plaatse van de beugel de muurplaat ondersabeld wordt door stelplaatjes of wiggen. In sommige gevallen wordt de gehele lengte van de muurplaat ondersabelt met PUR of krimpmortel. Vervolgens wordt het complete dakelement in positie gebracht, waarbij de sporen aan de muurplaat bevestigd worden door middel van een houtdraadbout. De sporen zijn niet in staat de axiale krachten direct aan de muurplaat over te brengen. De axiale krachten worden overgebracht aan de constructieve onderplaat, waarna deze ze doorgeeft aan de drukregel, welk in direct contact staat met de muurplaat. De afschuifkrachten worden wel direct van de sporen overgedragen aan de muurplaat. De muurplaat, drukregel en constructieve onderplaat zijn doorlopende elementen, in tegenstelling tot de beugels en de sporen. De afstand tussen beugels en sporen onderling wordt de hart-op-hart afstand van het element genoemd. Het verloop van de krachten kan gezien worden als een lokale belasting, die zich uitsmeerd over een bepaald afstand, waarna deze uiteindelijk tot een lokale kracht terugvloeit. Het concentreren van de krachten bij de beugels levert problemen op voor de muurplaat. Alhoewel de muurplaat een doorlopend element is, is het in staat slechts over een bepaalde afstand nabij de beugels de krachten over te dragen. Deze afstand wordt de meewerkende breedte van de muurplaat genoemd. De literatuur beperkt zich tot aannames omtrent de grootte van de meewerkende breedte, terwijl er ontwerpberekeningen in de praktijk zijn waarbij het gebruik van een meewerkende breedte achterwegen gelaten wordt. In plaats daarvan wordt de volledige lengte tussen de beugels als meewerkende breedte genomen, wat naast een onjuiste, zeker ook een onveilige aanname is. De hoofdvraag van het onderzoek is de bepaling van de weerstand van de muurplaat, met als deelvragen de bepaling van de meewerkende breedte van de muurplaat als ook de beïnvloedbaarheid van de meewerkende breedte door verscheidene variabelen omtrent het dakdetail. Denk hierbij aan de verschillende hart-op-hart afstanden van de beugels, verschil in dakhellingen en de hoogte van de stelruimte onder de muurplaat. Door middel van een literatuurstudie en anlytisch onderzoek wordt een tweetal formules opgesteld voor de bepaling van de weerstand van de muurplaat. De weerstand van de muurplaat wordt uitgedrukt in maximaal opneembare spanningen. De maximale drukspanningen zijn een sommatie van drukspanningen en buigspanningen, terwijl de maximale trekspanningen slechts bestaan uit buigspanningen. De buigspanningen zijn een resultaat van een inwendig buigend moment, wat ontstaat door het transleren van de samengestelde horizontale kracht in de top van de muurplaat naar de beugelflenzen halverwege en onderaan de muurplaat. Uit zowel het analytisch onderzoek als ook het numeriek onderzoek vloeit een bepaling voort voor de grootte van de 'arm' van het buigend moment. Het experimenteel onderzoek tracht door het meten van de rekken in de drukregel een overzicht te krijgen in het spanningsverloop in de drukregel en indirect de muurplaat. Dit is vervolgens door middel van een driedimensionaal numeriek model geprobeerd te valideren. Uit beide onderzoeken is een aanname voor de meewerkende breedte naar voor gekomen. Daarnaast blijken de dakhelling en de stelruimte geen invloed te hebben op de meewerkende breedte, in tegenstelling tot de hart-op-hart afstand van de beugels, wat weldegelijk een invloed heeft op de meewerkende breedte.

Acknowledgements

To become a graduate student from the master course Architecture, Building and Planning (Department of Structural Design) taught at the Technical University of Eindhoven, one needs to successfully perform a design or research project. As I see a future career in designing structures, I thought it would be an ideal opportunity to not only finish my educational course with a research project, but also test my research skills for a possible last time. Professor André Jorissen gave me the opportunity to graduate under his authority, for which I am very grateful. He has not only been responsible for the subject, he also arranged a valuable contact partner from practice (Mark Timmer). Many hours were spent discussing the development of the project in the early stages, which turned into discussions about the test results in the later stages. For all the effort put in both me and this project, I would like to thank him a lot.

Mark Timmer is the managing director from Vadeko and Domestic, and has been the outside contact partner from the start. There have been a few appointments, in which he has been able to give me the inside information regarding the subject of this research project by either showing me the factory or by granting design calculations from practice. Mark Timmer has also been able to provide me (on behalf of Vadeko) with test specimens for my experimental research. For all his help and effort I would like to thank him immensely.

Both Ad Leijten and Simon Wijte joined at a later stage of the project. Ad has been giving a lot of advice on the experimental research and the report, whereas Simon agreed to join the supervising committee to meet the commission requirements. Both their knowledge and expertise in the constructional world are highly appreciated.

I would also like to thank all the members from the 'Pieter van Musschenbroek Laboratory' for providing me space and equipment from their laboratory, as well as their help and knowledge in performing experimental tests. A special mention is in place for Johan, who has been my designated help in the period I have been hanging around in the laboratory.

At last I want to thank all friends and family for supporting me in the period of this project. An extra thanks to Ramses for reading my script and giving valuable comments.

Laurens Welmer

Deurne, July 21st 2016

List of symbols and abbreviations

Latin capitals

A	Cross section	[mm^2]
C	Constant	[-]
E	Modulus of elasticity	[N/mm^2]
F	Force	[N]
G	Shear Modulus	[N/mm^2]
H	Horizontal force	[N]
I	Moment of Inertia	[mm^4]
M	Bending moment	[Nmm]
N	Axial force	[N]
R	Resistance force	[N]
V	Shear force / Vertical force	[N]
W	Section modulus	[mm^3]

Latin lower case

b	Width	[mm]
e	Eccentricity	[mm]
f	Strength	[N/mm^2]
h	Fepth	[mm]
l	Length	[mm]
l_w	Effective width	[mm]
p	Areal load	[N/mm^2]
q	Line load	[N/mm]
s	Snow load	[N/mm^2]
w	Deformation	[mm]
x	variable length	[mm]
z	center of gravity	[mm]

Greek capitals

Σ	Sum	[-]
Υ	Sum of variables	[-]

Greek lower case

α	Rotation	[degrees]
χ	Factor	[-]
γ	Safety factor	[-]
γ	Shear angle	[-]
ε	Strain	[-]
κ	Curvature	[mm^{-1}]
μ	Snow factor	[-]
μ	Mean value	[-]
ν	Poisson's ratio	[-]
ρ	Density	[kg/m^3]
σ	Stress	[N/mm^2]
τ	Shear stress	[N/mm^2]
ψ	Factor	[-]
ω	Moisture content	[%]

Units

N	Newton
kN	Kilo Newton
m	Meter
mm	Millimter
kg	Kilograms

Indices

b	Upper
c	Compression
m	Bending
H	Horizontal
L	Longitudinal
o	Lower
R	Radial
t	Tension
T	Tangential
V	Vertical
x,y,z	Directions in coordinate system
y	Yield

Abbreviations

CTC	Center-to-center
F	F-bracket
SB	Supporting batten
SLS	Service limit state
SP	Supporting panel
ULS	Ultimate limit state
WP	Wall plate

Table of contents

Chapter 1 | Introduction

This chapter provides an introduction to the subject. First an overview of the matter is given. It starts with roofs in general and reduces the content repeatedly until a certain connection detail remains. Various alternative options not involving the matter of research will be disregarded. The overview is followed by the designation of the components involved. The chapter closes with the determination of the problem and setting the target for the research project. An overview of the thesis is added.

1.1 From roof to F-bracket

This research project focusses on the F-bracket and the timber made wall plate used in roof construction. To give the reader an insight on the topic, chapter one will attempt to give an introduction of constructional roofing by treating all components involved: from roofs in general to the constructional detail of a roof to floor connection. **Figure 1.1a** is added to give an overview of the components.

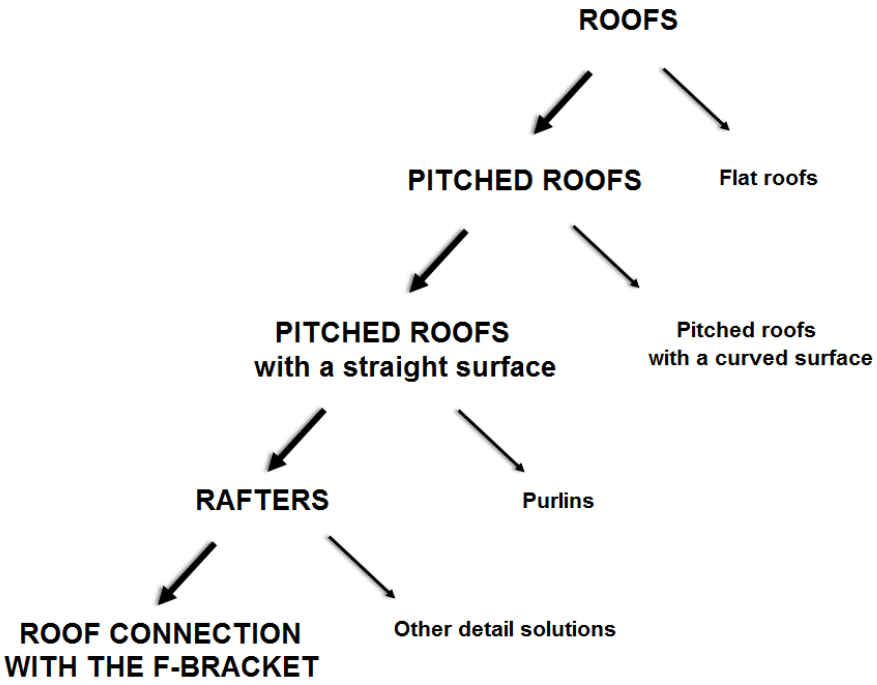

***Figure 1.1a**; From roof to F-bracket*

1.1.1 Function of a roof

A roof is part of a building or dwelling which function is to shut the space underneath from weather influences and unwanted intruders from outside. The shape of a roof varies in every project and is determined by a couple of factors. The most important factors are functional requirements (the space underneath the roof), esthetical requirements and technical requirements (the possibility to realize the span of the roofing, considering the economical consequence). The buildup of a roof consists of three main layers. First there is a water repelling layer, which function is to shield the space underneath from rain, snow or hail. This layer, commonly known as the paving of the roof, often consists of tiles for pitched roofs and

roofing felt for flat roofs. Of course there are many more materials available. The middle layer is a closing layer, also known as the sheathing of a roof. This layer consists of an isolation deck between wooden panels with various foils to keep the water and moisture on either side of the roof. This layer also has the purpose of locking out the space underneath from unwanted intruders such as wind, dust and vermin. It also keeps the heat inside in the winter and the cold inside in the summer. The third and last layer is the loadbearing layer, the construction of the roof. The layer is located either in or under the closing layer. The materials used for the construction of the roof vary from timber and steel, to aluminum and concrete. In this project, however, the focus is on timber as a construction material.

1.1.2 Technical requirements

A roof must meet a number of technical requirements. These requirements are the following **[15]**:

- Mechanical requirements
- Requirements regarding building physics
- Fire protection
- Sealability and burglary security

The last two requirements are straightforward and need no further explanation. Among the requirements regarding building physics are the resistance to water and wind penetration. Also the isolation of the space underneath the roof is an important requirement on which a roof must meet. The most important requirement is the mechanical requirement. Wrong implementation will result in heavy damage to the roof or worse, the total collapse of the building. To meet the requirement the following formula must hold:

$$S_d \leq R_d \tag{1.1}$$

In which:

S_d = the design load, force or stress that works on the construction
R_d = the design resistance of the construction

This formula is illustrated with **figure 1.1b**.

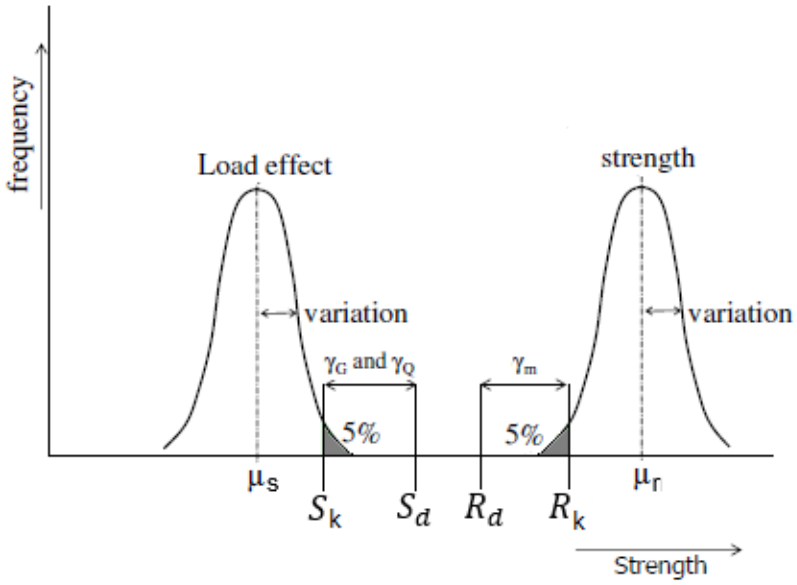

Figure 1.1b**; Determination of the design load and strength **[18]

The left normal distribution represents the scatter of various load effects in a predefined load situation and the right normal distribution represents the spread of material strength. The load effect consists of dead loads and live loads. The dead load of a roof is equal to the self-weight of the roof and the construction. The live load on the other hand consists of various load cases including snow, wind and local loading due to men or goods. The dead load can be determined very accurately, resulting in a small variation. The live load on the other hand is determined by generic models, which might not correspond to the load in the specific situation, resulting in a greater variation. For safety reasons, the upper 5% of the left distribution represents the characteristic load effect value (S_k). For equal reasons, the 5% lower value on the right distribution is taken as the characteristic strength value (R_k). The variation for homogeneous materials like steel and aluminum are relatively small. Timber however is an organic material and no tree is equal to another. Moreover, it is very difficult to accurately strength grade timber in a non-destructive way, therefore a higher variation in strength is present. To avoid the possibility of an unfortunate situation, in which case the characteristic strength has a lower value compared to the characteristic load, various safety factors (γ_G, γ_Q and γ_m) are introduced to create a certain buffer, resulting in both the design load (S_d) and the design resistance of a construction (R_d). Although it is important in construction design calculations that safety margins are implemented, for research purposes the actual load or strength value should be used.

1.1.3 Roof shapes

Roofs of buildings occur in many shapes. For instance, there are flat roofs, curved roofs, pitched roofs or roofs with a combination of shapes. For this research project only straight pitched roofs are considered, which are most commonly used for dwellings. An overview of several straight pitched roofs is given in **figure 1.1c**.

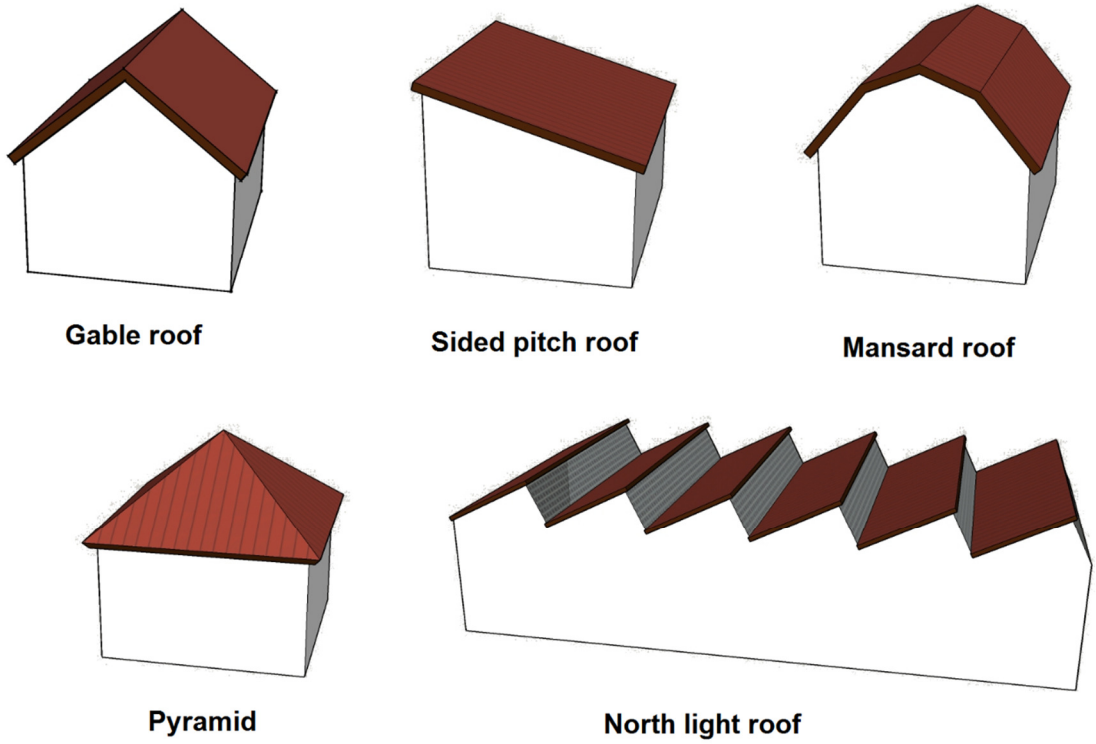

***Figure 1.1c**; Various shapes of straight pitched roofs*

The supporting structure of a straight pitched roof can roughly be subdivided into two main types of construction: rafters and purlins. Purlins are beams that span from wall to wall (sometimes supported by an intermediate truss). Rafters on the other side span from ridge to gutter. Residential roof structures consist of a high level of prefabrication. Often you will see the constructional elements used inside the prefabricated roof element. The roof elements are joined in pairs with a hinge connection, therefore commonly known as hinged roofs. The elements are positioned on top of the dwelling with a crane. By lifting the elements from the ground, the hinge will ensure the automatic unfolding of the roof.

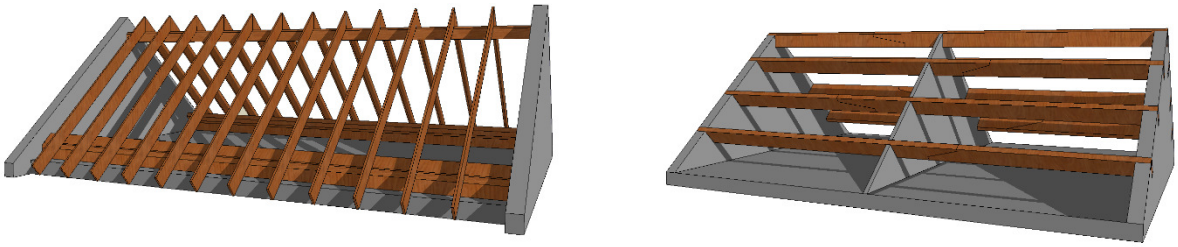

***Figure 1.1d**; Rafters (left) and purlins (right)*

1.1.4 Rafters

The rafters are made of sawn timber of strength class C18 to C24. Rafters with commonly used dimensions have a width-depth profile of 30mm x 220mm and a maximum span of four and a half meters. The dimensions of the rafters are adapted to the required strength of the roof structure. The center-to-center distance between separate rafters is approximately 600mm.
In some cases a supporting construction is added to avoid long spans of the rafters. This is achieved by either using under eaves or an attic. Both support types are primarily subjected to axial loading, reducing high moment stresses in the rafters. An attic is only used for high pitched roofs.

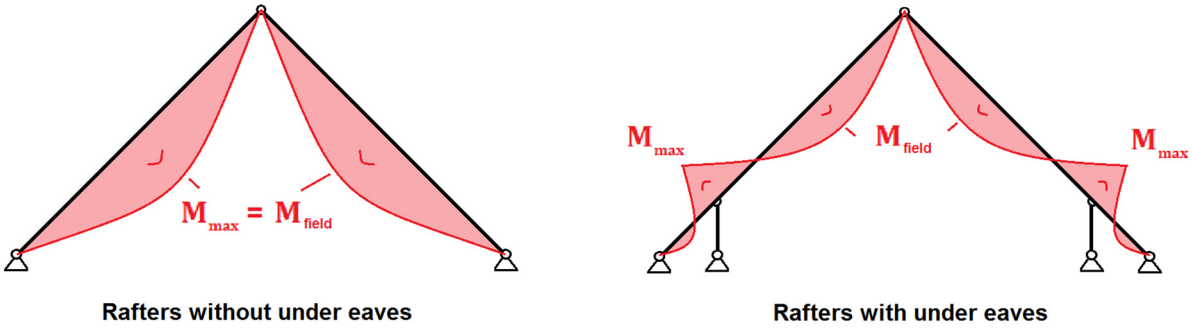

***Figure 1.1e**; Mechanical scheme of the moment stress distribution in the rafters*

1.1.5 Connection detail

The fixation of the roof to the underlying construction can be achieved in many ways. One should take into account the horizontal and vertical reaction forces, which should be adopted by the loadbearing wall and floor. In case there is no (continuous) floor, horizontal forces cannot be transferred. This will result in the connection acting like a roller support instead of a hinge support.
Our focus will be on a certain connection detail involving the wall plate and the F-bracket. The wall plate is a continuous timber element clamped into several steel-made brackets divided over the width of the floor. Forces due to loading are transferred through the rafters onto the wall plate. These forces can be divided into axial and shear forces. In the end, the load is transferred through the wall plate and the F-bracket onto the floor. To give an insight in the

buildup of the connection detail, **figure 1.1f** is added. The F-brackets and the rafters are non-continuous in the width-direction. Both the F-brackets and the rafters have a different center-to-center distance, varying per situation. The wall plate and supporting elements are continuous, and therefore capable of resisting larger forces. The effective width of the wall plate (see **figure 1.1f**) lies between the width of the bracket and the center-to-center distance of the brackets. The first assumption is cautious, the latter is under-dimensioned and therefore unsafe. The actual value of the effective width lies in between and is part of the research question. **Paragraph 1.2.5** will elaborate on this issue.

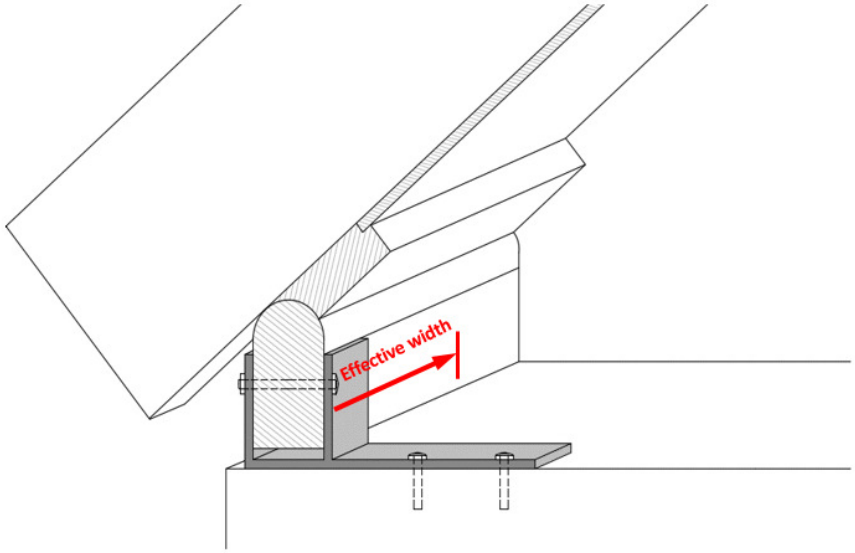

***Figure 1.1f**; Section plane of the F-bracket connection detail, the cut is located in the middle of the F-bracket*

The manner of load transfer is one of the main topics in this graduation project, which will be elaborated on in **chapter 2** and onwards.

1.1.6 Terminology

To clarify and unambiguously use the correct names, often recurring words are appointed into **figures 1.1g and 1.1h**.

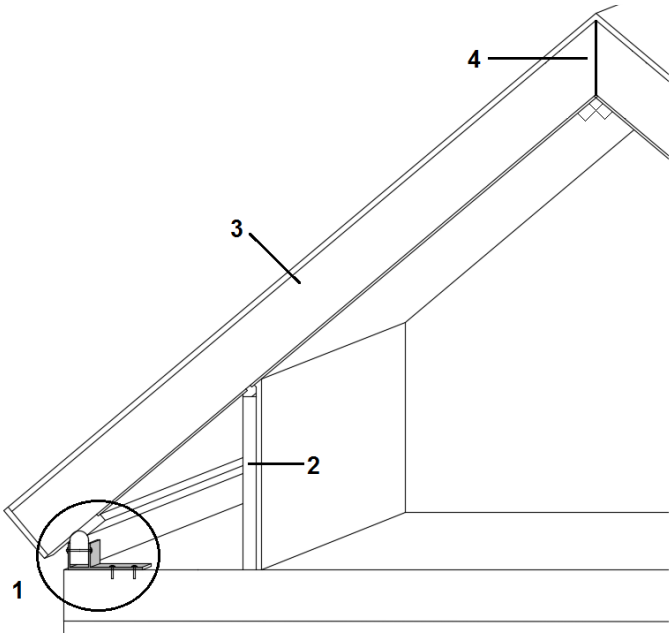

1. Connection detail

2. Supporting structure (under eaves)

3. Roof element (containing rafters and insulation material)

4. Ridge of the roof

***Figure 1.1g;** Terminology of the roofing*

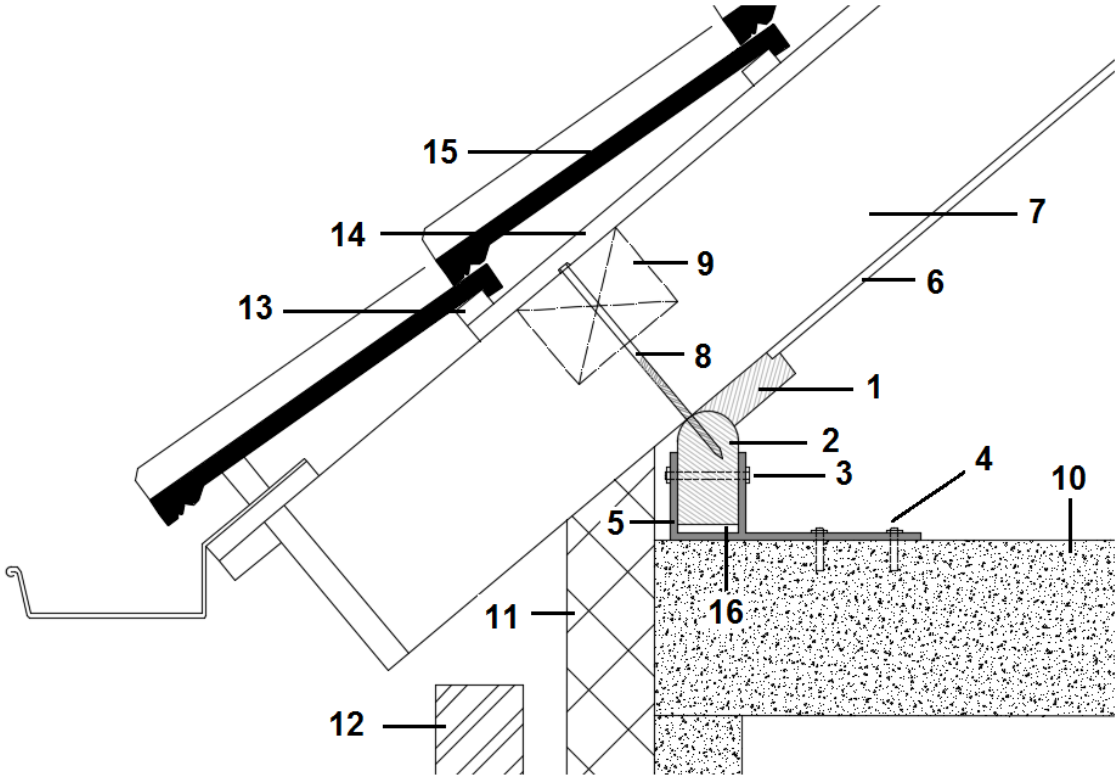

***Figure 1.1h**; Terminology of the connection detail*

1	Supporting batten	**7**	Rafters and insulation	**13**	Horizontal batten
2	Wall plate	**8**	Coach screw	**14**	Vertical batten
3	Nut-bolt connection	**9**	Spool	**15**	Tile
4	Expension rivet	**10**	Concrete floor	**16**	Adding
5	F-bracket	**11**	Insulation		
6	Supporting wooden panel	**12**	Facade (brick wall)		

***Table 1.1a**; Designation of parts in figure 1.1h*

1.2 F-bracket and wall plate

1.2.1 F-bracket

The F-bracket is a steel element. It consists of a flat strip and two upright baffles. One of the baffles is created by bending the extension of the strip. The other baffle is welded onto the strip with joints on both sides. The strip contains at least two holes. Expansion rivets are used to attach the bracket to the underlying floor. One hole is elongated in the axial direction for positioning during erection of the roof. The space between the baffles is reserved for clamping the wall plate. Both baffles are perforated and fastened with a bolt, locking down the wall plate. If you turn the brackets from **figure 1.2a** ninety degrees clockwise, you will see it forms an ‘F’. The bracket is a discontinuous element, with a common center-to-center distance of 600 to 1200 millimeters.

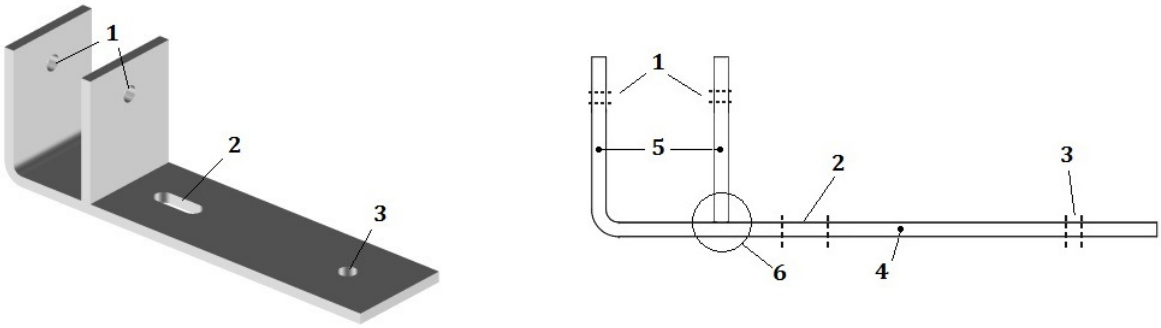

***Figure 1.2a**; Overview of the F-bracket and its section plane*

1	Perforated baffles	**3**	Normal hole	**5**	Baffles
2	Elongated hole	**4**	Strip	**6**	Welded joint

***Table 1.2a**; Designation of parts in figure 1.2a*

1.2.2 Wall plate

The wall plate is a sawn timber beam element with common dimensions of 70 millimeters in width and 120 to 150 millimeters in depth. De width of the wall plate matches the gap between the baffles of the F-bracket. The shape of the wall plate is rectangular, except for the top side. Two version are commonly used in practice. First, there is the double shaven top. It results in two plains, related with a right angle. One of the plains' angle must correspond to the pitch of the roof. Second, there is the round shaven top. The round top includes a matching (contra profile) supporting batten. The benefit of a round shaven top is that it is applicable for every roof angle, without changing the shape of the wall plate nor the supporting batten. The grain direction of the timber elements is perpendicular to the load direction.

***Figure 1.2b**; Pictures of a typical round shaven wall plate*

1.2.3 Coach screw

The coach screw serves as a fastener of the roof. It connects the bottom of the roof element with the wall plate. It is used to prevent the roof from lifting up due to the upward loading forced by wind suction. Because rafters are relatively small in width (~30mm), spools are used to thicken the body. Therefore, satisfying the minimal width required for applying the coach screw. One should consider the need of the spools, since the screw is not subjected to lateral loading. Pre-drilling the holes for the screws will prevent the rafters to split and will also aid the assembly positioning of the roof. It will reduce costs by saving material and labor.

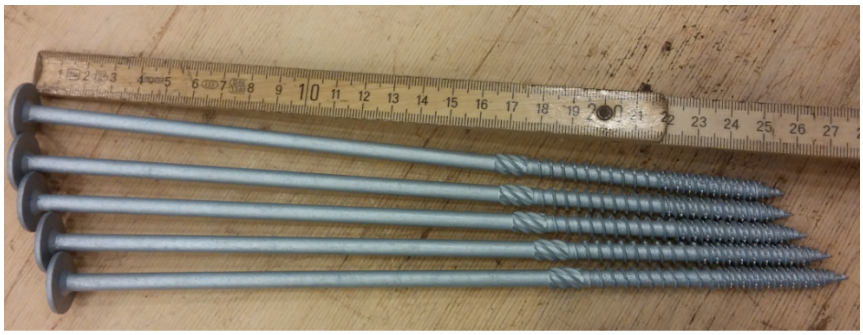

***Figure 1.2c**; Picture of exemplary coach screws*

1.2.4 Assembly of the connection detail

The assembly of the connection detail starts with the positioning of the F-bracket. As mentioned in **paragraph 1.2.1** an elongated hole is used to position the bracket in the axial direction (**Figure 1.2d; 1**). Therefore only one connector is fixed until the exact position is determined. Subsequently, the wall plate is placed in the bracket. To match the desired depth, wedges are used, only at the location of the bracket, to increase the depth of the wall plate (**Figure 1.2d; 2**). When the position of both elements is satisfactory, the second connector is set and the bolt retaining the wall plate is installed (**Figure 1.2d; 3**). To avoid leakages of air underneath the wall plate, the clearance is filled with either cement or PUR (see right **picture 1.2b**).

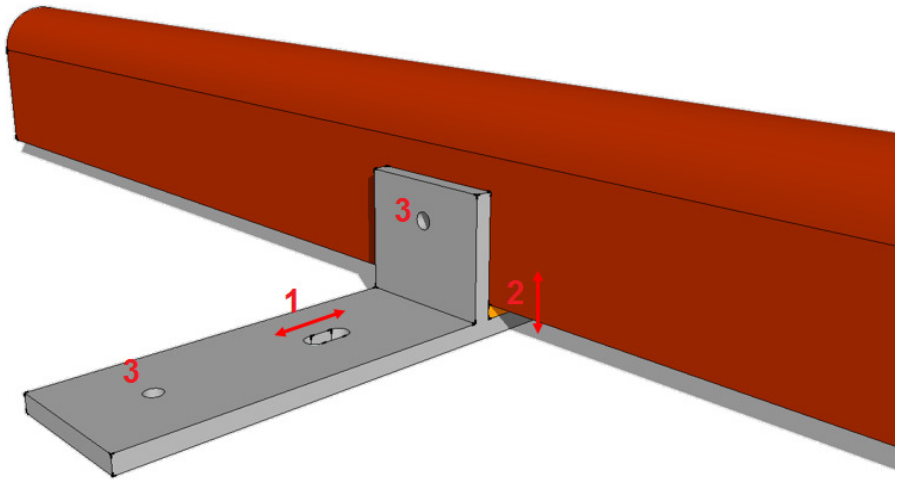

***Figure 1.2d**; Assembly of the detail*

1.2.5 Effective width of the wall plate

All stresses caused by the roof and the loads yield to the brackets. These brackets are considered to be hard points (attracting the stresses). The wall plate is the designated element to transfer these stresses towards the brackets. Near the brackets, the wall plate will be considered as a hard point as well, as it makes direct contact with the bracket. But the contribution of the wall plate will decrease as the distance to the brackets increases. At a certain point, the wall plate no longer contributes to the load transfer of the connection. The effective width is considered the width of the wall plate over which it contributes to the transfer of stresses towards the brackets. This is illustrated in **figure 1.2e**.

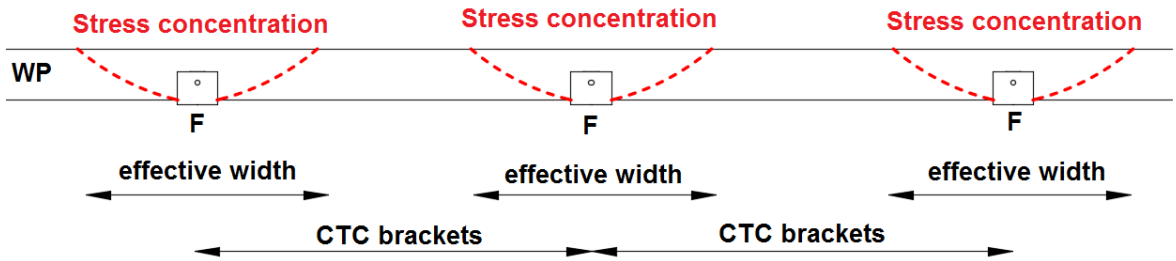

***Figure 1.2e**; Schematic top view of the wall plate (WP) and F-brackets (F). The effective width is determined by the stress distribution in the wall plate, which will be transmitted to the F-brackets. The F-brackets are discontinuous elements, separated by a distance known as the center-to-center distance (CTC) of the brackets*

1.3 Problem and goal

1.3.1 Problem and research question

The problem is the determination of the resistance of the wall plate, especially regarding the effective width of the wall plate. The forces in the wall plate are continuous and have to be distributed over the F-brackets. The brackets on the other hand have a varying center-to-center distance and are therefore discontinuous. The main research question will be:

- What is the resistance of the wall plate in combination with F-brackets?

And the sub-questions:

- What is the value of the effective width?
- Which variables have an effect on the effective width of the wall plate?

Variables as in: variation of roof inclination, positioning of the wall plate in the bracket (adding, see **figure 1.1h**, #16) and changing center-to-center distances of the brackets.

1.3.2 Aim of this research project

The aim of this project is to give an accurate determination of the resistance of the wall plate. This is necessary due to the fact that there has been a lack of research in the past. In addition, there is no agreed design method on this subject. This causes structural design agencies to design their own model for calculating the resistance, resulting in varied calculations in different cases. After examining these calculations, it is concluded that the results obtained using a non-conservative calculation method. This is obviously not acceptable in a sector where the failure of structures might result in life-threatening situations. No disastrous situations have been reported (yet). Still, less severe effects might result due to faulty design calculations (for example building physical deficiencies, like air or sound leakages).

1.3.3 Overview of the thesis

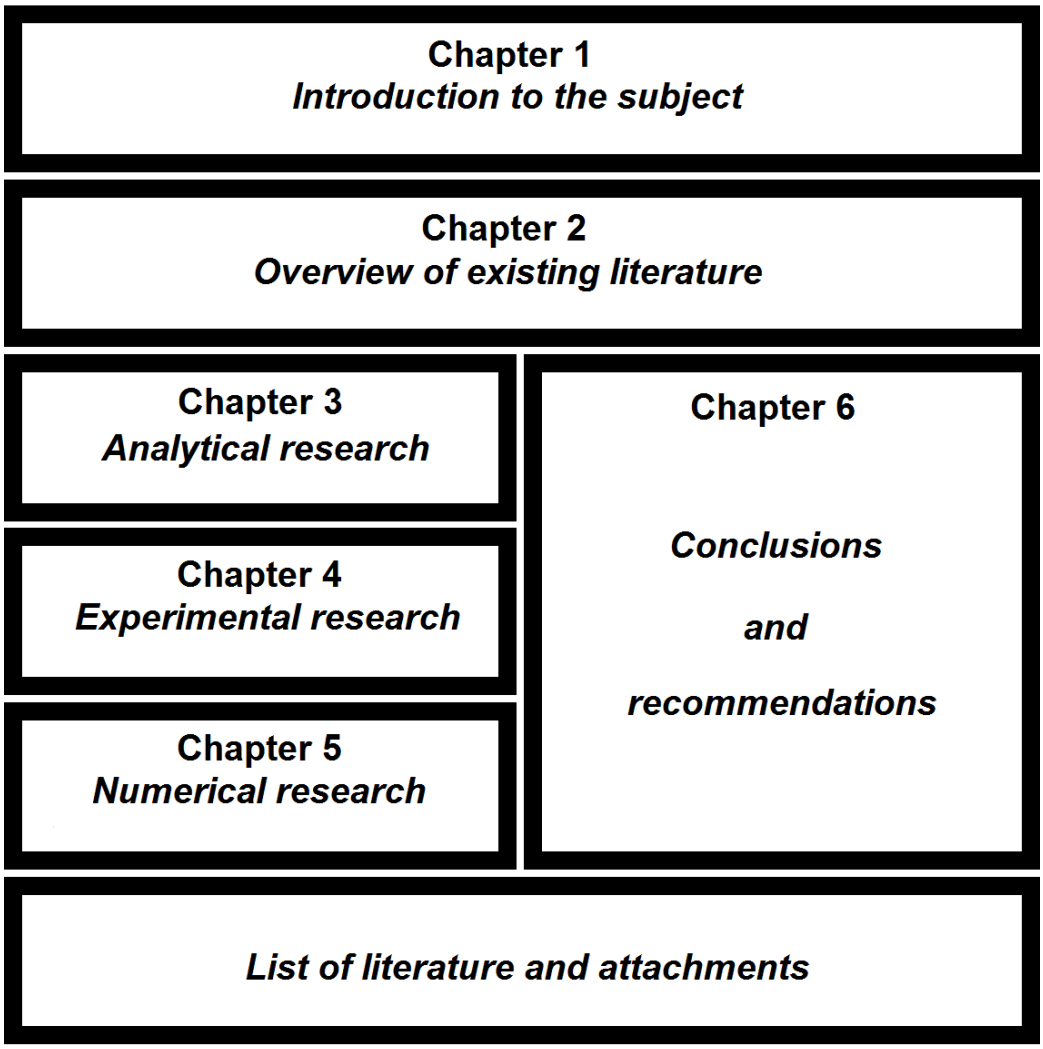

***Figure 1.3a**; Overview of the thesis*

- Chapter 2 Overview of existing literature

Chapter 2 gives a theoretical introduction on the subject regarding already existing literature. It provides a foundation for the research. However, some literature might be reviewed and revised. First, it starts with the basics of strength of materials. This is followed by literature provided by both the Technical University of Eindhoven and structural design agencies regarding the calculation of the connection detail.

- Chapter 3 Analytical research

Chapter 3 gives an analytical view on the erroneous assumptions detected in the existing literature from chapter 2. Also a starting point will be given for chapter 4 and 5, which will deal with the experimental and numerical research.

- Chapter 4 Experimental research

Chapter 4 deals with the preparation, execution and analysis of the experimental research. The preparation consists of the determination of material properties and geometry, the

development of the test set-up and the type of measurement. The execution of the experiments yield in results, whereafter the results are analyzed and concluded.

- Chapter 5 Numerical research

Chapter 5 deals with the preparation, execution and analysis of the numerical research. First a short introduction in the finite element method is give. Hereafter a two dimensional model is elaborated, which is the basis for the three dimensional model that follows afterwards. The chapter ends with conclusions and recommendations.

- Chapter 6 Conclusions and recommendations

Chapter 6 is divided in two parts. The first parts concludes the results obtained in chapters 3 to 5. This is followed by the answering of the research question and sub questions. The second part is giving recommendations for improvement regarding this research project and other future research subjects.

Chapter 2 | Overview of existing literature

This chapter gives a theoretical introduction on the subject regarding already existing literature. It provides a foundation for the research. However, some literature might be reviewed and revised. First, it starts with the basics of strength of materials. This is followed by literature provided by both the Technical University of Eindhoven and structural design agencies regarding the calculation of the connection detail.

2.1 Basics of strains and stresses

2.1.1 Linear elasticity for an isotropic material

As a result of normal forces, shear forces, bending moment and torsional moment on a constructional element, stresses appear in an imaginary small part of that element. This part is randomly taken at any position inside the material, but is therefore different in every case. Stresses are a force-per-unit-area and are indicated with Newton per squared meters or millimeters. Forces applied perpendicular to the surface are distinguished from forces applied parallel to the surface. These forces considered on a small element are called normal stresses and shear stresses respectively. Stresses are indicated with a vector. This means that they have a direction and magnitude. For simplification, the stresses are mostly indicated with only one arrow on a surface. Stresses are drawn in positive direction. This means that the normal stresses on a surface are interpreted as a pressure force and the normal stresses off a surface as a tension force. Normal stresses are indicated with a sigma (σ) and shear stresses with a tau (τ). Strain is the shortening or elongation of an element due to stresses. The strains related to normal stresses are indicated with an epsilon (ε) and strains related to shear stresses with a gamma ($\gamma; shear\ angle$). The elastic relation between stresses and strains are indicated in **equation 2.1**.

$$\sigma = E \cdot \varepsilon \tag{2.1a}$$

$$\tau = G \cdot \gamma \tag{2.1b}$$

'E' is the modulus of elasticity and 'G' is the shear modulus. Both moduli have the same dimension as the stresses. This results in the strains being dimensionless. The normal and shear stresses can be divided in three main directions. In an orthogonal coordinate system, these directions are called x, y and z. To indicate the matching stresses and strains, subscripts are added corresponding the axis direction. In a three dimensional model, the stress-strain relations for an isotropic material, such as steel, are written as follows **[13]**:

$$\begin{bmatrix} \varepsilon_x \\ \varepsilon_y \\ \varepsilon_z \\ \gamma_x \\ \gamma_y \\ \gamma_z \end{bmatrix} = \frac{1}{E} \cdot \begin{bmatrix} 1 & -\nu & -\nu & 0 & 0 & 0 \\ -\nu & 1 & -\nu & 0 & 0 & 0 \\ -\nu & -\nu & 1 & 0 & 0 & 0 \\ 0 & 0 & 0 & 2\cdot(1+\nu) & 0 & 0 \\ 0 & 0 & 0 & 0 & 2\cdot(1+\nu) & 0 \\ 0 & 0 & 0 & 0 & 0 & 2\cdot(1+\nu) \end{bmatrix} \cdot \begin{bmatrix} \sigma_x \\ \sigma_y \\ \sigma_z \\ \tau_x \\ \tau_y \\ \tau_z \end{bmatrix} \tag{2.2}$$

2.1.2 Linear elasticity for an orthotropic material

In the previous section, the relations between stress and strain for an isotropic material like steel or concrete were introduced. However, wood is an orthotropic material. This means that it contains different material properties in different perpendicular directions. There is a longitudinal (L), radial (R) and tangential (T) direction. The longitudinal direction is parallel to the grain direction, and therefore the strongest. The radial and tangential direction are perpendicular to the grain direction and contain only a fraction of the longitudinal strength. The radial direction is directed perpendicular to the growth rings of the tree. The tangential direction is perpendicular to the radial direction, tangential to the growth rings. The material properties for wood is therefore described with the following formula **[20]**:

$$\begin{bmatrix} \varepsilon_{LL} \\ \varepsilon_{RR} \\ \varepsilon_{TT} \\ \gamma_{LR} \\ \gamma_{LT} \\ \gamma_{RT} \end{bmatrix} = \begin{bmatrix} \frac{1}{E_L} & \frac{\nu_{RL}}{E_R} & \frac{\nu_{TL}}{E_Y} & 0 & 0 & 0 \\ \frac{\nu_{LR}}{E_L} & \frac{1}{E_R} & \frac{\nu_{TR}}{E_T} & 0 & 0 & 0 \\ \frac{\nu_{LT}}{E_L} & \frac{\nu_{RT}}{E_R} & \frac{1}{E_T} & 0 & 0 & 0 \\ 0 & 0 & 0 & \frac{1}{G_{LR}} & 0 & 0 \\ 0 & 0 & 0 & 0 & \frac{1}{G_{LT}} & 0 \\ 0 & 0 & 0 & 0 & 0 & \frac{1}{G_{RT}} \end{bmatrix} . \begin{bmatrix} \sigma_{LL} \\ \sigma_{RR} \\ \sigma_{TT} \\ \tau_{LR} \\ \tau_{LT} \\ \tau_{RT} \end{bmatrix} \quad (2.3)$$

2.2 Transfer of loads

The roof structure is exposed to several types of loading. As mentioned in paragraph **1.1.2** there are live loads and dead loads. The self-weight of the roof and its construction is considered a dead load, since it is always present. Loading due to snow, wind, rain and persons are live loads. These loads last for only short periods of time and vary in magnitude. Snow, wind and rain are often distributed uniformly on the construction, but loading due to persons is mostly local. The normative code prescribes certain rules for calculating maximum load combinations for a construction. Two decisive load combinations apply for a roof construction:

- Permanent load in combination with maximal snow load

The first load combination consists of maximum dead load with a maximal symmetric snow load. **Figure 2.2a** represents the moment, axial and shear distribution along the construction. Notice the redistribution of the moment stresses due to the supporting structure. This also results in a reduction of the axial and shear stresses in the floor-roof connection.

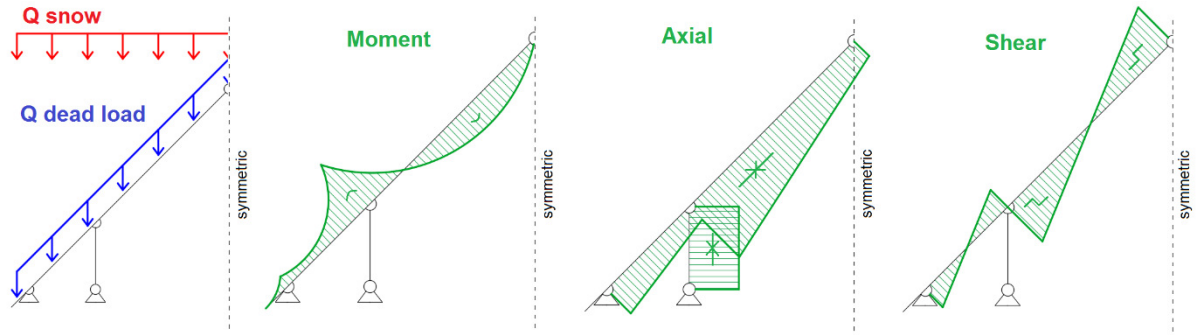

***Figure 2.2a**; Mechanical scheme for a pitched roof subdued to a maximal snow load*

- Permanent load in combination with maximal wind load

This load combination includes a maximum wind pressure on one side of the roof and a suction force on the other side. Add a minimal self-weight of the structure and an overpressure from the inside to obtain an upward force on the leeward side of the roof. The coach screw will prevent the roof from tilting, and is therefore the essential type of fastener.

The hinge support on the left in **figure 2.2a** represents the connection detail of the F-bracket and the wall plate. The connection detail is capable of transferring loads in a horizontal and vertical direction, but no bending moments. The loads are introduced in the rafters. The rafters are continuous structural elements. The loads are divided in axial forces and shear forces. The axial forces are transferred to the underlying supporting panel. The load will spread along the entire width of the roof element. Subsequently the load is passed on to the supporting batten, which on its turn transfers the load to the connecting wall plate. Finally the forces will be transferred to the F-bracket. Besides, there are the shear forces in the rafters. These forces are transported directly to the wall plate through surface contact. These forces are schematized as point loads on the wall plate, as the rafters are discontinuous in the direction of the wall plate. The flow of loads (and therefore stresses) is the main goal of this research.

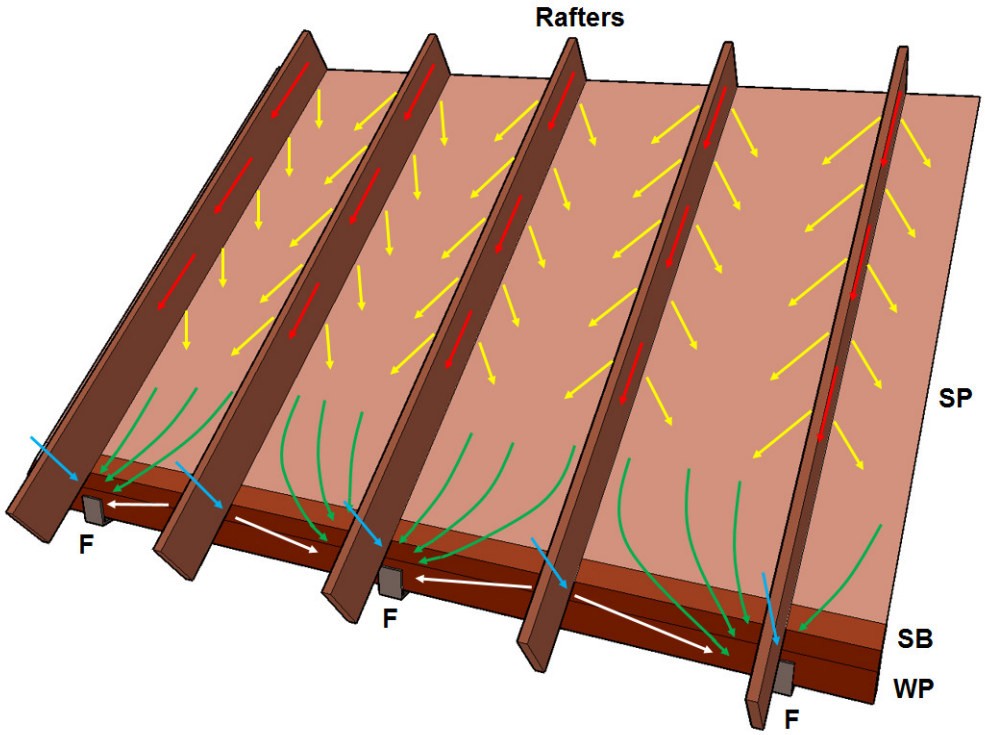

***Figure 2.2b**; Transfer of loads in the roof structure. The roof structure consists of rafters, a supporting panel (SP), a supporting batten (SB), a wall plate (WP) and F-brackets (F). The arrows represent the flow of forces:*

The arrows in **figure 2.2b** represent the following forces:

- Red arrow: the axial forces in the rafters
- Yellow arrow: Transfer of the axial force in the rafters to the supporting batten
- Green arrow: Transfer of the axial load from the supporting panel to the supporting batten, wall plate and subsequently the F-bracket.
- Blue arrow: the shear forces in the rafters, transferred directly to the wall plate
- White arrow: the translation of shear forces towards the F-brackets. Only applicable for shear forces in rafters position not directly above a bracket

2.3 Determination of the maximal allowed stresses

Although the calculation of the detail's strength is a three dimensional problem, it is often simplified in a two dimensional drawing. The calculation method described in this chapter is included in the study material for the course timber structures lectured at the Technical University of Eindhoven **[17]**:

2.3.1 Arrival of the forces at the wall plate

The initial axial and shear forces can be composed to a single equilibrium state (**figure 2.3a**). The axial forces are introduced by the supporting batten, whereas the shear forces are transferred by means of the rafters. Both forces are decomposed in a downward vertical force and an either positive or a negative horizontal thrust. This results in an increased downward vertical force and a positive horizontal thrust, as the axial force has a greater influence then the shear force. Note: the sear forces are introduced locally, as the rafters are discontinuous in the direction of the wall plate. The axial forces are assumed to spread evenly. However, this is most likely not the case due to the attraction of the stresses by the harder points in the structure.

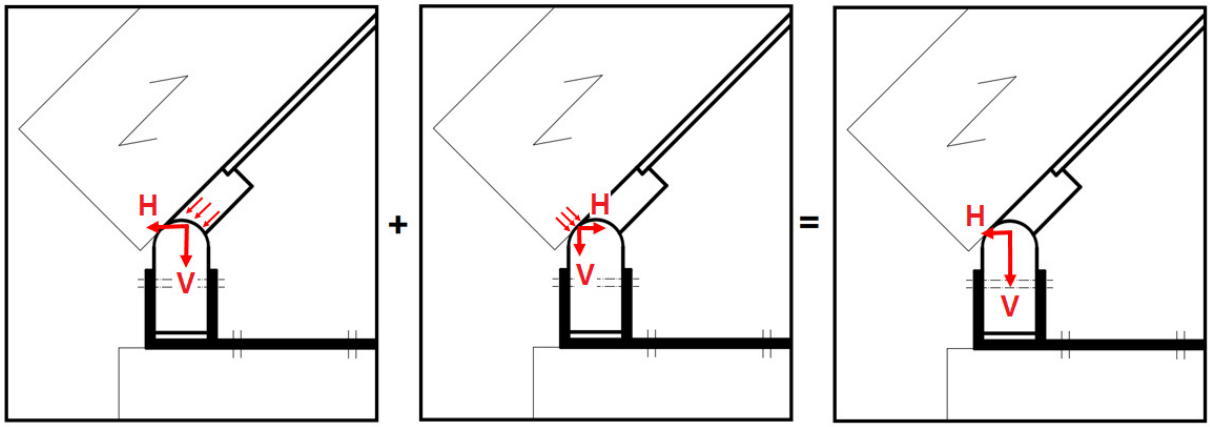

***Figure 2.3a**; Arrival of the forces in the wall plate. On the left: the axial forces obtained by the supporting batten. In the middle: the shear forces transferred by means of the rafter. On the right: the sum of the obtained forces*

2.3.2 Transfer of loads to the bracket and the floor

Once the forces arrive in the wall plate, they will be transferred to the bracket. The transfer of loads result in internal stresses in the wall plate, see **paragraph 2.3.3**. The vertical forces are transmitted by contact (with the interference of the adding) and are spread along the bottom surface of the bracket. The horizontal forces however have to be translated towards the top side of the baffles to be transferable. This will result in an internal bending moment in the wall plate.

Figure 2.3b explained:

The initial vertical force **(red V)** will spread into an equally divided vertical compressive stress **(blue V)**. The floor will give the corresponding reaction force **(green Rv1).** The initial horizontal force **(red H)** will be translated toward the upper side of the bracket's baffle **(blue H)**. This will result in moment stresses in the wall plate and the bracket **(Blue M)**. To equalize the moment in the bracket, two vertical reaction forces appear **(green Rv2 & Rv3)** by means of the rivets. These forces create a counter couple in the bracket **(Green M)**. To transfer the horizontal force, a reaction force in the outer rivet is present **(green Rh)**.

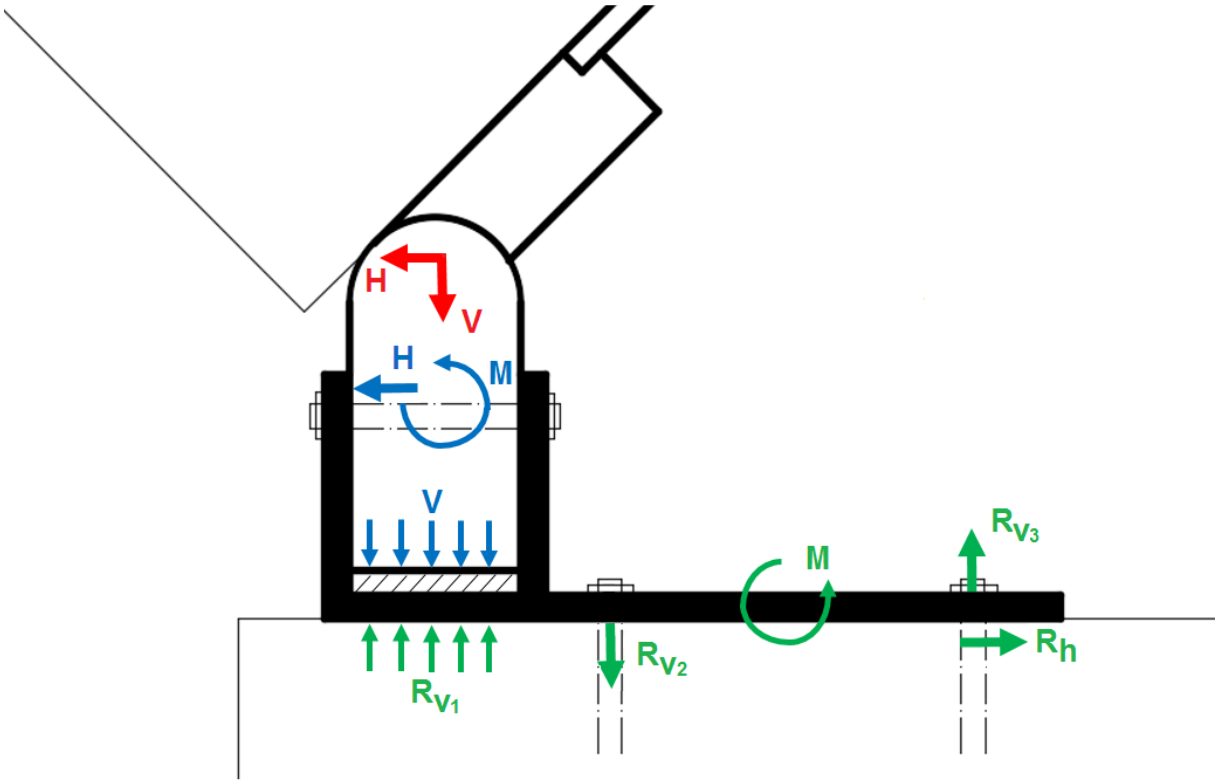

***Figure 2.3b**; Schematization of the transmission of loads to the bracket and the floor*

2.3.3 Stresses in the wall plate

The critical stresses in the wall plate consist of the stresses due to the vertical compression force and the stresses caused by the bending moment. The bending moment arises by transferring the horizontal force to the bracket. The stresses are obtained with the following formulas:

$$\sigma_c = \frac{V}{A} \tag{2.4}$$

$$\sigma_m = \frac{M}{W} \tag{2.5}$$

Where:

σ_c = Compressive stresses in the wall plate
V = Vertical compression force in the wall plate
A = Cross sectional area of the wall plate

σ_m = Bending stresses in the wall plate
M = Bending moment in the wall plate
W = Section modulus of the wall plate

And:

$$A = b_F \cdot b_{wp} \tag{2.6}$$

$$W = \frac{1}{6} \cdot l_{ef} \cdot (b_{wp})^2 \tag{2.7}$$

Where:

b_F = Width of the F-bracket
b_{wp} = Width of the wall plate
l_{ef} = Effective width of the wall plate (assumed 300mm)

The bending moment is equal to the following formula:

$$M = e \cdot H \tag{2.8}$$

Where:

e = The eccentricity of the horizontal force
H = The horizontal force which has to be translated to the bracket

The eccentricity e is subdivided in two parts (see **figure 2.3c**):

$$e_1 = b_{wp} \cdot \tan(\alpha) \tag{2.9a}$$

$$e_2 = \frac{H}{2 \cdot b_F \cdot f_{c,90}} \tag{2.9b}$$

Where:

α = roof inclination
$f_{c,90}$ = maximal compressive strength of wood perpendicular to the grain direction

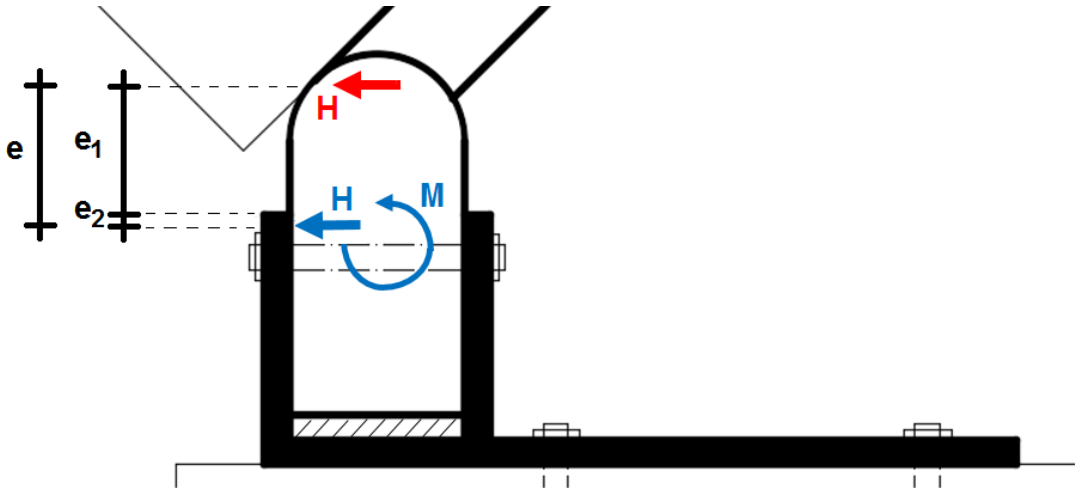

***Figure 2.3c**; Schematization of the transfer of the horizontal force, resulting in a bending moment*

The first element e_1 is obtained with help of the goniometric relation of the tangent. This is illustrated in **figure 2.3d (left)**. However, the graph on the right side of **figure 2.3d** shows the progressive increase of the eccentricity compared to the even increase of the roof inclination. Once it reaches a roof angle of 60 degrees, the value for e_1 is about 120mm. This is almost the complete depth of the wall plate, and therefore high unlikely. **Chapter 3** starts with an improvement of the formula and **Chapter 5** will give a more in depth solution.

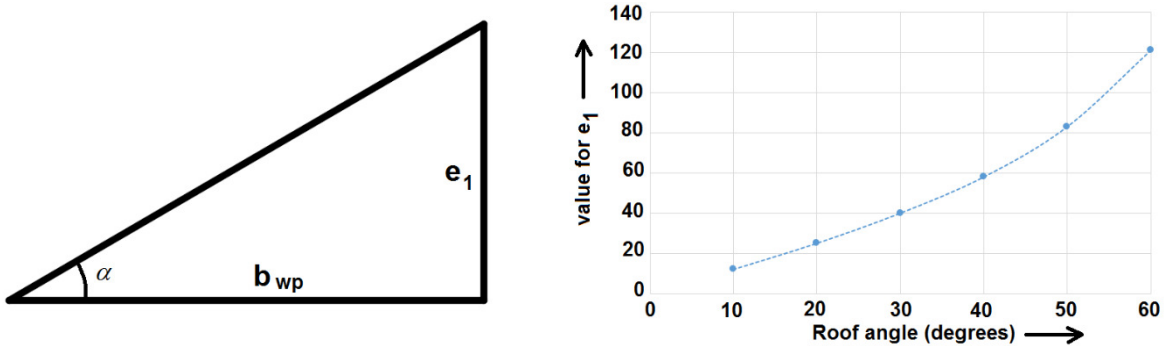

***Figure 2.3d**; Left: goniometric relation of the width of the wall plate and e_1. Right: relation between the value of e_1 and the roof angle. Depth of wall plate = 144mm, thickness of wall plate = 70mm*

The value for e_2 is determined with the minimal required area for the wood to transfer the horizontal load.

$$\sigma = \frac{F}{A} \tag{2.10}$$

Where:

σ = Maximal allowed compressive stress ($f_{c,90}$)
F = Horizontal force (H)
A = Minimal required area

So the minimal required area is obtained by the following formula:

$$A = h \cdot b_F \tag{2.11}$$

Where:

h = minimal required depth of wood to transfer the horizontal load.

As the center of gravity is located in the center of the area (see **figure 2.3e**), the depth is re-written as:

$$h = 2 \cdot e_2 \tag{2.12}$$

Combing formulas **2.10, 2.11 and 2.12** results in:

$$\sigma = f_{c,90} = \frac{H}{2 \cdot e_2 \cdot b_F} \tag{2.13}$$

Which is equal to:

$$e_2 = \frac{H}{2 \cdot b_F \cdot f_{c,90}} \tag{2.9b}$$

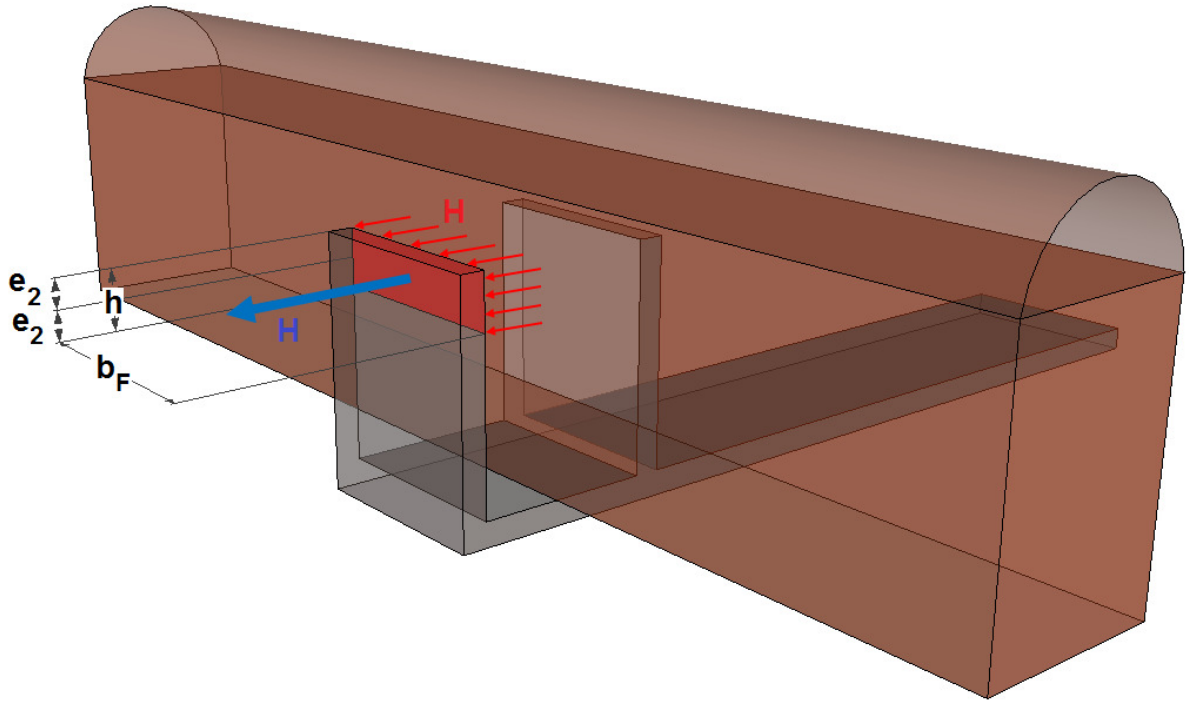

***Figure 2.3e**; Determination of e_2*

The critical stress combinations can now be determined. First there are the critical compressive stresses. These stresses are most likely to occur for a roof with a medium angle and a heavy load. Secondly, there are the critical tensional stresses. These are more likely to be present in case of a low pitched roof with a light roof. The critical stress combinations are provided in **formulas 2.14 and 2.15**. They are also illustrated in **figure 2.3f**.

$$\sigma_{c,90,d} = \frac{V}{b_F \cdot b_{wp}} + \frac{M}{1/6 \cdot l_{ef} \cdot (b_{wp})^2} \leq f_{c,90,d} \tag{2.14}$$

$$\sigma_{t,90,d} = \frac{M}{1/6 \cdot l_{ef} \cdot (b_{wp})^2} \leq f_{t,90,d} \tag{2.15}$$

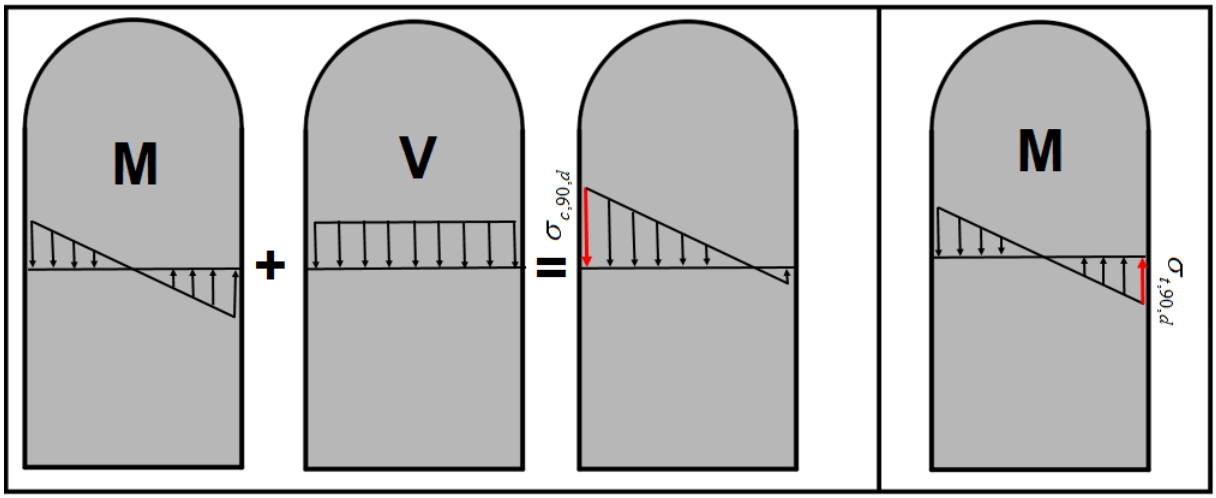

***Figure 2.3f**; Left: assembly of the critical compressive stress in the wall plate. Right: assembly of the critical tensile stress in the wall plate*

2.4 Calculation methods from practice

Five calculations of the connection detail, which are performed by structural design agencies, are analyzed. These calculations are given in **appendix 2.1** (Note: these calculations are in Dutch). It is worth mentioning that all SD-agencies perform their own list of design checks. There are resemblances, but also deviations in perception. This paragraph will sum up the most common checks performed. Besides an overview is given of erroneous assumptions.

2.4.1 Common checks performed

Although this research project focusses on the check of the wall plate, a list is made of all common checks performed by the SD-agencies. Not all checks are included in the performed calculations, eventhough it would be highly advisable to complete the list with the missing checks.

1) Check of the compressive stresses perpendicular to the grain direction in the wall plate
2) Check of the tensile stresses perpendicular to the grain direction in the wall plate
3) Check of the compressive stresses perpendicular to the grain direction in the supporting batten
4) Check of the connection between the wall plate and the supporting batten
5) Check of the connection between the supporting batten and the supporting panel
6) Check of the connection between the wall plate and the F-bracket
7) Check of the F-bracket and checks of individual components of the bracket
8) Check of the anchoring of the bracket to the floor
9) Check of the strength of the coach screw in combination with upward loading

The first two checks are elaborated upon in the previous paragraph. The third check verifies the strength of the supporting batten. Compressive stresses run through the batten, introduced by the supporting panel and leaving to the wall plate. A more in-depth treatment is given in **chapters 3 and 5**. Checks 4 to 6 validate the transference of the forces to another object. Normative is the minimal required area, similar as the determination of e_2 (**paragraph 2.3.3**). Check 7 and 8 focusses on the strength of the F-bracket. Components like baffles, welds and anchoring are considered. Check 9 makes sure the roof is not lifting upward. The coach screw is both checked for the pull out resistance and the shear strength.

2.4.2 Erroneous assumptions

- 2D schematization, not 3D

As in existing literature, the design agencies don't take the three dimensional aspect into account. If the detail was correctly simplified to a two dimensional model, it wouldn't be a problem. However, due to this simplification, certain important aspects, like the concentration of the stresses in the wall plate and the random position of the rafters, are disregarded.

- Neglecting the shear forces

All calculations assume the detail to transfer the axial loads in the rafters only. They neglect the influence of the rafters on the wall plate, or, in other words, the locally applied shear force. This is caused by a wrong interpretation of the schematization. Frame software is used to calculate the reaction forces in the detail, after which the initial force is composed out of the reaction forces. In these cases only the axial force is composed, instead of both the axial force and the shear force.

- No effective width of the wall plate

All checks of the wall plate or supporting batten have been performed with an overestimated width. The effective width is expected to be between the width of the bracket (conservative) and the center-to-center distance of the brackets (overestimate). The determination of the actual effective width is part of this research project.

- Assumption of the counter moment

Some calculations assume the vertical component in the wall plate to generate a counter bending moment, reducing the effect of the bending moment caused by the horizontal component. However, the vertical component is able to transfer the load directly to the underlying floor, without shifting of the working line, resulting in no bending moment.

2.5 Conclusions

- There is no uniformity in the way the design checks of the connection detail (with the wall plate and F-brackets) should be performed. Various structural design agencies interpret the detail in their own way, resulting in different (and in some cases erroneous) checks. A more uniform list of checks, and how they need to be performed, is required to prevent over-estimation of the design resistance as well as over-conservative designs.

- There is no information on the magnitude of the effective width, beside an assumed value. Design agencies often neglect the effective width of the wall plate by using the entire width of the wall plate, which is incorrect. This research project should help to correct this matter and provide a correct standard for the effective width of the wall plate.

- The determination of the bending moment in the wall plate, in particular the value for the eccentricity, needs improvement, as it is incorrect. **Chapters 3 and 5** will give an improved recommendation for defining the value of the eccentricity.

Chapter 3 | Analytical research

This chapter gives an analytical view on the defects detected in the existing literature from the previous chapter. Also a starting point will be given for the upcoming two chapters, which will deal with the experimental and numerical research.

3.1 Determination of the bending stresses in the wall plate

As mentioned in the previous chapter, this paragraph offers an improved formula for determining the bending moment in the wall plate. Again, it starts with the formula for the bending moment:

$$M = e \cdot H \tag{3.1}$$

Where:

M = Bending moment
e = The eccentricity of the horizontal force
H = The horizontal force, decomposed from the initial axial and shear forces, which has to be translated to the bracket

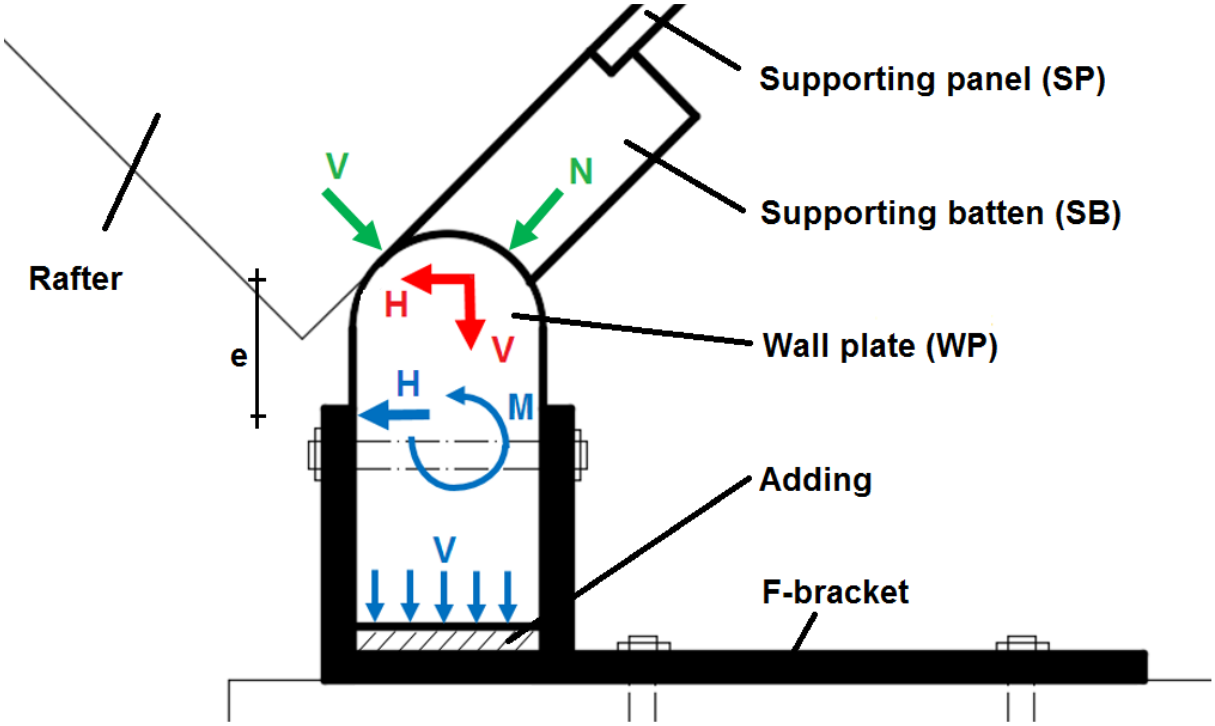

Figure 3.1a; *Determination of the bending moment. The green arrows represent the initial forces. The red arrows suggest the decomposed forces in the top of the wall plate. The blue arrows are the translated forces in the wall plate and the resulting bending moment*

As in the previous chapter, the eccentricity 'e' is divided in separate parts. Though, this time, it is distinguished in three parts:

$$e = e_{1a} + e_{1b} + e_2 \tag{3.2}$$

Where $e1_a$ and $e1_b$ suggest an improved version of the previous e_1, and e_2 being an addition to the e_2 given in **paragraph 2.3.3**.

So e1 consists of two parts. The first part e1a is defined by the dimensions of the connection detail (see **figure 3.1b**):

$$e_{1a} = h_{wp} + t_a + t_F - r - h_b \tag{3.3a}$$

Where:

h_{wp} = The depth of the wall plate

t_a = The thickness of the adding

t_F = The thickness of the F-bracket

r = The radius of the shaven wall plate (semicircle). It is equal to half the width of the wall plate = $\frac{1}{2} \cdot b_{wp}$

h_b = Depth of the baffles of the F-bracket

So:

$$e_{1a} = h_{wp} + t_a + t_F - \frac{1}{2} \cdot b_{wp} - h_b \tag{3.3b}$$

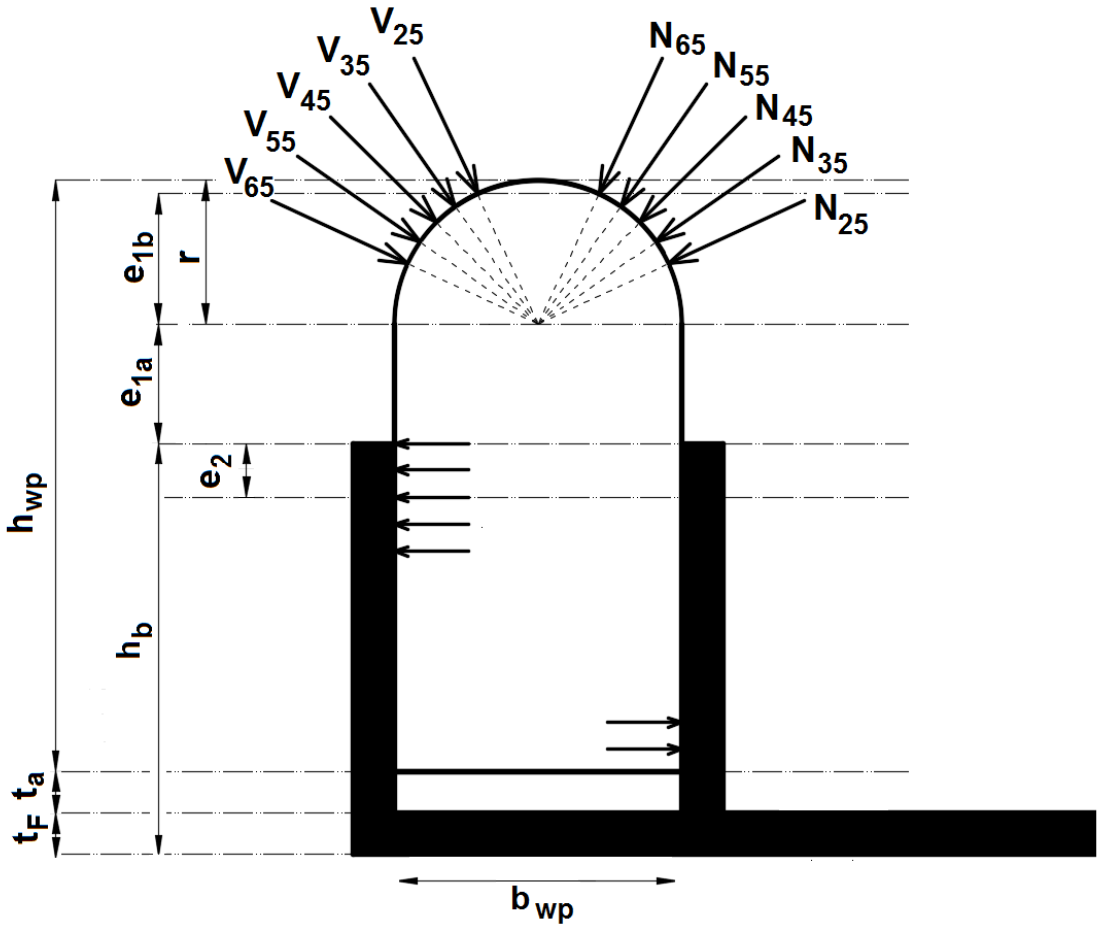

Figure 3.1b; *Dimensions of the connection detail. N represents the axial forces, whereas V represents the shear forces. The subscript equals the roof inclination*

The value for e_{1b} is harder to define. The position of the horizontal component introduced by the axial force is normative for the maximal depth of e_{1b}. However, the horizontal component caused by the shear force will induce a counter moment, eventually resulting in a reduction of e_{1b}. The location of the rafters, and therefore the shear forces, cannot be predetermined and are for simplicity reasons disregarded. This will result in an overestimation of e1b, however on the safe side. So the actual value for e1b will be between:

$$0 \le e_{1b,actual} \le e_{1b,assumed} = e_{1b} \tag{3.4}$$

The value for e_{1b} is determined with the help of **figure 3.1c**:

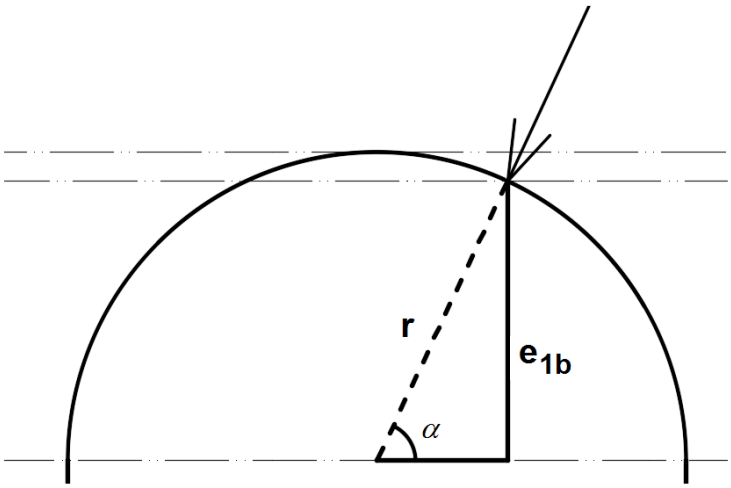

Figure 3.1c; *Determination of e_{1b} with goniometric relations*

$$e_{1b} = \sin(\alpha) \cdot r = \sin(\alpha) \cdot {}^{1}\!/_{2} \cdot b_{wp} \tag{3.5}$$

Where:

α = Roof angle (degrees)

In chapter 2 it was determined that e_2 is equal to:

$$e_2 = \frac{H}{2 \cdot b_F \cdot f_{c,90}} \tag{3.6}$$

This is according to the assumption that the reaction force at the top of the baffles is the only reaction force present. However, this is not the case. Beside the reaction force at the top of the baffles, there is also a reaction force present at the bottom of the baffles, resulting in an increased reaction force at the top of the baffles. This will also result in an increased value of e_2.

The sum of the horizontal forces is considered to be zero:

$$\Sigma F_H = 0 \qquad \rightarrow \qquad R_{H;1} = H + R_{H;2} \tag{3.7}$$

$R_{H;1}$ presents the new horizontal force in **formula 3.6**, resulting in:

$$e_2 = \frac{R_{H;1}}{2 \cdot b_F \cdot f_{c,90}} = \frac{H + R_{H;2}}{2 \cdot b_F \cdot f_{c,90}} \tag{3.8}$$

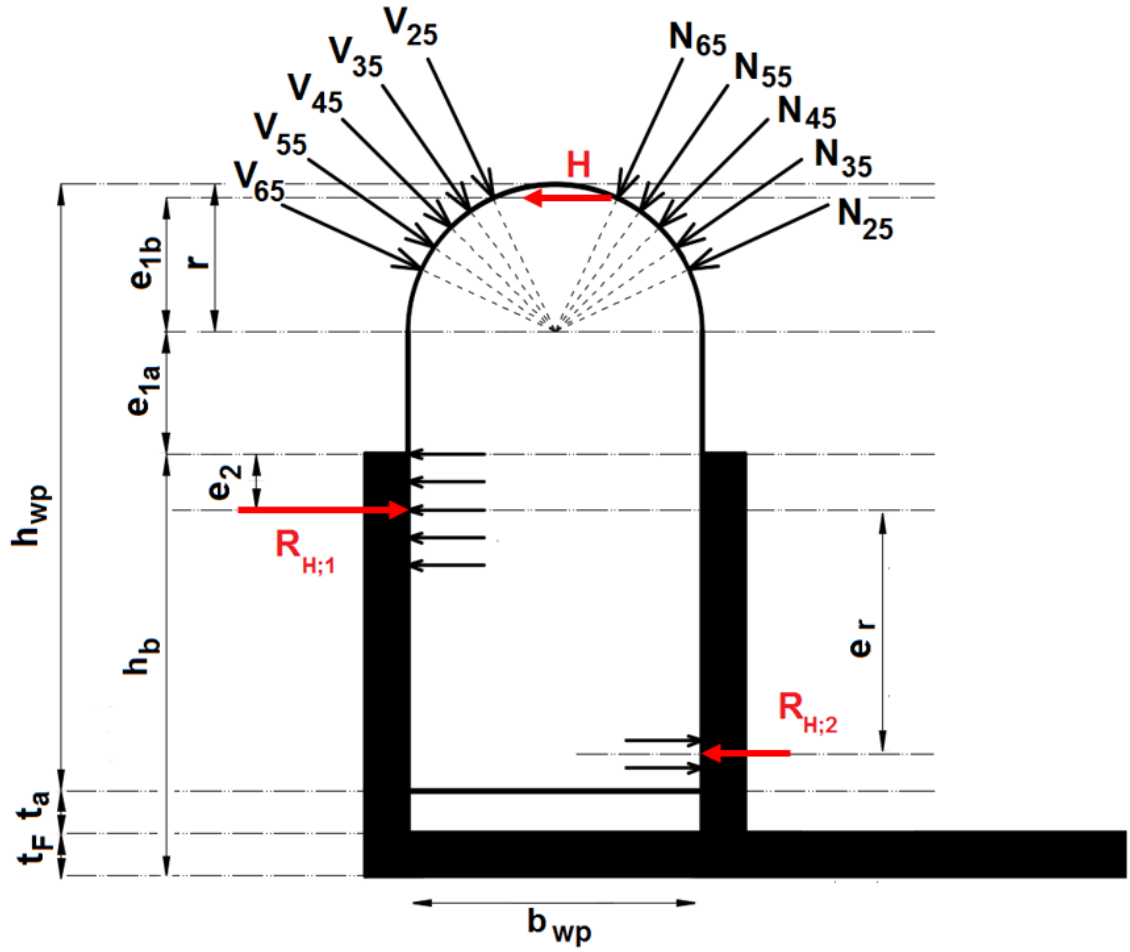

Figure 3.1d; *Initial force H and the reaction forces $R_{H;1}$ and $R_{H;2}$*

To define $R_{H;1}$, $R_{H;2}$ needs to be determined. Therefore the sum of the bending moment at $R_{H;1}$ is considered to be zero:

$$\Sigma M = 0 \qquad \rightarrow \qquad H \cdot e = R_{H;2} \cdot e_r \tag{3.9}$$

This can be re-written as:

$$R_{H;2} = \frac{H \cdot e}{e_r} \tag{3.10}$$

Where:

$$e_r = h_{wp} - r - e_{1a} - e_2 - \frac{R_{H;2}}{2 \cdot b_F \cdot f_{c,90}} \tag{3.11}$$

Resulting in:

$$R_{H;2} = \frac{H \cdot e}{h_{wp} - r - e_{1a} - e_2 - \dfrac{R_{H;2}}{2 \cdot b_F \cdot f_{c,90}}} \tag{3.12}$$

Although $R_{H;2}$ mathematically might be solvable, the values of e and e_{1a} are unknown, therefore the value of $R_{H;2}$ cannot be determined. So, as a possible solution, an estimated ratio is used for determining $R_{H;2}$:

$$R_{H;2} = \chi \cdot H \tag{3.13}$$

χ is obtained by using figure **3.1e**. One needs to determine ψ first:

$$\psi = \frac{e_{1a} + r}{h_{wp}} = \frac{h_{wp} + t_a + t_F - h_b}{h_{wp}} \tag{3.14}$$

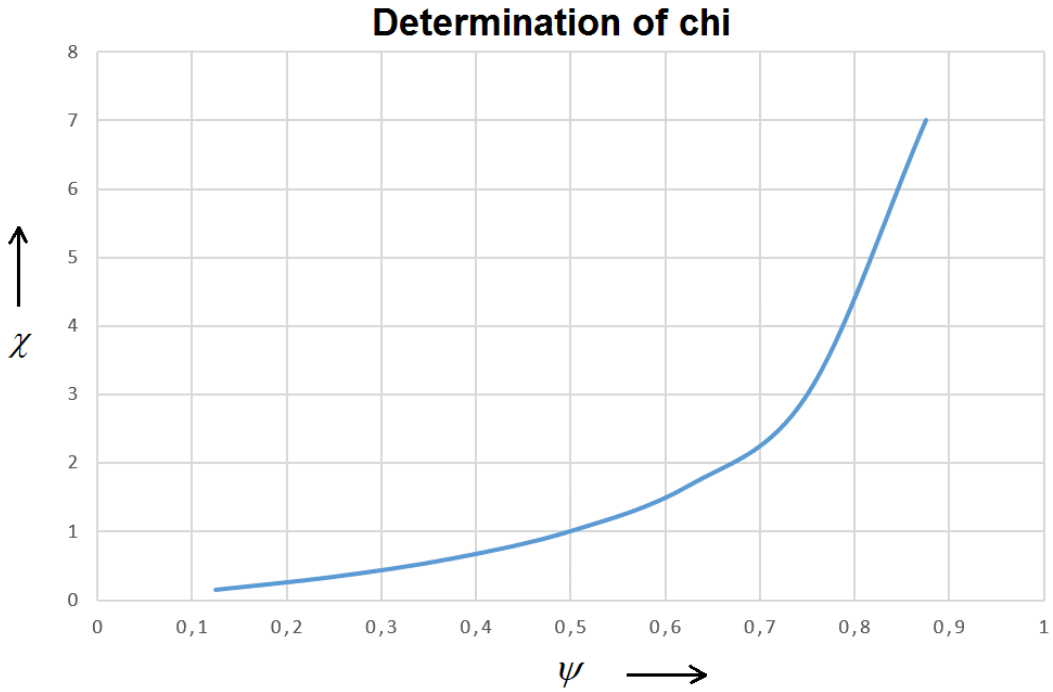

Figure 3.1e; *Determination of chi*

The ratio is based on the length of the wall plate rising above the bracket divided by the length of the wall plate still in the bracket.

Finally, this results in a formula for the eccentricity of the horizontal force:

$$e = h_{wp} + t_a + t_F - \tfrac{1}{2} \cdot b_{wp} - h_b + \sin(\alpha) \cdot \tfrac{1}{2} \cdot b_{wp} + \frac{(1+\chi) \cdot H}{2 \cdot b_F \cdot f_{c,90}} \tag{3.15}$$

For a couple of standard roof structures example calculations are made and added to **appendix 2.2**. The results are shown in **table 3.1a**. The decrease of the eccentricity for higher roof angles is caused by the decrease of the axial force in this particular load combination (dead load with maximum snow load).

Roof inclination	eccentricity
35 degrees	79,41mm
45 degrees	75,82mm
55 degrees	74,68mm

Table 3.1a; *Results for the eccentricity regarding the internal bending moment of the wall plate, the complete calculation is added to* ***appendix 3.1***

3.2 Transfer of load in the supporting batten

The role of the supporting batten has not been discussed yet, though, it plays an important role in the transfer of the loads. This paragraph will give a better insight into the usefulness of the batten. The axial forces in the rafters are transferred to the supporting panel, followed by the supporting batten, before they reach the wall plate. The supporting batten acts as a transition between the supporting panel and the wall plate. The benefits of this supporting batten are discussed here.

The supporting panel has an average thickness of 11 mm. In case no supporting batten is used, the axial force would arrive at the top of the batten, risking the wall plate to fail by shear. In addition, it would generate an increased bending moment in the wall plate, risking failure by either exceeding maximum compressive or tensile stresses of wood perpendicular to the grain direction. The supporting batten is four times thicker compared to the panel. It will operate as a distributor of forces for the wall plate. It will bend the forces to a more downward direction, reducing the size of the horizontal force (which leads to a bending moment in the wall plate). However, this results to a bending moment in the batten itself, as the forces are translated over a distance ‘e’ to a new working line, shown in **figure 3.2a**.

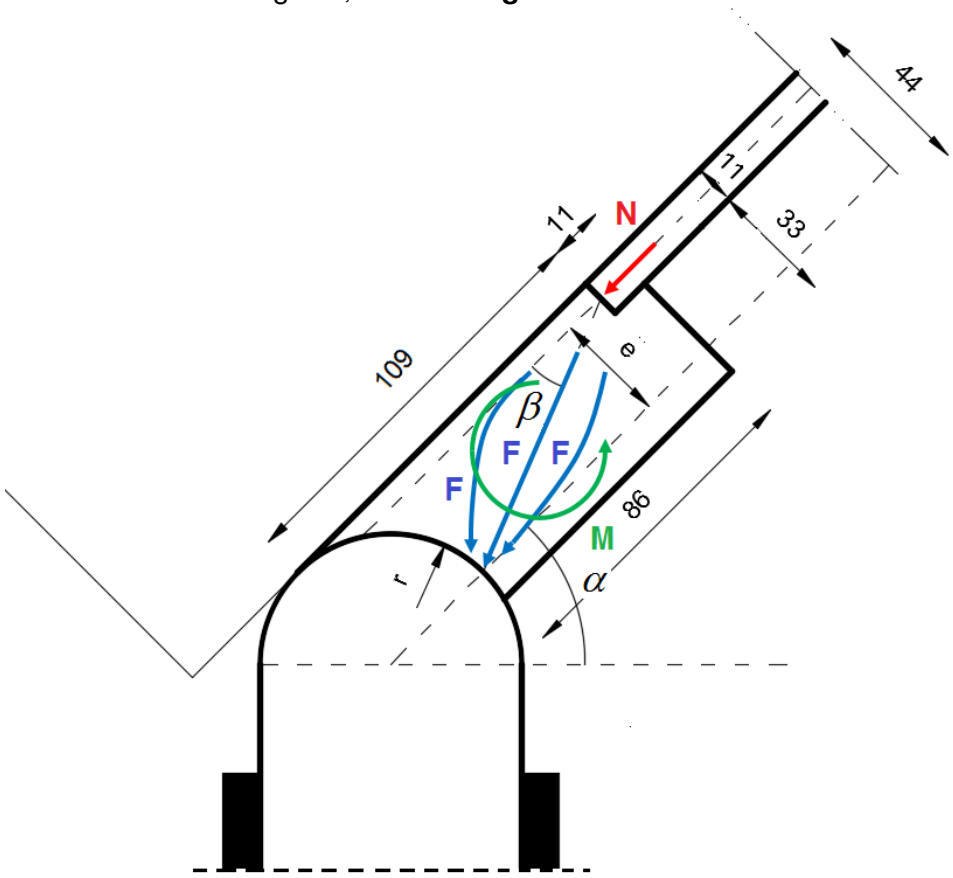

Figure 3.2a; *Transfer of loads in the supporting batten.*

By making a section cut halfway the batten, the internal stresses can be analyzed. As the forces take the path of the least resistance, in this case the shortest route, a higher stress will occur in the center of the wall plate. The effect of the bending moment should also be included. The distribution of stresses in **figure 3.2b** is a simple estimation, but **Chapter 5** gives a more accurate approximation.

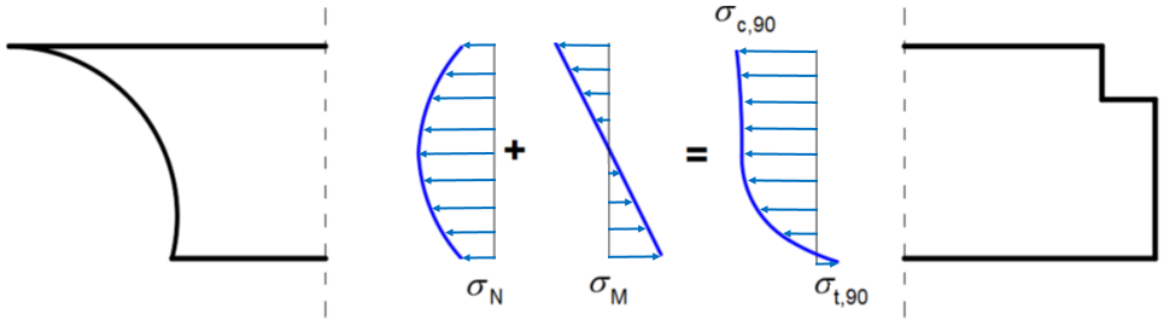

Figure 3.2b; *Stress distribution in the supporting batten.*

3.3 Standardized test set-up

The upcoming two chapters discuss the outcome of the experimental and numerical researches. This paragraph will function as a starting point for the experimental and numerical research, by presenting the test set-up. To be able to compare results it is important to have singularity in the boundary conditions. The outcome of these tests should give an answer (or at least give a direction) to the research question stated in **chapter 1**.

3.3.1 Test material and dimensions of the model

First a decision has to be made regarding what materials should be used for the test set-ups. Ideally a complete roof structure would be the best option for simulating reality. However, as this requires either a lot of space in the laboratory or computing capacity of the computer, this is not practical. Therefore, all non-structural elements are replaced by loads. After this reduction, all that is left is the connection detail and a roof structure. The roof structure consists of rafters, supporting panels and supporting battens, whereas the connection detail is made of the F-brackets and the wall plates. To reduce the size even further, only half a roof is dealt with. This is possible for symmetrical roof structures, with symmetrical load cases. The length of the roof is set at 4500mm without the supporting structure (under eaves).

3.3.2 Load cases

For the remainder of the research phase, only one load combination is considered. As the measuring is performed inside the material elastic range, there is no need work out the normative load. However, representative load distribution are necessary for valuable test results. As half the roof structure is considered, assuming a symmetrical roof structure, only a symmetrical load is applicable. For this reason the symmetrical snow load has been chosen as variable load for the roof structure. Beside the variable load, a dead load q_G is present as well. For a roof structure, the dead load consists of the weight of the roof deck and the own weight of the structure. The complete calculation of the variable and dead loads is attached in **appendix 3.2**.

$$q_G = 0,60 kN/m^2$$

$$q_{Snow,35} = 0,47 kN/m^2; \qquad q_{Snow,45} = 0,28 kN/m^2; \qquad q_{Snow,55} = 0,09 kN/m^2$$

This results in the following mechanical scheme:

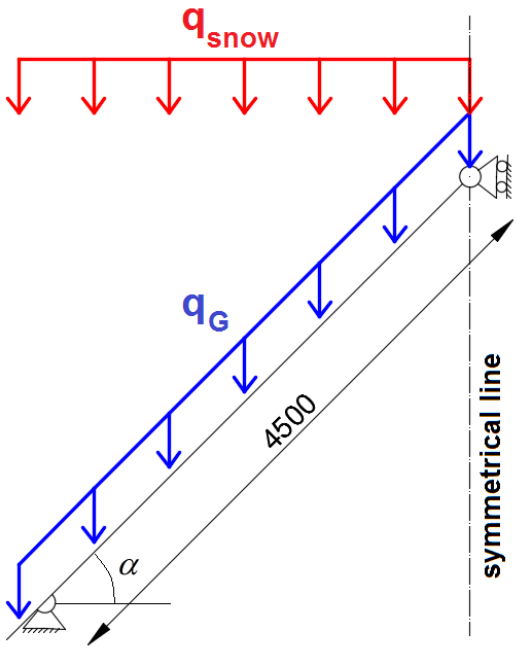

Figure 3.3a; *Mechanical scheme of the symmetrical roof structure*

3.3.3 Test variables

As mentioned in the second sub question (**paragraph 1.3**), various variables might have an influence on the strength of the connection. These variables are considered to be:

- Roof inclination
- Center-to-center distance of the F-bracket
- Depth of the adding

The roof inclination ranges from 15 to 70 degrees. Common center-to-center distances of the brackets lie between 600 and 1200 millimeters. The depth of the adding is dependent on the alignment on the building site (often a couple of centimeters). With these variables an enormous range of possible combinations are possible. To make this manageable, only a couple of frequent applied variables are used. The following variables are considered:

Roof inclination		CTC of the F-brackets		Depth of the adding
35 degrees		600mm		10mm
45 degrees		900mm		30mm
55 degrees		1200mm		

Table 3.3a; *Overview of the test variables*

As the roof inclination is the only variable influencing the load on the roof structure, the values for the axial and shear load are determined by using equilibrium states of the structure. The results are shown in **table 3.3b**, the calculations are given in **appendix A3.2**.

Roof inclination	Axial load (H)	Shear load (V)
35 degrees	5,323 kN/m	1,683 kN/m
45 degrees	3,872 kN/m	1,252 kN/m
55 degrees	2,983 kN/m	0,852 kN/m

Table 3.3b; *Overview of axial and shear load, belonging to the assigned roof inclination*

Chapter 4 | Experimental research

This chapter deals with the preparation, execution and analysis of the experimental research.

4.1 Material properties of sawn timber

The test set-up contains multiple sawn timber elements. It consists of the wall plate, the supporting batten and the rafters. Although the shape of some elements is almost identical, the material properties are not. This paragraph will provide the specific properties for each individual element.

4.1.1 Characteristic and mean values

The timber specimen are strength graded into class C24. This will give us an indication of the average and characteristic strength of the material. According to NEN6760 the following material properties apply **[4]**:

	$f_{m,0}$	$E_{0,mean}$	ρ	$f_{t,0}$	$f_{t,90}$	$f_{c,0}$	$f_{c,90}$	$f_{v;0}$	$E_{0,car}$	$E_{90,ser}$	G_{mean}
C24	24	11.000	350	14	0,5	21	2,5	2,5	7400	370	690
Unit	N/mm²	N/mm²	Kg/m³	N/mm²	N/mm²	N/mm²	N/mm²	N/mm²	N/mm²	N/mm²	N/mm²

***Table 4.1a**; Strength class C24 Sawn Timber*

Although these values give us a good indication of the expected strength of the materials, the exact strength of each specimen needs to be specified to be able to compare results.

4.1.2 Dimensions of specimen

As mentioned before, the specimen are subdivided into three groups. These groups are characterized with **M** for wall plate, **D** for supporting batten and **S** for rafters. Although the test set-up requires one wall plate, one supporting batten and five rafters, each group contains a spare element, in case one gets damaged. Cross-sectional dimensions are given in **figure 4.1a**. The length of the wall plate, supporting batten and rafters are respectively 2600mm, 2600mm and 1000mm.

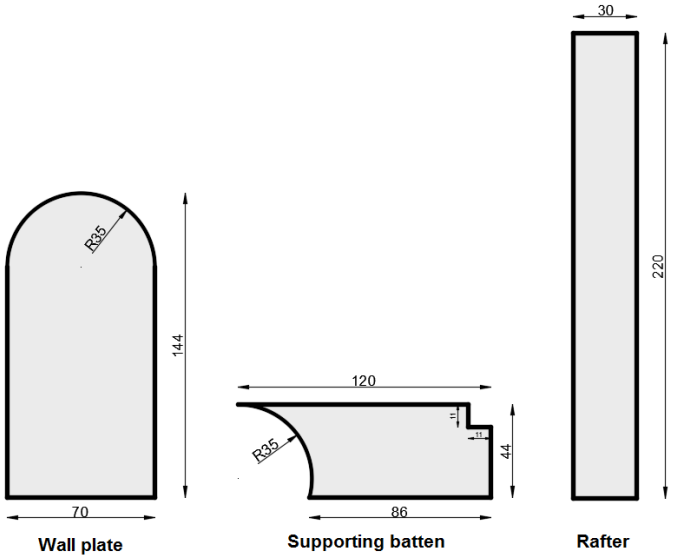

***Figure 4.1a**; Geometry of the sections in millimeters*

4.1.3 Moisture value

The moisture content of wood ω is the determined according to **equation 4.1**.

$$\omega = \frac{m_{\omega} - m_{\omega=0}}{m_{\omega=0}} \cdot 100\% \qquad (4.1)$$

The moisture content can also be determined directly with the use of the FME moisture meter.

***Figure 4.1b**; FME moisture meter*

The measurements are taken on three different positions of the specimen to specify a representative mean value.

Specimen	Measurement 1	Measurement 2	Measurement 3	Average value
M1	19,0%	18,6%	17,6%	18,4%
M2	18,4%	17,9%	17,4%	17,9%
D1	16,1%	15,3%	15,4%	15,6%
D2	15,4%	15,5%	15,9%	15,6%

***Table 4.1b**; Moisture level measurements*

In normal indoor circumstances the equilibrium moisture content is expected to be 12%. This means that the moisture content in the specimen, especially the wall plates, will drop a few percentages over a longer period of time, resulting in the specimen to shrink and become stronger and stiffer. However, this only applies at a moisture content below the fibre saturation point (~22-30%). This will be of no influence during testing, since the specimen have been in the laboratory for a couple of weeks to reach an equilibrium state. Besides, the testing will take only a couple of days, in which there is hardly any time for the specimen to vary in moisture content **[16]**.

4.1.5 Modulus of elasticity

To get an indication of the strength of each specimen, the Young's modulus is determined. The Young's modulus, or modulus of elasticity, is the relation between the stress and the strain of a material, as mentioned in **paragraph 2.1**. This relation holds only for that part where the timber is elastic. This means that the increase of stress results in an equal increase of deformation. Strength properties of wood are distinguished in four general directions: compression and tension either perpendicular or parallel to the grain direction. The strength of wood perpendicular to the grain direction is limited, having only a small region where the wood behaves elastic. On the other hand, wood loaded parallel to the grain direction is a lot stronger. However, the Young's modulus of compression and tension parallel to the grain direction are unequal, where the difference can increase up to 20%. For this reason there is an average modulus of elasticity. **[19]**

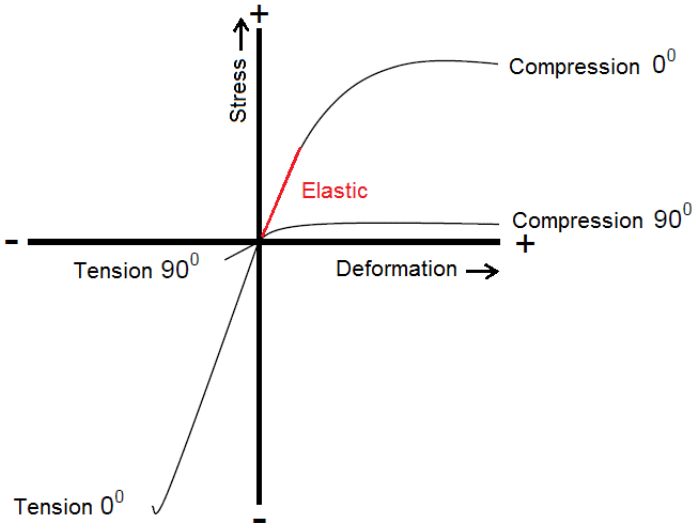

***Figure 4.1c**; Stress-strain relation of wood*

There are several ways to determine the Young's modulus of a specimen. As the actual tests required have not taken place yet, damaging or permanently deforming the specimens was not desirable, therefore limiting the options by which the modulus of elasticity could be determined. Two different assessments have been performed on each specimen, to increase the accuracy of the measurements. The first test uses the Mobile Timber Grader (MTG). The second test consists on a bending test of the specimen. The deformations remain in the elastic area, resulting in the specimen to take its original shape after unloading.

- Mobile Timber Grader

The Mobile Timber Grader is a device that is able to create and receive vibrations. After the input of a number of properties, the MTG is able to determine the Eigen frequency of the material and subsequently the modulus of elasticity. To use the MTG, it has to be calibrated first by using an appropriate reference object, of which the properties are known. After calibration, the geometry of the prospective test object has to be set. Finally the test can be performed by placing the MTG at the end grain face of the object. The results of the tests are shown in **table 4.1c**.

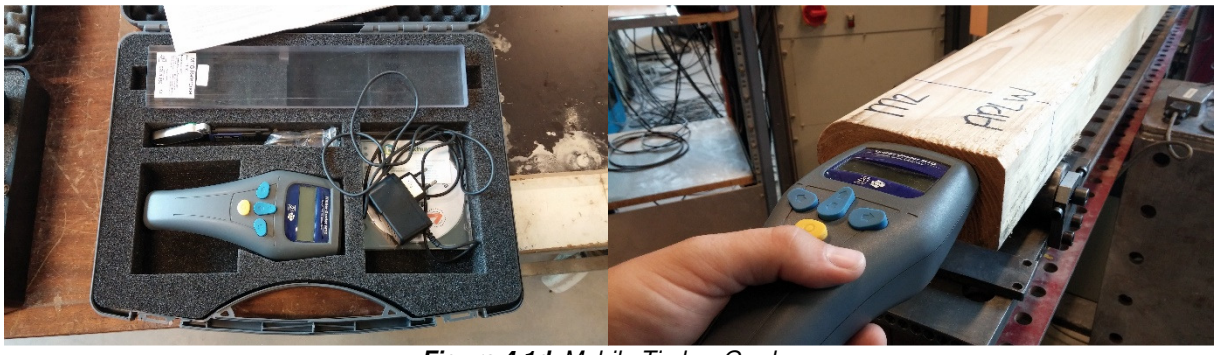

***Figure 4.1d**; Mobile Timber Grader*

Spc.	M1 (N/mm²)	M2 (N/mm²)	M3 (N/mm²)	M4 (N/mm²)	M5 (N/mm²)	**E_{AV} (N/mm²)**
M1	11.679	10.650	11.560	10.422	10.995	**11.061**
M2	12.694	12.570	12.694	10.943	12.694	**12.319**
D1	10.976	10.862	10.862	10.976	10.862	**10.908**
D2	12.697	12.599	12.599	12.599	12.599	**12.619**

***Table 4.1c**; Modulus of elasticity graded with the MTG*

- 4-point bending test

According to **EN408 [8]**, a 4 point bending test is schematized with **figure 4.1e**.

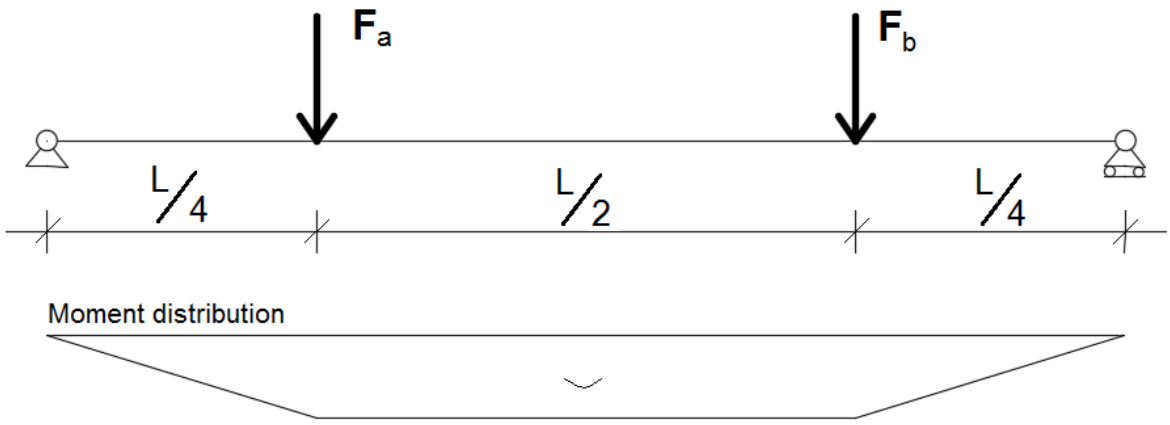

***Figure 4.1e**; Schematized 4 point bending test*

The forces cause the element to bend. The bending moment and curvature between the applied forces are constant. There is a relation between curvature, moment and bending stiffness:

$$\kappa = \frac{M}{E \cdot I} \tag{4.2a}$$

The forces which are applied are equal and measured. The bending moment is therefore easily determined with the following formula:

$$M = \frac{F_n \cdot L}{4} \tag{4.3}$$

With:

$F_n =$ The force applied on position a or b

$L =$ The length of the specimen

The moment of Inertia is dependent on the cross-section, and by measuring the deflection at the positions of the applied forces (Fa and Fb) and mid-span (M), the curvature can be determined. The deflection is measured by using linear variable differential transformers (LVDT's) on either side of the specimen to rule out the effect of twisting.

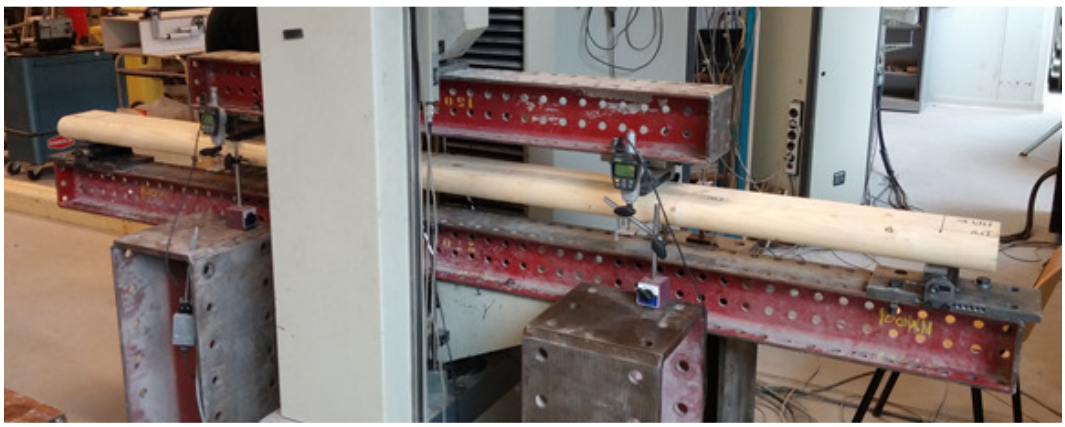

***Figure 4.1f**; Test setting of the 4 point bending test*

By changing the order of formula 4.2a, the Young's modulus can be determined:

$$E = \frac{M}{I \cdot \kappa} \tag{4.2b}$$

The complete calculation is given in **appendix 4.1.**The results of the 4 point bending test and the MTG are presented in **Table 4.1d**.

Specimen	MTG E (N/mm^2)	4-PBT E (N/mm^2)	**Average E (N/mm^2)**
M1	11.061	10.828	**10.945**
M2	12.319	12.249	**12.284**
D1	10.908	10.500	**10.704**
D2	12.619	12.649	**12.634**

***Table 4.1d**; Modulus of elasticity of the wall plates and supporting battens*

4.1.6 Knots and grain direction

The number of knots and the grain deviation affect the strength of the material. This is taken into account with the design of the test set-up, to avoid weak connections and bad measuring points.

4.1.7 Overview of properties

To give an overview, all properties have been inserted into **table 4.1e**.

Specimen	Length (mm)	Width (mm)	Depth (mm)	Moisture content (%)	Modulus of Elasticity (N/mm^2)
M1	2600	70	144	18,4	10.945
M2	2600	70	144	17,9	12.284
D1	2600	120	44	15,6	10.407
D2	2600	120	44	15,6	12.634
S1	1000	30	220	-	-
S2	1000	30	220	-	-
S3	1000	30	220	-	-
S4	1000	30	220	-	-
S5	1000	30	220	-	-
S6	1000	30	220	-	-

***Table 4.1e**; Material properties of the wall plate (M), supporting batten (D) and rafters (S)*

4.2 Material properties of other materials

Besides the wall plate, supporting batten and rafters, other materials are involved in the test set-up as well. The material properties are not tested individually, but obtained from reliable sources.

4.2.1 F-bracket

The F-bracket is made of steel. As steel isn't an organic material, the properties don't vary much, so documented properties can be considered to be accurate. Therefore, the material properties are taken from **[2]**, and are listed in **table 4.2a.** The brackets are labeled with the letter B followed by an identification number (up to 6).

	Type	E (N/mm^2)	f_y (N/mm^2)	f_t (N/mm^2)	ε after fracture (%)
F-bracket	S235	2,1.10^5	235	360	19

***Table 4.2a**; Material properties of steel*

The geometry of the bracket is displayed in **figure 4.2a.**

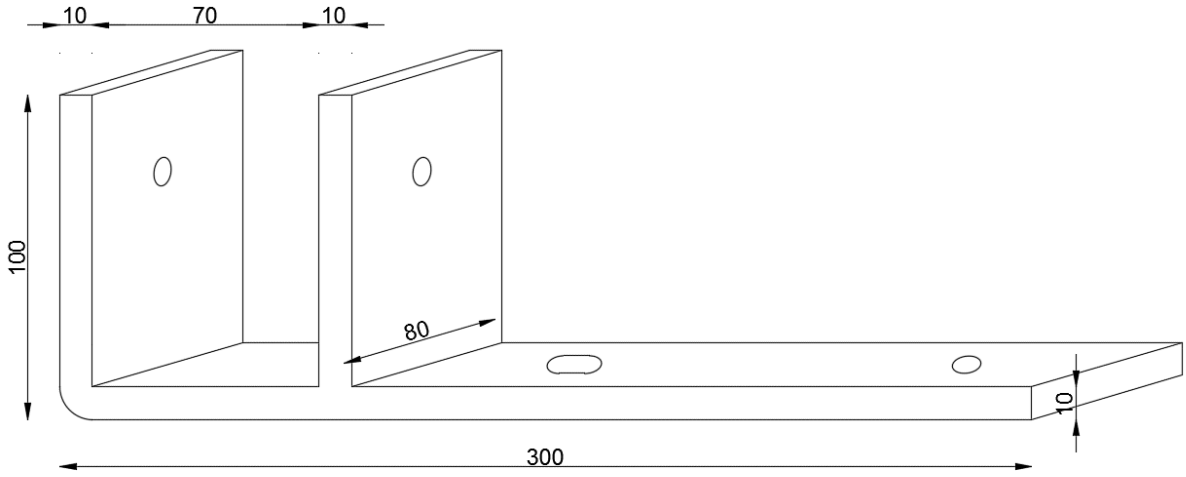

***Figure 4.2a**; Geometry of the F-bracket*

4.2.2 Supporting wooden panel

The supporting wooden panel is a particle board. According to **[7]**, the material properties of the board are given in **table 4.2b**. The dimensions of the particle board are 800mm x 2400mm with a thickness of 11mm.

	E (N/mm^2)	f_m (N/mm^2)	$f_{t,90}$ (N/mm^2)
Particle board (t = 11mm)	3.150	20	0,60

***Table 4.2b**; Material properties of the particle board*

4.2.3 Wedges

The wedges are used to adjust the position of the wall plate in the F-bracket. Once in place, they will transfer only vertical compressive loads. Therefore, Medium-Density Fibreboard is chosen as material for the wedges. **Table 4.2c** gives the material properties of MDF **[22]**.

***Figure 4.2b**; Position of the wedges in the F-bracket, underneath the wall plate*

	E_0 (N/mm^2)	f_m (N/mm^2)	$f_{t,90}$ (N/mm^2)	$f_{c,0}$ (N/mm^2)
MDF (t = 10mm)	2.800	32	0,80	>10,0

***Table 4.2c**; Material properties of MDF*

4.2.4 Bolts and nuts

To fasten the wall plate in the F-bracket, as well as the F-bracket to the frame support, socket head cap screws in combination with bolts are used. The screws fastening the wall plate have a smooth surface, except for the end. Material properties of the screws and nuts are shown in **figure 4.2c and table 4.2d [11][12]**.

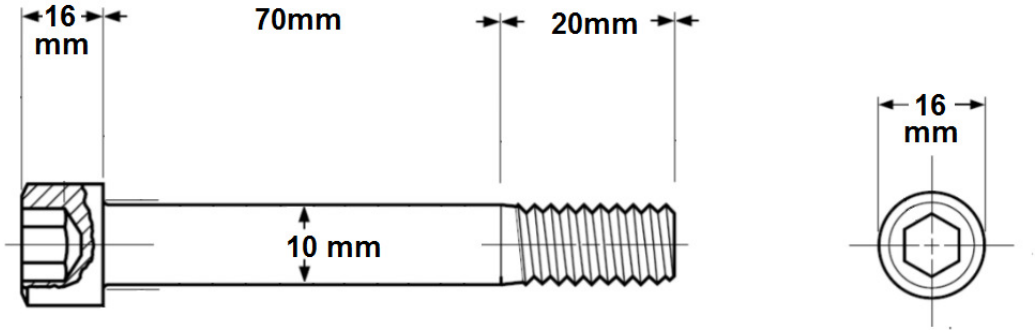

***Figure 4.2c**; Geometry of the socket head cap screw fastening the wall plate with the F-bracket*

	Proof Stress (N/mm^2)	Proof Load (kN)	Tensile Stress (N/mm^2)	Hardness (HRC)
SHC screw 8mm	580	21,2	800	22-32
SHC screw 10mm	580	34,1	800	22-32
Nut M8	870	31,8	-	30
Nut M10	880	51,7	-	30

Table 4.2d**; Material properties of the SCH screw and nuts. Proof stress and proof load are the maximum tensile strength of the bolts which will result in elastic deformation. This is typically between 85% and 95% of the yield strength **[21]

4.2.5 Coach screw

The coach screw is used to fasten the rafters to the wall plate. The screw has a length of 260mm and a diameter of 8,0mm. **Figure 1.2c** shows a couple of coach screws. The material properties are similar to the SCH screw 8mm in **table 4.2d**.

4.3 Test set-up and test-program

This paragraph deals with the design and development of the test set-up. At the end a test-program is included, which has been carried out for the purpose of this research project.

4.3.1 Dimensions of the test set-up

The most ideal situation would be a full size roof element, with an infinite width. However, due to limitations in available space in the laboratory, concessions must be made regarding frame size, costs and material dimensions. The reduced size of the test set-up should nevertheless resemble properties of a full size roof. A minimum width of at least 3 center-to-center distances of the F-bracket is necessary to have at least one bracket (the middle one) with symmetrical properties. The maximum center-to-center distance is 1200mm. Therefore, at least 2400mm of width is necessary. To tighten the wall plate, an extra 100 mm is added on either sides for both the wall plate and the supporting batten. The width of the supporting panel however is limited to 2500mm due to the maximum dimension of a particle board. The length of the roof element is set at about 1000mm. Instead of introducing the horizontal axial loads on the rafters, these loads will be introduced directly into the supporting panel. This will reduce the necessary length of the supporting panel. The combination of the rafters and the supporting panel is

significantly stiffer compared to the wall plate and supporting batten, resulting in the shortened roof element to satisfy the boundary conditions. The supporting batten and supporting panel are both connected to the parent rafters using wood screws. The supporting batten is fastened with two screws and the supporting panel is connected every 100 millimeters. These elements together are considered to be the substitute roof element.

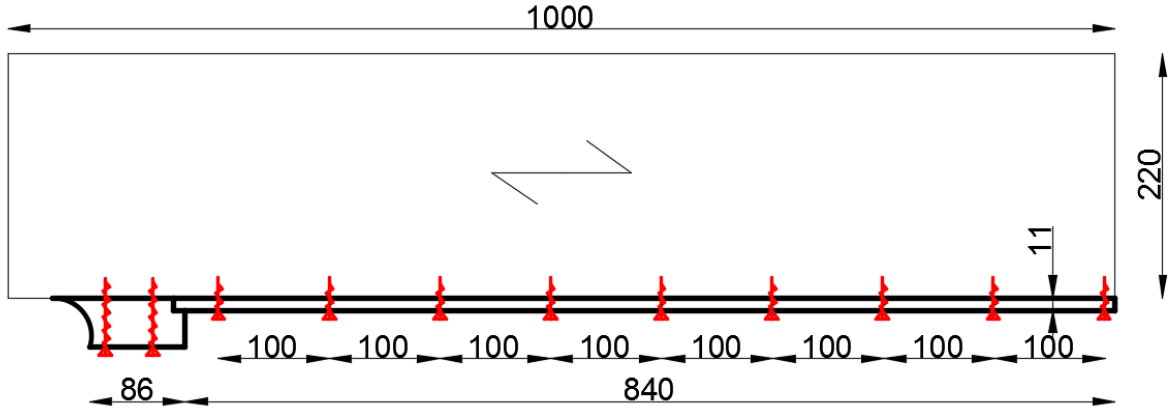

***Figure 4.3a**; The substitute roof element with its fasteners*

4.3.2 Development of the test set-up

The test set-up consists of the substitute roof element, the wall plate and the F-brackets. Two types of forces are applied on the assembly. The horizontal axial force and the vertical shear force. It is more convenient for the hydraulic actuator to be applied in an orthogonal manner. Therefore, the whole test orientation is rotated over 45 degrees. A cross section and a top view are shown in **figure 4.3b**.

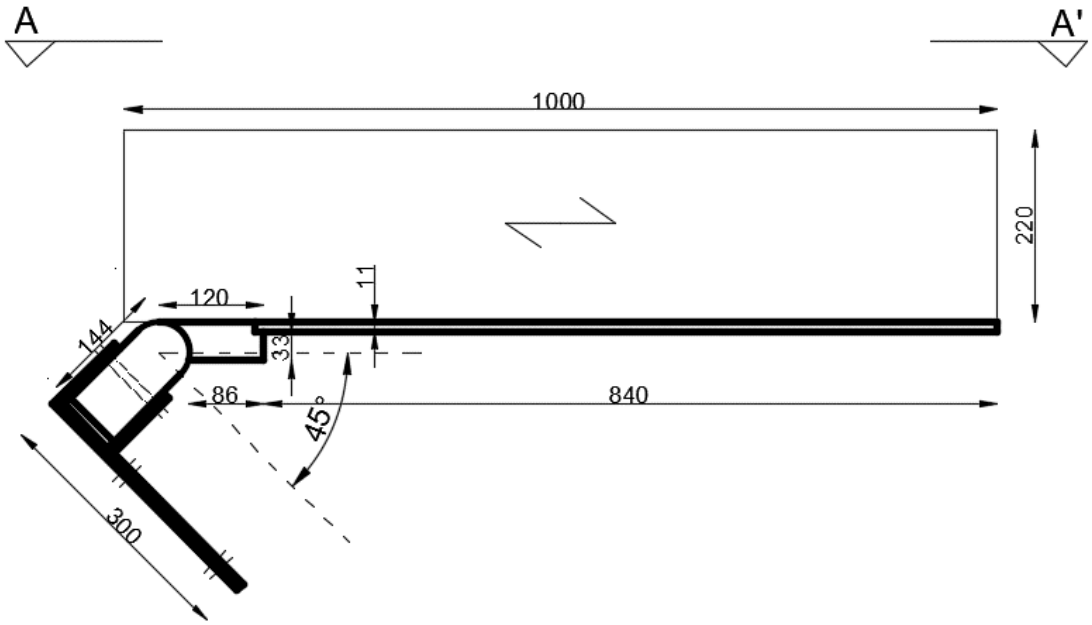

***Figure 4.3b**; Cross section of the rotated assembly. The roof angle is 45 degrees*

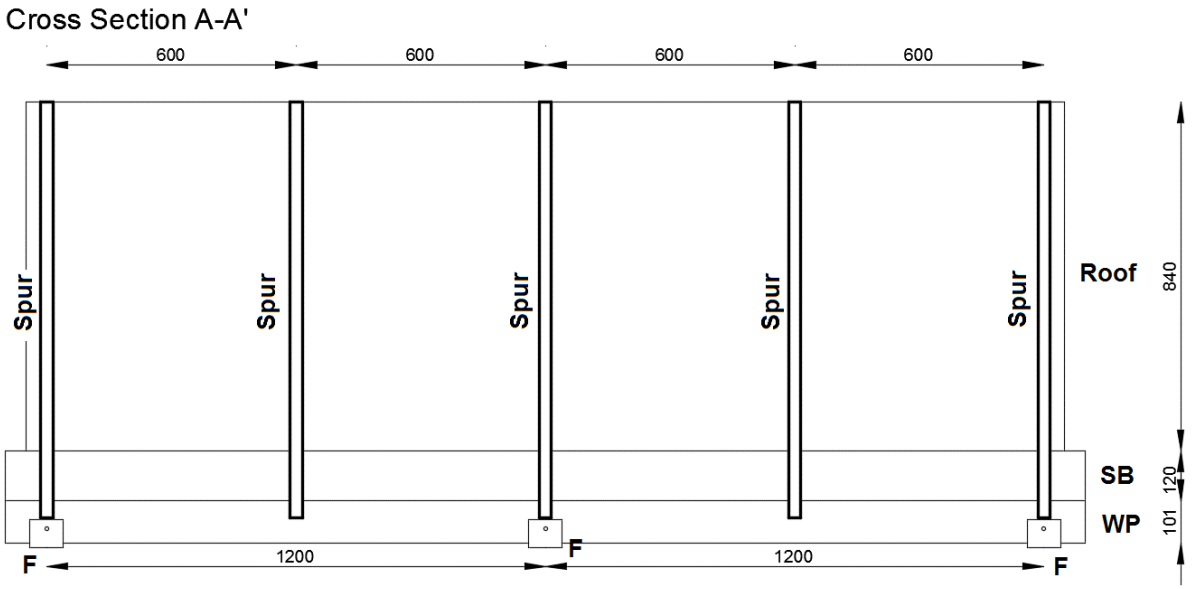

***Figure 4.3c**; Top view of the rotated assembly. The center-to-center distance is 1200mm*

The horizontal axial force, the greater of the two, is applied by two hydraulic actuators. These hydraulic actuators push against a series of almost frictionless steel beams with an increasing width to achieve an equal load spread on the substitute roof element. The steel beams are frictionless by using roller supports. The vertical shear force is applied to the rafters, directly above the wall plate, by the use of dead weight, as the load is relatively small to be performed by a jack. The dead load is obtained by using a series of pre-measured steel I-beams (see **figure 4.3e**). The use of a dead load prevents the test series from checking specific load cases. Though, as the path of the loading is present in the elastic section, corresponding load ratios may be simulated. The results are thereafter multiplied by a specified factor to match the results in case of the predetermined load cases (more will be explained in **paragraph 4.4**).
The test set-up requires the possibility of being adjustable between test series. Parameters to be adjusted are the alteration of the roof inclination, different center-to-center distances of the F-brackets and the use of different depth of adding. It is therefore not desirable for the substitute roof element to be attached to the wall plate, since this prevents making adjustments of the set-up, once it is fixed. The use of the coach screw is subsequently disregarded for nearly all tests. Only for the last test series the coach screw may be applied. The lock out of the coach screw is justified by the fact that it mainly serves in case of upward loading. Test results might prove otherwise though.
Before testing, since the assembly is not fixed, a gap is present between the wall plate and the supporting batten due to geometrical imperfections (see **figure 4.3d**). It is observed that approximately 2kN of horizontal force is required to fully close the gap.

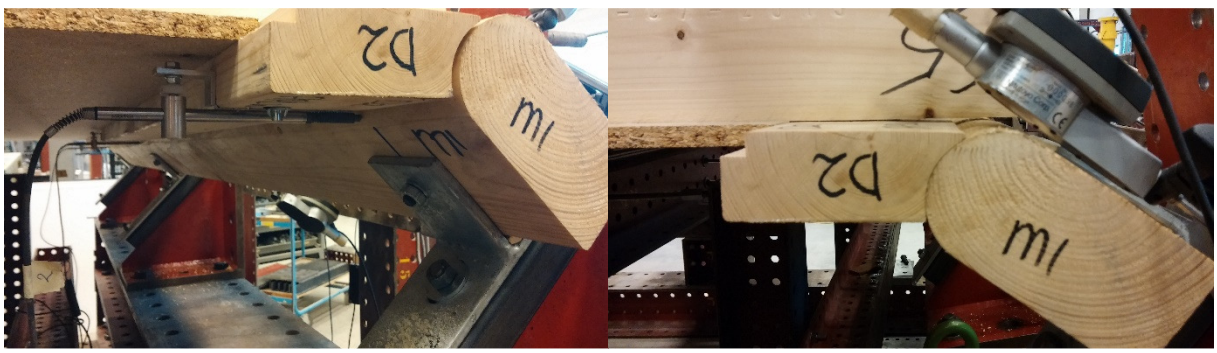

***Figure 4.3d**; Pictures of the wall plate M1 and supporting batten D2 and the existing gap on the left before testing, and the non-existing gap on the right once 2kN of horizontal axial force is applied*

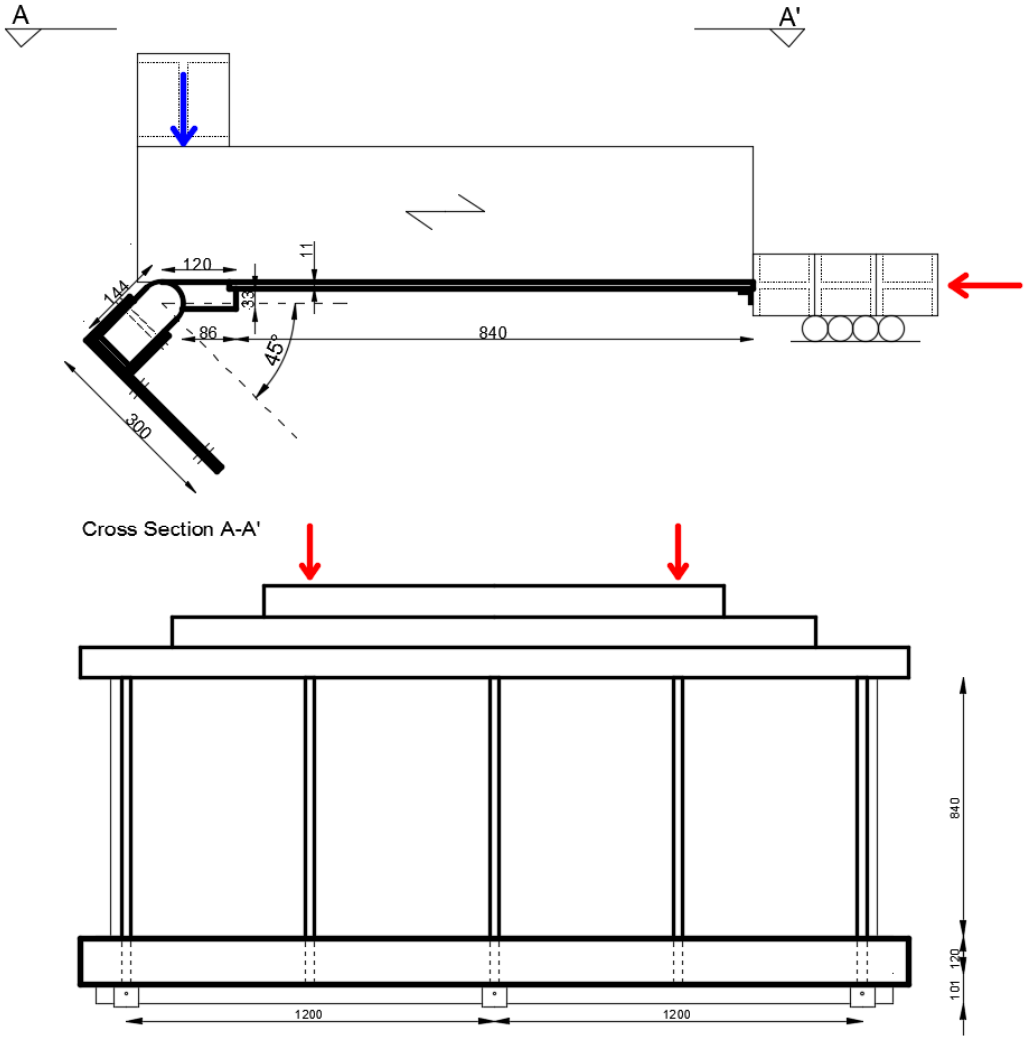

***Figure 4.3e**; Cross section and top view of the rotated assembly in combination with the applied forces. The red arrow represents the horizontal axial loads by means of a hydraulic actuator. The blue arrow embodies the vertical shear load by means of the steel I-beam.*

The test set-up, including the supporting frame, is schematized in **figure 4.3f.** Pictures of the set up and tests are depicted in **appendix 4.3**

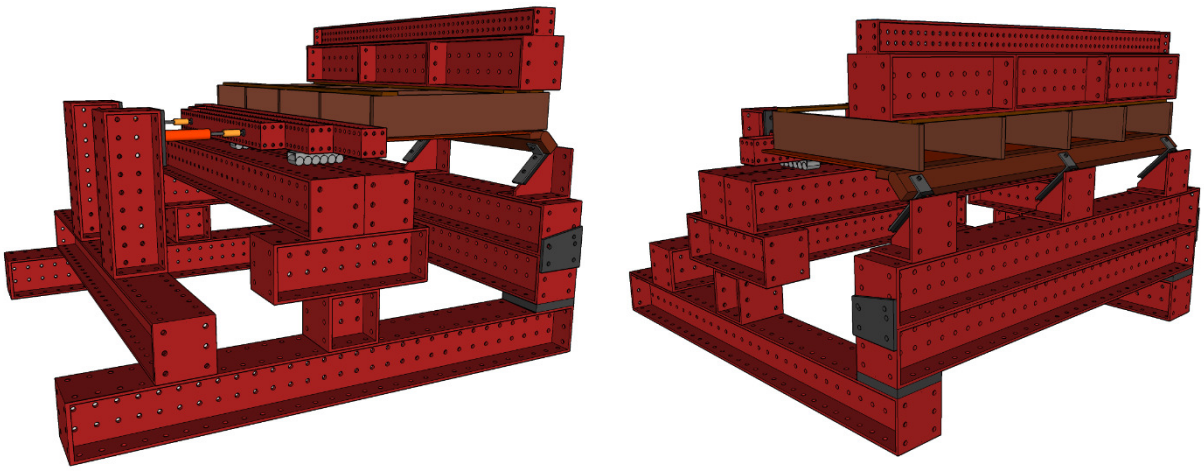

***Figure 4.3f**; Three dimensional model of the test set-up. Shown from two different sides*

4.3.3 Type of measurement

The goal of the research project is to get an insight in the stress distribution along the width of the wall plate. However, this is not a straightforward measurement on a full size model. Stresses can indirectly be obtained by either measuring the force over a certain area, or measuring the strains of a material with a known modulus of elasticity. The first option provides a problem, as measuring equipment needs to be positioned inside the model, which will affect its properties. In case this option was chosen, the measuring equipment would need to be as small as possible to limit the side effect. However, such measuring equipment was not available. The second option is measurable, however, the applicability is limited. To fully understand the course of the stresses, one needs to obtain the strain of the complete cross section of the material, including the exact material properties. As both conditions cannot be satisfied directly, another solution must be found:

- Solution 1: measuring the gaps

It was first believed that the gaps between the wall plate and the supporting batten would close at places where the loads are transferable, namely near a hard point (i.e. the F-bracket), and that the gap would remain at softer points, which lie in between the brackets. This belief was based on the assumption that the wall plate would suffer more deformation than the roof element. The length of gap to be closed between the wall plate and the supporting batten could be indicative of the effective width of the wall plate.

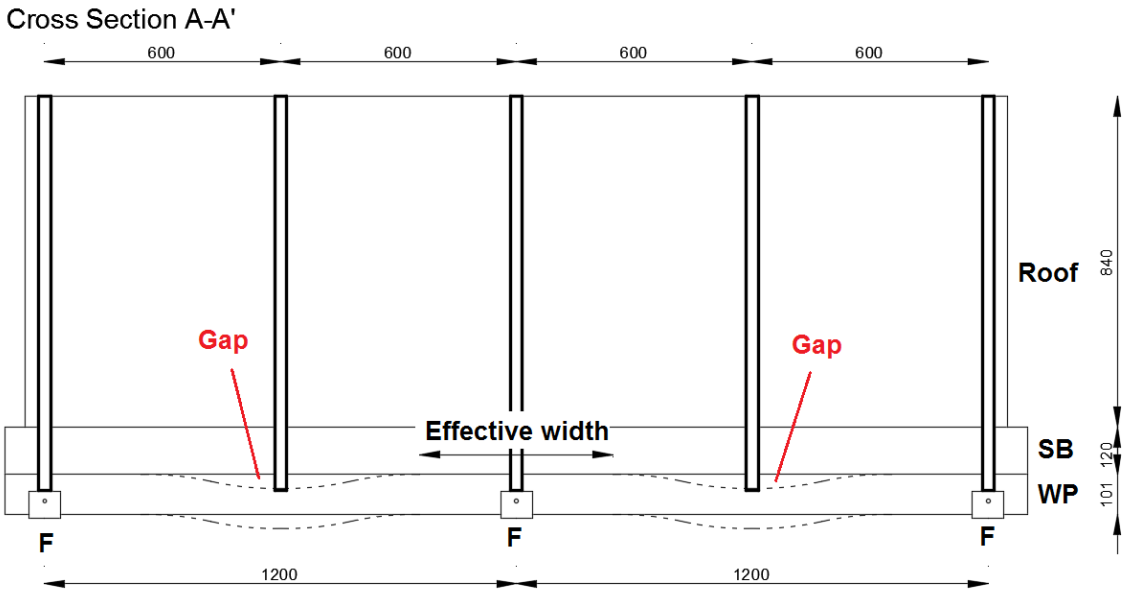

***Figure 4.3g**; Top view of the assembly with the deformed wall plate*

The gap was measured with LVDT's. The alignment of the measuring equipment is shown in **figure 4.3h**.

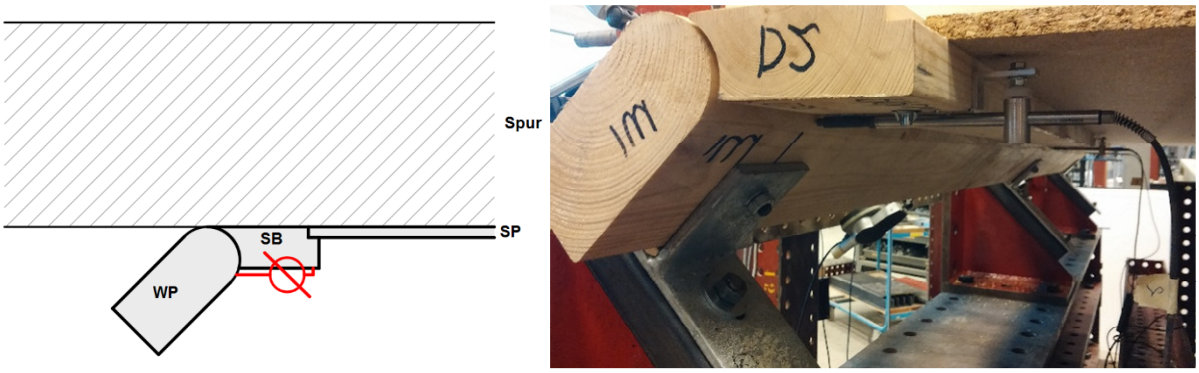

***Figure 4.3h**; Position of the LVDT to measure the gap between the wall plate and supporting batten*

However, after performing several tests, it was discovered that no gap remained over the entire length of the connection. Besides, it was concluded that whenever a gap would close, it would have no indication regarding the amount of stresses going through the connection, as a closed connection could transfer either a small load, or almost all of the load. For this reason it was decided to abandon this type of measurement.

- Solution 2: measuring strains along the width of the assembly

This solution involves several strain gauges along the width of the assembly. The strain gauges give a segmented overview of the present strains, and therefore stresses. The intermediate strains can be interpolated by connecting the measured strains at certain points. More strain gauges will give a more fluent overview of the present strains. The location of these gauges needs to be considered carefully, as the cost of an individual strain gauge is quite high. These costs work contradictory to our aim. Besides, the amount of strain gauges is limited by the data acquisition capacity of the present computer. It is therefore decided to use 16 strain gauges on the assembly. The positions of these strain gauges need to fulfill the following criteria:

- The directions of the strain gauges need to face the same direction as the direction of the stresses.
- The positions of these strain gauges need to be as close as possible to the wall plate, to give a more accurate prediction of the stresses in the wall plate.

The strain gauges can only take measurements on the surface of an object, therefore, it is desirable to attach the gauges to an object with a proportionally stress distribution, as this gives a better insight of the actual stress distribution.

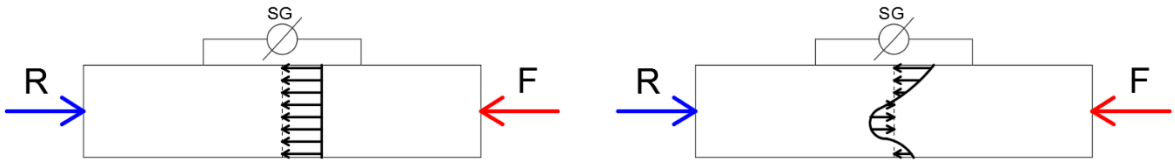

***Figure 4.3i**; The strain gauge on the left side will give a better indication of the present stresses in the object, compared to the right object.*

The possibility of placing strain gauges on the wall plate is disregarded, as it does not fulfill the first criteria. Besides, the deformation of the wall plate is considered to be unpredictable, resulting in strains and stresses that cannot be explained. The stresses in the supporting batten do not follow the same direction as the strain gauges, due to the transfer of loads considered in **chapter 3**. Though, positioning the gauges on the supporting panel might give mismatching results due to the greater distance to the wall plate, as demonstrated in **figure 4.3j**.

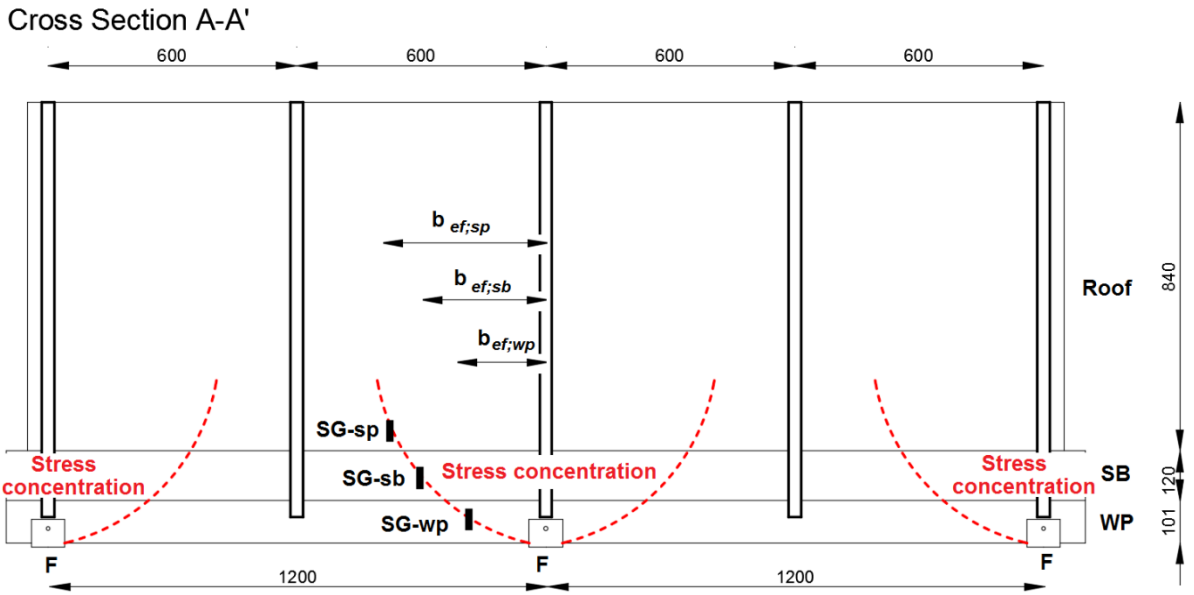

***Figure 4.3j**; Top view of the assembly with the predicted stress concentration towards the F-brackets. The strain gauges indicated on the elements show equal values for stresses, though the effective distance to the corresponding bracket varies a lot.*

The problem of the supporting batten might be solved by placing strain gauges on either side of the batten, and taking the average value of both measurements, excluding the influence of the moment stresses. This solution will limit the amount of measured locations even further. However, it is preferred to position the strain gauges on the supporting batten over the supporting panel. The strain gauges used have the following properties:

Gauge length (mm)	**Gauge width (mm)**	**Backing length (mm)**	**Backing width (mm)**
30	2.3	40	7
Operational Temperature	**Backing**	**Element**	**Strain limit**
-20°C up to +80°C	Polyester	Cu-Ni (wire)	2% (0,02 strain)

Table 4.3a: Strain gauge specifications

The strain gauges are positioned according to **figure 4.3k and 4.3L**. The top view shows the gauges to be on one side of the bracket. Assuming the results on either side to be the same, it is concluded that there is no necessity to measure both sides. The strain gauges are positioned 75 millimeters center-to-center, except for the last row, which is translated an extra 30 millimeters further due to the obstruction of the spur. The gauges closest to the middle bracket are numbered 1, the following gauges are numbered 2 and so on. The gauges on the upper side of the batten are given the subscript **b** and the gauges on the down side have subscript **o**.

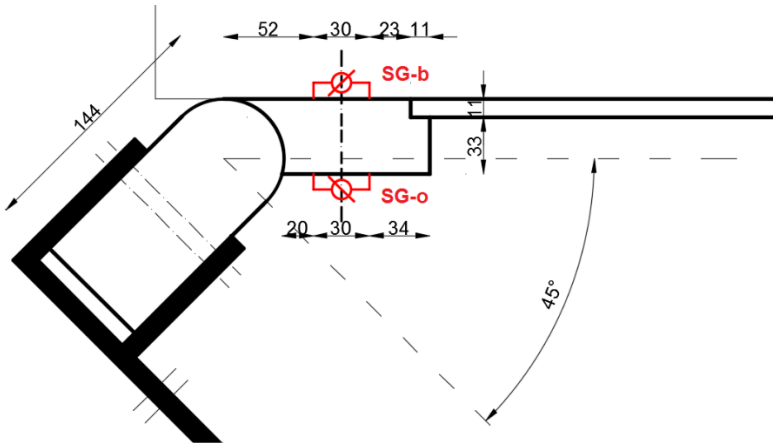

***Figure 4.3k**; Cross section of the assembly near the supporting batten with the positioning of the gauges on the upper side (b) and down side (o).*

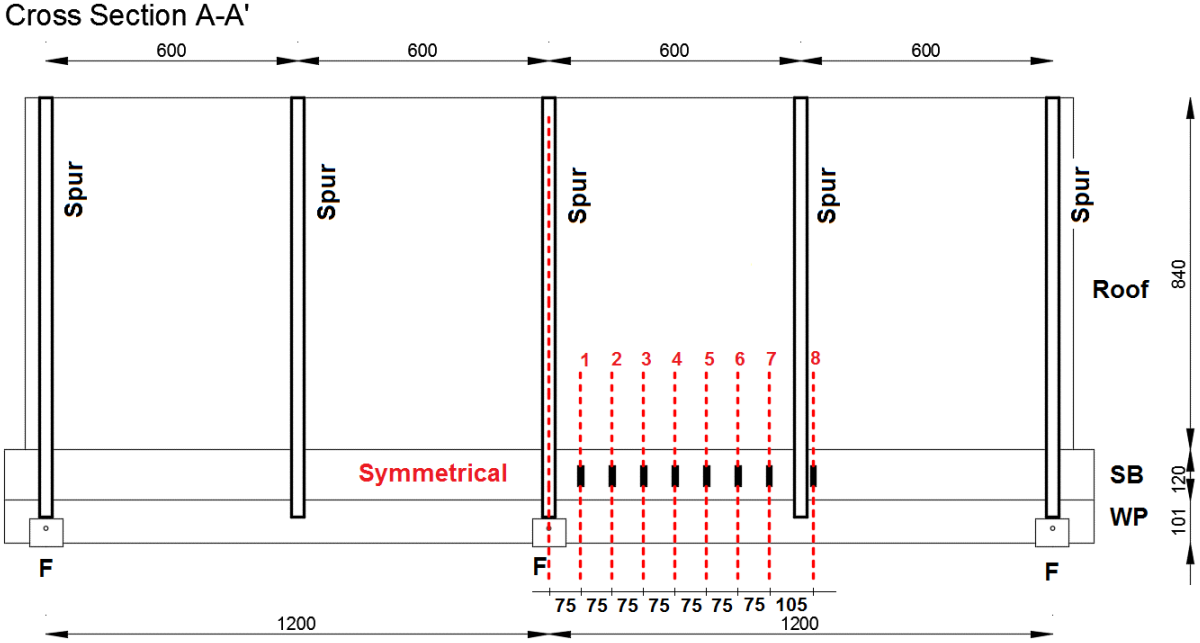

***Figure 4.3L**; Top view of the assembly with the positioning of the gauges and the accompanying rows.*

The forces applied by the hydraulic actuators are measured individually using load cells. The load cells have a capacity of up to 50kN each, eventhough the load required doesn't exceed 20kN. The weight of the dead load is measured on a scale. The exact amount of dead load transferred to the wall plate is uncertain, since a small part might escape through the roller support at the other end of the set-up. Therefore tests have been performed to link a specific position of the dead load to a certain amount of weight loss. The amount of dead weight on the rafters is circa 4.080N at the specific location shown in **figure 4.3M**. To be able to apply the dead load on the assembly, a crane is used.

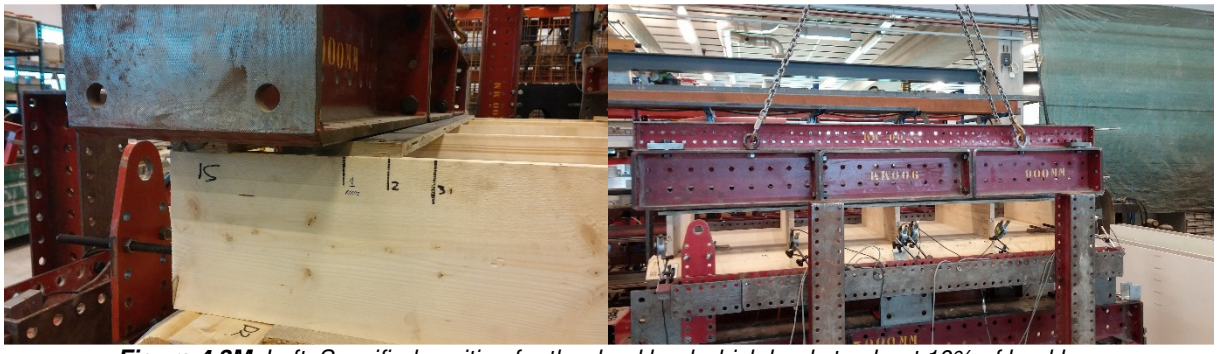

***Figure 4.3M**; Left: Specified position for the dead load which leads to about 10% of load loss*
Right: The dead load is applied with the use of a crane

During all tests, seven points on the set-up are measured with LVDT's to check for irregular behavior of the assembly. The first test will be considered to be a trial run. In case this test proceeds without incidents, the second and third tests will be considered to be actual measurement tests.

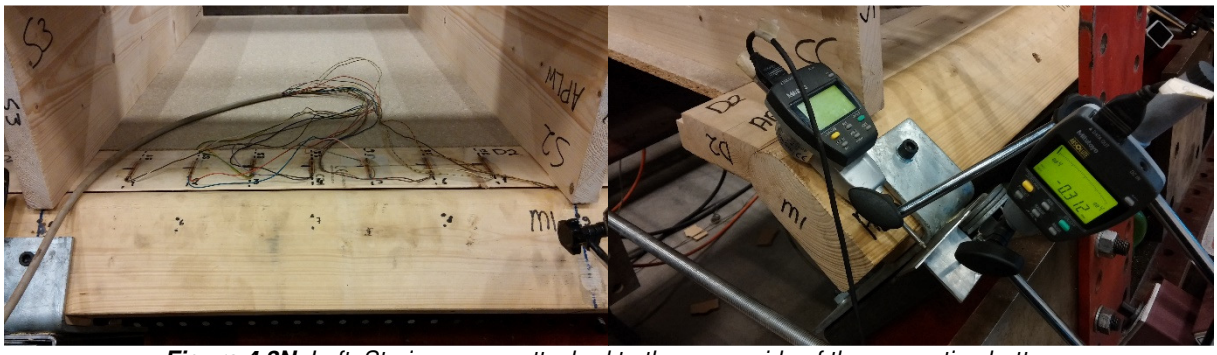

***Figure 4.3N**; Left: Strain gauges attached to the upper side of the supporting batten*
Right: LVDT's measuring the set-up for abnormal behavior

4.3.4 Test program

The following test series are performed:

35/600/L Roof Angle: 35° CTC: 600mm Adding: Low (10mm) Coach screw: No	**45/600/L** Roof Angle: 45° CTC: 600mm Adding: Low (10mm) Coach screw: No	**55/600/L** Roof Angle: 55° CTC: 600mm Adding: Low (10mm) Coach screw: No	**45/600/H** Roof Angle: 45° CTC: 600mm Adding: High (30mm) Coach screw: No	
35/900/L Roof Angle: 35° CTC: 900mm Adding: Low (10mm) Coach screw: No	**45/900/L** Roof Angle: 45° CTC: 900mm Adding: Low (10mm) Coach screw: No	**55/900/L** Roof Angle: 55° CTC: 900mm Adding: Low (10mm) Coach screw: No	**45/900/H** Roof Angle: 45° CTC: 900mm Adding: High (30mm) Coach screw: No	
35/1200/L Roof Angle: 35° CTC: 1200mm Adding: Low (10mm) Coach screw: No	**45/1200/L** Roof Angle: 45° CTC: 1200mm Adding: Low (10mm) Coach screw: No	**55/1200/L** Roof Angle: 55° CTC: 1200mm Adding: Low (10mm) Coach screw: No	**45/1200/H** Roof Angle: 45° CTC: 1200mm Adding: High (30mm) Coach screw: No	**45/1200/L/CS** Roof Angle: 45° CTC: 1200mm Adding: High (30mm) Coach screw: Yes

Table 4.3b: Overview of test series

The test set-ups vary in roof angle (35, 45 or 55 degrees), different center-to-center distances of the F-bracket (600mm, 900mm and 1200mm), variation in adding (10mm or 30mm) and the usage of the coach screw (yes or no). Every specific assembly has been tested three times. The first attempt serves as a test round, to check if all adjustments have been performed properly, and is therefore not included in the results. The successive attempts are recorded as test A and test B.

4.4 Analysis of the results

This paragraph deals with the way the tests are executed, explains how the results can be interpreted, evaluates various phenomenon which occur and finally rounds these up into a conclusion.

4.4.1 Execution of the tests

The execution of the tests can be subdivided into three steps:

- 1st step: Closing of the gaps. (**closing of the gap + axial force 1**)

By pumping oil through the system, both hydraulic actuators start to apply an evenly distributed force onto the roof element. Together they need to provide at least 2kN for the gaps to close. Once they reach a force of 4kN the first step ends. This process takes about 60 seconds.

- 2nd step: Applying the vertical shear force (**shear force**)

With help of the crane, the vertical shear force (the steel I-beam) is applied onto the rafters (see **figure 4.3m**). It will cause five 'point loads' on the rafters along the width of the test set-up. The application of the vertical shear force is instant.

- 3rd step: Continuing to apply the horizontal axial force (**axial force 2**)

The third step continues to apply the horizontal axial force onto the roof element. The value of the horizontal force needs to exceed a minimum amount to obtain the required horizontal to vertical ratio (see **paragraph 4.4.2**). This step is performed within 240 seconds.

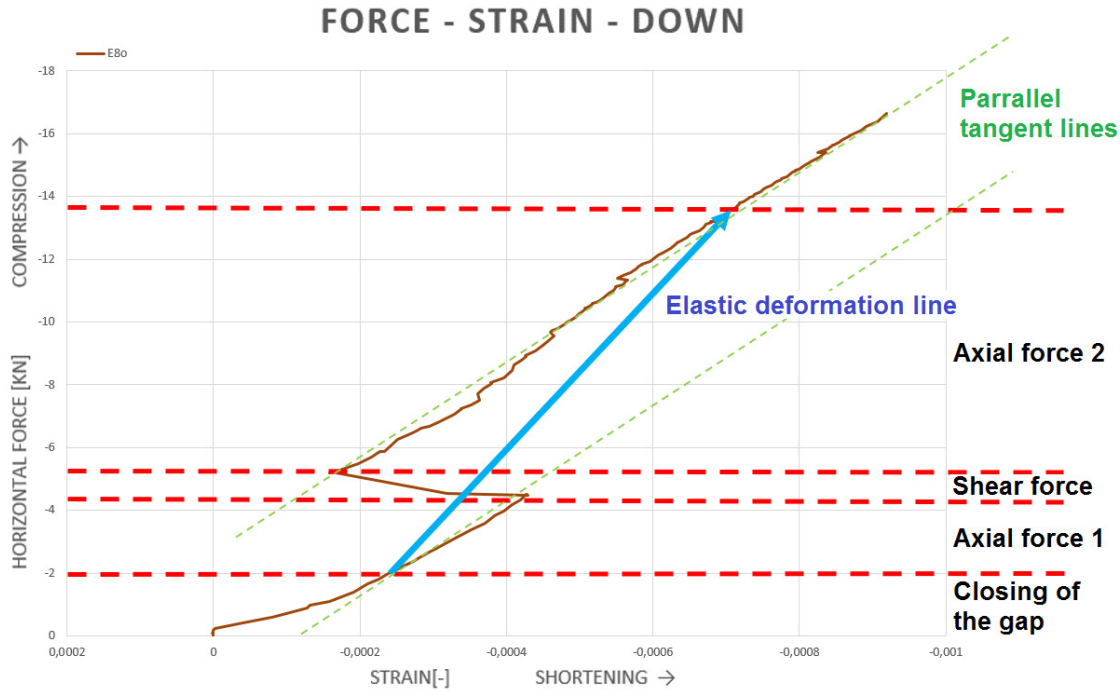

***Figure 4.4a**; Typical load deformation diagram for a specific point on the supporting batten*

The timing of the second step is important, as it prevents the roof element from lifting up. The process of the steps is reflected in the graph, shown in **figure 4.4a**. This is an example of a typical load-deformation diagram measured on a specific point on the supporting batten (position 1, upper side).

4.4.2 Initial results

As mentioned in chapter 3, a specific combination of loads is considered for the various roof angles.

Roof Angle	Horizontal axial force	Vertical shear force
35 degrees	13,840kN / 2,6m	4,376kN / 2,6m
45 degrees	10,067kN / 2,6m	3.255kN / 2,6m
55 degrees	7,756kN / 2,6m	2,215kN / 2,6m

Table 4.4a; *The load combinations for various roof angles*

To determine the matching strains with these load combinations, one should simply apply the specified forces in **table 4.4a**. Though, the value for the vertical shear force is fixed on 4,080kN / 2,6m. Therefore the horizontal axial forces are adjusted to equal the horizontal-vertical load ratio.

Roof Angle	Adjusted horizontal axial force	Adjusted vertical shear force
35 degrees	12,904kN / 2,6m	4,080kN / 2,6m
45 degrees	12,618kN / 2,6m	4,080kN / 2,6m
55 degrees	14,286kN / 2,6m	4,080kN / 2,6m

Table 4.4b; *The adjusted load combinations for various roof angles*

The strain on a specific location is determined as follows:

$$\varepsilon_i = \varepsilon_{i;N(adjusted+2kN)} - \varepsilon_{i;N(2kN)} \tag{4.4}$$

Where:

ε_i =	The strain on a specific location corresponding locations in **figure 4.3L**
$\varepsilon_{i;N(adjusted+2kN)}$ =	The strain corresponding with an adjusted axial force + 2kN
$\varepsilon_{i;N(2kN)}$ =	The strain corresponding with an axial force of 2kN
i =	Location indicator, consisting of a number (1 to 8) and a subscript (b = up and o = down)

The first 2kN is skipped due to strains related to the closing of the gaps. The subsequent route should match the elastic behavior of the supporting batten, in case the vertical and horizontal force were applied simultaneously. This route is indicated with a blue arrow in **figure 4.4a**, nominated as the Elastic deformation line.
Once all strains are measured for all positions, both up and down, one could draw two graphs. These graphs represent the progress of the strains along the width of the supporting batten.

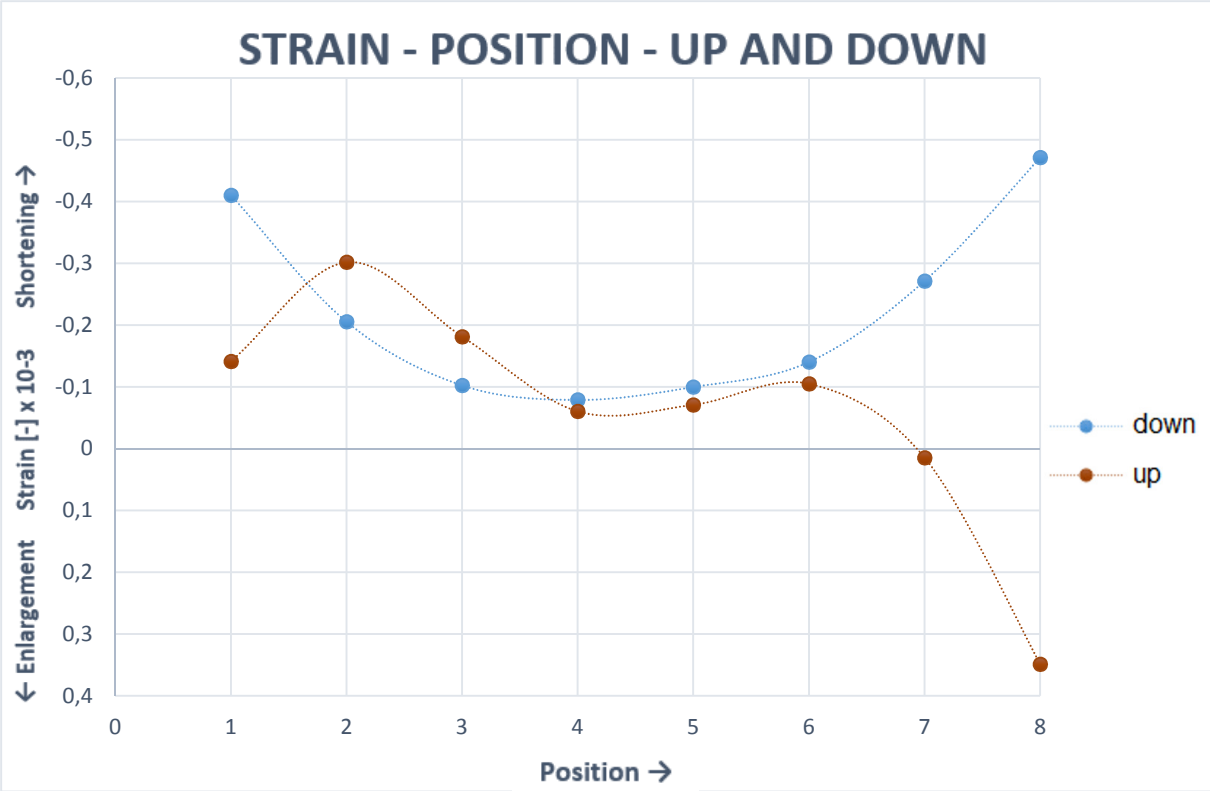

***Figure 4.4b**; Example of the strain progress along the width of the supporting batten for both the upper side and the down side*

To rule out the effect of moment stresses, the average value for all positions is determined and shown in f**igure 4.4c**.

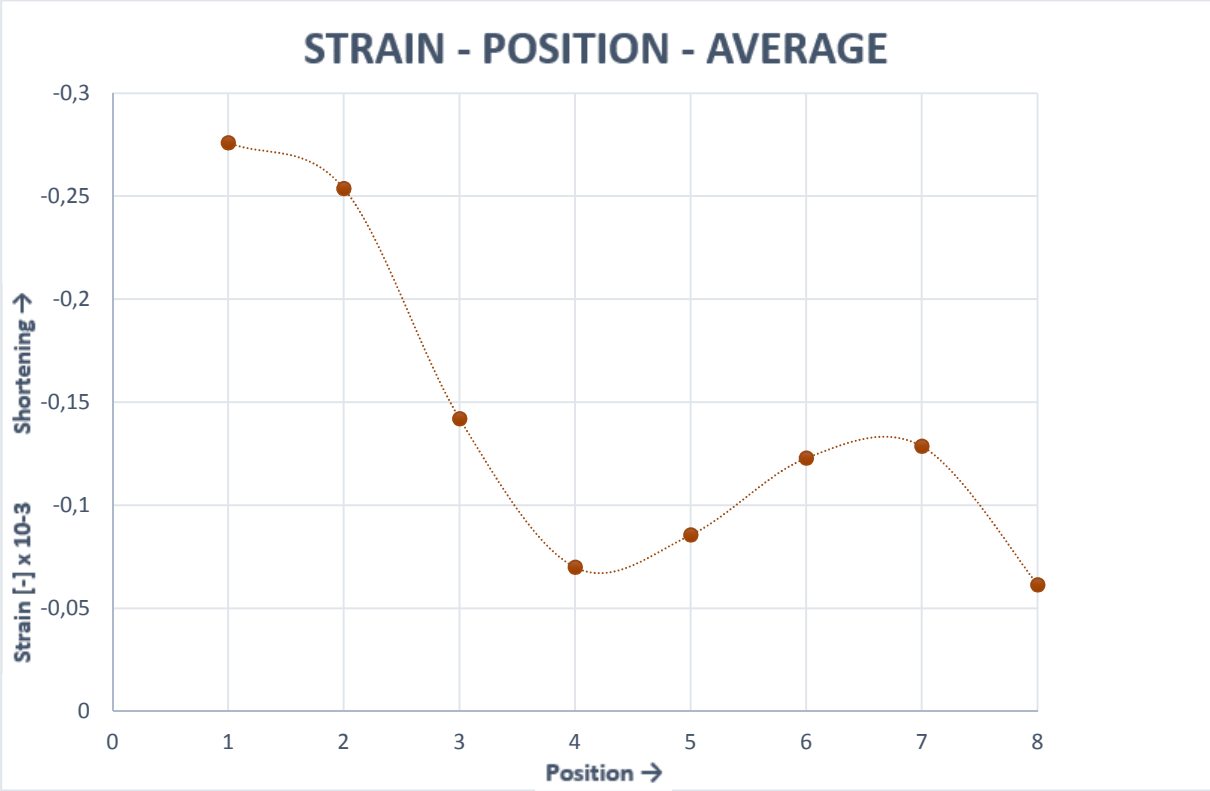

***Figure 4.4c**; Example of the average strain progress along the width of the supporting batten*

To compare the results, the strains retrieved from the adjusted forces are simply multiplied with the deviation to equal the strains from the intended forces of **table 4.4a**.

$$\varepsilon_{i;100\%} = \frac{N_{adjusted}}{N_{100\%}} \cdot \varepsilon_{i;adjusted} = \frac{V_{adjusted}}{V_{100\%}} \cdot \varepsilon_{i;adjusted} \tag{4.5}$$

4.4.3 Final results

The results of all tests are included in **appendix 4.2**. To be able to analyze the results, they are categorized into seven groups (Note, these are all multiplied according to **formula 4.2**). The lines correspond to the average value of the two test series.

Group	Parameters				
Roof inclination 35° (low adding)	600 CTC	900 CTC	1200 CTC		
Roof inclination 45° (low adding)	600 CTC	900 CTC	1200 CTC		
Roof inclination 55° (low adding)	600 CTC	900 CTC	1200 CTC		
Roof inclination 45° (high adding)	600 CTC	900 CTC	1200 CTC		
All 600 CTC	35° (L)	45° (L)	55° (L)	45° (H)	
All 900 CTC	35° (L)	45° (L)	55° (L)	45° (H)	
All 1200 CTC	35° (L)	45° (L)	55° (L)	45° (H)	45° (L+CS)

Table 4.4c; *Seven groups categorizing certain parameters for analysis*

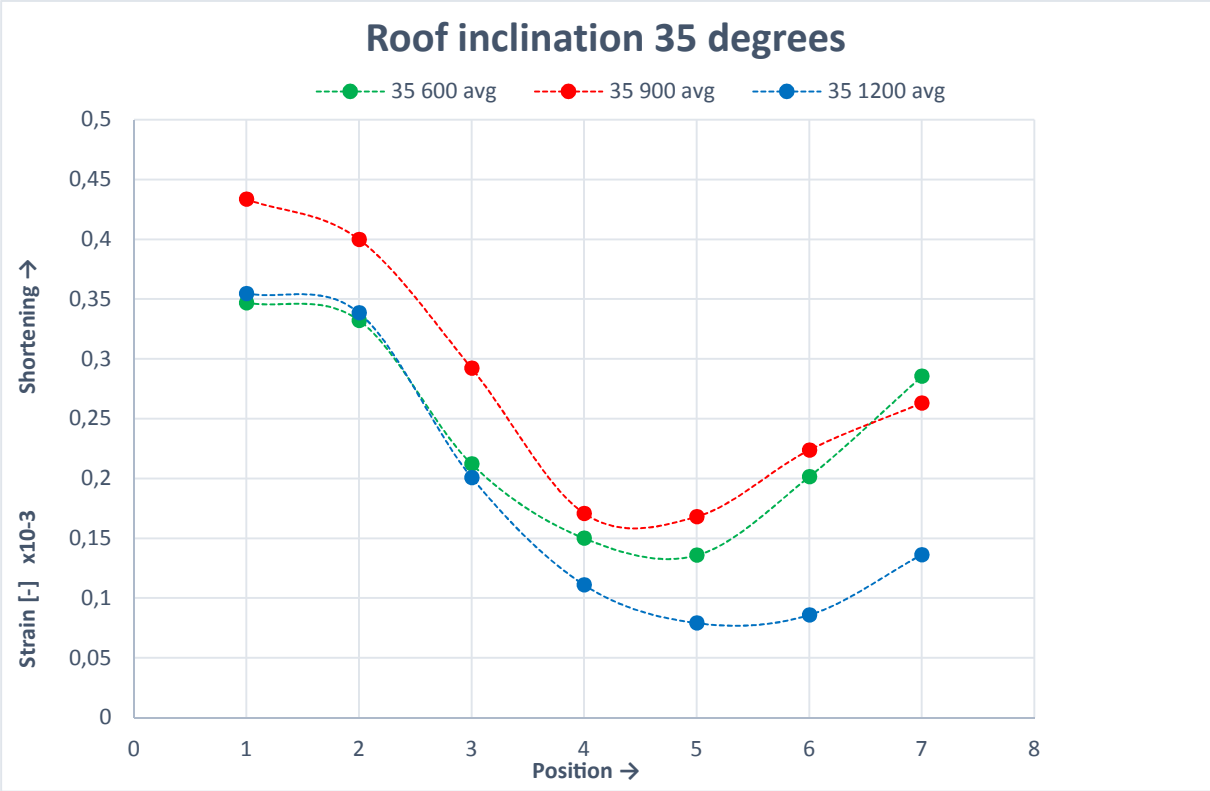

Figure 4.4d*; Average values of the strain corresponding the center-to-center distance of 600, 900 and 1200 millimeters with the roof angle of 35 degrees*

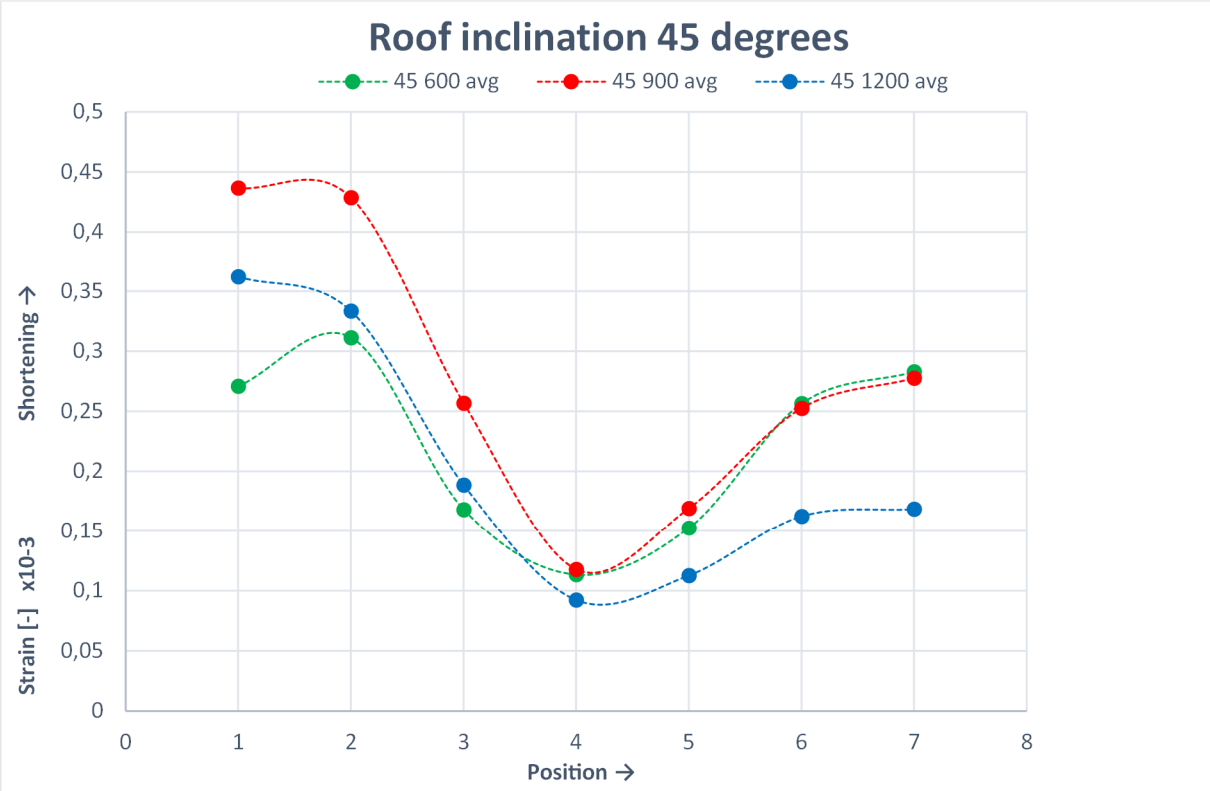

***Figure 4.4e**; Average values of the strain corresponding the center-to-center distance of 600, 900 and 1200 millimeters with the roof angle of 45 degrees*

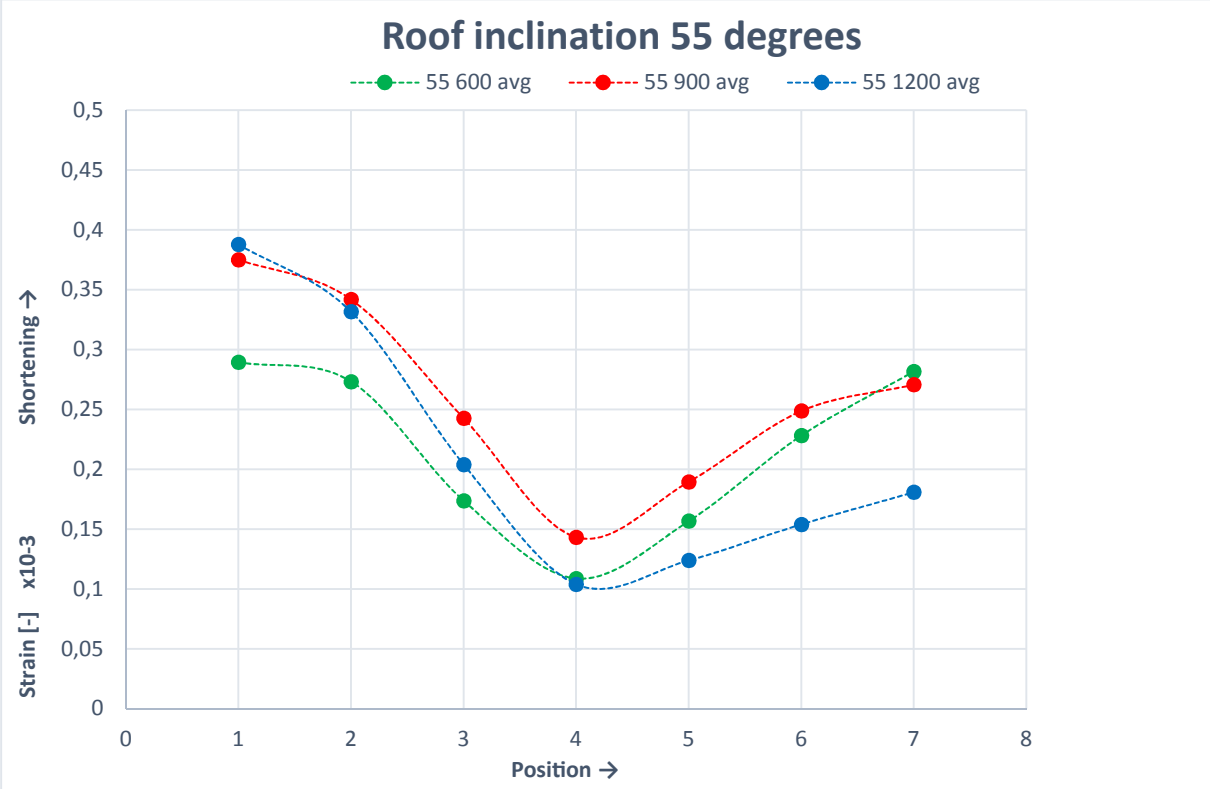

***Figure 4.4f**; Average values of the strain corresponding the center-to-center distance of 600, 900 and 1200 millimeters with the roof angle of 55 degrees*

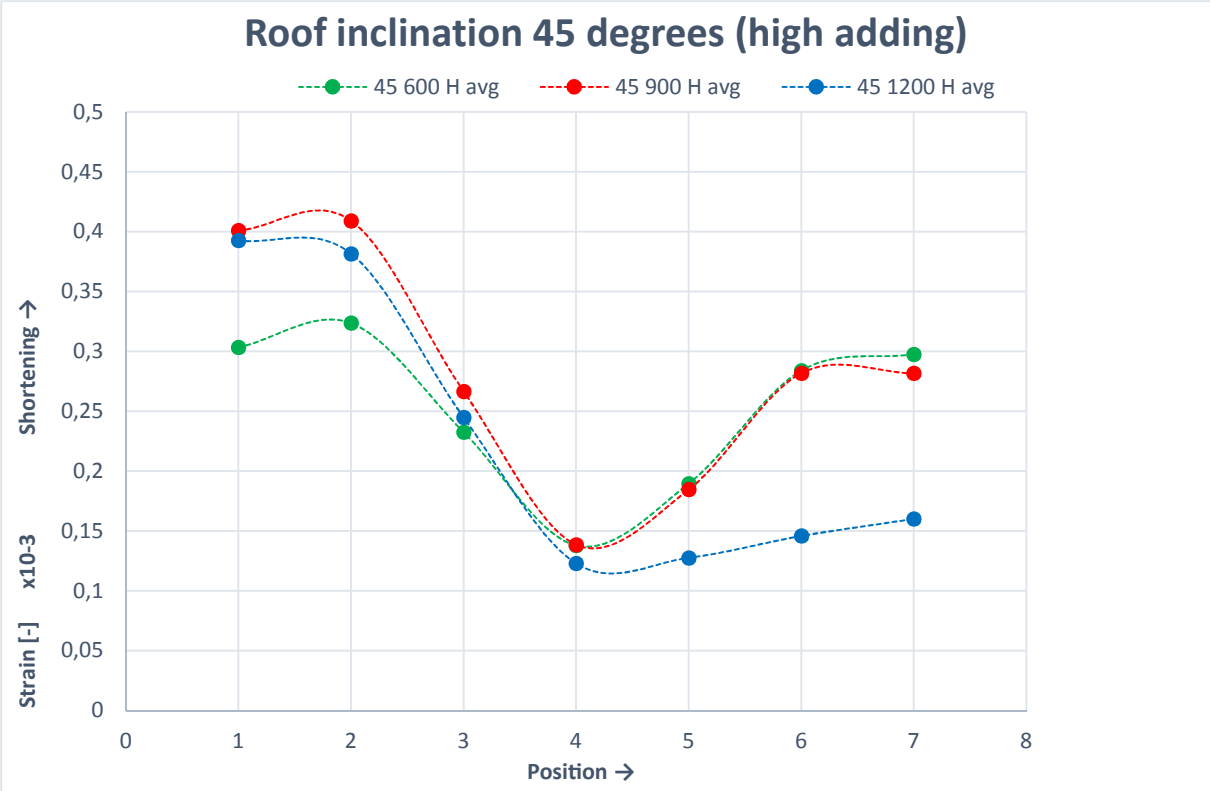

***Figure 4.4g**; Average values of the strain corresponding the center-to-center distance of 600, 900 and 1200 millimeters with the roof angle of 45 degrees and high adding of the wall plate*

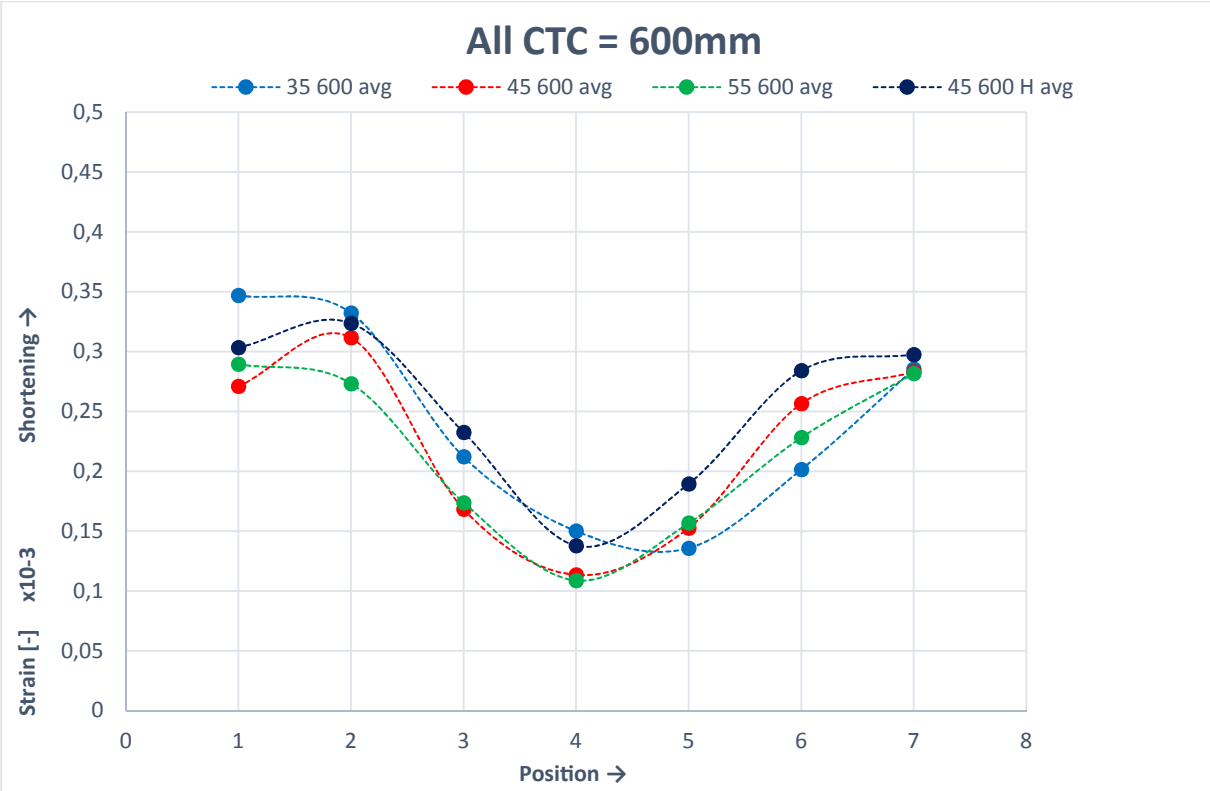

***Figure 4.4h**; Average values of the strain corresponding various roof angles with a CTC distance of 600mm*

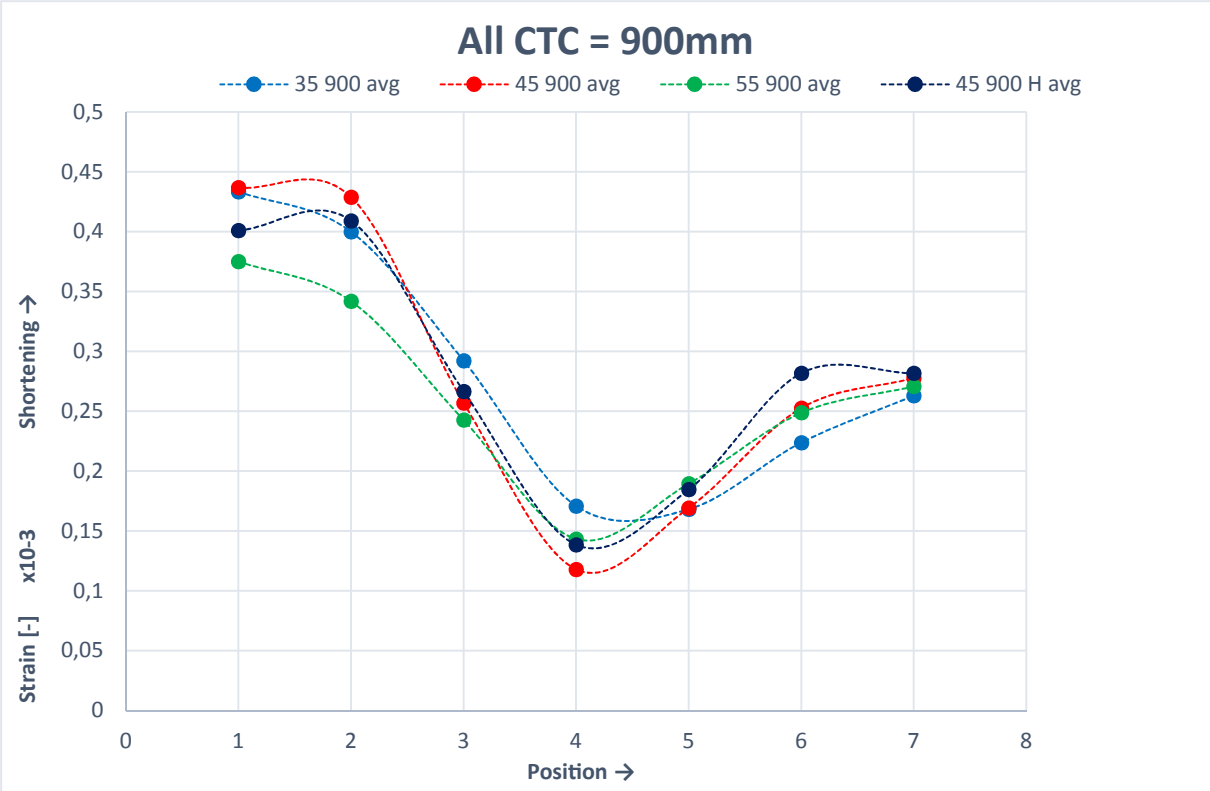

***Figure 4.4i**; Average values of the strain corresponding various roof angles with a CTC distance of 900mm*

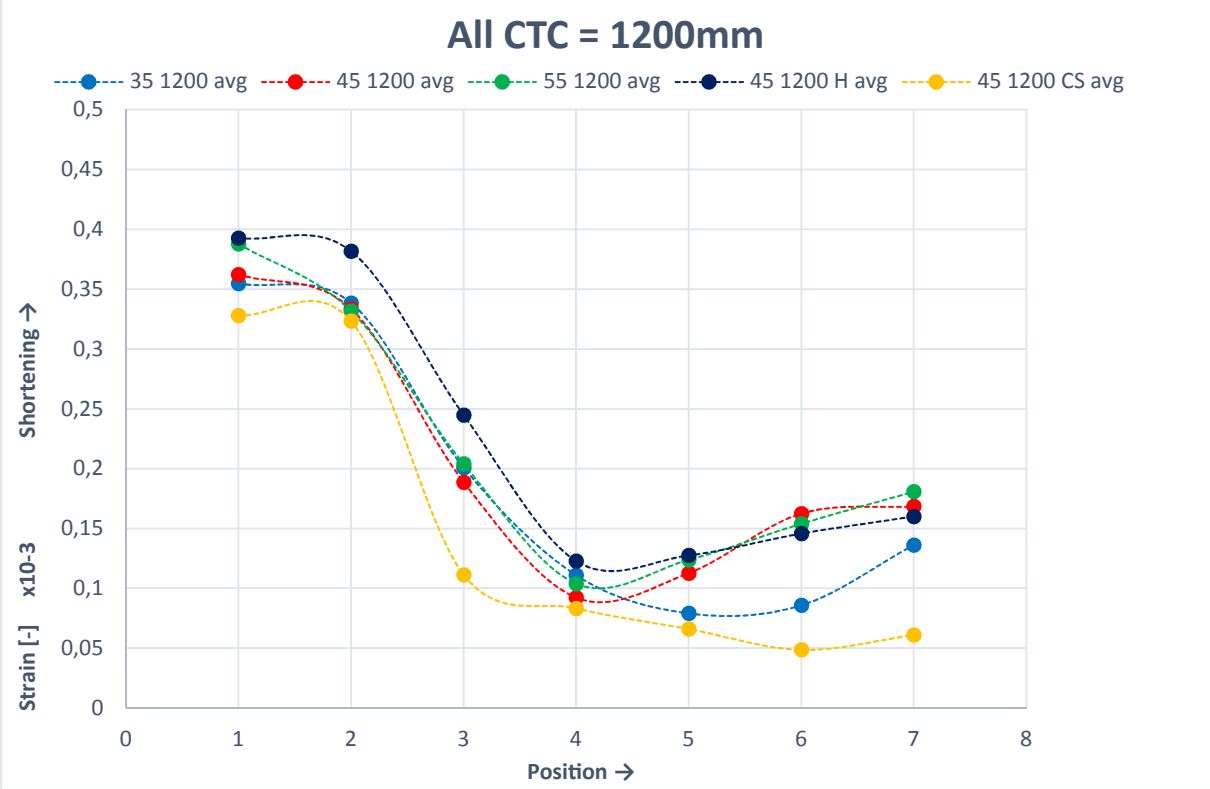

***Figure 4.4j;**; Average values of the strain corresponding various roof angles with a CTC distance of 1200mm including the coach screw*

4.4.4 Analysis of the results

Paragraph 4.4.3 contains several groupings regarding the results given in **appendix 4.2**. To be able to interpret these results, a series of possible boundary conditions are drafted. **Figure 4.4.k** shows a series of expected deformation progress lines regarding the various center-to-center distances of the brackets.

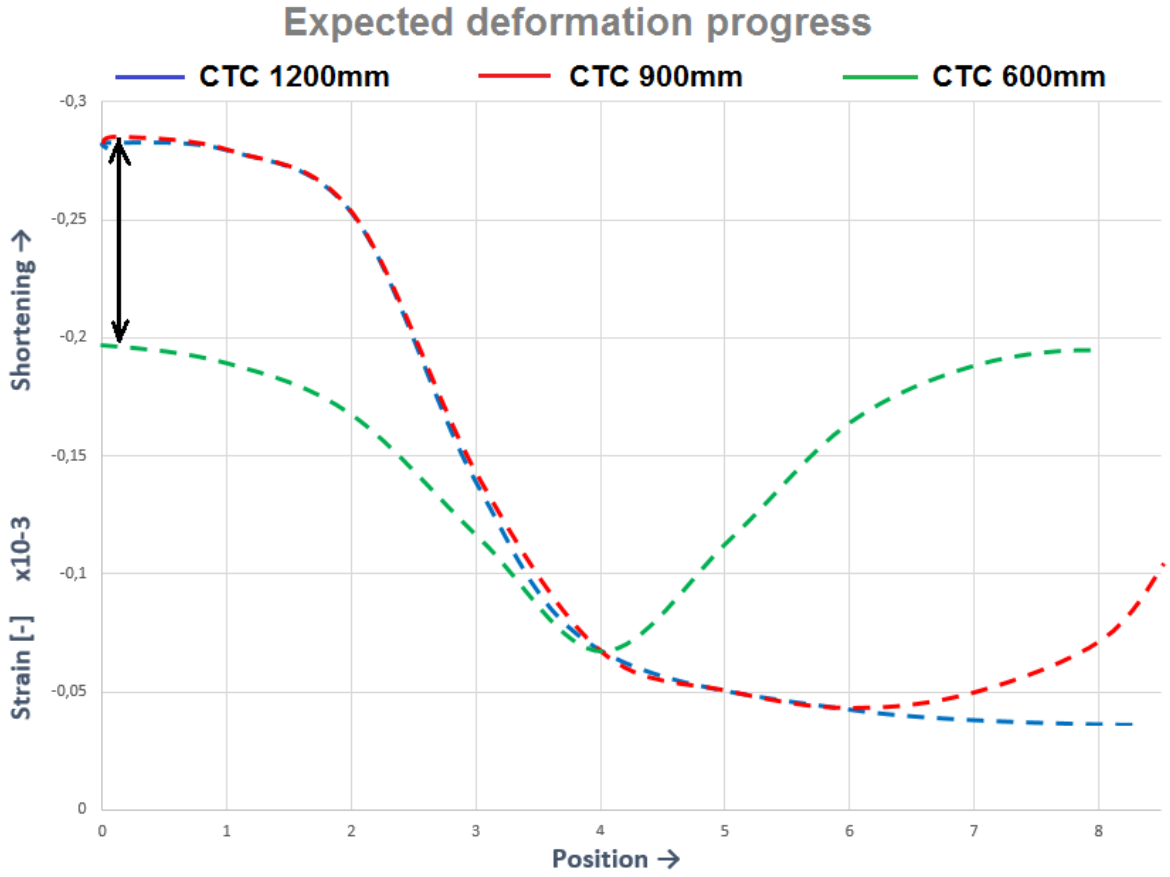

Figure 4.4k; *Expected deformation progress of the 600/900/1200 CTC distance of the brackets*

The following characteristic properties are established:

- Symmetry lines halfway between the brackets

As most stresses will be attracted by the brackets, and a minimum of stresses will be present halfway the brackets, a sinusoidal progress may be expected. With the top of the sine located at the position of the brackets (CTC 600 position 0 and 8, CTC 900 position 0 and CTC 12000 position 0) and a dale located halfway the brackets (CTC 600 position 4, CTC 900 position 6 and CTC 1200 position 8). This will result in a full sine for the CTC 600, a three quarter sine for the CTC 900 and a half sine for the CTC 1200. Subsequently, vertical symmetry lines can be drawn at the position of a dale

- Less top stresses for CTC 600 compared to CTC 900 and CTC 1200

As the test set-up contains 5 brackets in the CTC 600 specification and 3 brackets in the CTC 900 and CTC 1200 specifications, a reduced top stress (and therefore strain) is expected for the CTC 600 compared to the CTC 900 and CTC 1200. This reduction is visualized in **figure 4.4k** with a black arrow.

After comparing these characteristics with the results shown in **figure 4.4d to 4.4j** and analyzing all other results, the following findings are highlighted:

- The overall progress equals the predicted progress

The overall progress meets the expectations, though some remarks may be noted:

1) Position of the dale for the CTC 900 and CTC 1200 is out of place. This could partially be explained by the abnormal behavior of the strain gauges near position 8. This will be explained later on in this paragraph.

2) The strains of the CTC 1200 are considerably lower compared to the strains measured with the CTC 900. This effect can be ascribed to the finite width of the test set-up, resulting in asymmetrical stress distributions. However, this assumption cannot be validated due to a lack of measurements. A possible distribution is given in figure 4.4L.

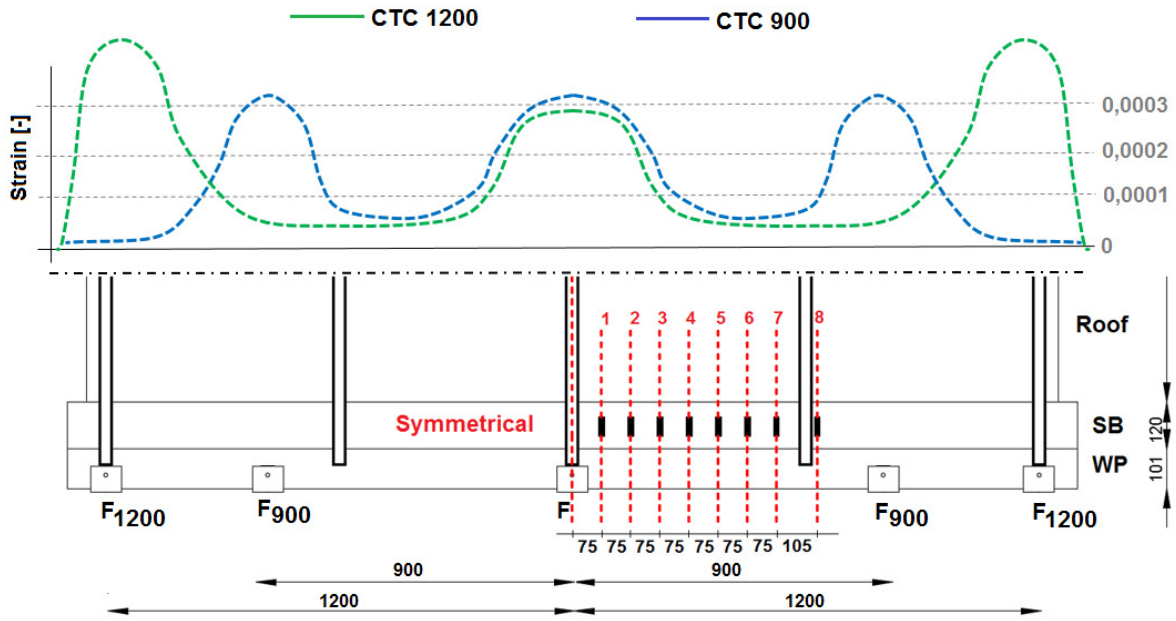

Figure 4.4L; *Possible strain progress along the width of the test set-up*

- The amount of strain is acceptable

To validate whether the measured strains are valid or not, the strain progress is compared with an average value for the strain. This average value is determined by applying the force on a cross sectional surface similar to the supporting batten and grant it the material properties obtained in **paragraph 4.1**:

$$\sigma = \frac{F}{A} \tag{4.6}$$

With:

F = Applied force by the hydraulic actuators (CTC 1200, roof angle 45 degrees, adding low)

A = Crosse sectional area of the supporting batten located at the gauges

$$E_{90;D2} = \frac{E_{0;D2}}{E_{0;mean}} \cdot E_{90,mean} \tag{4.7}$$

With:

$E_{90;D2}$ = Estimated modulus of elasticity for the supporting batten perpendicular to the grain direction

$E_{0;D2}$ = Determined modulus of elasticity for the supporting batten parallel to the grain direction (**paragraph 4.1**)

$E_{0;mean}$ = Modulus of elasticity for C24 timber parallel to the grain direction

$E_{90,mean}$ = Modulus of elasticity for C24 timber perpendicular to the grain direction

$$E_{90;D2} = \frac{12.634 N/mm^2}{11.000 N/mm^2} \cdot 370 N/mm^2 = 425 N/mm^2$$

$$\varepsilon_{average;D2} = \frac{\sigma}{E_{90;D2}} = \frac{0,103 N/mm^2}{425 N/mm^2} = 0,242 \cdot 10^{-3} \tag{4.8}$$

This is plotted in the strain progress diagram, displayed in **figure 4.4M**.

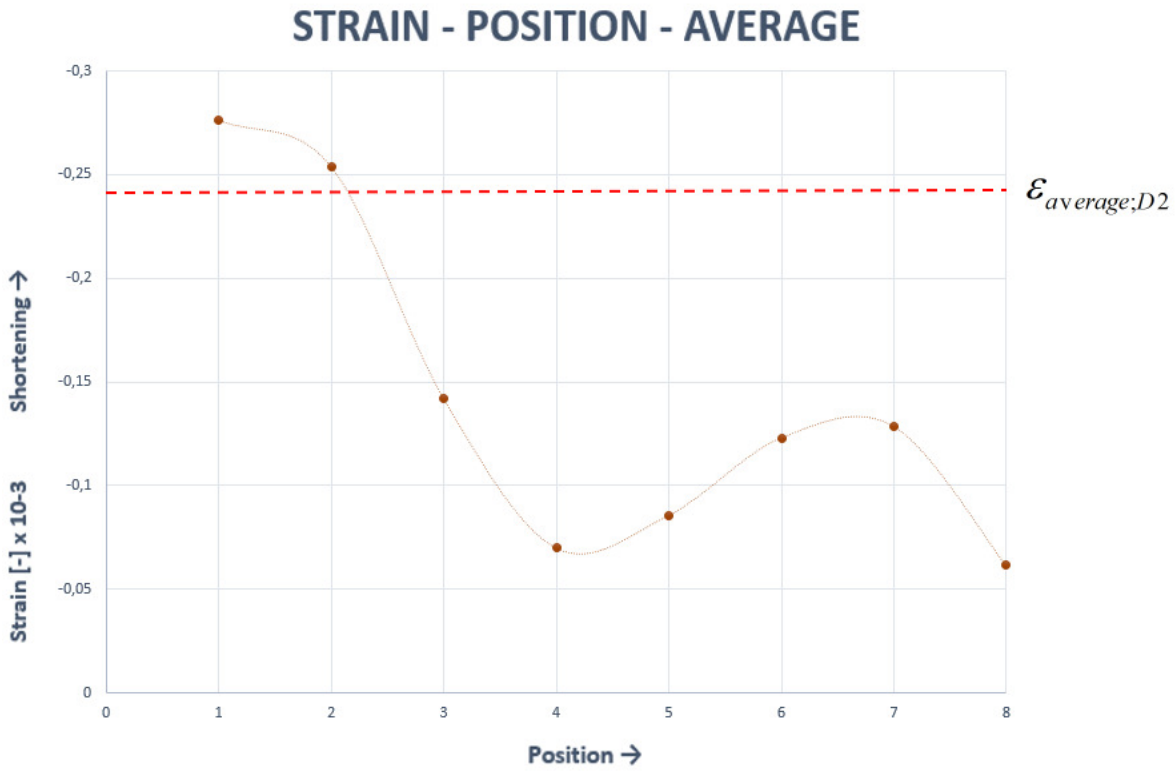

Figure 4.4m; *Average strain in the supporting batten compared with the strain progress of the batten along the width of the test set-up*

Although the value for the average strain seems too great to be plausible, the order of magnitude is in the same range, and therefore acceptable. Besides, there are two possible explanations why the average strain is greater than expected. The first reason is the an-isotropic behavior of the supporting batten (which will be explained later on in this paragraph), causing various strength properties in different directions and therefore a rather more

complicated relation between strain and stresses. Second, the peak stresses are located in the middle of the cross section, not on the outside. This is explained in **chapter 3**.

- Abnormal behavior of the strain gauges towards position 8

The progress lines for CTC 900 and CTC 1200 show an obvious upward movement towards position 8 contradictory to the expectations. A possible explanation could be the geometrical imperfection of the connection, resulting in side effect strains. This can be validated by looking at the results from the test series including the coach screw. By connecting the wall plate with the roof element beforehand, possible side effect strains might be excluded. And as the results show, the upward movement towards position 8 is diminished. Though, as the coach screw is only applied for one test series, it is incorrect to consider this explanation as the only possible and correct explanation. A second possible solution is the truss behavior of the roof element. The rafters have a center-to-center distance of 600 millimeters, located in the test set-up at both position 0 and 8. The rafters located not directly above the F-bracket might function as a pull rod, as they are connected with the supporting batten by means of fasteners. They will bring the forces back towards the supporting panel, where they redirects towards the brackets. This is illustrated in **figure 4.4N**.

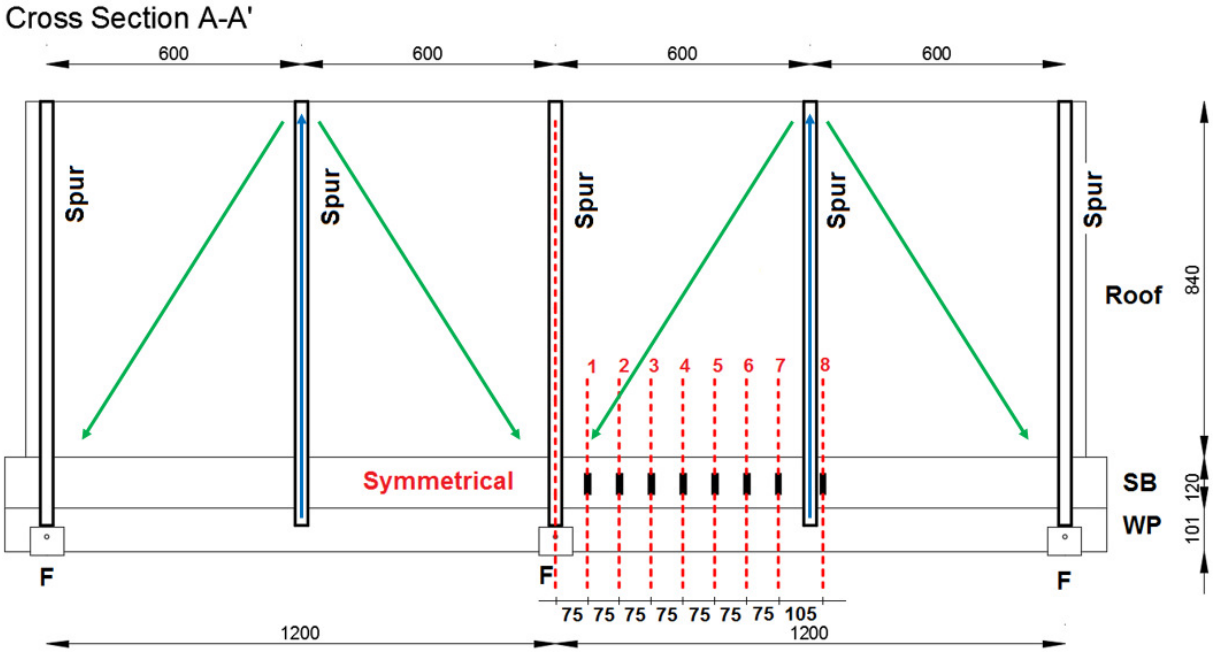

Figure 4.4n; *Truss-like behavior of the roof element. The blue arrow illustrates the possible forces in the rafters, acting like a pull rod. The green arrows visualizes the redistribution of the forces*

- Possible erroneous values for strain 8

The position of the 8th strain gauges are divergent to the first 7. This is because of the impediment of the rafters. Therefore the gauges have been relocated as close as possible near the predestined position. This however was, concluding afterwards, not the best solution. The measured strain values differ immensely to the other results. And as the measurements cannot be checked with the symmetrical counterpart (position 0), it is decided to disregard the results from these gauges.

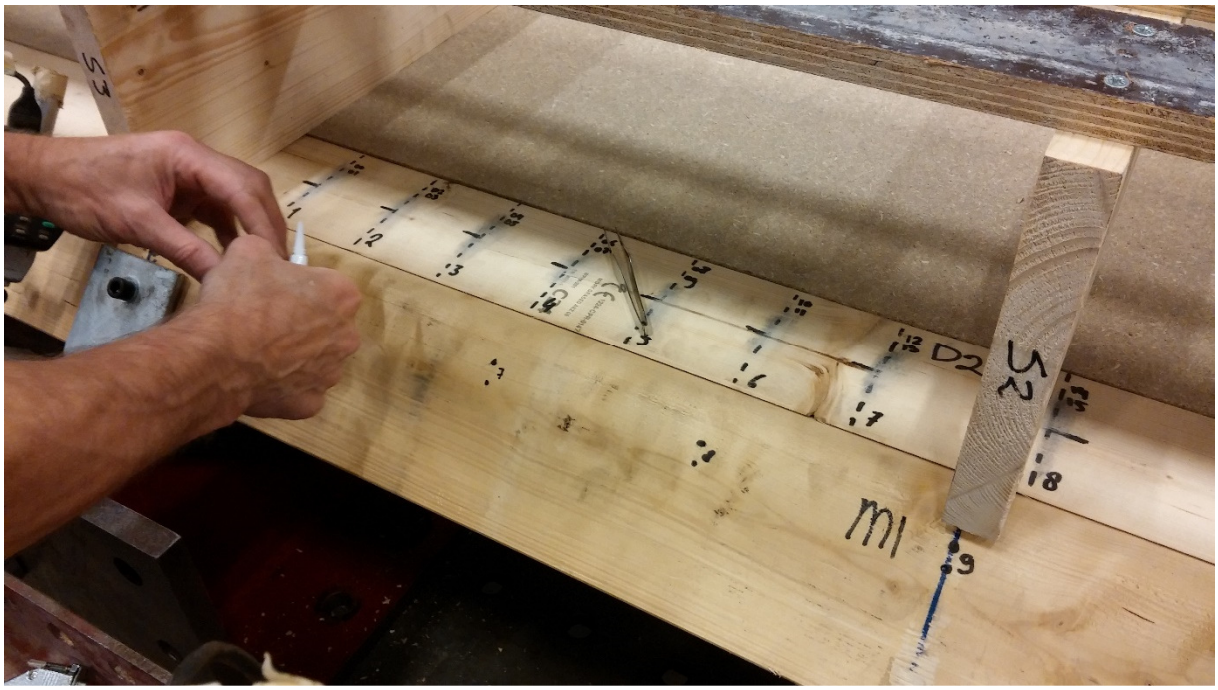

Figure 4.4o; *Positions of the strain gauges on the supporting batten. On the right side the dislocated position 8 giving abnormal results*

- Appearance of moment stresses in the supporting batten

The strain progress in **figure 4.4b** raises suspicions of moment stresses being present near the rafters. This is indicated by the opposite directions of the slopes near the positions of the rafters. For position 7, the relation between the force and strain has been highlighted in **figure 4.4p**.

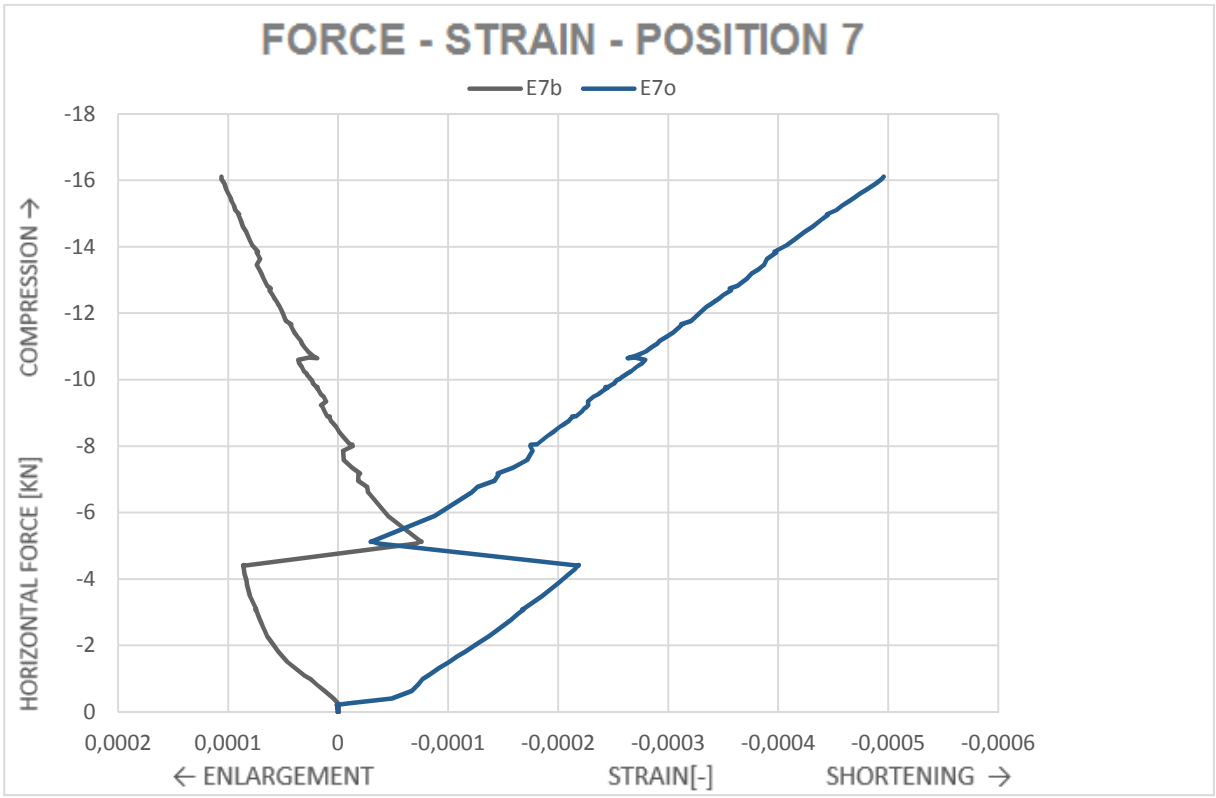

Figure 4.4p; *Force – strain relation at position 7 on the supporting batten. E7o is the strain gauges on the lower side, E7b is the strain gauges on the upper side*

An increase in horizontal force results in an elongation of the upper side of the supporting batten, while simultaneously the lower side contracts. This is due to the translation of the horizontal forces in the supporting batten, explained in **chapter 3**. The application of the vertical shear force results in an opposite effect, as the shear force is counteracting on the curvature. This is illustrated in **figure 4.4q**.

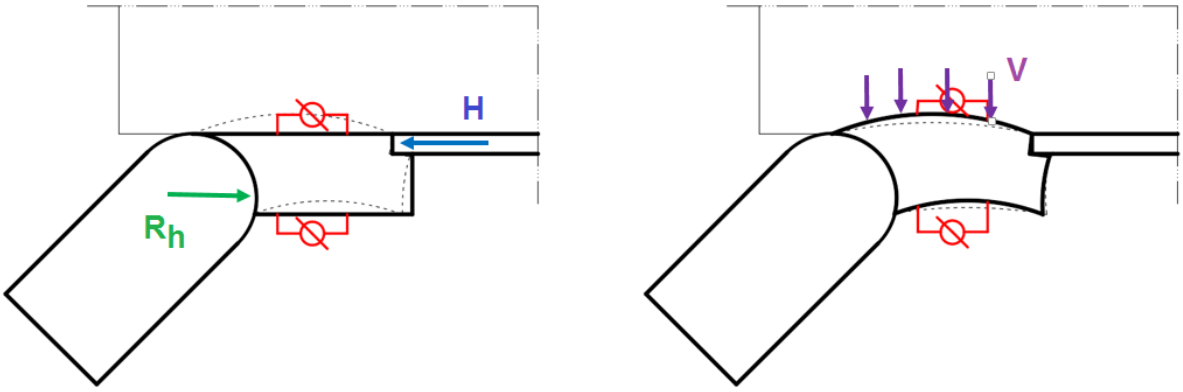

Figure 4.4q; *Left: curving of the supporting batten due to horizontal axial forces*
Right: counteracting on the curvature by the vertical shear force
Note: deformations are demonstrative

- An-isotropic properties of the supporting batten

Timber perpendicular to the grain direction is an-isotropic. This means that the strength properties in the radial direction differ from the tangential direction. Wood is about two times stiffer in the radial direction compared to the tangential direction **[5]**. That is why the relationship between the measured strains (especially between top and bottom) is different from the actual stresses. Secondly, the cross section of the supporting batten contains juvenile wood as well as mature wood. The ratio of modulus of elasticity between juvenile wood and mature wood ranges from 0,5 to 0,9. Especially towards the pith of the tree the wood becomes a lot less stiff **[9]**.

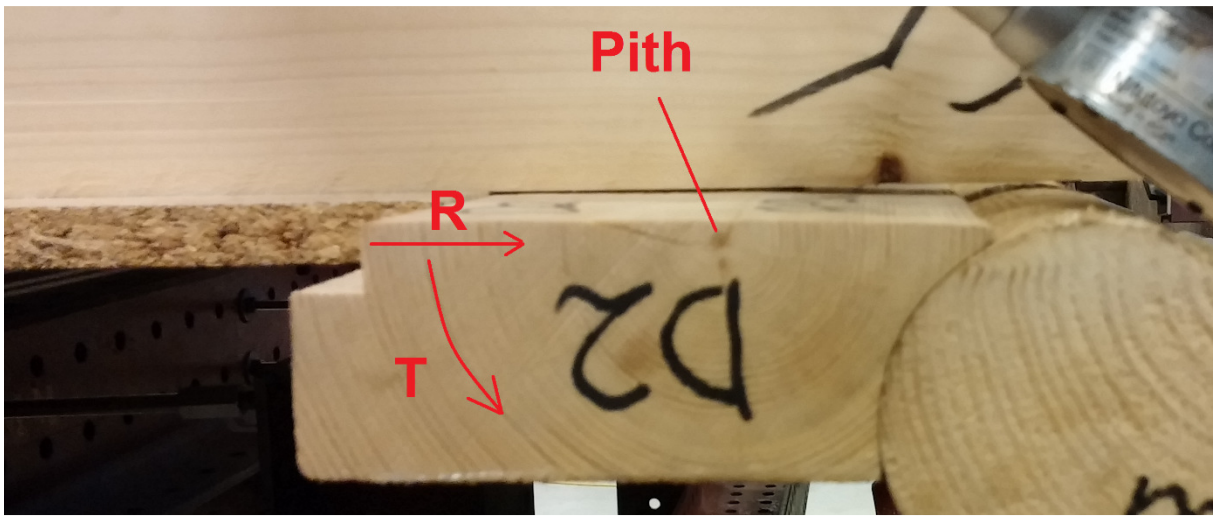

Figure 4.4r; *Orientation of the growth rings in the supporting batten. Indicated are the pith, the radial direction ® and the tangential direction (T)*

4.5 Conclusions and improvement points

This last paragraph summarizes all analytical findings. In addition, improvements are included to facilitate future experimental research.

4.5.1 Conclusions regarding the experimental research

Main conclusion:

- All test set-ups (varying in center-to-center distance of brackets, differing roof angles and changing depth of the adding) indicate a concentration of strains (and possibly stresses) near the F-brackets. The effective width lies somewhere between the 2 and 3 positions (meaning 150mm to 225mm) on each side of the bracket (resulting in an effective width between 300mm and 450mm).

- The variation in roof angle, amount of adding and the center-to-center distances have no obvious influence on the effective width

Side-notes:

- Various phenomena cannot be explained sufficiently. Phenomena such as the abnormal behavior of the strain gauges towards position 8, or the amount of strain for the CTC 1200 set-up being considerably lower compared to the CTC 900 set-up. The use of more measuring equipment or change of test materials might improve the certainty of the results.

- Afterwards it can be concluded that the choice of position of the gauges on the supporting batten was unfortunate, resulting in certain side-effects which were not foreseen or were overlooked. By positioning the gauges on the supporting panel, side-effects like the an-isotropic properties and moment stresses could have been avoided.

4.5.2 Improvement points regarding experimental research

- As mentioned in the side-notes, the following aspects would be an improvement in future research:

    1) Using more measuring equipment would improve the segmentation of the progress line
    2) Using the measuring equipment on other positions to be able to compare existing results.
    3) Using different test-materials to compare existing results
    4) Changing the location of the gauges towards the supporting panel

- The utilization of ESPI:

No usage has been made of ESPI. ESPI (Electronic speckle pattern interferometry) uses lasers and video detection to measure stresses and strains. It could lead to additional valuable test results.

- Alternative test set-up:

An alternative experimental test set-up has been developed to increase knowledge of the effective width of the supporting batten. This experimental research is more quantitative, compared to the executed research, which is more qualitative.

The test set-up consists of a single F-bracket, a wall plate and a supporting batten. The width of the wall plate and the supporting batten are similar.

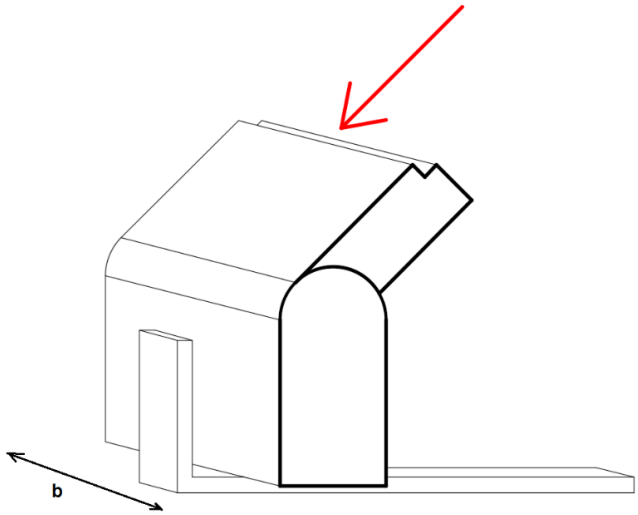

Figure 4.4s; *Test set-up for possible future research. B is the width of the wall plate and the supporting batten*

The goal of the test is to determine the force at which the connection will fail due to fracture. The first test series have a certain (preferably rather small) width. Once the failure strength is determined, the width of the set-up is increased, and again the failure strength is determined. It is most likely that the failure strength of the second series will have an increased failure strength:

$$F_{fracture,1} < F_{fracture,2} \tag{4.9}$$

This process is repeated until an increase of width doesn't affect the failure strength, so that:

$$F_{fracture,n} = F_{fracture,n+1} \tag{4.10}$$

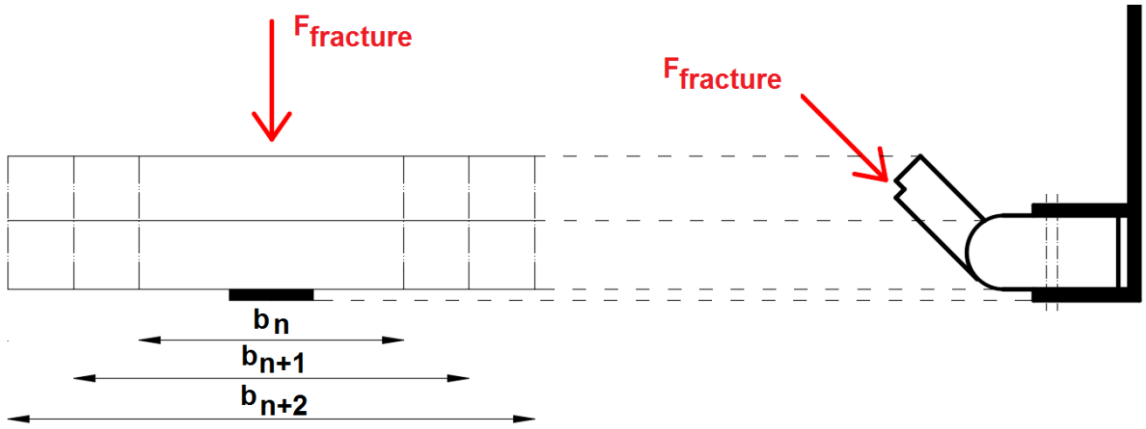

Figure 4.4t; *Test set-up for possible future research. Left is top view, right is rotated cross section*

Chapter 5 | Numerical research

This chapter deals with the preparation, execution and analysis of the numerical research. First a short introduction in the finite element method is given. Hereafter, a two dimensional model is elaborated, which is the basis for the three dimensional model that follows afterwards. The chapter ends with conclusions and recommendations.

5.1 Finite element method

The finite element method (FEM) is a method for finding solutions on material behavior like strains, stresses, thermal expansion and vibrations. This is achieved by dividing the problem into smaller elements and giving these elements properties in the available degrees of freedom. The system of elements is then solved by a selected solution method. An element is modeled by either a one, two or three dimensional model. Several different element types can be used for modeling the problem. A finer element net or a more complexed element type doesn't always result in a better representation of the reality, as it is easier to make an incorrect input. Besides, the size of the model has influence on the time it takes for the computer to get to a solution. The use of a finite element program should always be done cautiously, as various mistakes may occur, resulting in meaningless answers. One could think of idealization errors, input errors, discretization errors, geometrical errors, solve errors, display errors, interpretation errors or bugs in the software **[1]**. The finite element models are created and solved with the software package Abaqus 6.13 from Simulia **[A]**.

5.2 Two dimensional model

This paragraph serves as an introduction for the numerical study. A two dimensional model is developed as a basis for the three dimensional model, which will be elaborated on in the next paragraph. However, Results obtained by the two dimensional model will be analyzed.

5.2.1 Geometrics and material properties

First the size of the model needs to be specified. All materials that have no influence on the research goal, or that what can be substituted by means of a boundary condition, should be left out. As the goal is to know the stress distribution in the wall plate, the first part of the model is specified. Parts that have direct contact with the wall plate and therefore an influence on the behavior of the wall plate are the supporting batten and the F-bracket. Also the influence of the adding is included. The axial forces in the rafters will be transferred to the engaging point of the supporting batten, leaving out the rafters and the supporting panel. Though, to be able to introduce the shear force in the wall plate, a small part of the rafter is modeled. To simulate the deformation of the bracket properly, a small part of the concrete floor is implemented into the model (see **figure 5.2a** and **figure 5.2b**).

The parts are divided in three material property groups, listed in table **5.2a**:

Material property	Part
Timber C24 perpendicular to the grain direction	Wall plate, supporting batten, adding
Concrete	Floor
Steel	F-bracket

Table 5.2a; *Grouping of the parts by material property*

The material properties of all these materials are shown in **table 5.2b**. For the parts labeled as C24 perp. timber, no distinction is made between the tangential and radial direction. A separate material orientation is added to the supporting batten, as it makes an angle with the rest of the model (see **figure 5.2b**).

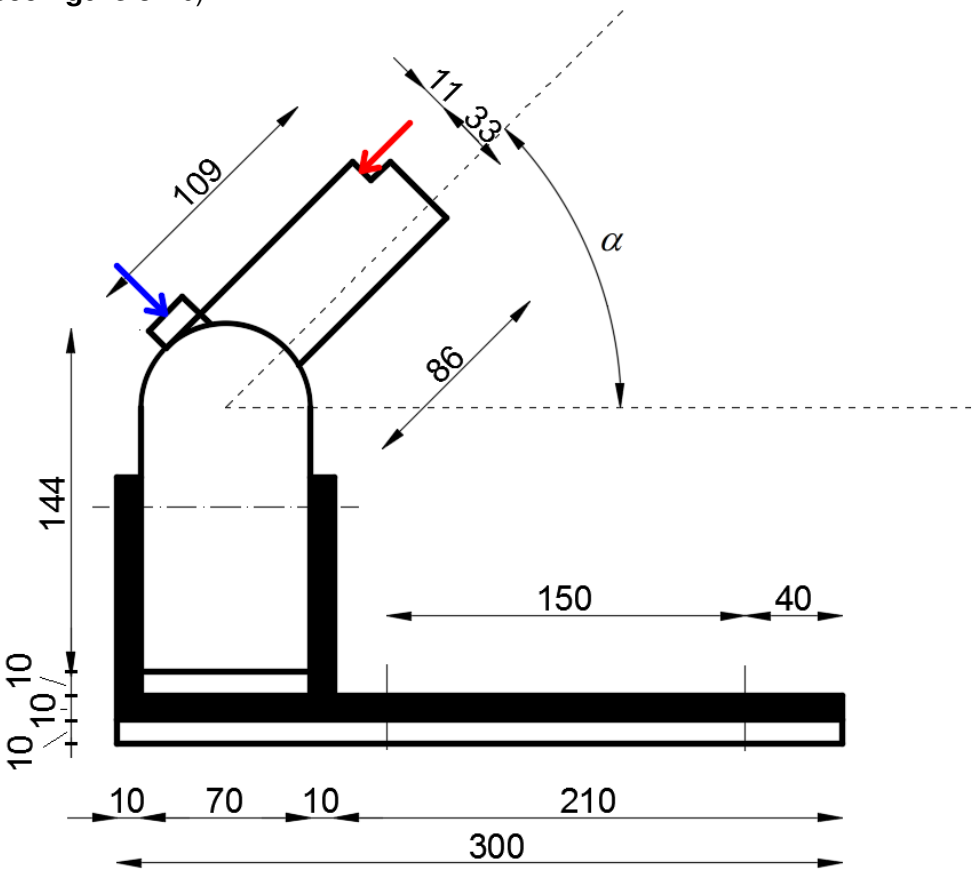

Figure 5.2a; *Dimensions of the assembly. Red arrow represents the axial force, the blue arrow the shear force.*

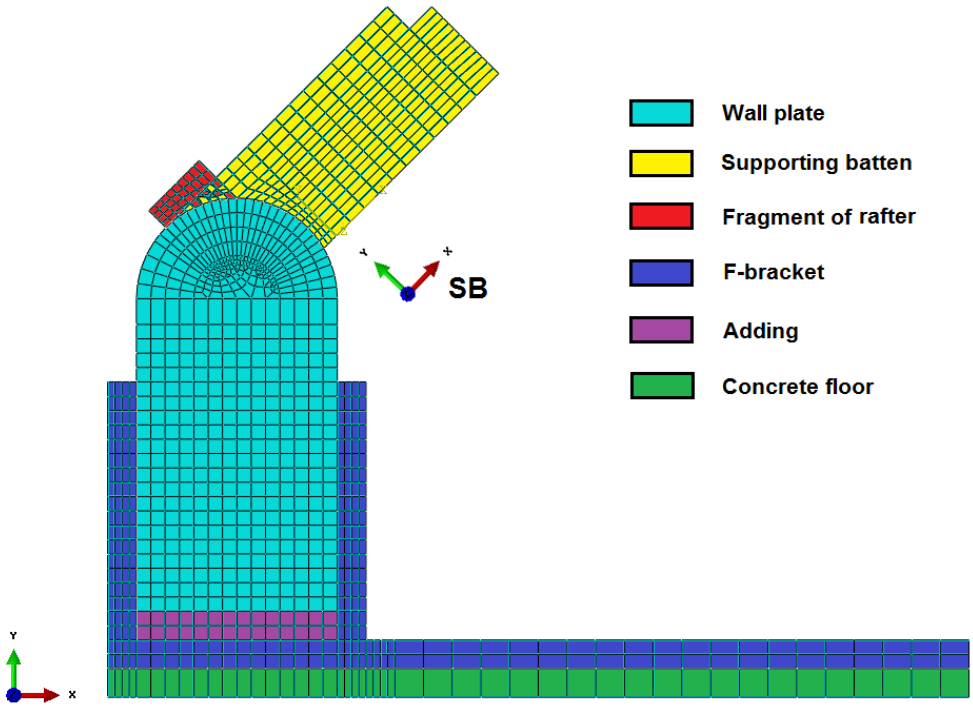

Figure 5.2b; *Meshing of the assembly. Note the separate material orientation of the supporting batten*

	C24 perp. timber	Concrete	Steel
Material behaviour	Elastic	Elastic	Elastic
Type	Isotropic	Isotropic	Isotropic
Young's modulus	370 N/mm^2	30.000 N/mm^2	210.000 N/mm^2
Poission's ratio	0,415	0,15	0,3

Table 5.2b; *Material properties used in the model. The Poisson's ratio for C24 perp. Timber is based on an average value of several softwood species* ***[6]***

5.2.2 Boundary conditions

To make sure the model is working as intended, several boundary conditions are established. The following boundary conditions are distinguished:

1) Contact boundary conditions

The contact properties are assigned to the elements to simulate the proper interaction behavior of the model.

Interaction Property	Tangential behavior	Normal behavior
Timber - Timber	Penalty, Friction coefficiënt: 0,5	Hard contact, Allow separation after contact
Steel - Timber	Penalty, Friction coefficiënt: 0,6	Hard contact, Allow separation after contact
Steel - Concrete	Penalty, Friction coefficiënt: 0,5	Hard contact, Allow separation after contact
Frictionless	Frictionless	Hard contact, Allow separation after contact

Table 5.2c; *Interaction properties of the surface-to-surface contacts between parts of the model. The friction coefficient are based on values posted at the Engineering Toolbox* ***[23].***

These surface-to-surface contacts are designated to the following part combinations:

Interactions	Combination of parts	Interaction property
Surface-to-surface	Wall plate - Supporting batten	Timber - Timber
Surface-to-surface	Wall plate - F-bracket	Steel - Timber
Surface-to-surface	Adding - F-bracket	Steel - Timber
Surface-to-surface	Adding - Wall plate	Frictionless
Surface-to-surface	Shear force - Wall plate	Timber - Timber
Surface-to-surface	F-bracket - Floor	Steel - Concrete

Table 5.2d; *Corresponding interaction properties for the combination of parts*

Figure 5.2b shows an overlap of the supporting batten and the rafter. As no interaction properties are assigned, these elements can move independently of each other.

2) Displacement and rotational boundary conditions

As the model is delimited in its size, several displacement and rotational boundary conditions are added to replace the original surrounding elements. **Figure 5.2c** shows the applied boundary conditions with the common mechanical symbols.

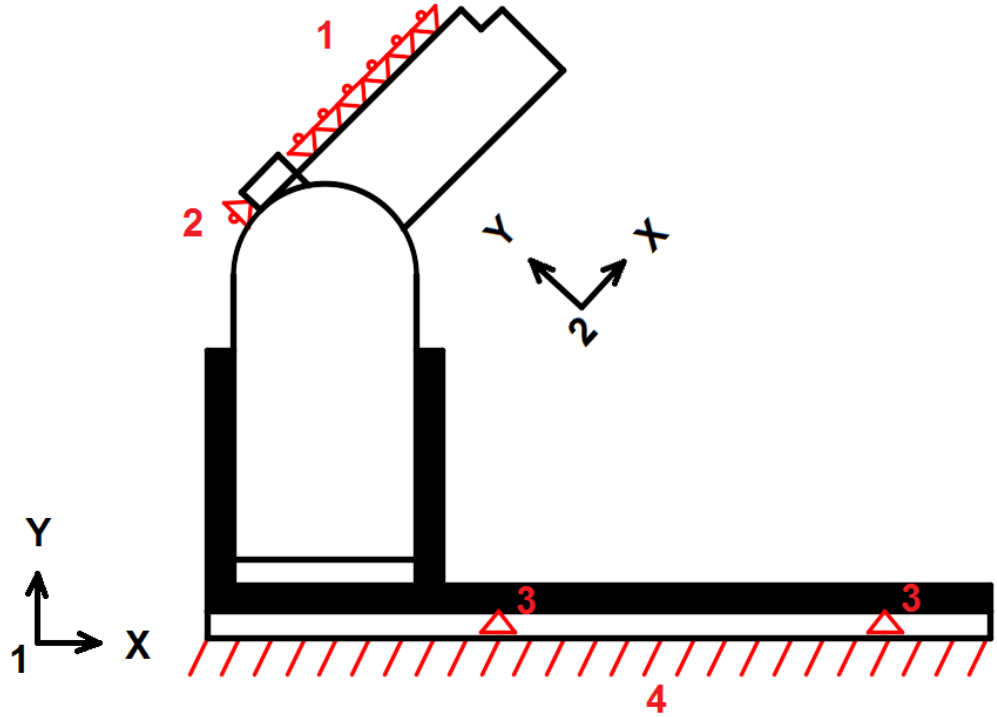

Figure 5.2c; *Applied boundary conditions. Note the dual coordinate system. The first coordinate system applies to the floor, F-bracket, adding and wall plate, whereas the second coordinate system applies to the rafter and supporting batten*

The applied boundary conditions are described in **table 5.2e**.

#	Location	Boundary condition
1	Roller support over a surface, the upper side of the supporting batten	Prohibited to move in the Y2-direction
2	Roller support over a surface, the lower side of the rafter	Prohibited to move in the X2-direction
3	Hinge supports for the F-bracket to floor connection	Prohibited to move in X1 and Y1-direction
4	Fixed support for the concrete floor	Prohibited to move in X1 and Y1-direction, also prohibited to rotate around the Z1-axis

Table 5.2d; *Description of the applied boundary conditions in* ***figure 5.2c***

3) Constraints

To imitate the bolted connection of the F-bracket and the wall plate, a constraint boundary condition is applied to the bracket. The constraint dictates two assigned nodes to copy their movements in the X1 and Y1-direction. This is illustrated in **figure 5.2d**.

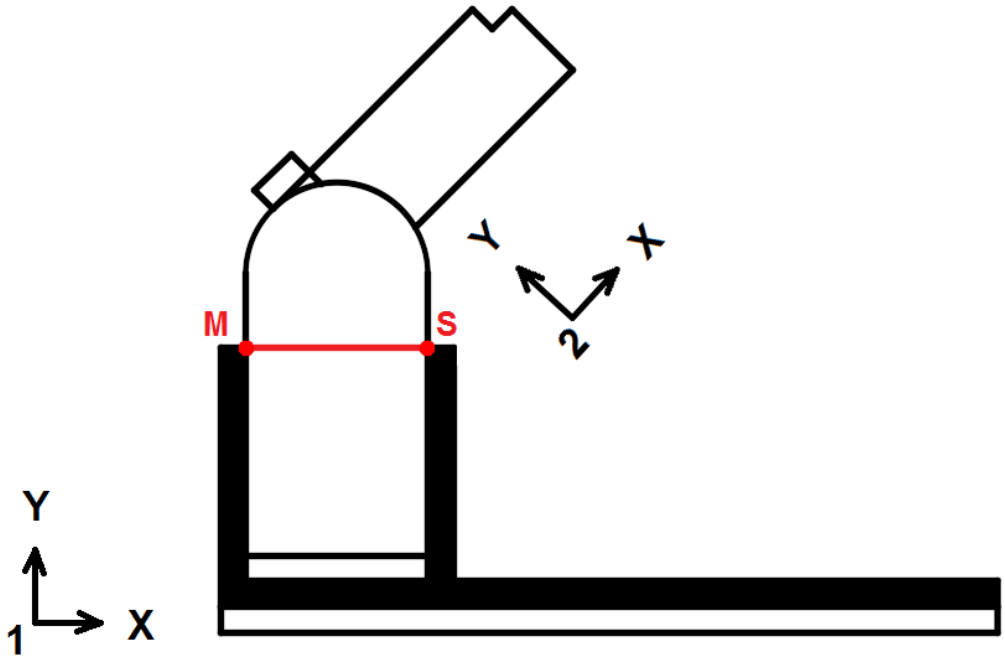

Figure 5.2d; *Constraint relation between two nodes. M is the master node and S is the slave node*

4) Loading

The axial and shear forces from the actual structure are modeled by two pressure loads, divided over the complete width of the point of engagement. This is shown in **figure 5.2e**.

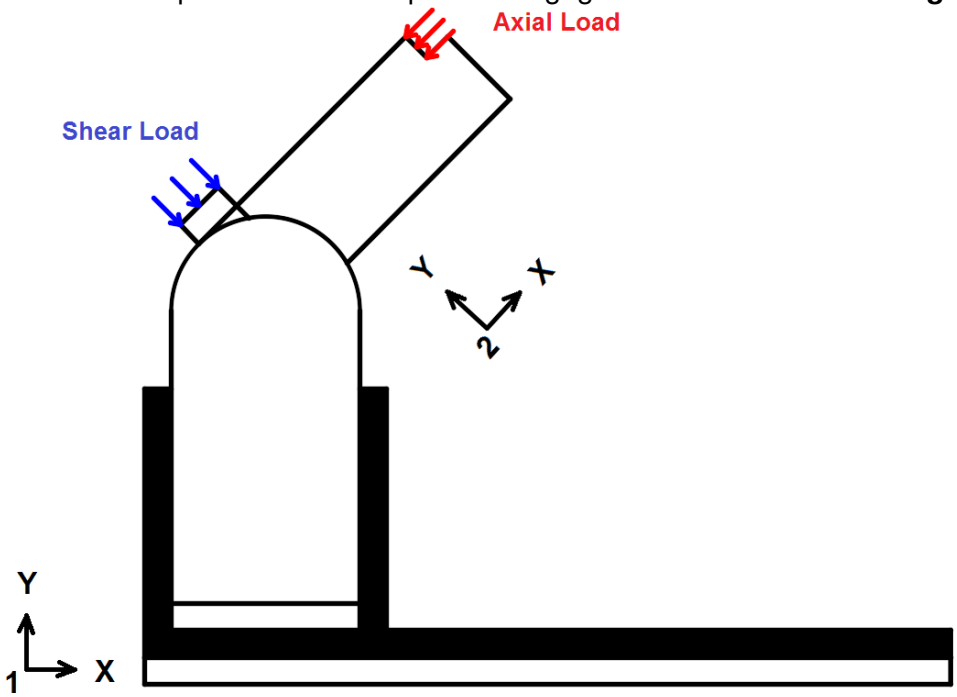

Figure 5.2e; *Applied pressure forces in the model*

The magnitude of the loads correspond to the loads determined in **chapter 3, table 3.3b**:

Roof inclination	(Axial load) **Corresponding pressure load**	(Shear load) **Corresponding pressure load**
35 degrees	(5,323 kN) **0,484 N/mm**	(1,683 kN) **0,0673 N/mm**
45 degrees	(3,872 kN) **0,352 N/mm**	(1,252 kN) **0,0501 N/mm**
55 degrees	(2,983 kN) **0,271 N/mm**	(0,852 kN) **0,0341 N/mm**

Table 5.2e; *Overview of axial and shear load, belonging to the assigned roof inclination*

5.2.3 FEM modelling

The previous paragraphs covered all the input required for Abaqus to submit a proper calculation, except for the mesh properties and the solution method, which will be discussed here:

- Meshing of the model

The determination of the mesh size is influenced by the goal of the research. A smaller mesh size will give a more fluent representation of the flow of strains and stresses, whereas a bigger mesh size will be more discreet. In case a smaller mesh size is used, the amount of elements increases together with the computational time for the computer to complete a calculation. For this reason, smaller mesh sizes are locally applied to regions with high interest. The goals for the numerical model consists of:

1) Getting a global overview of the flow of stresses in the connection detail

2) Making sure the nodes of various parts of the model connect to each other

As for the first goal, it results in a rather evenly distributed mesh pattern across the entire model (see **figure 5.2b**). Though, the second goal causes a disturbance in the region where the supporting batten meets the wall plate. As three different roof inclinations are tested, it is required for the connecting elements to match in all situations. This resulted in a radial mesh orientation at the top of the wall plate, which is shown in **figure 5.2f.** Between the top and the bottom of the model a free mesh is applied to enable a transition between the radial mesh orientation at the top and a structured rectangular mesh orientation for the rest of the model.

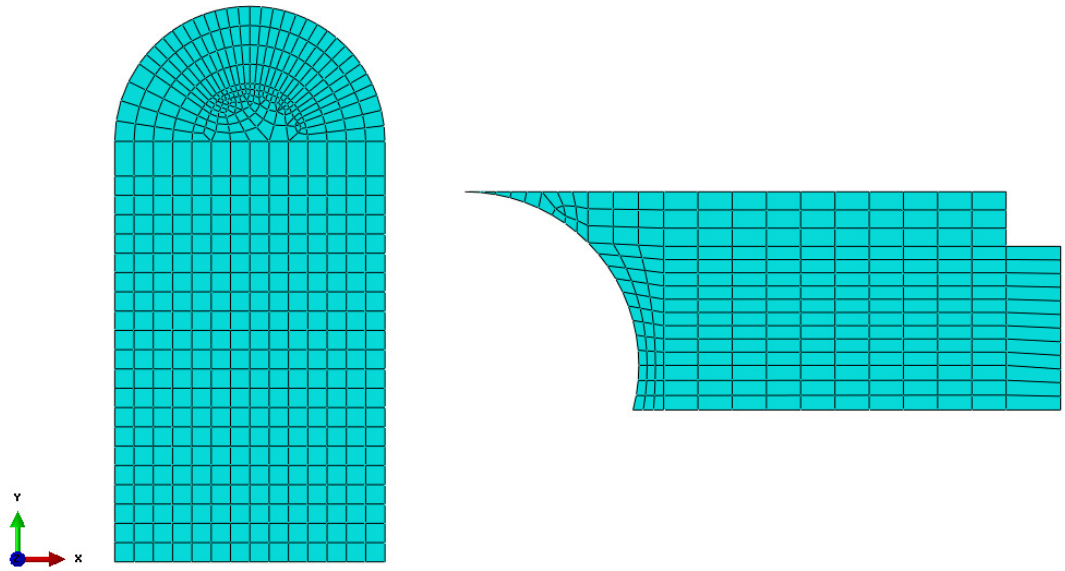

Figure 5.2f; *Mesh distribution of the wall plate (left) and the supporting batten (right)*

The type of element that is selected for the model is the CPS4R element. This element is a 4-node bilinear plane stress quadrilateral which is more than sufficient for solid elements. It also includes reduced integration, which reduces computational time at the cost of a slight degrade of results, and hourglass control, which disables the model to deform improperly. Although an 8-node quadratic element would possibly give a more accurate solution to the model, it is incompatible with the free mesh used in the middle of the wall plate **[10].**

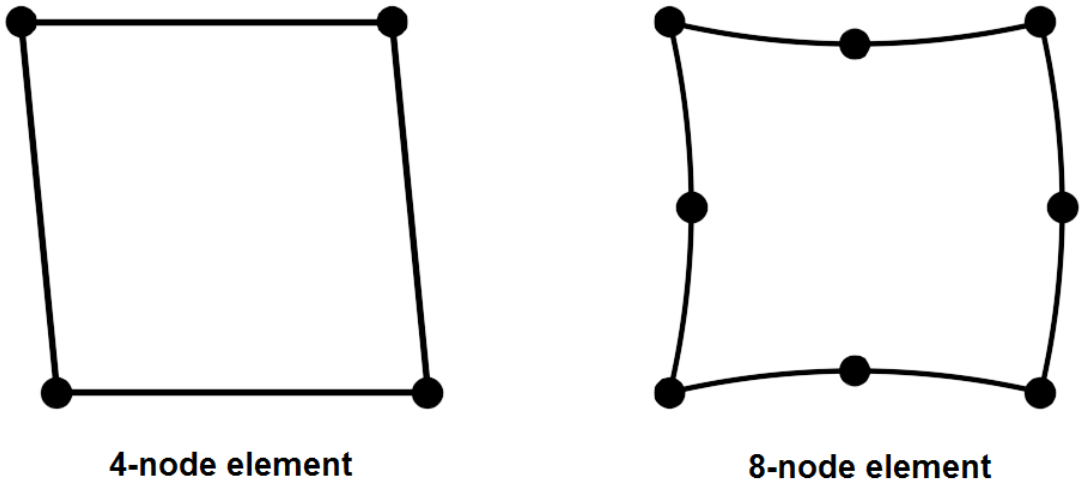

Figure 5.2g; *Difference between a 4-node and an 8-node element. The 4-node element behaves linear and therefore stiffer compared to the quadratic 8-node element, resulting in an improved representation of the stresses and strains for the 8-node element*

- Solution method

The model is solved with a static general analysis. As the model is subjected to loading in the elastic range, the nonlinear effect is disregarded, since no large displacements should occur. Therefore, the model being a linear static problem, a direct full Newton method is used as the solution method.

5.2.4 Results

There are several ways to get an indication of the stress flow through the connection detail. In this paragraph the stresses in the supporting batten and wall plate will be discussed. The numerical results of the supporting batten will be used to reflect on the experimental results obtained in the previous chapters, whereas the numerical results of the wall plate will be used as a verification for analytical assumptions made in **chapter 3.1**.

- Stress flow in the supporting batten

A first way of interpreting the stresses is by looking at the minimal principal stresses. As mentioned in **chapter 2.1**, the stresses on an infinitesimal small squared element are visualized with forces perpendicular on the surface and parallel to the surface. The perpendicular stresses are the axial stresses and the parallel stresses are the shear stresses. At a random position inside an object, all these stresses will be present. Though, by rotating the element with a certain angle, it is possible for the shear stresses to become zero, hereby increasing the axial stresses. An example is given in figure 5.2h.

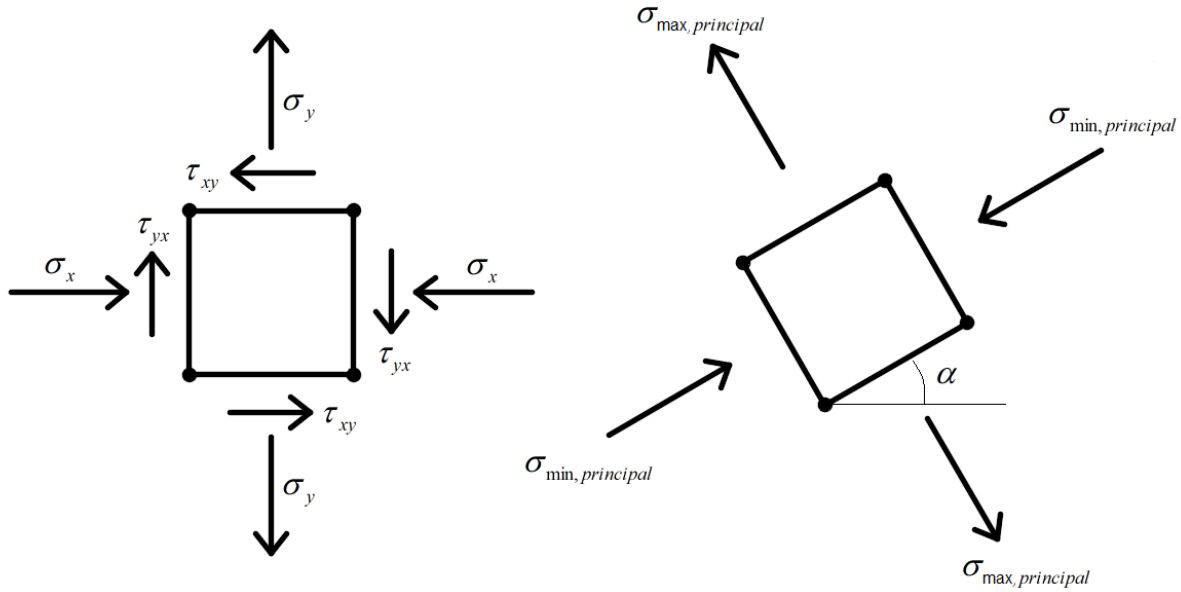

Figure 5.2h; *Left: infinitesimal small element subjected to axial stresses and shear stresses*
Right: rotated element with zero shear stresses

The formula for determining the minimal principal stress is as follows **[14]**:

$$\sigma_{\min,principal} = \frac{1}{2}\left(\sigma_x - \sigma_y\right) - \frac{1}{2}\sqrt{\left(\sigma_x - \sigma_y\right)^2 + 4\cdot\left(\tau_{xy}\right)^2} \qquad (5.1)$$

The concept of minimal principal stresses in Abaqus is based on the rotated element. The direction of the symbols is parallel to the minimal axial stresses. Minimal stresses equal compressive stresses, whereas maximal stresses equal tensile stresses. The bigger the symbol, the higher the magnitude of the compressive stress. **Figure 5.2i** shows the flow of stresses through the supporting batten for the model with a roof inclination of 45 degrees.

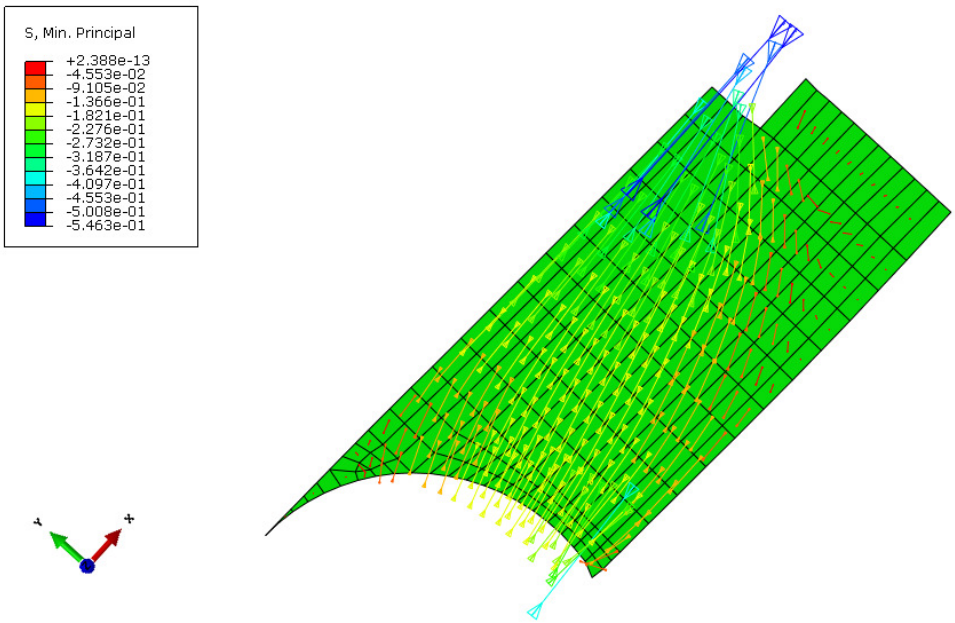

Figure 5.2i; *Minimal principal stresses in the supporting batten, 45 degrees roof inclination*

Another way of interpreting the results is by looking at either the stresses in a specified direction (for example the x, y or z direction of a coordinate system), or by checking all directions at once using the von Mises stresses criterium. The von Mises stresses are determined with the following formula **[3]**:

$$\sigma_{Mises} = \sqrt{\frac{\left(\sigma_x - \sigma_y\right)^2 + \left(\sigma_y - \sigma_z\right)^2 + \left(\sigma_z - \sigma_x\right)^2 + 6 \cdot \left(\tau_{xy}^2 + \tau_{yz}^2 + \tau_{zx}^2\right)}{2}} \tag{5.2}$$

Note that the von Mises stresses are always higher than zero. Von Mises stresses are used to determine the yield strength of a material, but in our case will give an insight in peak stresses present in the model**. Figure 5.2j** gives an overview of the von Mises stresses in the supporting batten and the stresses in the rotated X direction.

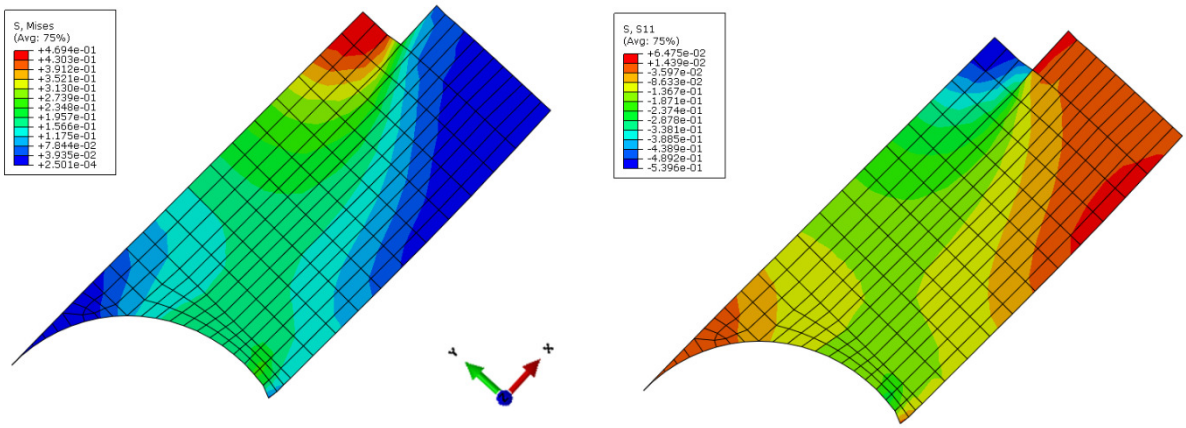

Figure 5.2j; *Left: von Mises stresses in the supporting batten, roof inclination 45 degrees*
Right: stresses in the rotated X-direction, roof inclination 45 degrees

An overview of all the results is added in **appendix 5.1.**

By taking a closer look at the stresses in the X-direction, it is possible to make cuts at the cross section to get an overview of the stress distribution over the depth of the batten. This is illustrated in **figure 5.2k.** In this case, two different cuts are made, to be able to compare these results.

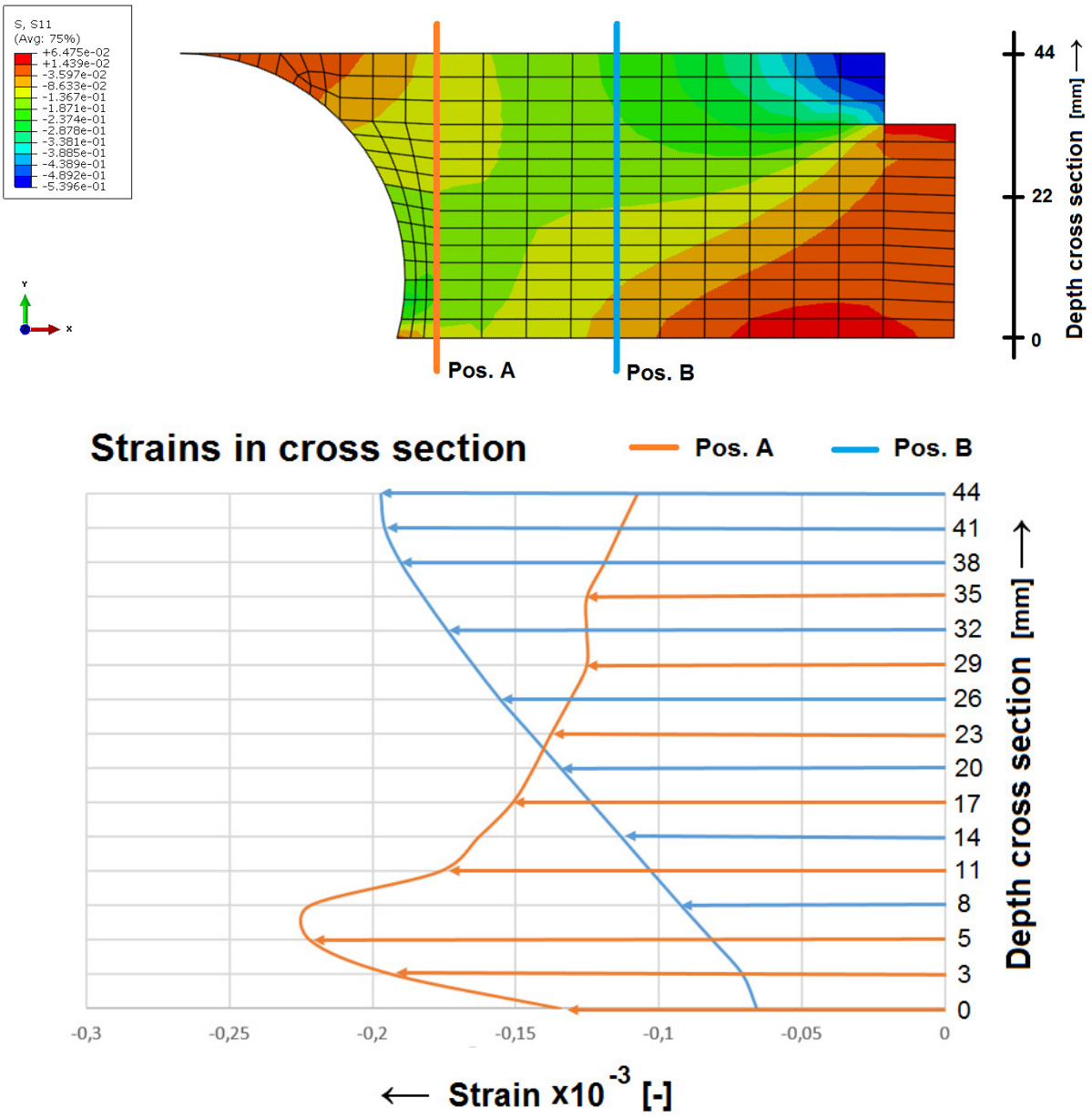

Figure 5.2k; *Stresses in X-direction at specified cuts through the cross section. Position A is located near the connection with the wall plate, whereas position B is located at the middle of the batten*

It is obvious that the stresses start in the upper right corner, where the supporting panel introduces the forces into the supporting batten. Over the width of the supporting batten the stresses start to spread across the depth of the batten, but the peak stresses remain in the upper side of the batten (blue stress distribution). Though, once the stresses reach the wall plate, the stresses transfer to the lower side of the batten, hereby causing an internal moment (red stress distribution).

It should be mentioned that the stresses in the pointed end of the batten are negligible. Therefore, the pointed end has been omitted from the three dimensional model.

- Stress flow in the wall plate

The same strategy is applied for the wall plate. **Figure 5.2L** shows the stresses in X and Y direction for the wall plate only subjected by axial loading through the supporting batten.

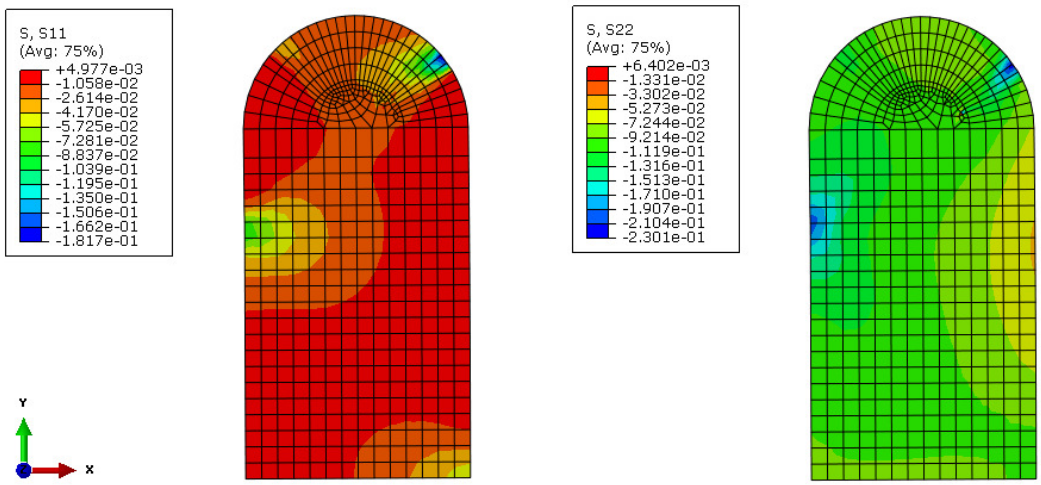

Figure 5.2L; *Stresses in X (left) and Y (right) direction at the wall plate, roof inclination 45 degrees*

The stresses in the X-direction show peak stresses at the location where the supporting batten introduces the load (N) and the reaction forces from the bracket (R1 and R2) (**figure 5.2M**). The stresses in the Y-direction show the identical location for the peak stresses regarding the introduction load. These stresses spread out toward the bottom of the wall plate.

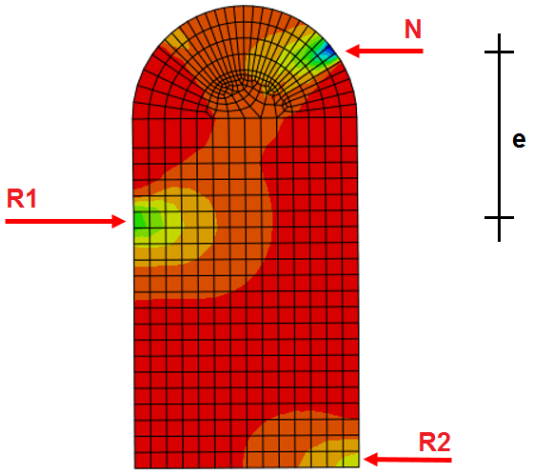

Figure 5.2M; *Stresses in X direction for the wall plate, illustrating the introduction force and the reaction forces. Roof inclination 45 degrees. e is the eccentricity for the internal bending moment*

Table 5.2f gives an overview of the magnitude of the eccentricity for the internal bending moment, illustrated in **figure 5.2M**.

Roof inclination	eccentricity (mm)
35 degrees	55,07
45 degrees	57,23
55 degrees	61,74

Table 5.2f; *eccentricity regarding the internal bending moment of the wall plate for various roof inclinations*

5.3 Three dimensional model

This paragraph discusses the three dimensional numerical model created in Abaqus. It is an expansion to the two dimensional model from the previous paragraph.

5.3.1 Geometrics and material properties

The cross section of the model equals the geometry of the model created in the previous paragraph. Though, a small addition is made for the introduction of the forces by implementing a substitution for the supporting panel, this will be discussed later in this paragraph. The length of the model however is dependent on the determined center-to-center distance of the F-bracket. In the previous chapter three center-to-center distances have been discussed, namely 600, 900 and 1200mm. To limit the size of the model, only half of the center-to-center distance is used as the length of the model due to symmetry, whenever this is possible (see **figure 5.3a**). For the CTC-distances of 600mm and 1200mm this is no problem. However, for the 900mm specification symmetry is hard to find. This is illustrated in **figure 5.3b**. An overview of the created models is given in **table 5.3a**:

Name of the model	Roof Angle (degrees)	Center-to-center distance (mm)	Adding (mm)	Coach screw
35/600/L	35	600	10	no
35/1200/L	35	1200	10	no
45/600/L	45	600	10	no
45/1200/L	45	1200	10	no
55/600/L	55	600	10	no
55/1200/L	55	1200	10	no

***Table 5.3a**; Overview of all performed tests*

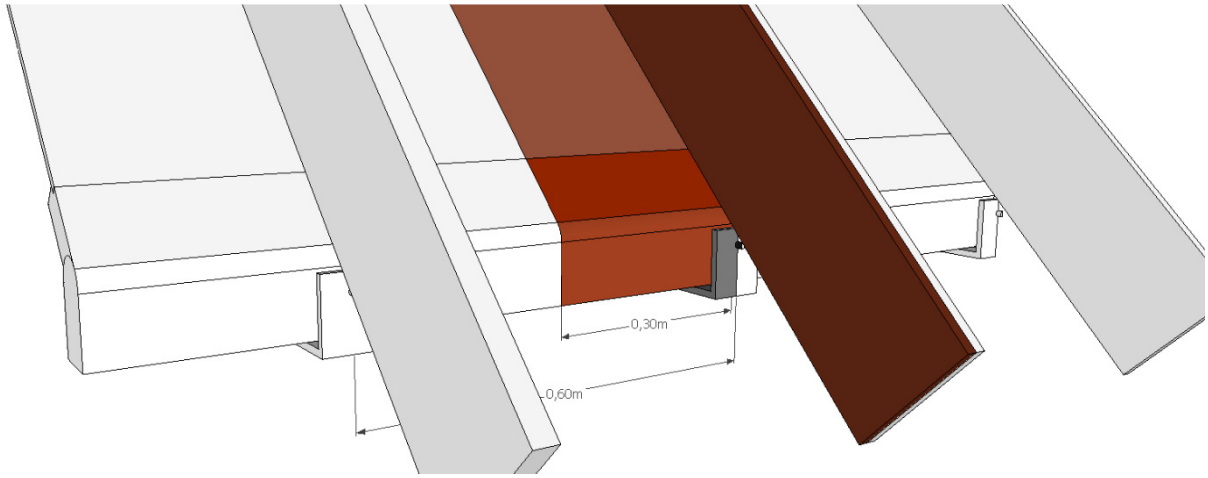

***Figure 5.3a**; Due to symmetry, only half of the center-to-center distance is modeled. In this case a CTC-distance of 600mm is schematized, with the colored part to be modeled*

The reduction of the model due to symmetry needs to be replaced by corresponding boundary conditions, which will be mentioned in the next paragraph.

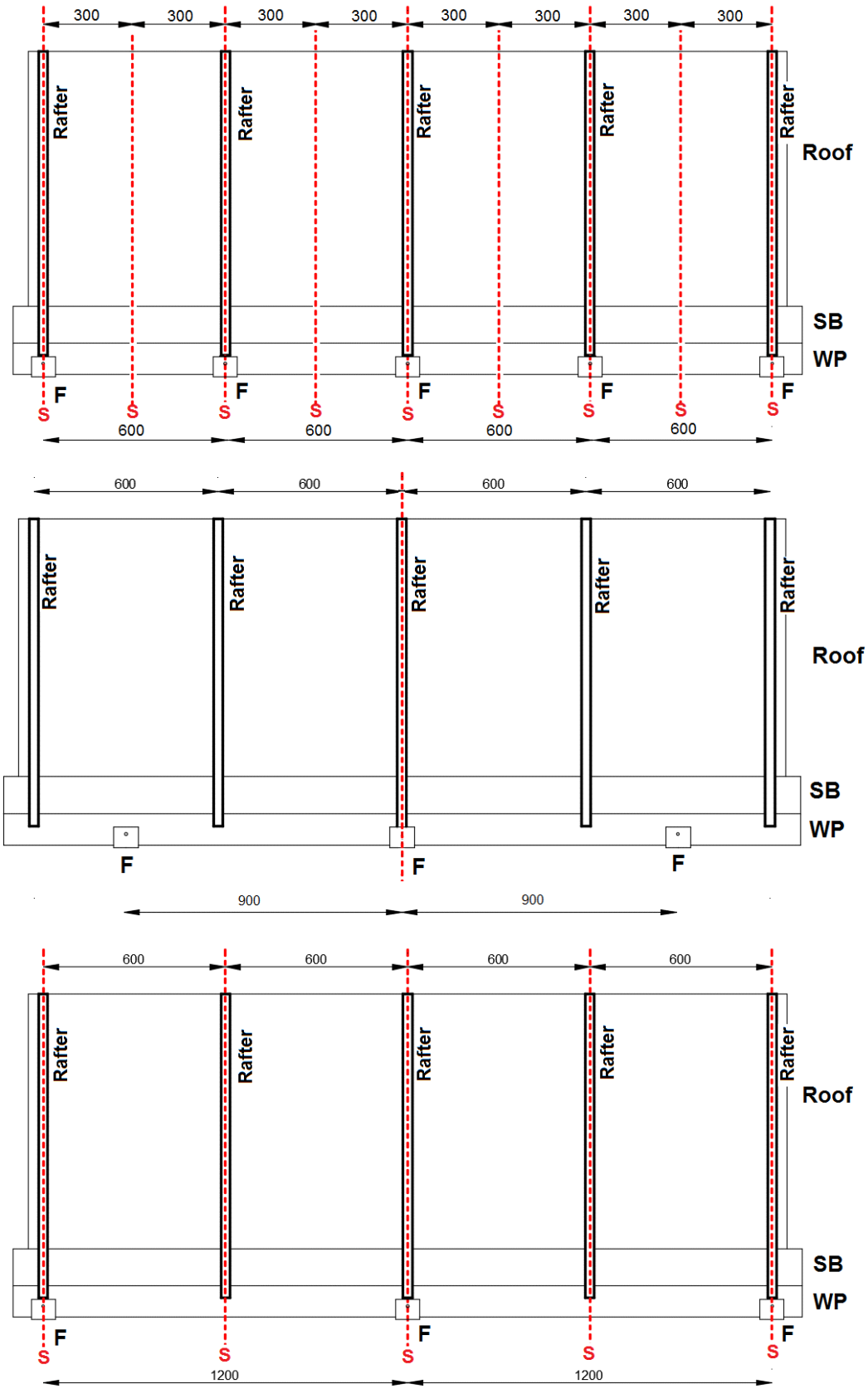

***Figure 5.3b**; Top view of the roof connection for CTC 600mm, 900mm and 1200mm. The dashed red line shows the present symmetry lines in the model. The 900mm CTC has only one symmetry line, resulting in an oversized numerical model*

The length of the supporting panel is almost as long as the length of the entire roof element. Therefore, the length is reduced. To equal the material properties for the normal and substituting panel, substituting material properties are implemented. The following formula applies:

$$(E \cdot I)_{original} = (E \cdot I)_{substitute} \tag{5.3}$$

With:

$E_{original} = 3.150 N / mm^2$ (particle board)

$$I_{original} = \frac{1}{12} \cdot b \cdot h^3 = \frac{1}{12} \cdot (11mm) \cdot (4000mm)^3 = 5,866 \cdot 10^{10} mm^4$$

And the length of the substitute supporting batten is set at 200mm, it results in the following values:

$$I_{substitude} = \frac{1}{12} \cdot b \cdot h_{sub}{}^3 = \frac{1}{12} \cdot (11mm) \cdot (200mm)^3 = 7,333 \cdot 10^6 mm^4$$

$$E_{substitude} = \frac{3.150 N / mm^2 \cdot 5,866 \cdot 10^{10} mm^4}{7,333 \cdot 10^6 mm^4} = 25.200.000 N / mm^2$$

An overview of all parts of the model is illustrated in **figure 5.3c**.

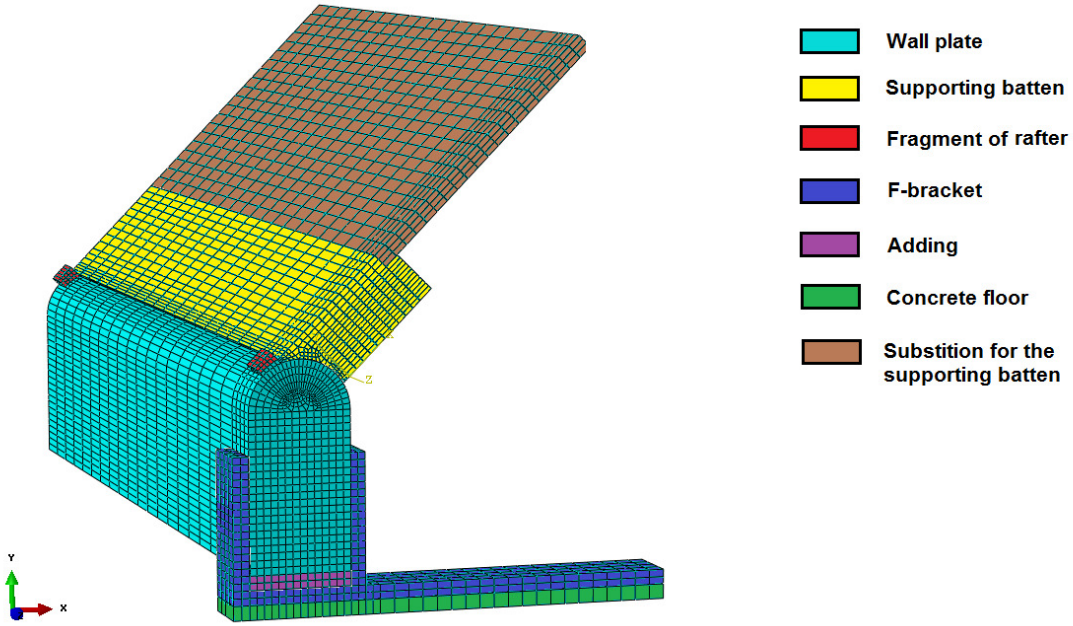

***Figure 5.3c**; All parts of the three dimensional model. Roof inclination 45 degrees, CTC 1200mm*

The parts are divided in four material property groups, listed in table **5.2a**:

Material property group	Part
Timber C24	Wall plate, supporting batten, adding
Concrete	Floor
Steel	F-bracket
Substitude particle board	Substitute for the supporting batten

Table 5.3b *Grouping of the parts by material property*

The material properties of the groups are as follows:

- Timber C24

Wood is an orthotropic material, with the material properties described by **formula 2.3**. Abaqus uses the same principal for input to the model. The following variables are required:

$$
\begin{aligned}
D1111 &= E_1 \cdot (1 - \nu_{23} \cdot \nu_{32}) \cdot \Upsilon \\
D2222 &= E_2 \cdot (1 - \nu_{13} \cdot \nu_{31}) \cdot \Upsilon \\
D3333 &= E_3 \cdot (1 - \nu_{12} \cdot \nu_{21}) \cdot \Upsilon \\
D1122 &= E_1 \cdot (\nu_{21} + \nu_{31} \cdot \nu_{23}) \cdot \Upsilon \\
D1133 &= E_1 \cdot (\nu_{31} + \nu_{21} \cdot \nu_{32}) \cdot \Upsilon \\
D2233 &= E_2 \cdot (\nu_{32} + \nu_{12} \cdot \nu_{31}) \cdot \Upsilon \\
D1212 &= G_{12} \\
D1313 &= G_{13} \\
D2323 &= G_{23} \\
\Upsilon &= \frac{1}{1 - \nu_{12} \cdot \nu_{21} - \nu_{23} \cdot \nu_{32} - \nu_{31} \cdot \nu_{13} - 2 \cdot \nu_{21} \cdot \nu_{32} \nu_{13}}
\end{aligned}
\qquad (5.4)
$$

With:

$E_1 = E_R = 710N/mm^2$	$\nu_{13} = \nu_{RL} = 0{,}03$	$\nu_{31} = \nu_{LR} = 0{,}38$	$G_{12} = G_{RT} = 23N/mm^2$
$E_2 = E_T = 430N/mm^2$	$\nu_{23} = \nu_{TL} = 0{,}03$	$\nu_{32} = \nu_{LT} = 0{,}51$	$G_{13} = G_{RL} = 500N/mm^2$
$E_3 = E_L = 10.700N/mm^2$	$\nu_{12} = \nu_{RT} = 0{,}51$	$\nu_{21} = \nu_{TR} = 0{,}31$	$G_{23} = G_{TL} = 620N/mm^2$

Table 5.3c *Material properties of Spruce wood* ***[6]***

The longitudinal direction is in the Z-direction, whereas the radial and tangential direction are respectively in the local X- and Y-direction.

- Steel

Elastic isotropic material properties with:

$$E = 210.000 N / mm^2$$
$$\nu = 0{,}3$$

- Concrete

Elastic isotropic material properties with:

$$E = 30.000 N / mm^2$$

$\nu = 0,15$

- Substitute particle board

Elastic isotropic material properties with:

$E_{substitute} = 25.20.000 N / mm^2$
$\nu = 0,3$

5.3.2 Boundary conditions

Again the following boundary conditions are distinguished:

1) Contact boundary conditions

The contact properties are assigned to the elements to simulate the proper behavior of the model. These surface-to-surface contacts are given a specific interaction property.

Interaction Property	**Tangential behavior**	**Normal behavior**
Timber - Timber	Penalty, Friction coefficiënt: 0,5	Hard contact, Allow separation after contact
Steel - Timber	Penalty, Friction coefficiënt: 0,6	Hard contact, Allow separation after contact
Steel - Concrete	Penalty, Friction coefficiënt: 0,5	Hard contact, Allow separation after contact
Frictionless	Frictionless	Hard contact, Allow separation after contact

Table 5.3d; *Interaction properties of the surface-to-surface contacts between parts of the model. The friction coefficient are based on values posted at the Engineering Toolbox* ***[23].***

These surface-to-surface contacts are designated to the following combinations of parts:

Interactions	**Combination of parts**	**Interaction property**
Surface-to-surface	Wall plate - Supporting batten	Timber - Timber
Surface-to-surface	Wall plate - F-bracket	Steel - Timber
Surface-to-surface	Adding - F-bracket	Steel - Timber
Surface-to-surface	Adding - Wall plate	Frictionless
Surface-to-surface	Shear force - Wall plate	Timber - Timber
Surface-to-surface	F-bracket - Floor	Steel - Concrete
Surface-to-surface	Sup. panel substitute - Sup. batten	Frictionless

Table 5.3e; *Corresponding interaction properties for the combination of parts*

2) Displacement ,rotational boundary conditions and symmetry

The same displacement and rotational boundary conditions apply to the three dimensional model as these were applied to the two dimensional model. However, in the three dimensional model the boundary conditions apply for the entire surface of the model. Also an additional boundary condition is created for the substitute supporting panel.

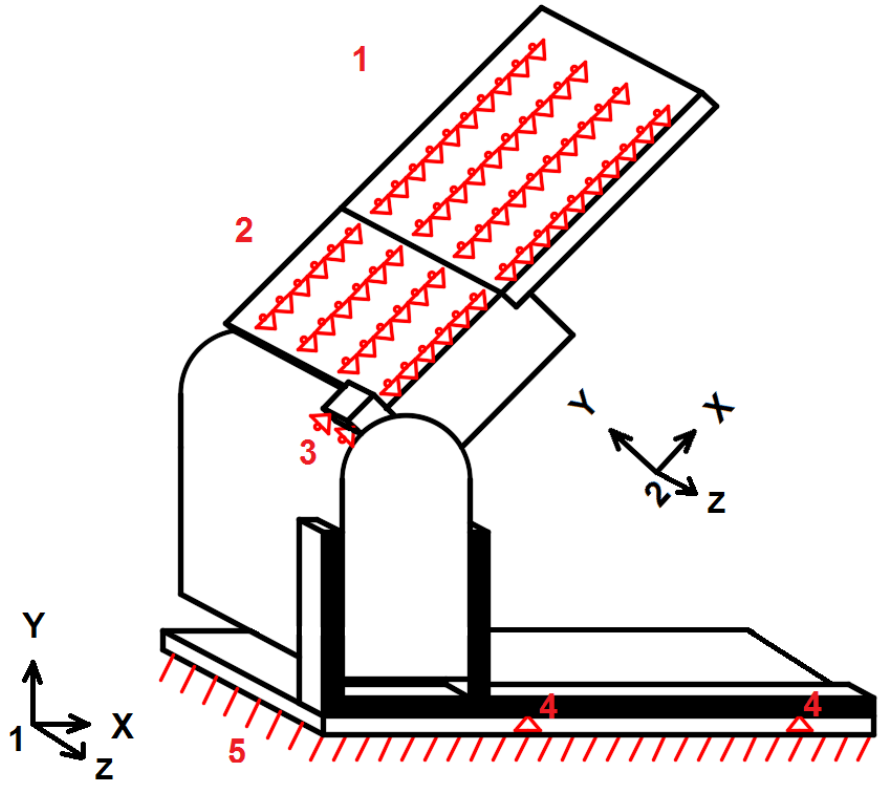

Figure 5.3d; *Applied boundary conditions. Note the dual coordinate system. The first coordinate system applies to the floor, F-bracket, adding and wall plate, whereas the second coordinate system applies to the rafter and supporting batten. Roof inclination 45 degrees, CTC 600mm*

The applied boundary conditions are described in **table 5.3f**.

#	Location	Boundary condition
1	Roller support over a surface, the upper side of the substitute supporting panel	Prohibited to move in the Y2-direction
2	Roller support over a surface, the upper side of the supporting batten	Prohibited to move in the Y2-direction
3	Roller support over a surface, the lower side of the rafter	Prohibited to move in the X2-direction
4	Hinge supports for the F-bracket to floor connection	Prohibited to move in X1 and Y1-direction
5	Fixed support for the concrete floor	Prohibited to move in X1 and Y1-direction, also prohibited to rotate around the Z1-axis

Table 5.3f; *Description of the applied boundary conditions in* ***figure 5.3d***

The symmetry boundary conditions apply for all surface of elements created by the cut of the symmetry line. The conditions dictate that:

- The surface is prohibited to displace in the Z-direction
- The surface is prohibited to rotate around their respective X-axis
- The surface is prohibited to rotate around their respective Y-axis

3) Constraints

To imitate the bolted connection of the F-bracket and the wall plate, a series of constraint boundary conditions are applied to the bracket. The constraint dictates two assigned nodes to copy their movements in the X1 and Y1-direction. This is illustrated in **figure 5.3e**.

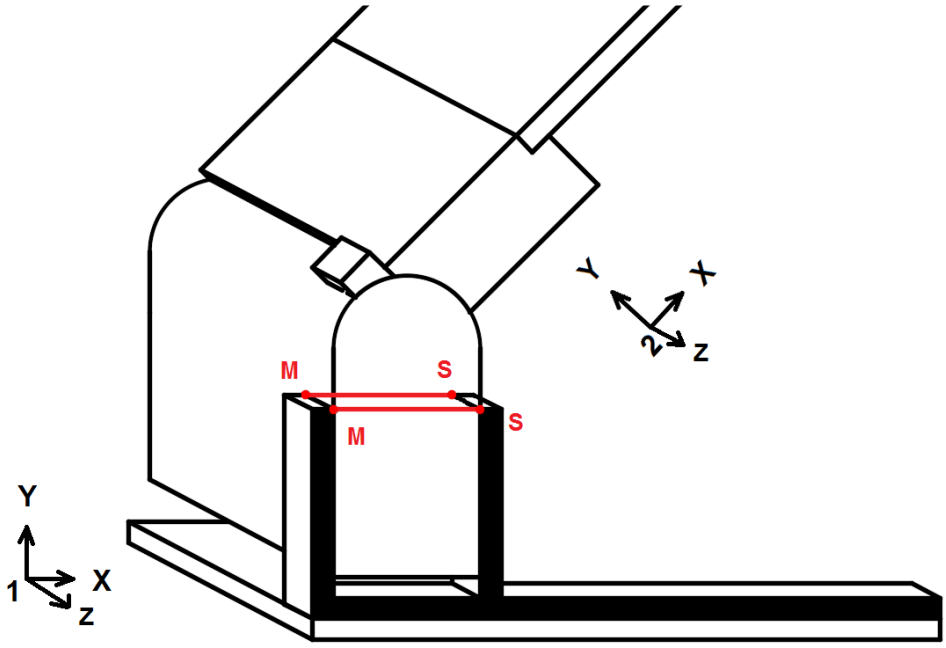

Figure 5.3e; *Constraint relation between two nodes. M is the master node and S is the slave node. Roof inclination 45 degrees, CTC 600mm*

4) Loading

The axial and shear forces from the real time structure are modeled by either two or three pressure loads (depending on the CTC distance, 600mm = two, 1200mm = three). The axial load is applied to the top surface of the substitute supporting batten. The shear load is applied to the top surface of the fragmented rafter. This is shown in **figure 5.3f**. The magnitude of the loads correspond to the loads determined in **chapter 3, table 3.3b**:

Roof inclination	(Axial load) **Corresponding pressure load**	(Shear load) **Corresponding pressure load**
35 degrees	(5,323 kN) **0,484 N/mm²**	(1,683 kN) **2,805 N/mm²**
45 degrees	(3,872 kN) **0,352 N/mm²**	(1,252 kN) **2,087 N/mm²**
55 degrees	(2,983 kN) **0,271 N/mm²**	(0,852 kN) **1,420 N/mm²**

Table 5.3g; *Overview of axial and shear load, belonging to the assigned roof inclination*

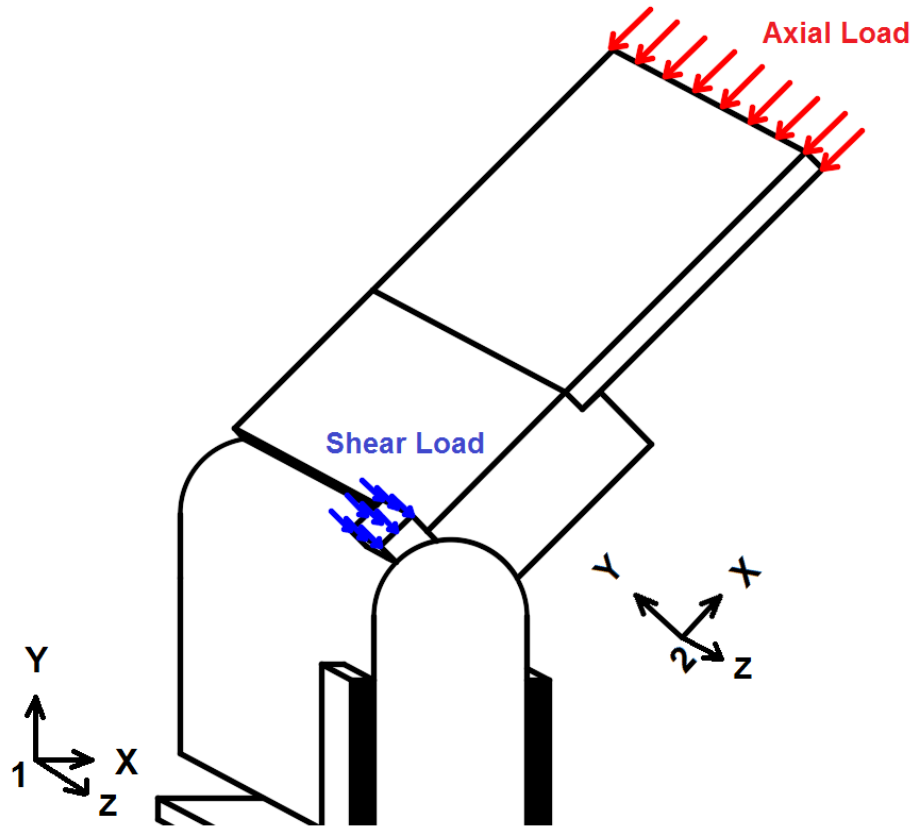

Figure 5.3f; *Applied pressure forces in the model. Roof inclination 45 degrees, CTC 600mm*

5.3.3 Fem modelling

In this paragraph the mashing and the solution method is discussed.

- Meshing of the model

The goals for the three dimensional numerical model consists of:

1) Getting an overview of the spread of the stresses in the wall plate

2) Measure the strains in the supporting batten for comparison

An evenly mashed model will satisfy these goals, with a higher concentration of elements near the brackets to avoid discreet element mashing. The mashing near the connection of the wall plate and the supporting batten is a copy of the mashing applied in the two dimensional model. This is illustrated in **figure 5.3c**.

The C3D8R element is the selected element for this model. The element is an 8-node linear brick which is applicable for solid three dimensional elements. It also includes reduced integration and hourglass control. The 8-node quadratic element is incompatible with the free mesh used in the middle of the wall plate **[10].**

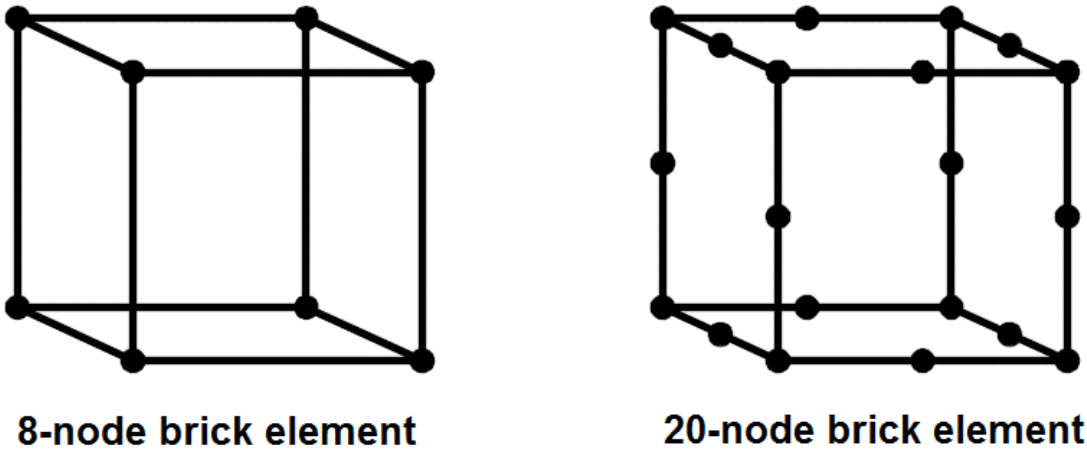

Figure 5.3g; *Difference between an 8-node and a 20-node element. The 8-node element behaves linear and therefore stiffer compared to the quadratic 20-node element, resulting in an improved representation of the stresses and strains for the 20-node element*

- Solution method

The model is solved with a static general analysis. As the model is subjected to loading in the elastic range, the nonlinear effect is disregarded, since no large displacements should occur. Therefore, the model being a linear static problem, a direct full Newton method is used as the solution method.

5.3.4 Results

The results of the three dimensional model are analyzed for stress and strain distribution.

- Stress analysis

By analyzing parts of the model individually, it is possible to get an understanding of the stress flow in the connection detail. First, the substitute supporting panel is considered, illustrated in **figure 5.3h**. The axial stresses (x-direction) indicate an evenly distributed stress on the top side of the element, which redistributes towards the connection with the supporting batten at the bottom. Although a small stress remains on the entire length of the element, the increase in stress might give an indication for the effective width in the wall plate.

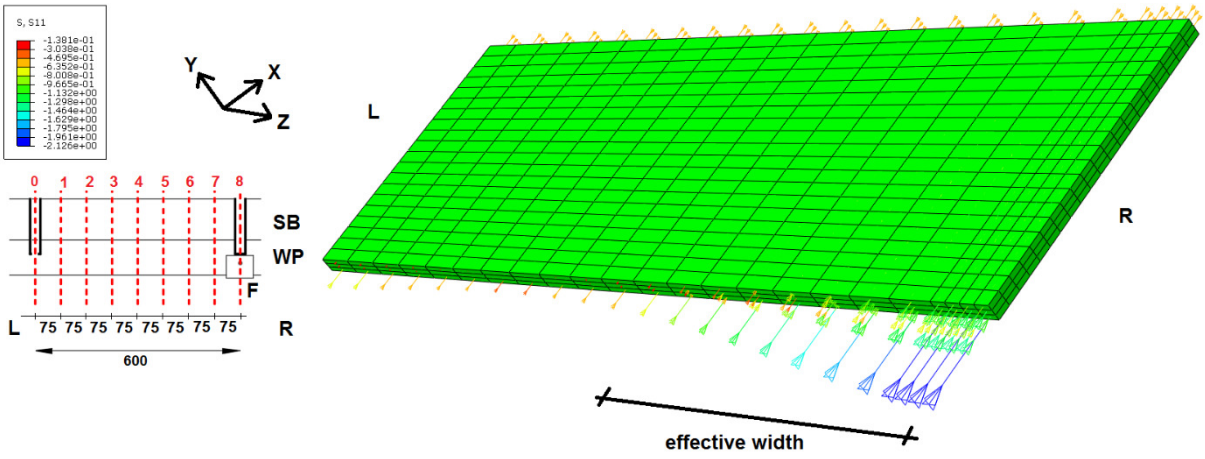

Figure 5.3h; *Three dimensional view of the sub. supporting panel. The arrows indicate the axial stresses (in X-direction). R represents the right side of the model (side of the bracket) and L represents the left side of the model (halfway the CTC distance of the brackets). Roof inclination 45 degrees, CTC 1200mm*

Secondly, the supporting batten is considered. The minimal principal stresses for this part are shown in **figure 5.3i**. Four areas of concentrated stresses are distinguished:

1) The introduction of stresses transferred by the supporting panel, corresponding with the effective width illustrated in **figure 5.3h**.
2) The cluster of stresses transferring towards the wall plate
3) Stresses remain the entire length of the model
4) Stresses resulting from the rafter halfway the center to center distance of the bracket

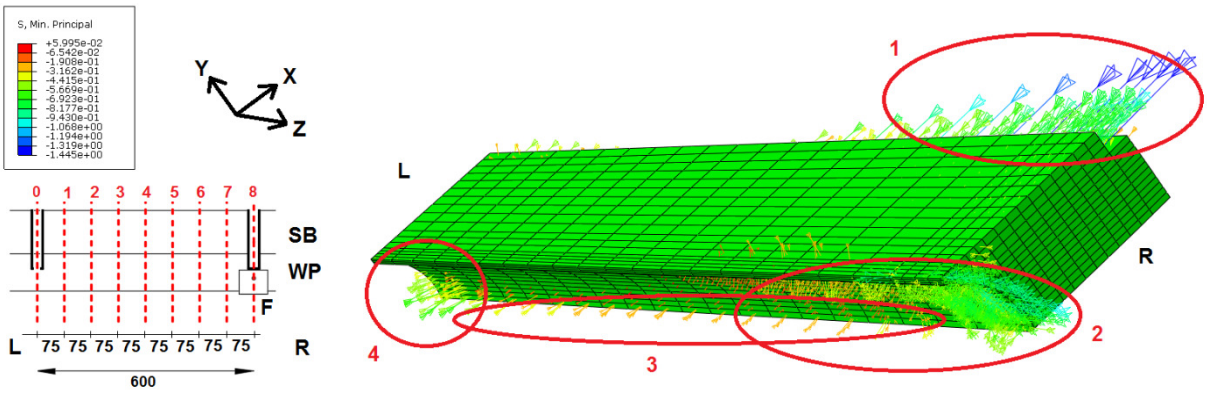

Figure 5.3i; *Three dimensional view of the supporting batten. The arrows represent the minimal principal stresses. R represents the right side of the model (side of the bracket) and L represents the left side of the model (halfway the CTC distance of the brackets). Roof inclination 45 degrees, CTC 1200mm*

Thirdly, the wall plate is considered. **Figure 5.3j** shows the present von Mises stresses. Three areas are distinguished:

1) Stress concentration caused by the rafter located above the bracket and the concentration of axial forces introduced by the supporting batten
2) Stress concentration caused by the rafter located halfway the center to center distance of the brackets.
3) Stress concentration for transferring the stresses towards the brackets.

The stress concentration of the first area gives a second indication for the effective width in the wall plate. The indication for the effective width derived from the wall plate, as well as the supporting panel, are given in **table 5.3h**.

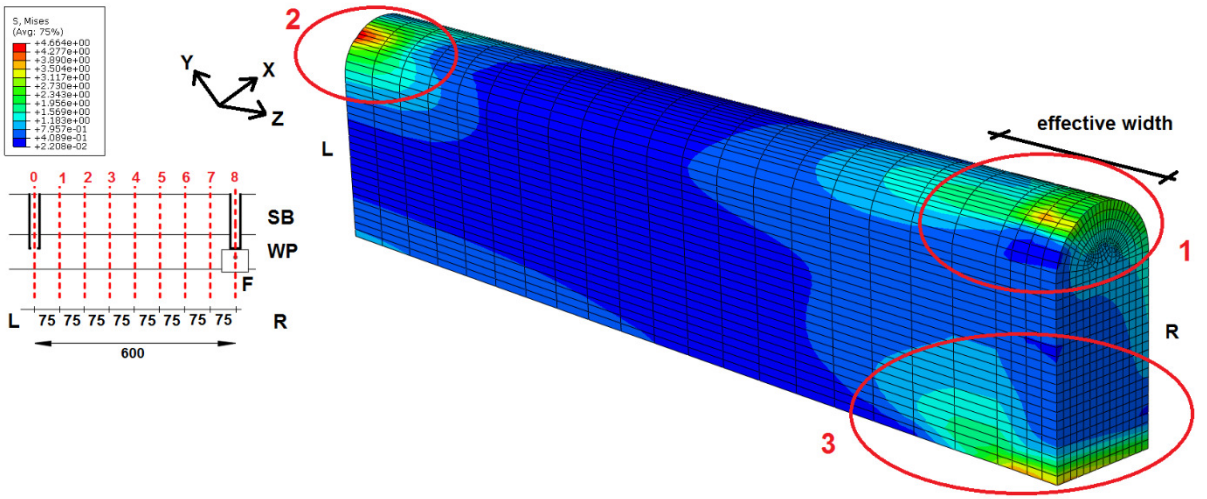

Figure 5.3j; *Three dimensional view of the Wall plate. The colors represent the von Mises stresses. R represents the right side of the model (side of the bracket) and L represents the left side of the model (halfway the CTC distance of the brackets). Roof inclination 45 degrees, CTC 1200mm*

Name of the model	Possible effective width at the supporting panel (mm)	Possible effective width at the wall plate (mm)
35/600/L	156	84 – 141
35/1200/L	229	128 – 172
45/600/L	214	84 – 141
45/1200/L	243	128 – 172
55/600/L	214	69 – 141
55/1200/L	272	128 – 185

Table 5.3h; *Approximations of measured effective width. The effective width for the supporting panel is determined by the increase of axial stresses for the panel-batten connection. The effective width for the wall plate is determined by measuring the distance from the symmetry axis located at the bracket up to the first and second lowest color category.*

- Strain analysis

Strains obtained from the model are used to compare with the experimental results. The strains are measured in the local X-direction. The position of the measurement is shown in **figure 5.3k up to 5.3m**:

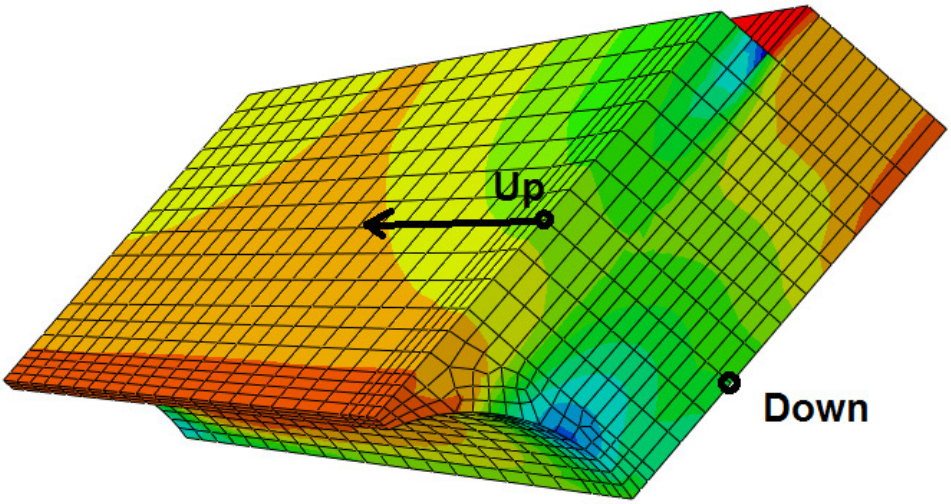

Figure 5.3k*; Location of the measurements in three dimensional perspective*

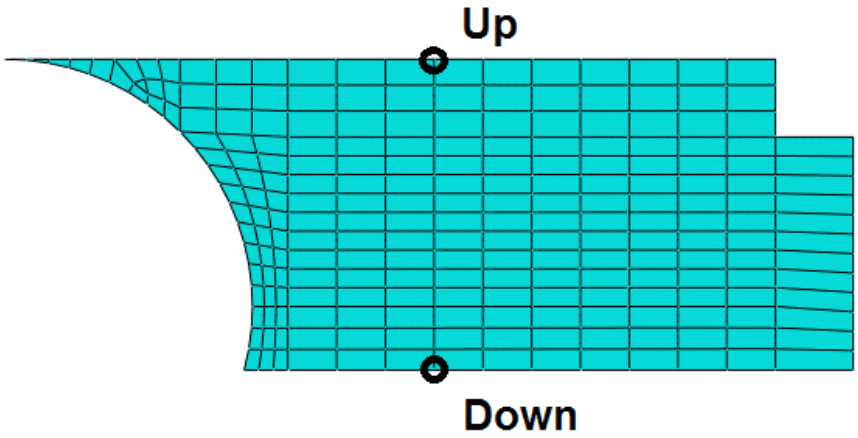

Figure 5.3L*; Location of the measurements in two dimensional perspective, viewed from the side*

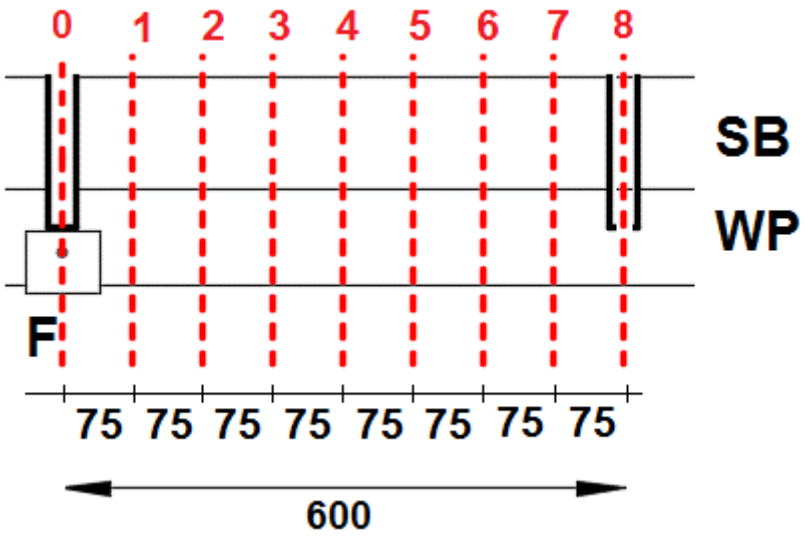

***Figure 5.3m**; Location of the measurements in two dimensional perspective, viewed from the top side. The red line shows the location of the positions*

The measurements are taken at the top and bottom side of the batten, from which the average value is established. The results are added to **appendix 5.2**. An overview of the average values is given in **figure 5.3n**.

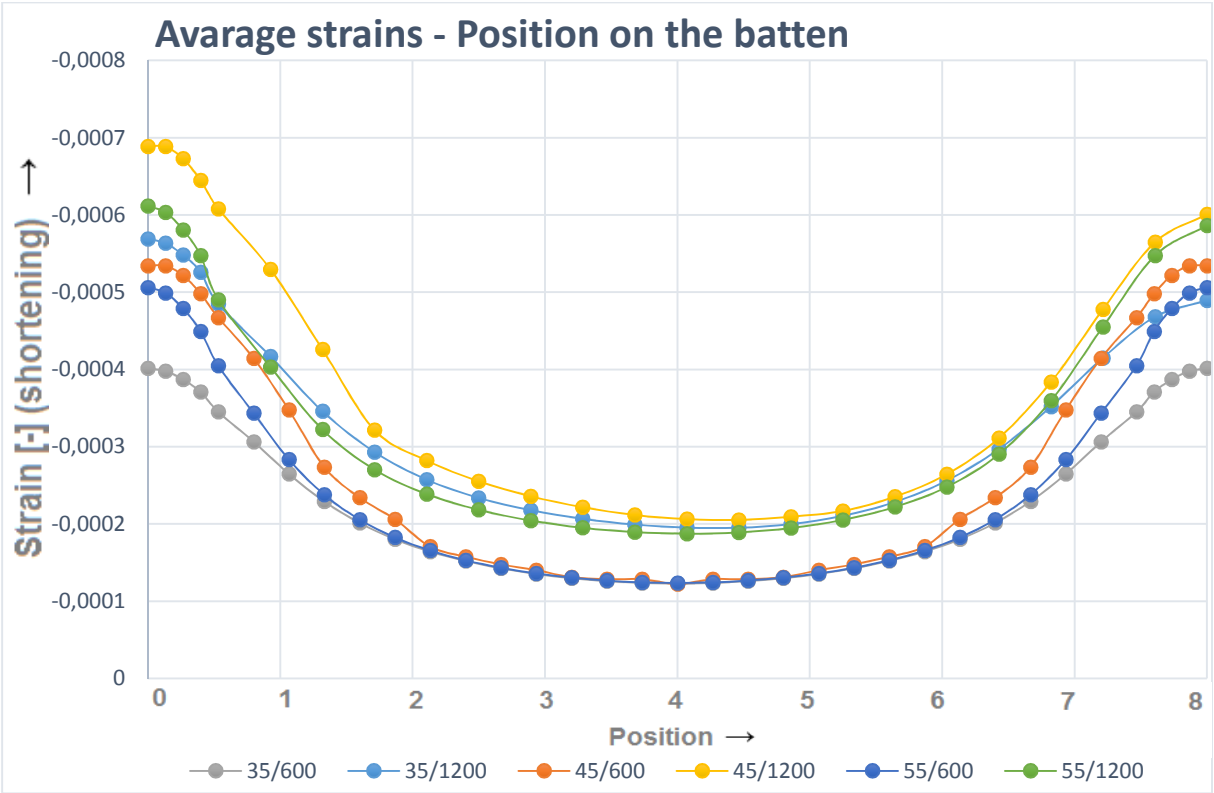

***Figure 5.3n;** An overview of the strains measured in the models. The legend indicates the roof inclination (35, 45 or 55 degrees) and the center to center distance of the brackets (600mm or 1200mm)*

The results for positions 4 to 8 regarding all the CTC-600mm-models are a symmetrical duplicate from the results obtained for position 0 to 4. The figure shows that there are maximum strains near the bracket, as well as near the positions of the rafters (for CTC 1200mm). However, the high strains near the rafters are a result of high peak strains at the bottom of the batten (see **appendix 5.2**). These strains are probably less representative compared to the

strains near the bracket. This dissimilarity is visualized with the linear and random strain progress in **figure 5.2k**.

5.4 Conclusions and recommendations

This paragraph summarizes the conclusions obtained by the results from the numerical model. It ends with recommendations for future development regarding these models.

5.4.1 Conclusion regarding the 2D model

- The two dimensional model shows a translation of stresses inside the supporting batten, resulting in an internal bending moment.
- By measuring the strains halfway the supporting batten on the top and bottom side, an accurate average value can be obtained (for most cases).
- The axial load on the wall plate results in two counter forces caused by the F-bracket. See figure 5.2M
- The stresses in the pointed end of the batten are rather small compared to stresses in other parts of the batten and therefore negligible.

5.4.2 Conclusions regarding the 3D model

- The stresses in the wall plate indicate an effective width up to 150mm for a CTC-600mm-model and up to 200mm for a CTC-1200mm-model. This is illustrated in **figure 5.4a**.

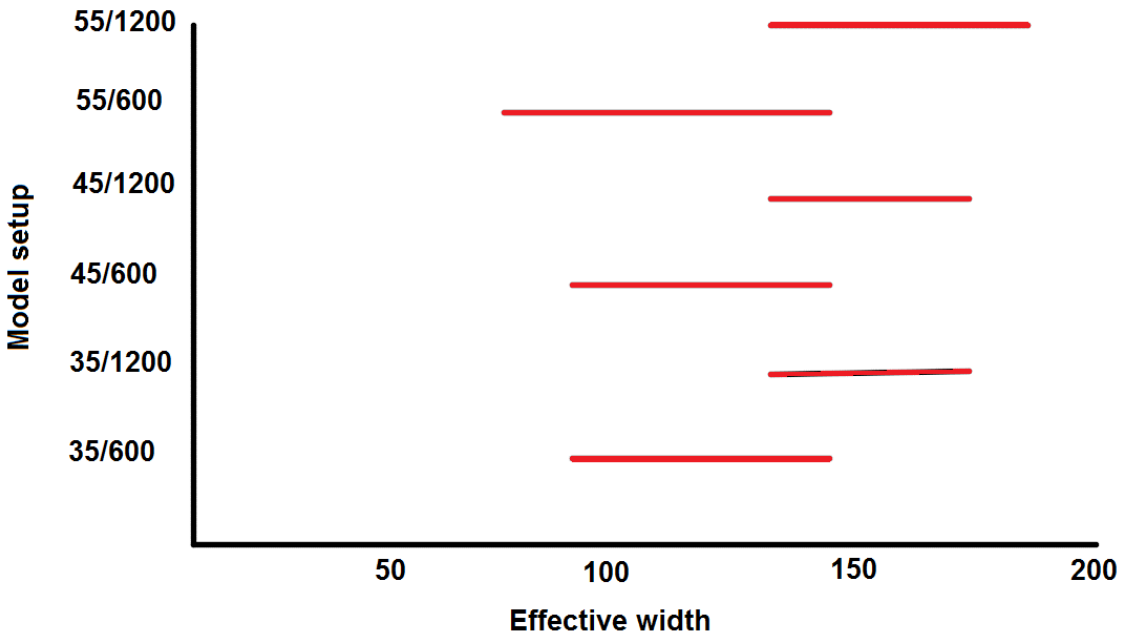

Figure 5.4a; *Approximate ranges of effective width for various test setups. Values obtained by the results given in* ***paragraph 5.3.4***

- The average strains measured in the supporting batten show a steep decrease up to position 2, whereafter the graph is smoothened until reaching either the next bracket or the rafter. The distance from position 0 to position 2 equals 150mm.

Note: the effective widths related to the numerical model are one-sided. They should be multiplied by two to become the actual effective width.

5.4.3 Recommendations for future research

- Finer mashing equal a higher accuracy of test results. However, it also increases computing time. A mash-density optimization could give improved test results, whenever the hardware is capable of computing the results.

- A different mash geometry of the wall plate could result in the capability to use the 20-node brick elements, resulting possibly in a higher accuracy of test results.

- The position of the rafters are a copy of the positions used in the experimental research. A study of random assigned positions for the rafter could result in a better understanding of the influence of the rafters on the stresses and strains in the wall plate and supporting batten.

Chapter 6 | Conclusions and recommendations

This chapter is divided in two paragraphs. The first paragraph concludes the results obtained in chapters 3 to 5. This is followed by the answering of the research question and sub questions. The second paragraph is giving recommendations for improvement regarding this research project and other future research subjects.

6.1 Conclusions

6.1.1 Determination of the eccentricity in the wall plate

The analytical results, as well as the numerical results, show the presence of two counter forces working on the wall plate.

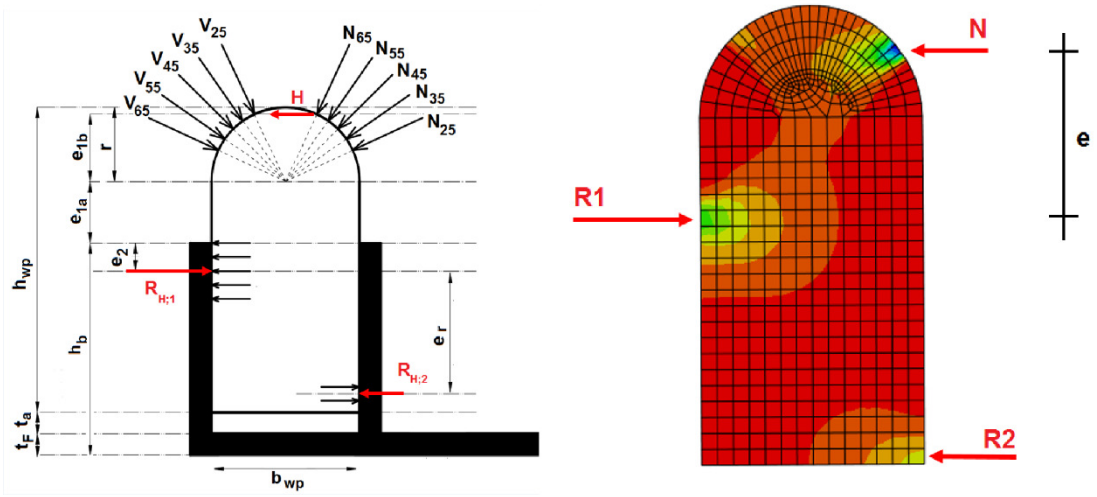

***Figure 6.1a**; Visualization of the axial load (N) and the reaction forces (Rh) on the wall plate. The left figure is the analytical model, and the right figure is the numerical model*

Values for the eccentricity '**e**' are shown in **figure 6.1b**:

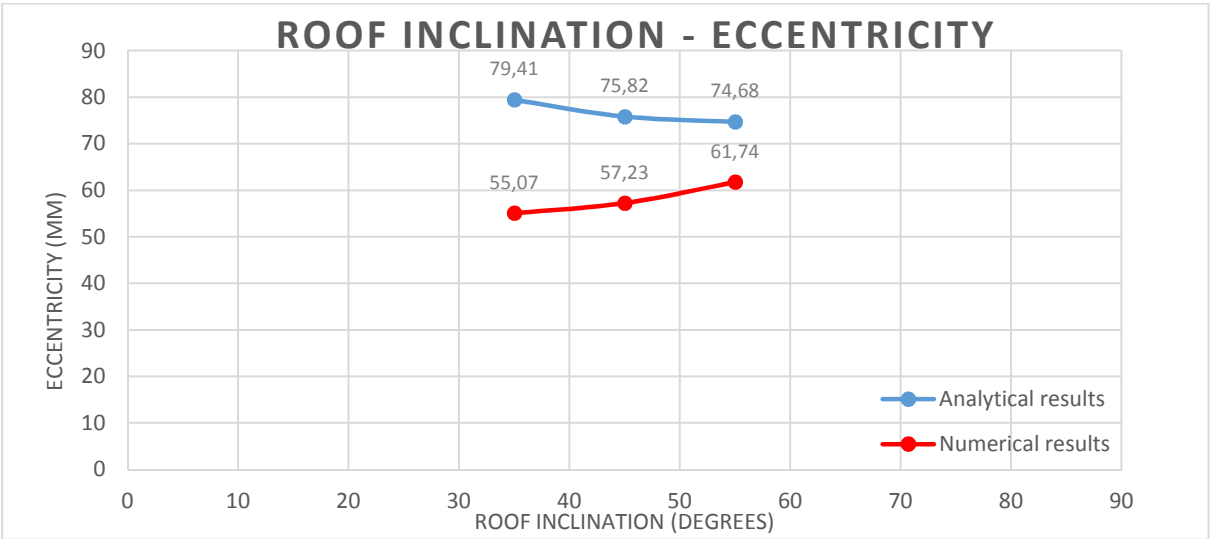

***Figure 6.1b**; Results for the eccentricity in figure 6.1a. The blue line represents the analytical results, whereas the red line represents the numerical results. Dimensions of the wall plate are: 70mm x 144mm*

The analytical results show higher values for the eccentricity, compared to the numerical results. The cause for this phenomena is due to the fact that the results obtained by the analytical model are retrieved in a conservative manner. The results obtained by the numerical model represent the actual value for the eccentricity in the wall plate, therefore should always be lower than the analytical results. As this is the case, the analytical formula is validated. For save assumptions of the eccentricity in the wall plate, the following formula can be used:

$$e = h_{wp} + t_a + t_F - \tfrac{1}{2} \cdot b_{wp} - h_b + \sin(\alpha) \cdot \tfrac{1}{2} \cdot b_{wp} + \frac{(1+\chi) \cdot H}{2 \cdot b_F \cdot f_{c,90}} \tag{6.1}$$

With the value of χ determined with **formula 6.2** and **figure 6.1c**:

$$\psi = \frac{e_{1a} + r}{h_{wp}} = \frac{h_{wp} + t_a + t_F - h_b}{h_{wp}} \tag{6.2}$$

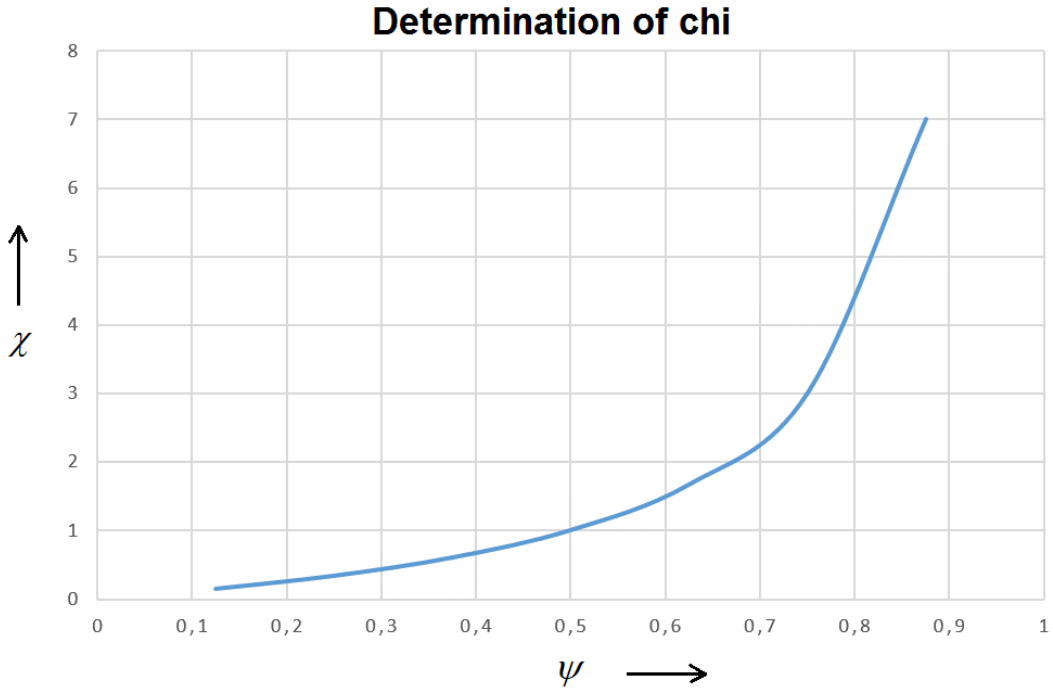

Figure 6.1c; *Determination of chi*

6.1.2 Stress flow inside the supporting batten

Figures 6.1d and 6.1e show the flow of stresses inside the supporting batten. **Figure 6.1d** represents the analytical assumption of the stress flow. The assumption visualizes a translation of the working line of the axial force (N). The translation of the axial force results in an internal bending moment. **Figure 6.1e,** retrieved by the numerical model, shows an almost identical flow of stresses.

Figures 6.1f and 6.1g illustrate the stress distribution over the depth of the supporting batten. **Figures 6.1f** is an analytical assumption based on **figure 6.1d**. The assumed total stress distribution is obtained by adding the stresses from the axial load and the internal bending moment. The results from the numerical model in **figure 6.1g** show comparable results. The total stress distribution halfway the supporting batten has a similar progress along the depth of the batten. Though, the effect of the internal bending moment is not too much of an influence to result in tensile stresses at the bottom of the batten. **Figure 6.1g** also shows different results

for the stress distribution at different positions for the section cut. Strain results from the experimental research contradict the expected stress distribution by showing shortening of the batten at the upper side instead of the bottom side. This is probably due to the orthotropic behavior of the batten used for the experimental tests. However, it is concluded that one should be extra cautious analyzing stress and strain results regarding the supporting batten.

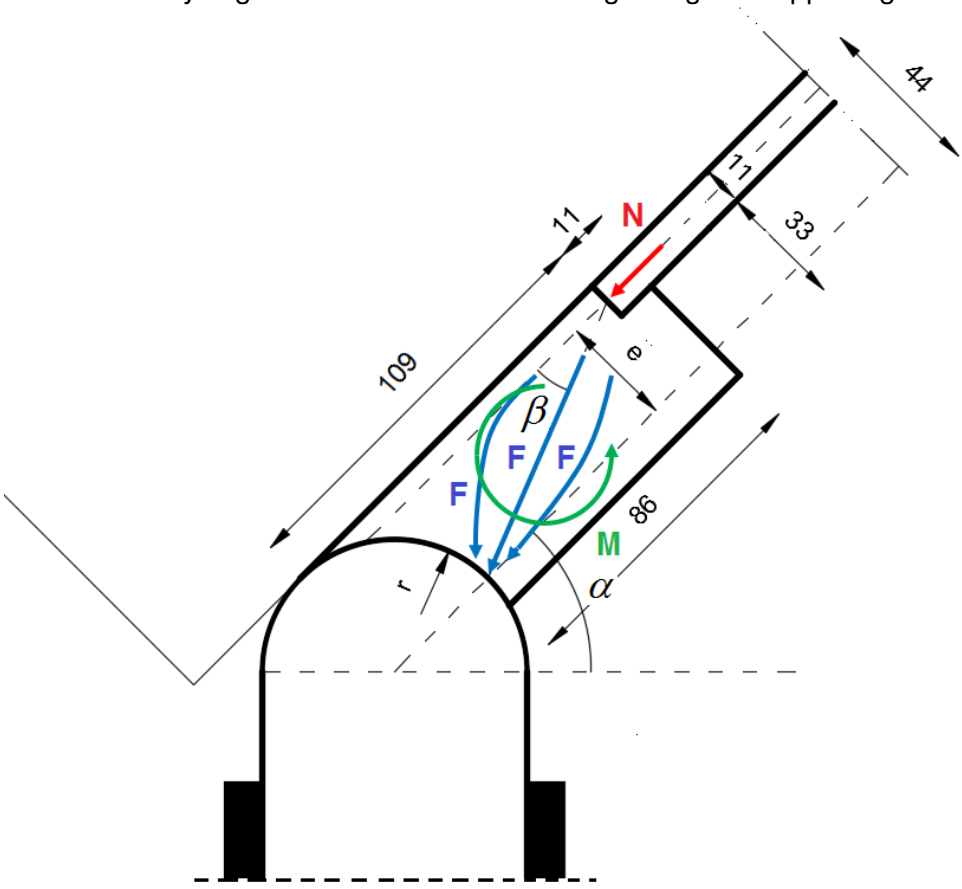

Figure 6.1d; *Analytical assumption on the stress flow in the supporting batten*

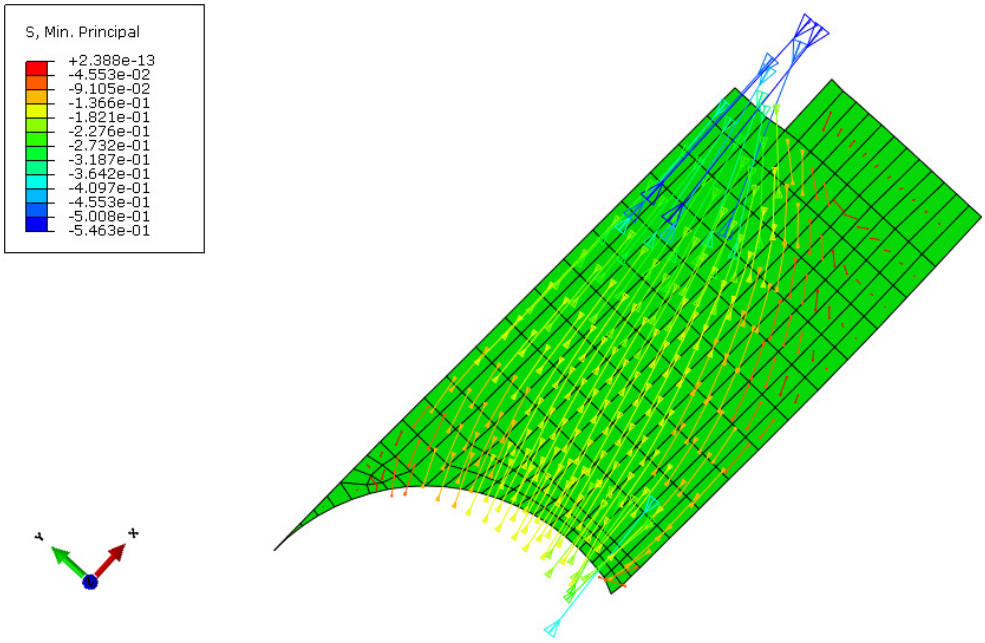

Figure 6.1e; *Flow of minimal principal stresses in the wall plate*

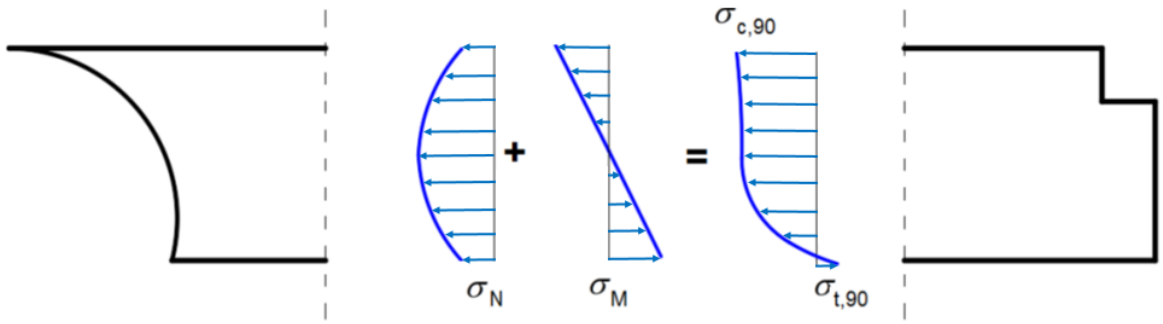

Figure 6.1f; *Stresses in X-direction at the cross section*

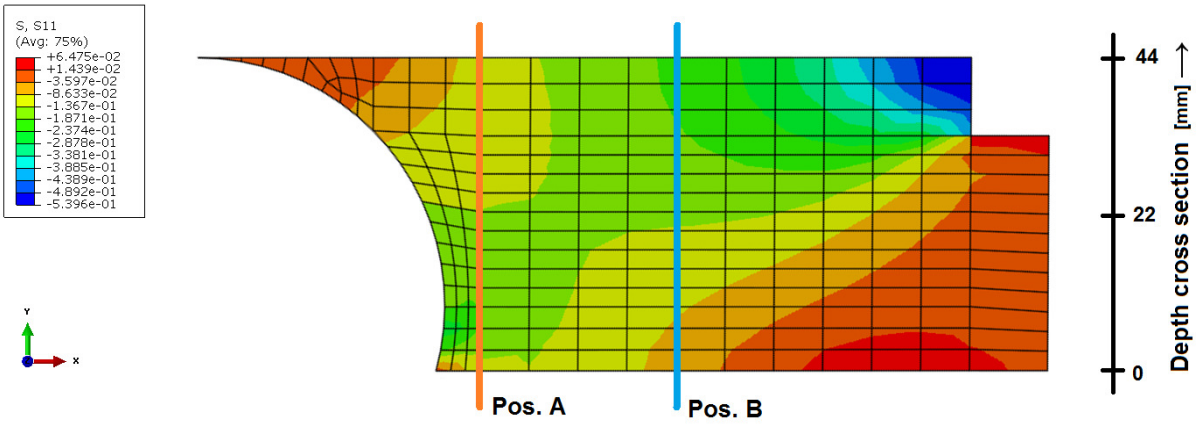

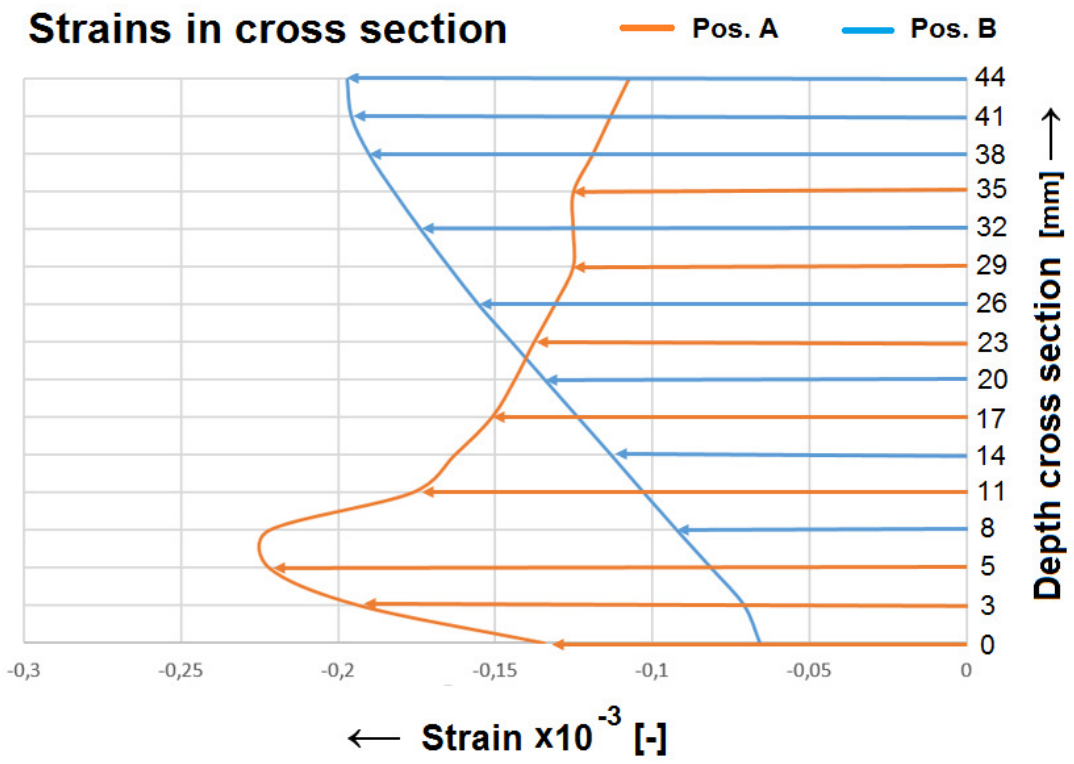

Figure 6.1g; *Stresses in X-direction at specified cuts through the cross section. Position A is located near the connection with the wall plate, whereas position B is located at the middle of the batten*

6.1.3 Comparison of the strains

Figures 6.1i to 6.1n show the average strain measured along the width of the supporting batten. The numbers of the positions correspond to the numbers illustrated in **figure 6.1h**.

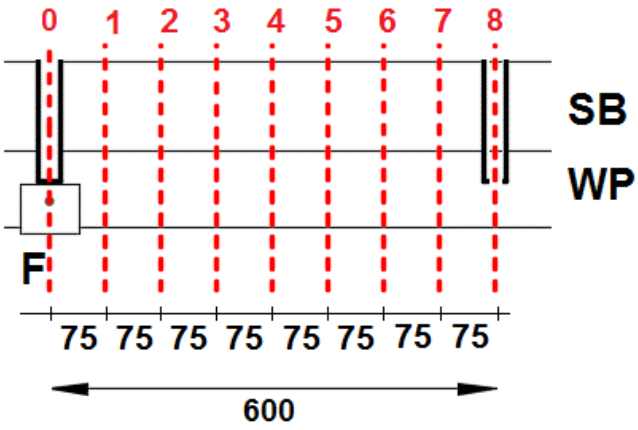

Figure 6.1h; *Position of the measurements at the supporting batten. The CTC 1200 set-up shows no F-bracket at position 8, whereas the CTC 600 set-up does*

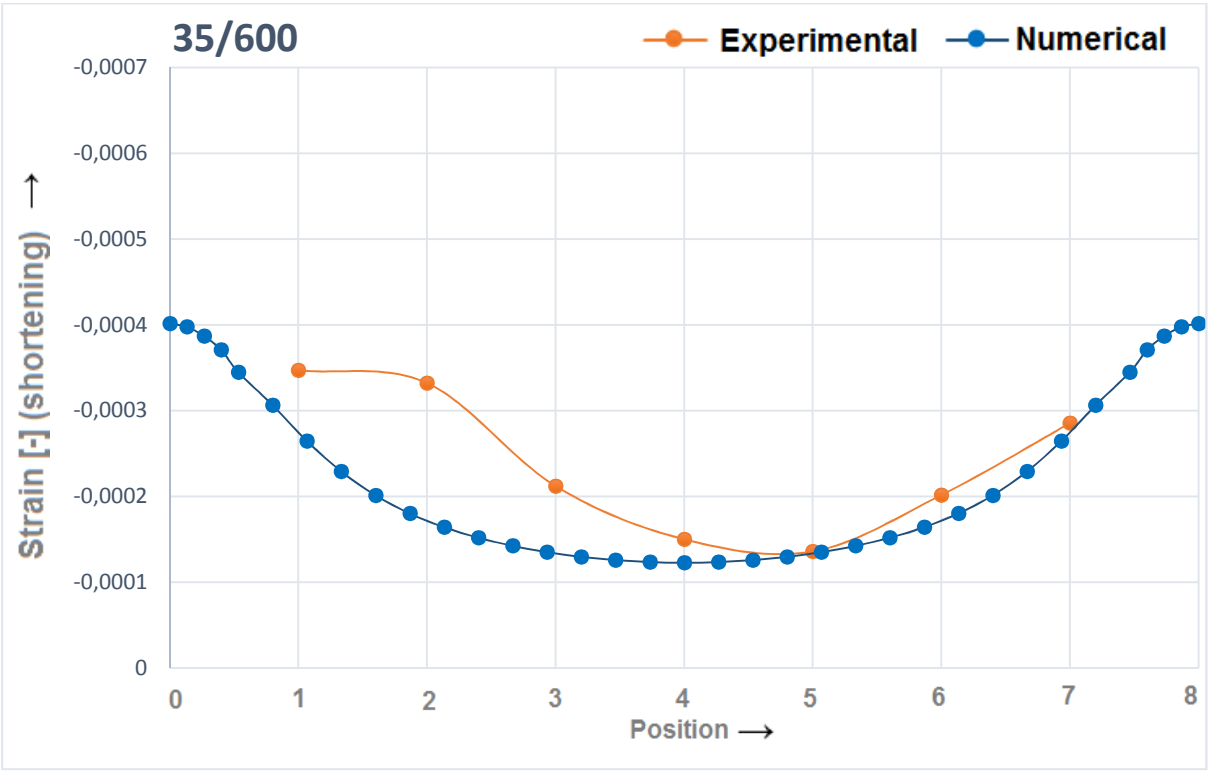

Figure 6.1i; *Strains measured at the supporting batten. The orange line corresponds to the experimental results, whereas the blue line corresponds to the numerical results. Specifications: Roof inclination 35 degrees, CTC distance of the brackets is 600mm, adding is 10mm.*

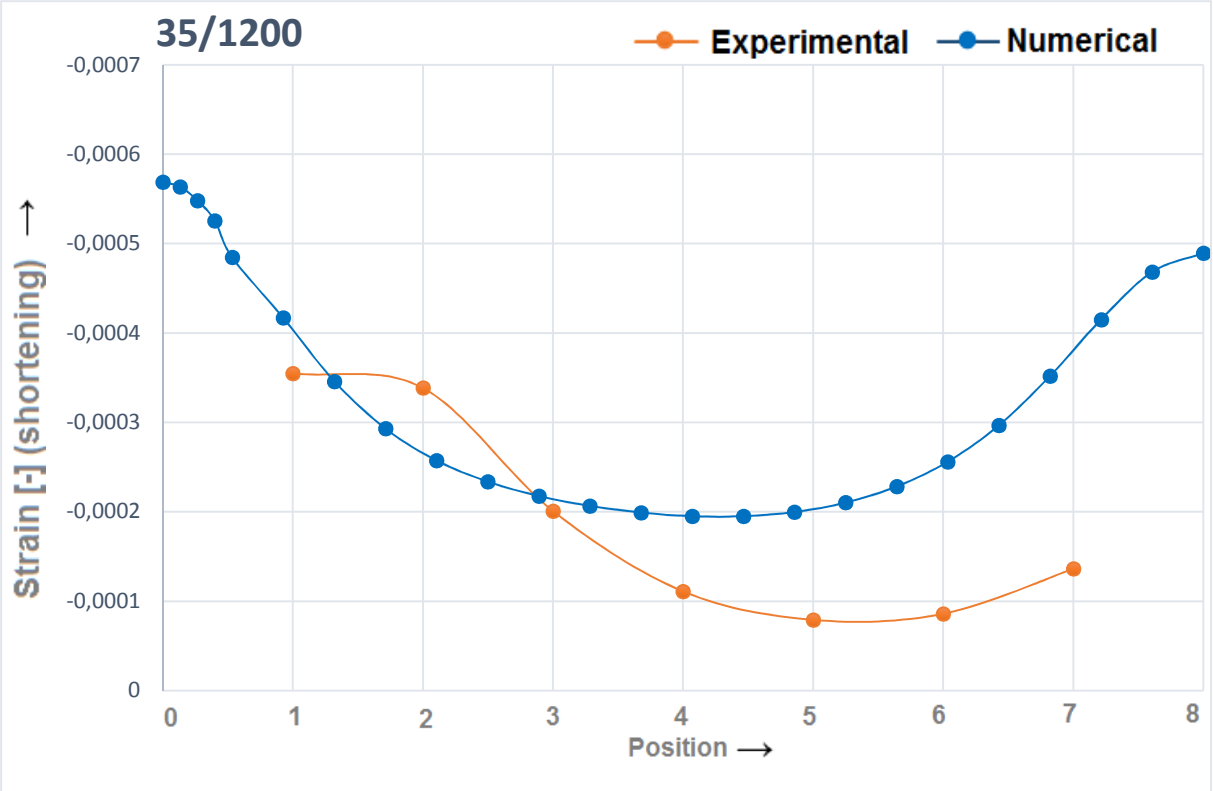

Figure 6.1j; *Strains measured at the supporting batten. The orange line corresponds to the experimental results, whereas the blue line corresponds to the numerical results. Specifications: Roof inclination 35 degrees, CTC distance of the brackets is 1200mm, adding is 10mm.*

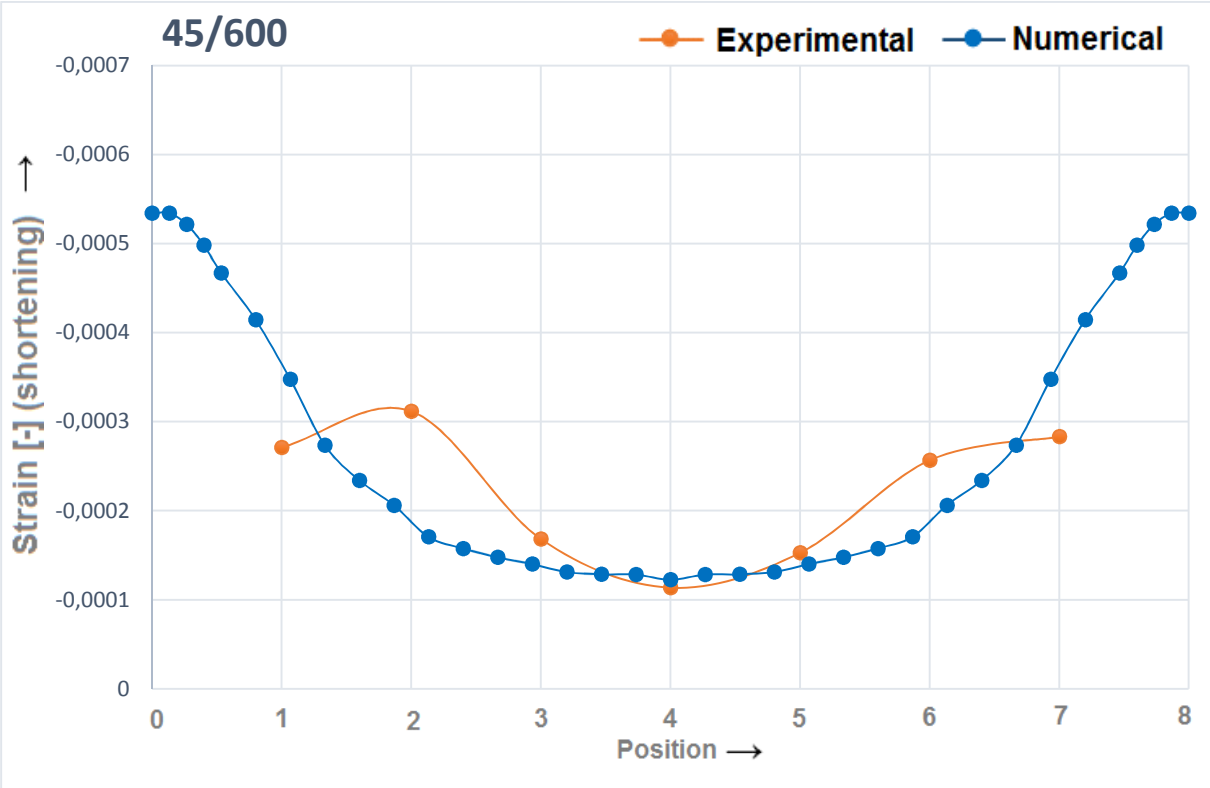

Figure 6.1k; *Strains measured at the supporting batten. The orange line corresponds to the experimental results, whereas the blue line corresponds to the numerical results. Specifications: Roof inclination 45 degrees, CTC distance of the brackets is 600mm, adding is 10mm.*

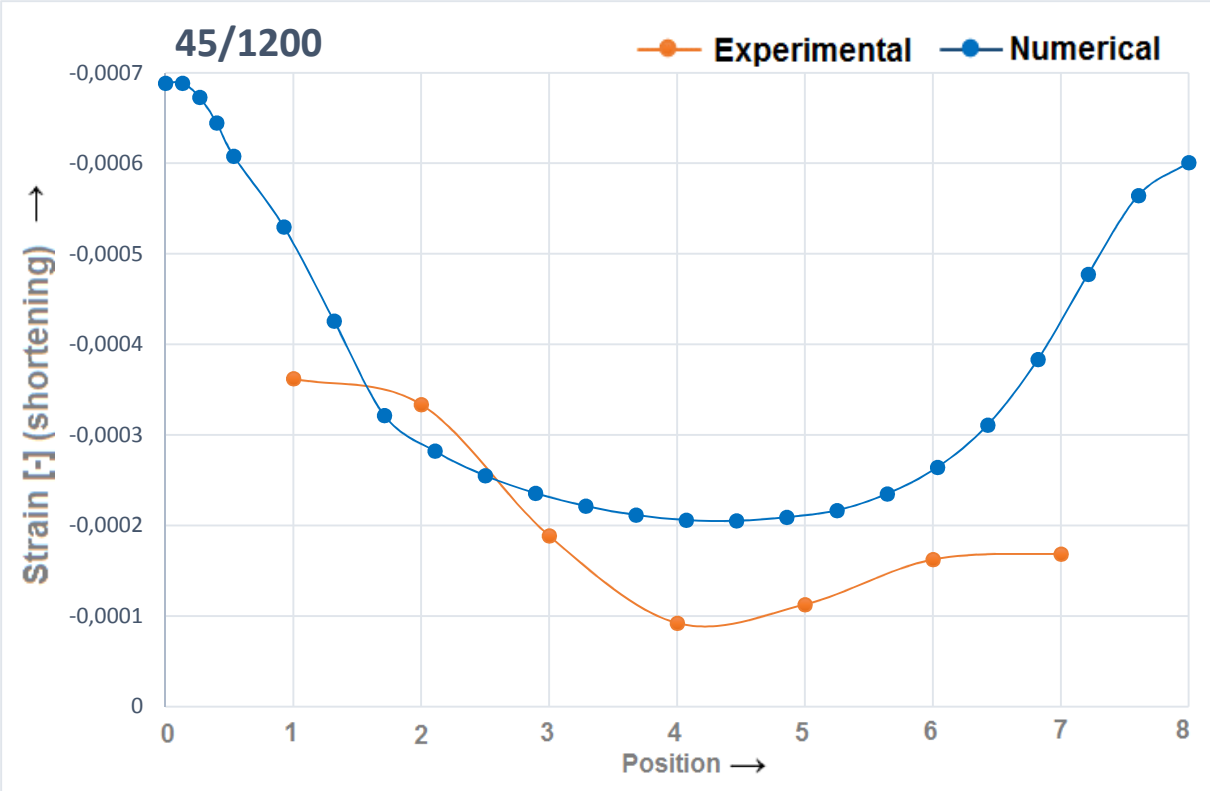

Figure 6.1L; *Strains measured at the supporting batten. The orange line corresponds to the experimental results, whereas the blue line corresponds to the numerical results. Specifications: Roof inclination 45 degrees, CTC distance of the brackets is 1200mm, adding is 10mm.*

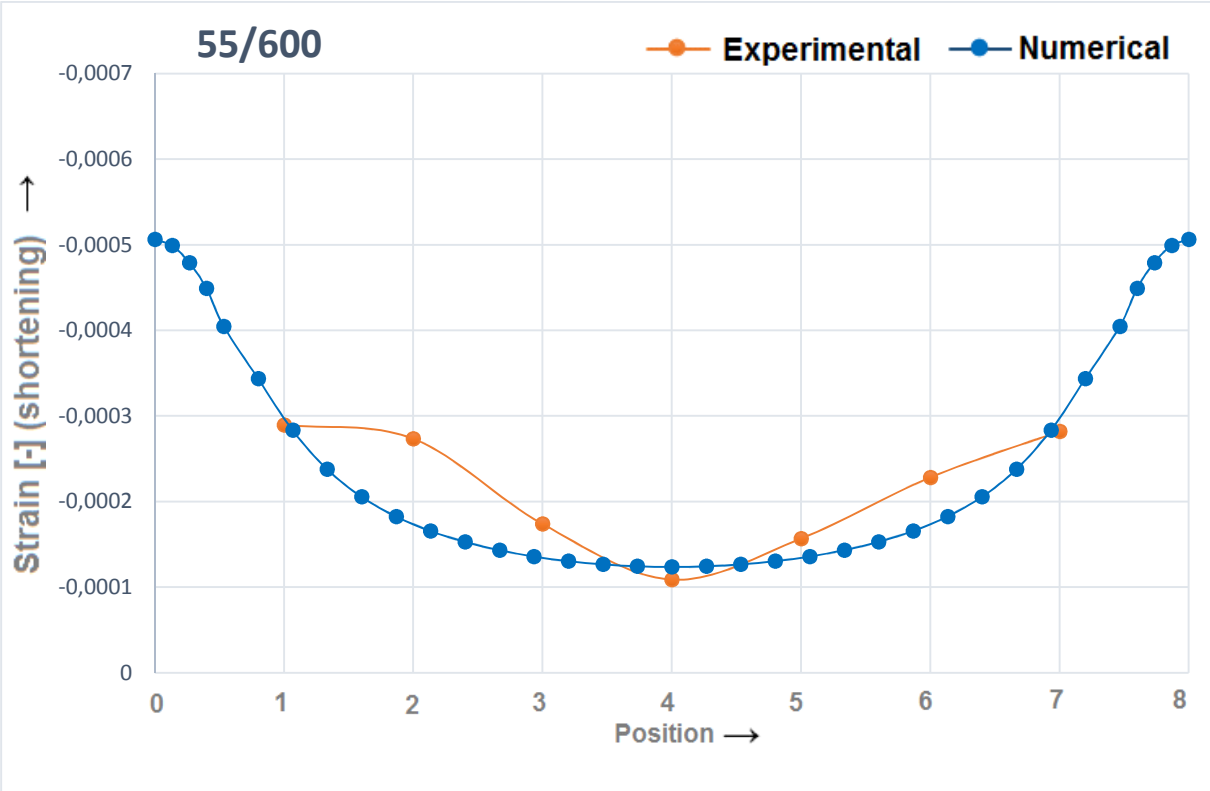

Figure 6.1n; *Strains measured at the supporting batten. The orange line corresponds to the experimental results, whereas the blue line corresponds to the numerical results. Specifications: Roof inclination 55 degrees, CTC distance of the brackets is 600mm, adding is 10mm.*

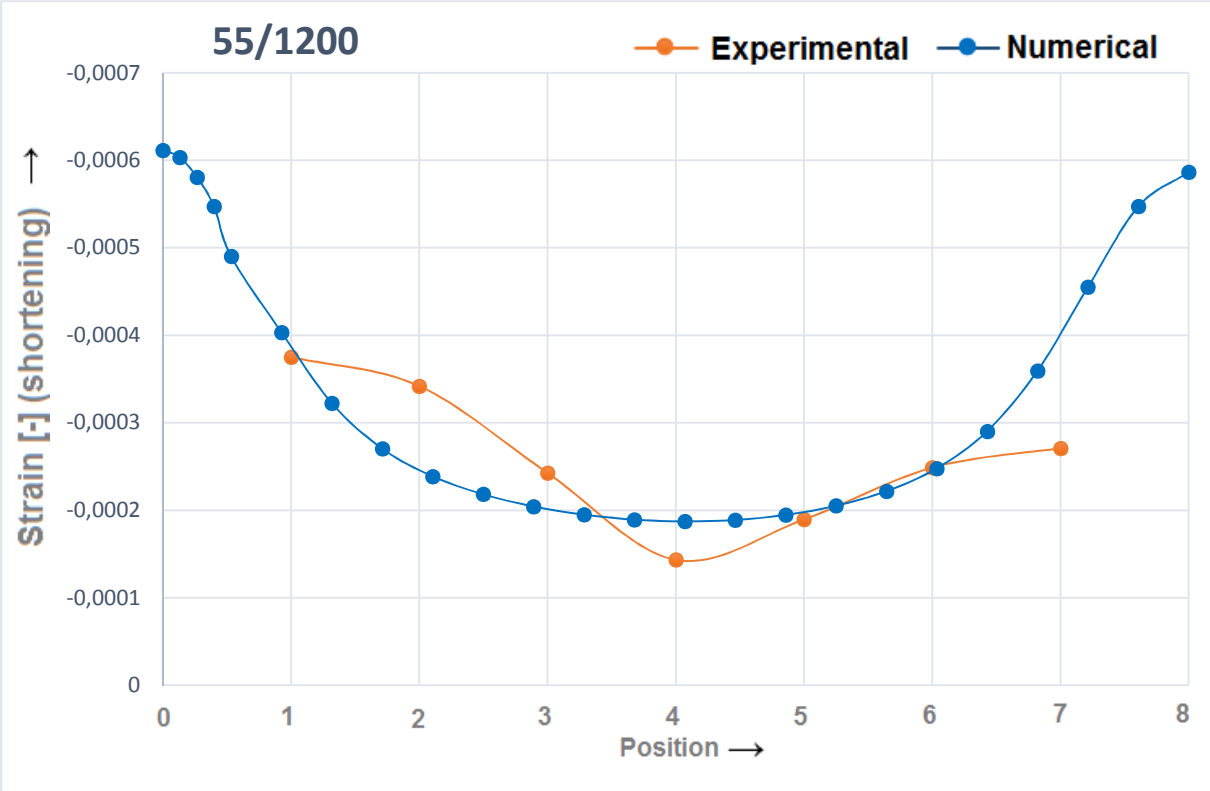

Figure 6.1n; *Strains measured at the supporting batten. The orange line corresponds to the experimental results, whereas the blue line corresponds to the numerical results. Specifications: Roof inclination 55 degrees, CTC distance of the brackets is 1200mm, adding is 10mm.*

The results obtained from both the experimental and numerical models lie in the same range, with small deviations for the 35/1200 and 45/1200 set-ups, which is encouraging. Though, more measurements for the experimental set-up, especially closer to the brackets (positions 0 and 8) would give more certainty for the results retrieved by the numerical model.

6.1.4 Effective width

In the course of this report, several effective widths have been obtained. **Figure 6.1o** shows an overview of the results.

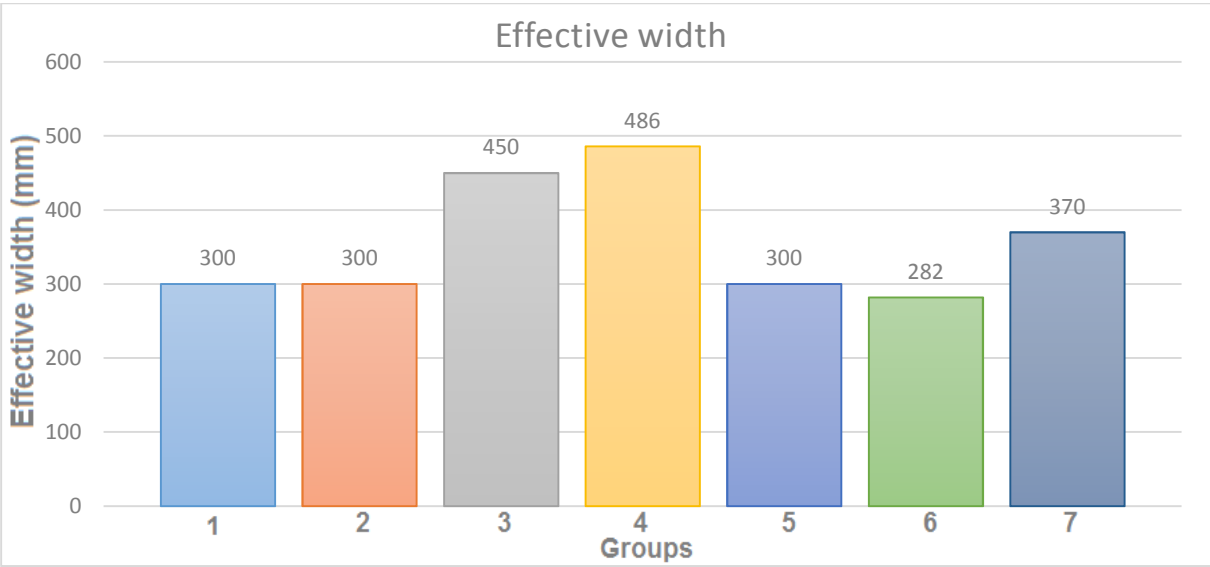

Figure 6.1o; *Effective widths, categorized in seven groups*

1) Literature study – Wall plate

The 300 millimeters effective width is the assumed value in the existing literature.

2) Experimental study – Supporting batten, high end

The measured strains on the supporting batten show high values up to the 2nd position (meaning an effective width of 300 millimeters), whereafter a steep drop shows lower values for positions 3 and further.

3) Experimental study – Supporting batten, cautious

As no measurements are available between positions 2 and 3, a cautious approach would suggest to take the first lower value for the strain, which in this case would mean position 3. This results in an effective width of 450 millimeters.

4) Numerical study – Supporting panel

The minimal principal stresses in the three dimensional model show a decrease of peak stresses at the connection with the supporting batten up to 486mm

5) Numerical study – Supporting batten

The measured strains on the supporting batten show a decrease in value up to position 2, corresponding to an effective width of 300 millimeters.

6) Numerical study – Wall plate, CTC 600mm

The von Mises stresses for a CTC 600mm model show a concentration of stresses at the top of the wall plate up to a 141 millimeters distant from the heart of the bracket, resulting in an effective width of 282 millimeters.

7) Numerical study – Wall plate, CTC 1200mm

The von Mises stresses for a CTC 1200mm model show a concentration of stresses at the top of the wall plate up to a 185 millimeters distant from the heart of the bracket, resulting in an effective width of 370 millimeters.

The effective width decreases as the distance to the wall plate becomes smaller. This is in correspondence with the assumption made in the experimental phase, illustrated in **figure 6.1p**.

As the effective width of the wall plate is the matter of interest, it is concluded that the lowest value measured at the wall plate only is used as the proposed value in future calculations. This results in:

- Effective width for a wall plate with a center-to-center distance of 600 millimeters for the F-bracket: **282 millimeters**.

- Effective width for a wall plate with a center-to-center distance of 1200 millimeters for the F-bracket: **370 millimeters**.

Intermediate values for the center-to-center distance of the F-brackets should be interpolated.

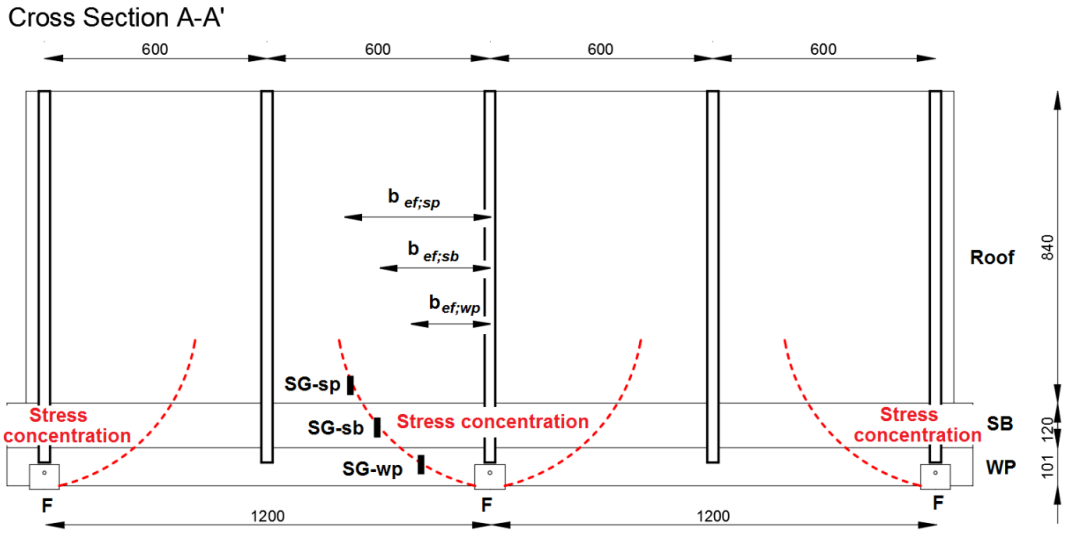

Figure 6.1p; *Top view of a roof structure. The red line illustrates the stress concentration towards the wall plate. The strain gauges at the wall plate (WP), supporting batten (SB) and supporting panel (SP) show identical results. However, the effective width increases as the distance to the wall plate increases.*

6.1.5 Answering the research questions

The research question is formulated as:

- What is the resistance of the wall plate in combination with F-brackets?

And the sub questions are:

- What is the size of the effective width?
- Which variables have an effect on the effective width of the wall plate?

The resistance of the wall plate is formulated with the existing formulas:

$$\sigma_{c,90,d} = \frac{V}{b_F \cdot b_{wp}} + \frac{M}{\frac{1}{6} \cdot l_{ef} \cdot (b_{wp})^2} \leq f_{c,90,d} \tag{6.3}$$

$$\sigma_{t,90,d} = \frac{M}{\frac{1}{6} \cdot l_{ef} \cdot (b_{wp})^2} \leq f_{t,90,d} \tag{6.4}$$

With a reformulated value for the eccentricity determining the internal bending moment:

$$e = h_{wp} + t_a + t_F - \frac{1}{2} \cdot b_{wp} - h_b + \sin(\alpha) \cdot \frac{1}{2} \cdot b_{wp} + \frac{(1+\chi) \cdot H}{2 \cdot b_F \cdot f_{c,90}} \tag{6.5}$$

With the value of χ determined with **formula 6.6** and **figure 6.1c**:

$$\psi = \frac{e_{1a} + r}{h_{wp}} = \frac{h_{wp} + t_a + t_F - h_b}{h_{wp}} \tag{6.6}$$

Also, new values for the effective width are proposed:

- Effective width for a wall plate with a center-to-center distance of 600 millimeters for the F-bracket: **282 millimeters**.

- Effective width for a wall plate with a center-to-center distance of 1200 millimeters for the F-bracket: **370 millimeters**.

Intermediate values for the center-to-center distance of the F-brackets should be interpolated.

Other than the center-to-center distance of the F-brackets, the angle of the roof or the size of the adding seem to have no effect on the effective width of the wall plate. The position of the rafters might have an influence on the effective width, but it has not been tested sufficiently.

6.2 Recommendations

6.2.1 Recommendations regarding this research project

- Extensive work on the experimental research

As mentioned in the recommendation section of **chapter 4**, the execution of the experimental research has not been optimized. Points which could improve the experimental results are:

5) Using more measuring equipment would improve the segmentation of the progress line
6) Using the measuring equipment on other positions to be able to compare existing results.
7) Using different test-materials to compare existing results
8) Changing the location of the gauges towards the supporting panel

- Alternative experimental test set-up:

An alternative experimental test set-up has been developed to increase knowledge of the effective width of the supporting batten. This experimental research is more quantitative, compared to the executed research, which is more qualitative.

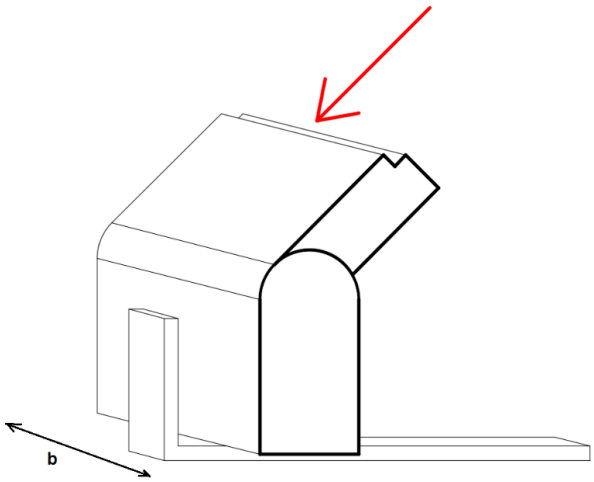

Figure 6.2a; *Test set-up for possible future research. B is the width of the wall plate and the supporting batten*

The test set-up consists of a single F-bracket, a wall plate and a supporting batten. The width of the wall plate and the supporting batten are similar.

The goal of the test is to determine the force at which the connection will fail due to fracture. The first test series have a certain (preferably rather small) width. Once the failure strength is determined, the width of the set-up is increased, and again the failure strength is determined. It is most likely that the failure strength of the second series will have an increased failure strength:

$$F_{fracture,1} < F_{fracture,2} \tag{6.7}$$

This process is repeated until an increase of width doesn't affect the failure strength, so that:

$$F_{fracture,n} = F_{fracture,n+1} \tag{6.8}$$

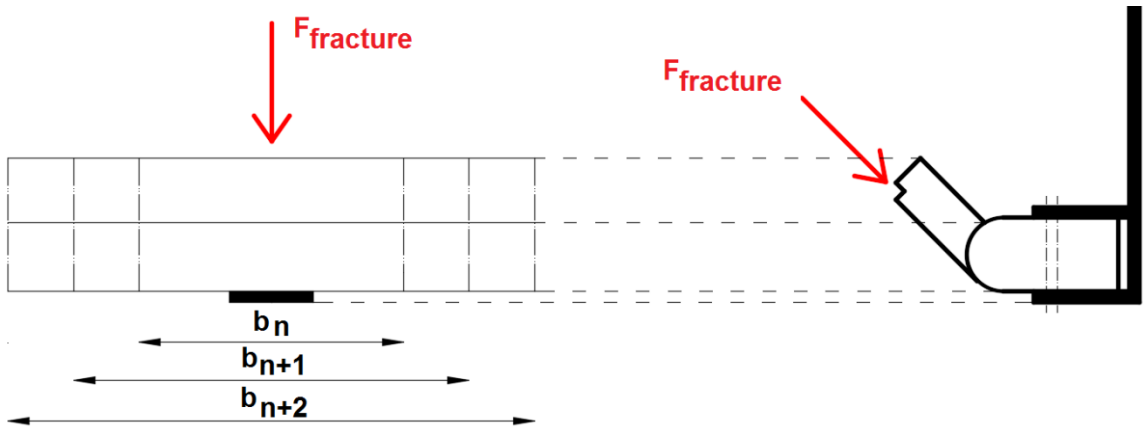

Figure 6.2b; *Test set-up for possible future research. Left is top view, right is rotated cross section*

- Positioning of the rafters

The variable positioning of the rafters has been left out this research project. However, the results obtained by the experimental and numerical models show interesting phenomena that might be explained by further research.

6.2.2 Recommendations for other research subjects

- Coach screw

From the construction sector there is a demand for more information regarding the connection of the coach screw with the rafters and the wall plate. The code prescribes the use of minimal width of the rafters to avoid rupture of the rafters caused by the screws. This is solved by locally using spools to increase the minimal width of the rafter. However, the use of spools increases the material costs and labor time (which indirectly increases the costs). Further research on this subject might give an improved code description, which allows the constructor to omit the use of spools.

List of literature and software

Literature

[1] **Bakker, M.C.M. Kerstens, J.G.M. Hofmeyer, H.** (2003), *Finite Element Method: Linear (Eindige Elementen Methode: Lineair) – Mechanica 8*. p. 1 – 17: Technical University of Eindhoven, Faculty Building Engineering.

[2] **Bouwen met staal** (2004), *Spanning Steel, Part 1: Book of basics (Overspannend staal, Deel 1: Basisboek)*. p. 53: Rotterdam, Bouwen met staal. ISBN: 90 72830 45 8 Fouth press, second edition.

[3] **Capinc** (2014), *Frequently Asked Questions on Von Mises Stress Explained*. url: www.capinc.com/2014/02/12/frequently-asked-questions-on-von-mises-stress-explained

[4] **Centrum Hout** (2007), *Strength properties of wood (Sterktegegevens van hout).* p.2: Almere, Centrum Hout.

[5] **Danielsson, H.** (2013) *Perpendicular to grain fracture analysis of wooden structural elements – Models and applications*, p. 10 – 11: Lund, Sweden. Department of Construction Sciences. ISBN 978 91 7473 475 1

[6] **Danielsson, H.** (2013) *Perpendicular to grain fracture analysis of wooden structural elements – Models and applications*, p. 10: Lund, Sweden. Department of Construction Sciences. ISBN 978 91 7473 475 1

[7] **EN 312** (2010), *Particleboards, Specifications*. BSI publishing, ISBN 978 0 580 67603 1

[8] **EN 408** (2011), *Timber structures – Structural timber and glued laminated timber – Determination of some physical and mechanical properties*. BSI publishing, ISBN 978 0 580 76731 9.

[9] **Green, D.W. Winandy, J.E. Kretschmann D.E.** (1999)*: Wood Handbook Chapter 4 – Mechanical Properties of Wood*. p. 4 – 32: Madison, US. Department of Agriculture, Forest Service, Forest Products Laboratory.

[10] **Imechanica** (2005), *Abaqus – Lecture 2: Elements. Slides 3 – 31*: Abaqus inc.

[11] **ISO 898-1:2013** (2013), *Mechanical properties of fasteners made of carbon steel and alloy steel – Part 1: Bolts, screws and studs with specified property classes – Coarse thread and fine pitch thread.* Geneva, International Organization for Standardization.

[12] **ISO 898-2:2012** (2012), *Mechanical properties of fasteners made of carbon steel and alloy steel – Part 2: Nuts with specified property classes – Coarse thread and fine pitch thread.* Geneva, International Organization for Standardization.

[13] **Janssen, H.J.M.** (2010), *Constructional behavior of elements – Mechanica 4 (Constructief gedrag van elementen – Mechanica 4).* p. 7 – 51: Technical University of Eindhoven, Faculty Building Engineering.

[14] **Janssen, H.J.M.** (2010), *Constructional behavior of elements – Mechanica 4 (Constructief gedrag van elementen – Mechanica 4).* p. 22: Technical University of Eindhoven, Faculty Building Engineering.

[15] **Jellema 4A** (2005), *Housing – Performence requirements / Roofings (Omhulling – Prestatie-eisen/Daken).* p. 54 – 86: Utrecht/Zutphen, Thiememeulenhoff. ISBN: 90 06 95043 2. Second press, first edition.

[16] **Jorissen, A.J.M.** (2012-2013), *Lecture Notes – Timber structures 3, General topics.* p. 11 – 14: Technical University of Eindhoven, Faculty Architecture, Building and Planning.

[17] **Jorissen, A.J.M.** (2012-2013), *Presentation slides – Timber structures 3, Roof loads.* Slides 49 and 50. Technical University of Eindhoven, Faculty Architecture, Building and Planning.

[18] **Jorissen, A.J.M.** (2012-2013), *Presentation slides – Timber structures 3, Strength grading*. Slides 51 and 52. Technical University of Eindhoven, Faculty Architecture, Building and Planning.

[19] **Leijten, A.J.M.** (2010), *Lecture Notes – Timber structures 2, Chapter 3: Mechanical Properties (Mechanisch eigenschappen).* p. 7 – 8. Technical University of Eindhoven, Faculty Building Engineering.

[20] **Marianon, F. Fortino, S. and Toratti, T.** (2008), *A method to model wood by using Abaqus finite element software. Part 1. Constitutive and computational details.* p. 16 – 18: Julkaisija, VTT Technical Research Center of Finland. ISBN 978 951 38 7107 9. url: http://www.vtt.fi/publications/index.jsp.

[21] **Smartbolts** (2016) *Fundamentals of Basic Bolting – What is proof load and how is it different from yield strength and ultimate strength*. url: www.smartbolts.com/fundamentals/

[22] **Spanolux** (2011), *MDF Manual*. p. 14: Vielsalm, Spanolux NV.

[23] **The Engineering Toolbox** (2016) *Friction and Friction Coefficients – Friction theory and coefficients of friction for ice, aluminum, steel, graphite and other common materials and material combinations*. url: www.engineeringtoolbox.com/friction-coefficients-d_778.html

Software

[A] **Abaqus** (2016), *Abaqus Unified FEA – Complete solutions for realistic simulation*. 3DS:

[B] **Autocad** (2016), *Autocad Design every detail*. Autodesk productions

[C] **Microsoft Office** (2016), *Excel, Powerpoint, Word.* Microsoft

Appendices

This report contains the following appendices:

- **Appendix 2.1**
- **Appendix 3.1**
- **Appendix 3.2**
- **Appendix 4.1**
- **Appendix 4.2**
- **Appendix 4.3**
- **Appendix 5.1**
- **Appendix 5.2**

A compact disc is attached to the hardcopy version of this report. It contains the digital version of this report, as well as results from the numerical and experimental experiments. Also the software files from the analytical and numerical models.

Appendix 2.1

This appendix contains the calculations of the structural design agencies. There a five different projects (Note: the calculations are in Dutch):

- 20 woningen te Schoonbeek
- 12 huurwoningen Borgele te Deventer
- Unnamed project
- 32 woningen Ruyschenberg te Helmond
- 8 woningen Lent, woningtype 4.1

Algemeen:

Afmeting muurplaat:	70 ×	170	mm² (rond)
Afmeting oplegregel	45 ×	95	mm²
dikte plaatmateriaal		11	mm
stelruimte onder muurplaat		15	mm
dakhelling		41	graden
h.o.h beugels		590	mm

Maatgevende U.C. **0,99**

Hout:

Houtsterkteklasse:	**C18**	
k_{mod}	**0,85**	
$f_{t;90;u;d}$	**0,31**	N/mm²
$f_{c;90;t;d}$	**3,12**	N/mm²

Staal

Staalkwaliteit S 235

Geometrie

t_{staal}	10	mm	A	**188**	mm
a_{las}	4	mm	B	**88**	mm
breedte	80	mm	C	**90**	mm
$d_{gat\ anker}$	14	mm	D	**56**	mm
			E	**14**	mm
$e_{Fv;\ muurplaat}$	20,7	mm	F	**45**	mm
$e_{FH;\ muurplaat\ vlak\ B}$	88,2	mm	G	**55**	mm
			H	**170**	mm
Ankers:	Fischer FHII M8NL, FHY M8, Spit Dynabolt M10*55 of MEA ZA/S		I	**30**	mm
h.o.h. afstand	= 170	mm	J	**300**	mm
randafstand	= 100	mm	K	**0**	mm
$F_{bu;d}$	= 4,00	kN			

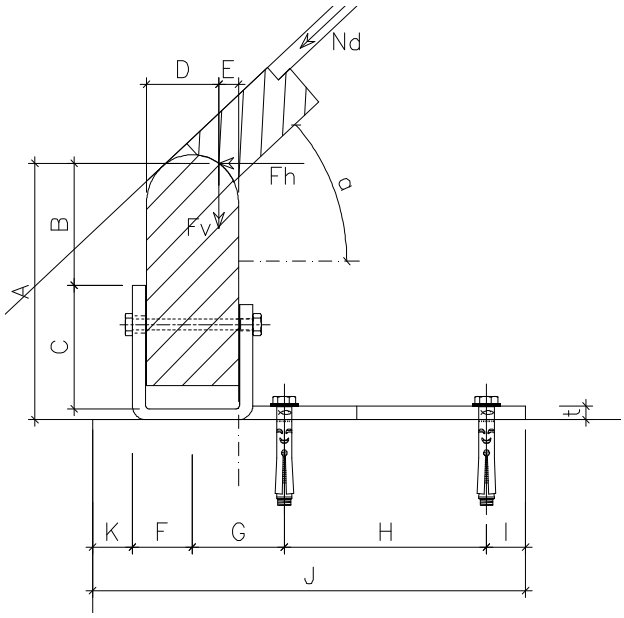

bouten bevestiging muurplaat aan F-anker

Diameter	=	8 mm
Lengte	=	100 mm
aantal	=	1 stuks
$F_{v;u;d}$	=	3,29 kN/bout

(Technosoft) h.o.h. stijlen: **0,61** m

Belastingen	C1 (max $F_{H)}$	C2 (Max $F_{V)}$	C3 min(Neg)
$F_{H;d}$ (kN)	2,24	2,24	-0,10
$F_{V;d}$ (kN)	1,52	1,52	-1,53

Belastingen per meter

	C1	C2	C3
$F_{H;d}$ (kN/m)	**3,67**	**3,67**	**-0,16**
$F_{V;d}$ (kN/m)	**2,49**	**2,49**	**-2,51**

Controle spanningen in schotjes (positieve krachten) **(Strip 80 × 10)**

$M_{d;\ 1\ strip}$	= 3,67 ×	0,590 ×	0,188	=	0,41	kNm per strip		
$W_{elastisch}$	= 1/6 ×	80 ×	10 ²	=	1333,33	mm³		
$W_{elastisch}$	= 1/6 ×	25 ×	10 ²	=	416,667	mm³ +		
					1750,00	mm³		
$M_{y;u;d;\ opneembaar}$	= 235 ×	1750,00 /	10^6	=	0,41	kNm per strip	**U.C. =** **0,99**	**Voldoet**

Controle spanningen in lassen volgens NEN 6770

t	= 10	mm	β	=	0,8	lasfactor	
a_{las}	= 4	mm	$f_{t;d}$	=	360	N/mm²	
$l_{t;ef}$	= 80	mm	$f_{w;u;d}$	=	207	N/mm²	
Spanningen in las afschuiving			Spanningen in las moment				
$F_{s;d}$	= 1,08	kN	$M_{s;d}$	=	0,20	kNm	
σ_l	= 1,20	N/mm²	σ_l	=	32,71	N/mm²	
τ_l	= 1,20	N/mm²	τ_l	=	32,71	N/mm²	
τ_2	= 0,00		τ_2	=	0,00		
			b*	=	13,77	mm	
$\sigma_{w;s;d}$	= 39,16	N/mm²	< $f_{w;u;d}$	=	207	N/mm²	**U.C. =** **0,19** **Voldoet**

Controle spanningen vlak A in F-anker (negatieve krachten)

$F_{H;d}$	= -0,10	kN	$e_{FH\ t.o.v.\ A}$	=	183,211	mm		
$F_{v;d}$	= -1,48	kN	$e_{FV;To.v.\ A}$	=	34,284	mm		
			$M_{t.o.v.\ A}$	=	-0,068	kNm		
$Wy_{;beugel;pl}$	= ¼×b×h² =	0,25 ×	66 × 10 ^2	=	1650	Nmm³		
$\sigma_{s;d}$	= 1,00 ×	68455 /	1650	=	41,49	N/mm²		**Voldoet**
$f_{t;u;d}$	= 235	N/mm²					**U.C. =** **0,18**	**-**

Controle anker ter plaatse van vlak A en vlak B

Fischer FHII M8NL, FHY M8, Spit Dynabolt M10*55 of MEA ZA/S12 (og)

Vloertype	=	kanaalplaat	
F_{bu}	=	2,5	kN
h.o.h. afstand	=	170	mm
randafstand	=	100	mm
reductie rand	=	n.v.t	-
reductie h.o.h.	=	n.v.t	-
Betonkwaliteit minimaal		C45/55	
$F_{bu;d}$	=	4,00	kN

$F_{H;d1}$	=	2,17	kN	$e_{FH\ t.o.v.\ C}$	=	188	mm
$F_{V;d1}$	=	1,47	kN	$e_{FV;To.v.\ C}$	=	66	mm
$M_{d;1;t.o.v.C}$	=	0,31	kNm	$e_{anker\ A;\ t.o.v.\ C}$	=	100	mm
$F_{axiaal;d;anker\ A}$	=	3,11	kN/anker	$F_{axiaal;d;anker\ B}$	=	0,00	kN/anker
$F_{afschuiving;d;Anker\ A}$	=	0,00	kN/anker	$F_{afschuiving;d;Anker\ B}$	=	2,17	kN/anker
$F_{id;A}$	=	3,11	kN	$F_{id;A}$	=	2,17	kN

U.C. = 0,78 Voldoet **U.C. = 0,54** **U.C. = 0,78 Voldoet**

Controle buiging vlak D in muurplaat t.g.v. Combinatie 1

							trekspanning			
$M_{d1;tgv\ FH}$	=	0,088	×	3,67	=	0,32 kNm/m	$\sigma_{t;90;d}$	=	0,40	N/mm²
$M_{d2;tgv\ FV}$	=	-0,021	×	2,49	=	-0,05 kNm/m	$\sigma_{t;90;d}$	=	-0,06	N/mm²
$F_{V;d1}$	=				=	-2,49 kN/m	$\sigma_{t;90;d}$	=	-0,04	N/mm²
							$\sigma_{t;90;d}$	=	0,30	N/mm² **U.C. = 0,95 Voldoet**
							$f_{t;90;u;d}$	=	0,31	N/mm²

Controle buiging vlak D in muurplaat t.g.v. combinatie 2

$M_{d1;tgv\ FH}$	=	0,088	×	3,67	=	0,32 kNm/m	$\sigma_{t;90;d}$	=	0,40	N/mm²
$M_{d2;tgv\ FV}$	=	-0,021	×	2,49	=	-0,05 kNm/m	$\sigma_{t;90;d}$	=	-0,06	N/mm²
$F_{V;d1}$	=				=	-2,49 kN/m	$\sigma_{t;90;d}$	=	-0,04	N/mm²
							$\sigma_{t;90;d}$	=	0,30	N/mm² **U.C. = 0,95 Voldoet**
							$f_{t;90;u;d}$	=	0,31	N/mm²

Controle muurplaat vlak D t.g.v. BG 3

							Trekspanningen			
$M_{d3;\ tgv\ FH}$	=	0,088	×	-0,16	=	-0,0145 kNm/m	$\sigma_{t;90;d}$	=	0,02	N/mm²
$M_{d4;tgv\ FV}$	=	0,021	×	-2,51	=	-0,0520 kNm/m	$\sigma_{t;90;d}$	=	0,06	N/mm²
$F_{v;3}$	=				=	-2,5082 kN/m	$\sigma_{t;90;d}$	=	0,04	N/mm²
$\sigma_{t;90;d}$	=						$\sigma_{t;90;d}$	=	0,12	N/mm² **Voldoet**
							$f_{t;90;u;d}$	=	0,31	N/mm² **U.C. = 0,37 -**

Controle aansluiting beugel - muurplaat (drukkracht)

$F_{H;d}$	=	2,17	kN	A	=	80 ×	90	=	7200	mm²
$\sigma_{c;90;d}$	=	0,30	N/mm²							
$f_{c;90;u;d}$	=	3,12	N/mm²							**U.C. = 0,10 Voldoet**

Controle bevestiging muurplaat - F-anker

Muurplaat bevestigen aan anker dmv bout

Diameter:	8	mm	$F_{v;u;d}$	=	**3,29**	kN/bout
Lengte	100	mm	$F_{v;u;d;tot}$	=	3,29	kN
aantal	1	stuks	$F_{v;d}$	=	-1,48	kN **U.C. = 0,45 Voldoet**

Belastingen

Veiligheidsklasse, belastingfactoren, referentieperiode:

Type bouwwerk : Woning
Gevolgklasse : 1 F_{fi} = 0,9
Referentieperiode : 50 jaar

Gegevens dakelement:

Breedte rib	= 30 mm¹
Hoogte rib	= 220 mm¹
h.o.h. ribben	= 610 mm¹
Daktype	= zadeldak
Dakpannen type	= Koramic OVH
Afmetingen bovenplaat	= n.v.t.
Plaattype	= n.v.t.
Afmetingen onderplaat	= 11 mm¹
Plaattype	= Houtspaanplaat
Dakhelling	= 45°

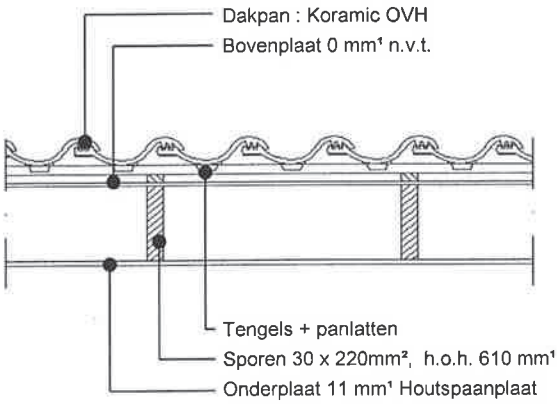

Dak met helling 45° (zadeldak)

Permanent:

Dakpannen type: Koramic OVH	=	0,41	kN/m²
Tengels en panlatten inclusief isolatie	=	0,06	kN/m²
Bovenplaat: n.v.t.	=	0,00	kN/m²
Sporen: Afmeting 30 x 220mm², h.o.h. 610 mm¹	=	0,05	kN/m²
Onderplaat: plaatdikte 11 mm (0,011 x 7,0 kN/m³)	=	0,08	kN/m²
	=	0,60	kN/m²

Veranderlijk:

Sneeuw: (ψ_0=0 ψ_1=0,2 ψ_2=0) = 0,28 kN/m²
μ1 =0,4 (0,4 x 0,70 x 1 x 1 = 0,28)
μ1*0,5 =0,2 (0,2 x 0,70 x 1 x 1 = 0,14)

Wind: (ψ_0=0 ψ_1=0,2 ψ_2=0)
Windgebied : 3 = 0,73 kN/m²
Onbebouwd
Bouwwerkhoogte : 11 m¹
Bouwwerkbreedte : 0,61 m¹
Uitgangspunt in de berekening in zone H en I.
qp(ze) = 0,73 kN/m¹ $c_s c_d$ = 1

Uitwendige drukcoëfficiënten ($c_{pe,10}$)

$C_{pe(druk)}$	= 0,60
$C_{pe(zuiging)}$	= -0,90
$C_{pe(onderdruk)}$	= 0,30
$C_{pe(overdruk)}$	= -0,20

Druk + onderdruk :	Cp,net = 0,9	=	0,66 kN/m²
Zuiging + overdruk :	Cp,net = -1,1	=	-0,80 kN/m²

Reparatie: (ψ_1=0 ψ_2=0 ψ_3=0) = 0,00 kN/m²
Dakhelling 45°

ES

Detailberekening aansluiting staande muurplaat - sporen

Omschrijving: **Detail 1**

Algemeen:

Afmeting muurplaat	= 70 x 120 mm²
Afmeting oplegregel	= 44 x 120 mm²
Dikte plaatmateriaal	= 11mm
Dakhelling α	= 45°

Hout:

Houtsterkteklasse	= C24
K_{mod}	= 0,9
Treksterkte $f_{t;90;d}$	= 0,31 N/mm²
Druksterkte $f_{c;90;d}$	= 1,52 N/mm²

Verankering:

Strippen beugels	= strip 80 x 8, hoogte 100mm¹, staalkwaliteit S235
Voetplaat beugels	= strip 80 x 8, lengte 315mm¹, staalkwaliteit S235
Verstijving beugels	= Beugels NIET verstijfd d.m.v. schotje
Ankertype	= Fischer TA M8 3 ankers toepassen
Toelaatbare ankerkracht	= 4 kN

Geometrie:

A	= 33 mm¹
B	= 23 mm¹
C	= 23 mm¹
D	= 47 mm¹
E	= 47 mm¹
F	= 66 mm¹
G	= 109 mm¹
ondersabelen	= 30 mm¹

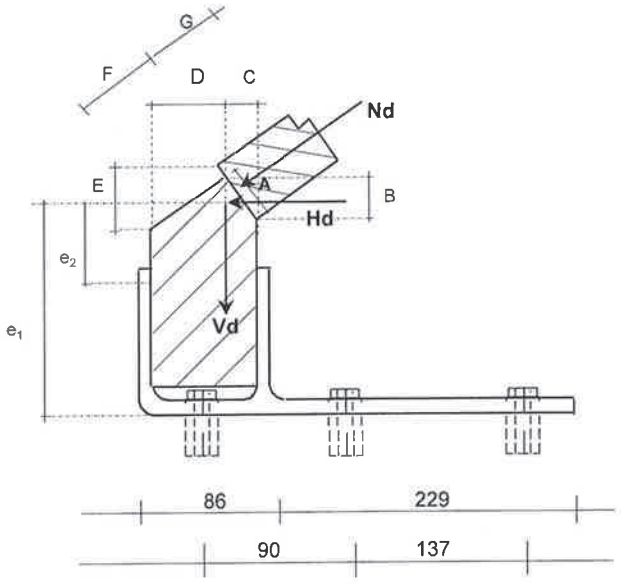

Excentriciteiten:

Excentriciteit e_1	= 131 mm¹
Excentriciteit e_2	= 44 mm¹

Fundamentele belastingen:

b.c.	Hd [kN/m¹]	(KN/spoor)	Vd [kN/m¹]	(KN/spoor)	Nd [kN/m¹]	(KN/spoor)
12	2,84	(1,73)	2,90	(1,77)	4,06	(2,48)
26	-1,70	(-1,04)	-2,00	(-1,22)	n.v.t.	(n.v.t.)
-	0,00	()	0,00	()	0	(0)
-	0,00	()	0,00	()	0	(0)
Permanent	1,08	(0,66)	0,97	(0,59)	1,45	(0,88)

Bepaling h.o.h. afstand beugels: *(Maatgevende belastingcombinatie 12)*

$F_{d;\ toelaatbaar\ ankers}$	= 9,23 kN	(incl. reductiefactoren)
$H_{d;\ maatgevend}$	= 2,84 kN	
H.o.h. afstand maximaal	= 9,23 / 2,84	(Ankers Fischer TA M8, Fd (max) = 4 kN)
	= 3,25 m¹	3 Ankers in rekening gebracht
Keuze h.o.h. afstand	**= 0,9 m¹**	
u.c	= 0,28	(≤1,0 Voldoet)

ES

Controle spanningen in beugels: **(Strip 80 x 8)** *(Maatgevende belastingcombinatie 12)*

M_{ed} = (2,84 x 0,131) x 0,9 m¹ = 0,33 kNm

M_{rep} = (2,32 x 0,131) x 0,9 m¹ = 0,27 kNm

--> Moment op te nemen door 2 strippen

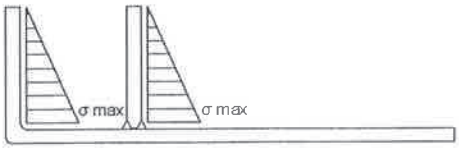

$W_{y;strip;pl}$ = 1280 mm³ => Plastisch weerstandsmoment

$W_{y;strip;el}$ = 853 mm³ => Elastisch weerstandsmoment

M_{Rd} = 2 x {(1280 x 235) / 1000000} = 0,6 kNm

$M_{rep,Rd}$ = 2 x {(853 x 235) / 1000000} = 0,4 kNm

u.c $_{UGT}$ = 0,55 (≤1,0 Voldoet)

u.c $_{BGT}$ = 0,68 (≤1,0 Voldoet)

Controle spanningen in lassen: *(Maatgevende belastingcombinatie 12)*

t = 8 mm¹

totale lasdikte = 2 x a minimale totale lasdikte = t + 2

$a_{min.}$ = (t + 2) / 2 = 5 mm¹

a = 6 mm¹

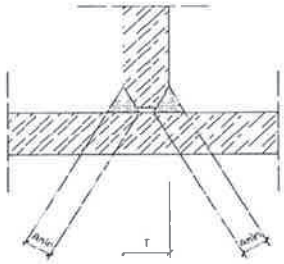

$\sigma_{optr.}$ = (0,706 x 0,33 x 1000000) / (6 x 80 x $\sqrt{2}$) = 35,54 N/mm²

σ_{toel} = 207 N/mm²

u.c = 0,17 (≤1,0 Voldoet)

Controle spanningen muurplaat: **(70 x 120 mm²)** *(Maatgevende belastingcombinatie 26)*

Med_1 = 1,7 x 0,044 = 0,075 kNm

N_{ed1} = -2 kN (Druk)

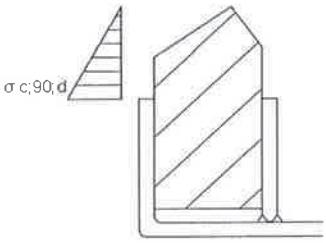

$\sigma_{t;90;d}$ = -0,09 + -0,03 = -0,12 N/mm²

$f_{t;90;d}$ = 0,31 N/mm²

u.c = -0,12 / 0,31 = 0,39 (≤1,0 Voldoet)

Controle houten oplegregel: **(44 x 120 mm²)** *(Maatgevende belastingcombinatie 12)*

$N_{ed;max}$ = 4,06 x 0,9 m¹

= 3,654 kN (opnemen over oppervlak 212 x 33 mm²)

$\sigma_{t;90;d}$ = 0,52 N/mm²

$f_{t;90;d}$ = 2,66 N/mm²

u.c = 0,52 / 2,66 = 0,2 (≤1,0 Voldoet)

Controle aansluiting plaatmateriaal - oplegregel:

$N_{ed;max}$ = 4,06 x 0,9 m¹

= 3,654 kN (opnemen over oppervlak 430 x 22 mm²)

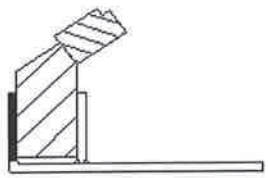

$\sigma_{t;90;d}$ = 0,39 N/mm²

$f_{t;90;d}$ = 2,66 N/mm²

u.c = 0,39 / 2,66 = 0,15 (≤1,0 Voldoet)

ES

Controle opwaaiverankering: (Verankering met houtdraadbouten ø 10, h.o.h. 610 mm¹)

d_{nom} = 10 mm¹

$F_{ax,Rk}$ = 7,31 kN (zie berekening houtdraadbouten)

$F_{ax,Rd}$ = 5,06 KN

Lokale windzuiging:

qp(ze) = 0,73 kN/m²

$C_{pe(zuiging)}$ = -0,9

$C_{pe(Overdruk)}$ = -0,2

$q_{p;Ed}$ = {(-0,9) + (-0,2)} x 0,73 kN/m²
= -0,8 kN/m²

Permanent:

$p_{g;Ed}$ = 0,6 kN/m²

Rekenwaarde belasting:

p_{Ed} = 0,9 x (0,6x cos45°) + 1,35 x (-0,8)
= -0,7 kN/m²

Dakstrook = 6,5 m¹

F_{Ed} = -4,55 kN/m²

Kracht per houtdraadbout:

$F_{ax,Ed}$ = 0,61 m¹ x -4,55
= -2,78 kN/bout

u.c = 0,55 (≤1,0 Voldoet)

Overzicht belastingen evenwijdig en loodrecht dakvlak op te nemen met houtdraadbouten:

Reacties fundamentele combinaties: (in kN/m¹)

Richting:	FC 1	FC 2	FC 3	FC 4	FC 5	FC 6	
Horizontaal naar buiten (-)	0,00	-1,70	0,00	0,00	0,00	0,00	
Horizontaal naar binnen (+)	2,84	0,00	0,00	0,00	0,00	0,00	
Verticaal naar buiten (+)	2,90	0,00	0,00	0,00	0,00	0,00	
Verticaal naar binnen (-)	0,00	-2,00	0,00	0,00	0,00	0,00	
Evenwijdig aan dakvlak	**4,06**	**-2,62**	**0**	**0**	**0**	**0**	(+ = omhoog)
Loodrecht op dakvlak	**0,05**	**-0,21**	**0**	**0**	**0**	**0**	(+ = buiten)

Maximale waarden per houtdraadbout:

$F_{v;Ed,\ //\ omhoog}$ = 1,5982 kN/bout toepassen houtdraadbouten ø 10 h.o.h. 610 mm¹

$F_{v;Ed,\ //\ omlaag}$ = 2,4766 kN/bout (op te nemen door knellat)

$F_{ax;Ed,\ \perp\ naar\ buiten}$ = 0,1281 kN/bout

$F_{ax;Ed,\ \perp\ naar\ binnen}$ = 0,0305 kN/bout (op te nemen door knellat)

ES

Controle beugel tpv punt C bij negatieve krachten (3 ankers):

Horizontale optredende kracht = -1,7 kN/m¹
Arm = 131 mm¹
Verticale optredende kracht = -2 kN/m¹
Arm = 90 mm¹

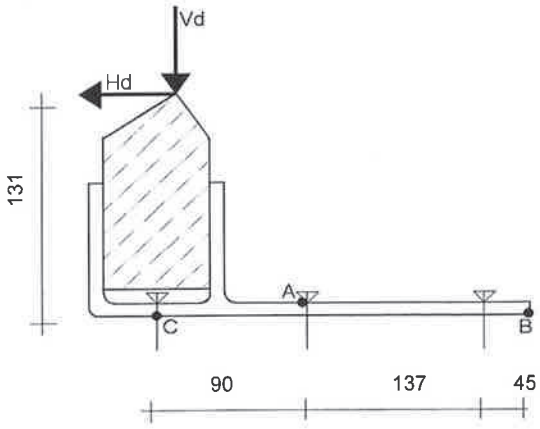

Moment t.o.v. punt B
Moment t.g.v. Hd = -1,7 x 0,9 x (131 / 1000)
= -0,2 kNm
Moment t.g.v. Vd = -2 x 0,9 x (90 / 1000)
= -0,49 kNm
Moment totaal optredend = -0,2 + -0,49
= -0,69 kNm

Moment op te nemen door 2 strippen
$W_{y;strip;pl}$ = 1/4 x (80) x 8²
= 1280 mm³
$W_{y;2\ strippen;pl}$ = 2560 mm³
$\sigma_{optr.}$ = -0,2 x 1000000 / 2560
= 78,13 N/mm²
$\sigma_{toel.}$ = 235 N/mm²

u.c. = 0,33 (≤1,0 Voldoet)

Controle ankers bij negatieve krachten (3 ankers):

Som van de momenten t.o.v punt B
Moment t.g.v. Hd = -1,7 x 0,9 x (131 / 1000)
= -0,2 kNm
Moment t.g.v. Vd = -2 x 0,9 x (272 / 1000)
= -0,49 kNm
Moment totaal optredend = -0,2 + -0,49
= -0,69 kNm

Toelaatbare ankerkrachten
Anker C F_d = 1,77 kN
Anker A F_d = 1,18433823529412 kN
$M_{opneembaar}$ = Fd;anker C x a + Fd;Anker A x a
= 0,7 kNm

u.c. = 0,99 (≤1,0 Voldoet)

ES

DETAILBEREKENING AANSLUITING MUURPLAAT - SPOREN

Omschrijving: **Muurplaat detail Go-1 type E10**

Algemeen:

Afmeting muurplaat	= 70 x 145 mm²
Afmeting oplegregel	= 48 x 95 mm²
Dikte plaatmateriaal	= 11mm
Dakhelling α	= 37,5°

Hout:

Houtsterkteklasse	= C18
K_{mod}	= 0,85
Treksterkte $f_{t;90;u;d}$	= 0,35 N/mm²
Druksterkte $f_{c;90;u;d}$	= 3,12 N/mm²

Verankering:

Strippen beugels	= strip 60 x 10, hoogte 100mm¹, staalkwaliteit S235
Voetplaat beugels	= strip 60 x 10, lengte 435mm¹, staalkwaliteit S235
Verstijving beugels	= Beugels NIET verstijfd d.m.v. schotje
Ankertype	= MEA ZA S12/10 ELVZ of Fischer FH II 12/10
Toelaatbare ankerkracht	= 6 kN 2 ankers toepassen

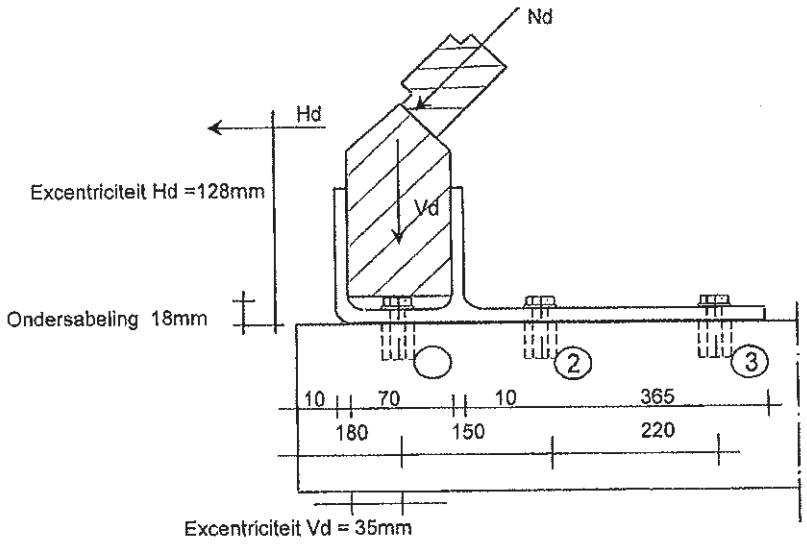

Fundamentele belasting per m¹:

b.c.	Hd [kN/m¹]	Vd [kN/m¹]	Nd [kN/m¹]	bij 2 of 3 ankers pos. Md [kNm/m¹]
1	-0,73	-0,40	0	0,00
7	3,65	1,98	4,24	0,40
10	0,65	-1,61	0	0,08
12	2,76	2,16	3,62	0,28

b.c.	Hd [kN/m¹]	Vd [kN/m¹]	Nd [kN/m¹]	bij 2 of 3 ankers neg. Md [kNm/m¹]
1	-0,73	-0,40	0	-0,09
7	3,65	1,98	4,24	0,00
10	0,65	-1,61	0	0,00
12	2,76	2,16	3,62	0,00

h.o.h. afstanden van de beugels:

Afhankelijk van de hierna volgende berekeningen zijn de h.o.h. afstande van de beugels bepaald

Gekozen is voor een h.o.h. afstand van : **850 mm¹**

SM

Schema t.b.v. berekening krachten bij een positief moment

(Maatgevende belastingcombinatie = 7)

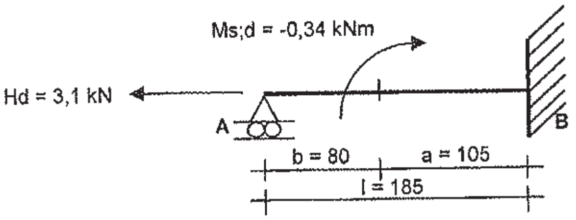

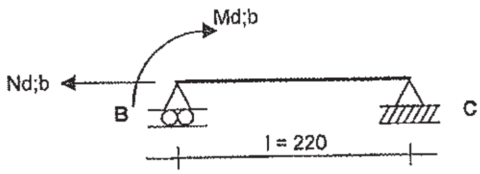

$V_{d;b} = \dfrac{3\,M_d\,(l^2 - b^2)}{2l^3} = -2{,}24$ kN

$V_{d;a} = \dfrac{-3\,M_d\,(l^2 - b^2)}{2l^3} = 2{,}24$ kN

$M_{d;b} = \dfrac{-M_d\,(l^2 - 3b^2)}{2l^2} = 0{,}07$ kNm

$N_{d,b} = H_d =$ 3,10 kN

$V_{d;b} = \dfrac{-M_{d;b}}{l} = 0{,}32$ kN

$V_{d;c} = \dfrac{M_{d;b}}{l} = -0{,}32$ kN

$M_{d;veld} = \dfrac{M_{d;b}}{2} = -0{,}04$ kN

$N_{d;c} = N_{d;b} =$ 3,10 kN

Controle spanningen in beugels (volgens NEN 6770): **(Strip 60 x 10)**

$M_d = 0{,}34$ kNm

b/t = 6 < 10 (plastisch rekenmodel)

$W_{y;strip} = 1500\ mm^3$ => Plastisch weerstandsmoment

$\sigma_{y;s;d} = \dfrac{M_d}{W_{y;strip}} = \dfrac{340000}{1500} = 226{,}7\ N/mm^2$

$\sigma_{z;s;d} = \dfrac{H_d}{A_{netto}} = \dfrac{3100}{600} = 5{,}2\ N/mm^2$

$\sigma_{vgl;s;d} = \sqrt{\sigma_{y;s;d}^2 + \sigma_{z;s;d}^2} = \sqrt{226{,}7^2 + 5{,}2^2} = 226{,}8\ N/mm^2$

u.c. = $\sigma_{vgl;s;d} / f_{y;d}$ = 226,8 / 235 = 0,96 **(<1,0 akkoord)**

Controle spanningen in stompe lassen (volgens NEN 6770)

t = 10 mm^1

totale lasdikte = 2 x a minimale totale lasdikte = t + 2

$a_{min.} = (t + 2) / 2 = 6\ mm^1$

a = 6 mm^1

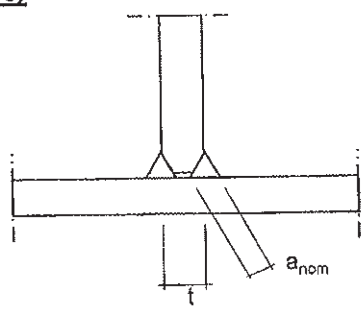

$f_{t;d} = 360\ N/mm^2$

$\beta = 0{,}8$

$f_{w;u;d} = 0{,}46 \times f_{t;d} / \beta = 207\ N/mm^2$

$t^* = t + 2/3a \times \sqrt{2} = 15{,}66$ mm

$F_d = \sqrt{((M_{s;d} / 2) / t^*)^2 + (0{,}5 \times (H_d/2))^2} = 10885{,}6$ N

$A_{ef} = L_{l;ef} \times a = 360\ mm^2$

$\sigma_{w;s;d} = F_d / A_{ef} = 30{,}2\ N/mm^2$

u.c. = $\sigma_{w;s;d} / f_{w;u;d}$ = 30,2 / 207 = 0,15 **(<1,0 akkoord)**

SM

Schema t.b.v. berekening krachten bij een negatief moment bij 2 ankers

(Maatgevende belastingcombinatie = 1)

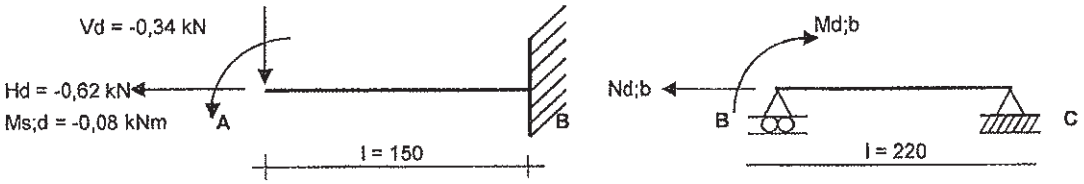

$V_{d;b}$ = -0,34 kN

$M_{d;b}$ = $- M_d - V_d \times l$ = 0,13 kNm

$N_{d;b} = H_d$ = -0,62 kN

$V_{d;b} = \frac{- M_{d;b}}{l}$ = -0,59 kN

$V_{d;c} = \frac{M_{d;b}}{l}$ = 0,59 kN

$M_{d;veld} = \frac{M_{d;b}}{2}$ = 0,07 kNm

$N_{d;c} = N_{d;b}$ = -0,62 kN

Controle spanningen in beugels (volgens NEN 6770): (Strip 60 x 10)

M_d = 0,13 kNm

b/t = 6 < 10 (plastisch rekenmodel)

$W_{y;strip}$ = 1150 mm³ => Netto Plastisch weerstandsmoment

$\sigma_{y;s;d} = \frac{M_d}{W_{y;strip}} = \frac{130000}{1150}$ = 113 N/mm²

$\sigma_{z;s;d} = \frac{H_d}{A_{netto}} = \frac{620}{600}$ = 1 N/mm²

$\tau_{y;s;d} = \frac{V_d}{A_{netto}} = \frac{340}{600}$ = 0,6 N/mm²

$\sigma_{vgl;s;d} = \sqrt{\sigma_{y;s;d}^2 + \sigma_{z;s;d}^2 + 3\,\tau_{y;s;d}^2} = \sqrt{113^2 + 1^2 + 3 \times 0{,}6^2}$ = 113 N/mm²

u.c. = $\sigma_{vgl;s;d} / f_{y;d}$ = 113 / 235 = 0,48 **(<1,0 akkoord)**

Controle spanningen in stompe lassen (volgens NEN 6770)

t = 10 mm¹

totale lasdikte = 2 x a minimale totale lasdikte = t + 2

$a_{min.}$ = (t + 2) / 2 = 6 mm¹

a = 6 mm¹

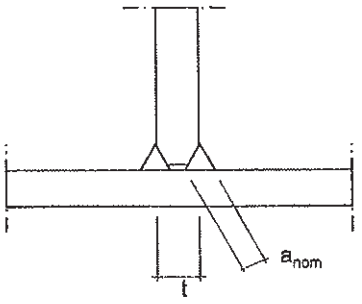

$f_{t;d}$ = 360 N/mm²

β = 0,8

$f_{w;u;d}$ = 0,46 x $f_{t;d}$ / β = 207 N/mm²

t* = t + 2/3a x √2 = 15,66 mm

$F_d = \sqrt{((M_{s;d} / 2) / t^*)^2 + (0{,}5 \times (H_d/2))^2}$ = 2559,7 N

$A_{ef} = L_{j;ef} \times a$ = 360 mm²

$\sigma_{w;s;d} = F_d / A_{ef}$ = 7,1 N/mm²

u.c. = $\sigma_{w;s;d} / f_{w;u;d}$ = 7,1 / 207 = 0,03 **(<1,0 akkoord)**

SM

Controle ankers in breedplaatvloer: MEA ZA S12/10 ELVZ of Fischer FH II 12/10

Krachten zijn afkomstig uit de krachtberekeningen van de beugels

Toelaatbare Ankerkrachten incl. reductiefactoren voor rand en h.o.h. afstanden

$F_{t;u;d} = F_{v;u;d} = 0$ kN	Anker 1
$F_{t;u;d} = 6$ kN	Anker 2 (met slobgat)
$F_{t;u;d} = F_{v;u;d} = 6$ kN	Anker 3

Optredende Ankerkrachten bij een positief moment (maatgevende belastingcombinatie = 7)

$F_{v;s;d} = 0$ kN	Anker 1	u.c. =	$F_{v;s;d} / F_{v;u;d} = 0$	**(<1,0 akkoord)**
$F_{t;s;d} = 1{,}92$ kN	Anker 2	u.c. =	$F_{t;s;d} / F_{t;u;d} = 0{,}32$	**(<1,0 akkoord)**
$F_{v;s;d} = 3{,}1$ kN	Anker 3	u.c. =	$F_{v;s;d} / F_{v;u;d} = 0{,}52$	**(<1,0 akkoord)**

Optredende Ankerkrachten bij een negatief moment (maatgevende belastingcombinatie = 1)

$F_{t+v;s;d} = 0$ kN	Anker 1	u.c. =	$F_{t+v;s;d} / F_{t+v;u;d} = 0$	**(<1,0 akkoord)**
$F_{t;s;d} = 0{,}93$ kN	Anker 2	u.c. =	$F_{t;s;d} / F_{t;u;d} = 0{,}16$	**(<1,0 akkoord)**
$F_{v;s;d} = 0{,}62$ kN	Anker 3	u.c. =	$F_{v;s;d} / F_{v;u;d} = 0{,}1$	**(<1,0 akkoord)**

Controle spanningen muurplaat: (70 x 145 mm²)

(Maatgevende belastingcombinatie = 12)

M_d	= 3,65 x 0,028= 0,1 kNm/m¹		
N_d	= 4,24 kN/m¹		
$W_{y;muurplaat}$	= 816667 mm³		
A_{netto}	= 70000 mm²		
$\sigma_{t;90;s;d}$	$= M_d / W_{y;muurplaat} - N_d / A_{netto}$	= 0,06 N/mm²	
$\sigma_{c;90;s;d}$	$= M_d / W_{y;muurplaat} + N_d / A_{netto}$	= 0,18 N/mm²	
$f_{t;90;u;d}$	= 0,35 N/mm²	u.c. = $\sigma_{t;90;s;d} / f_{t;90;u;d} = 0{,}17$	**(<1,0 akkoord)**
$f_{c;90;u;d}$	= 3,12 N/mm²	u.c. = $\sigma_{c;90;s;d} / f_{c;90;u;d} = 0{,}06$	**(<1,0 akkoord)**

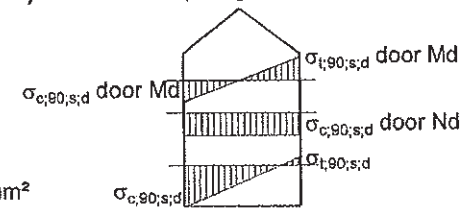

Controle knellat: (48 x 95 mm²)

(Maatgevende belastingcombinatie = 7)

$N_{c;d;max}$	= 4,24 x 0,85 m¹		
	= 3,604 kN (opnemen over oppervlak 316 x 37 mm²)		
$\sigma_{c;90;d}$	= 0,31 N/mm²		
$f_{c;90;u;d}$	= 3,12 N/mm²		
u.c	= 0,31 / 3,12	= 0,1	**(<1,0 akkoord)**

Controle aansluiting plaatmateriaal - oplegregel:

$N_{c;d;max}$	= 4,24 x 0,85 m¹		
	= 3,604 kN (opnemen over oppervlak 386 x 11 mm²)		
$\sigma_{c;90;d}$	= 0,85 N/mm²		
$f_{c;90;u;d}$	= 3,12 N/mm²		
u.c	= 0,85 / 3,12	= 0,27	**(<1,0 akkoord)**

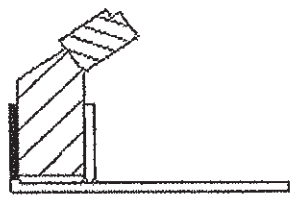

SM

Controle opwaaiverankering: (Verankering met houtdraadbouten ø 10, h.o.h. 620 mm¹)

d_{nom} = 10 mm
$F_{t;u;rep}$ = 5,23 kN (zie berekening houtdraadbouten)
$F_{t;u;d}$ = 3,7 KN

Lokale windzuiging:

p_w = 0,86 kN/m²
C_{dim} = 1
$C_{pe;loc}$ = -1 C_{eq} = 1
C_{pi} = -0,3 ϕ_0 = 1
$p_{w;rep}$ = {(-1) + (-0,3)} x 0,86 kN/m²
= -1,12 kN/m²

Permanent:

$p_{g;rep}$ = 0,67 kN/m²

Rekenwaarde belasting:

p_d = 0,9 x (0,67x cos37,5°) + 1,3 x (-1,12)
= -0,98 kN/m²
Dakstrook = 5,7 m¹

F_d = -5,59 kN/m²

Kracht per houtdraadbout:

$F_{t;d}$ = 0,62 m¹ x -5,59
= -3,47 kN/bout

u.c. = 0,94 **(<1,0 akkoord)**

Overzicht belastingen evenwijdig en loodrecht op het dakvlak

Reacties fundamentele combinaties: (in kN/m¹)							
Richting:	FC 1	FC 2	FC 3	FC 4	FC 5	FC 6	
Horizontaal naar buiten (-)	-0,73	0,00	0,00	0,00	0,00	0,00	
Horizontaal naar binnen (+)	0,00	3,65	0,65	2,76	0,00	0,00	
Verticaal naar buiten (+)	0,00	1,98	0,00	2,16	0,00	0,00	
Verticaal naar binnen (-)	-0,40	0,00	-1,61	0,00	0,00	0,00	
Evenwijdig aan dakvlak	**-0,82**	**4,1**	**-0,47**	**3,5**	**0**	**0**	(+ = omhoog)
Loodrecht op dakvlak	**0,12**	**-0,65**	**-1,67**	**0,04**	**0**	**0**	(+ = buiten)

Maximale waarden per houtdraadbout:

$F_{v;d,\ //\ omhoog}$ = 0,5084 kN/bout toepassen houtdraadbouten ø 10 h.o.h. 620 mm¹
$F_{v;d,\ //\ omlaag}$ = 2,542 kN/bout (op te nemen door knellat)

$F_{t;d,\ \perp\ naar\ buiten}$ = 1,0354 kN/bout
$F_{t;d,\ \perp\ naar\ binnen}$ = 0,0744 kN/bout (op te nemen door knellat)

SM

Muurplaat

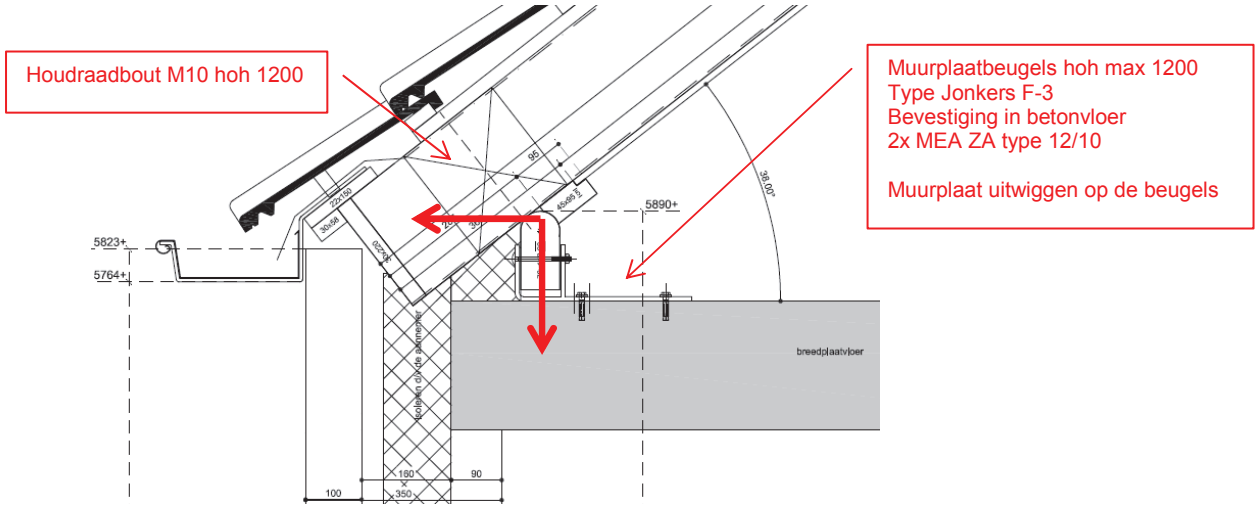

1. Geometrie

Afmeting spoor:

Afmeting muurplaat:

Afmeting stuikregel:

Dikte plaatmateriaal:

Dakhelling:

Variabelen:

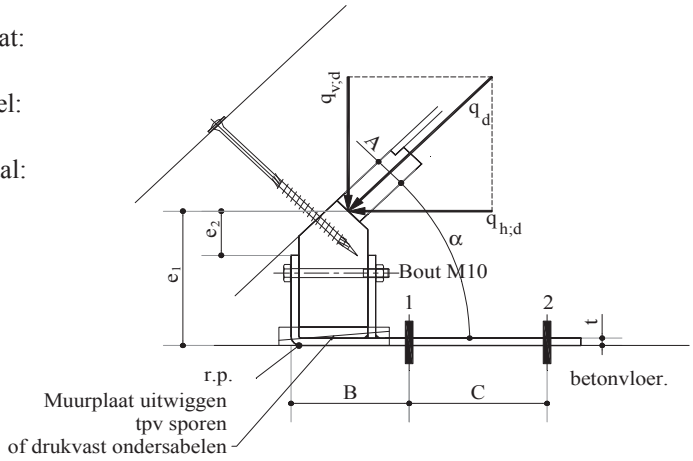

b:	30	mm
h:	220	mm
b:	70	mm
h:	140	mm
b:	45	mm
h:	95	mm
d:	11	mm
α:	38	graden
A:	38	mm (stuikr.)
B:	120	mm (rand)
C:	150	mm (tussen)
e_1:	140	mm
e_2:	40	mm

2. Belastingen

Normaalkracht spoor (inclusief veiligheidsfactoren), N_d:	2,1	kN
H.o.h. afstand spoor:	610	mm
Belasting per strekkende meter, $q_d = N_d * 1000$ /hoh afst. spant =	3,44	kN/m

Reacties

	comb.	R_x (kN)	R_z (kN)	$q_{h;d}$ (kN/m^1)	$q_{v;d}$ (kN/m^1)
druk	2	1,6	1,3	2,69	2,05
trek					

3. Houtkwaliteit

Houtsterkteklasse (C14 t/m C50):	C18	
Treksterkte (rep.) loodrecht op de vezel, $f_{t;90;rep}$:	0,50	N/mm^2
Druksterkte (rep.) loodrecht op de vezel, $f_{c;90;rep}$:	2,20	N/mm^2
K_{mod}:	0,90	
Materiaalfactor, γ_m:	1,30	
Treksterkte loodrecht op de vezel, $f_{t;90;ud} = (f_{t;90;rep}*K_{mod})/\gamma_m$:	0,35	N/mm^2
Druksterkte loodrecht op de vezel, $f_{c;90;ud} = (2*f_{c;90;rep}*K_{mod})/\gamma_m$:	3,05	N/mm^2

4. Verankering (standaard type F1)

Stripafmeting:	b:	80	mm
	t:	8	mm
Type vloer (MO=Monoliet, KA=Kanaalplaatvloer)		KA	
Totaal aantal ankers: MEA ZA, type 12/-- -M8 of gelijkwaardig		2	

Reductiefactoren/anker:

Anker:	$F_{bu;rep}$ [kN]	Randafst.:	Tussenafst.:	Red. rand.:	Red. hoh.:	Σred.:	$F_{bu;d}$ [kN]*	
1	6	120	150	0,92	0,84	0,77	4,00	kN
2	6	270	150	1,00	0,84	0,84	4,00	kN

Momentcapaciteit per stripbeugel, $M_{u;strip} = 2*^1/4*b*t^2*235*10^{-6}$:		0,602	kNm
Optredend moment, $M_{h1;d} = q_{h,d} * e_1 - q_{v;d} * 0,667 * b_{muurplaat}$ =		0,28	kNm/m
Maximale h.o.h. afstand stripbeugels:	<	2143	mm
Gekozen h.o.h. afstand stripbeugels:		1200	mm

*: I.g.v. kanaalplaatvloer, $F_{bu,rep} < 4$ kN.

5. Toetsing muurplaatdetail

5.1 Trekspanning in muurplaat (berekend per m.):

A:			70000	mm^2	
$W_y = 1/6*b*h^2$ =			816667	mm^3	
$M_{h2;d} = q_{h;d}*e_2$ =			0,11	kNm/m	
$q_{v;d} = \sin\alpha * q_d$ =			2,05	kN/m	
$\sigma_{t;90;d} = -\frac{M_{h2;d}}{W_y} + \frac{q_{v;d}}{A}$ =	0,13	+ -0,03 =	0,10	N/mm^2	trekspanning
$f_{t;90;ud}$:			0,35	N/mm^2	

UC1 = $f_{c;90;ud} / \sigma_{c;90;d}$	**0,30**	**< 1.00 : OK**	

5.2 Spanning in 1 beugel:

Momentcapaciteit /stripbeugel, $M_{u;strip} = 2*^1/4*b*t^2*235*10$	0,60	kNm	
Optredent moment, $M_{h1;d} = q_{h,d} * e_1$ =	0,28	kNm/m	
Optr. moment/ beugel, $M_{b;d}$ = ($M_{h1;d}$ * hoh afst. beugels)/100	0,34	kNm	

UC2 = $M_{b;d} / M_{u;strip}$ =	**0,56**	**< 1.00 : OK**	

5.3 Drukspanning houten oplegregel (berekend per spoor):

A = Maat "A" * 2/3 * h.o.h afst. spoor =	15453	mm^2	
$\sigma_{c;90;d} = N_d / A$ =	0,14	N/mm^2	
$f_{c;90;ud}$ =	3,05	N/mm^2	

UC3 = $f_{c;90;ud} / \sigma_{c;90;d}$	**0,04**	**< 1.00 : OK**	

Edisonweg 3, 8501 XG Joure
Tel: 0513-434202 / Fax: 0513-434227
E-mail: info@tekwoods.nl

5.4 Trekcapaciteit anker 1:

Optr. moment/ beugel, $M_{b;d}$ = ($M_{h1;d}$ * hoh afst. beugels)/10(	0,34	kNm	
Trekbelasting anker 1, $F_{t1;d} = \frac{M_{b;d}}{(B-t)}$ =	3,01	kN	trek in anker 1
Capaciteit anker 1, $F_{bu,d}$ =	4,00	kN	
UC4 = $F_{t1;d}$ / $F_{bu;d}$ =	**0,75**	**<**	**1.00 : OK**

5.5 Afschuifcapaciteit anker 2:

Afschuifbel. anker 2, $F_{h1;d}$ = ($q_{h;d}$ * hoh afst. beugels) / 1000	3,23	kN	
Capaciteit anker 2, $F_{bu,d}$ =	4,00	kN	
UC5 = $F_{h1;d}$ / $F_{bu;d}$ =	**0,81**	**<**	**1.00 : OK**

Algemeen:

Afmeting muurplaat:	70 ×	140	mm² (rond)
Afmeting oplegregel	45 ×	95	mm²
dikte plaatmateriaal		11	mm
stelruimte onder muurplaat		15	mm
dakhelling		38	graden
h.o.h beugels		750	mm

Maatgevende U.C. 0,97

Hout:

Houtsterkteklasse:	C18
k_{mod}	0,85
$f_{t;90;u;d}$	0,31 N/mm²
$f_{c;90;t;d}$	3,12 N/mm²

Staal

Staalkwaliteit S 235

Geometrie

t_{staal}	10	mm	A	157	mm
a_{las}	4	mm	B	57	mm
breedte	80	mm	C	90	mm
$d_{gat\ anker}$	14	mm	D	57	mm
			E	13	mm
$e_{Fv;\ muurplaat}$	22,2	mm	F	45	mm
$e_{FH;\ muurplaat\ vlak\ B}$	57,1	mm	G	55	mm
			H	170	mm
Ankers:	Fischer FHII M8NL, FHY M8, Spit Dynabolt M10*55 of MEA ZA/S		I	30	mm
h.o.h. afstand	= 170	mm	J	300	mm
randafstand	= 100	mm	K	0	mm
$F_{bu;d}$	= 2,50	kN			

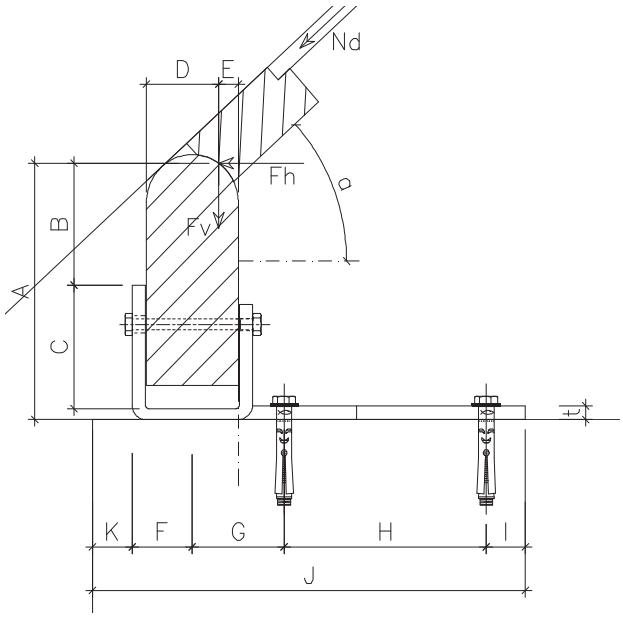

bouten bevestiging muurplaat aan F-anker

Diameter	=	8	mm
Lengte	=	100	mm
aantal	=	1	stuks
$F_{v;u;d}$	=	3,29	kN/bout

(Technosoft) h.o.h. stijlen: 0,61 m

Belastingen	C1 (max $F_{H)}$	C2 (Max $F_{V)}$	C3 min(Neg)
$F_{H;d}$ (kN)	1,89	1,89	-0,27
$F_{V;d}$ (kN)	1,49	1,49	-0,05

Belastingen per meter

	C1	C2	C3
$F_{H;d}$ (kN/m)	**3,10**	**3,10**	**-0,44**
$F_{V;d}$ (kN/m)	**2,44**	**2,44**	**-0,08**

Controle spanningen in schotjes (positieve krachten) (**Strip 80 × 10**)

$M_{d;\ 1\ strip}$	= 3,10 ×	0,750 ×	0,157	=	0,37	kNm per strip		
$W_{elastisch}$	= 1/6 ×	80 ×	10^2	=	1333,33	mm³		
$W_{elastisch}$	= 1/6 ×	25 ×	10^2	=	416,667	mm³ +		
					1750,00	mm³		
$M_{y;u;d;\ opneembaar}$	= 235 ×	1750,00 /	10^6	=	0,41	kNm per strip	**U.C. =** **0,89**	**Voldoet**

Controle spanningen in lassen volgens NEN 6770

t	= 10	mm	β	=	0,8	lasfactor	
a_{las}	= 4	mm	$f_{t;d}$	=	360	N/mm²	
$l_{t;ef}$	= 80	mm	$f_{w;u;d}$	=	207	N/mm²	
Spanningen in las afschuiving			Spanningen in las moment				
$F_{s;d}$	= 1,16	kN	$M_{s;d}$	=	0,18	kNm	
σ_l	= 1,28	N/mm²	σ_l	=	29,29	N/mm²	
τ_l	= 1,28	N/mm²	τ_l	=	29,29	N/mm²	
τ_2	= 0,00		τ_2	=	0,00		
			b*	=	13,77	mm	
$\sigma_{w;s;d}$	= 35,30	N/mm²	< $f_{w;u;d}$	=	207	N/mm²	**U.C. =** **0,17** **Voldoet**

Controle spanningen vlak A in F-anker (negatieve krachten)

$F_{H;d}$	= -0,33	kN	$e_{FH\ t.o.v.\ A}$	=	152,088	mm		
$F_{v;d}$	= -0,06	kN	$e_{FV;To.v.\ A}$	=	32,8359	mm		
			$M_{t.o.v.\ A}$	=	-0,053	kNm		
$Wy_{;beugel;pl}$	= ¼×b×h² =	0,25 ×	66 × 10 ^2	=	1650	Nmm³		
$\sigma_{s;d}$	= 1,00 ×	52507 /	1650	=	31,82	N/mm²		**Voldoet**
$f_{t;u;d}$	= 235	N/mm²					**U.C. =** **0,14**	-

Controle anker ter plaatse van vlak A en vlak B

Fischer FHII M8NL, FHY M8, Spit Dynabolt M10*55 of MEA ZA/S12 (og)

Vloertype	=	kanaalplaat	
F_{bu}	=	2,5	kN
h.o.h. afstand	=	170	mm
randafstand	=	100	mm
reductie rand	=	n.v.t	-
reductie h.o.h.	=	n.v.t	-
Betonkwaliteit minimaal		C45/55	
$F_{bu;d}$	=	2,50	kN

$F_{H;d1}$	=	2,32	kN	$e_{FH\ t.o.v.\ C}$	=	157	mm
$F_{V;d1}$	=	1,83	kN	$e_{FV;To.v.\ C}$	=	67	mm
$M_{d;1;t.o.v.C}$	=	0,24	kNm	$e_{anker\ A;\ t.o.v.\ C}$	=	100	mm
$F_{axiaal;d;anker\ A}$	=	2,42	kN/anker	$F_{axiaal;d;anker\ B}$	=	0,00	kN/anker
$F_{afschuiving;d;Anker\ A}$	=	0,00	kN/anker	$F_{afschuiving;d;Anker\ B}$	=	2,32	kN/anker
$F_{id;A}$	=	2,42	kN	$F_{id;A}$	=	2,32	kN

U.C. = 0,97 Voldoet **U.C. = 0,93** **U.C. = 0,97 Voldoet**

Controle buiging vlak D in muurplaat t.g.v. Combinatie 1

							trekspanning			
$M_{d1;tgv\ FH}$	=	0,057	×	3,10	=	0,18 kNm/m	$\sigma_{t;90;d}$	=	0,22	N/mm²
$M_{d2;tgv\ FV}$	=	-0,022	×	2,44	=	-0,05 kNm/m	$\sigma_{t;90;d}$	=	-0,07	N/mm²
$F_{V;d1}$	=				=	-2,44 kN/m	$\sigma_{t;90;d}$	=	-0,03	N/mm²
							$\sigma_{t;90;d}$	=	0,12	N/mm² **U.C. = 0,37 Voldoet**
							$f_{t;90;u;d}$	=	0,31	N/mm²

Controle buiging vlak D in muurplaat t.g.v. combinatie 2

$M_{d1;tgv\ FH}$	=	0,057	×	3,10	=	0,18 kNm/m	$\sigma_{t;90;d}$	=	0,22	N/mm²
$M_{d2;tgv\ FV}$	=	-0,022	×	2,44	=	-0,05 kNm/m	$\sigma_{t;90;d}$	=	-0,07	N/mm²
$F_{V;d1}$	=				=	-2,44 kN/m	$\sigma_{t;90;d}$	=	-0,03	N/mm²
							$\sigma_{t;90;d}$	=	0,12	N/mm² **U.C. = 0,37 Voldoet**
							$f_{t;90;u;d}$	=	0,31	N/mm²

Controle muurplaat vlak D t.g.v. BG 3

							Trekspanningen			
$M_{d3;\ tgv\ FH}$	=	0,057	×	-0,44	=	-0,0253 kNm/m	$\sigma_{t;90;d}$	=	0,03	N/mm²
$M_{d4;tgv\ FV}$	=	0,022	×	-0,08	=	-0,0018 kNm/m	$\sigma_{t;90;d}$	=	0,00	N/mm²
$F_{v;3}$	=				=	-0,0820 kN/m	$\sigma_{t;90;d}$	=	0,00	N/mm²
$\sigma_{t;90;d}$	=						$\sigma_{t;90;d}$	=	0,03	N/mm² **Voldoet**
							$f_{t;90;u;d}$	=	0,31	N/mm² **U.C. = 0,11 -**

Controle aansluiting beugel - muurplaat (drukkracht)

$F_{H;d}$	=	2,32	kN	A	=	80 ×	90	=	7200	mm²
$\sigma_{c;90;d}$	=	0,32	N/mm²							
$f_{c;90;u;d}$	=	3,12	N/mm²							**U.C. = 0,10 Voldoet**

Controle bevestiging muurplaat - F-anker

Muurplaat bevestigen aan anker dmv bout

Diameter:	8	mm	$F_{v;u;d}$	=	**3,29**	kN/bout	
Lengte	100	mm	$F_{v;u;d;tot}$	=	3,29	kN	
aantal	1	stuks	$F_{v;d}$	=	-0,06	kN	**U.C. = 0,02 Voldoet**

Appendix 3.1

For a couple of standard roof structures, the formula for determining the eccentricity of the internal bending moment of the wall plate is applied. The following roof structures are considered:

- 35 degrees roof inclination
- 45 degrees roof inclination
- 55 degrees roof inclination

Properties of an exemplary connection detail:

Depth of wall plate h_{wp}	144mm	**Thickness of bracket t_F**	10mm
Width of wall plate b_{wp}	70mm	**Width of bracket b_F**	80mm
Adding t_a	10mm	**Chi**	0,9
Depth of baffles h_b	100mm	**CTC bracket**	1200mm
$f_{c,90}$	2,5N/mm^2		

Table A3.1a; *Specifications for the exemplary connection detail*

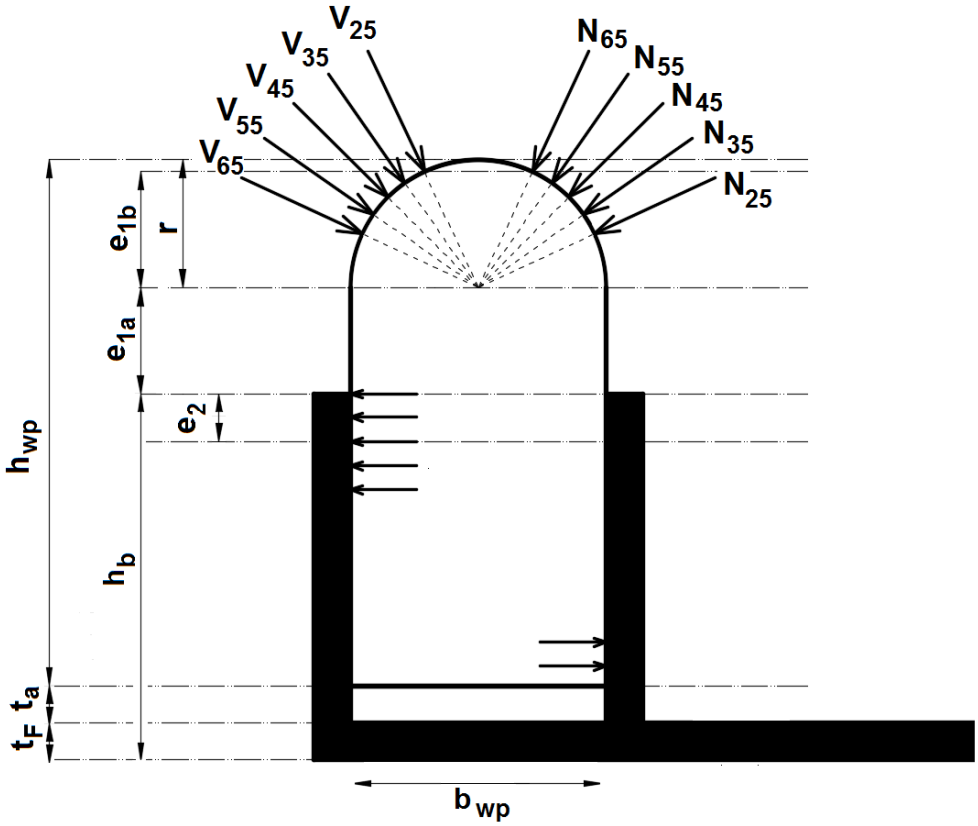

Figure A3.1a; *Corresponding dimensions to the properties shown in* ***table A3.1a***

The formula for determining the eccentricity is as follows:

$$e = h_{wp} + t_a + t_F - \tfrac{1}{2} \cdot b_{wp} - h_b + \sin(\alpha) \cdot \tfrac{1}{2} \cdot b_{wp} + \frac{(1+\chi) \cdot H}{2 \cdot b_F \cdot f_{c,90}} \qquad \text{(A3.1.1)}$$

All variables are known, except for chi (χ) and the axial force (H). The latter is dependent on the roof angle. Values for the loading are taken from **chapter 3.3**:

Roof inclination	Axial load / meter (H)	Axial load / bracket
35 degrees	5,323 kN/m	6,387 kN/bracket
45 degrees	3,872 kN/m	4,646 kN/bracket
55 degrees	2,983 kN/m	3,580 kN/bracket

Table A3.1b; *Overview of the axial, either per meter or per bracket with a CTC of 1200mm*

The value for chi is obtained by using **figure A3.1b** and formula for calculating psi:

$$\psi = \frac{h_{wp} + t_a + t_F - h_b}{h_{wp}} = \frac{144mm + 10mm + 10mm - 100mm}{144mm} = 0,444 \qquad \text{(A3.1.2)}$$

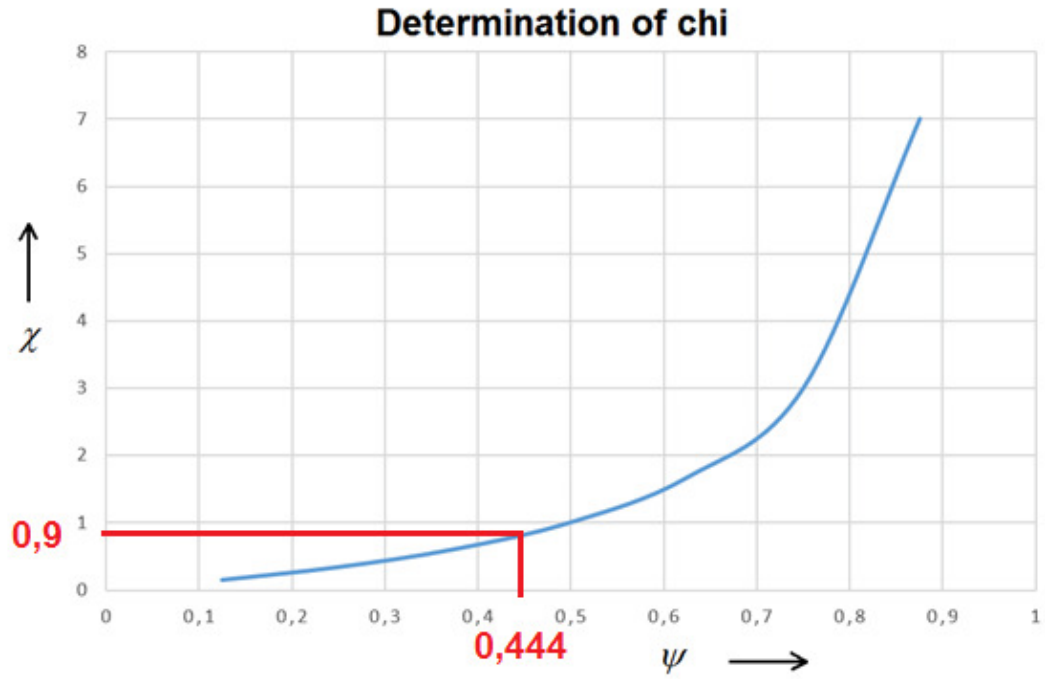

Figure A3.1b; *Determination of chi with psi*

Now the eccentricities can be calculated, using formula **A3.1.1**:

- 35 degrees roof inclination

$$e_{35} = 140mm + 10mm + 10mm - \tfrac{1}{2} \cdot 70mm - 100mm + \sin(35^o) \cdot \tfrac{1}{2} \cdot 70mm + \frac{(1+0,9) \cdot 6387N}{2 \cdot 80mm \cdot 2,5N/mm^2}$$

$$e_{35} = 79,41mm$$

- 45 degrees roof inclination

$$e_{45} = 140mm + 10mm + 10mm - \tfrac{1}{2} \cdot 70mm - 100mm + \sin(45^o) \cdot \tfrac{1}{2} \cdot 70mm + \frac{(1+0,9) \cdot 4646N}{2 \cdot 80mm \cdot 2,5N/mm^2}$$

$$e_{45} = 75,82mm$$

- 55 degrees roof inclination

$$e_{55} = 140mm + 10mm + 10mm - \tfrac{1}{2} \cdot 70mm - 100mm + \sin(55^o) \cdot \tfrac{1}{2} \cdot 70mm + \frac{(1+0,9) \cdot 3580N}{2 \cdot 80mm \cdot 2,5N/mm^2}$$

$$e_{55} = 74,68mm$$

Appendix 3.2

This appendix contains the determination of the live and dead load on the construction, as well as the calculation of the axial and shear load of the structure.

Determination of the dead load

Properties roof element:

Width of the rafter:	30mm
Depth of the rafter:	220mm
Center-to-center distance of rafters:	600mm
Type of roof tiles:	Ceramic
Thickness of the supporting panel:	11mm
Material of the supporting panel:	particle board
Roof inclination:	35/45/55 degrees

Roof tiles	=	0,41kN/m^2
Vertical and horizontal battens	=	0,06 kN/m^2
Rafters	=	0,05 kN/m^2
Isolation	=	0,00 kN/m^2
Supporting panel	=	0,08 kN/m^2 +
Total	**=**	**0,60 kN/m^2**

Values for the weight of the materials are based on values used in project 2 of **appendix 2.1**.

Live load

Type of load:	snow
Load combination:	symmetrical
Roof inclination:	35/45/55 degrees

Snow load = $\mu_1 \cdot C_e \cdot C_t \cdot s_k$

$\mu_{1;35} = 0{,}666;\ \mu_{1;45} = 0{,}4;\ \mu_{1;55} = 0{,}133$

$C_e = 1{,}0$

$C_t = 1{,}0$

s_k =0,7kN/m^2

Snow load 35 degrees = 0,47kN/m^2
Snow load 45 degrees = 0,28kN/m^2
Snow load 55 degrees = 0,09kN/m^2

Values for the determination of the snow load are based on **NEN-EN 1991-1-3 [Bron].**

Roof inclination 35 degrees SLS

The roof structure has the following properties:

Dead load q_G	0,60kN/m²	**Length of structure (L)**	4500mm
Snow load: q_{snow}	0,47kN/m²	**Length a (La)**	3686mm
Roof angle (alpha)	35 degrees	**Length b (Lb)**	2581mm

TableA3.2a; *structure properties*

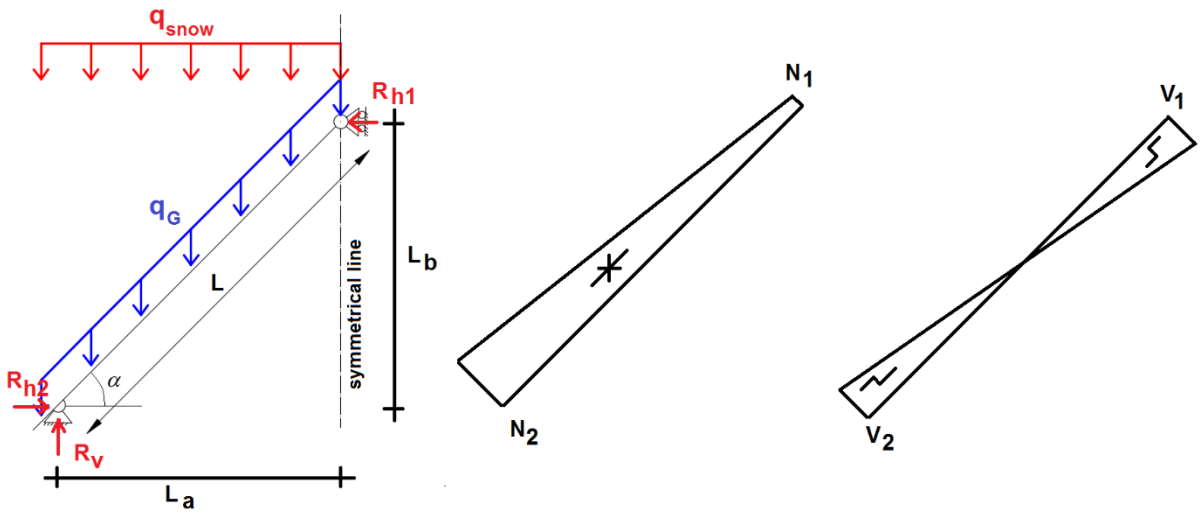

Figure A3.2a; *Left: geometry of the structure. Right: distribution of the axial and shear forces*

To obtain values for N_2 and V_2, equilibrium for the external forces on a structure is applied:

$$\Sigma H = 0 \rightarrow R_{H1} = R_{H2}$$

$$\Sigma V = 0 \rightarrow R_v = q_G \cdot L + q_{snow} \cdot L_A$$

$$R_v = 0,60kN/m^2 \cdot 4,5m + 0,47kN/m^2 \cdot 3,686m = 4,432kN/m$$

$$\Sigma M_1 = 0 \rightarrow R_V \cdot L_A = R_{H2} \cdot L_B + q_G \cdot L \cdot 0,5 \cdot L_A + q_{snow} \cdot 1,5 \cdot L_A$$

$$R_{H2} = \frac{R_V \cdot L_A - q_G \cdot L \cdot 0,5 \cdot L_A - q_{snow} \cdot 1,5 \cdot L_A}{L_B} = R_{H1}$$

$$R_{H2} = 3,395kN/m = R_{H1}$$

N2 and V2 result from decomposing R_{H2} and R_V:

$$N_2 = R_V \cdot \cos(55^o) + R_{H2} \cdot \cos(35^o) = 5,323kN/m$$

$$V_2 = R_V \cdot \cos(35^o) - R_{H2} \cdot \cos(55^o) = 1,683kN/m$$

Roof inclination 45 degrees SLS

The roof structure has the following properties:

Dead load q_G	0,60kN/m²	**Length of structure (L)**	4500mm
Snow load: q_{snow}	0,28kN/m²	**Length a (La)**	3182mm
Roof angle (alpha)	45 degrees	**Length b (Lb)**	3182mm

TableA3.2b; *structure properties*

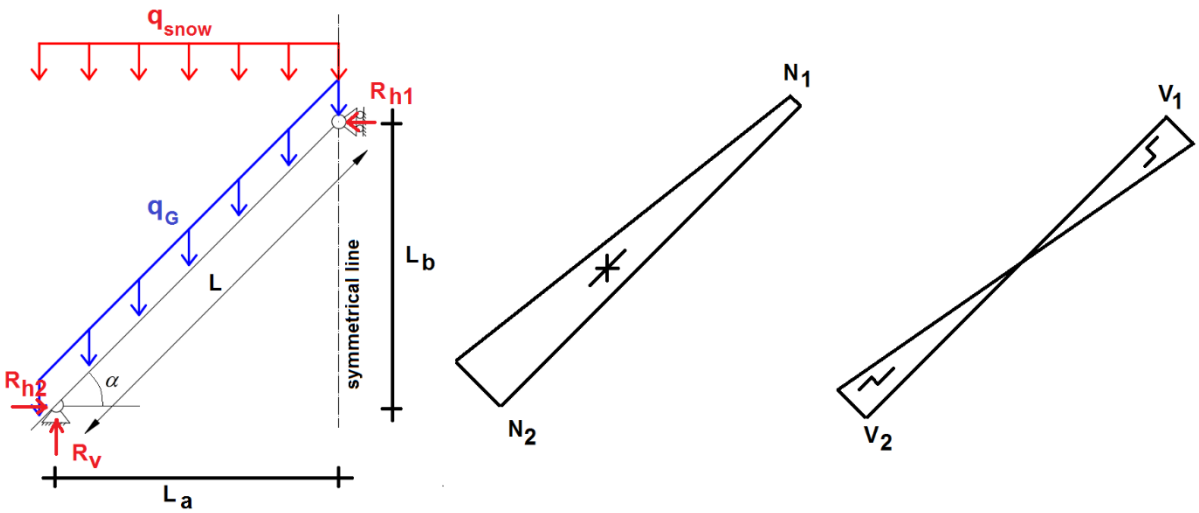

Figure A3.2b; *Left: geometry of the structure. Right: distribution of the axial and shear forces*

To obtain values for N_2 and V_2, equilibrium for the external forces on a structure is applied:

$$\Sigma H = 0 \rightarrow R_{H1} = R_{H2}$$

$$\Sigma V = 0 \rightarrow R_v = q_G \cdot L + q_{snow} \cdot L_A$$

$$R_v = 0,60kN/m^2 \cdot 4,5m + 0,28kN/m^2 \cdot 3,182m = 3,591kN/m$$

$$\Sigma M_1 = 0 \rightarrow R_V \cdot L_A = R_{H2} \cdot L_B + q_G \cdot L \cdot 0,5 \cdot L_A + q_{snow} \cdot 1,5 \cdot L_A$$

$$R_{H2} = \frac{R_V \cdot L_A - q_G \cdot L \cdot 0,5 \cdot L_A - q_{snow} \cdot 1,5 \cdot L_A}{L_B} = R_{H1}$$

$$R_{H2} = 1,821kN/m = R_{H1}$$

N2 and V2 result from decomposing R_{H2} and R_V:

$$N_2 = R_V \cdot \cos(45^o) + R_{H2} \cdot \cos(45^o) = 3,827kN/m$$

$$V_2 = R_V \cdot \cos(45^o) - R_{H2} \cdot \cos(45^o) = 1,252kN/m$$

Roof inclination 55 degrees SLS

The roof structure has the following properties:

Dead load q_G	0,60kN/m²	**Length of structure (L)**	4500mm
Snow load: q_{snow}	0,09kN/m²	**Length a (La)**	2581mm
Roof angle (alpha)	55 degrees	**Length b (Lb)**	3686mm

TableA3.2c; *structure properties*

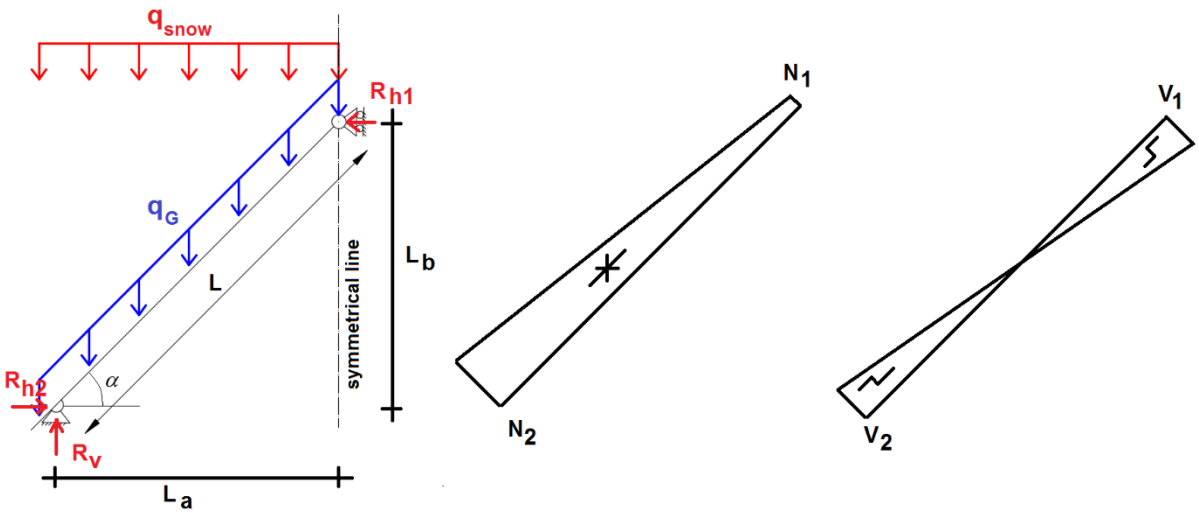

Figure A3.2c; *Left: geometry of the structure. Right: distribution of the axial and shear forces*

To obtain values for N_2 and V_2, equilibrium for the external forces on a structure is applied:

$$\Sigma H = 0 \rightarrow R_{H1} = R_{H2}$$

$$\Sigma V = 0 \rightarrow R_v = q_G \cdot L + q_{snow} \cdot L_A$$

$$R_v = 0,60kN/m^2 \cdot 4,5m + 0,09kN/m^2 \cdot 2,581m = 2,932kN/m$$

$$\Sigma M_1 = 0 \rightarrow R_V \cdot L_A = R_{H2} \cdot L_B + q_G \cdot L \cdot 0,5 \cdot L_A + q_{snow} \cdot 1,5 \cdot L_A$$

$$R_{H2} = \frac{R_V \cdot L_A - q_G \cdot L \cdot 0,5 \cdot L_A - q_{snow} \cdot 1,5 \cdot L_A}{L_B} = R_{H1}$$

$$R_{H2} = 1,013kN/m = R_{H1}$$

N2 and V2 result from decomposing R_{H2} and R_V:

$$N_2 = R_V \cdot \cos(35^o) + R_{H2} \cdot \cos(55^o) = 2,983kN/m$$

$$V_2 = R_V \cdot \cos(55^o) - R_{H2} \cdot \cos(35^o) = 0,852kN/m$$

Appendix 4.1

Calculation of the Young's modulus with the use of a 4 point bending test

The 4 point bending test is used on both the wall plate and the supporting batten. The bending test is schematized with figure A4.1a.

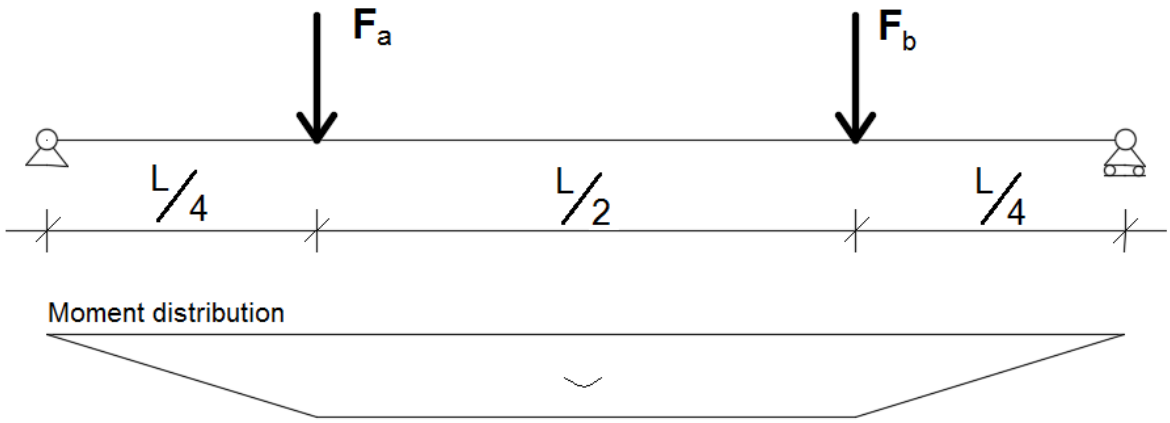

***Figure A4.1a**; Schematized 4 point bending test*

To avoid the specimens receiving any damage due to the 4 point bending test, they are rotated 90 degrees around their axis, so that the support and load introduction have a flat surface.

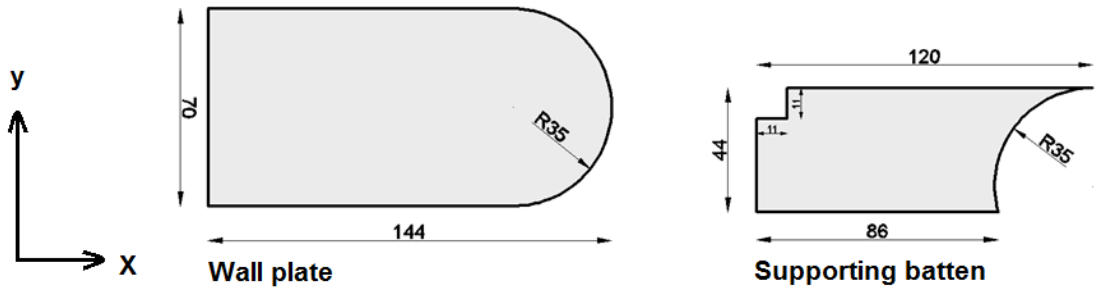

***Figure A4.1b**; Section plane of the rotated wall plate and supporting batten*

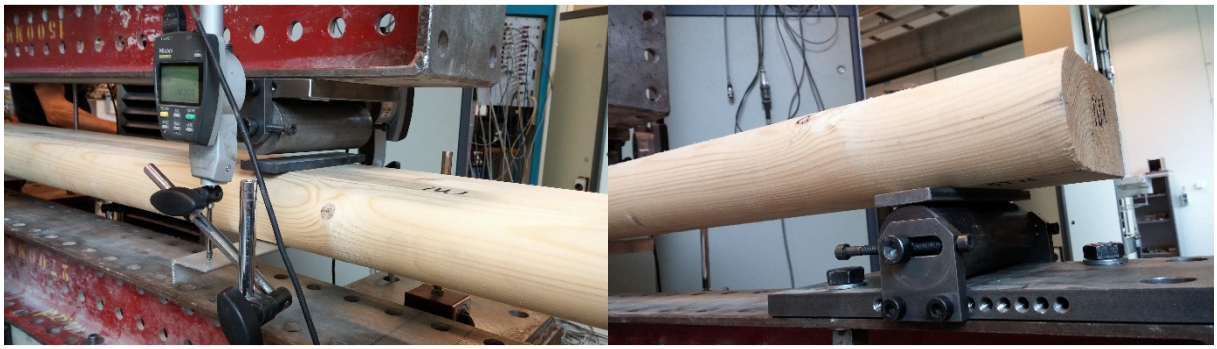

***Figure A4.1c**; Picture of the load introduction (left) and support (right)*

The Young's modulus can be calculated with the following formula:

$$E = \frac{M}{I \cdot \kappa} \qquad \text{(A4.1.1)}$$

With:
M = Constant moment along the curvature
I = Moment of Inertia
κ = Curvature

To fulfill the requirements of this formula, only the section between the forces is considered.

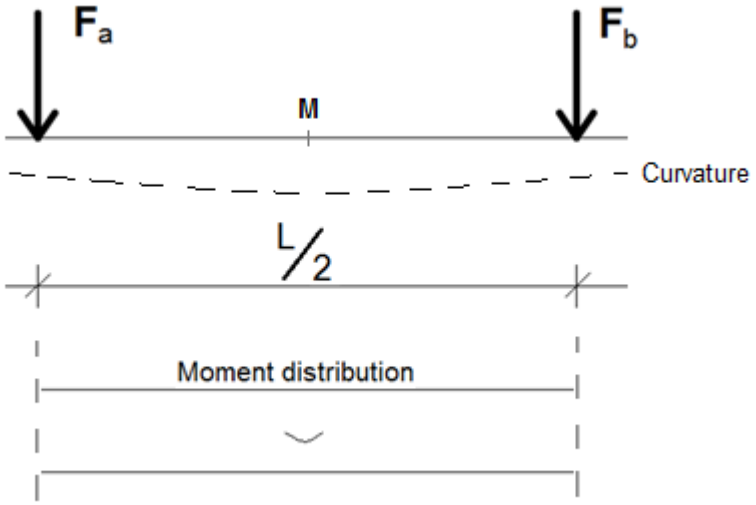

***Figure A4.1d**; Curved section of the specimen with constant moment*

The constant moment is determined with the following formula:

$$M = \frac{F_n \cdot L}{4} \qquad \text{(A4.1.2)}$$

With:
F_n = The force applied on position a or b
L = The length of the specimen = 2400mm

The forces applied to the specimen, with the corresponding moments are as followed:

Specimen	Load F_a (N)	Load F_b (N)	Moment (Nmm)
M1	787,91	787,91	472.748
M2	787,91	787,91	472.748
D1	353,20	353,20	211.918
D2	353,20	353,20	211.918

***Table A4.1a**; Load and moment on the specimen*

The curvature is determined with the following formula:

$$\kappa = \frac{1}{R} \qquad \text{(A4.1.3)}$$

With:

$R =$ Radius of the curvature

The radius is determined with the help of geometrics:

$$R = \frac{L/4}{\cos(\beta - \alpha)} \qquad \text{(A4.1.4)}$$

With:

$$\alpha = \tan^{-1}\left(\frac{w_{max}}{L/4}\right)$$

And

$$\beta = \tan^{-1}\left(\frac{L/4}{w_{max}}\right)$$

And

$L =$ 2400mm
$w_{max} =$ Difference between the deflection of points a and b with mid-span

The radius of the curvature is defined with **figure A4.1e**.

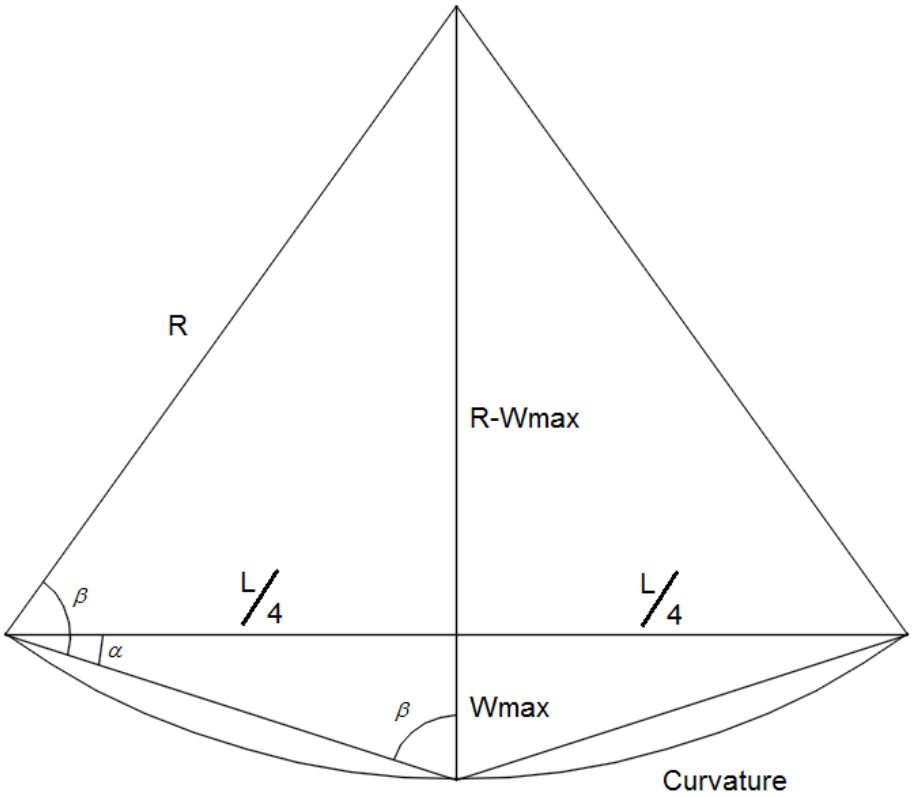

***Figure A4.1e**; Geometry lines to determine the radius of the curvature*

The deflection of points a, b and mid-span are shown in **table A4.1b.** The deflection is measured on two sides of the specimen (left and right). The average value is the average of

left and right. The maximum deflection is the deflection of mid-span minus the average deflection of left and right.

Specimen	W(a,left)	W(a,right)	W(a,av.)	W(b,left)	W(b,right)	W(b,av.)
M1	8,340	5,503	6,922	7,567	5,768	6,668
M2	5,993	6,191	6,092	5,105	7,578	6,342
D1	5,880	5,865	5,873	5,880	5,527	5,704
D2	5,816	5,227	5,522	5,076	5,579	5,328

***Table A4.1b (1)**; Deflection of points a and b in millimeters*

Specimen	W(M,left)	W(M,right)	W(M,av.)	W(a+b,av.)	**W(max)**
M1	9,952	7,880	8,916	6,795	**2,121**
M2	7,460	8,724	8,092	6,217	**1,875**
D1	8,049	7,848	7,949	5,788	**2,161**
D2	7,287	7,149	7,218	5,425	**1,793**

***Table A4.1b (2)**; Deflection of mid-span and Wmax*

By inserting the value of w_{max} into **formula A4.1.3 and A4.1.4** the curvature is determined:

Specimen	β (°)	α (°)	β – α (°)	R (mm)	**κ (-)**
M1	89,797	0,203	89,595	84.856	**$1{,}17846e^{-5}$**
M2	89,821	0,179	89,642	95.993	**$1{,}04174e^{-5}$**
D1	89,794	0,206	89,587	83.315	**$1{,}20026e^{-5}$**
D2	89,829	0,171	89,657	100.366	**$9{,}96352e^{-6}$**

***Table A4.1c**; Determination of the curvature*

The final variable that needs to be determined is the moment of Inertia for both specimen.

- Moment of Inertia of the wall plate

The moment of Inertia of the wall plate can be determined by adding the moment of Inertia of two separate sections of the wall plate, shown in **figure A4.1f**:

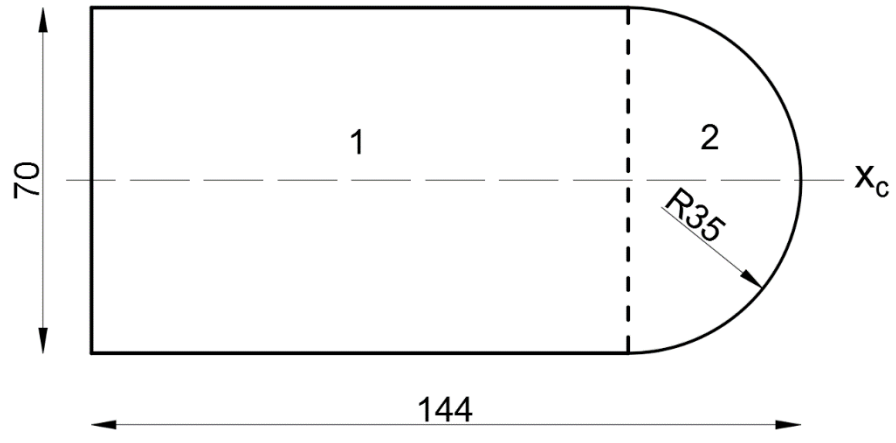

***Figure A4.1f**; Cross section of the wall plate, divided in two sections*

The centroid of both sections, as well as the wall plate itself is located at the same place. Therefore the moment of Inertia are simply added:

$$I_x = I_{x,1} + I_{x,2} \qquad \text{(A4.1.5)}$$

With:

$I_{x,n}$ = Moment of Inertia of a certain part of the section plane (**Fig A4.1f**)

$$I_x = \frac{1}{12} \cdot 109mm \cdot (70mm)^3 + \frac{1}{8} \cdot \pi \cdot (35mm)^4 = 3.704.877mm^4$$

- Moment of Inertia of the supporting batten

To determine the moment of inertia of the supporting batten, Steiner's law **[bron]** is applied:

$$I_x = I_{x,1} + (z_1)^2 \cdot A_1 - I_{x,2} - (z_2)^2 \cdot A_2 - I_{x,3} - (z_3)^2 \cdot A_3 - I_{x,4} - (z_4)^2 \cdot A_4 \qquad \text{(A4.1.6)}$$

With:

$I_{x,n}$ = Moment of Inertia of a certain part of the section plane (**Fig A4.1g**)

z_n = Distance between the centroid of section n and the centroid of the supporting batten

A_n = Surface of section n

Before the formula can be solved, the centroid of the section plane needs to be defined. F**igure A4.1g** is used to clarify the issue:

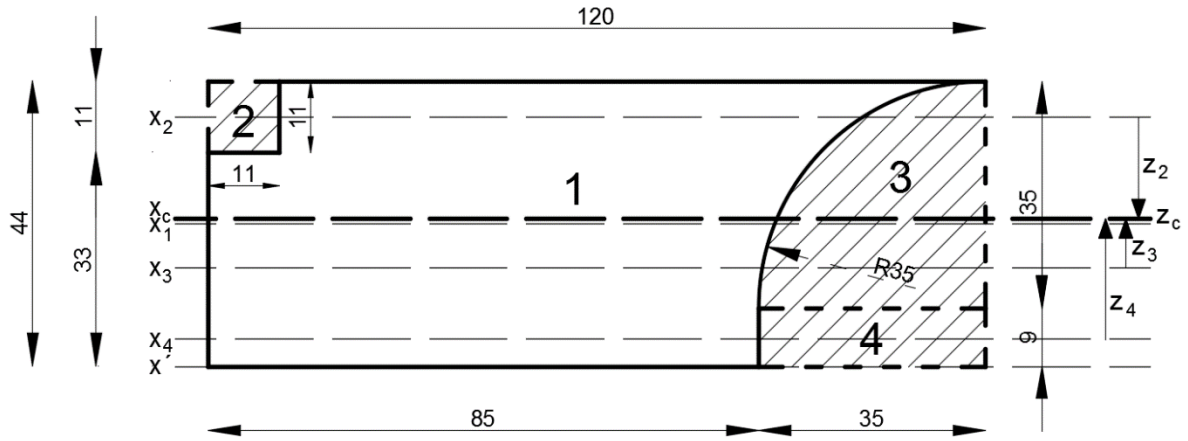

***Figure A4.1g**; The sections of the supporting batten's cross section. Note: section 1 is 120mm x 44mm*

The centroid of the supporting batten is determined as follows:

$$z_c = \frac{S_{x'}}{A_{sb}} \qquad \text{(A4.1.7)}$$

With:

$S_{x'}$ = Linear surface moment of the supporting batten to line x'

A_{sb} = Section area of the supporting batten

And:

$$S_{x'} = z_1' \cdot A_1 - z_2' \cdot A_2 - z_3' \cdot A_3 - z_4' \cdot A_4$$

$$A_{sb} = A_1 - A_2 - A_3 - A_4$$

With:

z_n' = Distance between the centroid of section n to line x'

	z_1' (mm)	z_2' (mm)	z_3' (mm)	z_4' (mm)	A_1 (mm)	A_2 (mm)	A_3 (mm)	A_4 (mm)
D1+D2	22	38,5	23,854	4,5	5280	121	962	315

***Table A4.1d**; Distance between center lines and line x'; surface area of sections 1 to 4*

This results in:

$$z_c = \frac{S_{x'}}{A_{sb}} = \frac{87.133mm^3}{3882mm^2} = 22,445mm$$

Now the distance of each section's centroid to the centroid of the supporting batten can be determined. Also the moment of Inertia for each section is given:

	z_1 (mm)	z_2 (mm)	z_3 (mm)	z_4 (mm)	I_{x1} (mm^4)	I_{x2} (mm^4)	I_{x3} (mm^4)	I_{x4} (mm^4)
D1+D2	0,445	16,055	1,4	17,945	851.840	1.220	294.647	2126

***Table A4.1e**; Distance between center lines of sections 1 to 4 and center line of the supporting batten; Moment of Inertia of sections 1 to 4*

By inserting all variables into **formula A4.1.6**, the moment of Inertia of the supporting batten is given:

$$I_x = 420.381mm^4$$

Finally the modulus of Elasticity can be determined:

$$E = \frac{M}{I \cdot \kappa} \qquad \text{(A4.1.1)}$$

Specimen	Moment M (Nmm)	Curvature κ (-)	Inertia I_x (mm4)	**E (N/mm^2)**
M1	472.748	1,17846e^{-5}	3.704.877	**10.828**
M2	472.748	1,04174e^{-5}	3.704.877	**12.249**
D1	211.918	1,20026e^{-5}	420.381	**10.500**
D2	211.918	9,96352e^{-6}	420.381	**12.649**

***Table A4.1f**; All parameters for determining the modulus of Elasticity of each specimen*

Appendix 4.2

This appendix includes all contributing experimental tests performed in the laboratory.

Several different test set-ups have been tested. The assemblies may differ in roof angle, position of the wall plate in the bracket (amount of adding), center-to-center distances of the F-brackets and the usage of the coach screw. Every specific assembly has been tested three times. The first attempt serves as a test round, to check if all adjustments have been performed properly, and is therefore not included in the results. The successive attempts are mentioned as test A and test B. The following tests are included:

	Roof Angle (degrees)	Center-to-center distance (mm)	Adding (mm)	Coach screw
35/600/L/A	35	600	10	no
35/600/L/B	35	600	10	no
35/900/L/A	35	900	10	no
35/900/L/B	35	900	10	no
35/1200/L/A	35	1200	10	no
35/1200/L/B	35	1200	10	no
45/600/L/A	45	600	10	no
45/600/L/B	45	600	10	no
45/900/L/A	45	900	10	no
45/900/L/B	45	900	10	no
45/1200/L/A	45	1200	10	no
45/1200/L/B	45	1200	10	no
45/600/H/A	45	600	30	no
45/600/H/B	45	600	30	no
45/900/H/A	45	900	30	no
45/900/H/B	45	900	30	no
45/1200/H/A	45	1200	30	no
45/1200/H/B	45	1200	30	no
45/1200/L/CS/A	45	1200	10	yes
45/1200/L/CS/B	45	1200	10	yes
55/600/L/A	55	600	10	no
55/600/L/B	55	600	10	no
55/900/L/A	55	900	10	no
55/900/L/B	55	900	10	no
55/1200/L/A	55	1200	10	no
55/1200/L/B	55	1200	10	no

***Table A4.2a**; Overview of all performed tests*

Specifications of the assemblies

- Adding, roof angle and center-to-center distances

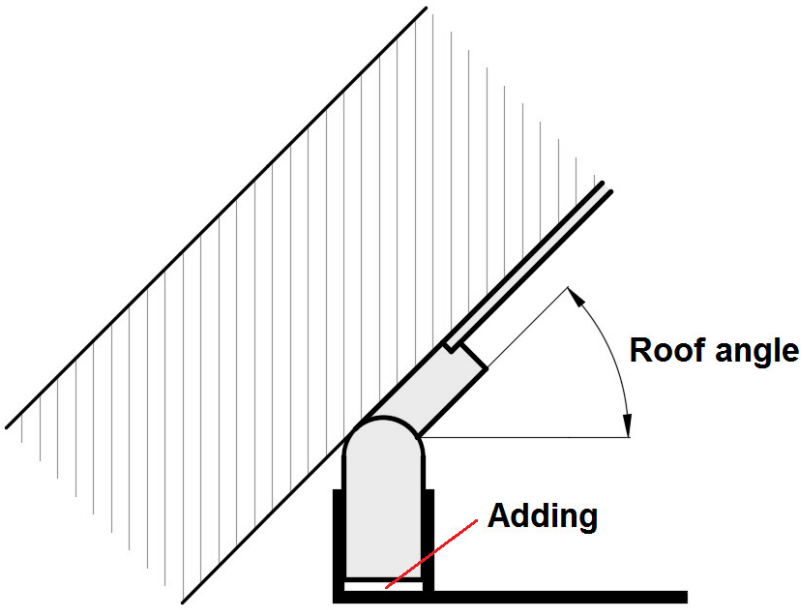

***Figure A4.2a**; Section of the detail to indicate the change in roof angle and adding*

Figure A4.2a gives an attempt to clarify the position of the adding and the variety of roof pitch. The following roof angles are used: 35º, 45º and 55º. The adding of the wall plate is either 10mm (low) or 30mm (high). **Figure A4.2b** demonstrates a top view of the wall plate and brackets. The dotted red line indicates the position of the strain gauge, the dotted blue line presents the position of the rafters. All dimensions are in millimeters.

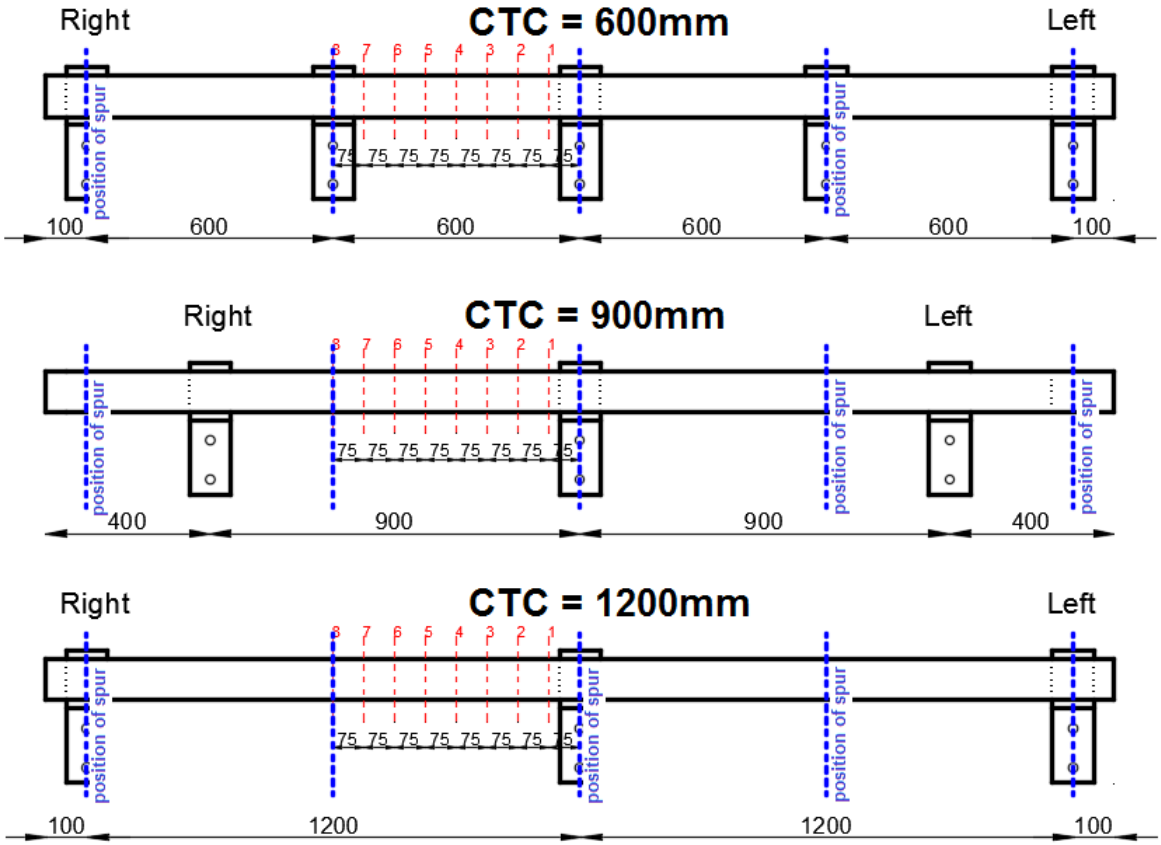

***Figure A4.2b**; Top view of the wall plate and brackets concerning different center-to-center distances*

- Coach screw

The test are performed with and without the use of the coach screw. In case the coach screw has been used, a pre-compression of 2kN has been performed to connect the wall plate with the roof deck, before applying the actual screw. Hereafter, the set-up was unloaded before starting the actual test.

- Position of gauges

The strain gauges are positioned on either side of the supporting batten. As shown in **figure A4.2c**, the gauges span 30mm of length, and are located in the middle of the batten.

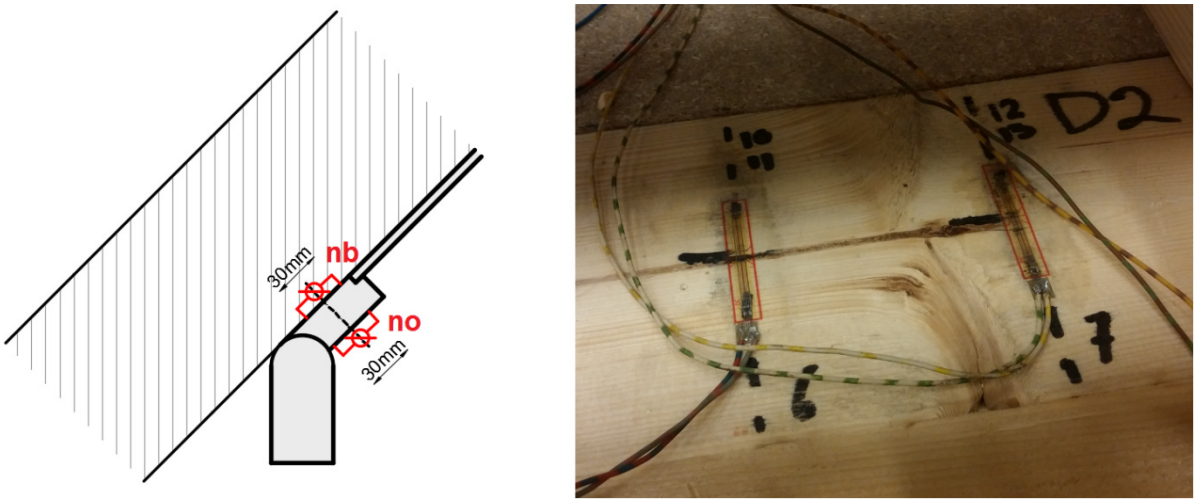

***Figure A4.2c**; Left: Position of the strain gauges on the supporting batten. nb = position number, up. no = position number, down. Note: n = a variable Right: Picture taken of the test set-up involving the gauges in the laboratory*

- Materials used

The test set-up contains several materials, which are listed in **table A4.2b**. The material properties are mentioned in **paragraph 4.1 and 4.2**

Wall Plate	M1
Supporting batten	D2 (**see par. 4.1**)
F-Bracket	B1, B2, B3, B4, B5. Note: B4 and B5 only with CTC = 600 (**see par. 4.1**)
Rafters	S1, S2, S3, S4, S5 (**see par. 4.2.3**)
Supporting panel	Particle board (**see par. 4.2.2**)
Coach screw	5 x Coach screw (**see par. 4.2.5**). Note: Only when the screws are applied

***Table A4.2b**; Overview of all materials used*

- Loading deviation

The loading of the various test set-ups need to fulfill the standardized load case mentioned in **chapter 3**. Though, the vertical shear component is fixed due to the self-weight. To satisfy the correct horizontal axial force to vertical shear force ratio, the magnitude of the loading is adjusted, deviating with the original load case. To be able to compare results in a later stage, the results are simply multiplied with a certain amount to become equal.

Roof Angle	**Deviation**
35 degrees	69,94% of original situation
45 degrees	76,30% of original situation
55 degrees	108,68% of original situation

***Table A4.2c**; Overview of load deviation*

35/600/L/A

Angle of the roof:	35°
Center-to-center distance brackets:	600mm
Position of the wall plate in the bracket:	Low (adding = 10mm)
Test series:	A
Coach screw	No
Load deviation:	69,94%

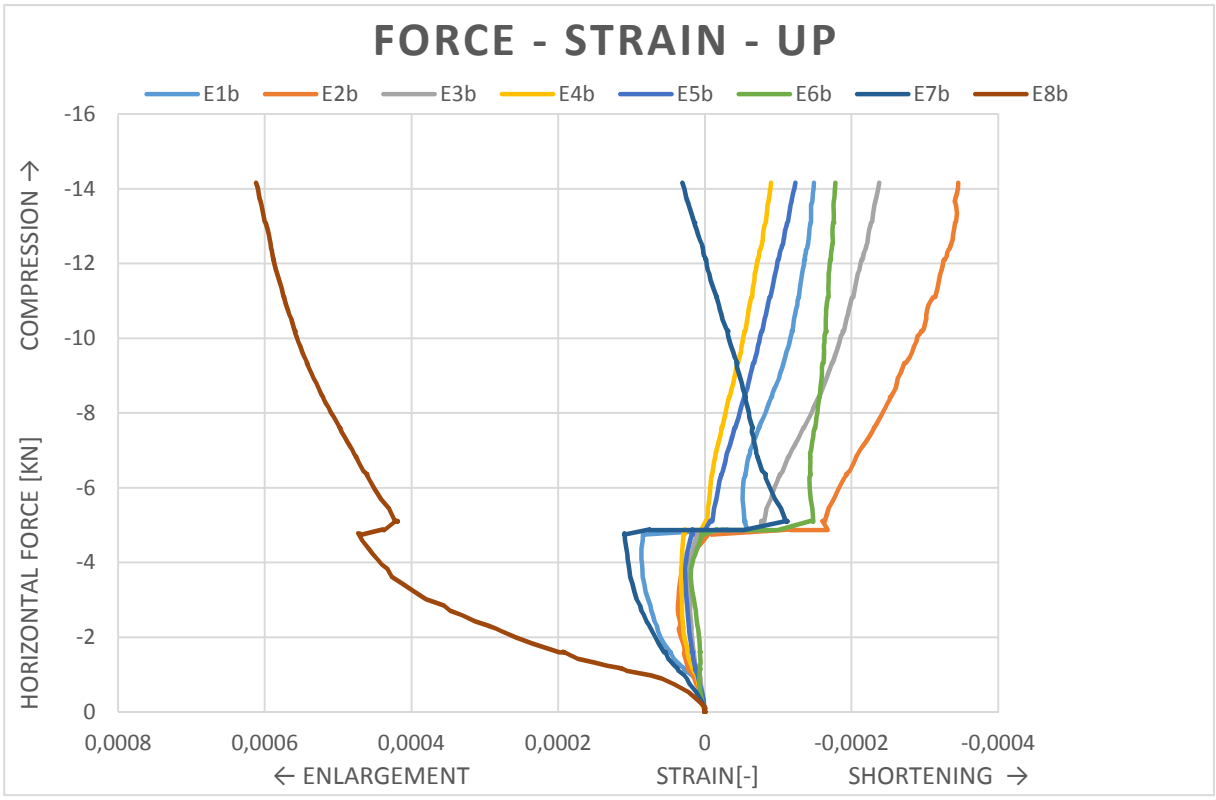

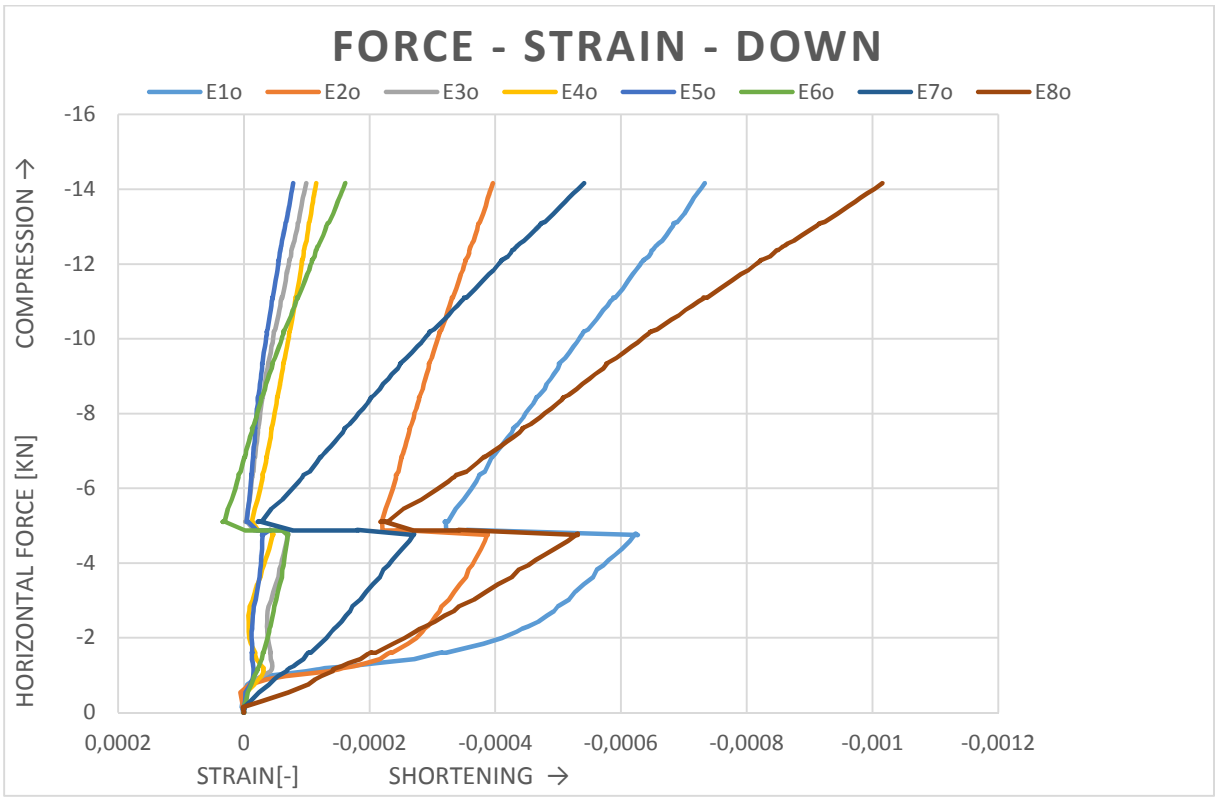

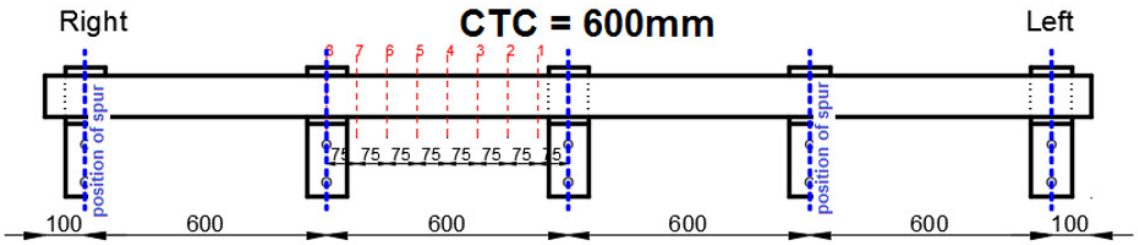
Right
CTC = 600mm
Left
8 7 6 5 4 3 2 1
75 75 75 75 75 75 75 75
position of spur
position of spur
100
600
600
600
600
100

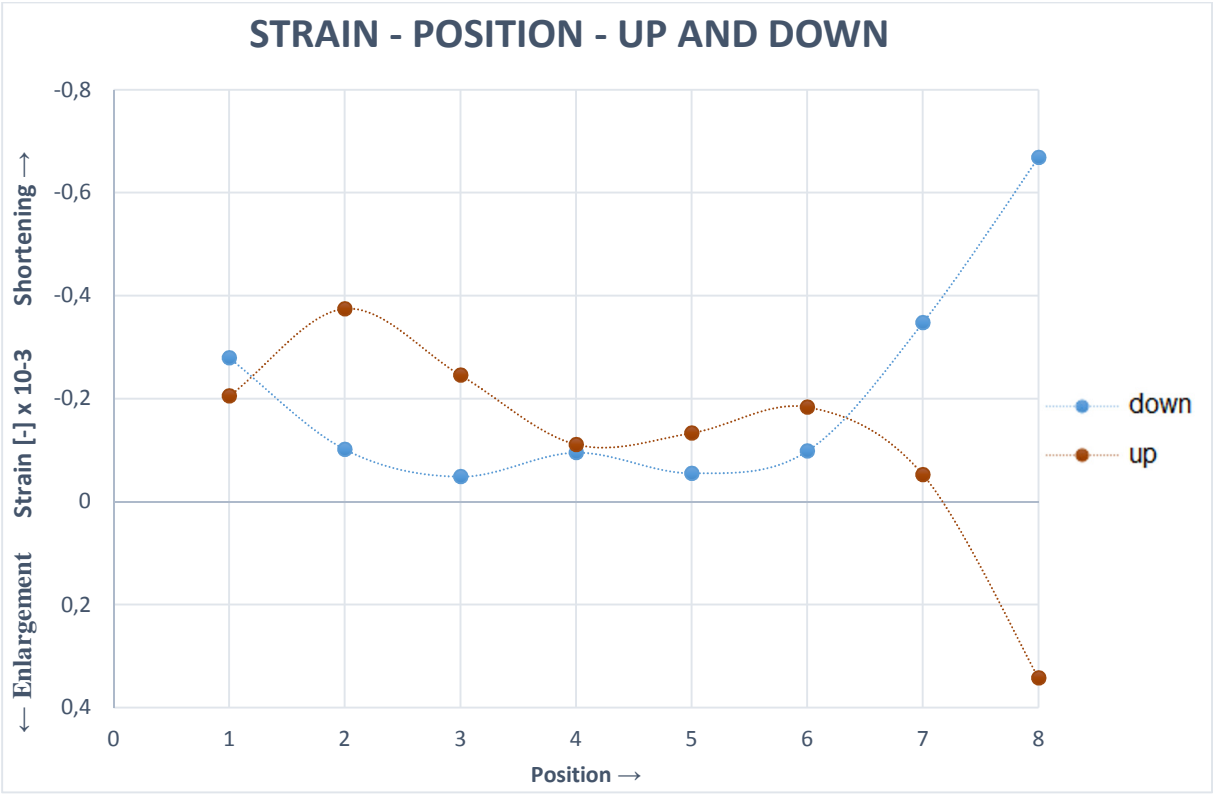
STRAIN - POSITION - UP AND DOWN
-0,8
-0,6
-0,4
-0,2
0
0,2
0,4
← Enlargement Strain [-] x 10-3 Shortening →
0
1
2
3
4
5
6
7
8
Position →
down
up

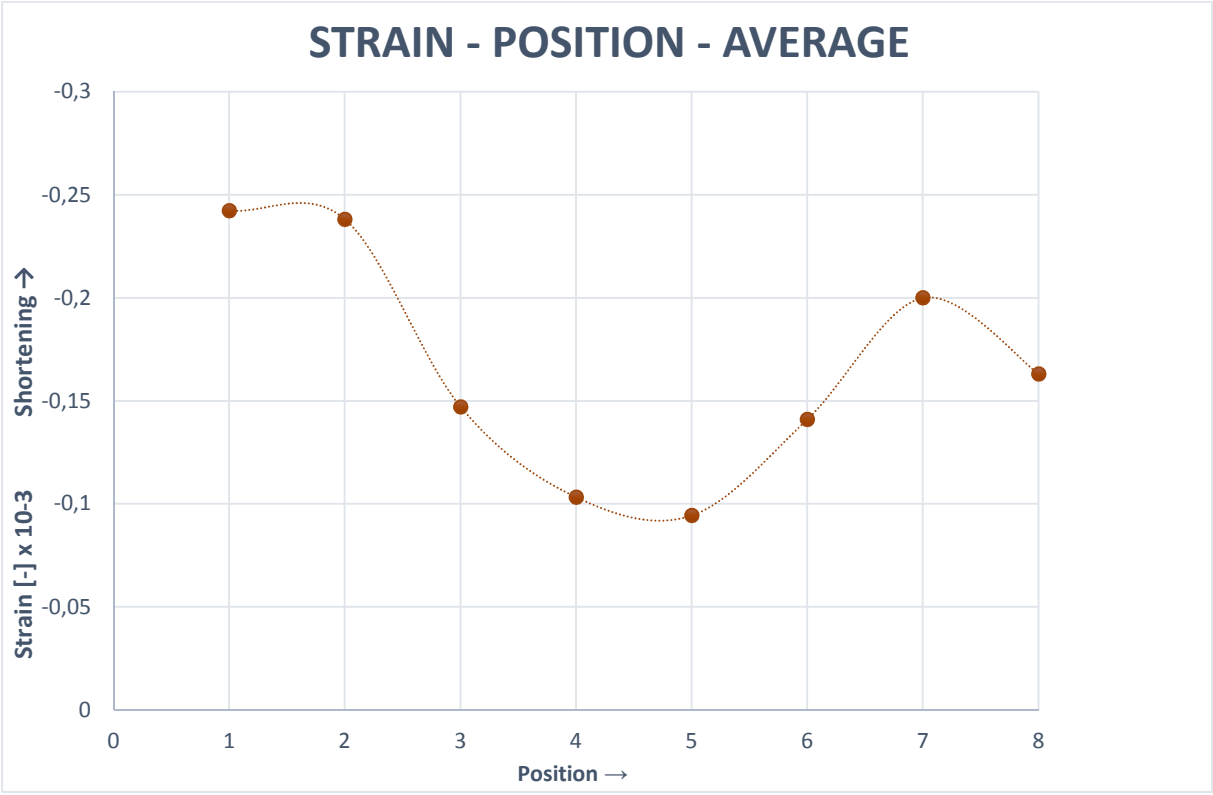
STRAIN - POSITION - AVERAGE
-0,3
-0,25
-0,2
-0,15
-0,1
-0,05
0
Strain [-] x 10-3 Shortening →
0
1
2
3
4
5
6
7
8
Position →

35/600/L/B

Angle of the roof:	35°
Center-to-center distance brackets:	600mm
Position of the wall plate in the bracket:	Low (adding = 10mm)
Test series:	B
Coach screw	No
Load deviation:	69,94%

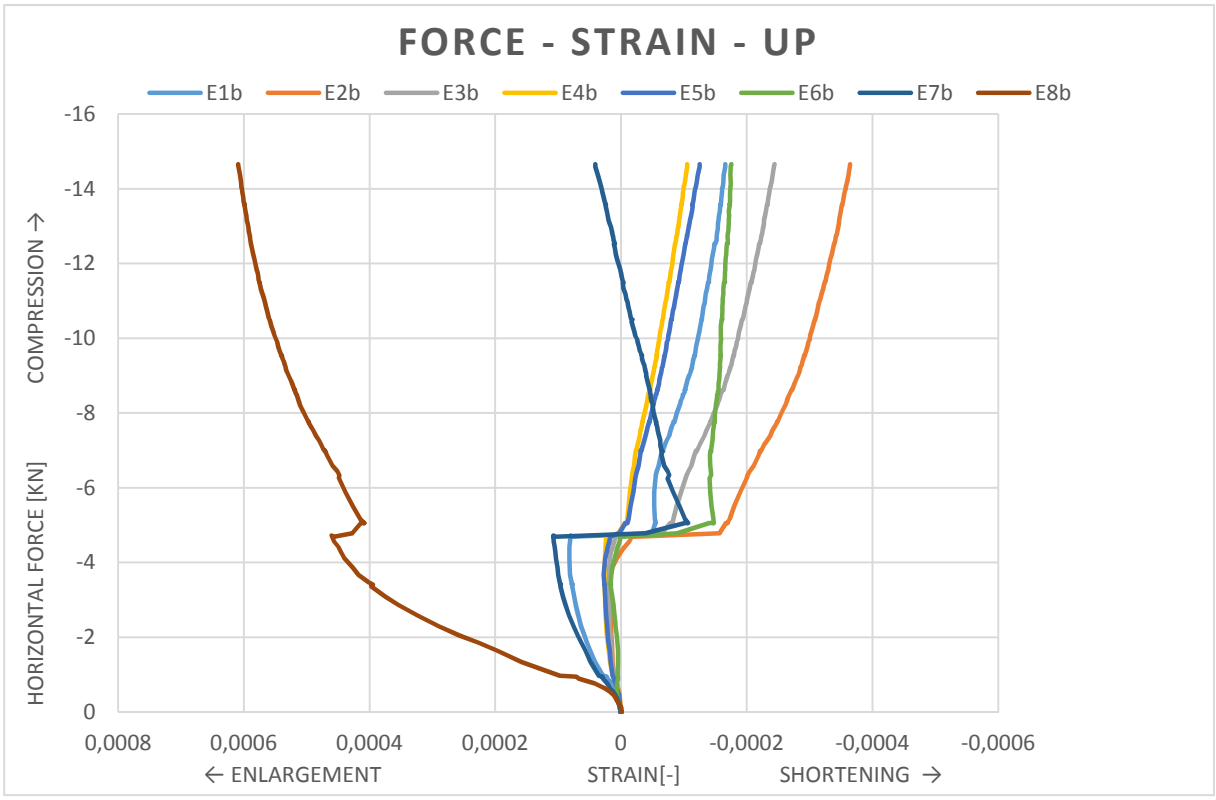

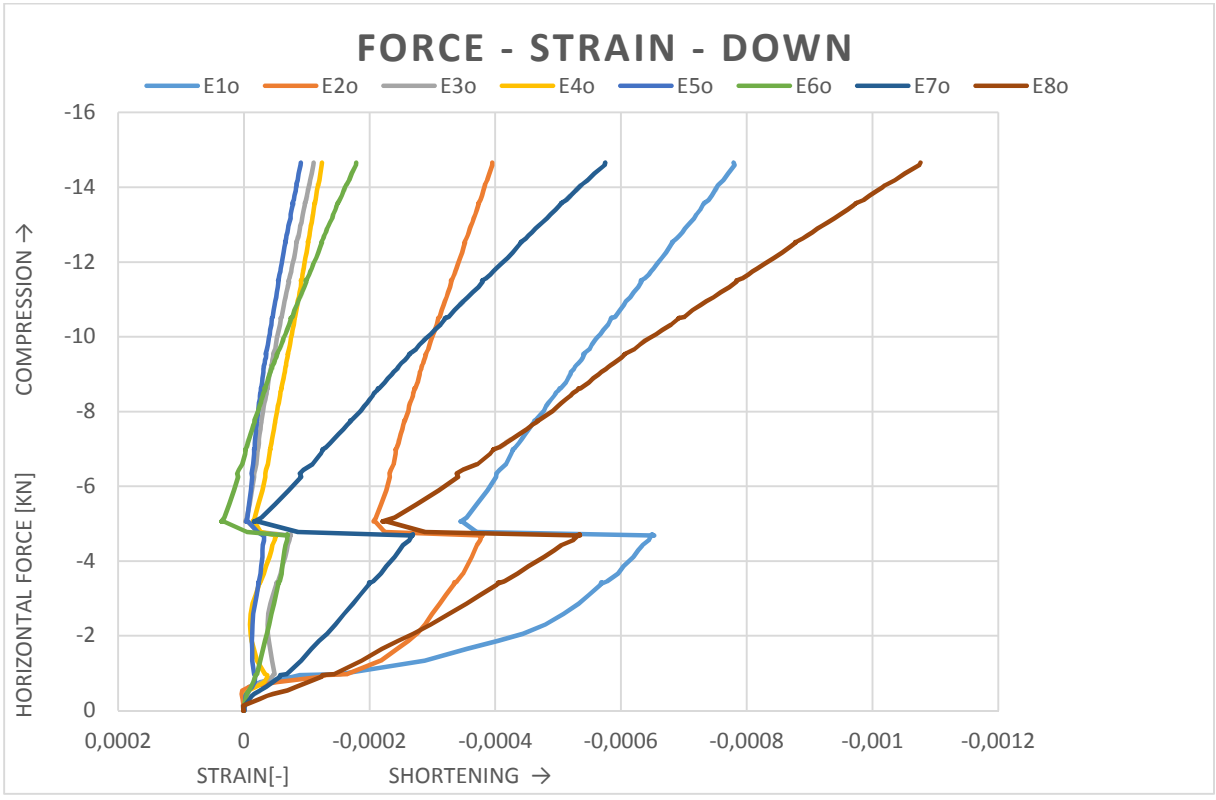

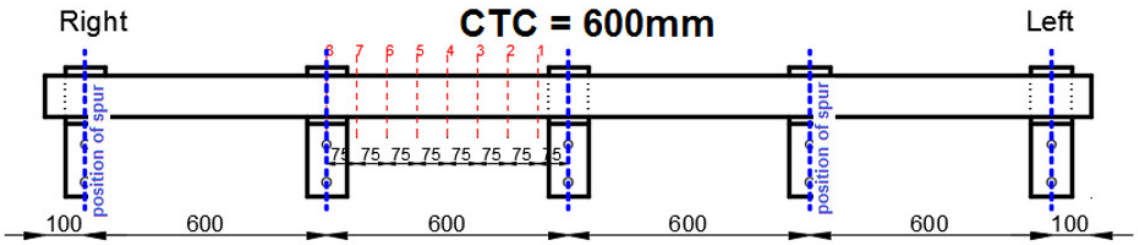
Right
CTC = 600mm
Left
8 7 6 5 4 3 2 1
75 75 75 75 75 75 75 75
position of spur
position of spur
100
600
600
600
600
100

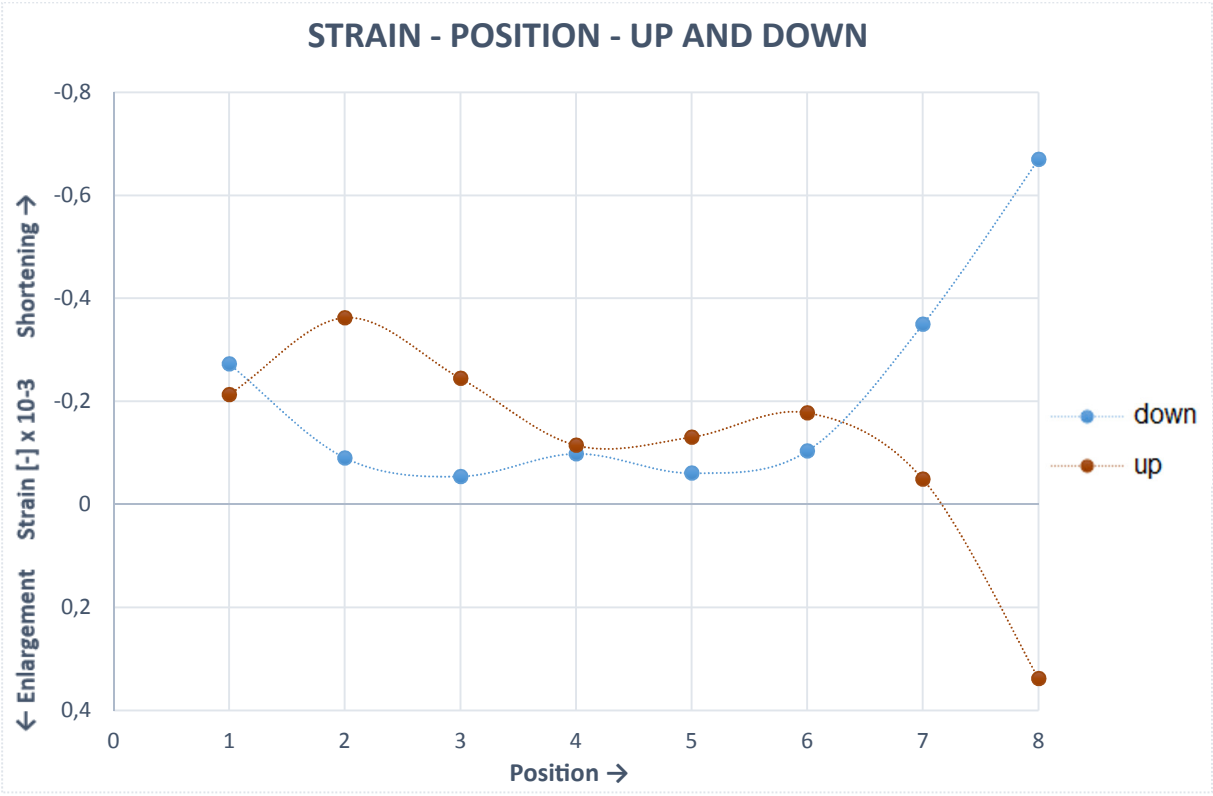
STRAIN - POSITION - UP AND DOWN
-0,8
-0,6
-0,4
-0,2
0
0,2
0,4
← Enlargement Strain [-] x 10-3 Shortening →
0
1
2
3
4
5
6
7
8
Position →
down
up

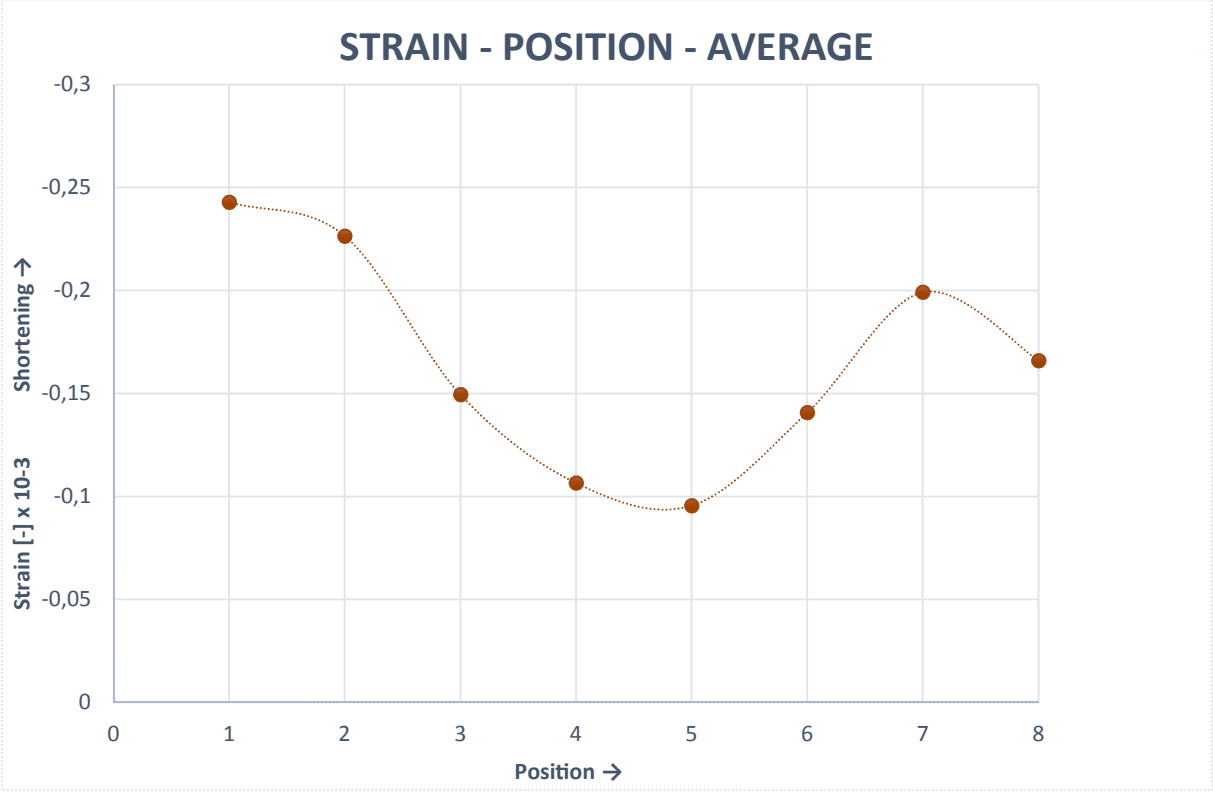
STRAIN - POSITION - AVERAGE
-0,3
-0,25
-0,2
-0,15
-0,1
-0,05
0
Strain [-] x 10-3 Shortening →
0
1
2
3
4
5
6
7
8
Position →

35/900/L/A

Angle of the roof:	35°
Center-to-center distance brackets:	900mm
Position of the wall plate in the bracket:	Low (adding = 10mm)
Test series:	A
Coach screw	No
Load deviation:	69,94%

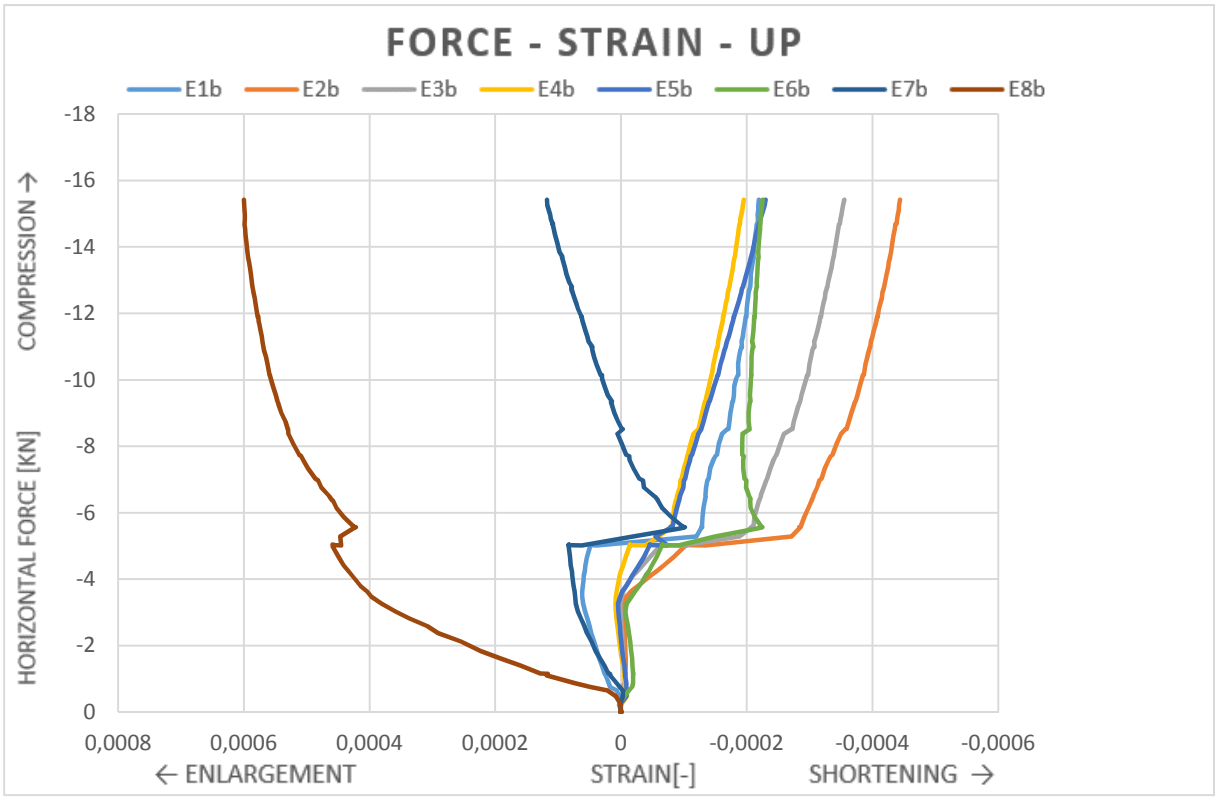

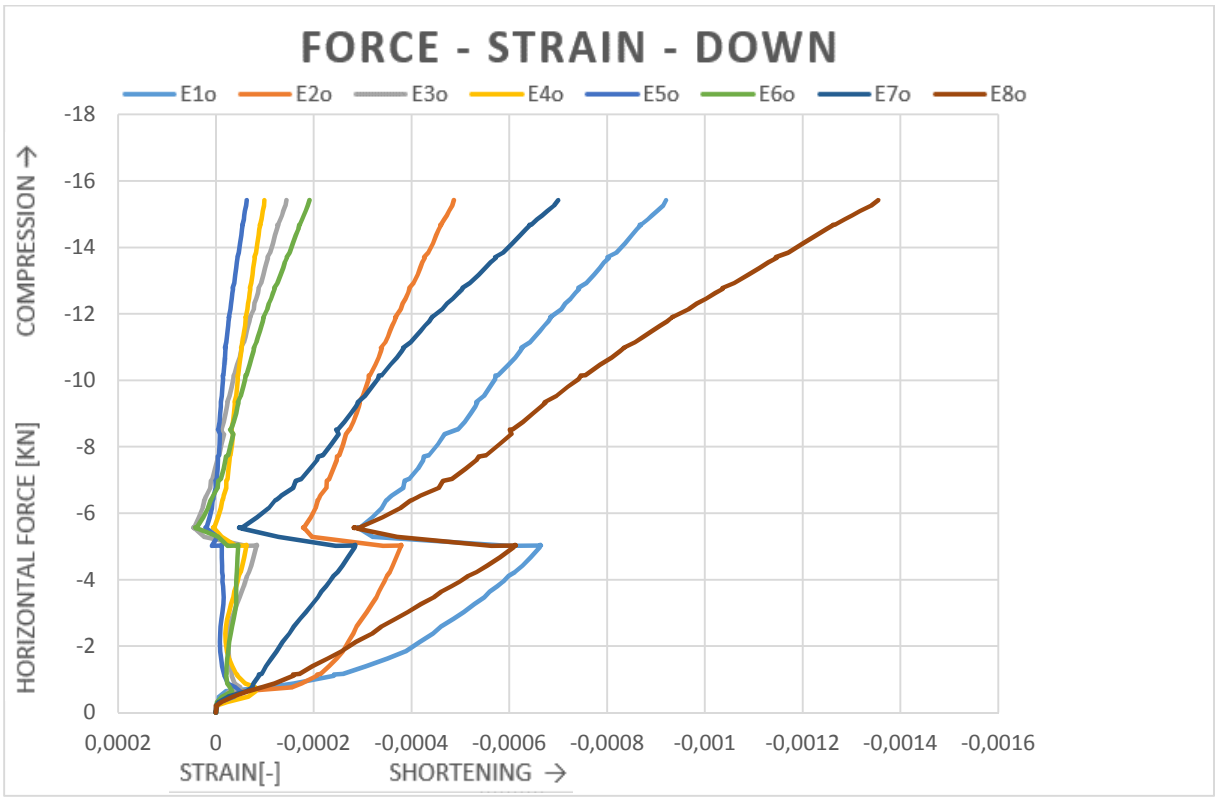

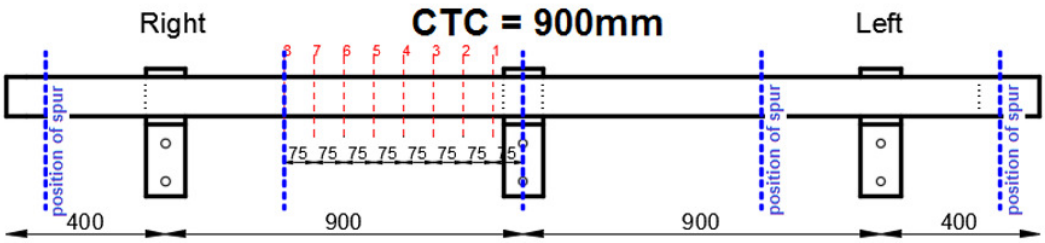
Right
CTC = 900mm
Left
8 7 6 5 4 3 2 1
75 75 75 75 75 75 75 75
position of spur
position of spur
position of spur
400
900
900
400

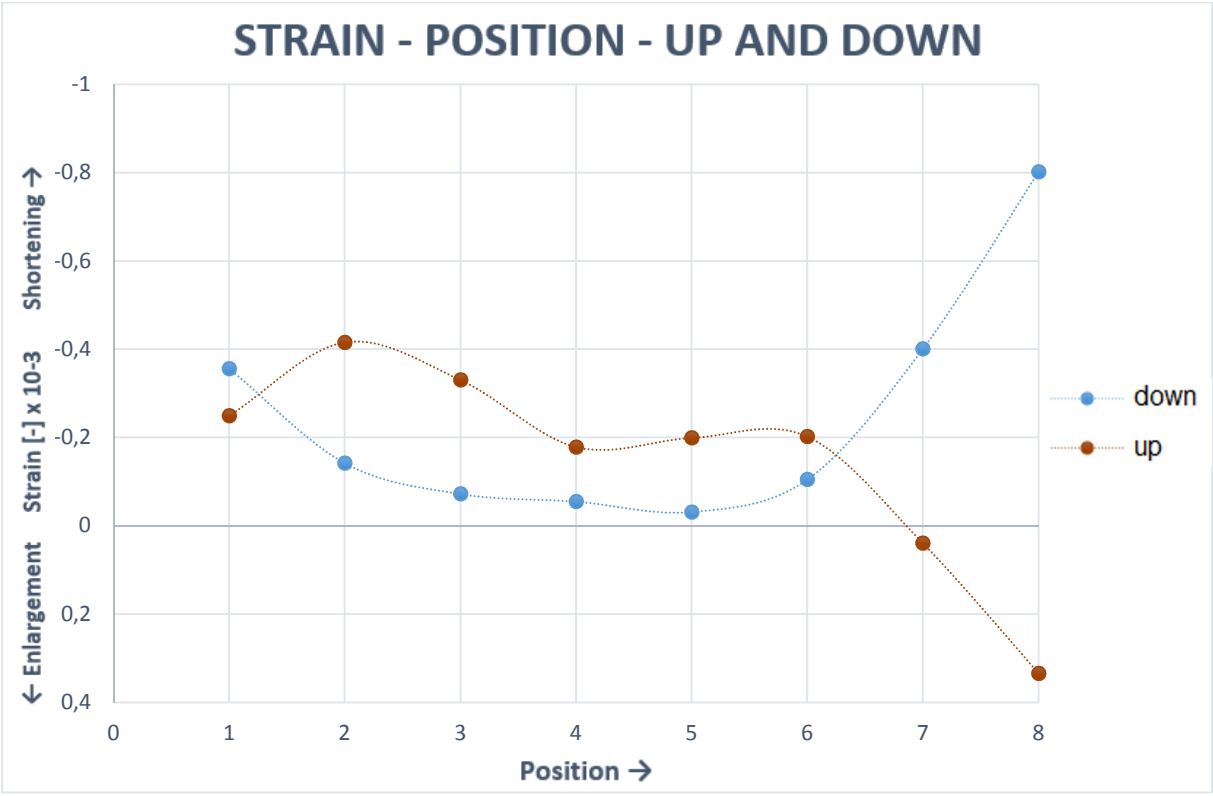
STRAIN - POSITION - UP AND DOWN
← Enlargement Strain [-] x 10-3 Shortening →
-1
-0,8
-0,6
-0,4
-0,2
0
0,2
0,4
0
1
2
3
4
5
6
7
8
Position →
down
up

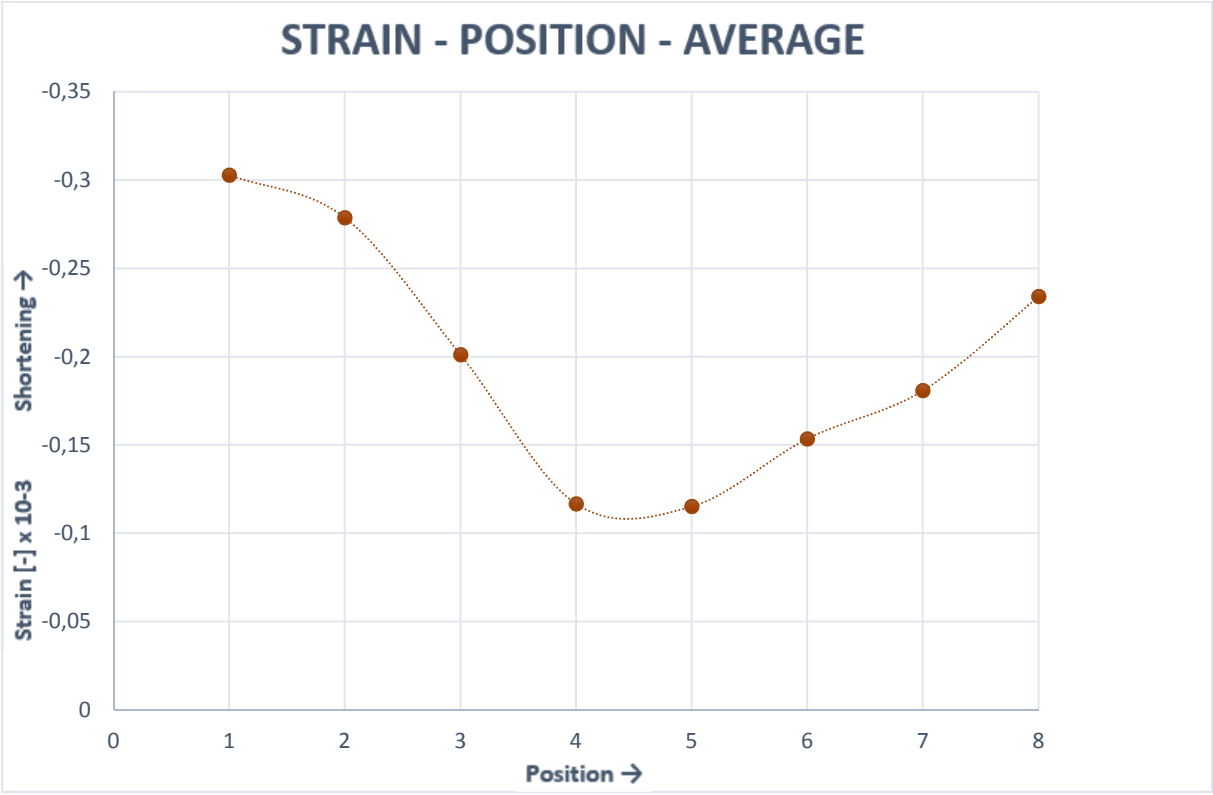
STRAIN - POSITION - AVERAGE
Strain [-] x 10-3 Shortening →
-0,35
-0,3
-0,25
-0,2
-0,15
-0,1
-0,05
0
0
1
2
3
4
5
6
7
8
Position →

35/900/L/B

Angle of the roof:	35°
Center-to-center distance brackets:	900mm
Position of the wall plate in the bracket:	Low (adding = 10mm)
Test series:	B
Coach screw	No
Load deviation:	69,94%

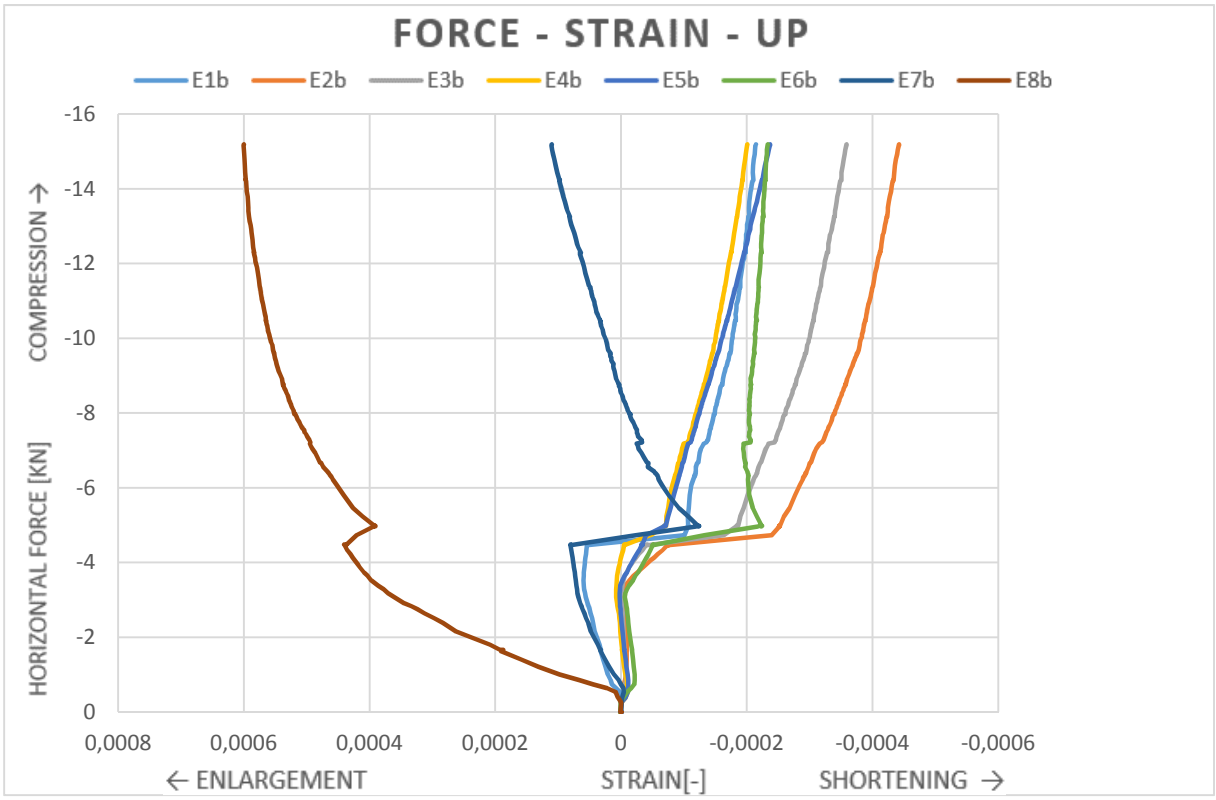

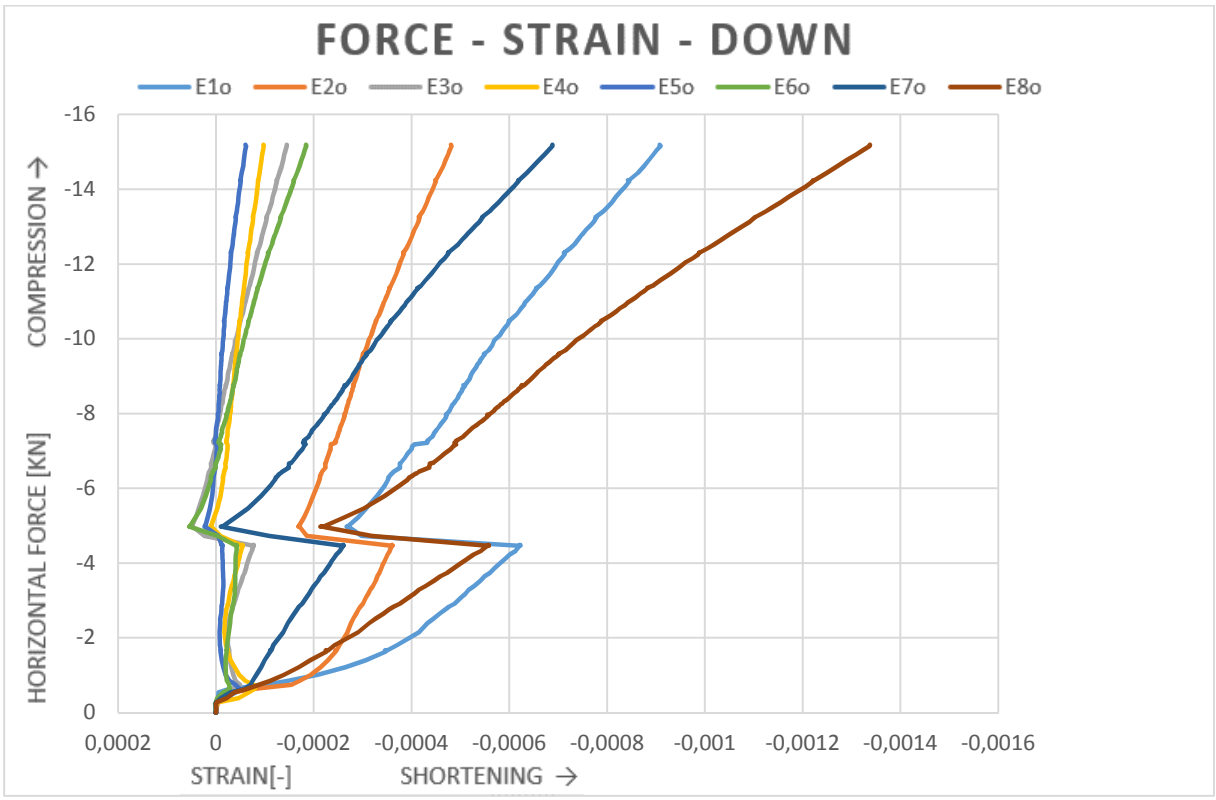

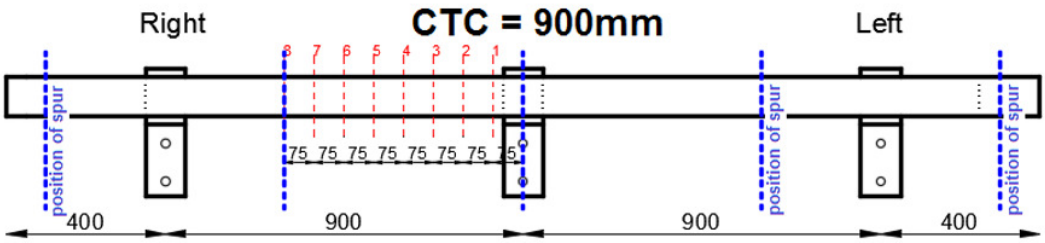
Right
CTC = 900mm
Left
8 7 6 5 4 3 2 1
75 75 75 75 75 75 75 75
position of spur
position of spur
position of spur
400
900
900
400

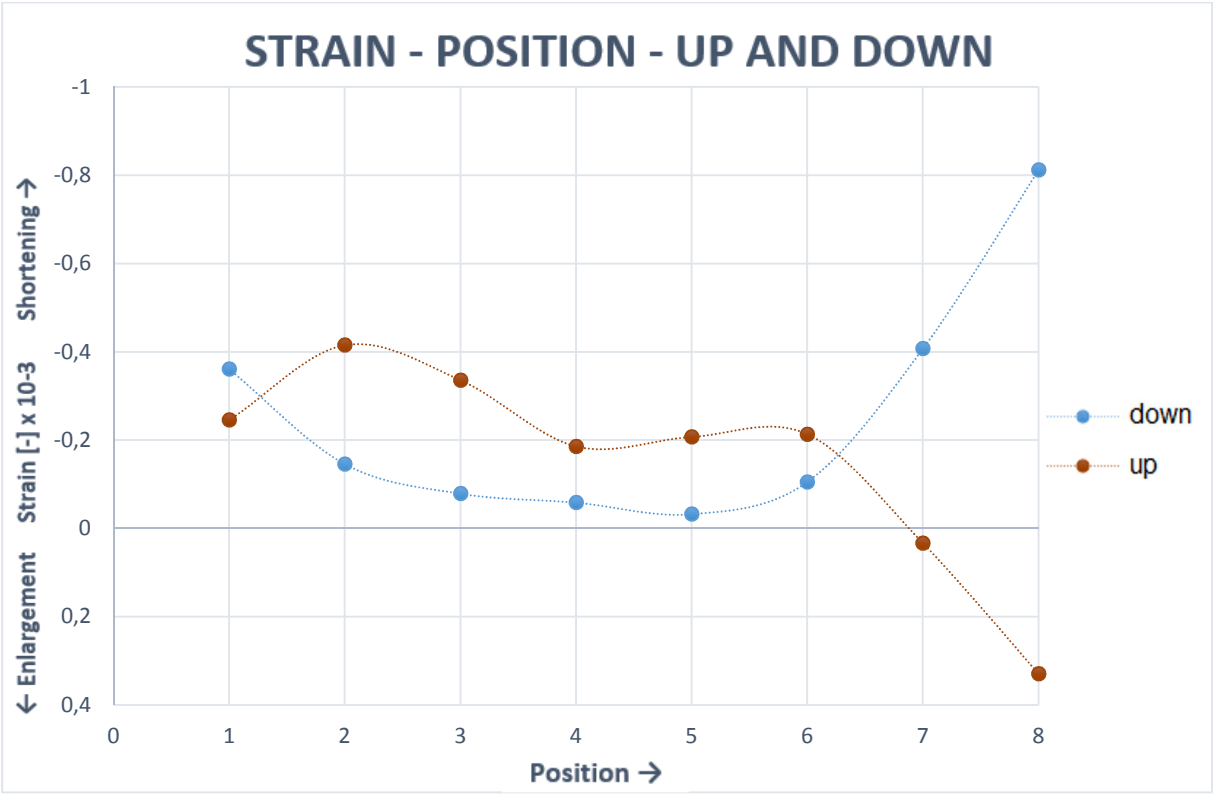
STRAIN - POSITION - UP AND DOWN
-1
-0,8
-0,6
-0,4
-0,2
0
0,2
0,4
← Enlargement Strain [-] x 10-3 Shortening →
0
1
2
3
4
5
6
7
8
Position →
down
up

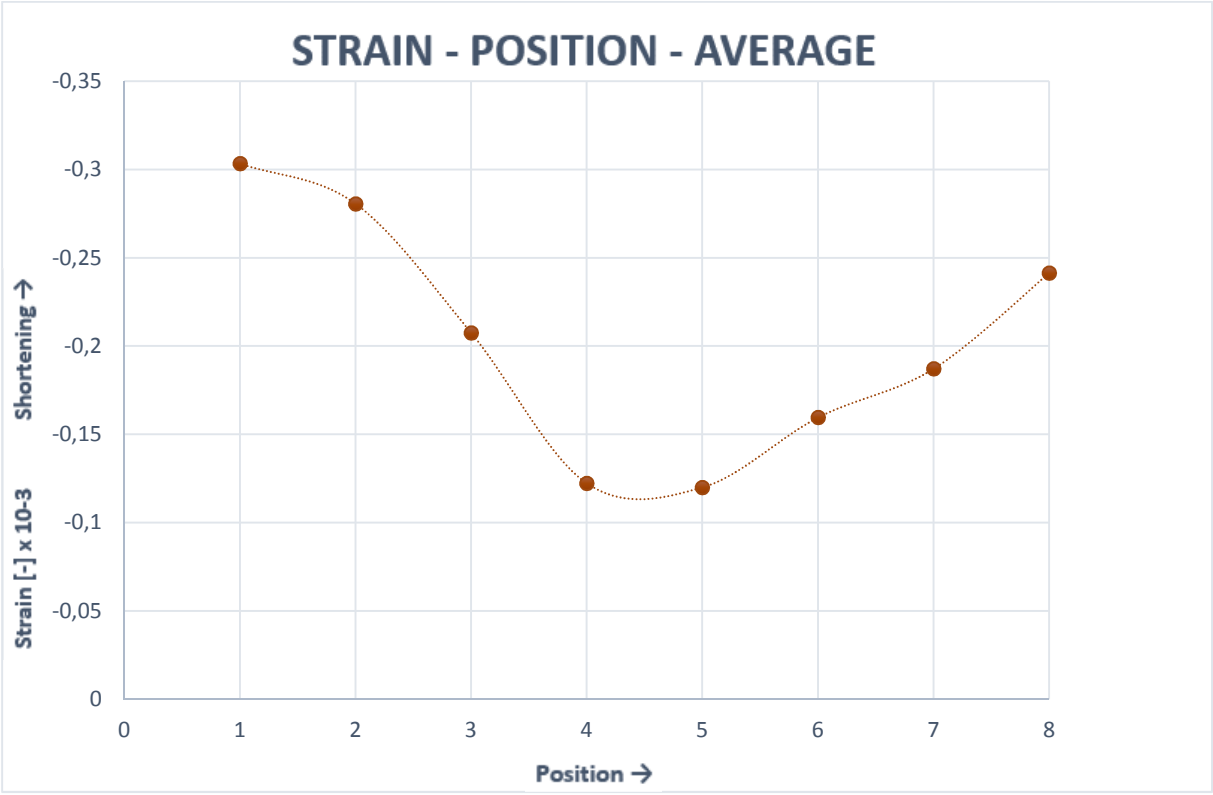
STRAIN - POSITION - AVERAGE
-0,35
-0,3
-0,25
-0,2
-0,15
-0,1
-0,05
0
Strain [-] x 10-3 Shortening →
0
1
2
3
4
5
6
7
8
Position →

35/1200/L/A

Angle of the roof:	35°
Center-to-center distance brackets:	1200mm
Position of the wall plate in the bracket:	Low (adding = 10mm)
Test series:	A
Coach screw	No
Load deviation:	69,94%

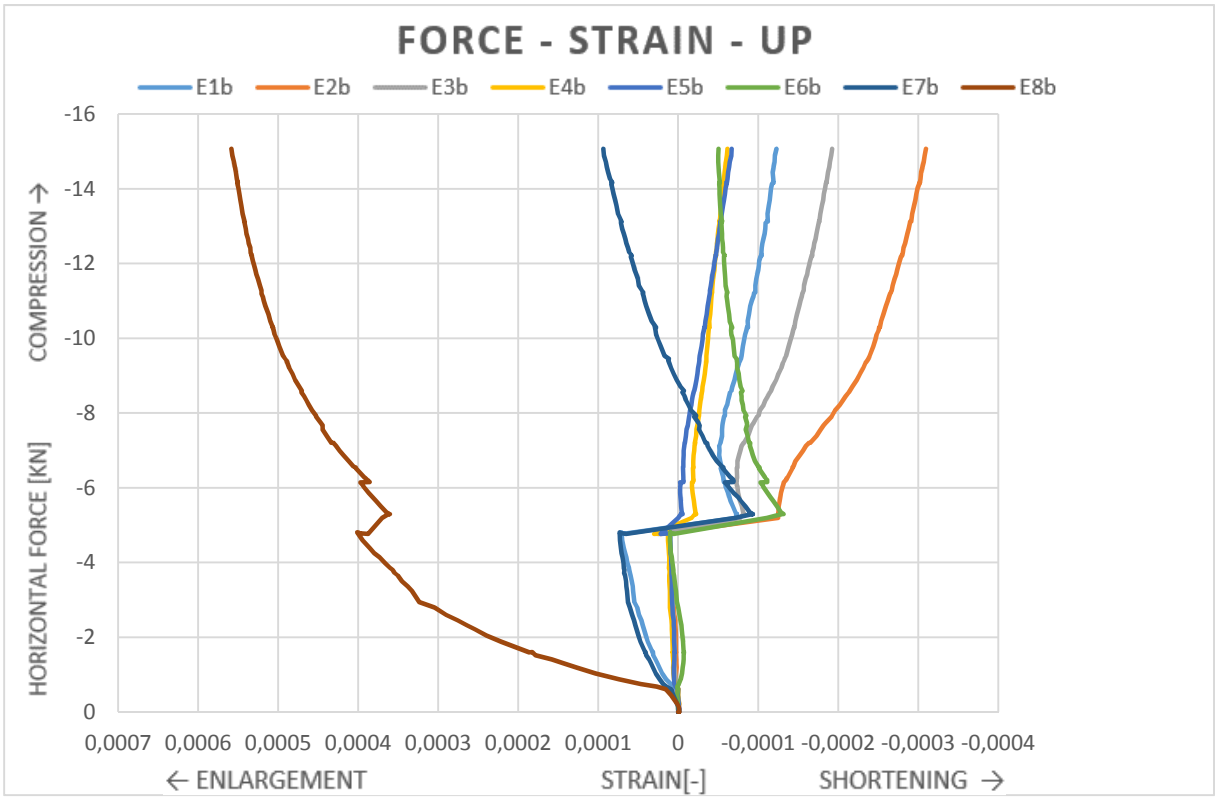

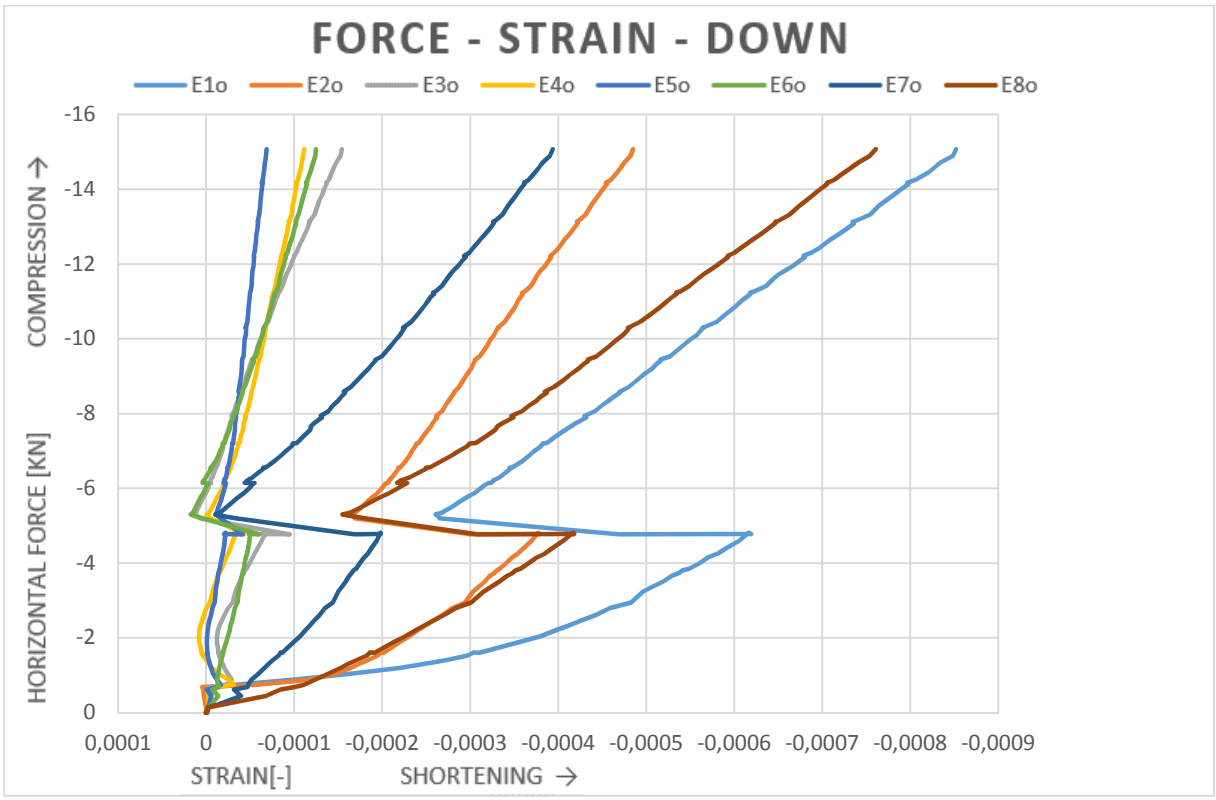

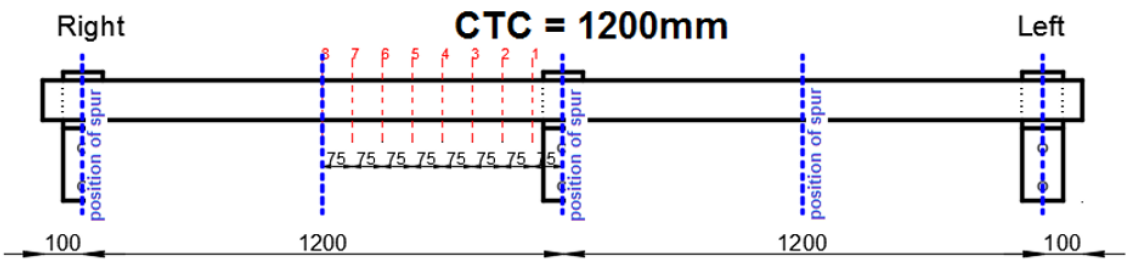
Right
CTC = 1200mm
Left
8 7 6 5 4 3 2 1
75 75 75 75 75 75 75 75
position of spur
position of spur
position of spur
100
1200
1200
100

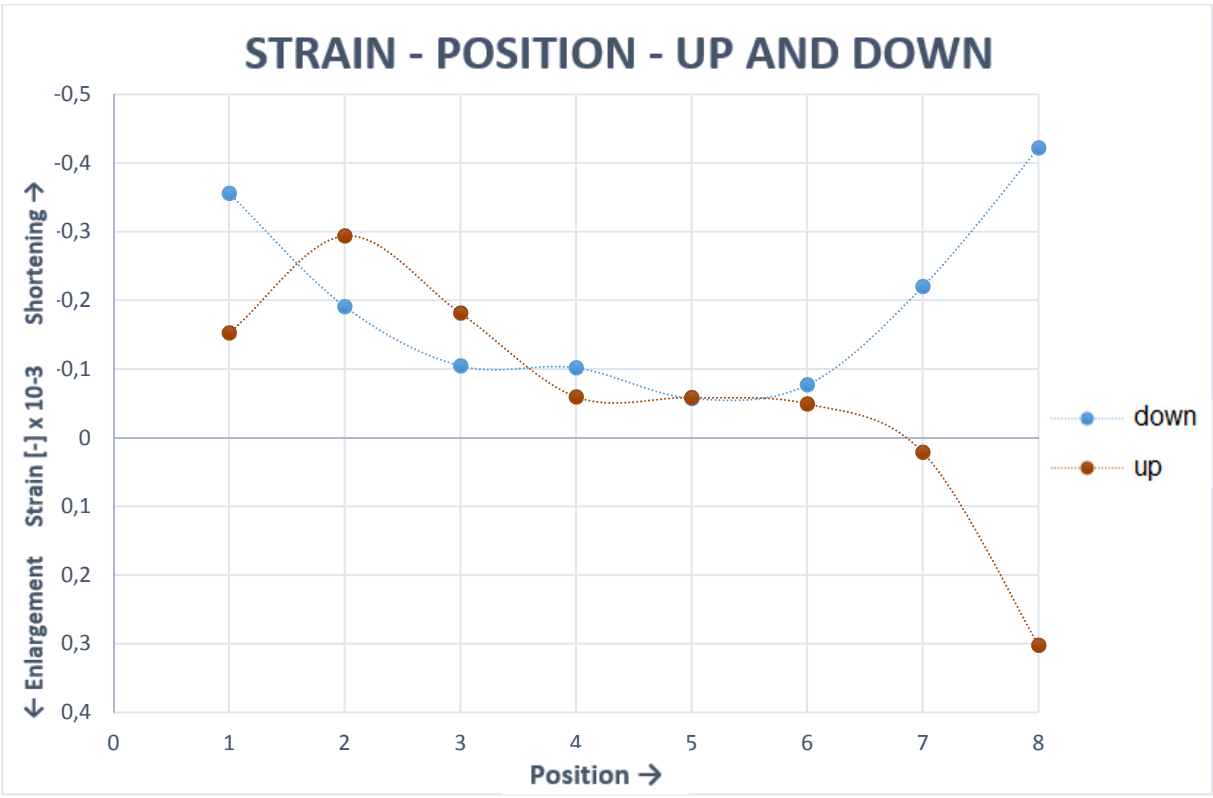
STRAIN - POSITION - UP AND DOWN
-0,5
-0,4
-0,3
-0,2
-0,1
0
0,1
0,2
0,3
0,4
Shortening →
Strain [-] x 10-3
← Enlargement
0
1
2
3
4
5
6
7
8
Position →
down
up

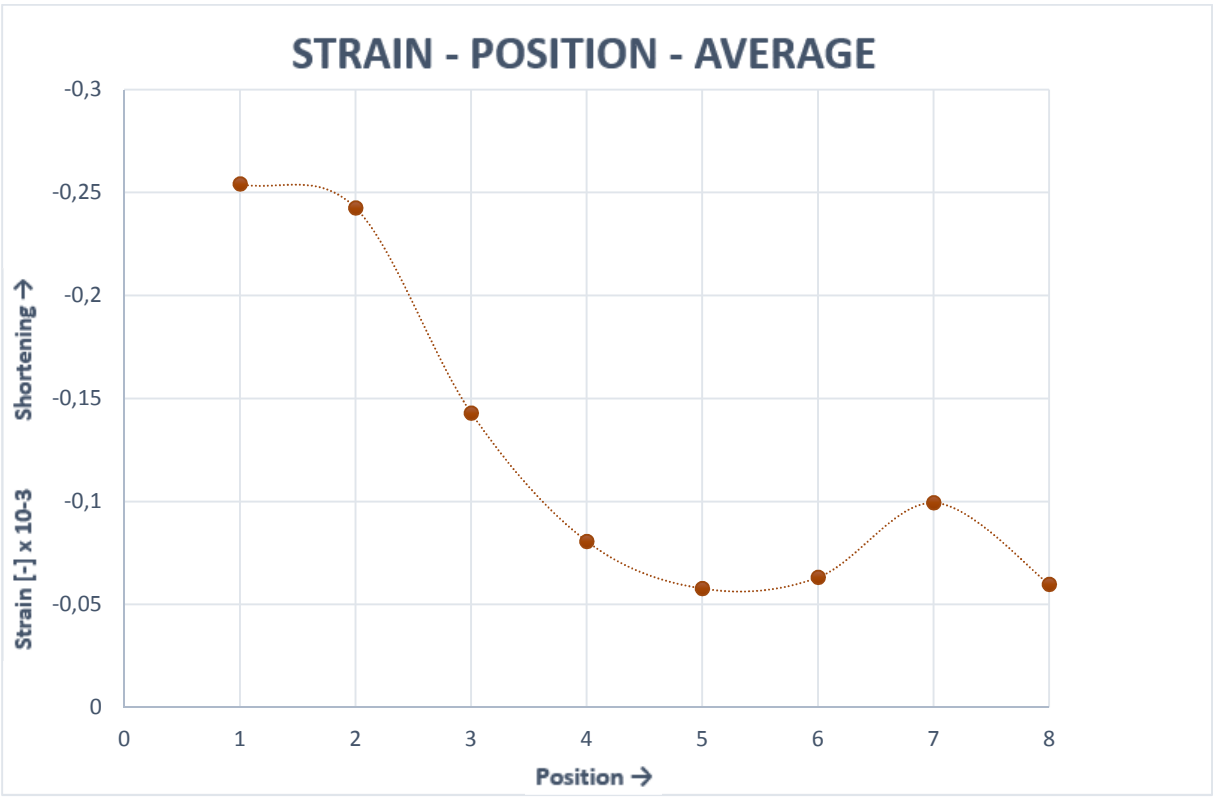
STRAIN - POSITION - AVERAGE
-0,3
-0,25
-0,2
-0,15
-0,1
-0,05
0
Shortening →
Strain [-] x 10-3
0
1
2
3
4
5
6
7
8
Position →

35/1200/L/B

Angle of the roof:	35°
Center-to-center distance brackets:	1200mm
Position of the wall plate in the bracket:	Low (adding = 10mm)
Test series:	B
Coach screw	No
Load deviation:	69,94%

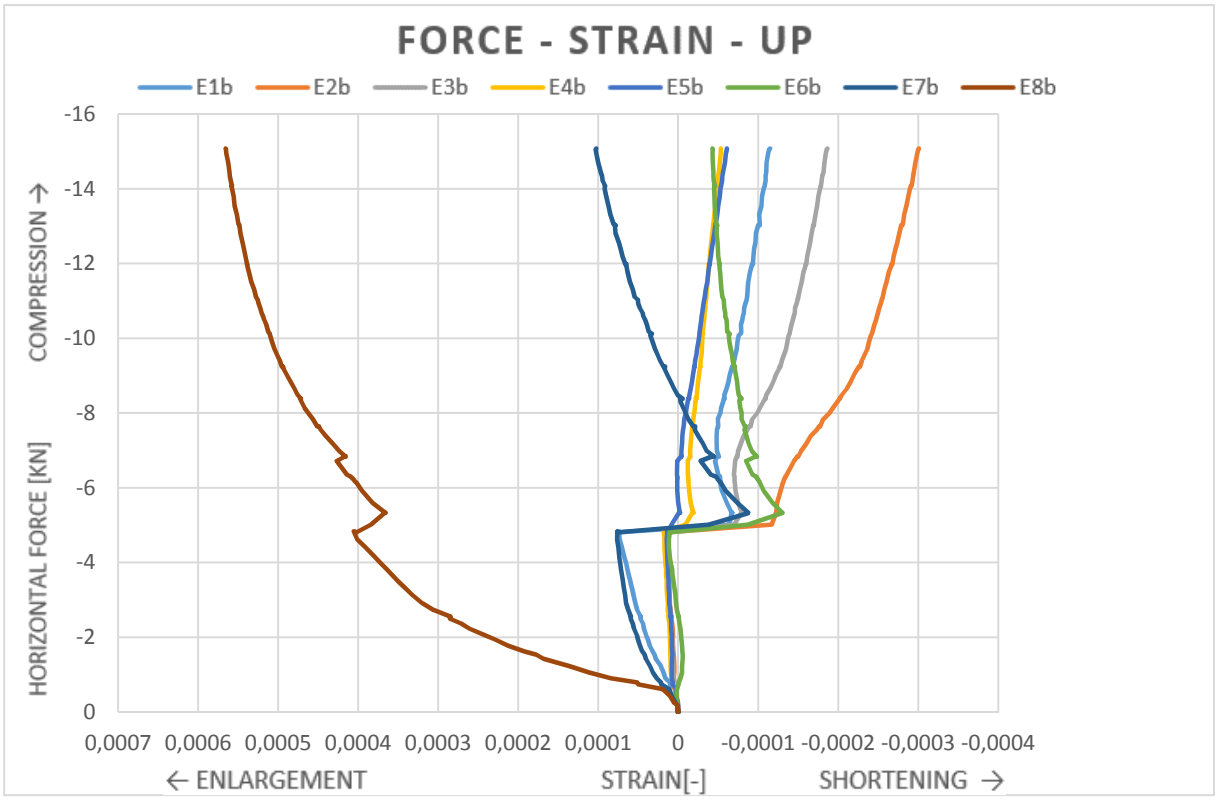

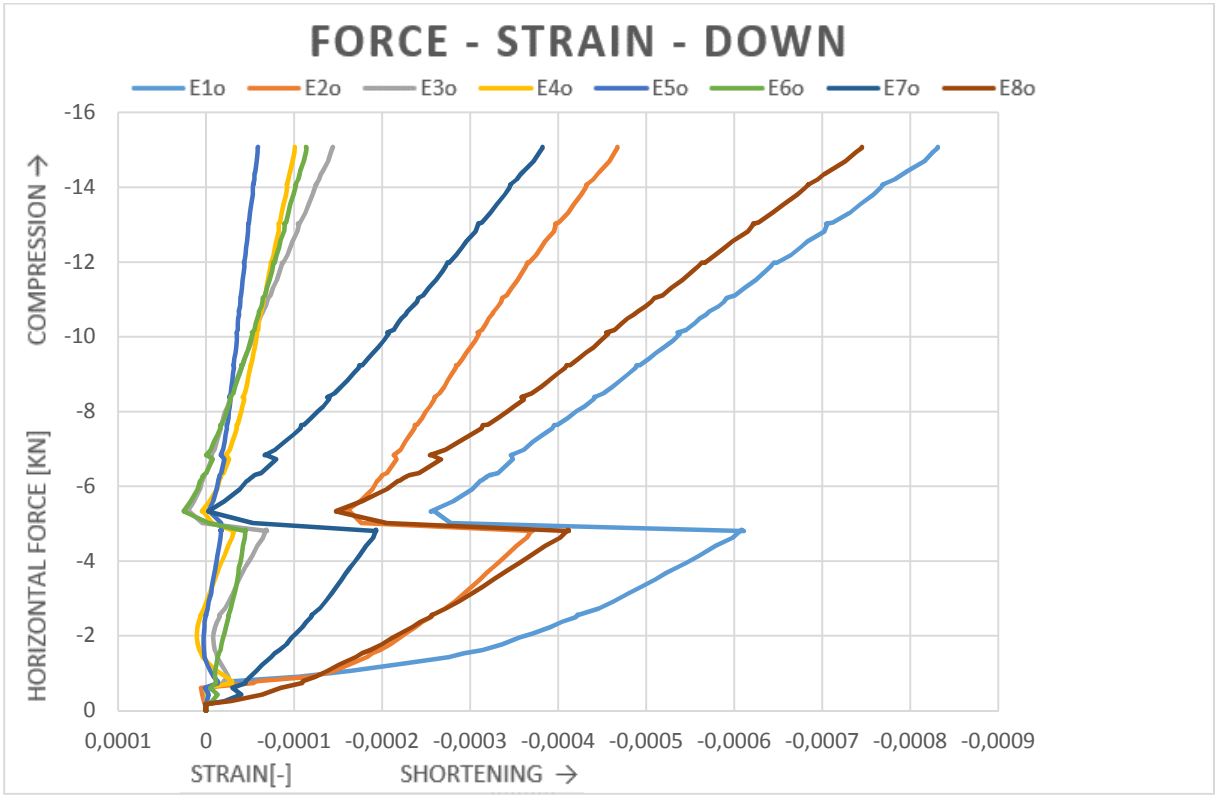

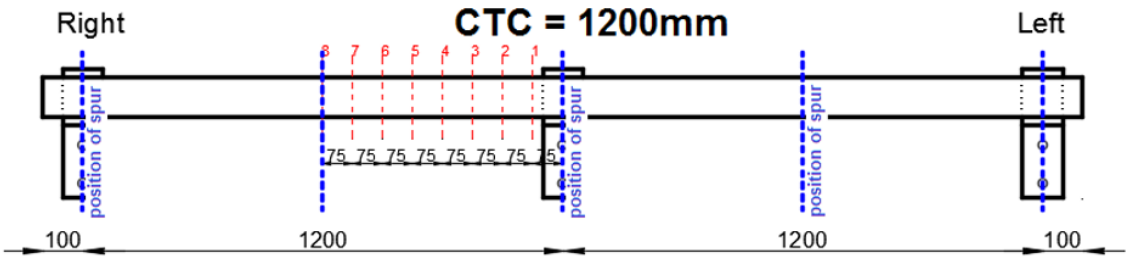
Right
CTC = 1200mm
Left
8 7 6 5 4 3 2 1
75 75 75 75 75 75 75 75
position of spur
position of spur
position of spur
100
1200
1200
100

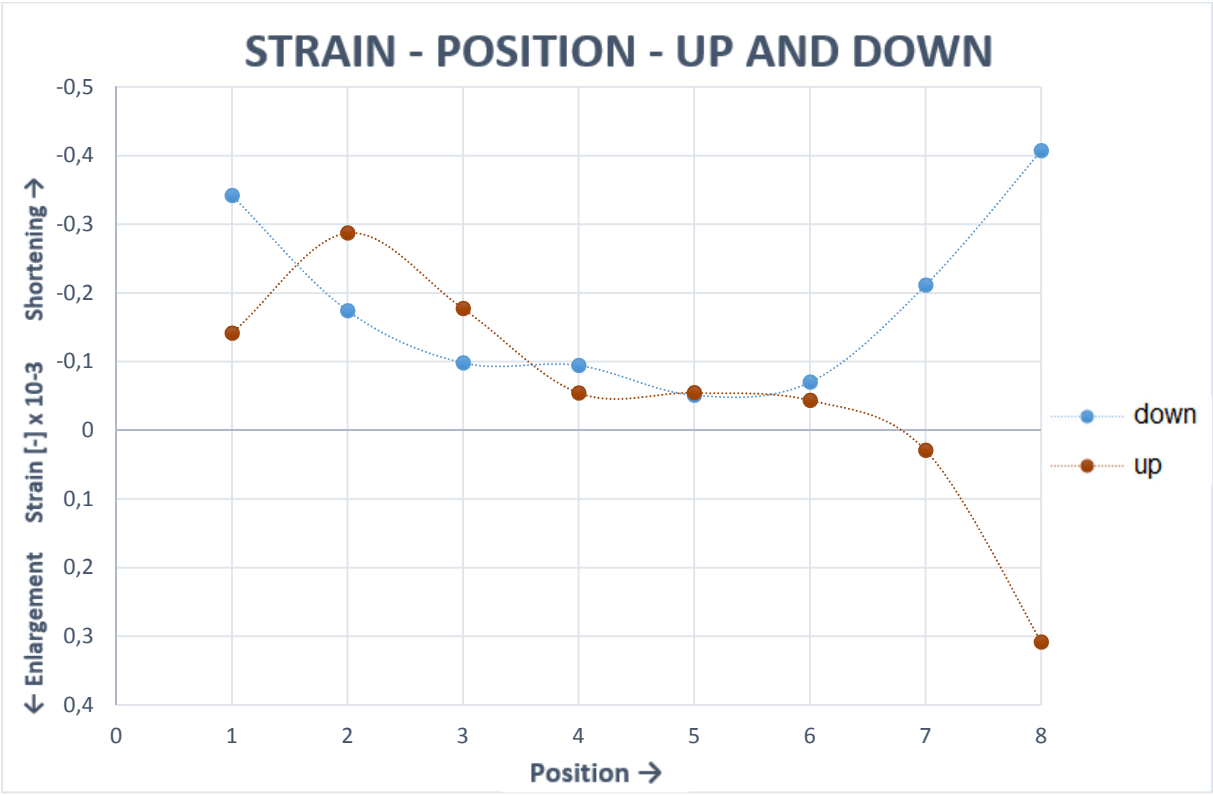
STRAIN - POSITION - UP AND DOWN
-0,5
-0,4
-0,3
-0,2
-0,1
0
0,1
0,2
0,3
0,4
Shortening →
Strain [-] x 10-3
← Enlargement
0
1
2
3
4
5
6
7
8
Position →
down
up

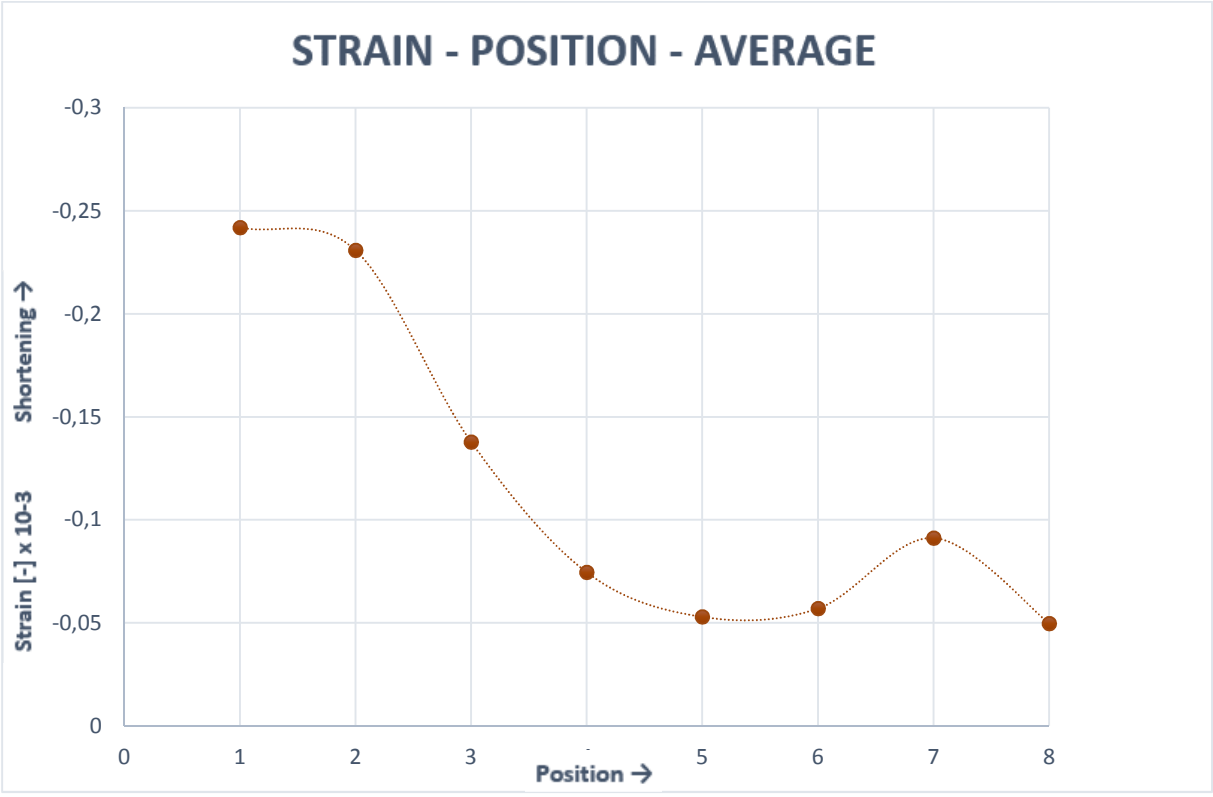
STRAIN - POSITION - AVERAGE
-0,3
-0,25
-0,2
-0,15
-0,1
-0,05
0
Shortening →
Strain [-] x 10-3
0
1
2
3
5
6
7
8
Position →

45/600/L/A

Angle of the roof:	45°
Center-to-center distance brackets:	600mm
Position of the wall plate in the bracket:	Low (adding = 10mm)
Test series:	A
Coach screw	No
Load deviation:	76,30%

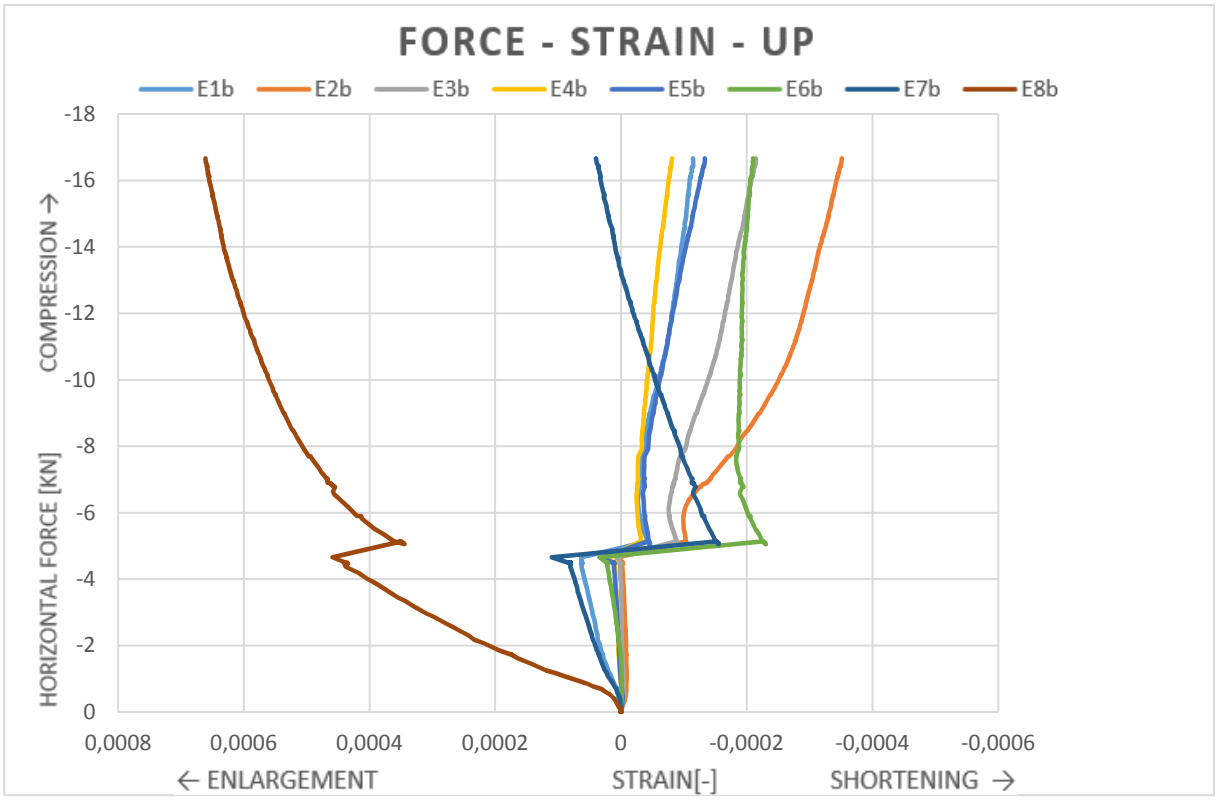

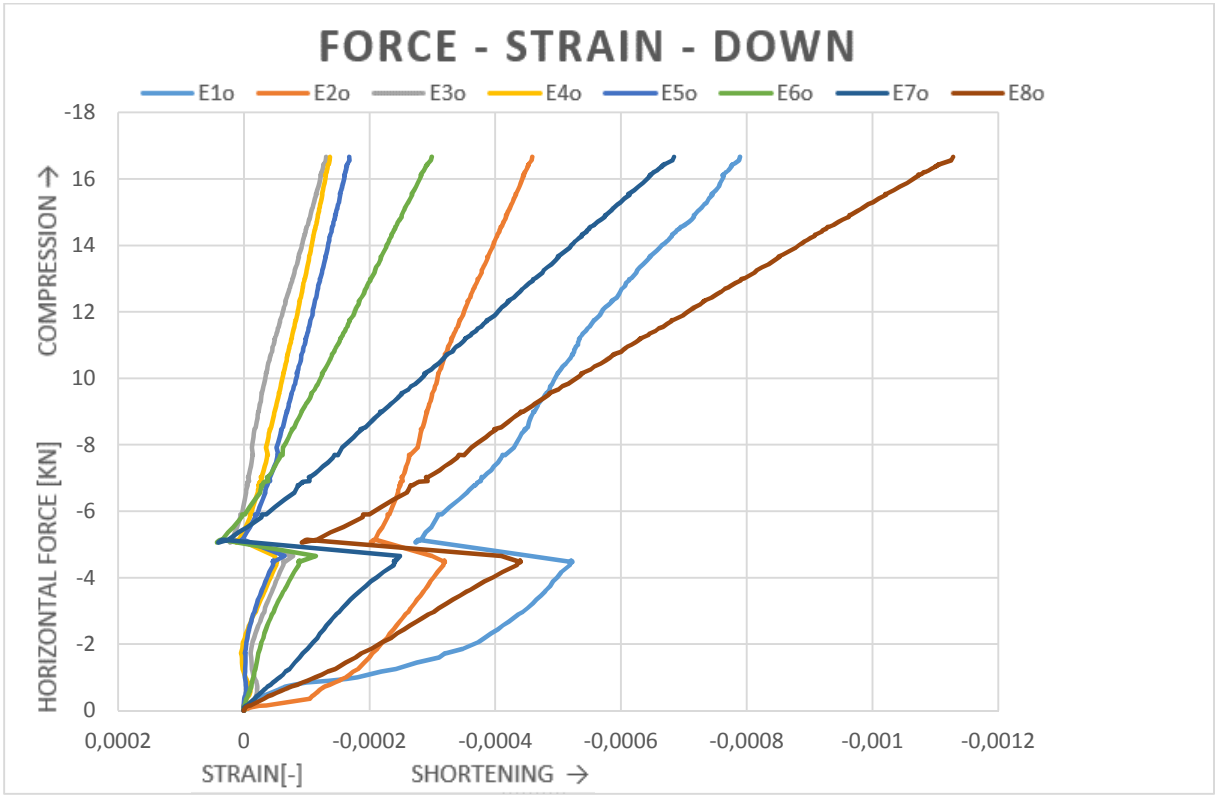

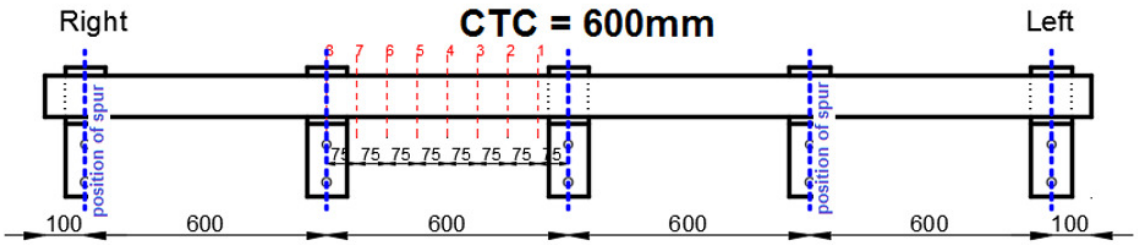
Right
CTC = 600mm
Left
8 7 6 5 4 3 2 1
75 75 75 75 75 75 75 75
position of spur
position of spur
100
600
600
600
600
100

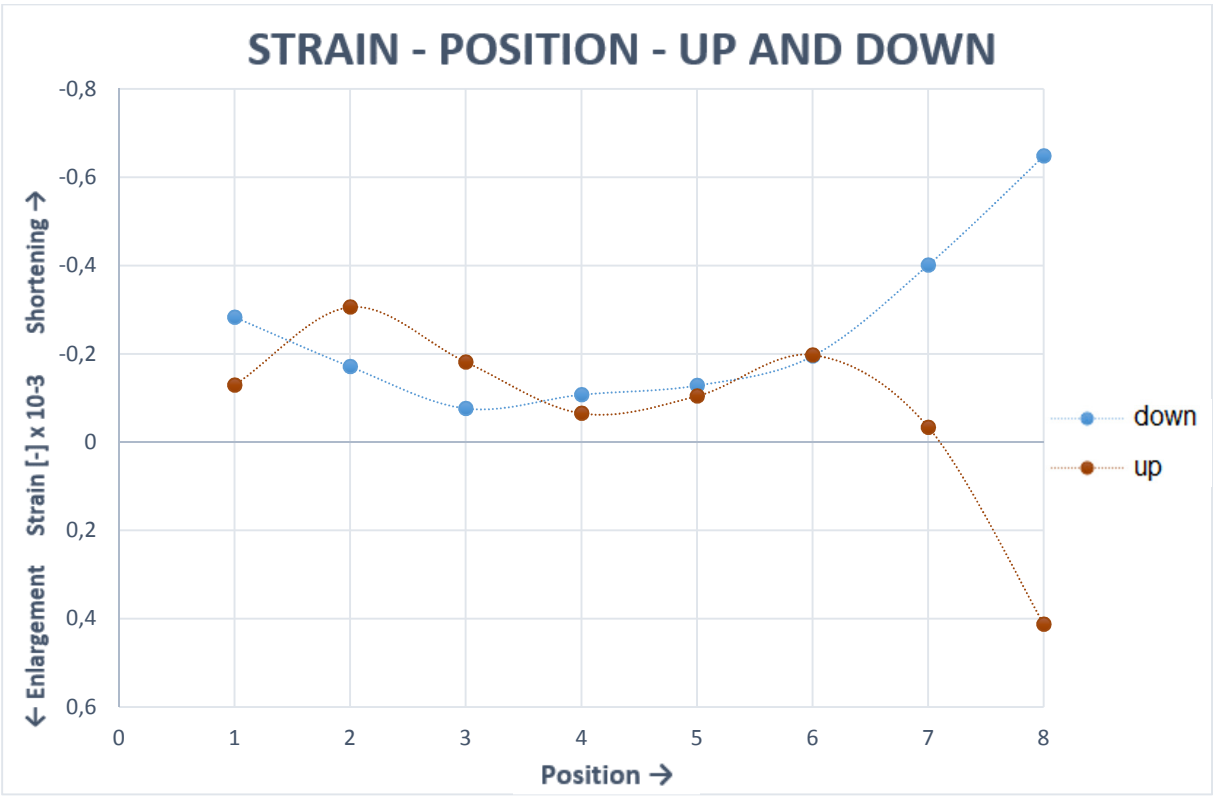
STRAIN - POSITION - UP AND DOWN
-0,8
-0,6
-0,4
-0,2
0
0,2
0,4
0,6
← Enlargement Strain [-] x 10-3 Shortening →
0
1
2
3
4
5
6
7
8
Position →
down
up

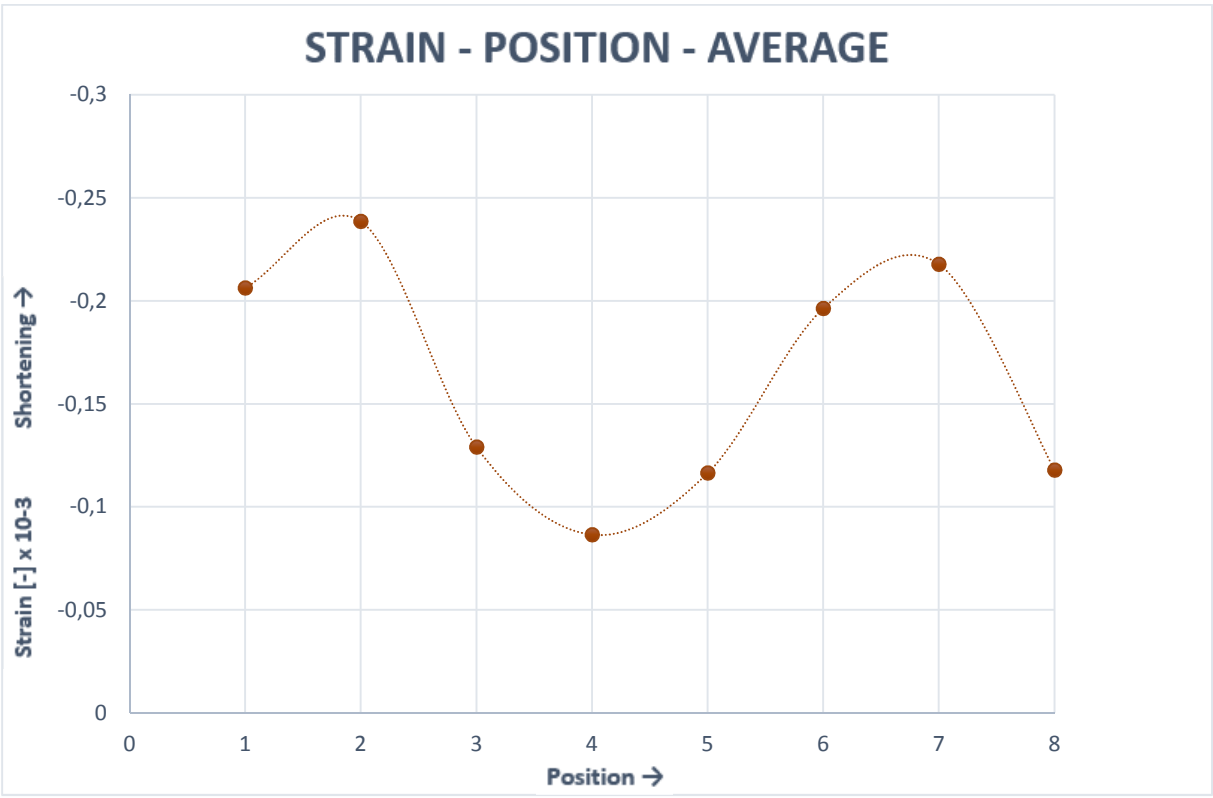
STRAIN - POSITION - AVERAGE
-0,3
-0,25
-0,2
-0,15
-0,1
-0,05
0
Strain [-] x 10-3 Shortening →
0
1
2
3
4
5
6
7
8
Position →

45/600/L/B

Angle of the roof:	45°
Center-to-center distance brackets:	600mm
Position of the wall plate in the bracket:	Low (adding = 10mm)
Test series:	B
Coach screw	No
Load deviation:	76,30%

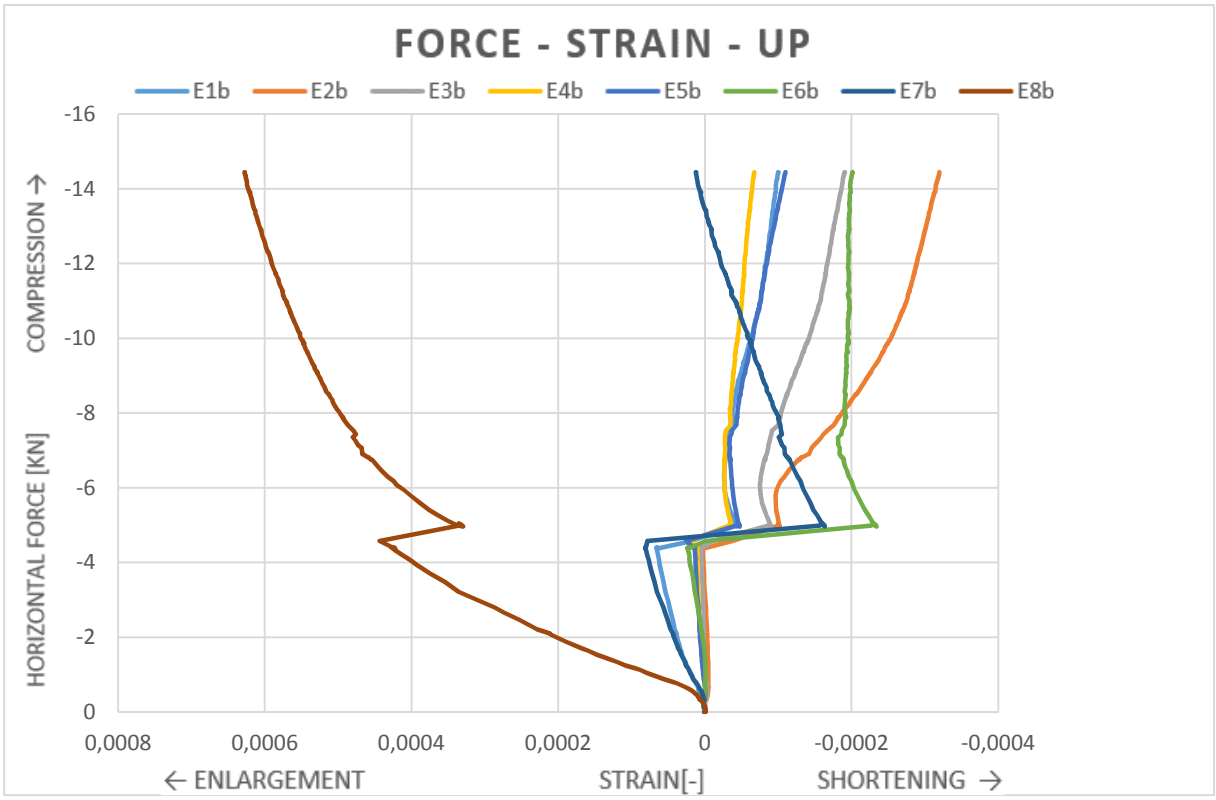

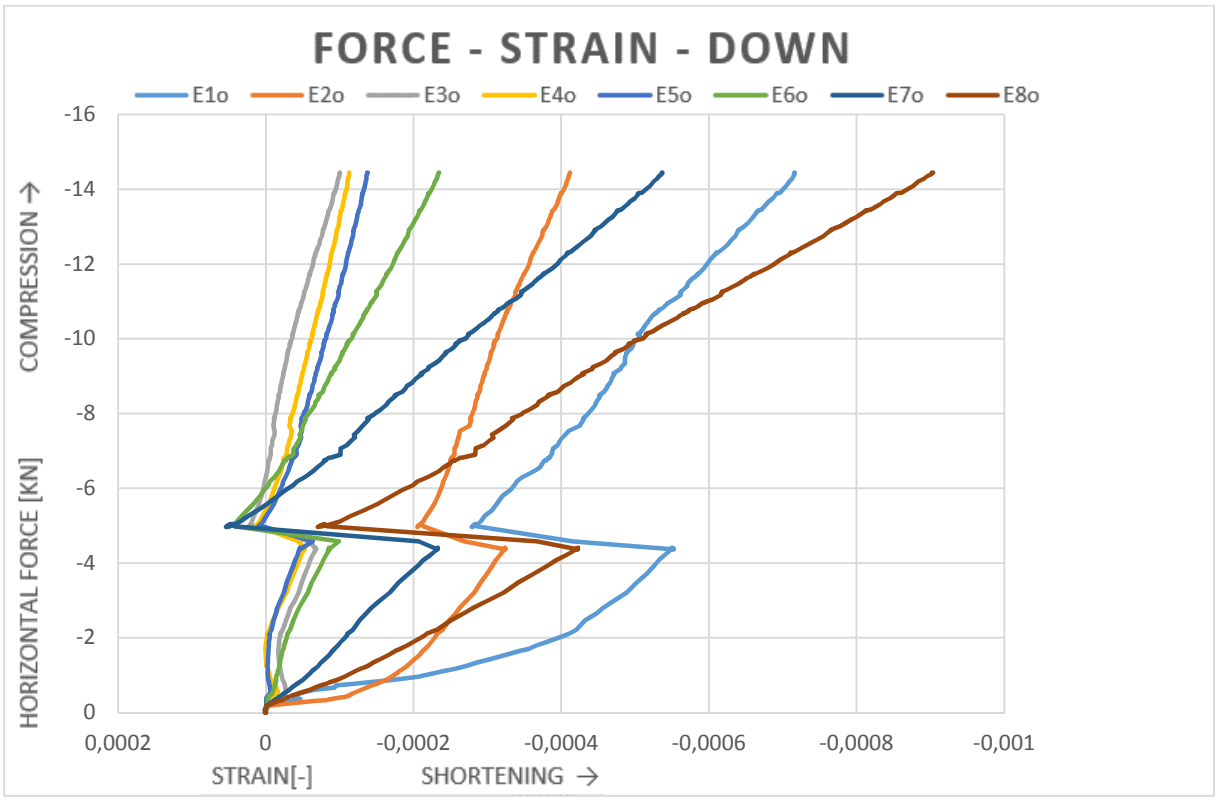

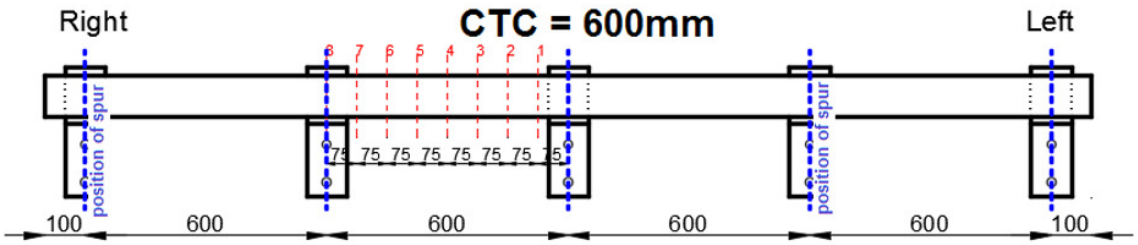
Right
CTC = 600mm
Left
8 7 6 5 4 3 2 1
75 75 75 75 75 75 75 75
position of spur
position of spur
100
600
600
600
600
100

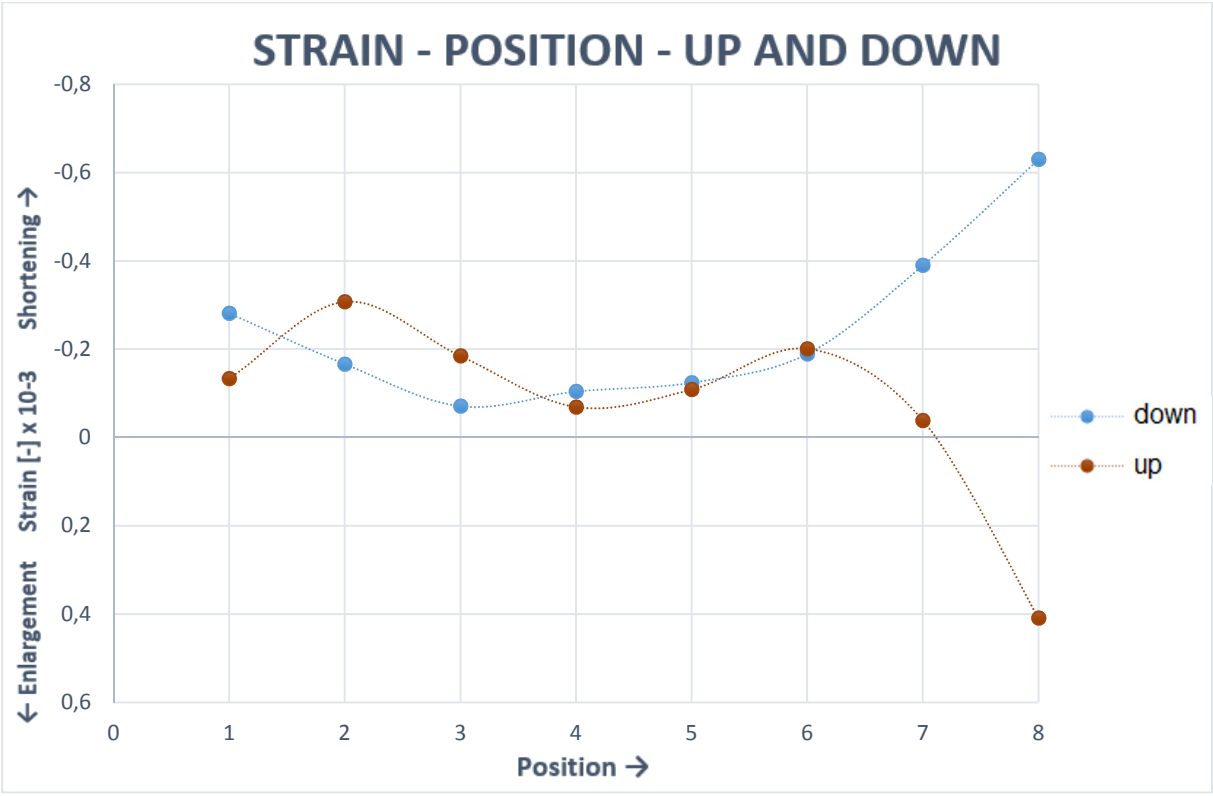
STRAIN - POSITION - UP AND DOWN
-0,8
-0,6
-0,4
-0,2
0
0,2
0,4
0,6
← Enlargement Strain [-] x 10-3 Shortening →
0
1
2
3
4
5
6
7
8
Position →
down
up

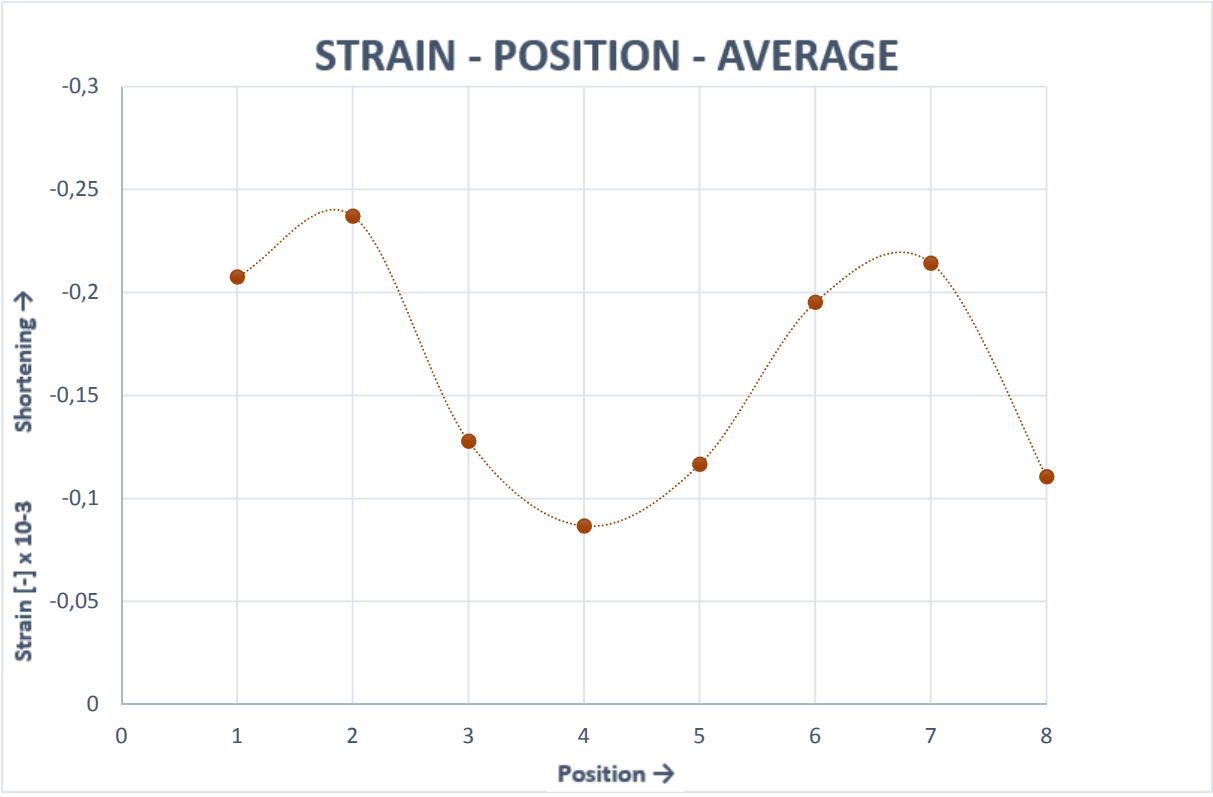
STRAIN - POSITION - AVERAGE
-0,3
-0,25
-0,2
-0,15
-0,1
-0,05
0
Strain [-] x 10-3 Shortening →
0
1
2
3
4
5
6
7
8
Position →

45/900/L/A

Angle of the roof:	45°
Center-to-center distance brackets:	900mm
Position of the wall plate in the bracket:	Low (adding = 10mm)
Test series:	A
Coach screw	No
Load deviation:	76,30%

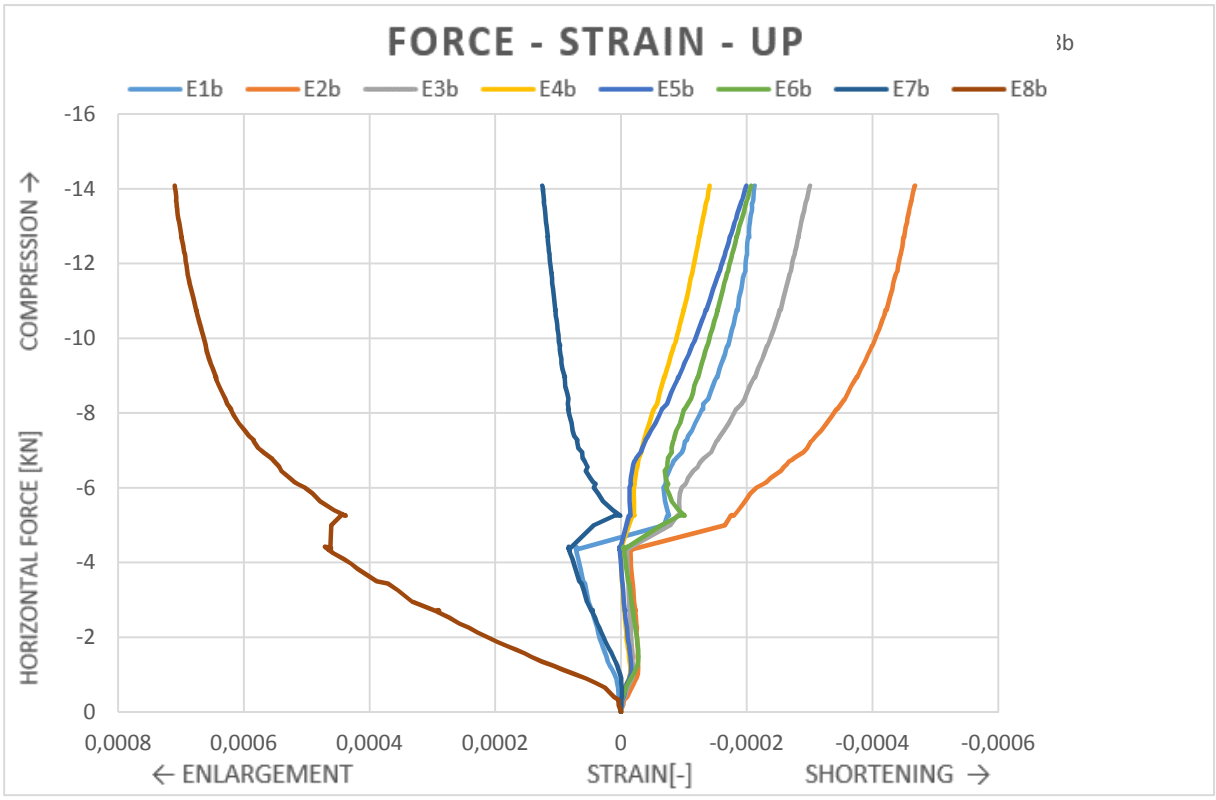

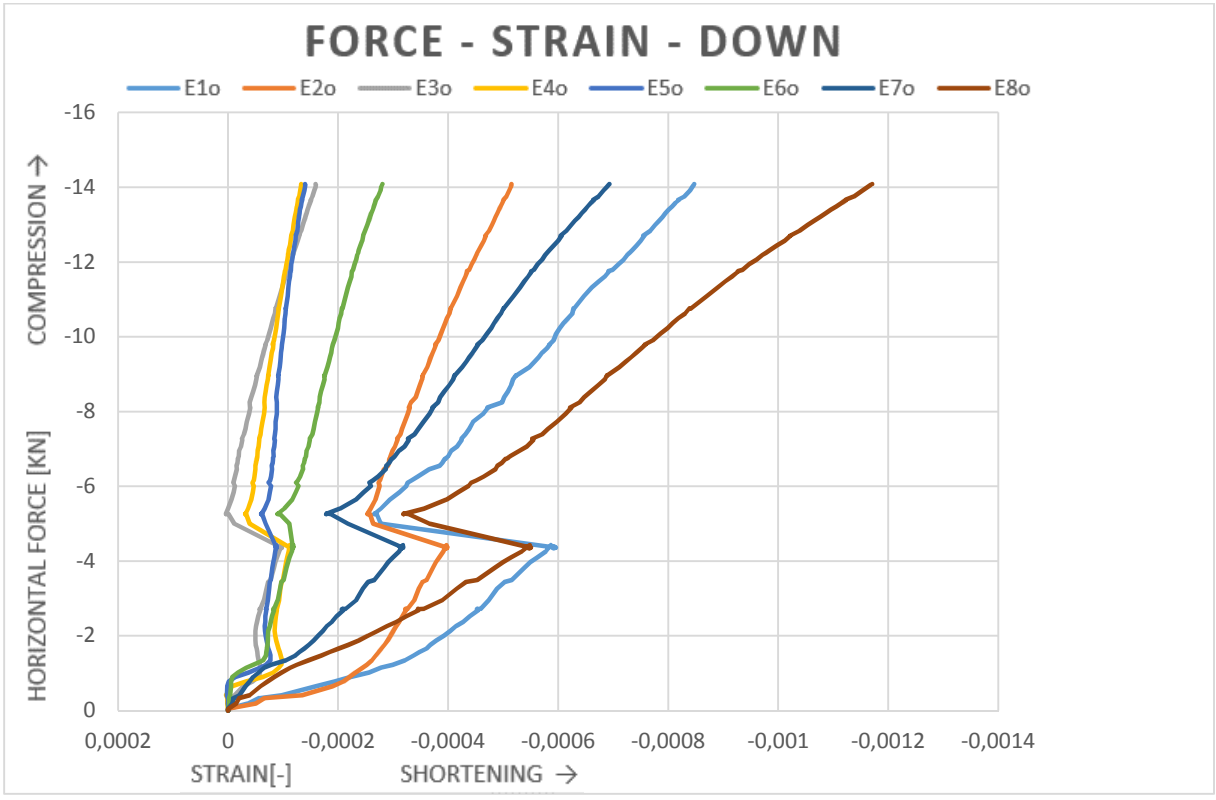

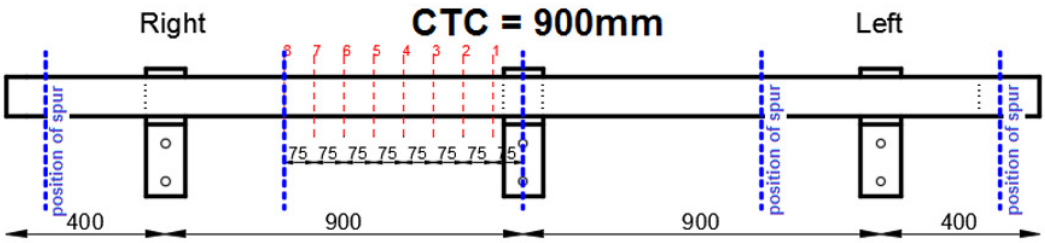
Right
CTC = 900mm
Left
8 7 6 5 4 3 2 1
75 75 75 75 75 75 75 75
position of spur
position of spur
position of spur
400
900
900
400

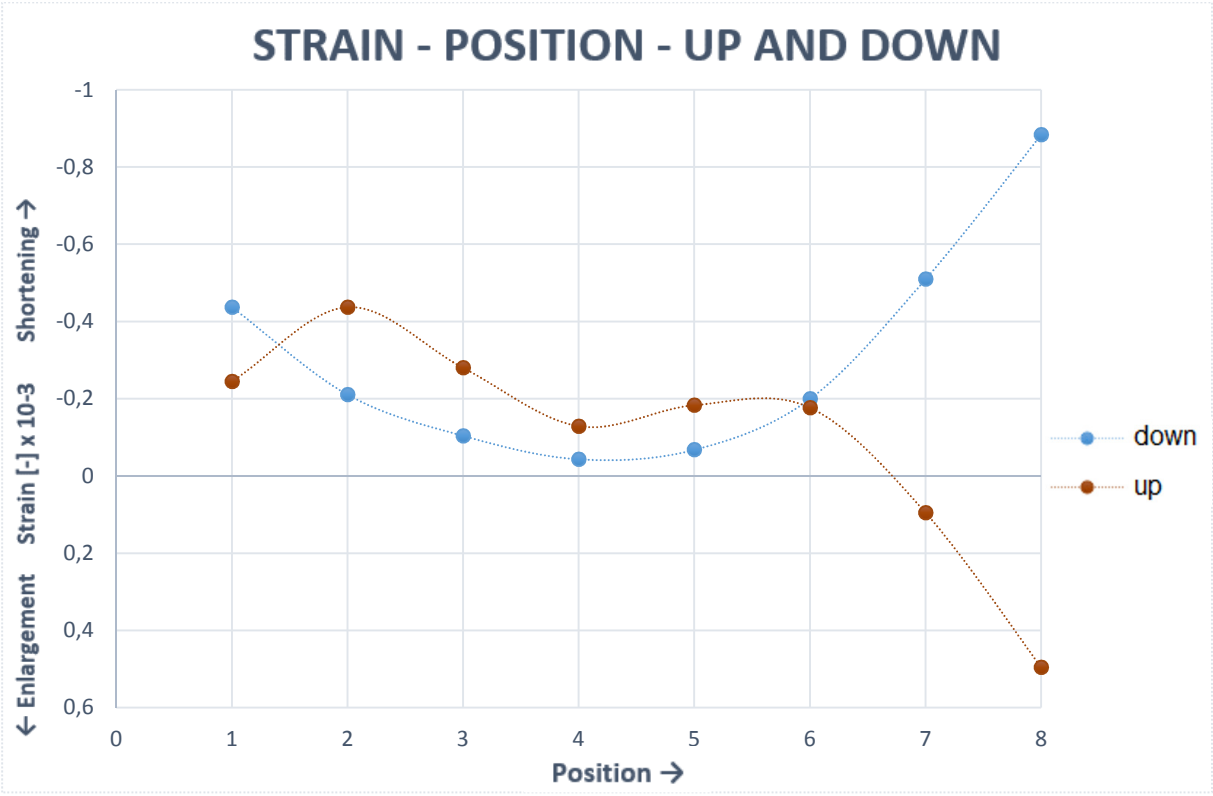
STRAIN - POSITION - UP AND DOWN
-1
-0,8
-0,6
-0,4
-0,2
0
0,2
0,4
0,6
← Enlargement Strain [-] x 10-3 Shortening →
0
1
2
3
4
5
6
7
8
Position →
down
up

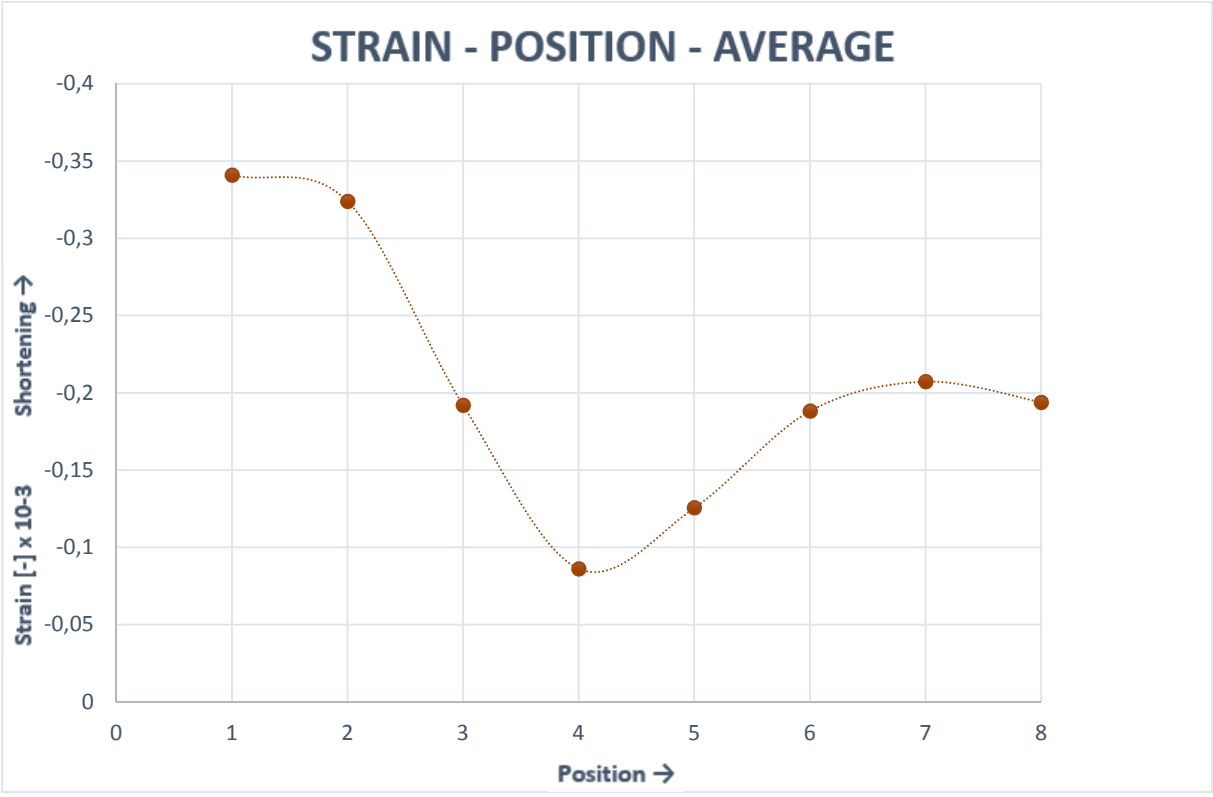
STRAIN - POSITION - AVERAGE
-0,4
-0,35
-0,3
-0,25
-0,2
-0,15
-0,1
-0,05
0
Strain [-] x 10-3 Shortening →
0
1
2
3
4
5
6
7
8
Position →

45/900/L/B

Angle of the roof:	45°
Center-to-center distance brackets:	900mm
Position of the wall plate in the bracket:	Low (adding = 10mm)
Test series:	B
Coach screw	No
Load deviation:	76,30%

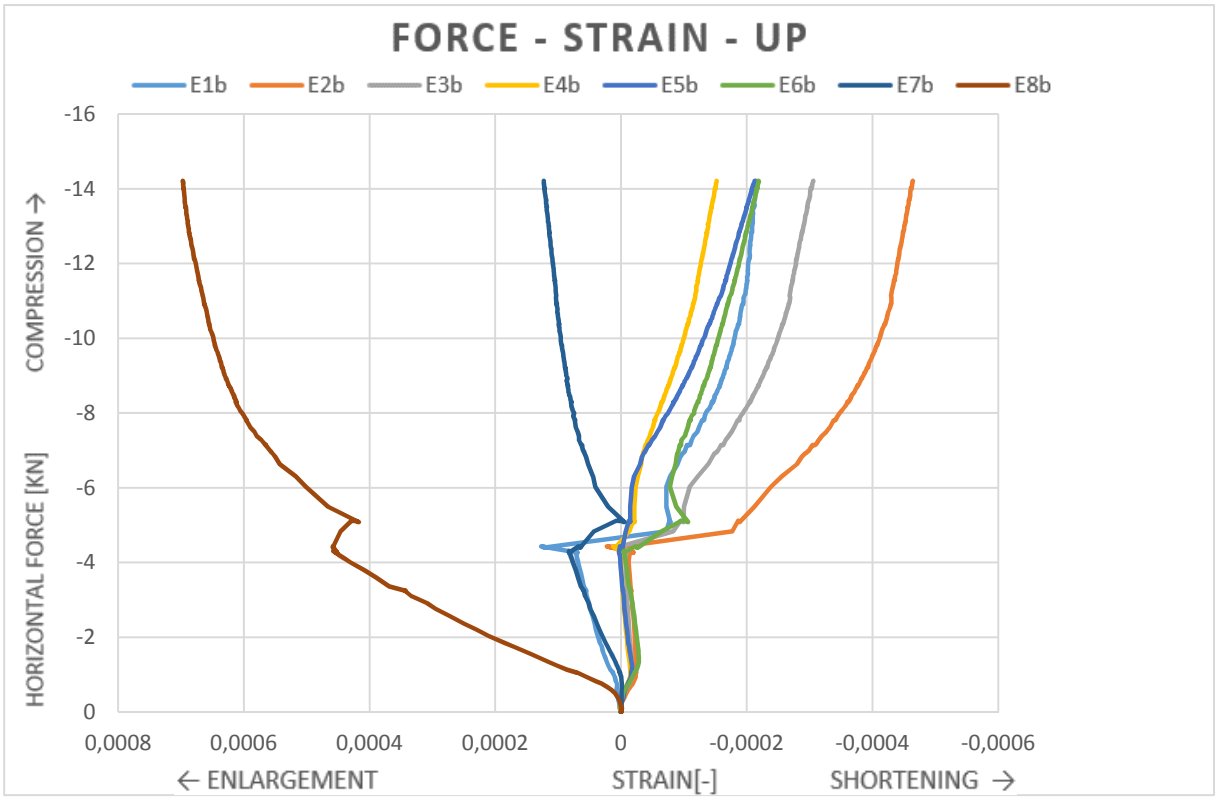

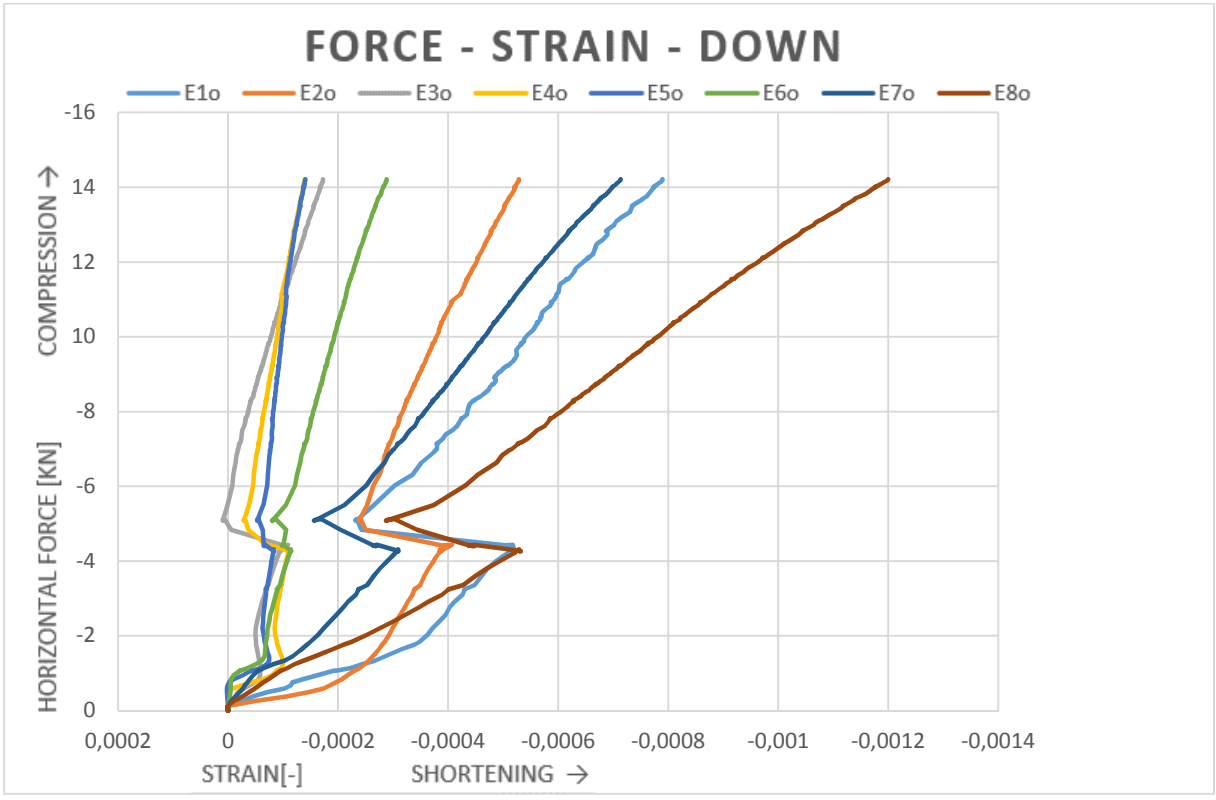

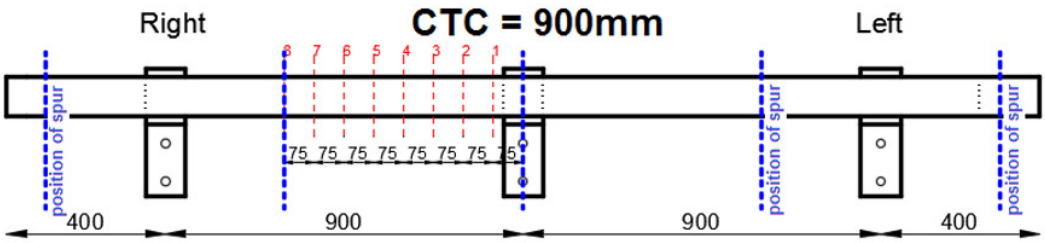
Right
CTC = 900mm
Left
8 7 6 5 4 3 2 1
75 75 75 75 75 75 75 75
position of spur
position of spur
position of spur
400
900
900
400

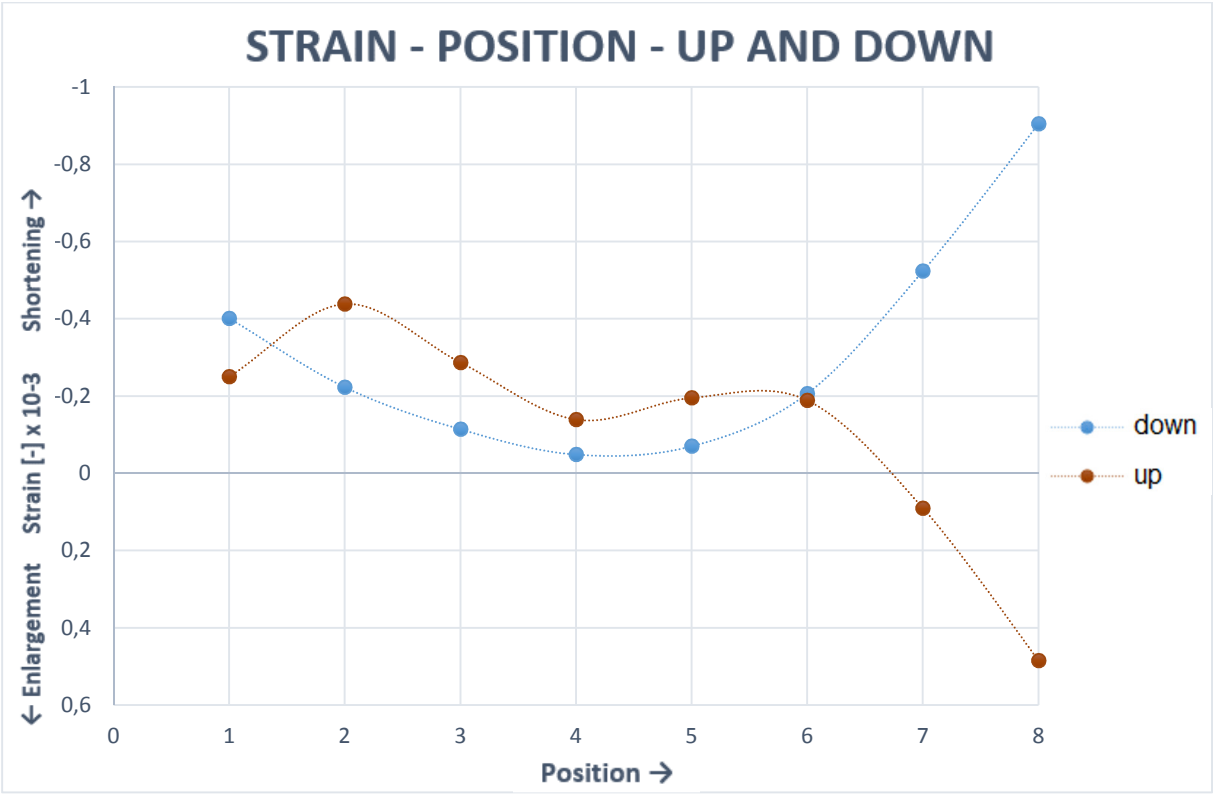
STRAIN - POSITION - UP AND DOWN
-1
-0,8
-0,6
-0,4
-0,2
0
0,2
0,4
0,6
← Enlargement Strain [-] x 10-3 Shortening →
0
1
2
3
4
5
6
7
8
Position →
down
up

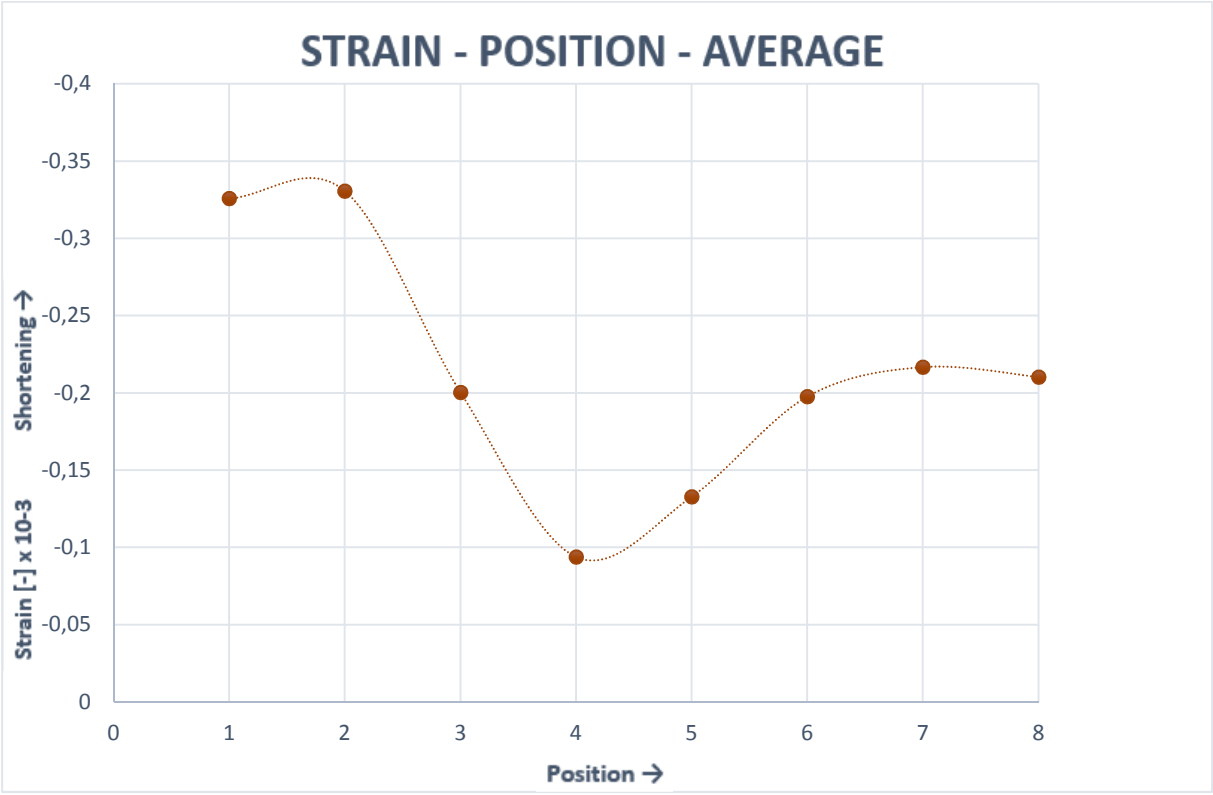
STRAIN - POSITION - AVERAGE
-0,4
-0,35
-0,3
-0,25
-0,2
-0,15
-0,1
-0,05
0
Strain [-] x 10-3 Shortening →
0
1
2
3
4
5
6
7
8
Position →

45/1200/L/A

Angle of the roof:	45°
Center-to-center distance brackets:	1200mm
Position of the wall plate in the bracket:	Low (adding = 10mm)
Test series:	A
Coach screw	No
Load deviation:	76,30%

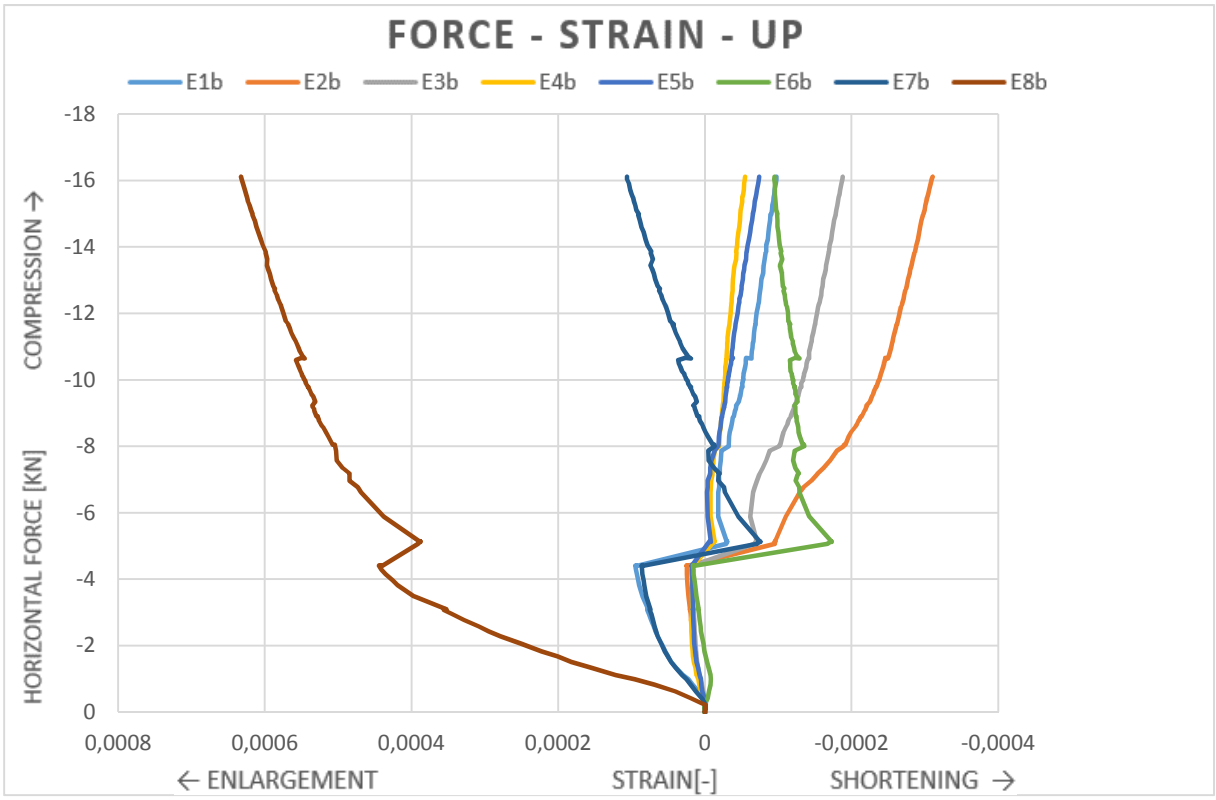

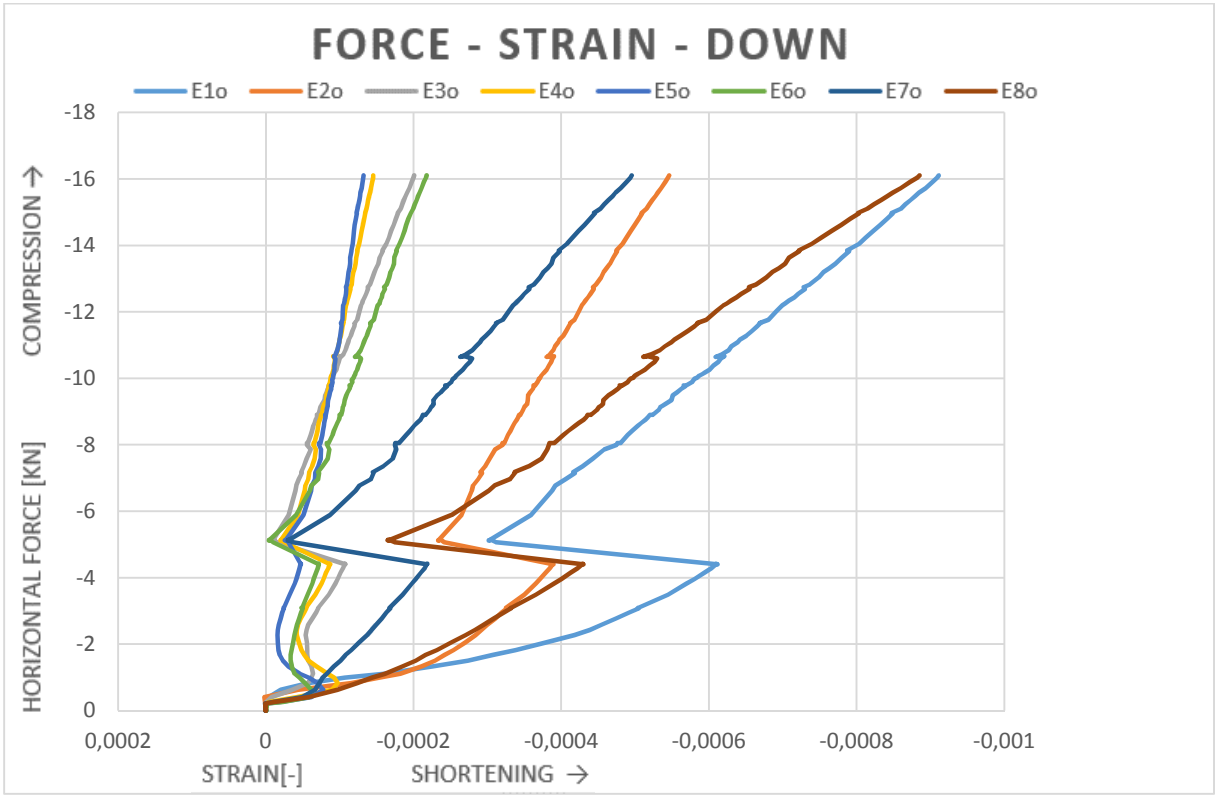

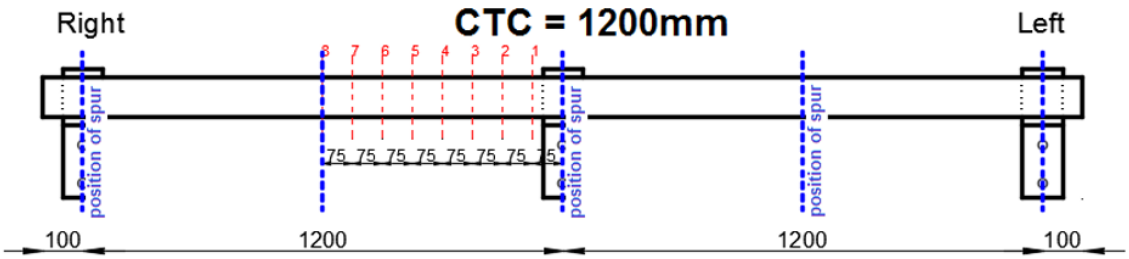
Right
CTC = 1200mm
Left
8 7 6 5 4 3 2 1
75 75 75 75 75 75 75 75
position of spur
position of spur
position of spur
100
1200
1200
100

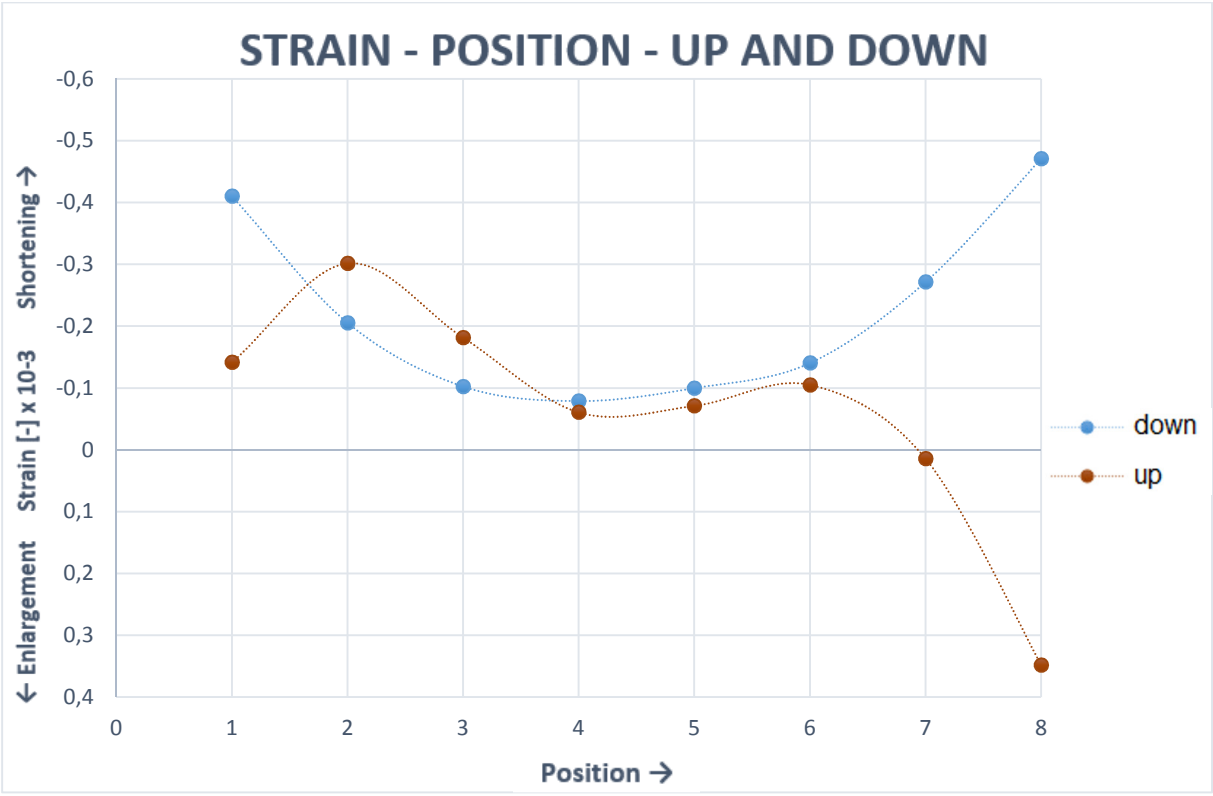
STRAIN - POSITION - UP AND DOWN
-0,6
-0,5
-0,4
-0,3
-0,2
-0,1
0
0,1
0,2
0,3
0,4
← Enlargement Strain [-] x 10-3 Shortening →
0
1
2
3
4
5
6
7
8
Position →
down
up

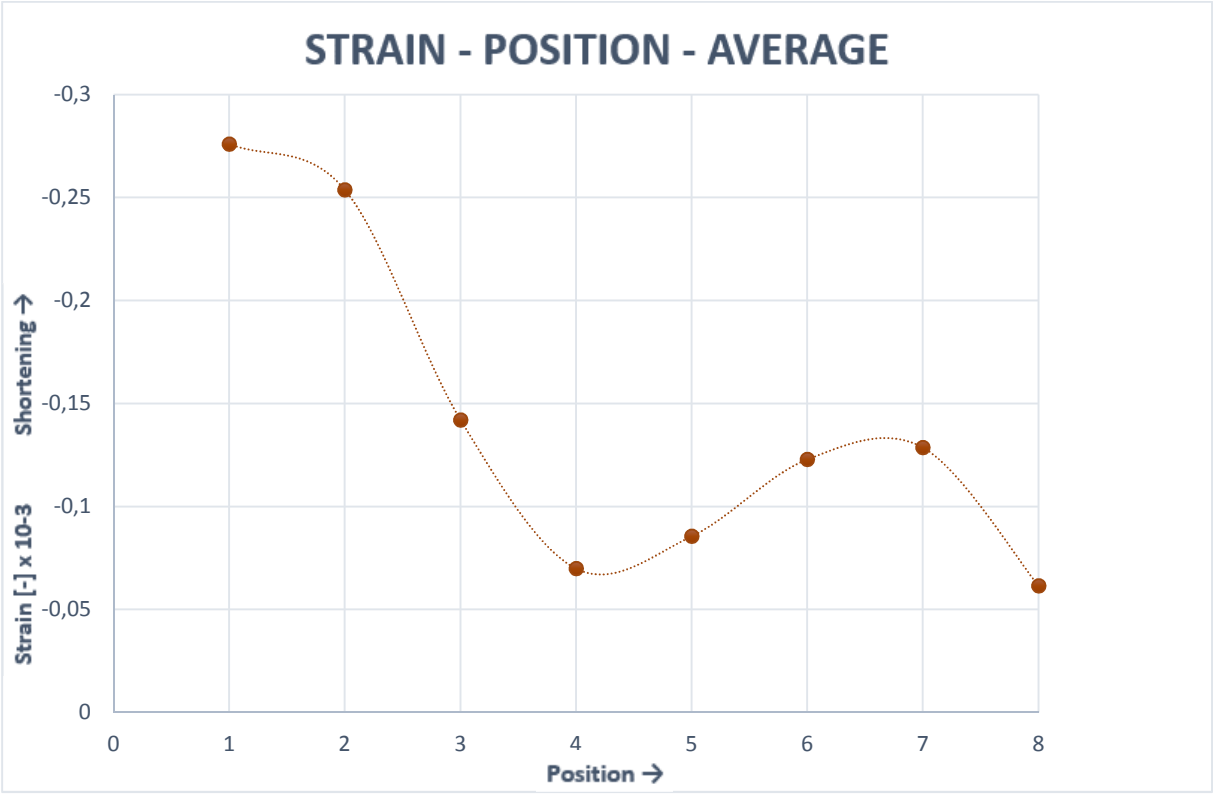
STRAIN - POSITION - AVERAGE
-0,3
-0,25
-0,2
-0,15
-0,1
-0,05
0
Strain [-] x 10-3 Shortening →
0
1
2
3
4
5
6
7
8
Position →

45/1200/L/B

Angle of the roof:	45°
Center-to-center distance brackets:	1200mm
Position of the wall plate in the bracket:	Low (adding = 10mm)
Test series:	B
Coach screw	No
Load deviation:	76,30%

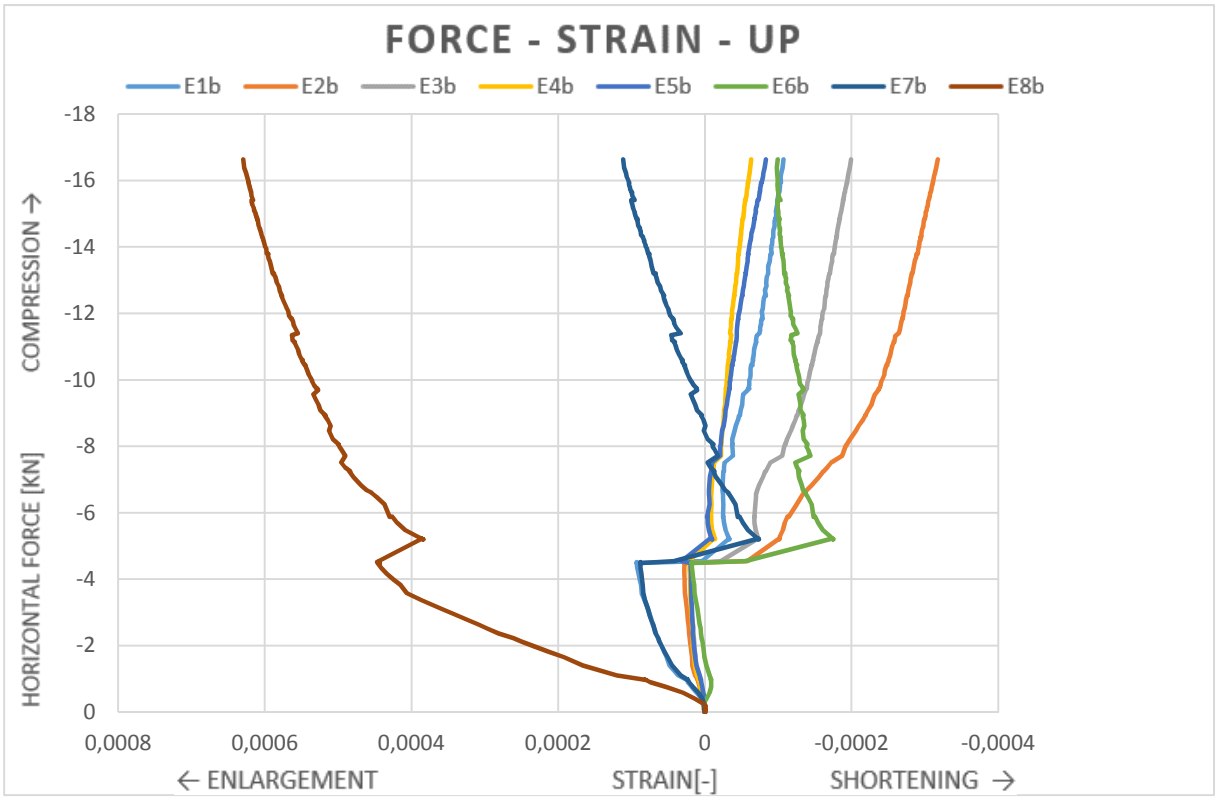

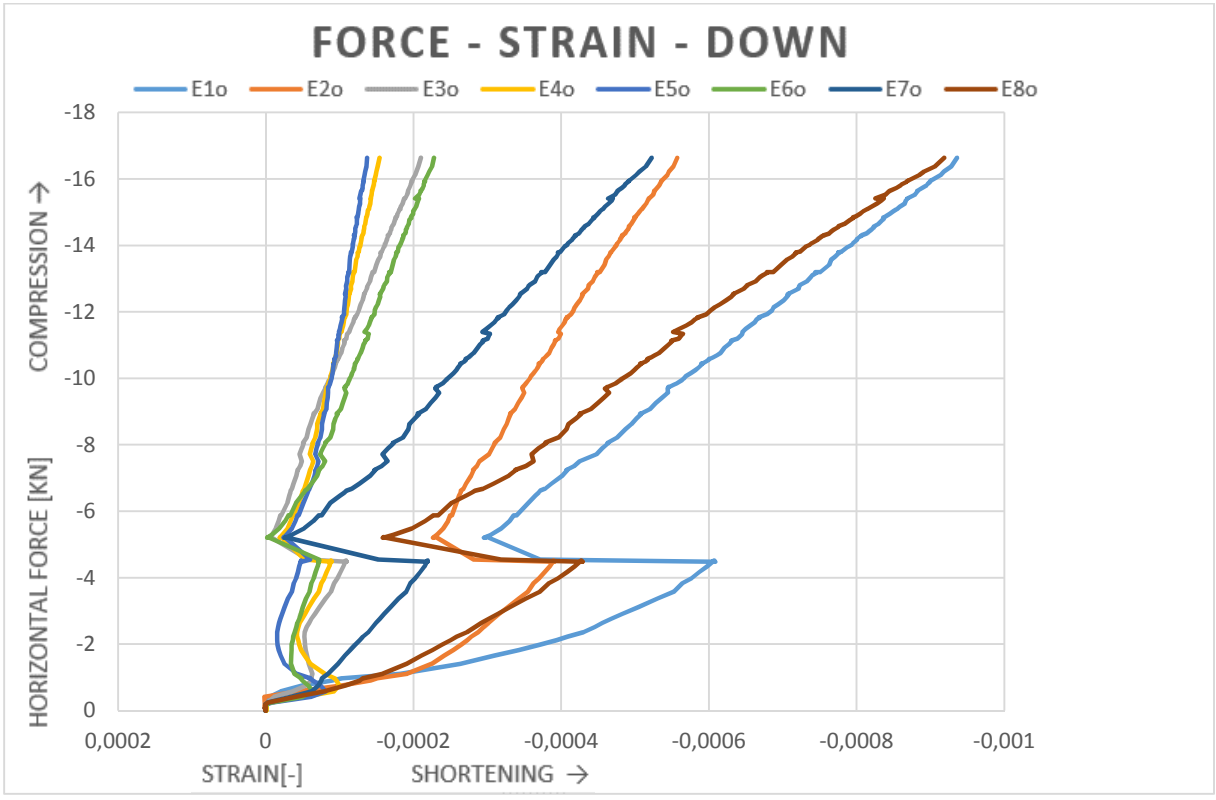

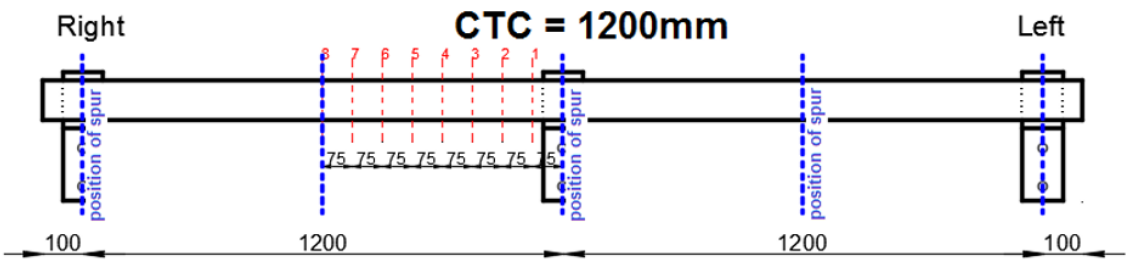
Right
CTC = 1200mm
Left
8 7 6 5 4 3 2 1
75 75 75 75 75 75 75 75
position of spur
position of spur
position of spur
100
1200
1200
100

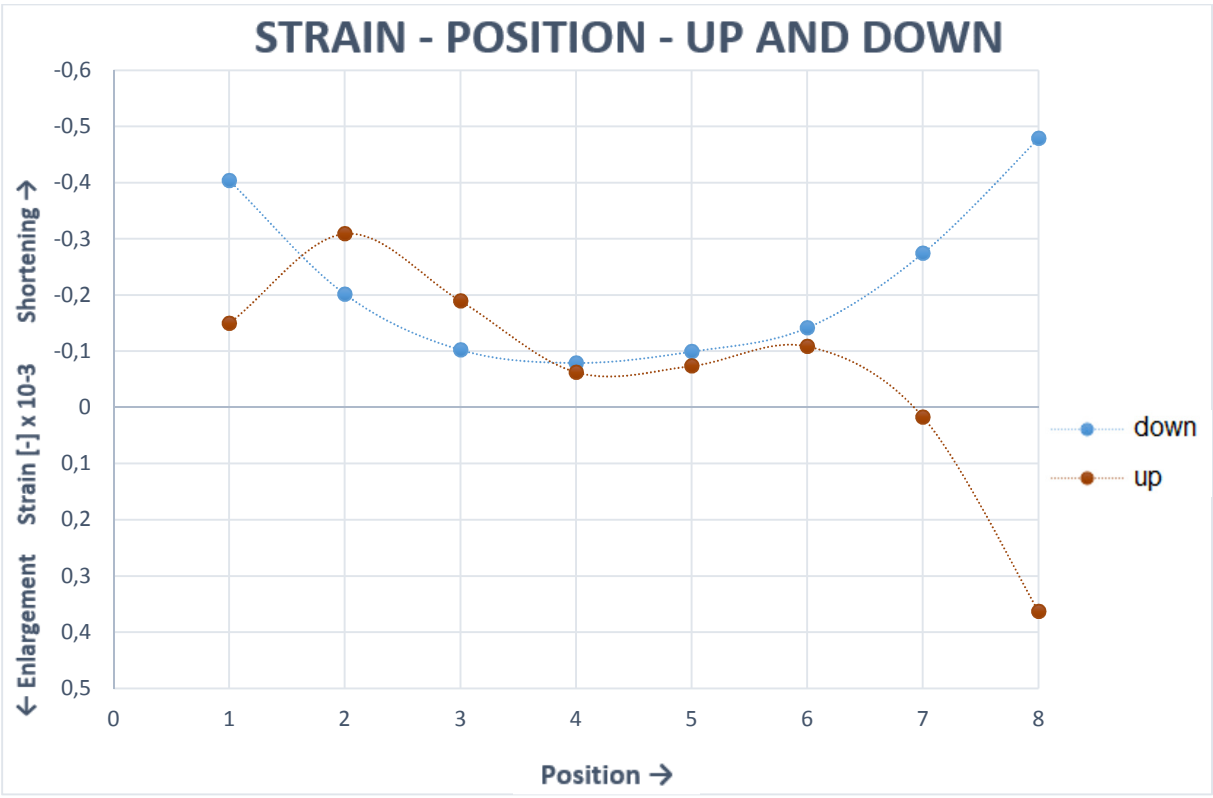
STRAIN - POSITION - UP AND DOWN
-0,6
-0,5
-0,4
-0,3
-0,2
-0,1
0
0,1
0,2
0,3
0,4
0,5
← Enlargement Strain [-] x 10-3 Shortening →
0
1
2
3
4
5
6
7
8
Position →
down
up

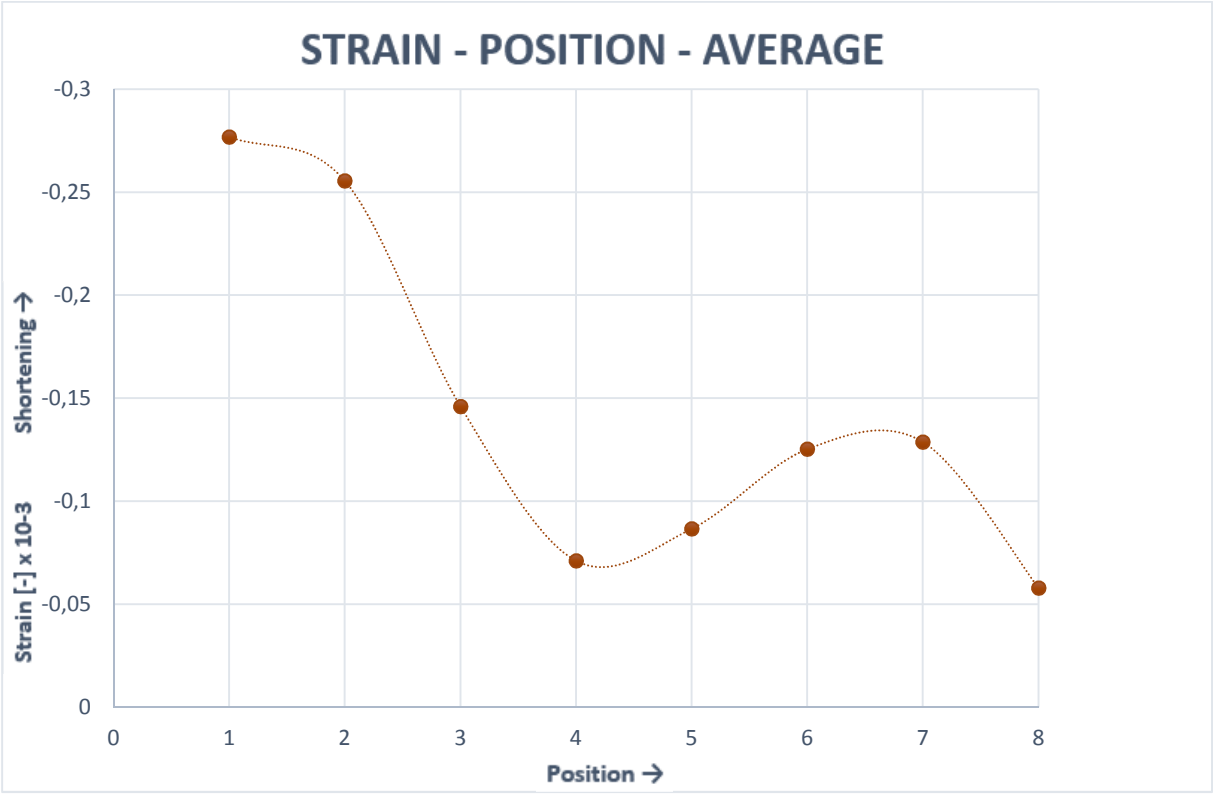
STRAIN - POSITION - AVERAGE
-0,3
-0,25
-0,2
-0,15
-0,1
-0,05
0
Strain [-] x 10-3 Shortening →
0
1
2
3
4
5
6
7
8
Position →

45/600/H/A

Angle of the roof:	45°
Center-to-center distance brackets:	600mm
Position of the wall plate in the bracket:	High (adding = 30mm)
Test series:	A
Coach screw	No
Load deviation:	76,30%

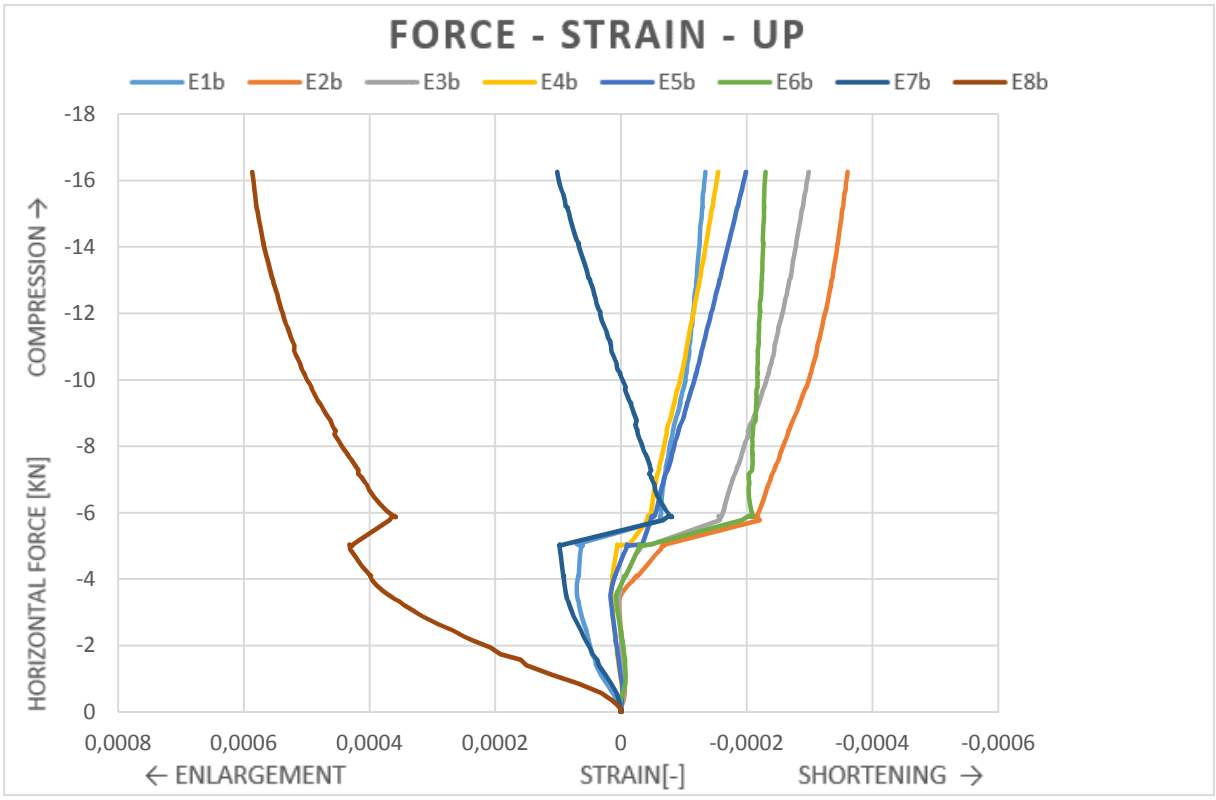

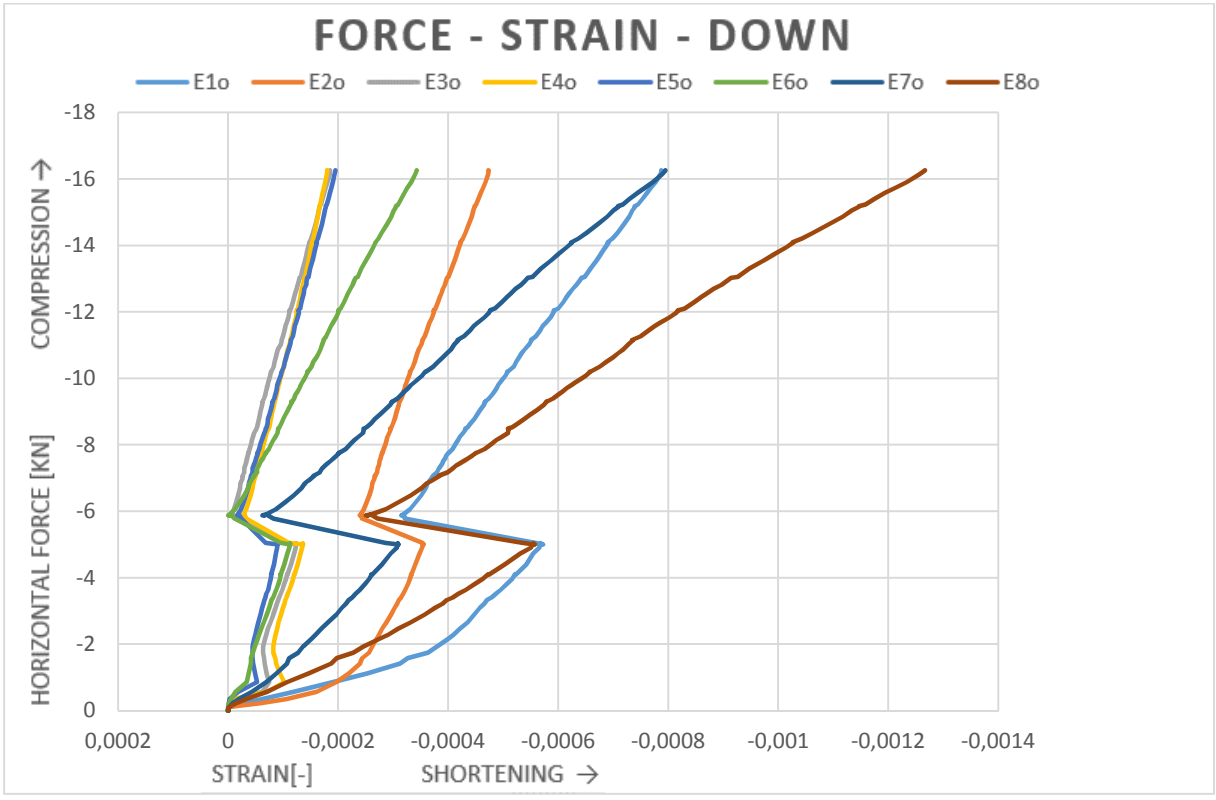

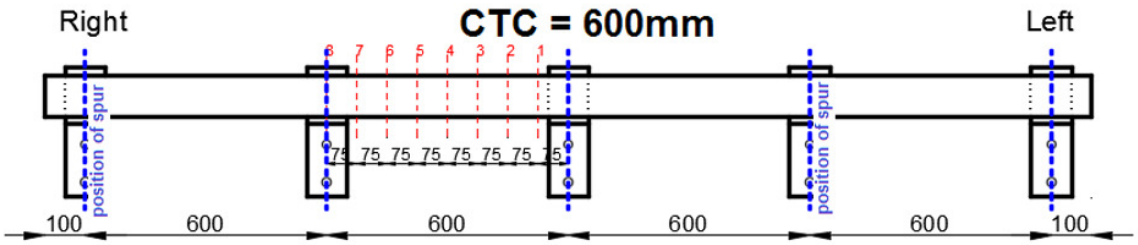
Right
CTC = 600mm
Left
8 7 6 5 4 3 2 1
75 75 75 75 75 75 75 75
position of spur
position of spur
100
600
600
600
600
100

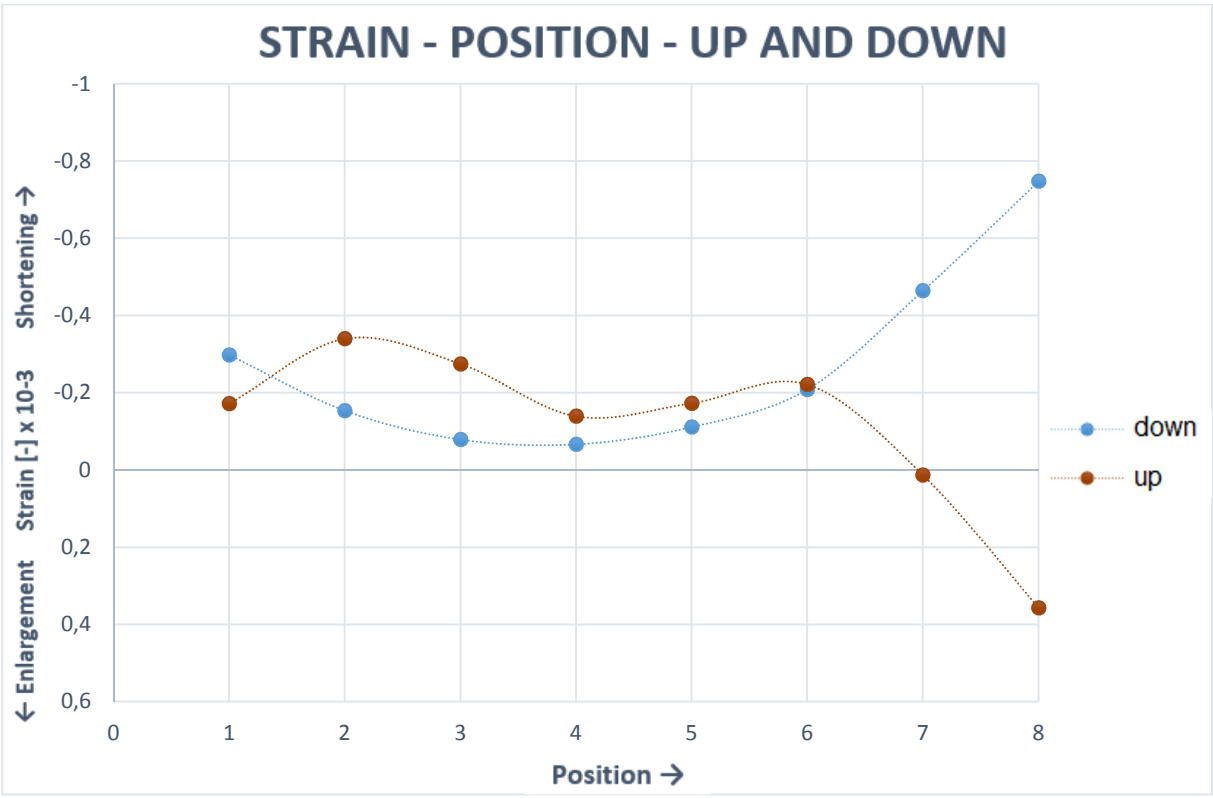
STRAIN - POSITION - UP AND DOWN
-1
-0,8
-0,6
-0,4
-0,2
0
0,2
0,4
0,6
← Enlargement Strain [-] x 10-3 Shortening →
0
1
2
3
4
5
6
7
8
Position →
down
up

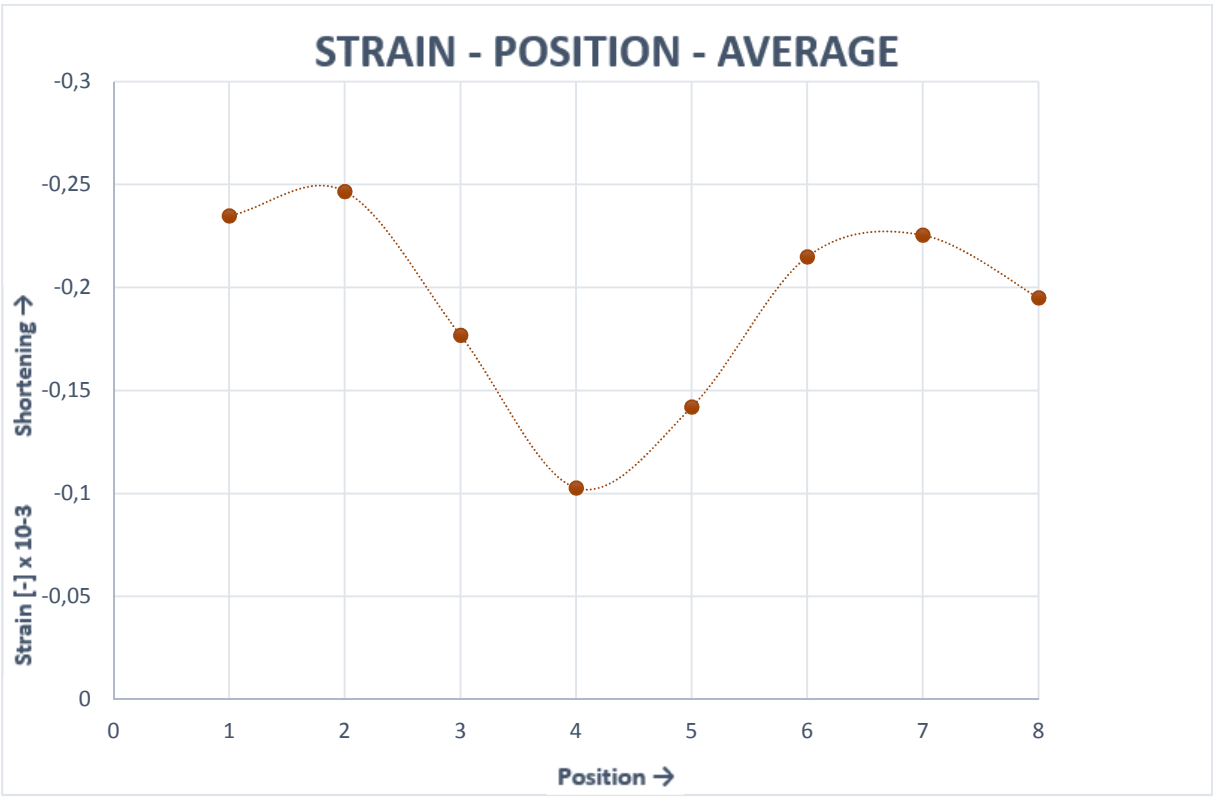
STRAIN - POSITION - AVERAGE
-0,3
-0,25
-0,2
-0,15
-0,1
-0,05
0
Strain [-] x 10-3 Shortening →
0
1
2
3
4
5
6
7
8
Position →

45/600/H/B

Angle of the roof:	45°
Center-to-center distance brackets:	600mm
Position of the wall plate in the bracket:	High (adding = 30mm)
Test series:	B
Coach screw	No
Load deviation:	76,30%

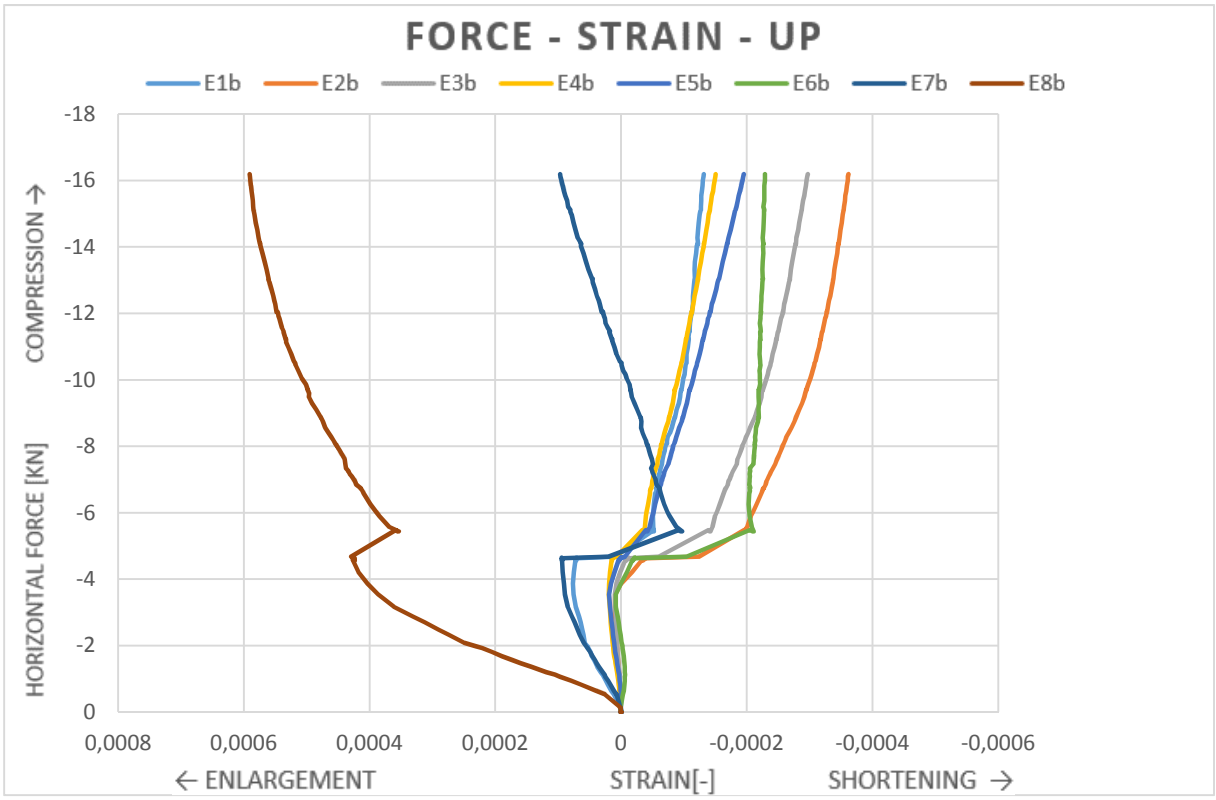

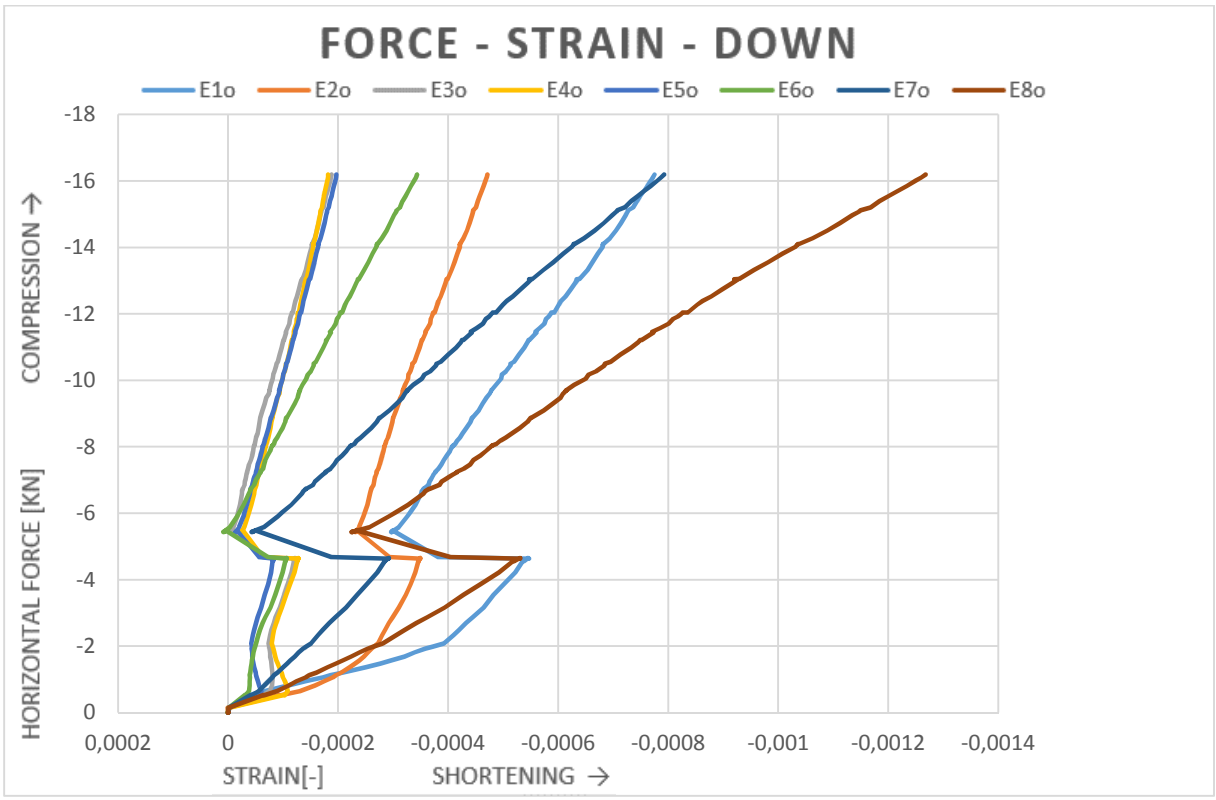

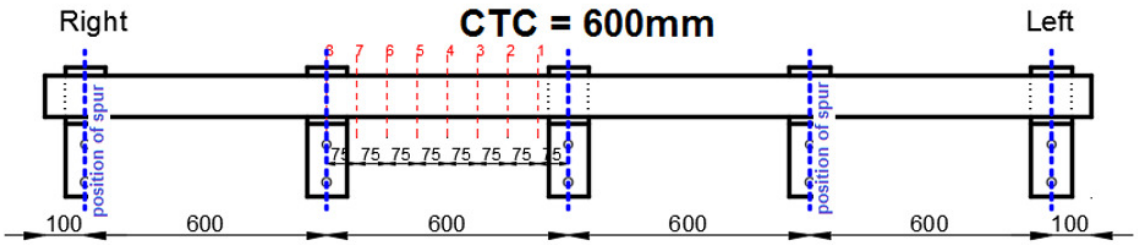
Right
CTC = 600mm
Left
8 7 6 5 4 3 2 1
75 75 75 75 75 75 75 75
position of spur
position of spur
100
600
600
600
600
100

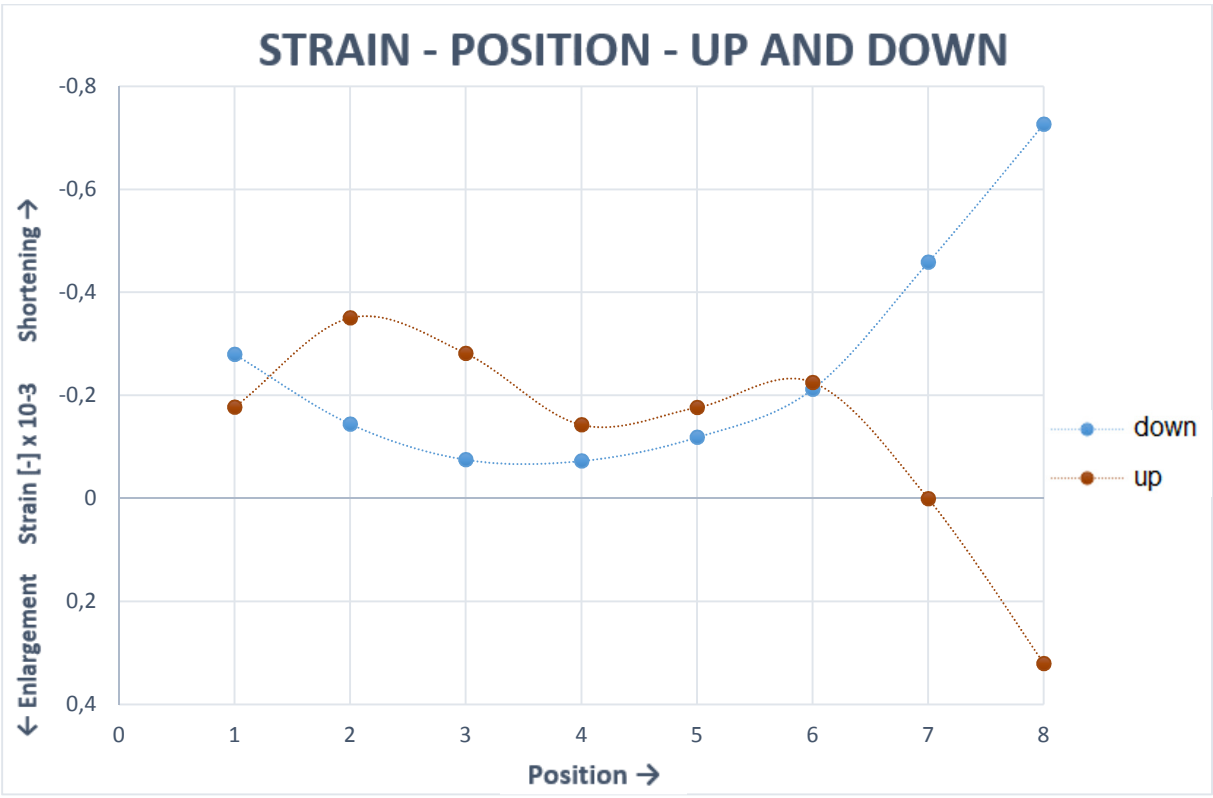
STRAIN - POSITION - UP AND DOWN
-0,8
-0,6
-0,4
-0,2
0
0,2
0,4
← Enlargement Strain [-] x 10-3 Shortening →
0
1
2
3
4
5
6
7
8
Position →
down
up

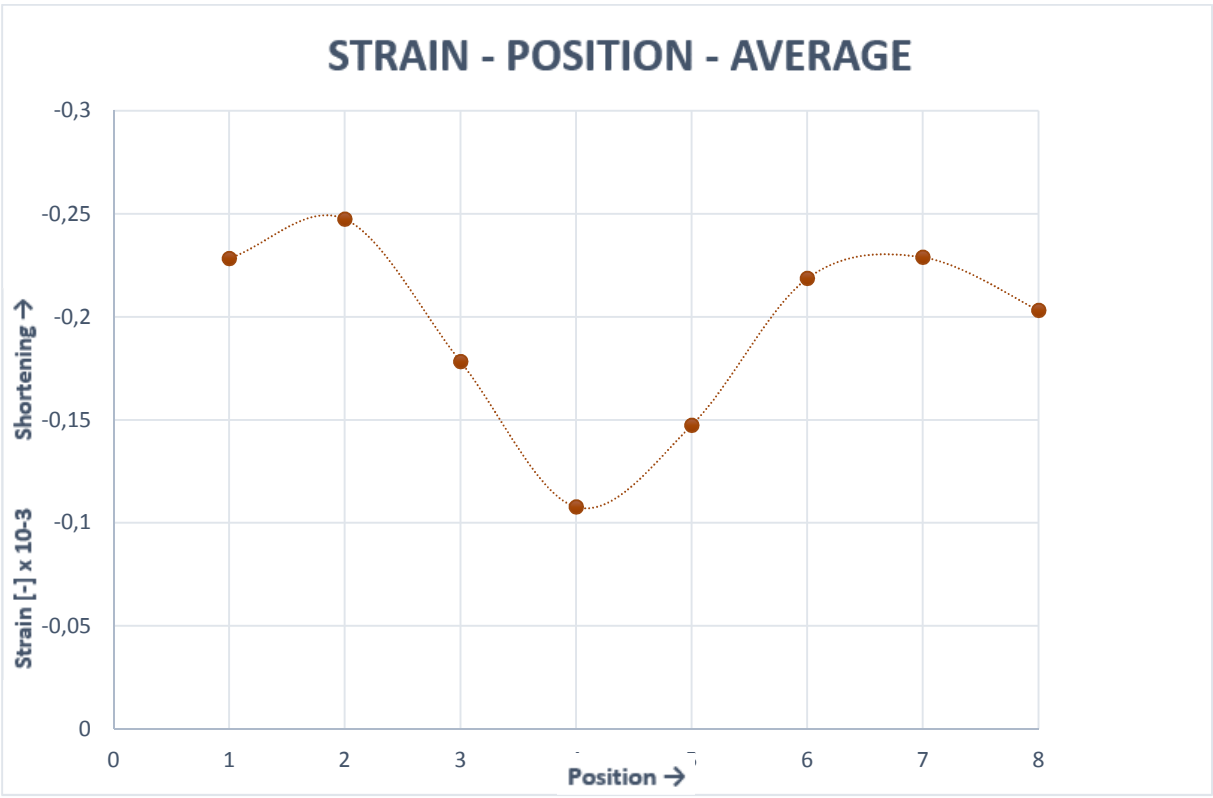
STRAIN - POSITION - AVERAGE
-0,3
-0,25
-0,2
-0,15
-0,1
-0,05
0
Strain [-] x 10-3 Shortening →
0
1
2
3
6
7
8
Position →

45/900/H/A

Angle of the roof:	45°
Center-to-center distance brackets:	900mm
Position of the wall plate in the bracket:	High (adding = 30mm)
Test series:	A
Coach screw	No
Load deviation:	76,30%

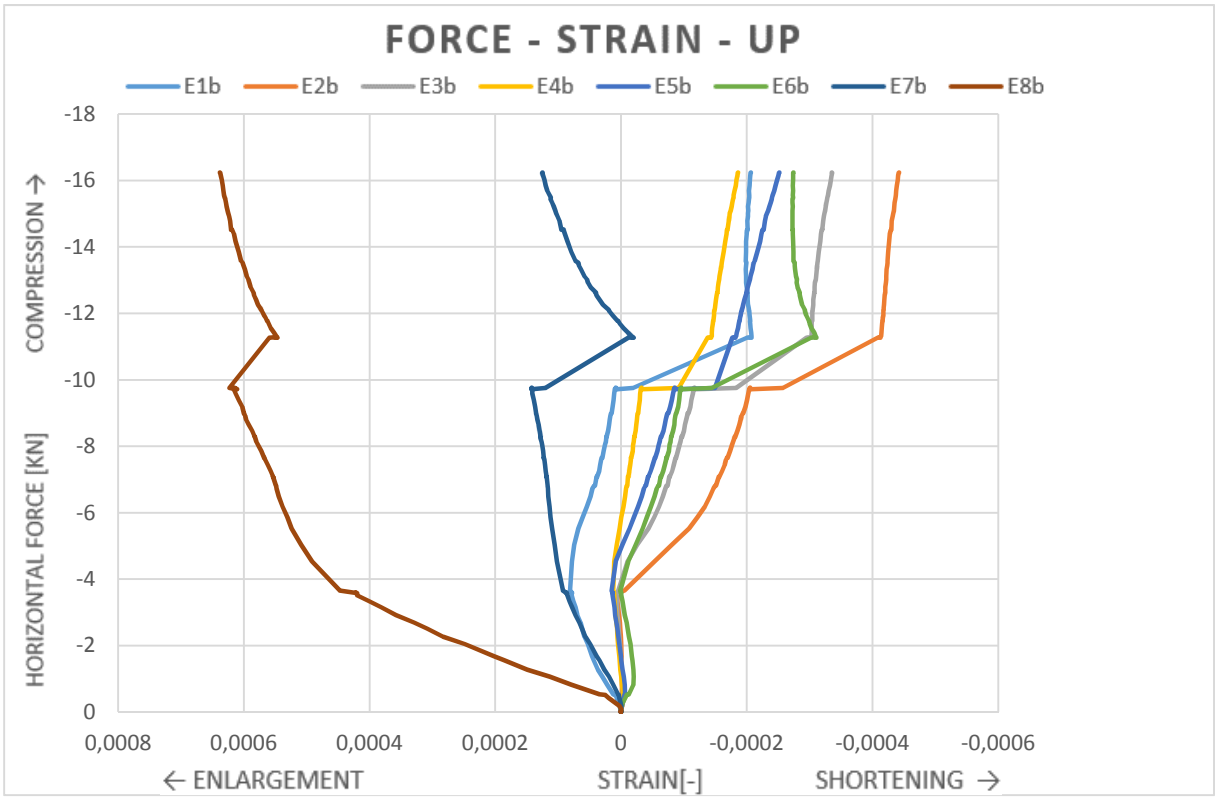

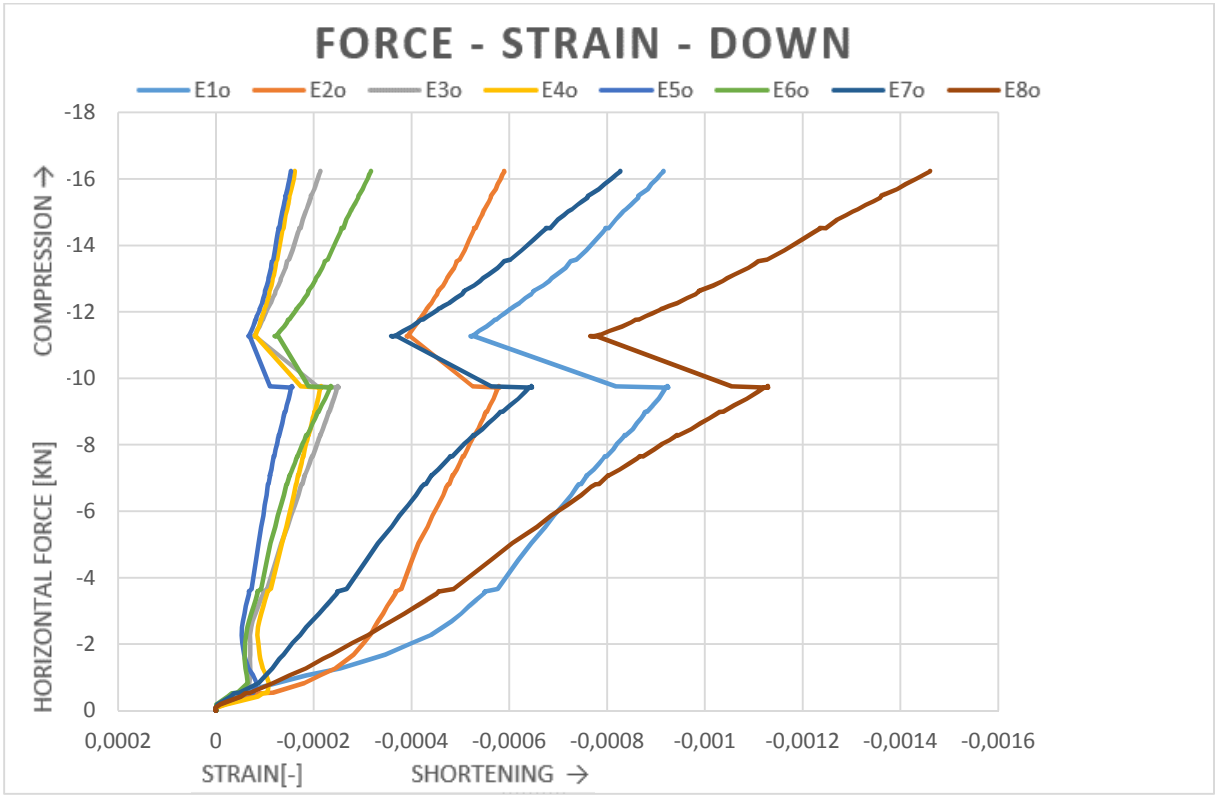

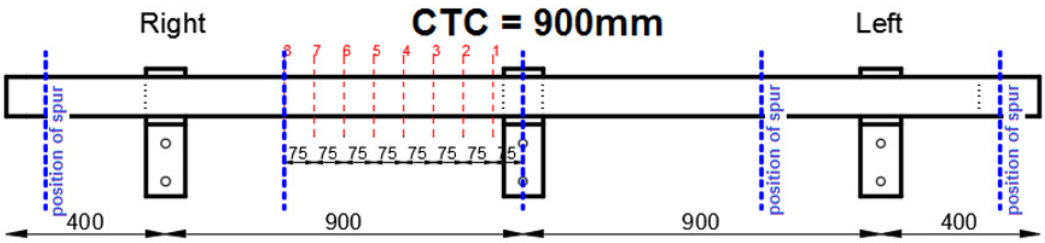
Right
CTC = 900mm
Left
8 7 6 5 4 3 2 1
75 75 75 75 75 75 75 75
position of spur
position of spur
position of spur
400
900
900
400

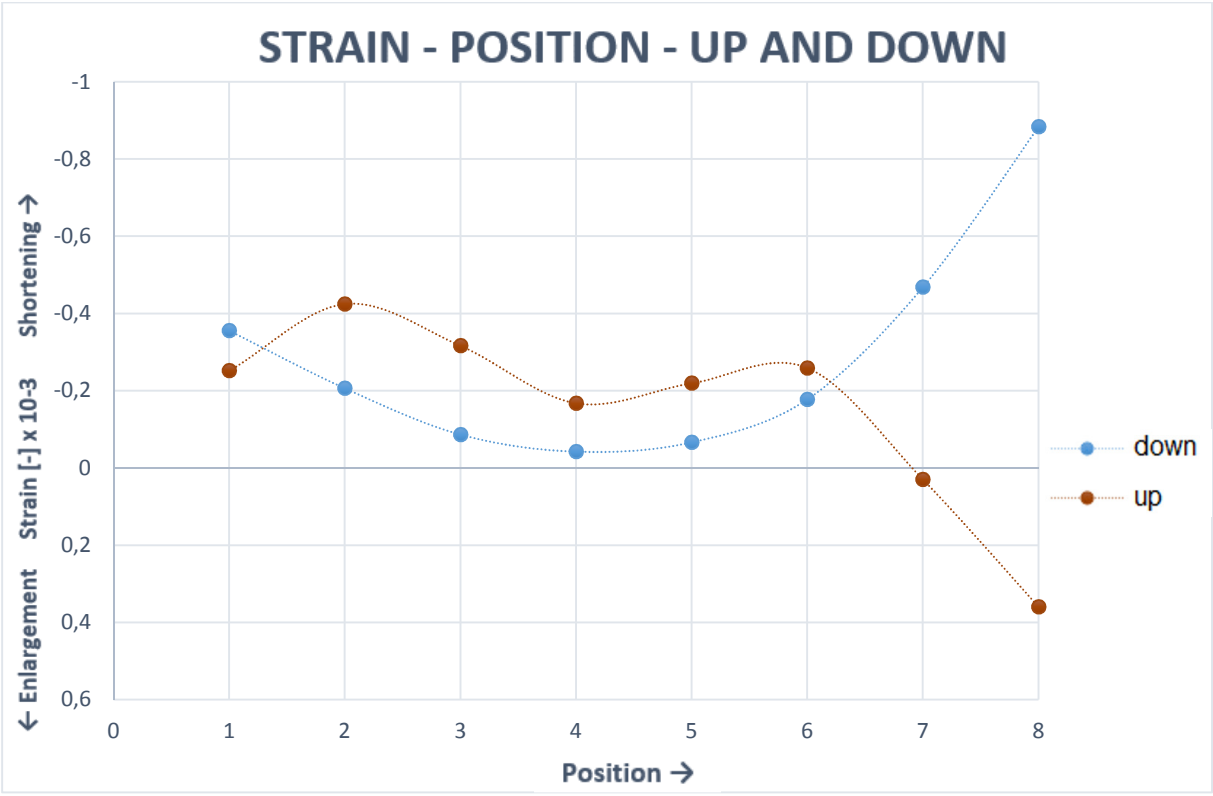
STRAIN - POSITION - UP AND DOWN
-1
-0,8
-0,6
-0,4
-0,2
0
0,2
0,4
0,6
← Enlargement Strain [-] x 10-3 Shortening →
0
1
2
3
4
5
6
7
8
Position →
down
up

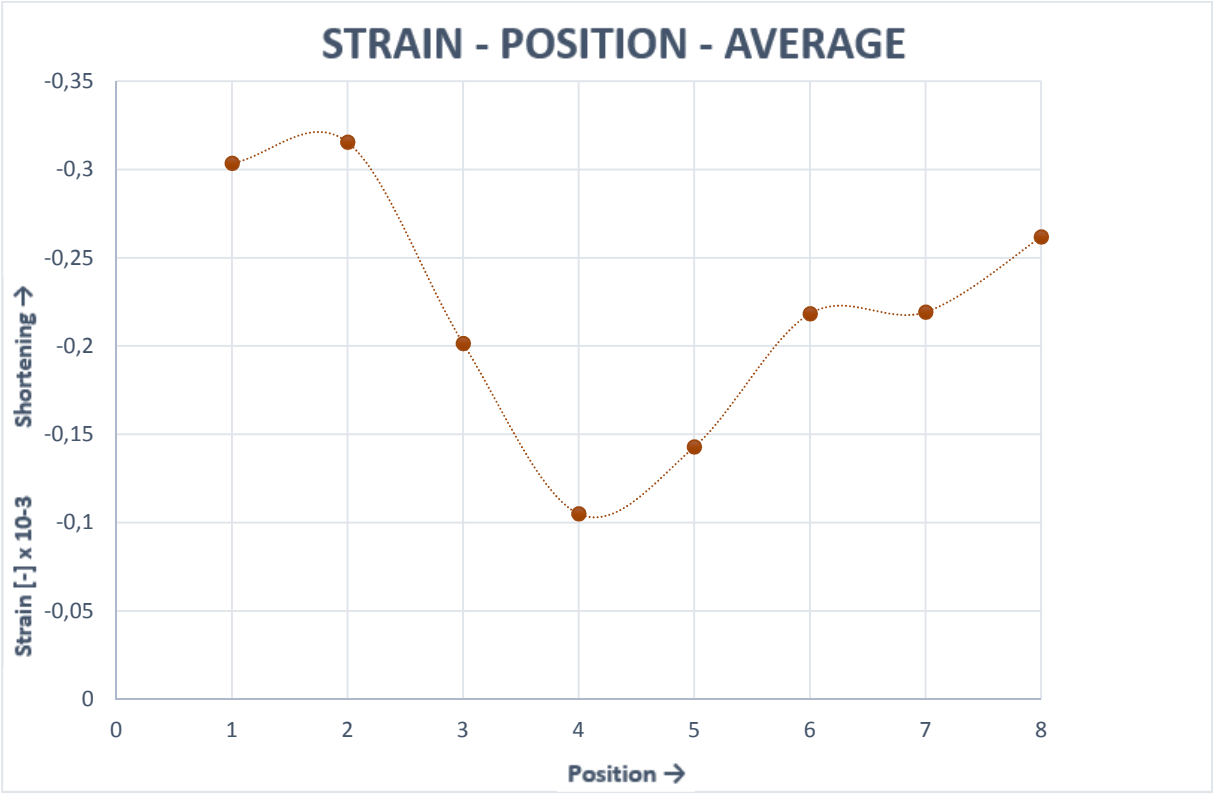
STRAIN - POSITION - AVERAGE
-0,35
-0,3
-0,25
-0,2
-0,15
-0,1
-0,05
0
Strain [-] x 10-3 Shortening →
0
1
2
3
4
5
6
7
8
Position →

45/900/H/B

Angle of the roof:	45°
Center-to-center distance brackets:	900mm
Position of the wall plate in the bracket:	High (adding = 30mm)
Test series:	B
Coach screw	No
Load deviation:	76,30%

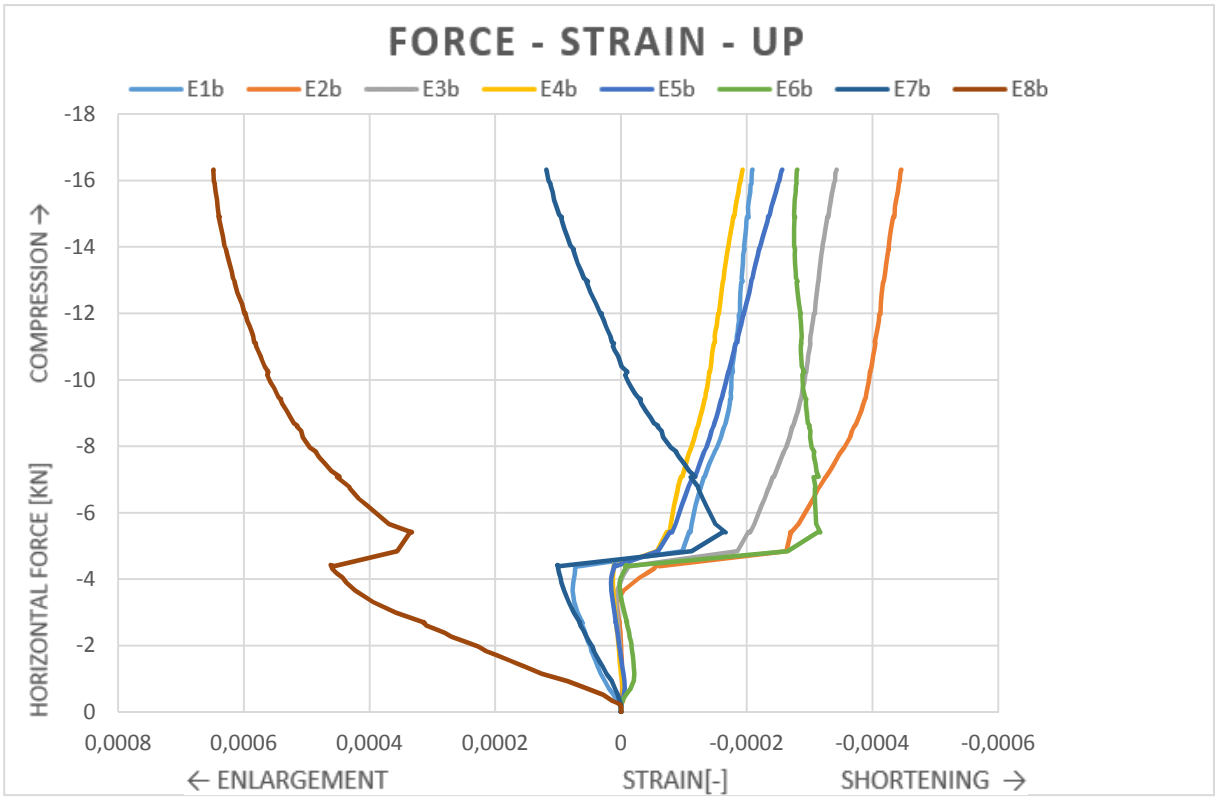

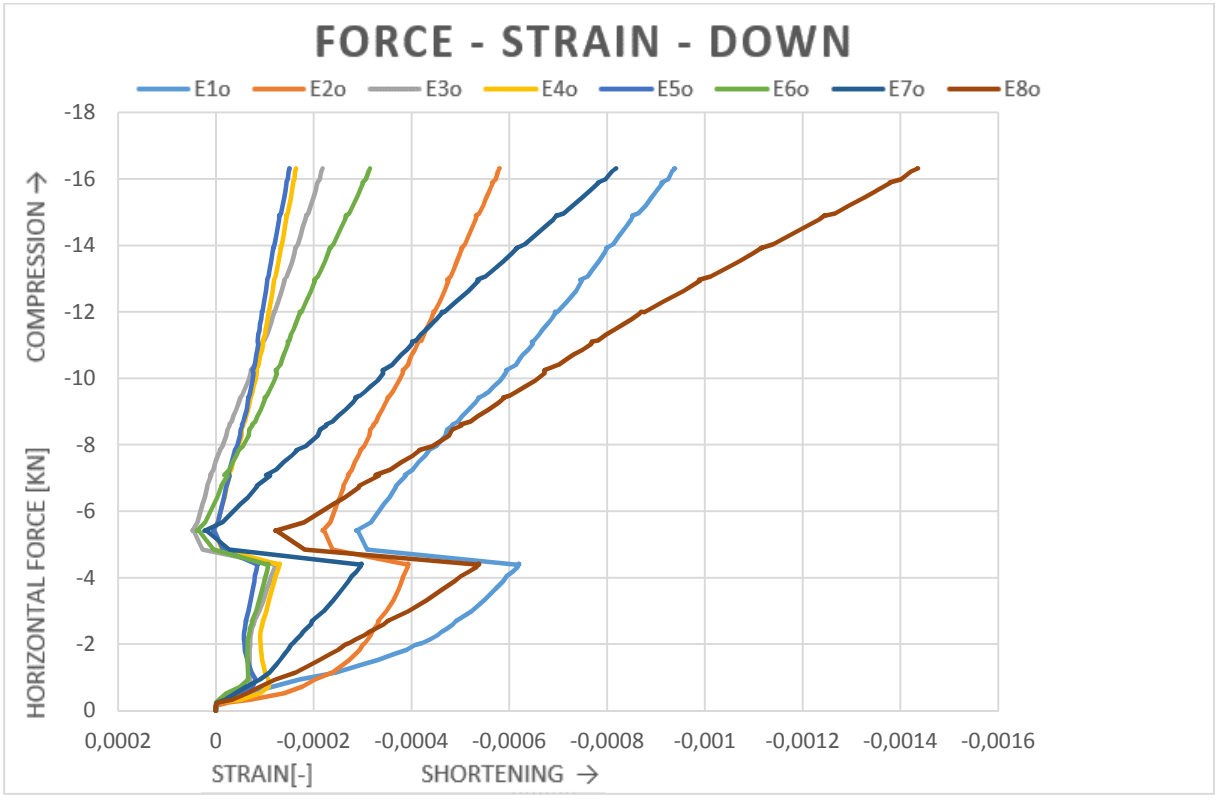

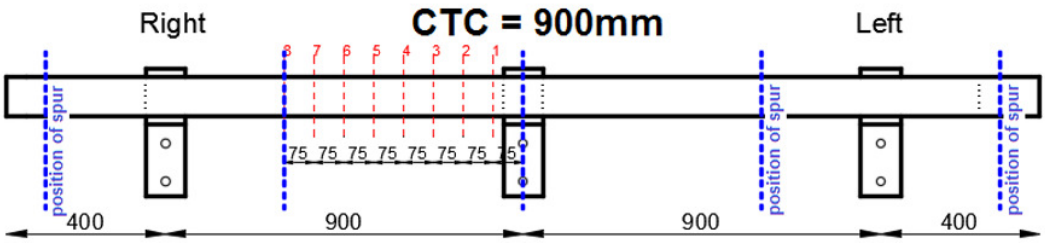
Right
CTC = 900mm
Left
8 7 6 5 4 3 2 1
75 75 75 75 75 75 75 75
position of spur
position of spur
position of spur
400
900
900
400

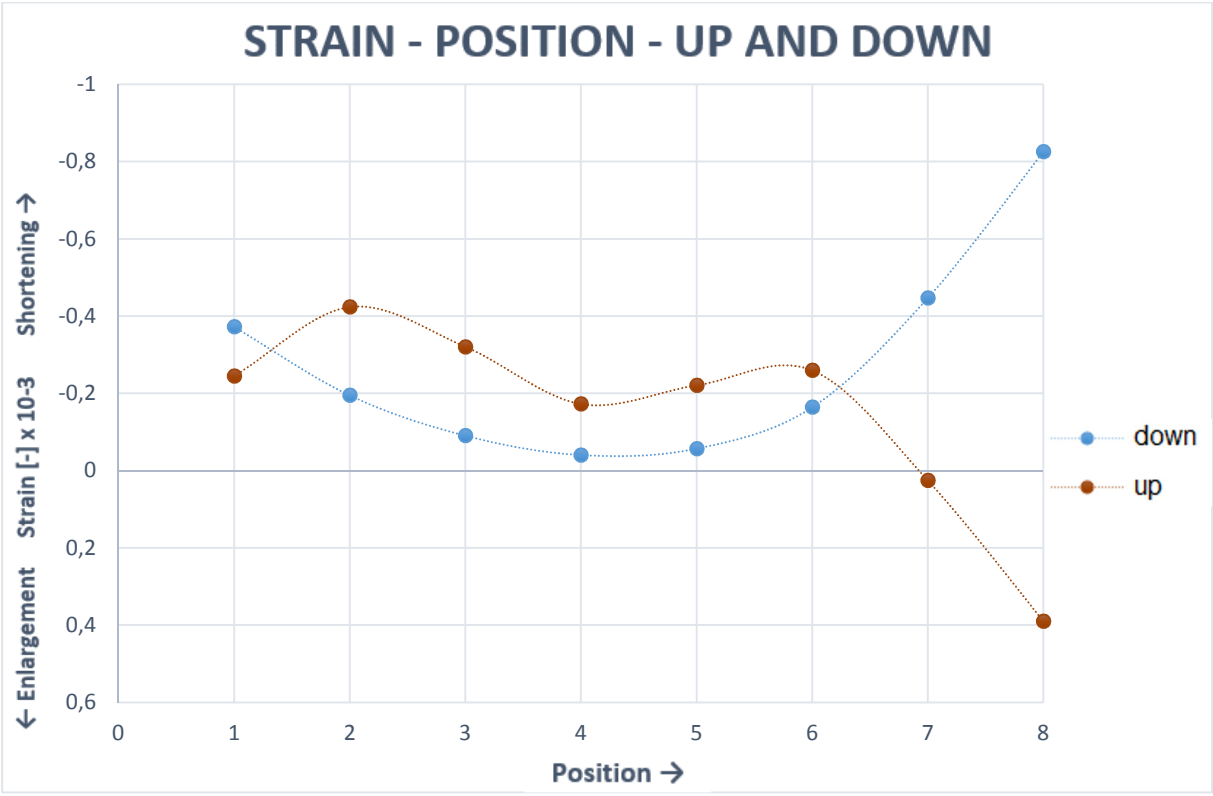
STRAIN - POSITION - UP AND DOWN
-1
-0,8
-0,6
-0,4
-0,2
0
0,2
0,4
0,6
← Enlargement Strain [-] x 10-3 Shortening →
0
1
2
3
4
5
6
7
8
Position →
down
up

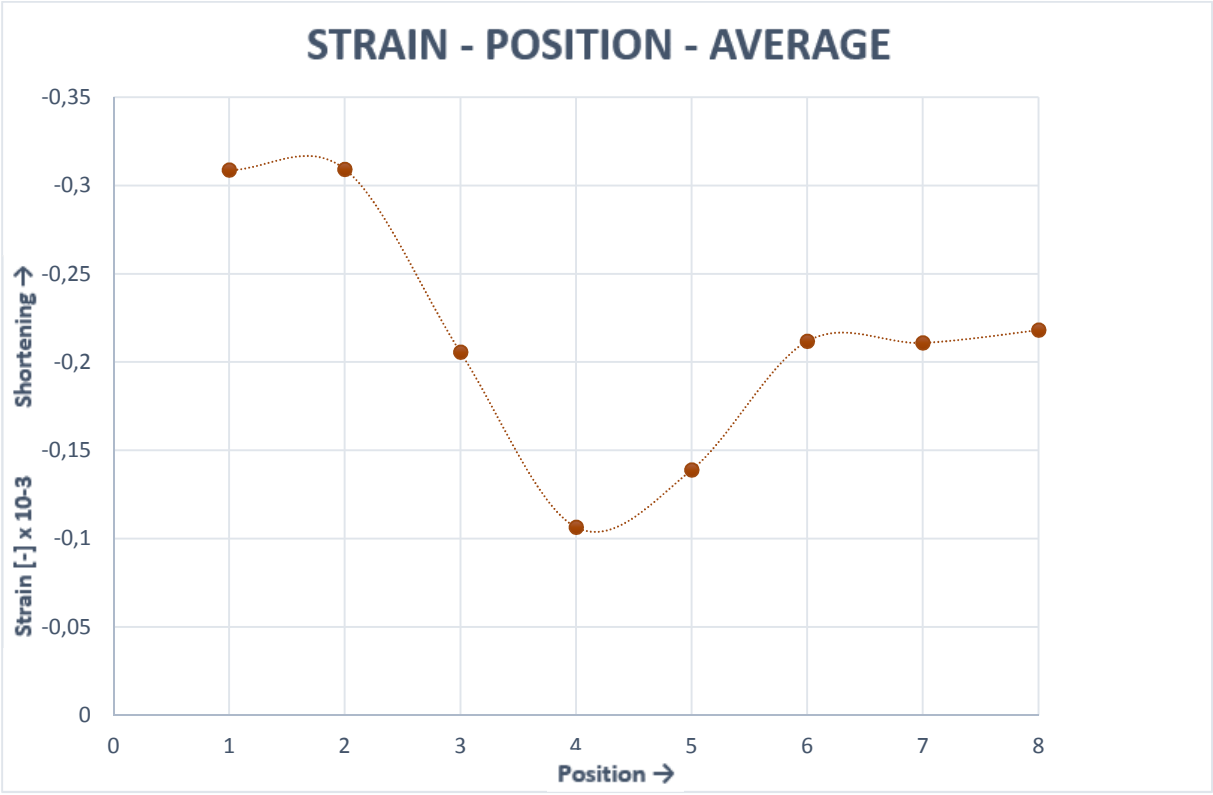
STRAIN - POSITION - AVERAGE
-0,35
-0,3
-0,25
-0,2
-0,15
-0,1
-0,05
0
Shortening → Strain [-] x 10-3
0
1
2
3
4
5
6
7
8
Position →

45/1200/H/A

Angle of the roof:	45°
Center-to-center distance brackets:	1200mm
Position of the wall plate in the bracket:	High (adding = 30mm)
Test series:	A
Coach screw	No
Load deviation:	76,30%

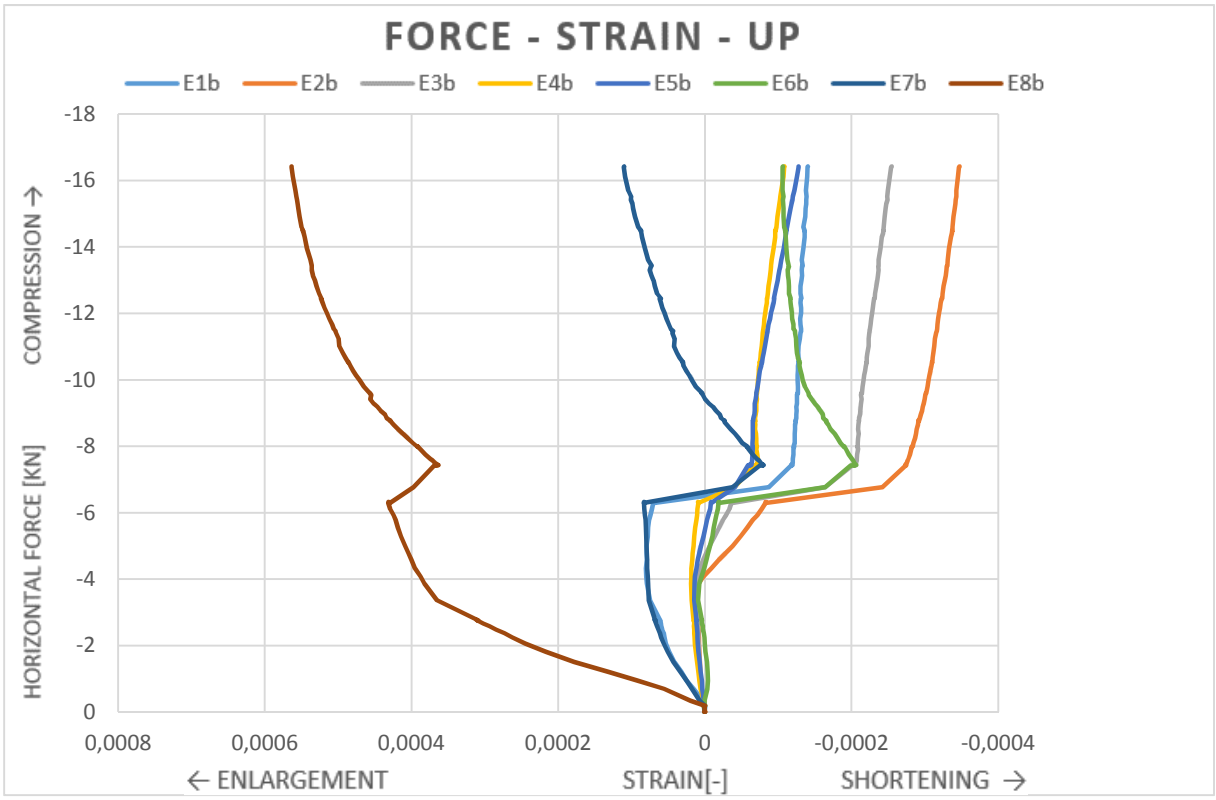

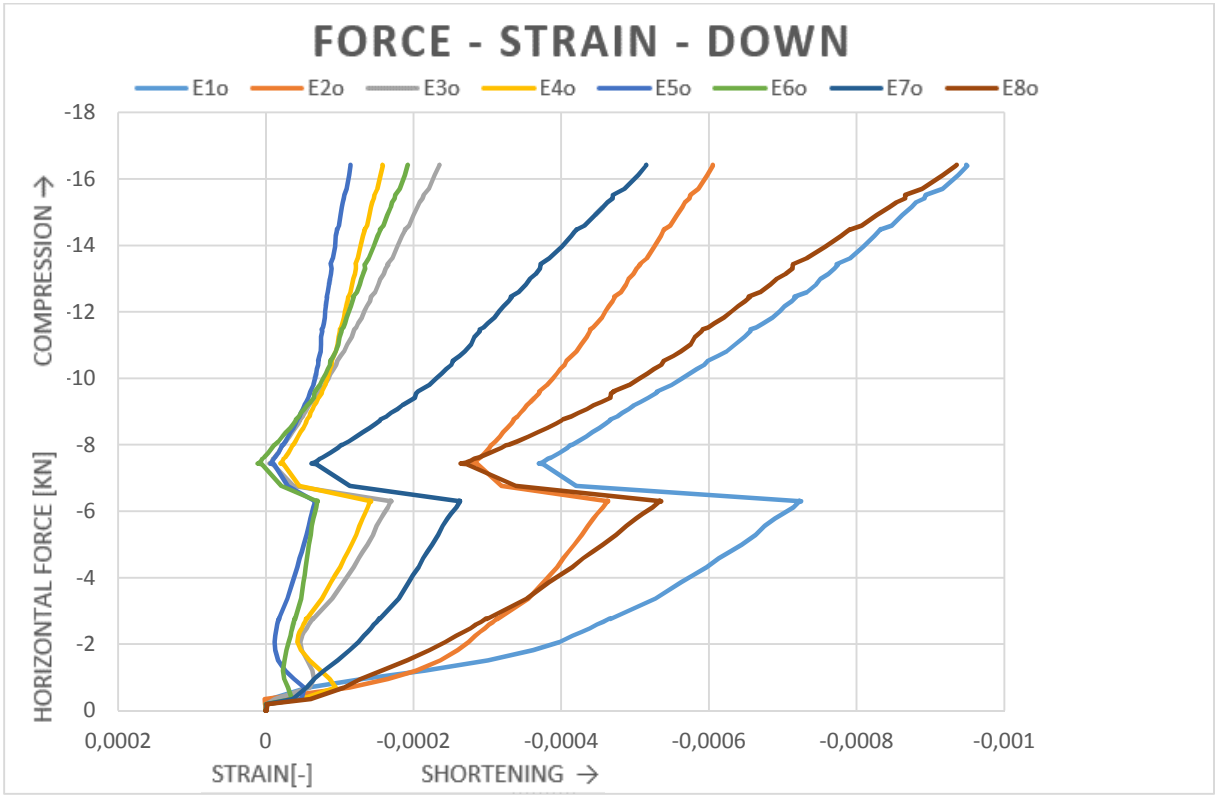

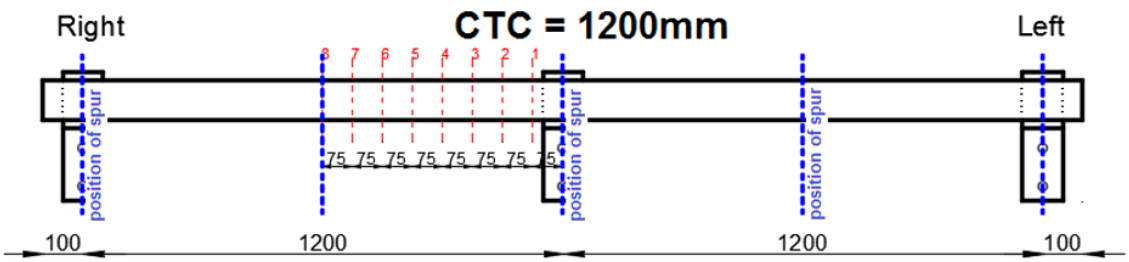
Right
CTC = 1200mm
Left
8 7 6 5 4 3 2 1
75 75 75 75 75 75 75 75
position of spur
position of spur
position of spur
100
1200
1200
100

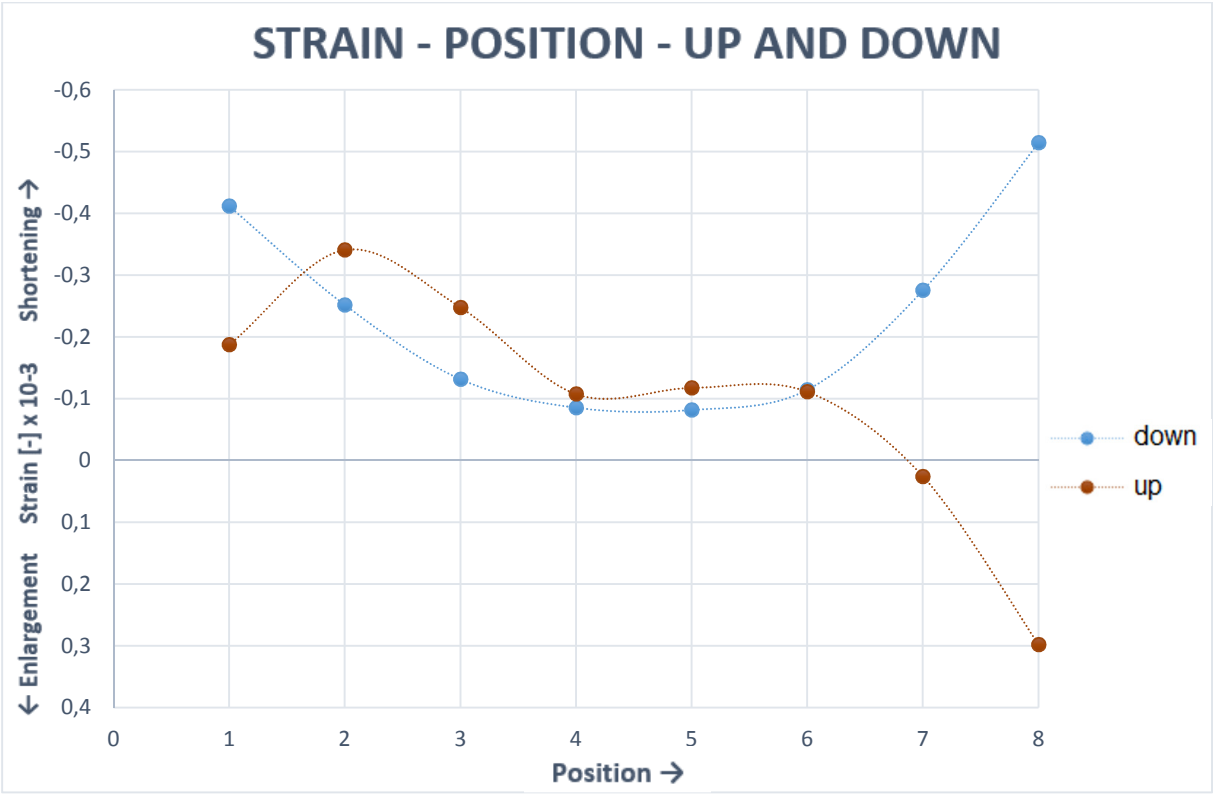
STRAIN - POSITION - UP AND DOWN
-0,6
-0,5
-0,4
-0,3
-0,2
-0,1
0
0,1
0,2
0,3
0,4
← Enlargement Strain [-] x 10-3 Shortening →
0
1
2
3
4
5
6
7
8
Position →
down
up

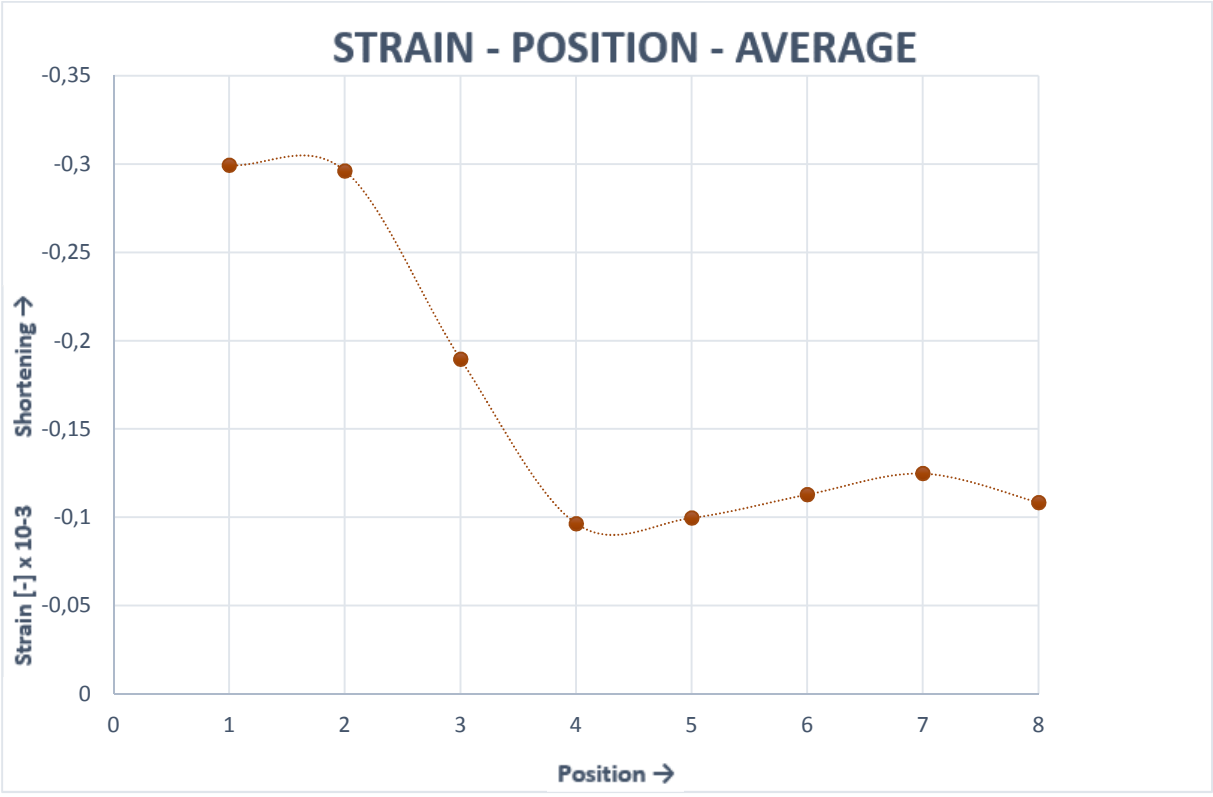
STRAIN - POSITION - AVERAGE
-0,35
-0,3
-0,25
-0,2
-0,15
-0,1
-0,05
0
Shortening →
Strain [-] x 10-3
0
1
2
3
4
5
6
7
8
Position →

45/1200/H/B

Angle of the roof:	45°
Center-to-center distance brackets:	1200mm
Position of the wall plate in the bracket:	High (adding = 30mm)
Test series:	B
Coach screw	No
Load deviation:	76,30%

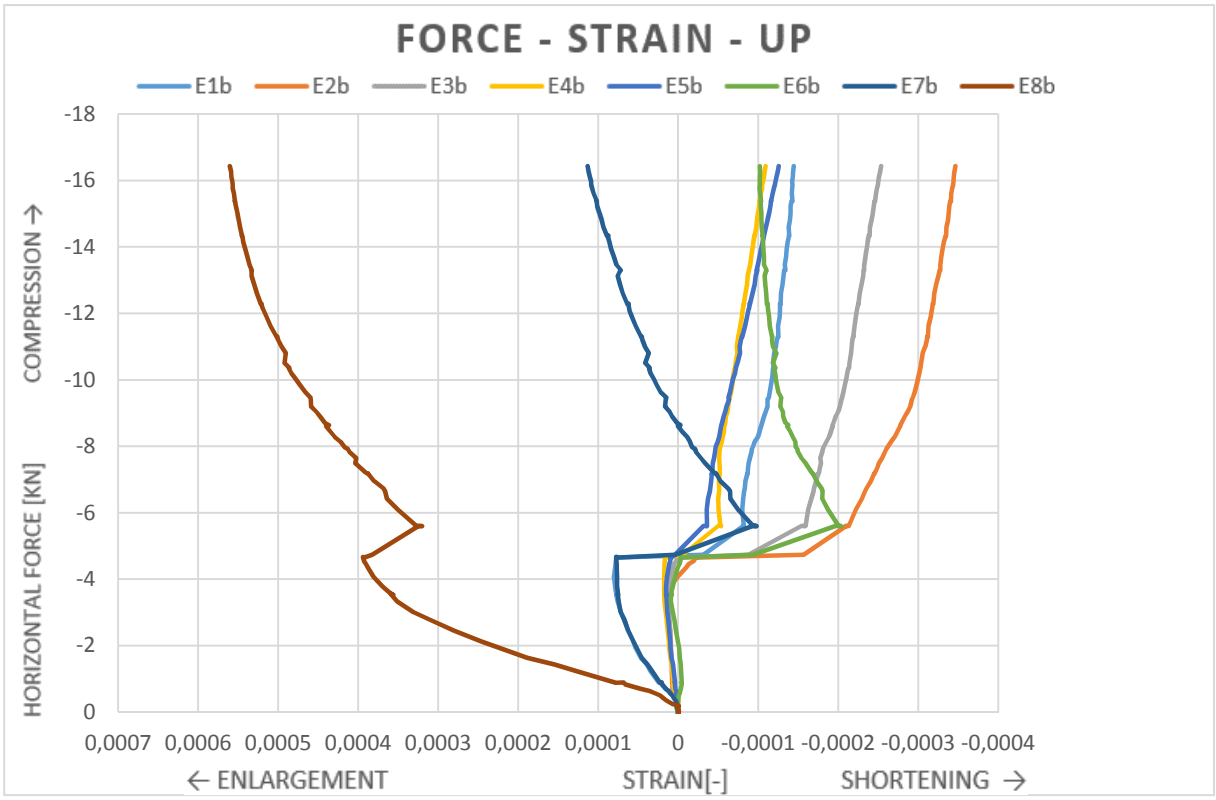

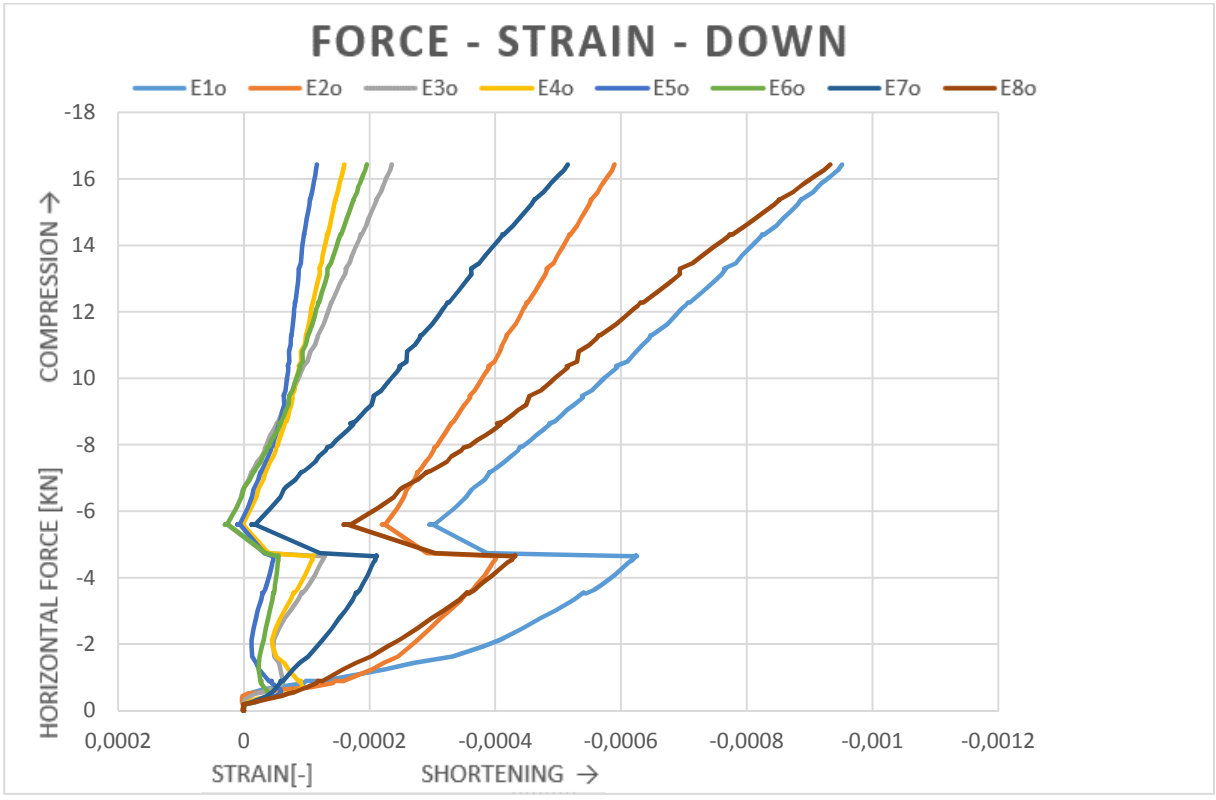

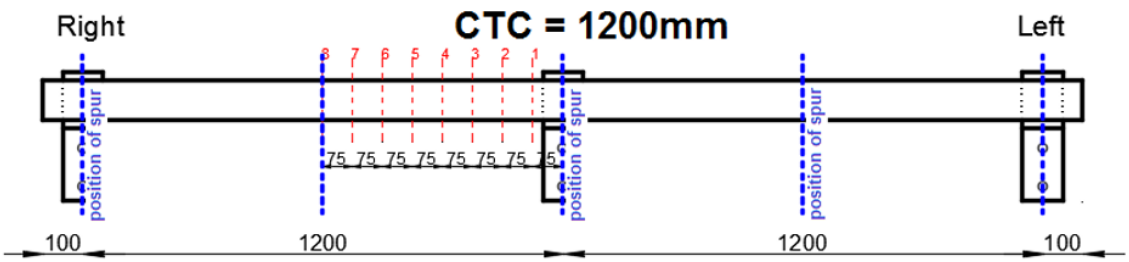
Right
CTC = 1200mm
Left
8 7 6 5 4 3 2 1
75 75 75 75 75 75 75 75
position of spur
position of spur
position of spur
100
1200
1200
100

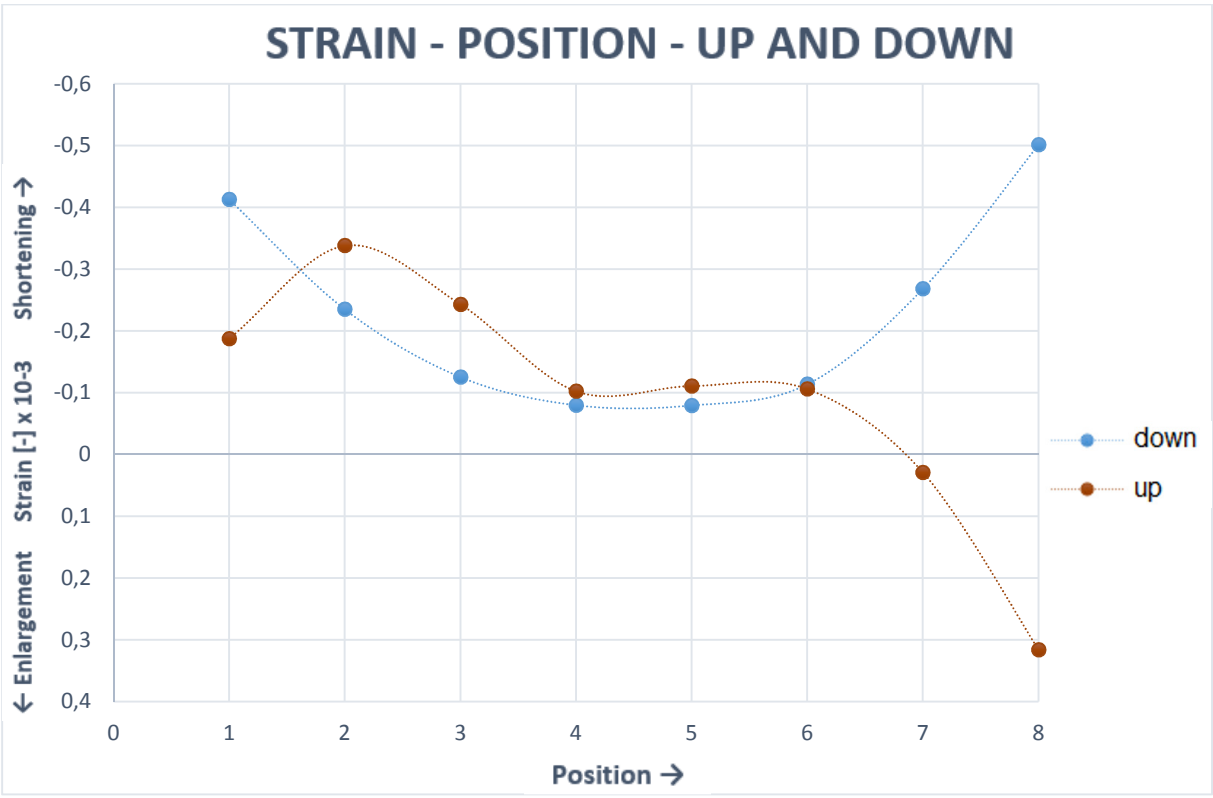
STRAIN - POSITION - UP AND DOWN
-0,6
-0,5
-0,4
-0,3
-0,2
-0,1
0
0,1
0,2
0,3
0,4
← Enlargement Strain [-] x 10-3 Shortening →
0
1
2
3
4
5
6
7
8
Position →
down
up

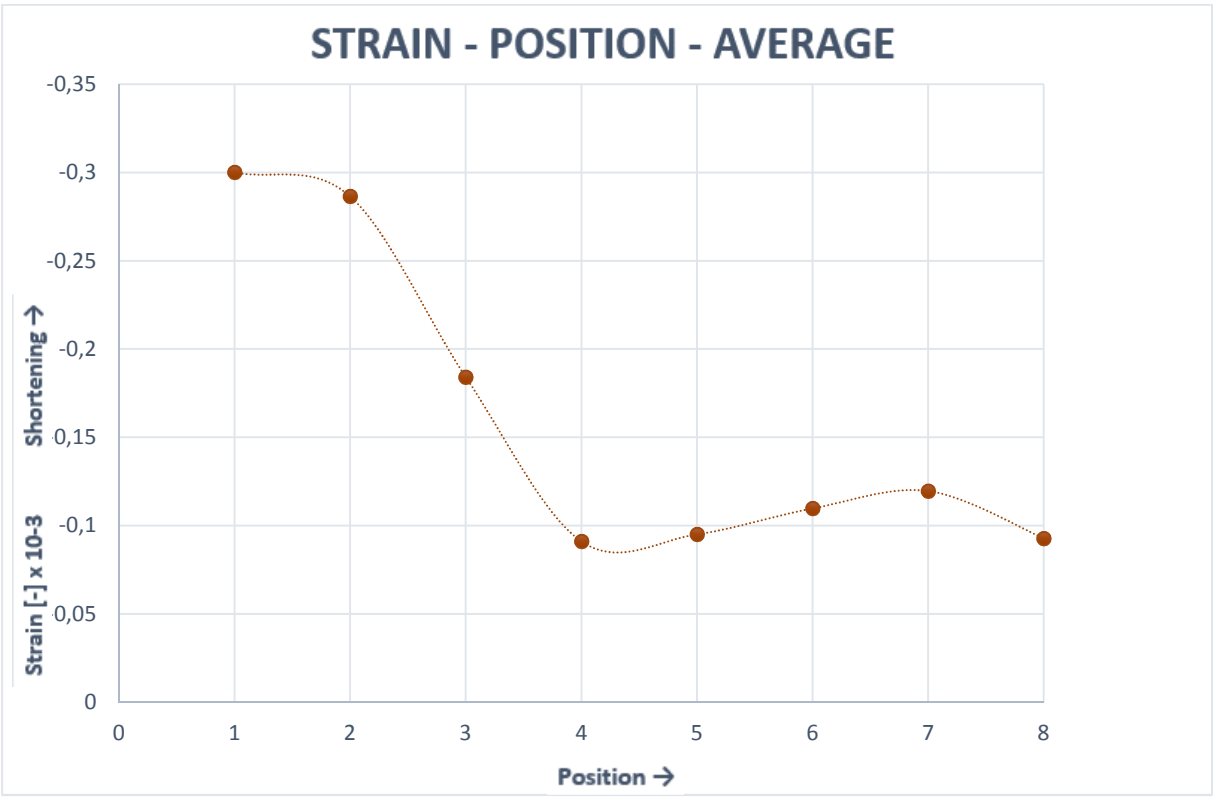
STRAIN - POSITION - AVERAGE
-0,35
-0,3
-0,25
-0,2
0,15
-0,1
0,05
0
Strain [-] x 10-3 Shortening →
0
1
2
3
4
5
6
7
8
Position →

45/1200/L/CS/A

Angle of the roof:	45°
Center-to-center distance brackets:	1200mm
Position of the wall plate in the bracket:	Low (adding = 10mm)
Test series:	A
Coach screw	Yes
Load deviation:	76,30%

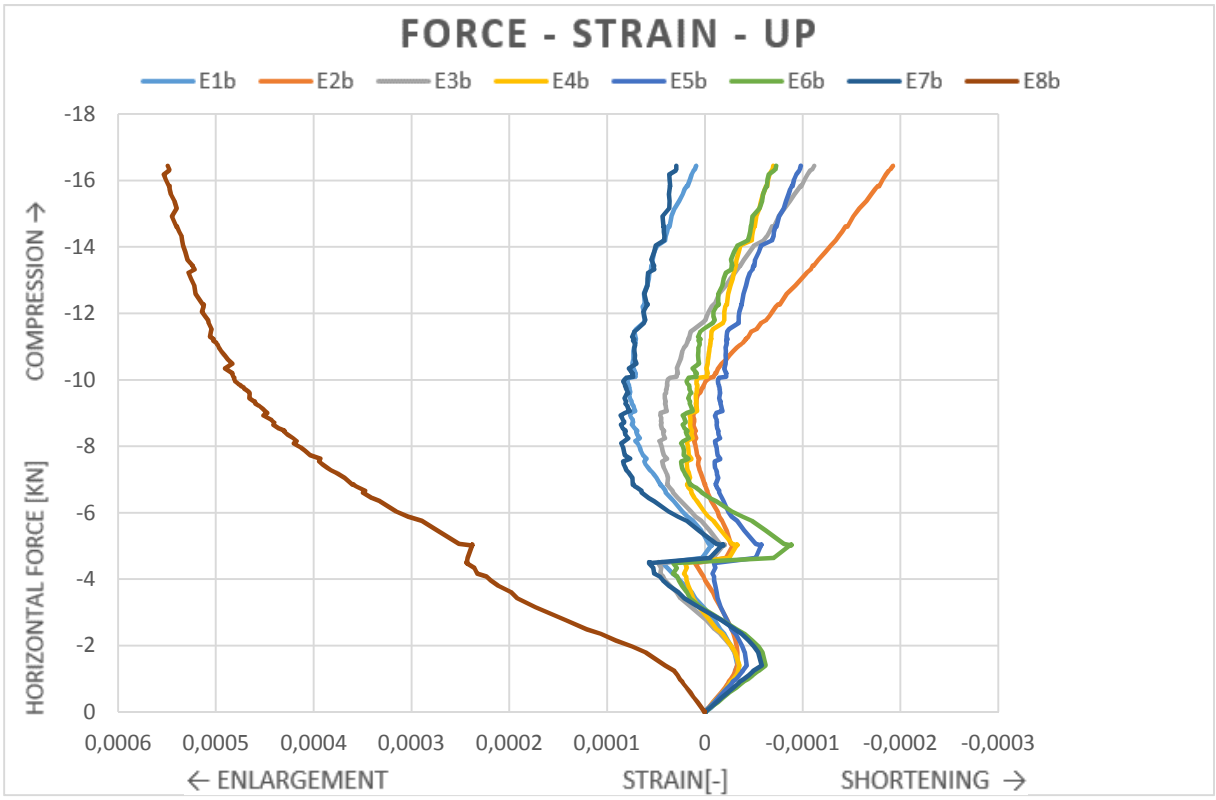

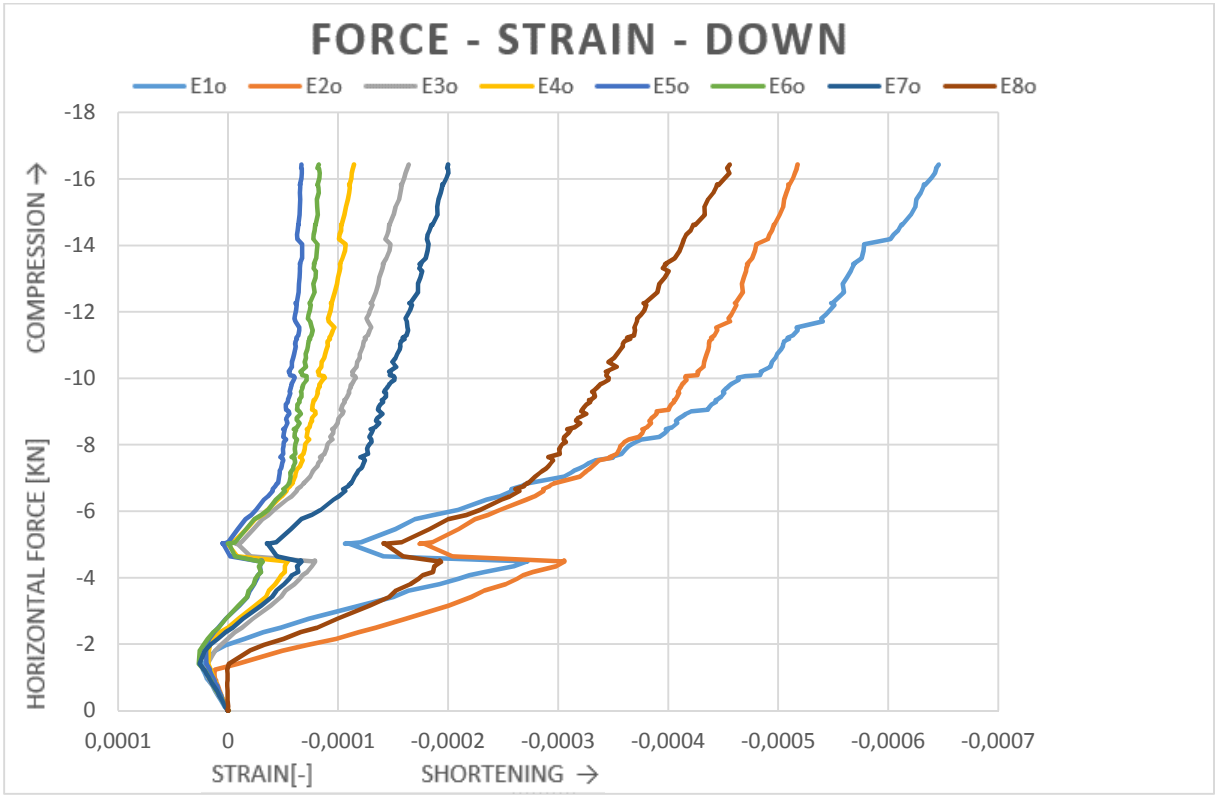

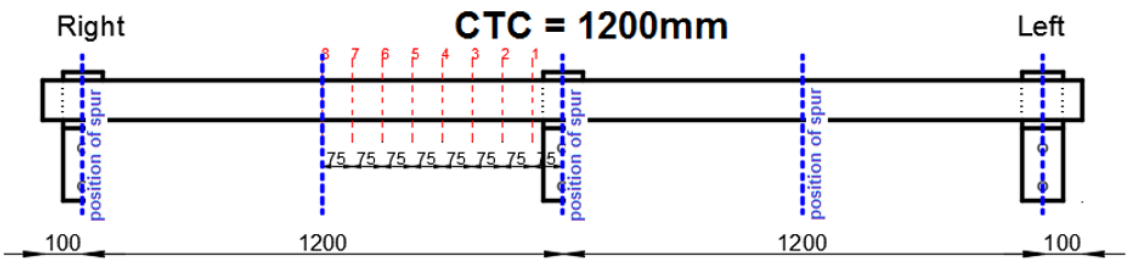
Right
CTC = 1200mm
Left
8 7 6 5 4 3 2 1
75 75 75 75 75 75 75 75
position of spur
position of spur
position of spur
100
1200
1200
100

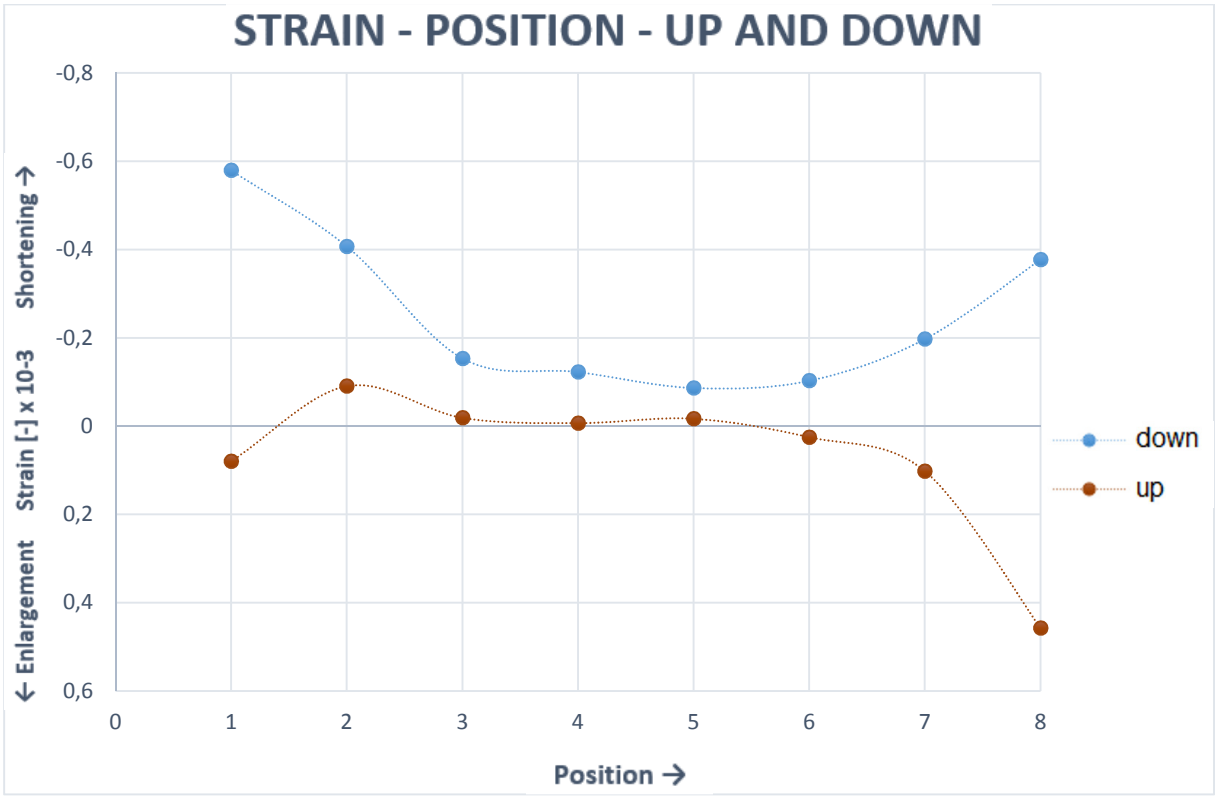
STRAIN - POSITION - UP AND DOWN
-0,8
-0,6
-0,4
-0,2
0
0,2
0,4
0,6
← Enlargement Strain [-] x 10-3 Shortening →
0
1
2
3
4
5
6
7
8
Position →
down
up

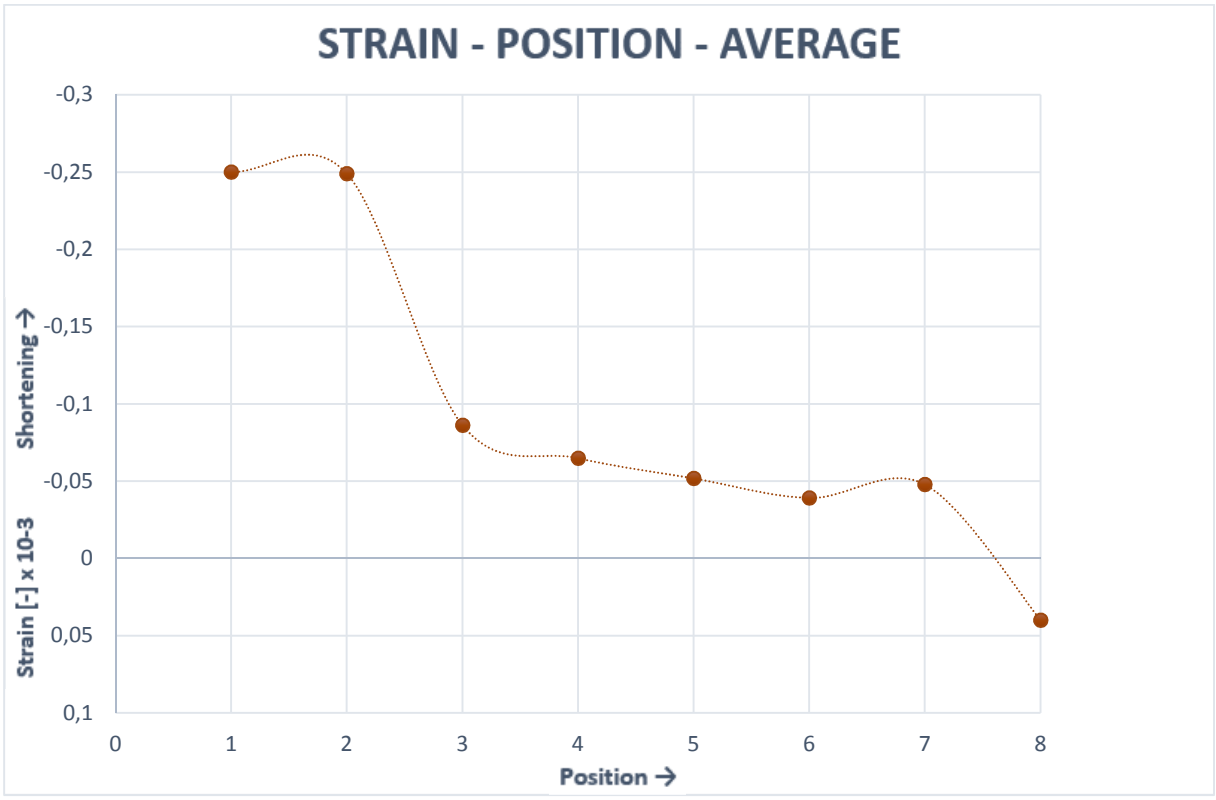
STRAIN - POSITION - AVERAGE
-0,3
-0,25
-0,2
-0,15
-0,1
-0,05
0
0,05
0,1
Strain [-] x 10-3 Shortening →
0
1
2
3
4
5
6
7
8
Position →

45/1200/L/CS/B

Angle of the roof:	45°
Center-to-center distance brackets:	1200mm
Position of the wall plate in the bracket:	Low (adding = 10mm)
Test series:	B
Coach screw	Yes
Load deviation:	76,30%

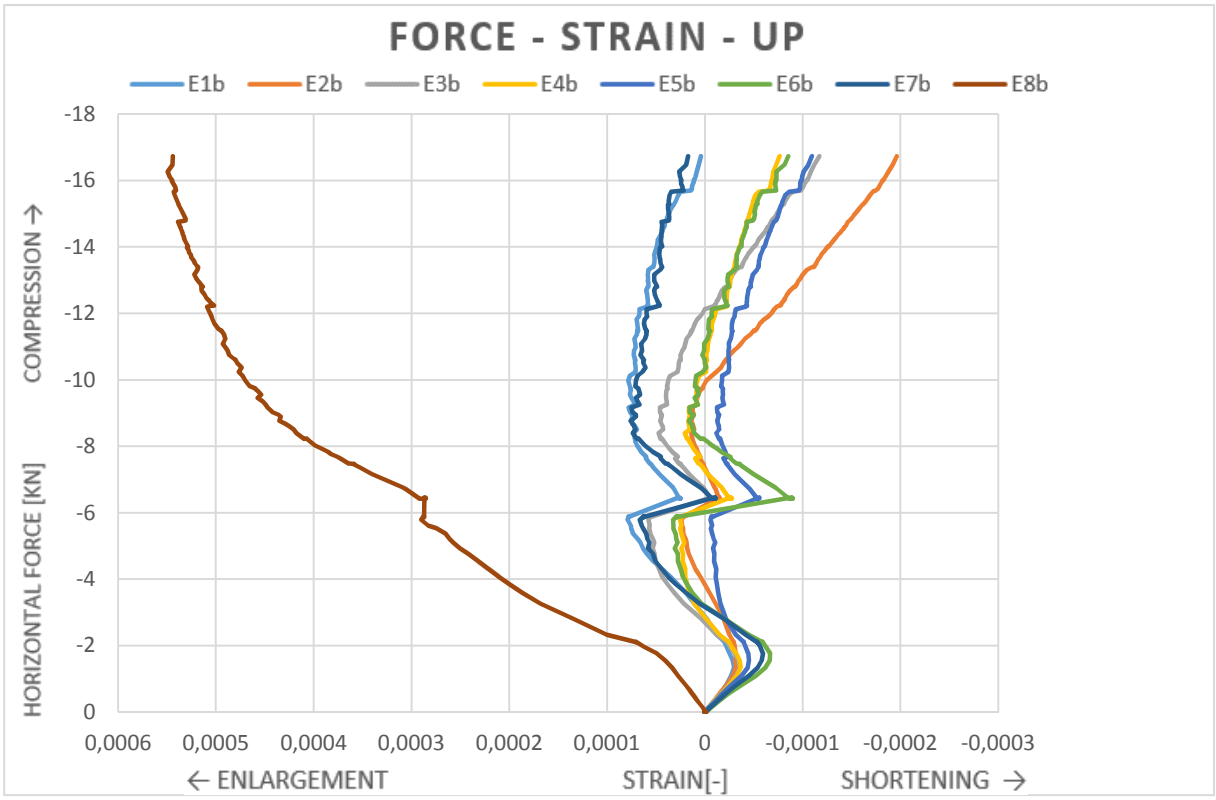

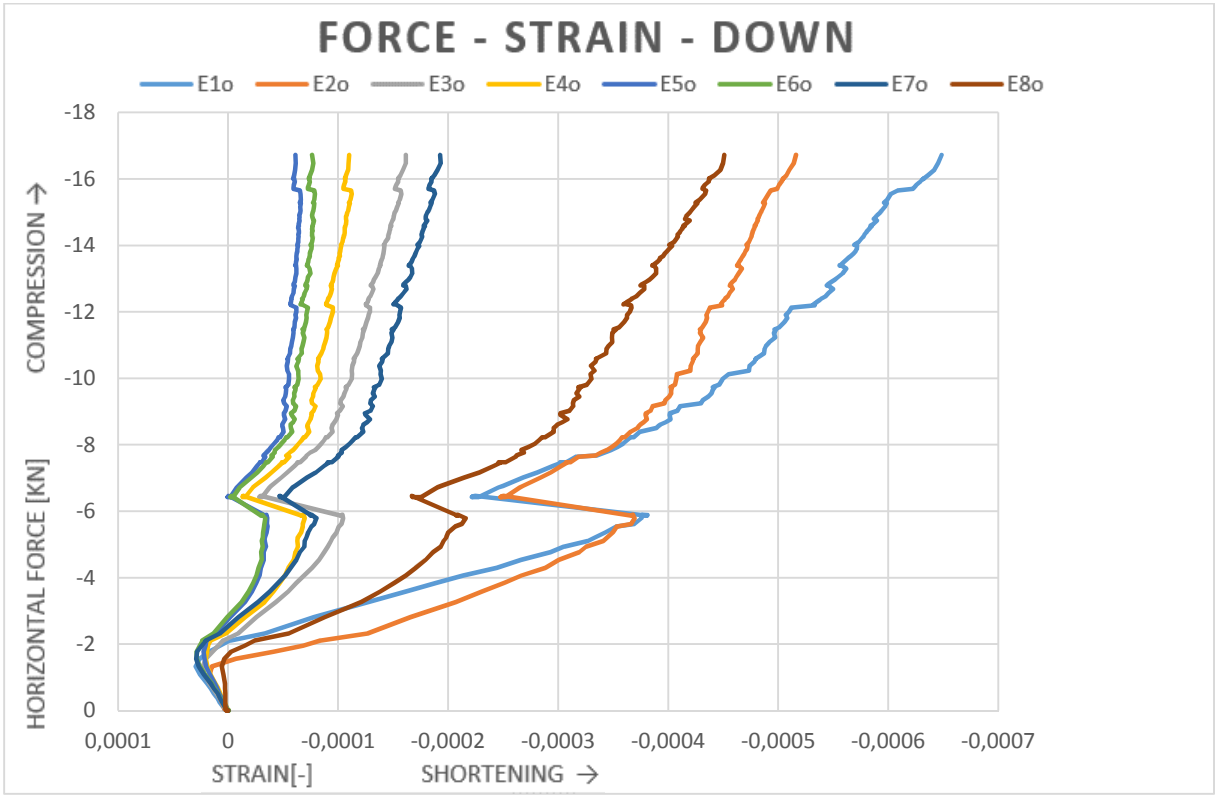

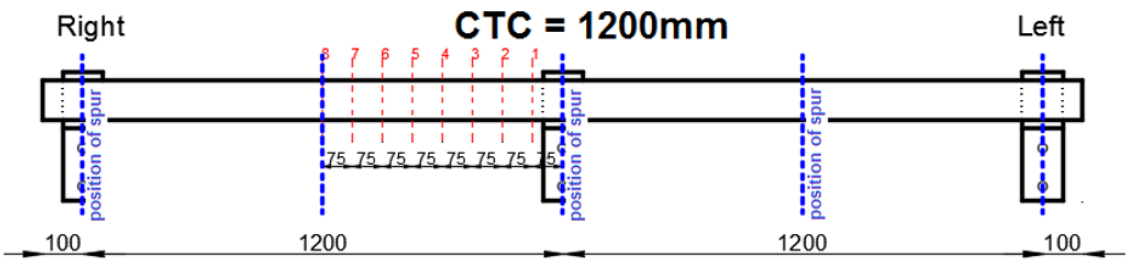
Right
CTC = 1200mm
Left
8 7 6 5 4 3 2 1
75 75 75 75 75 75 75 75
position of spur
position of spur
position of spur
100
1200
1200
100

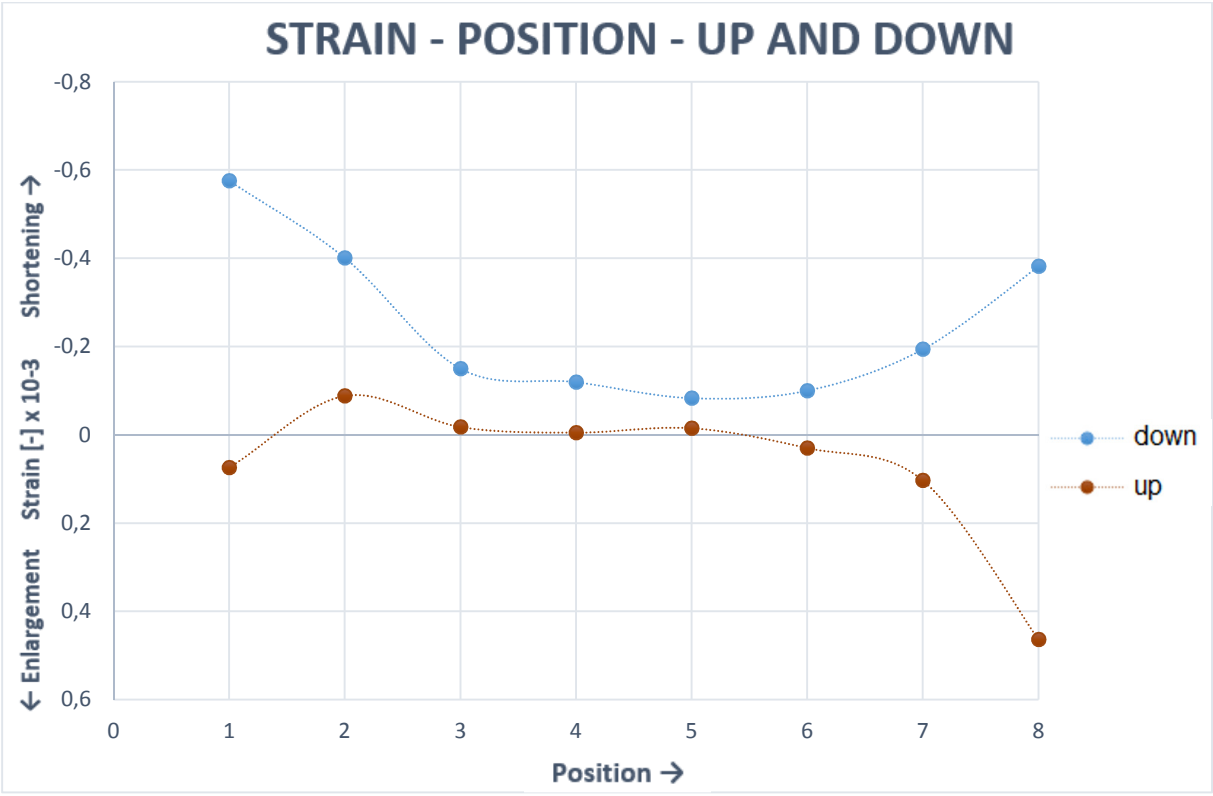
STRAIN - POSITION - UP AND DOWN
-0,8
-0,6
-0,4
-0,2
0
0,2
0,4
0,6
← Enlargement Strain [-] x 10-3 Shortening →
0
1
2
3
4
5
6
7
8
Position →
down
up

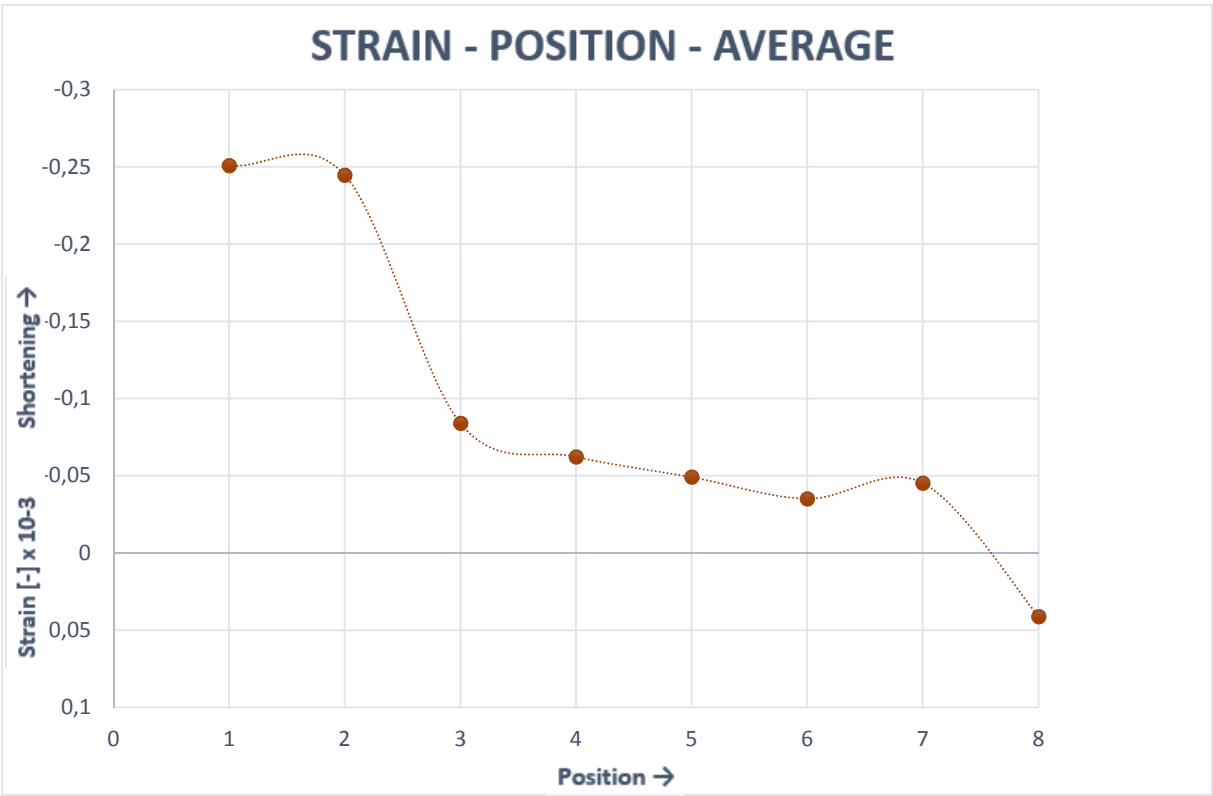
STRAIN - POSITION - AVERAGE
-0,3
-0,25
-0,2
-0,15
-0,1
-0,05
0
0,05
0,1
Shortening → Strain [-] x 10-3
0
1
2
3
4
5
6
7
8
Position →

55/600/L/A

Angle of the roof:	55°
Center-to-center distance brackets:	600mm
Position of the wall plate in the bracket:	Low (adding = 10mm)
Test series:	A
Coach screw	No
Load deviation:	108,68%

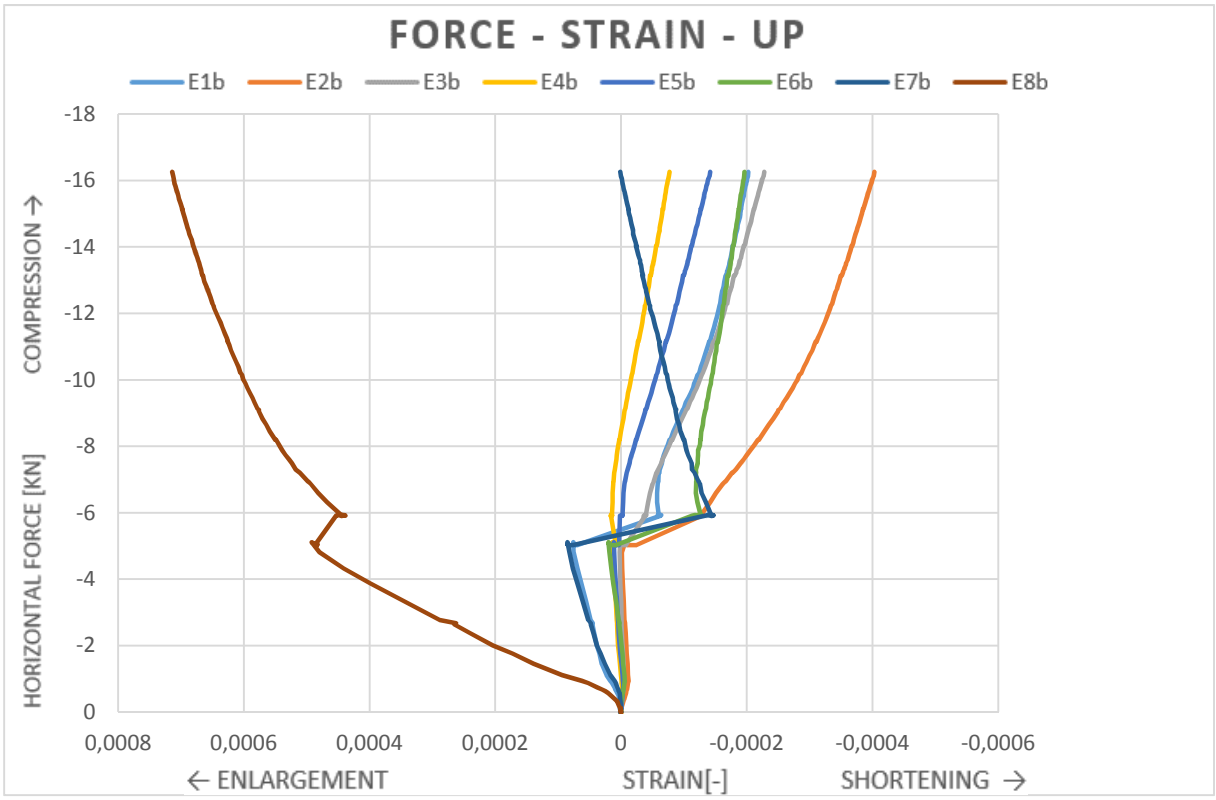

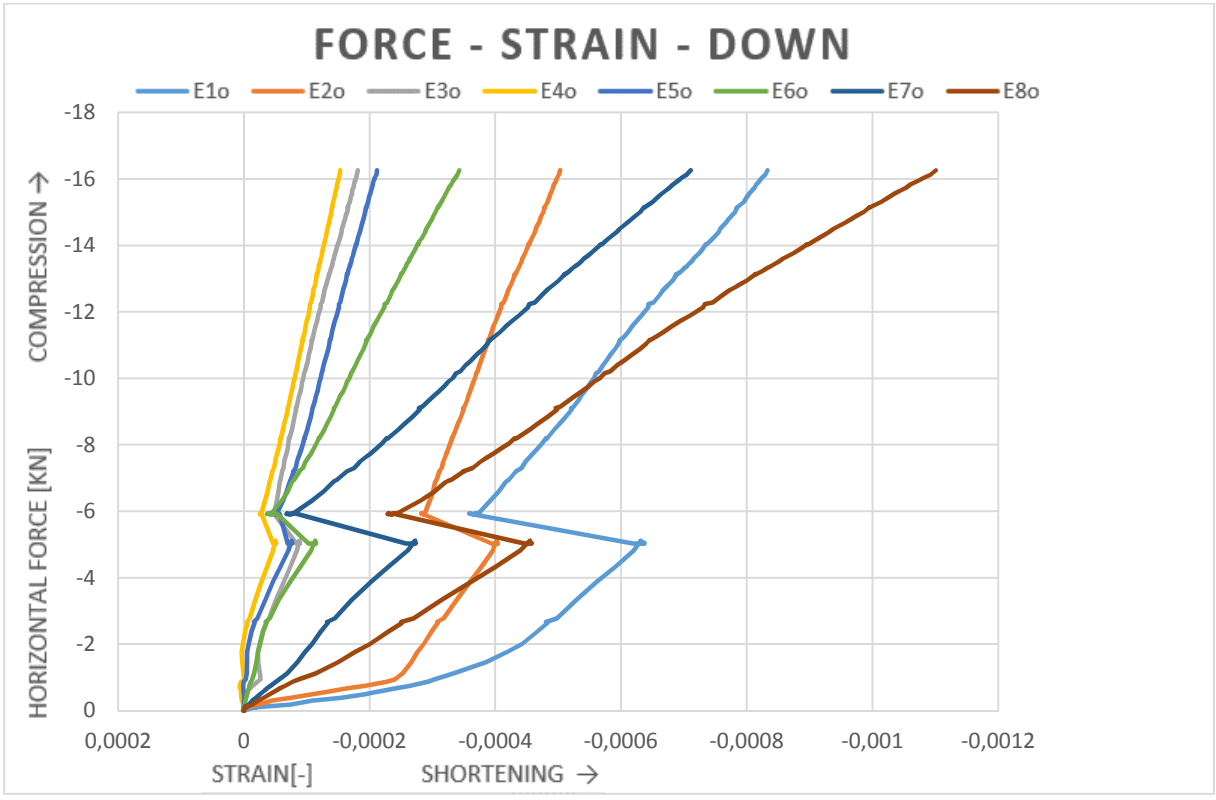

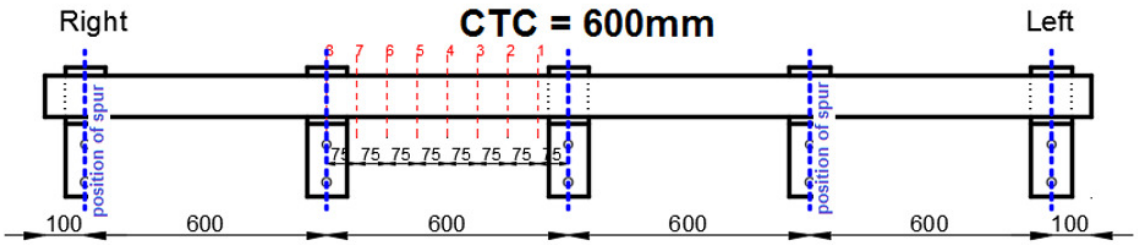
Right
CTC = 600mm
Left
8 7 6 5 4 3 2 1
75 75 75 75 75 75 75 75
position of spur
position of spur
100
600
600
600
600
100

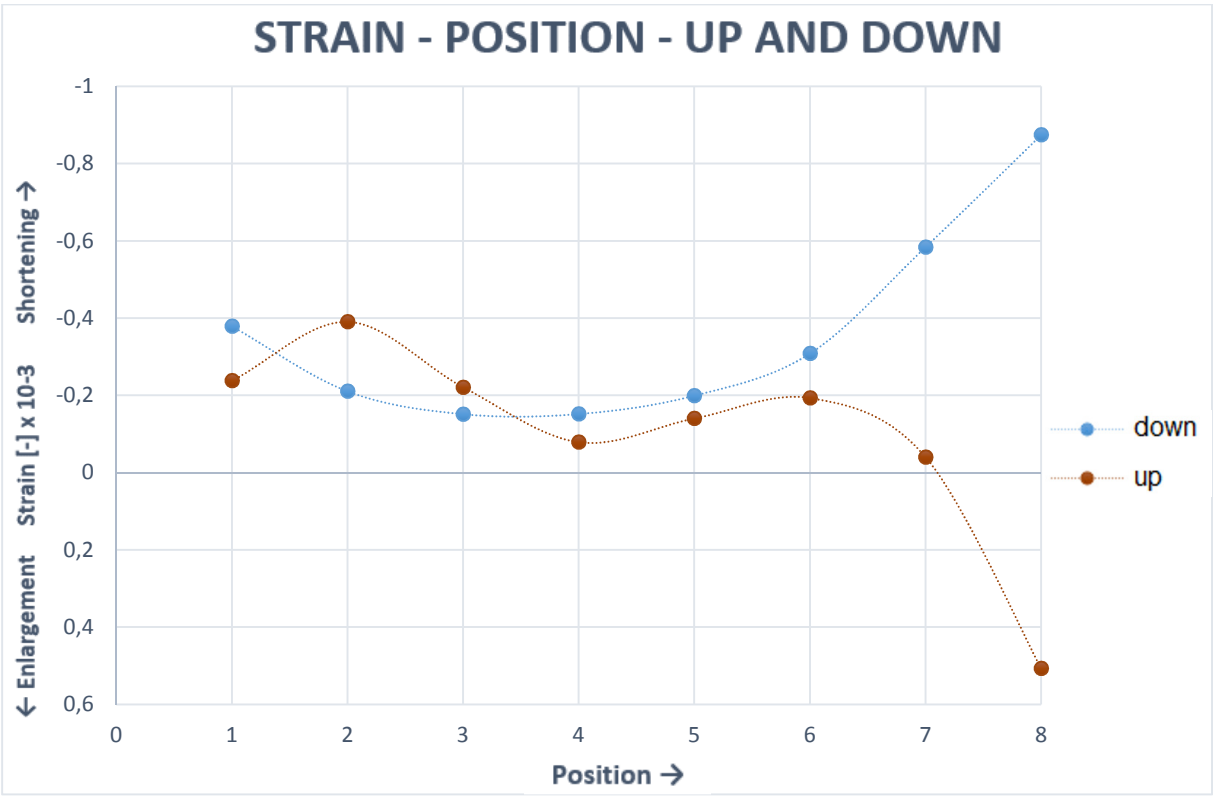
STRAIN - POSITION - UP AND DOWN
-1
-0,8
-0,6
-0,4
-0,2
0
0,2
0,4
0,6
← Enlargement Strain [-] x 10-3 Shortening →
0
1
2
3
4
5
6
7
8
Position →
down
up

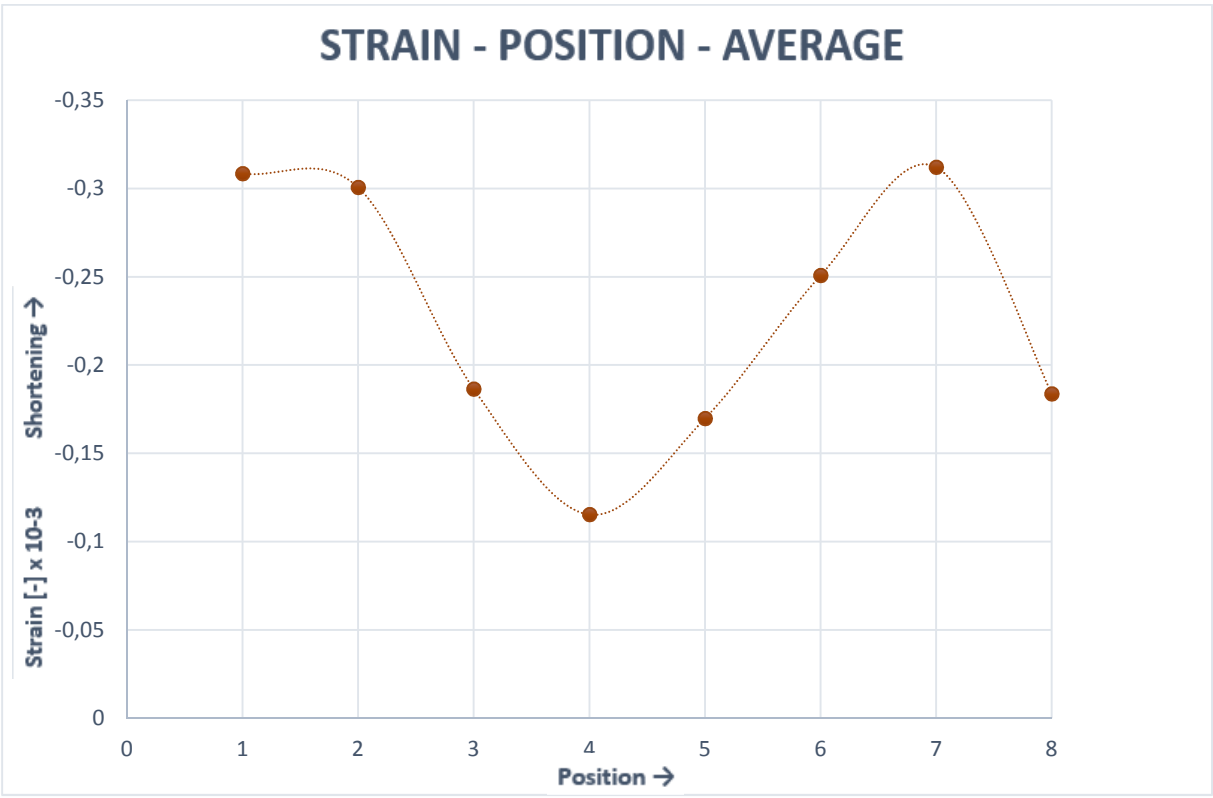
STRAIN - POSITION - AVERAGE
-0,35
-0,3
-0,25
-0,2
-0,15
-0,1
-0,05
0
Strain [-] x 10-3 Shortening →
0
1
2
3
4
5
6
7
8
Position →

55/600/L/B

Angle of the roof:	55°
Center-to-center distance brackets:	600mm
Position of the wall plate in the bracket:	Low (adding = 10mm)
Test series:	B
Coach screw	No
Load deviation:	108,68%

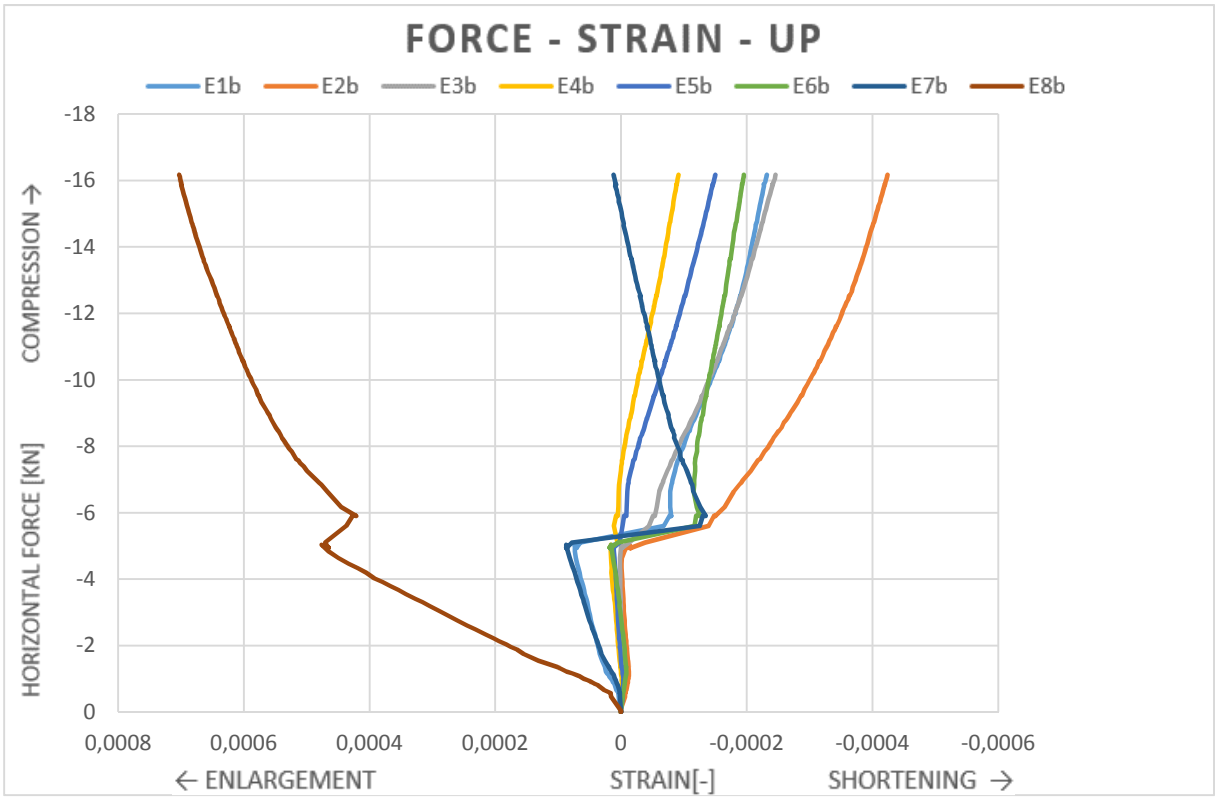

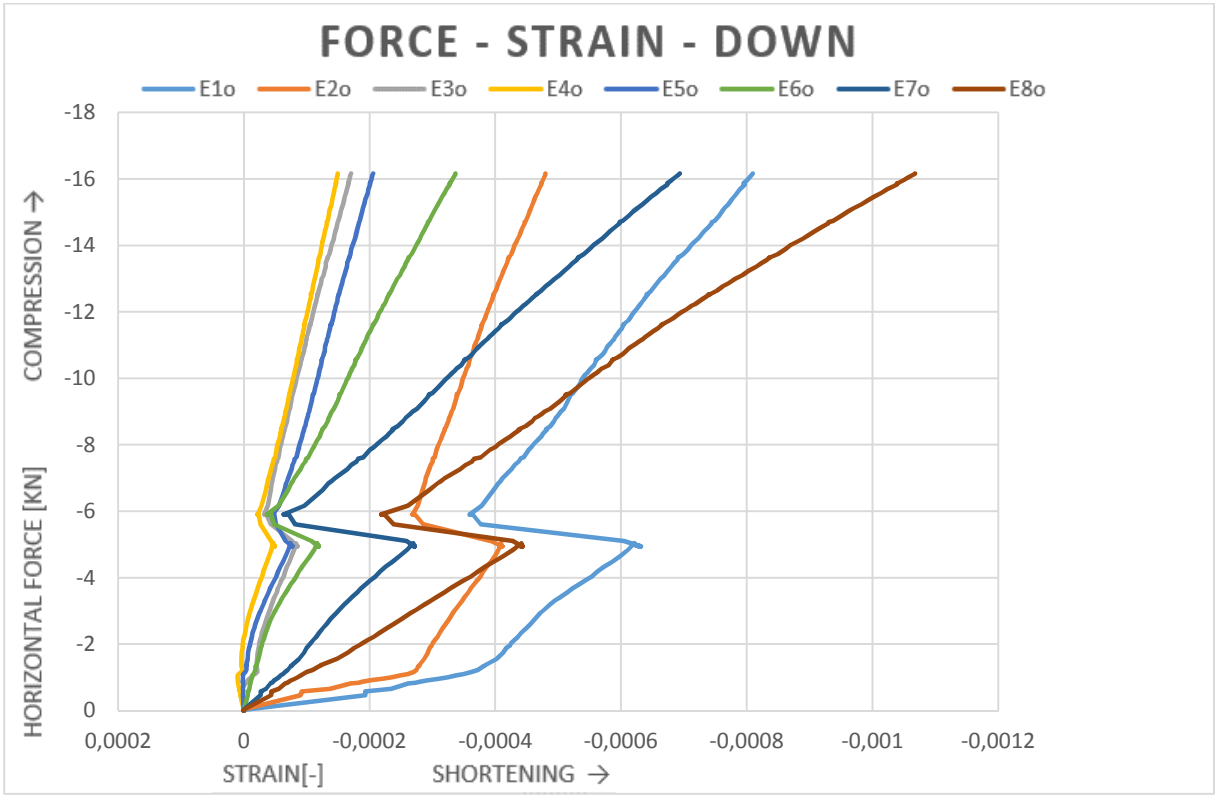

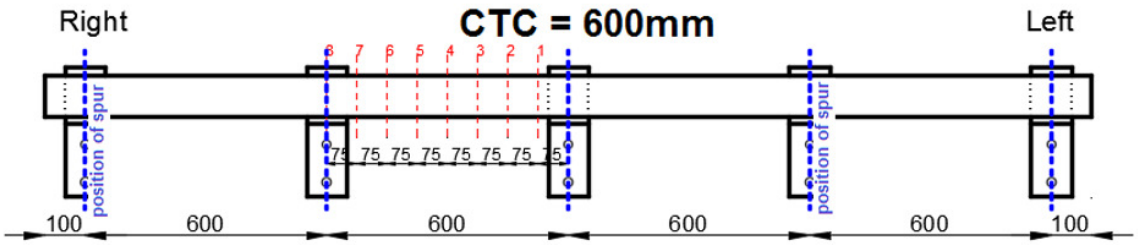
Right
CTC = 600mm
Left
8 7 6 5 4 3 2 1
75 75 75 75 75 75 75 75
position of spur
position of spur
100
600
600
600
600
100

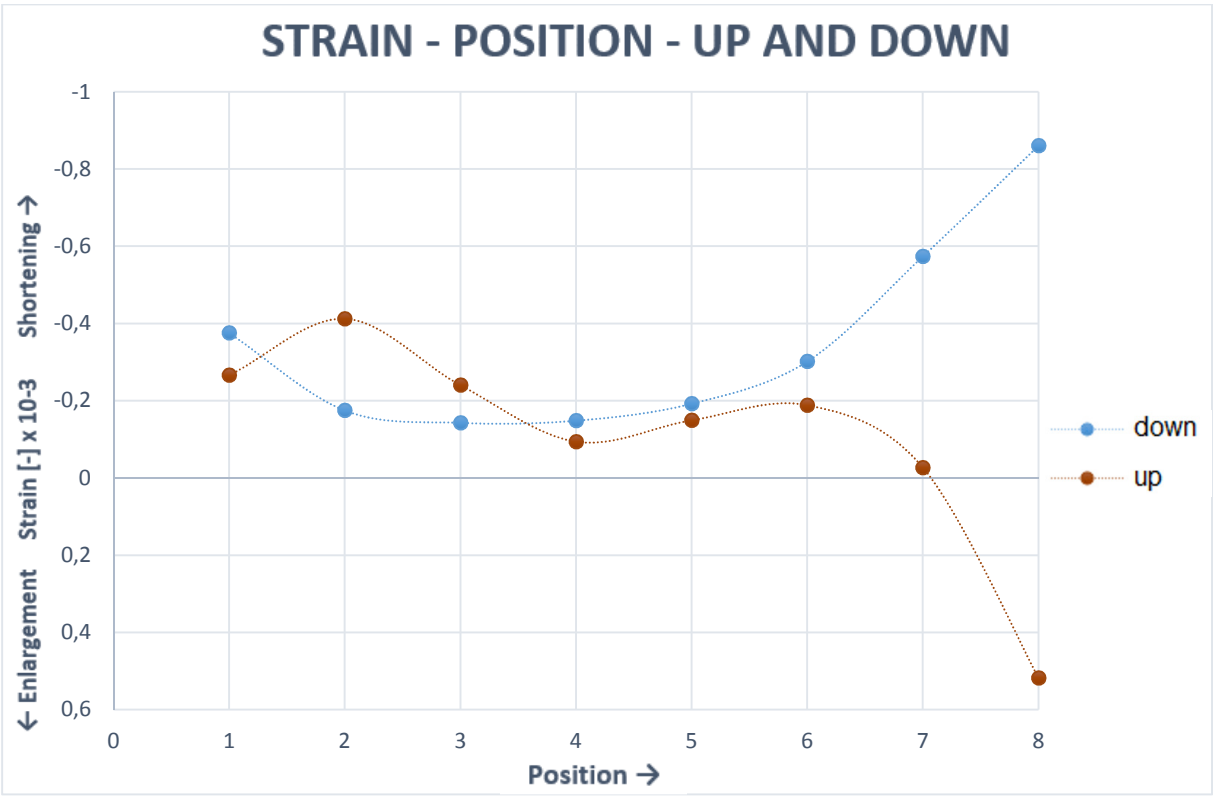
STRAIN - POSITION - UP AND DOWN
-1
-0,8
-0,6
-0,4
-0,2
0
0,2
0,4
0,6
← Enlargement Strain [-] x 10-3 Shortening →
0
1
2
3
4
5
6
7
8
Position →
down
up

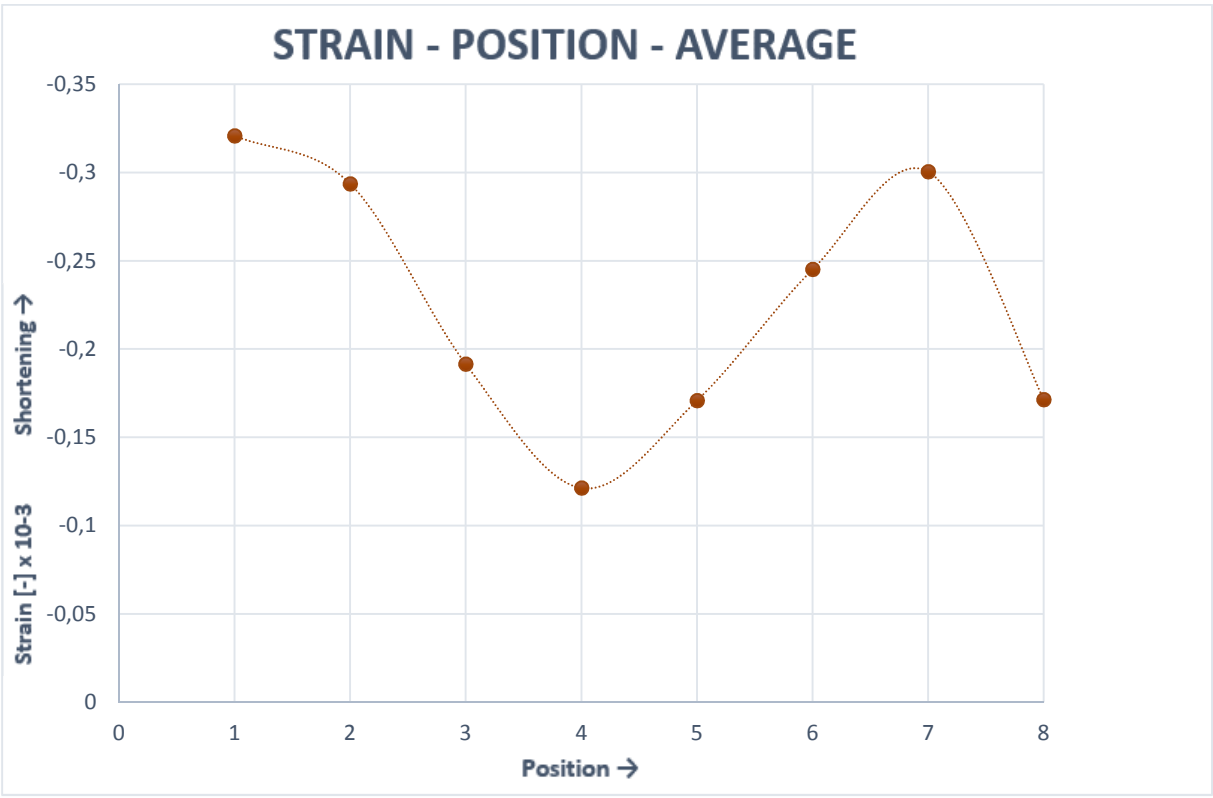
STRAIN - POSITION - AVERAGE
-0,35
-0,3
-0,25
-0,2
-0,15
-0,1
-0,05
0
Strain [-] x 10-3 Shortening →
0
1
2
3
4
5
6
7
8
Position →

55/900/L/A

Angle of the roof:	55°
Center-to-center distance brackets:	900mm
Position of the wall plate in the bracket:	Low (adding = 10mm)
Test series:	A
Coach screw	No
Load deviation:	108,68%

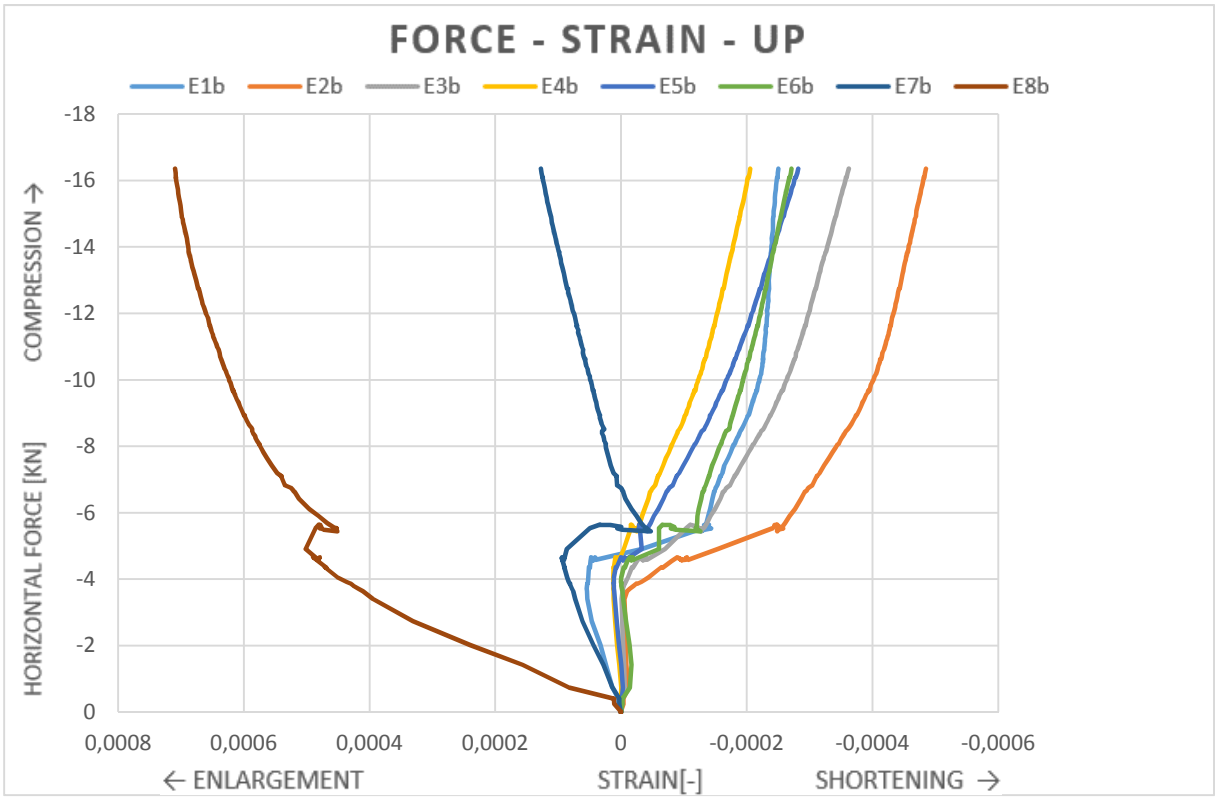

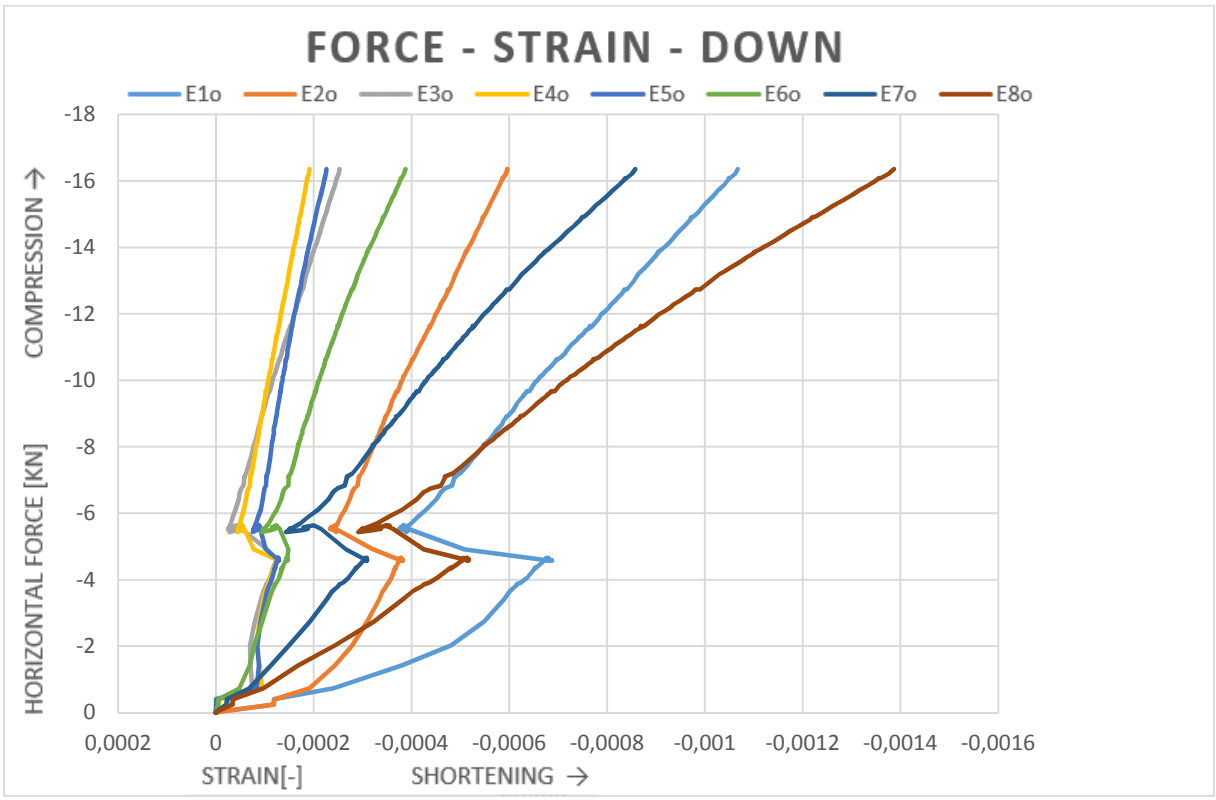

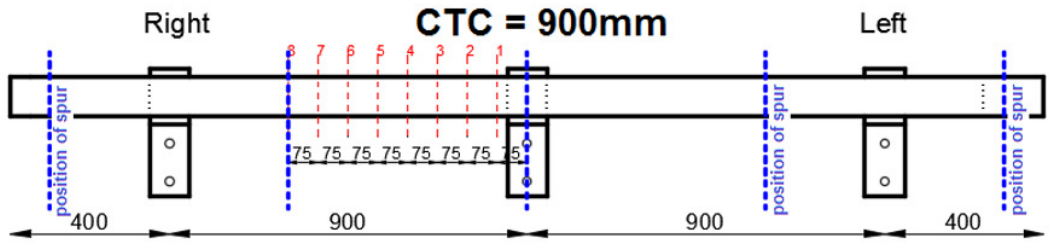
Right
CTC = 900mm
Left
8 7 6 5 4 3 2 1
75 75 75 75 75 75 75 75
position of spur
position of spur
position of spur
400
900
900
400

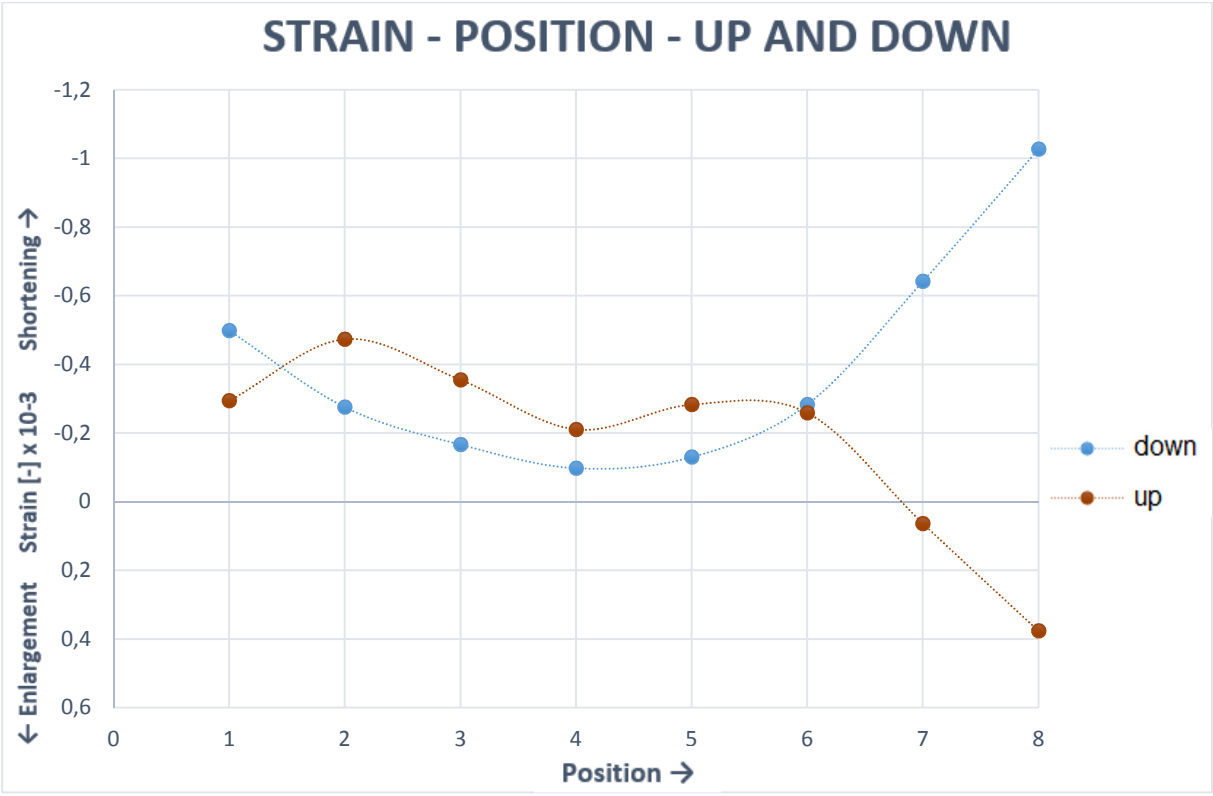
STRAIN - POSITION - UP AND DOWN
-1,2
-1
-0,8
-0,6
-0,4
-0,2
0
0,2
0,4
0,6
← Enlargement Strain [-] x 10-3 Shortening →
0
1
2
3
4
5
6
7
8
Position →
down
up

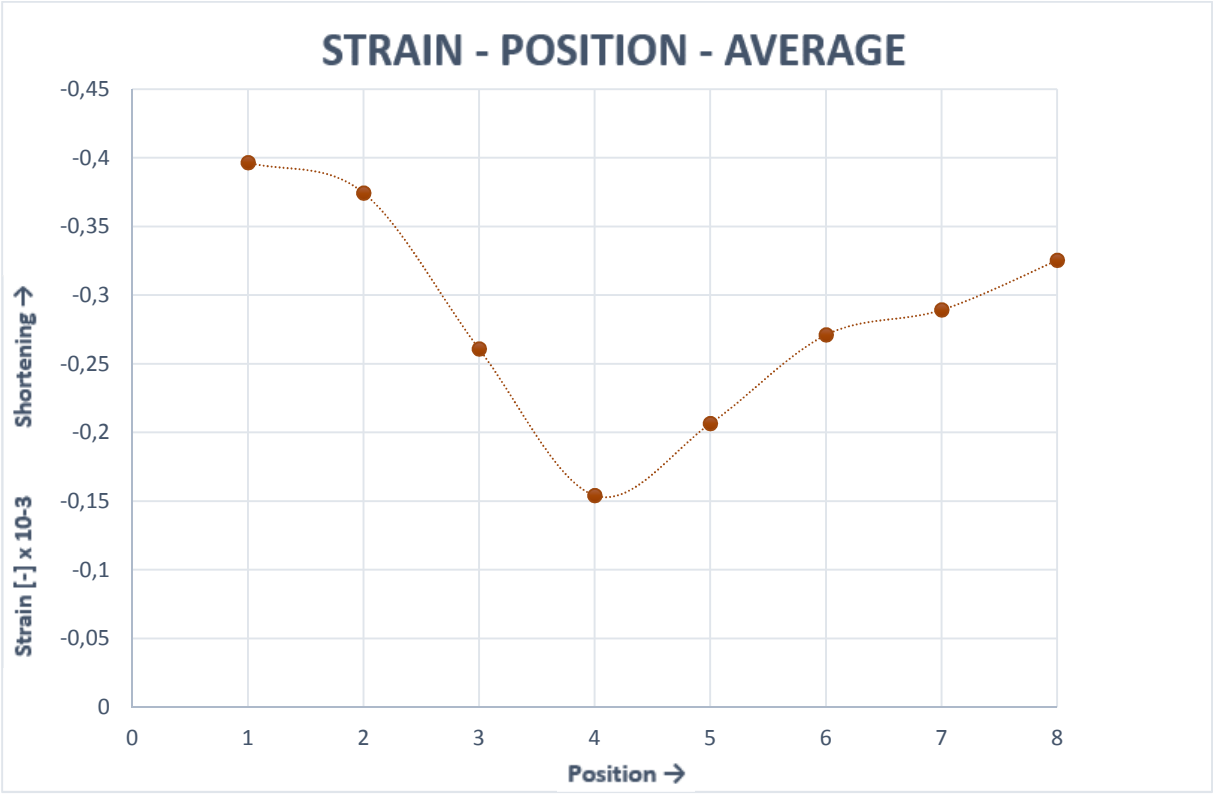
STRAIN - POSITION - AVERAGE
-0,45
-0,4
-0,35
-0,3
-0,25
-0,2
-0,15
-0,1
-0,05
0
Strain [-] x 10-3 Shortening →
0
1
2
3
4
5
6
7
8
Position →

55/900/L/B

Angle of the roof:	55°
Center-to-center distance brackets:	900mm
Position of the wall plate in the bracket:	Low (adding = 10mm)
Test series:	B
Coach screw	No
Load deviation:	108,68%

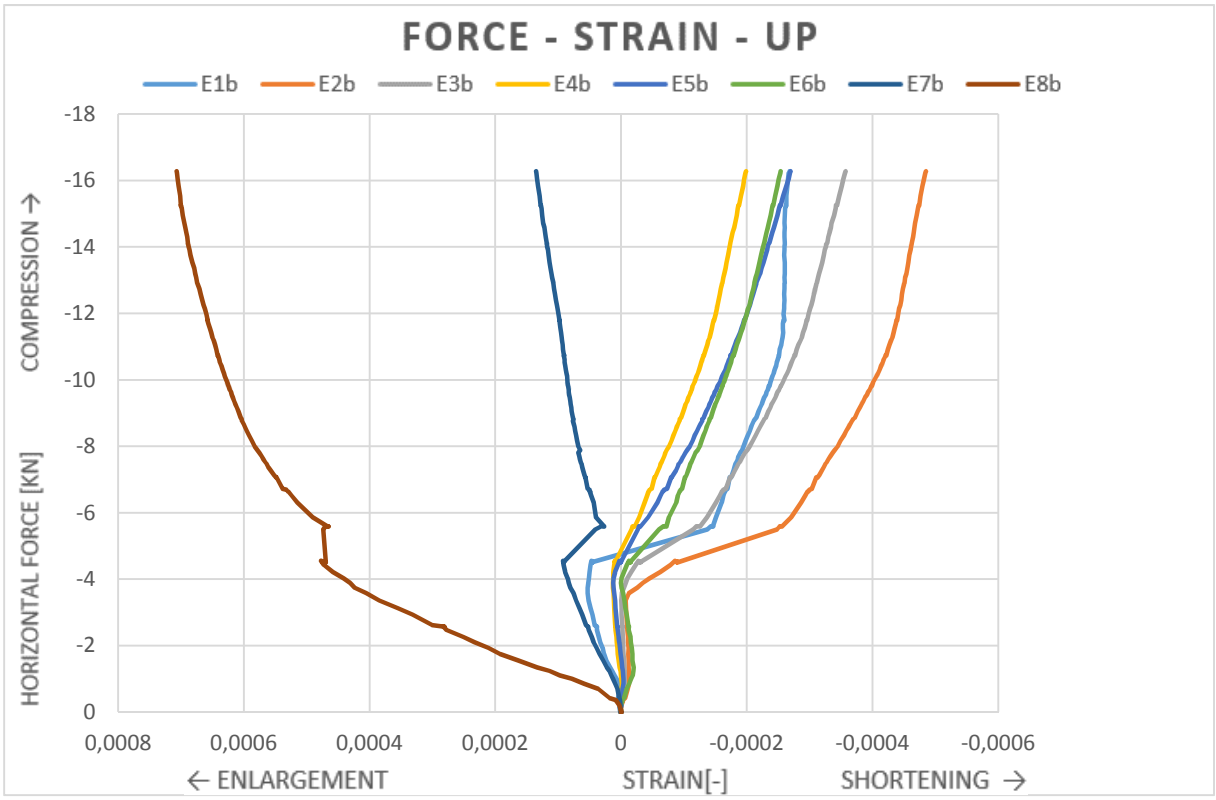

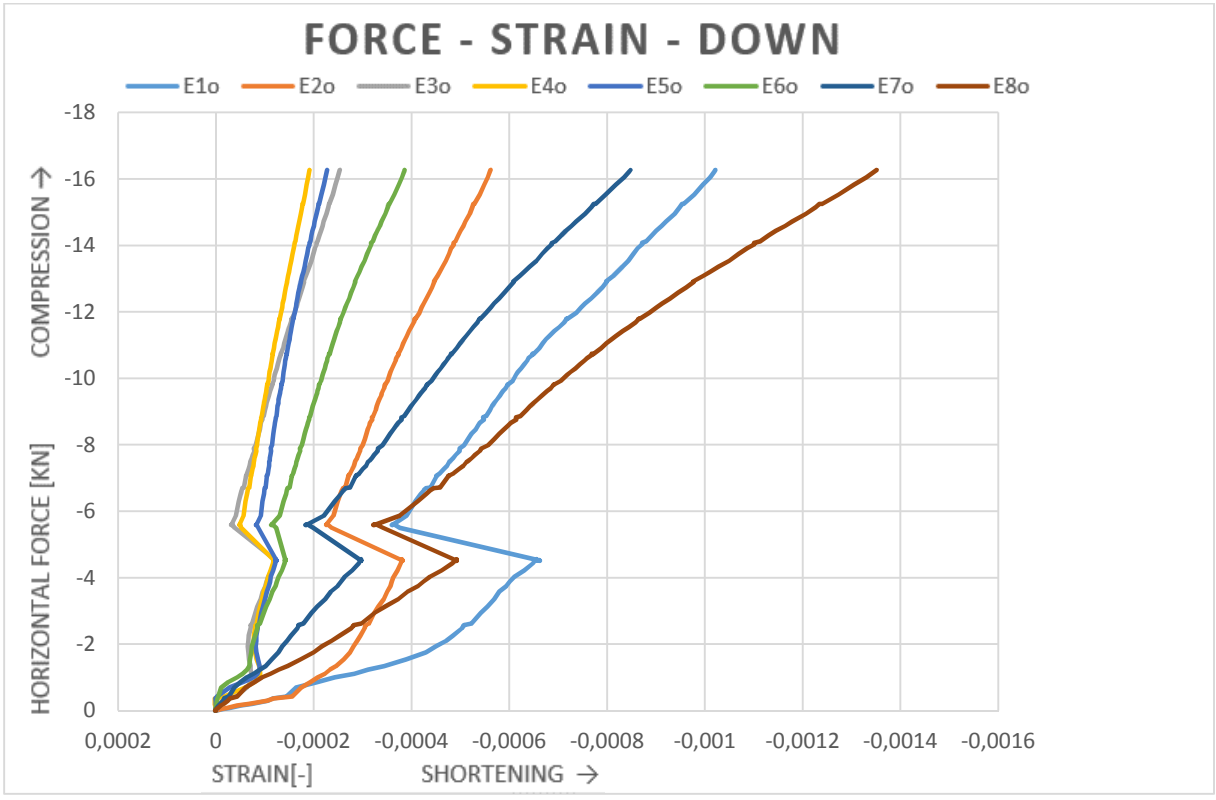

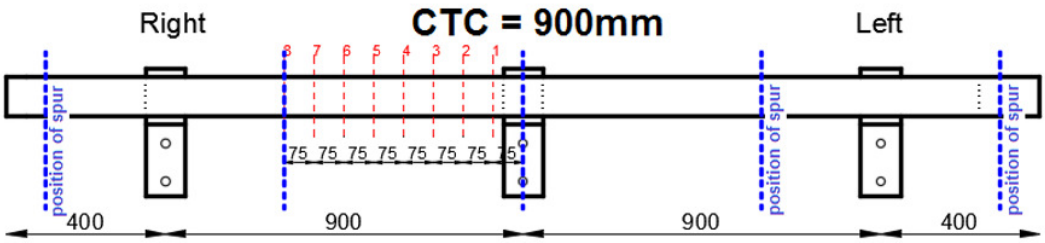
Right
CTC = 900mm
Left
8 7 6 5 4 3 2 1
75 75 75 75 75 75 75 75
position of spur
position of spur
position of spur
400
900
900
400

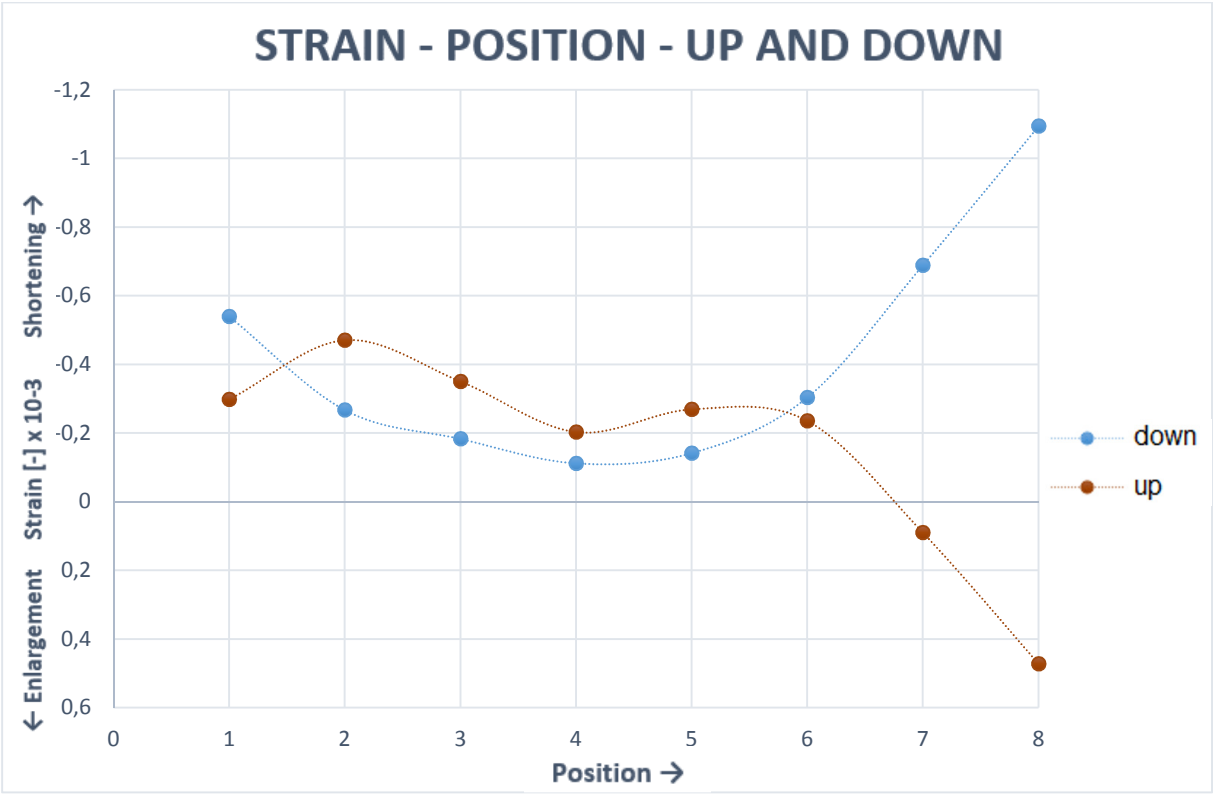
STRAIN - POSITION - UP AND DOWN
-1,2
-1
-0,8
-0,6
-0,4
-0,2
0
0,2
0,4
0,6
← Enlargement Strain [-] x 10-3 Shortening →
0
1
2
3
4
5
6
7
8
Position →
down
up

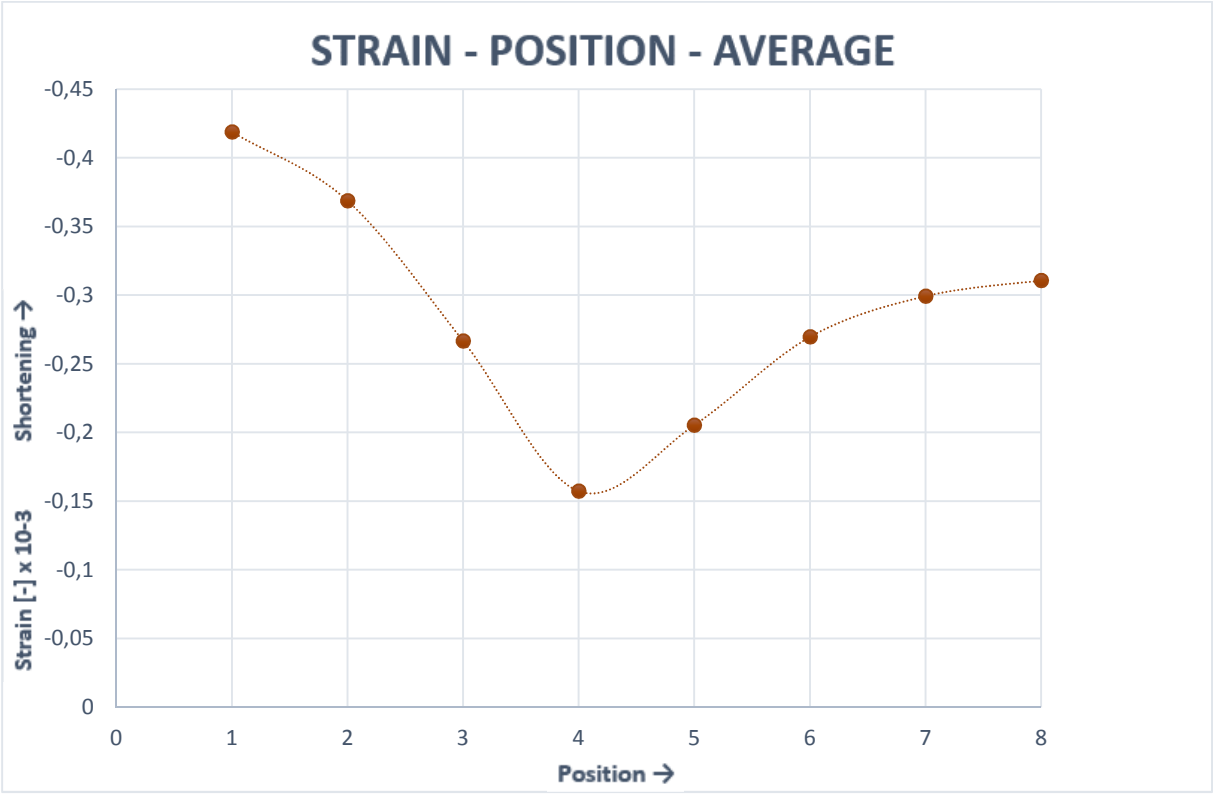
STRAIN - POSITION - AVERAGE
-0,45
-0,4
-0,35
-0,3
-0,25
-0,2
-0,15
-0,1
-0,05
0
Strain [-] x 10-3 Shortening →
0
1
2
3
4
5
6
7
8
Position →

55/1200/L/A

Angle of the roof:	55°
Center-to-center distance brackets:	1200mm
Position of the wall plate in the bracket:	Low (adding = 10mm)
Test series:	A
Coach screw	No
Load deviation:	108,68%

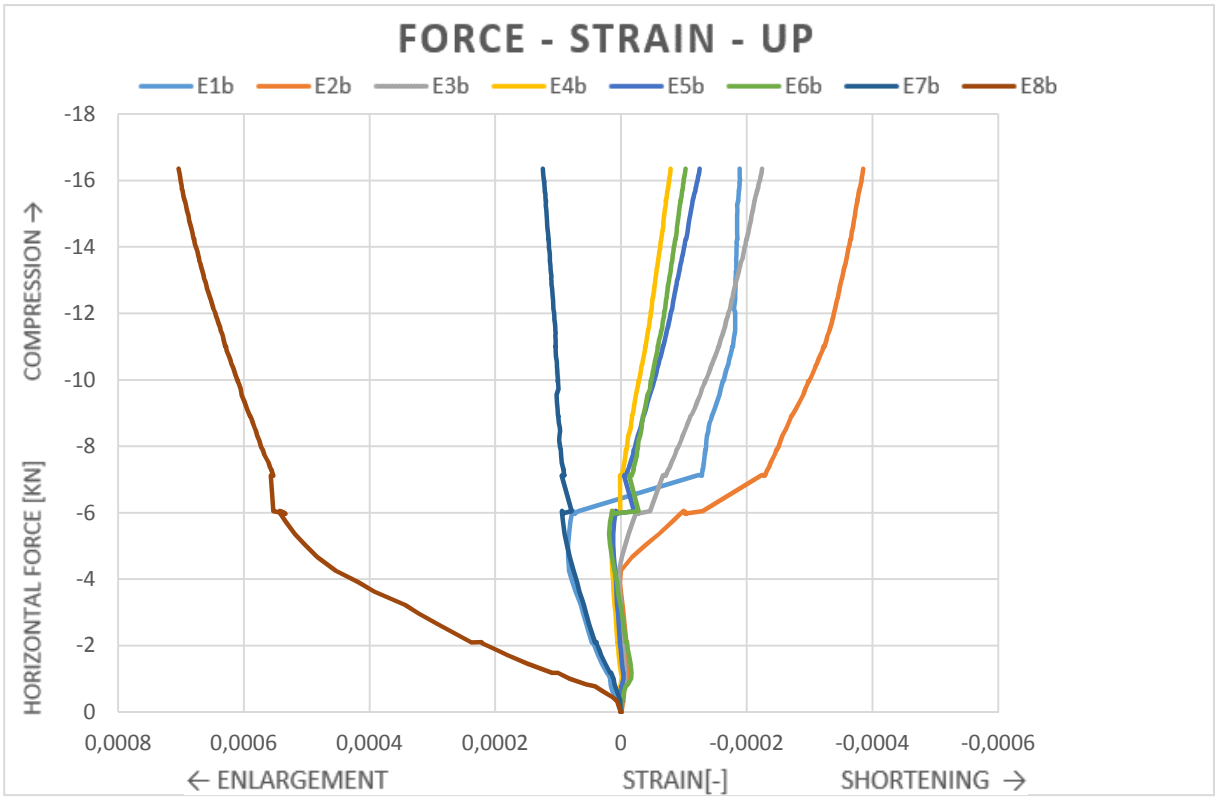

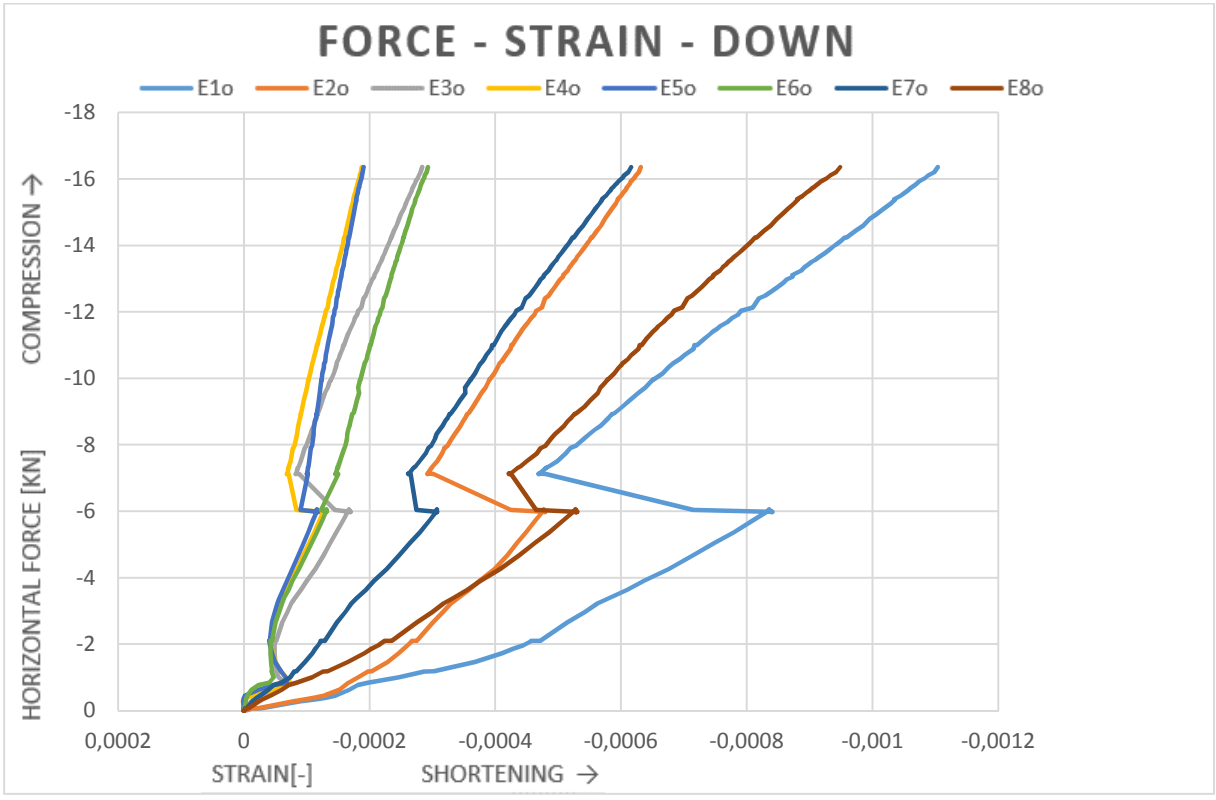

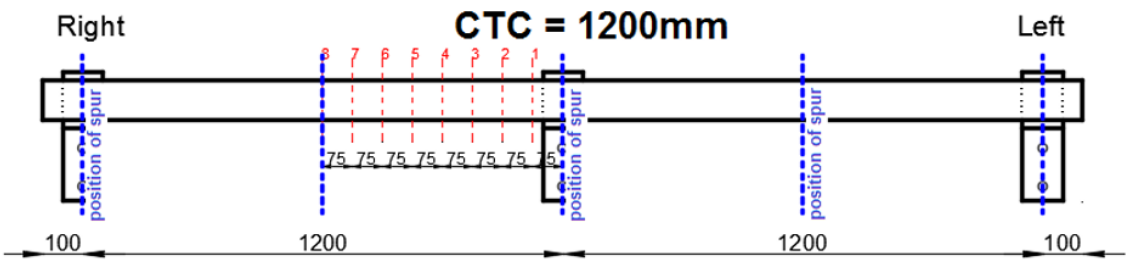
Right
CTC = 1200mm
Left
8 7 6 5 4 3 2 1
75 75 75 75 75 75 75 75
position of spur
position of spur
position of spur
100
1200
1200
100

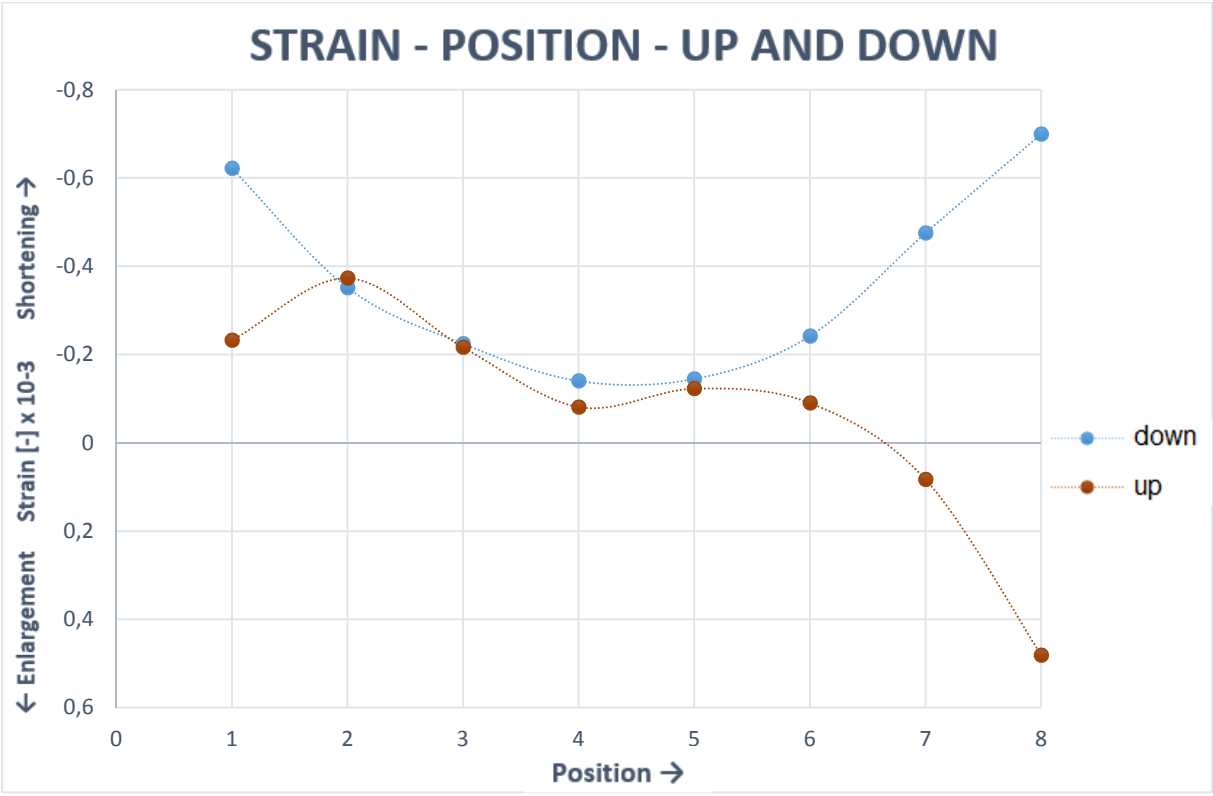
STRAIN - POSITION - UP AND DOWN
-0,8
-0,6
-0,4
-0,2
0
0,2
0,4
0,6
← Enlargement Strain [-] x 10-3 Shortening →
0
1
2
3
4
5
6
7
8
Position →
down
up

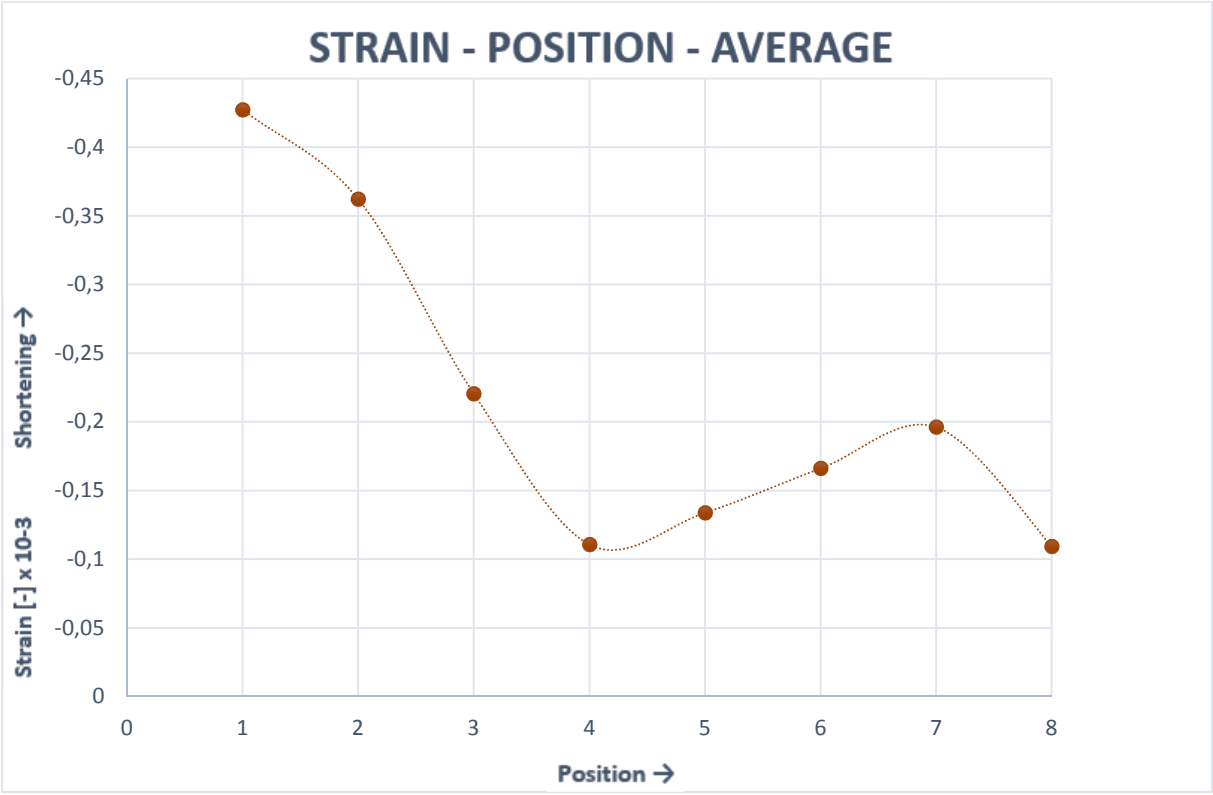
STRAIN - POSITION - AVERAGE
-0,45
-0,4
-0,35
-0,3
-0,25
-0,2
-0,15
-0,1
-0,05
0
Strain [-] x 10-3 Shortening →
0
1
2
3
4
5
6
7
8
Position →

55/1200/L/B

Angle of the roof:	55°
Center-to-center distance brackets:	1200mm
Position of the wall plate in the bracket:	Low (adding = 10mm)
Test series:	B
Coach screw	No
Load deviation:	108,68%

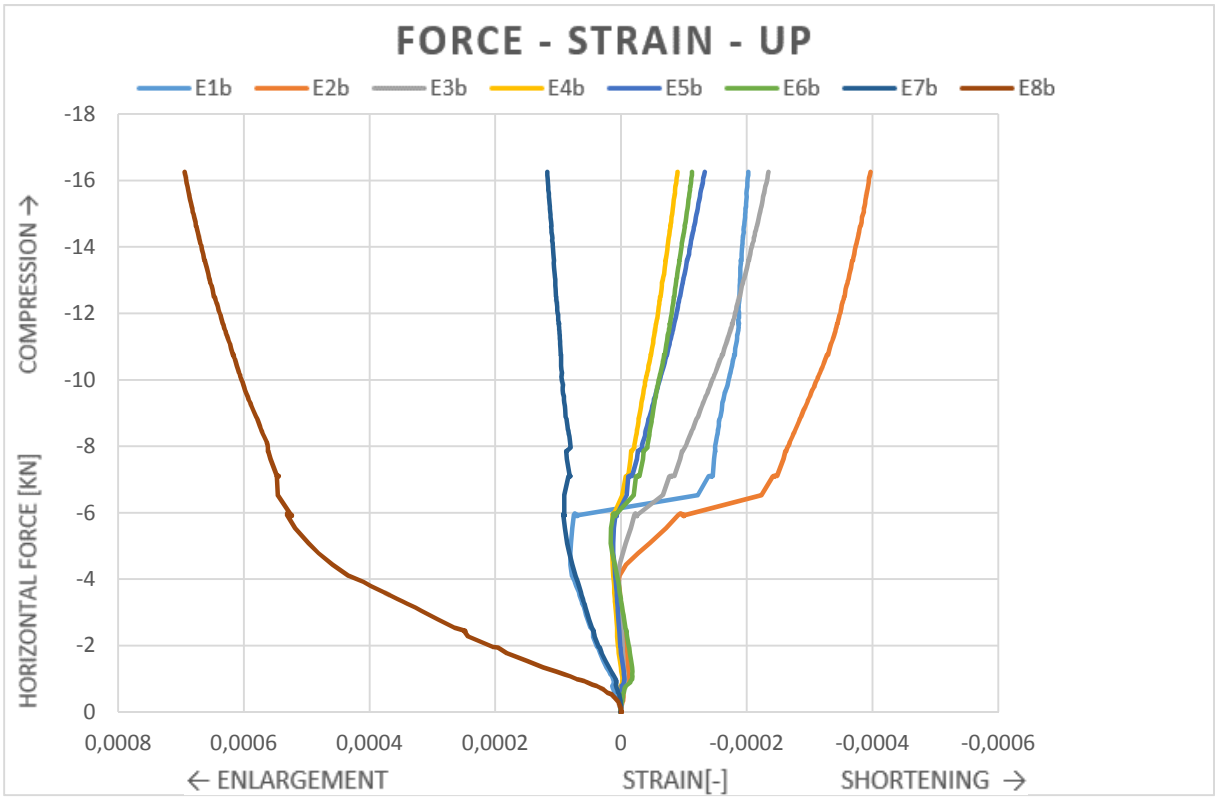

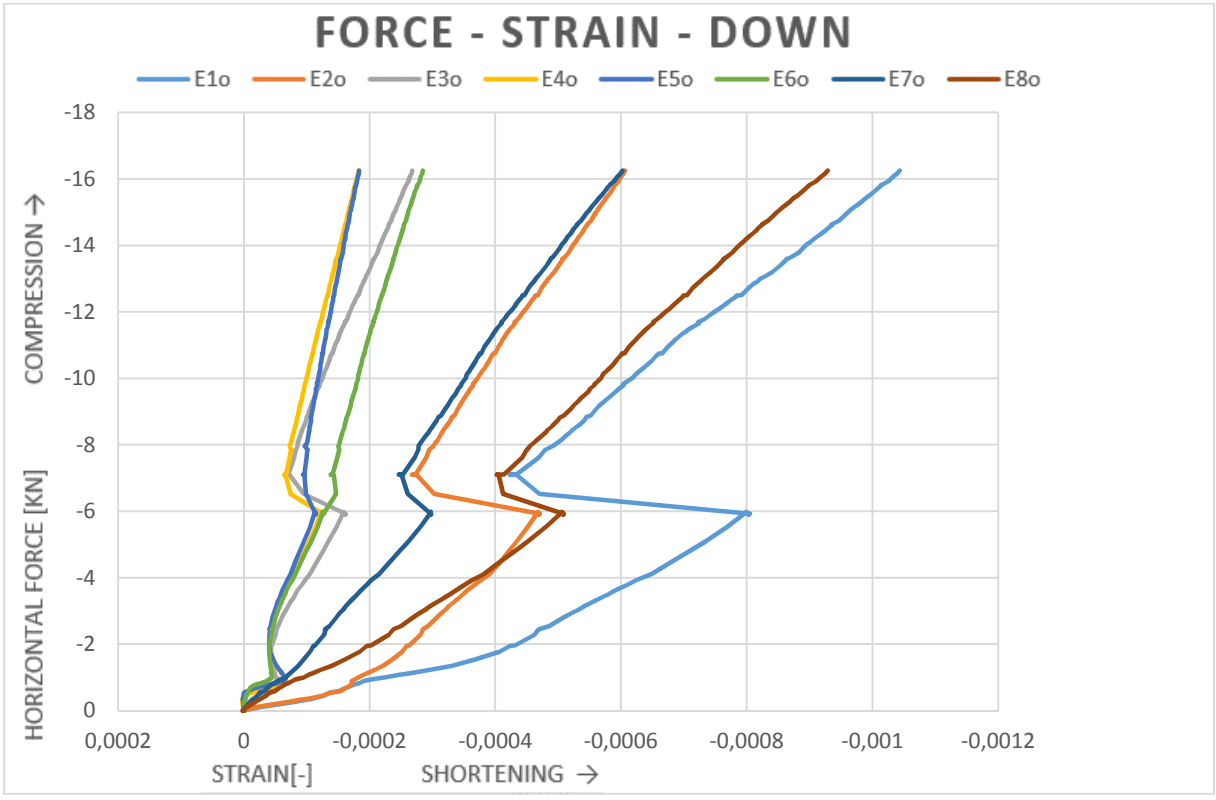

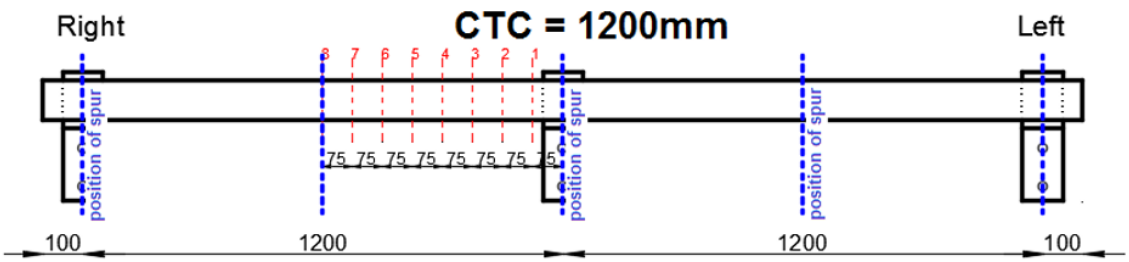
Right
CTC = 1200mm
Left
8 7 6 5 4 3 2 1
75 75 75 75 75 75 75 75
position of spur
position of spur
position of spur
100
1200
1200
100

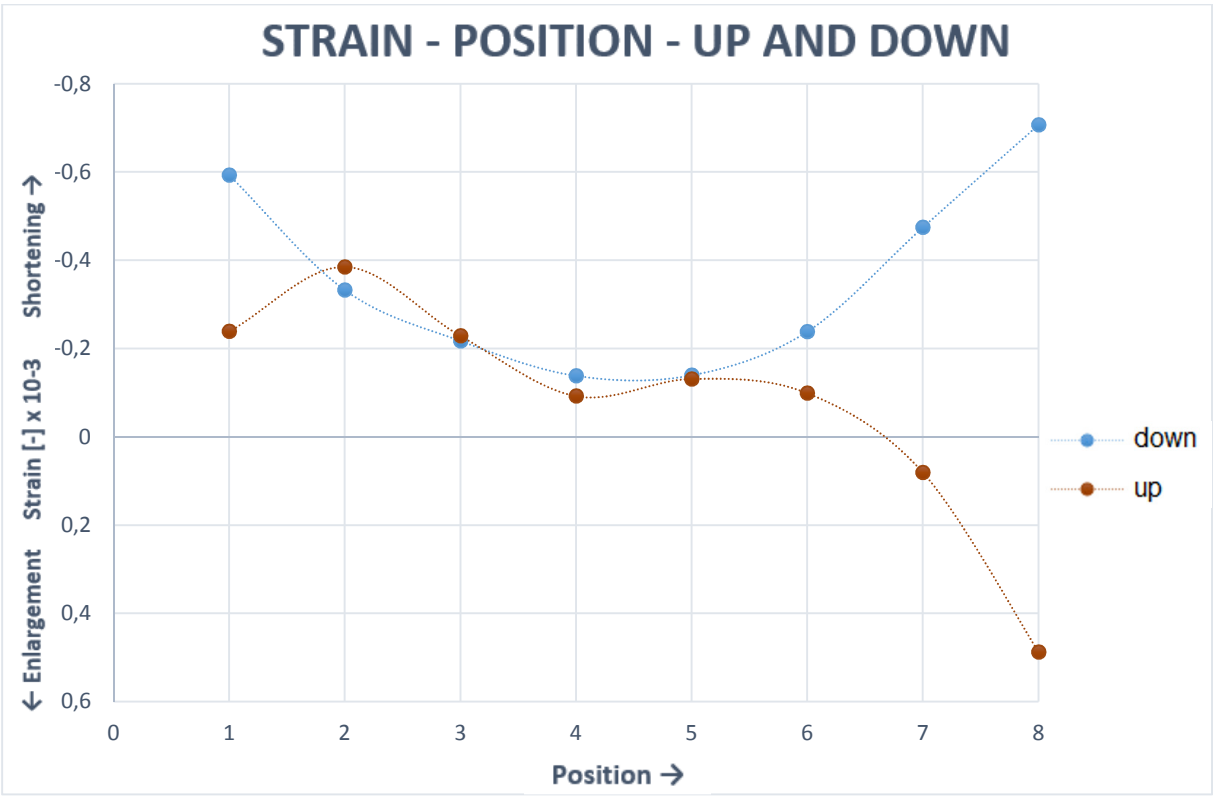
STRAIN - POSITION - UP AND DOWN
-0,8
-0,6
-0,4
-0,2
0
0,2
0,4
0,6
← Enlargement Strain [-] x 10-3 Shortening →
0
1
2
3
4
5
6
7
8
Position →
down
up

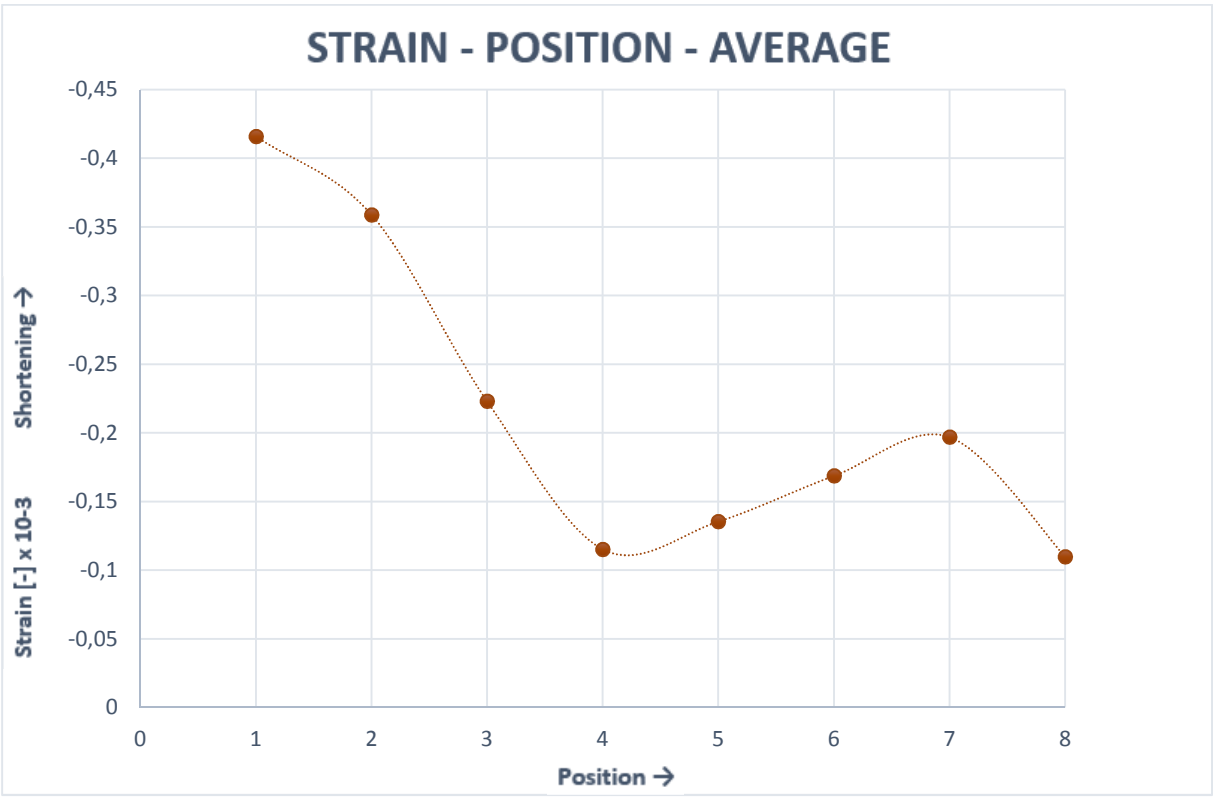
STRAIN - POSITION - AVERAGE
-0,45
-0,4
-0,35
-0,3
-0,25
-0,2
-0,15
-0,1
-0,05
0
Strain [-] x 10-3 Shortening →
0
1
2
3
4
5
6
7
8
Position →

Appendix 4.3

This appendix includes all pictures taken before and during testing in the laboratory.

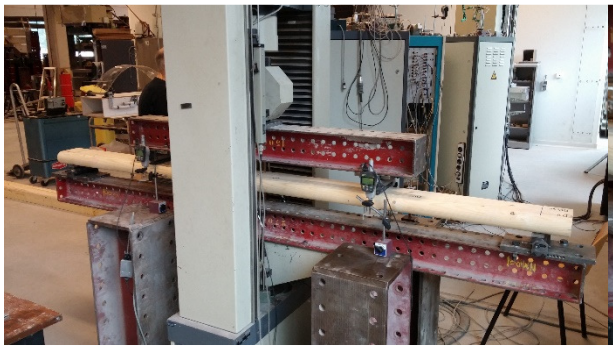





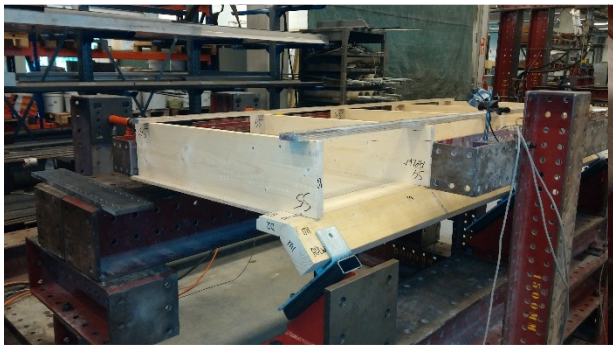



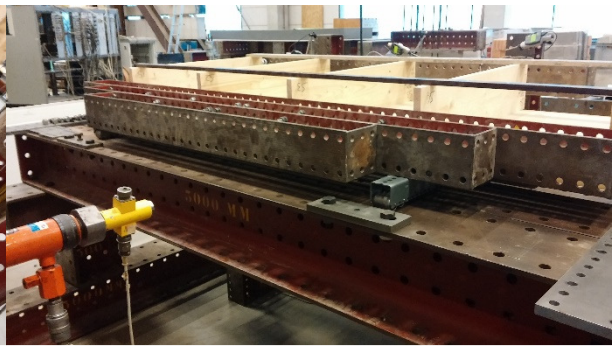
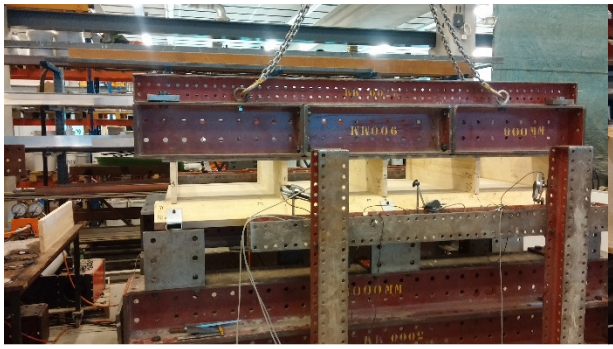
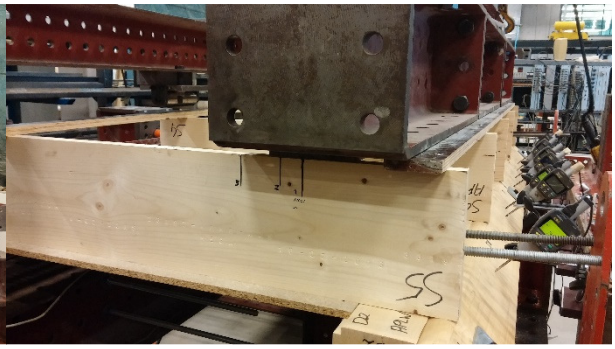




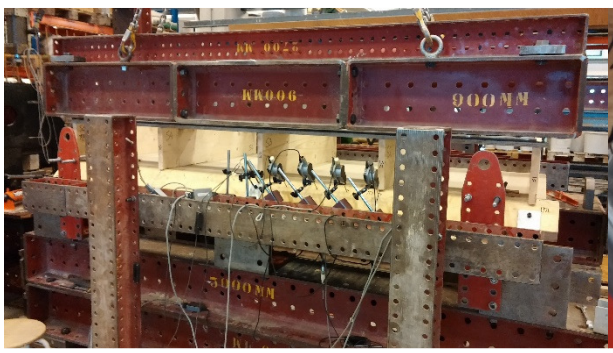



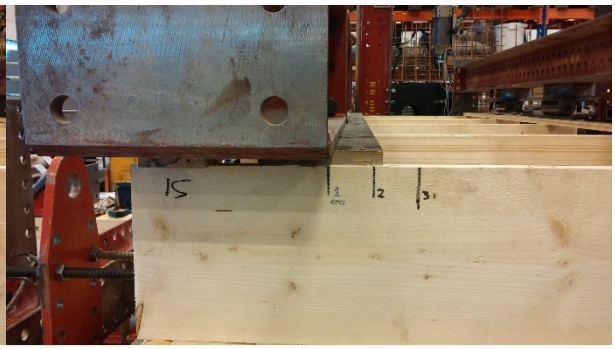

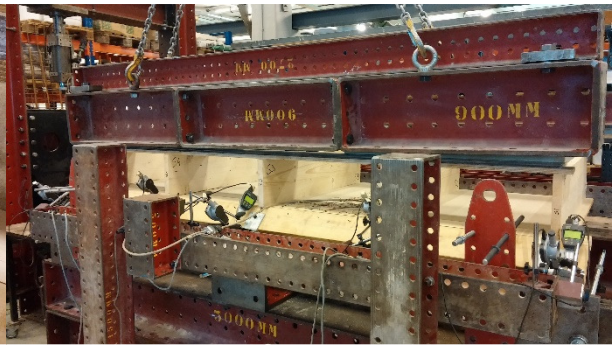
900MM
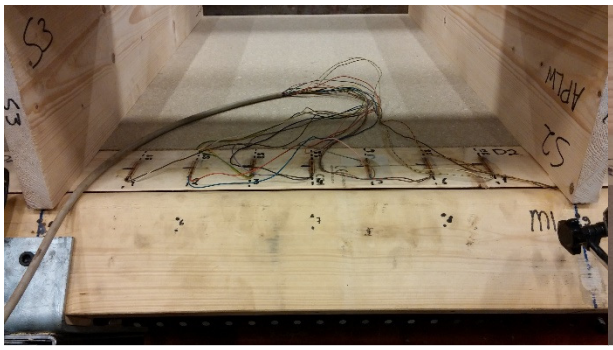
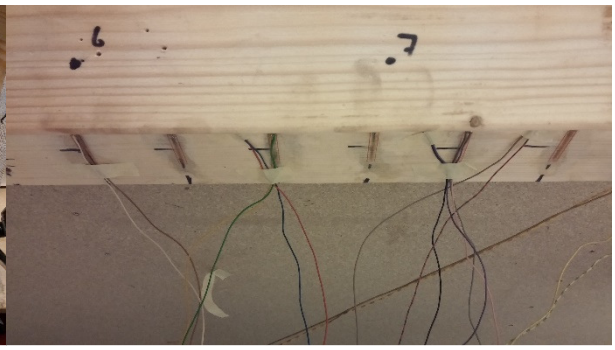

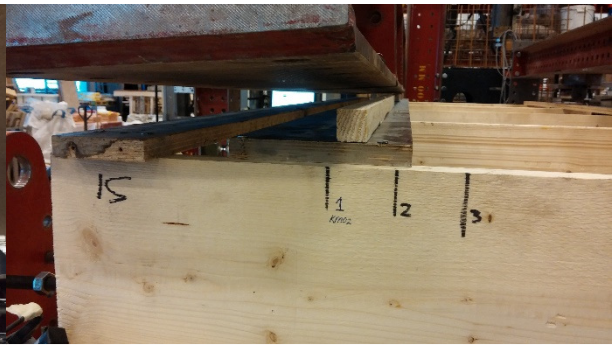
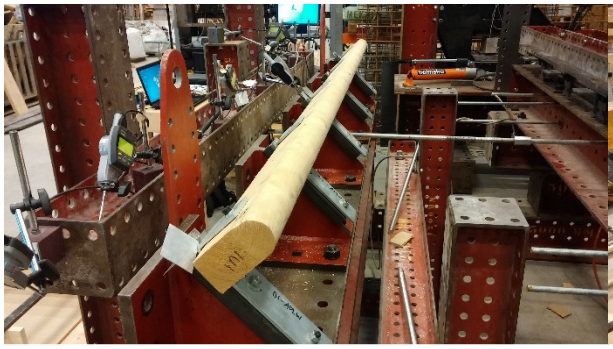


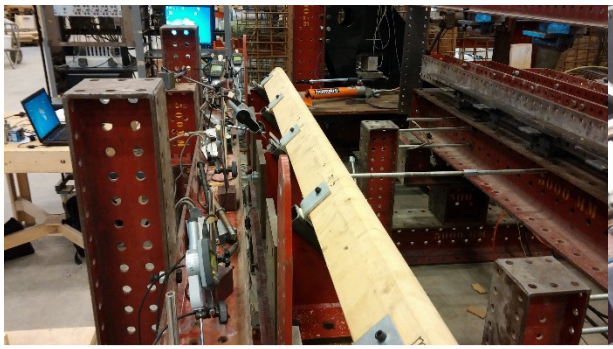

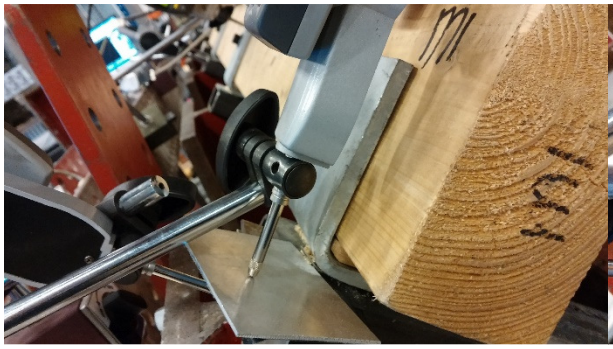
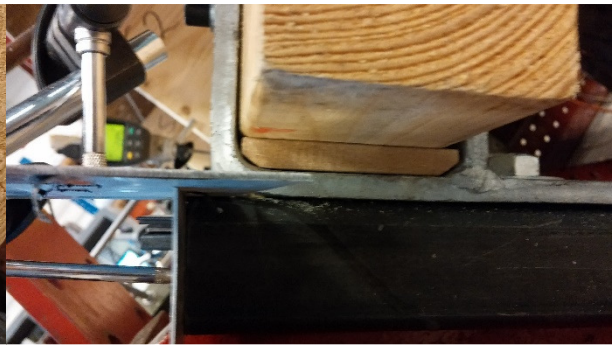

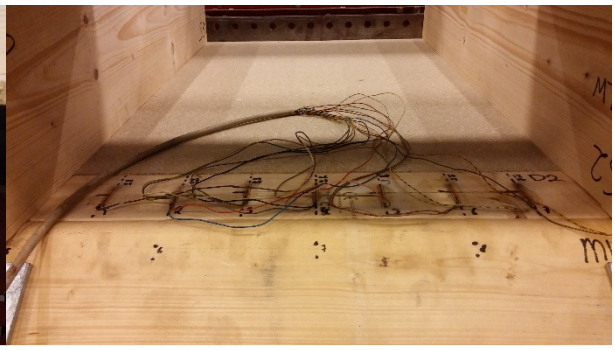


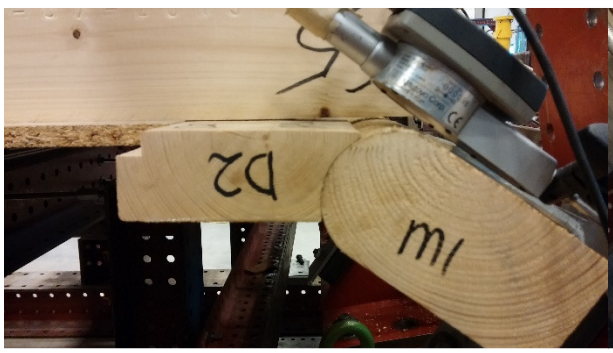
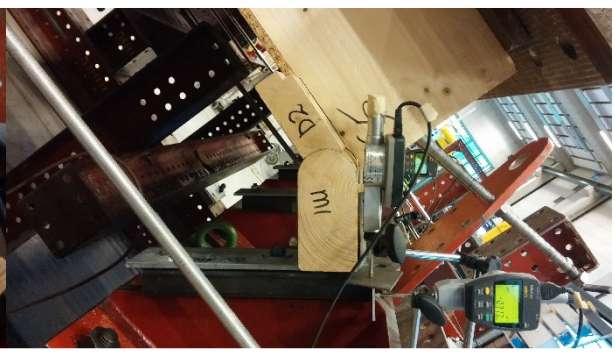


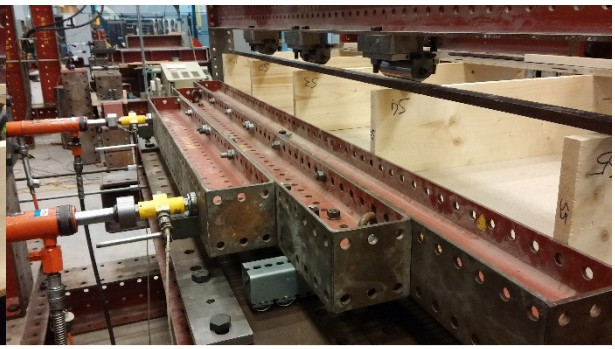


MADE IN
FRANCE
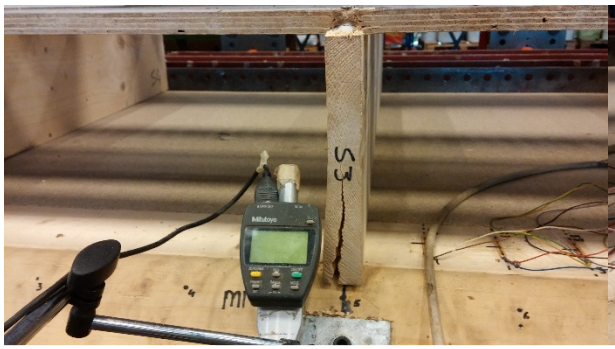
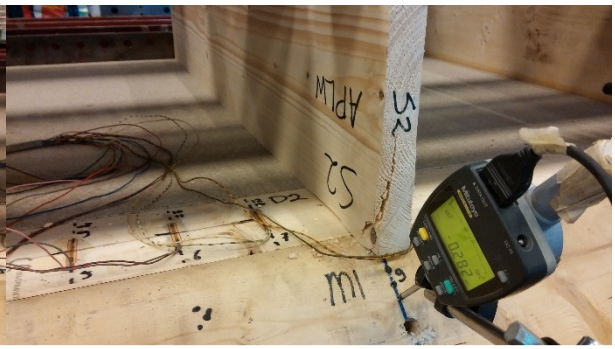



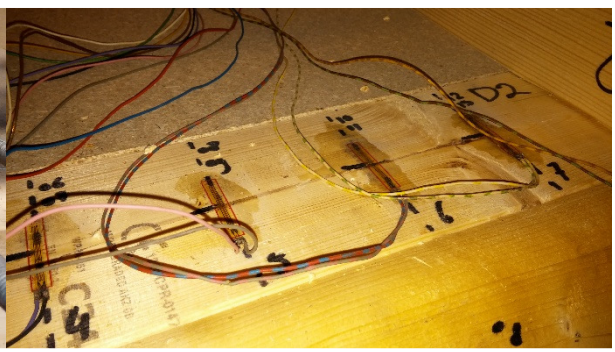


D2
D2
M1


S2
S2
M1
M1


S5
S4
APLW
M1
APLW
S5
D2


S3
APLW
S2
APLW
M1

Appendix 5.1

This appendix includes all results regarding the stresses in the supporting batten and the wall plate of the two dimensional model created with Abaqus.

The following test set ups have been tested:

	Roof Angle (degrees)	Adding (mm)	Coach screw
35/L	35	10	no
45/L	45	10	no
55/L	55	10	no

***Table A5.1a**; Overview of all performed tests*

For each test set up, the following figures are included:

- Minimal principal stresses of the supporting batten
- Von Mises stresses of the supporting batten
- Stresses in local X-direction of the supporting batten
- Von Mises stresses of the wall plate
- Stresses in local X-direction of the wall plate
- Stresses in local Y-direction of the wall plate

The complete test set up is show in figure **A5.1a**:

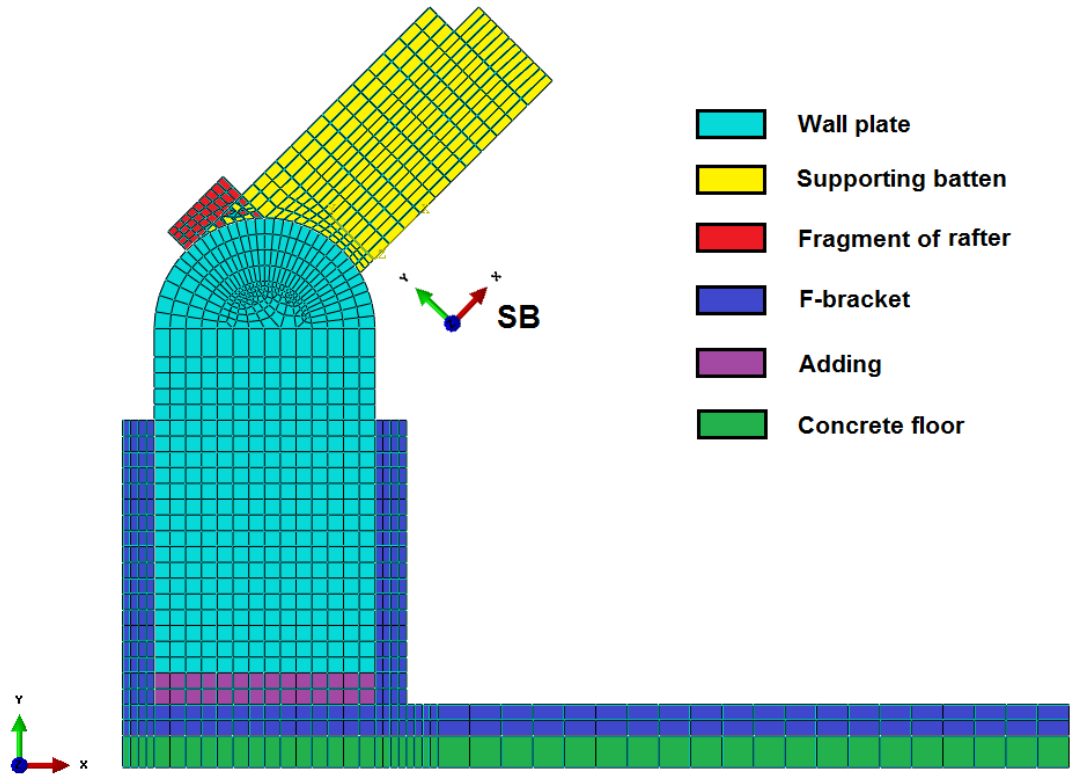

***Figure A5.1a**; Complete test set up. The angle of the supporting batten and rafter with the wall plate is variable*

Roof inclination 35 degrees

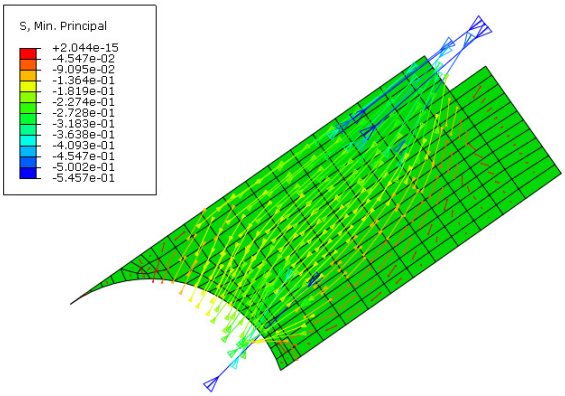

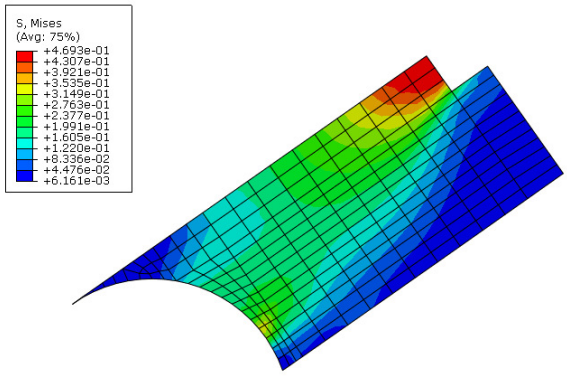

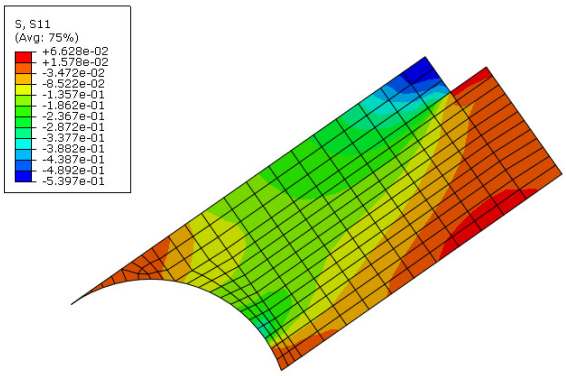

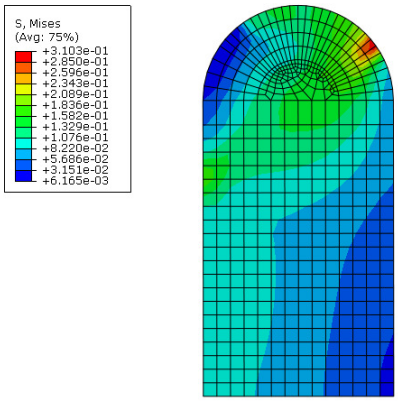

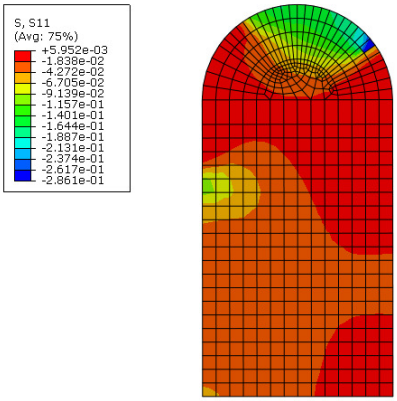

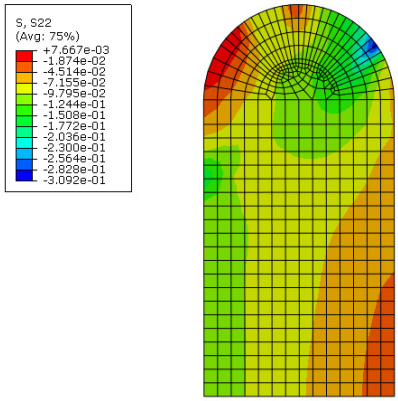

Roof inclination 45 degrees

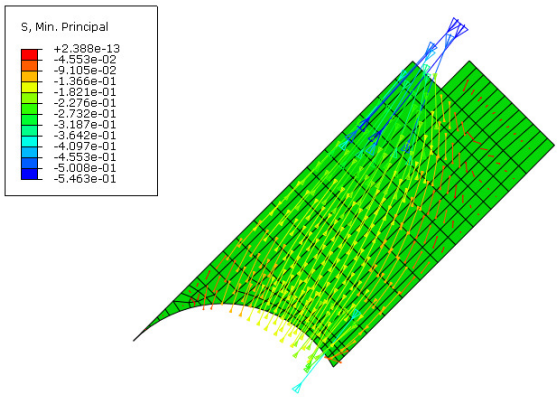

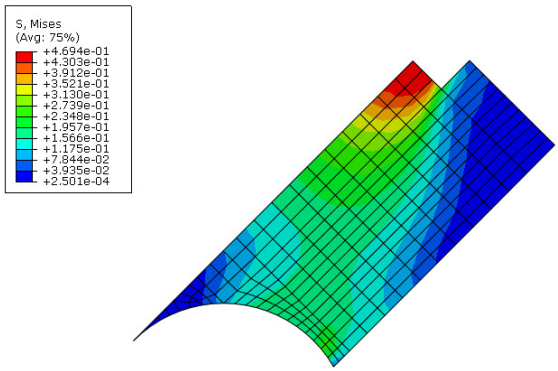

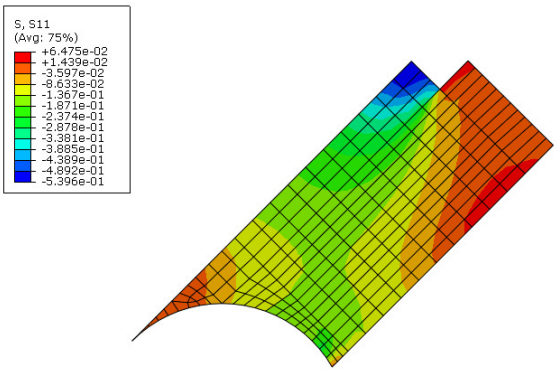

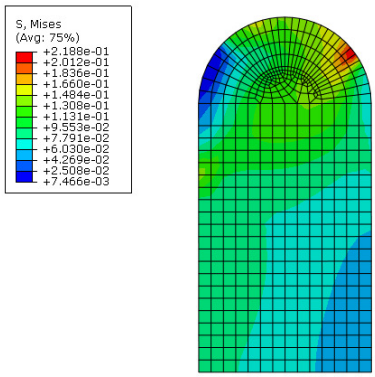

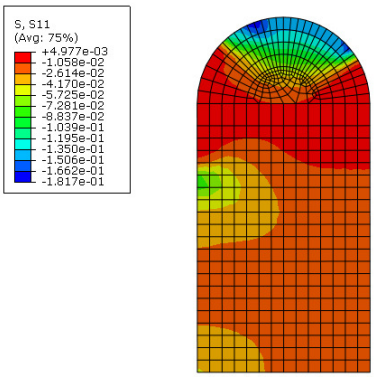

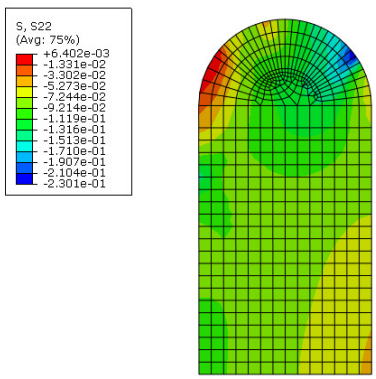

Roof inclination 55 degrees

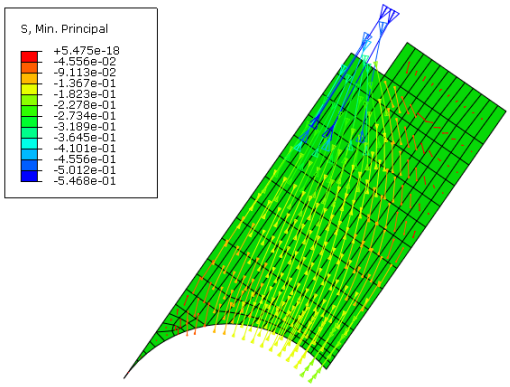

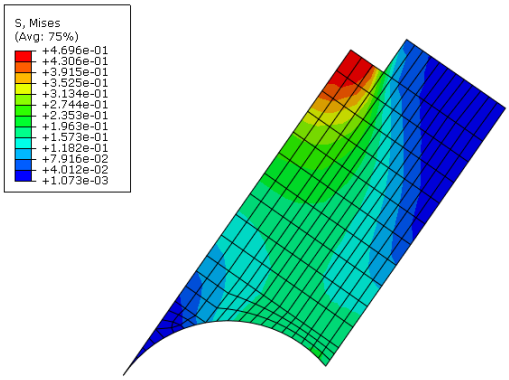

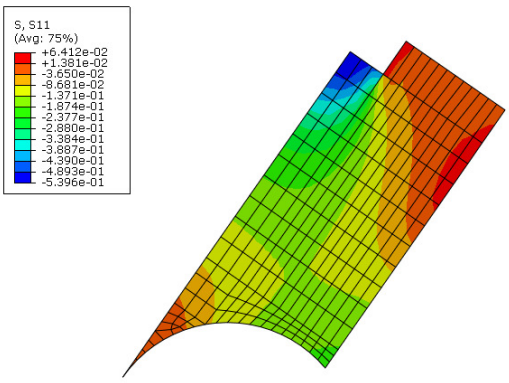

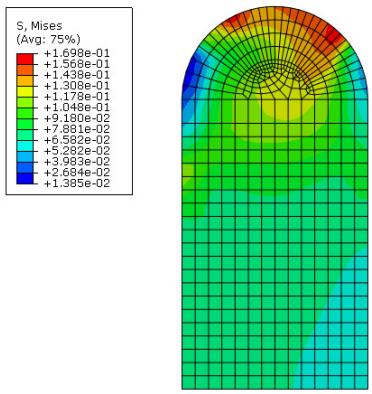

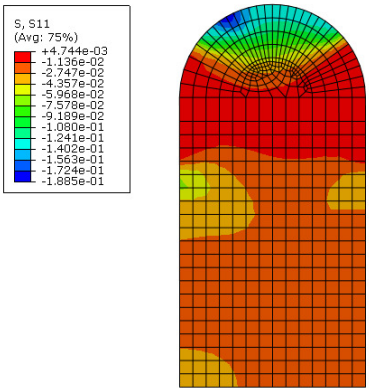

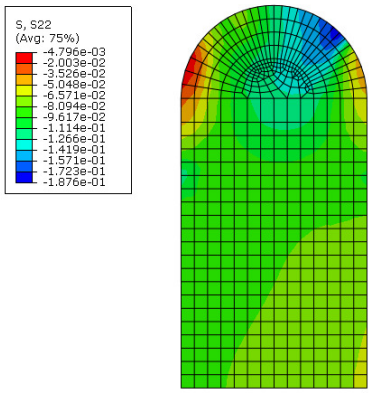

Appendix 5.2

This appendix includes all results regarding the strains in the supporting batten of the three dimensional model created with Abaqus

Several different test set-ups have been tested. The assemblies may differ in roof angle or center-to-center distances of the F-brackets.

	Roof Angle (degrees)	Center-to-center distance (mm)	Adding (mm)	Coach screw
35/600/L	35	600	10	no
35/1200/L	35	1200	10	no
45/600/L	45	600	10	no
45/1200/L	45	1200	10	no
55/600/L	55	600	10	no
55/1200/L	55	1200	10	no

***Table A5.2a**; Overview of all performed tests*

The position of the measurement is shown in **figure A5.2a up to A5.2c**:

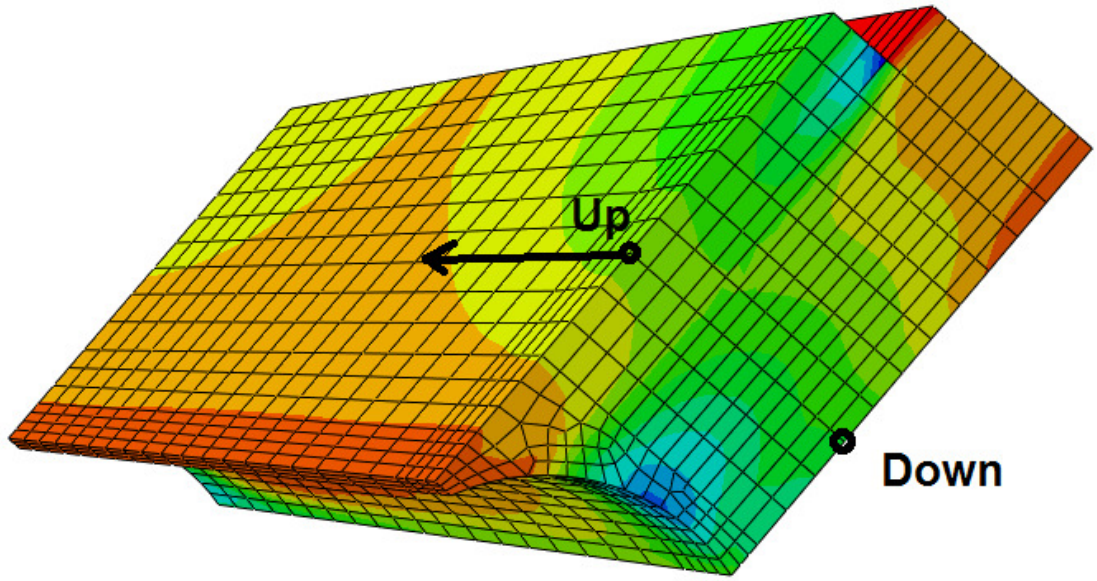

***Figure A5.2a**; Location of the measurements in three dimensional perspective*

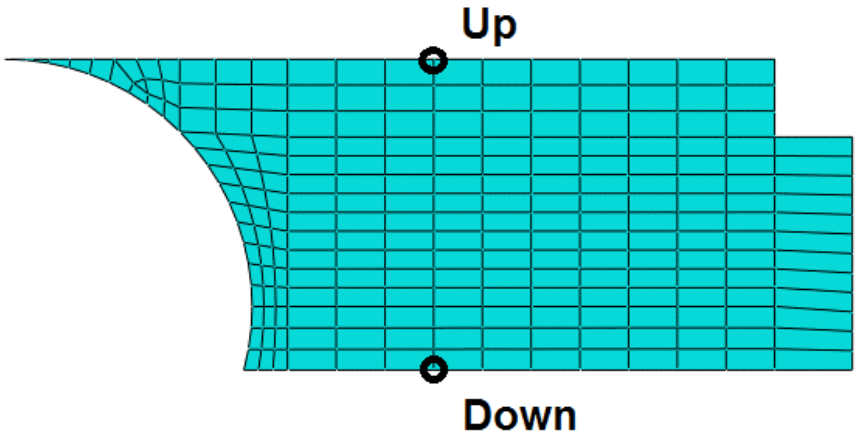

***Figure A5.2b**; Location of the measurements in two dimensional perspective, viewed from the side*

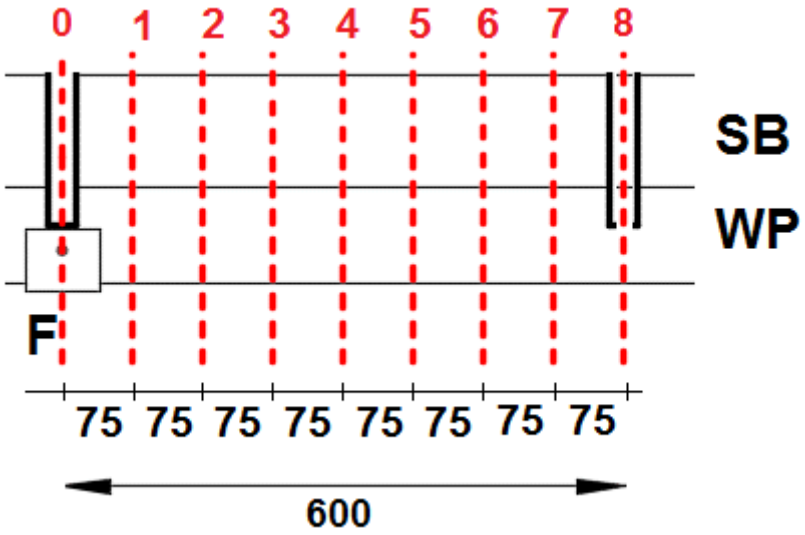

***Figure A5.2c**; Location of the measurements in two dimensional perspective, viewed from the top side. The red line shows the location of the positions*

35/600/L

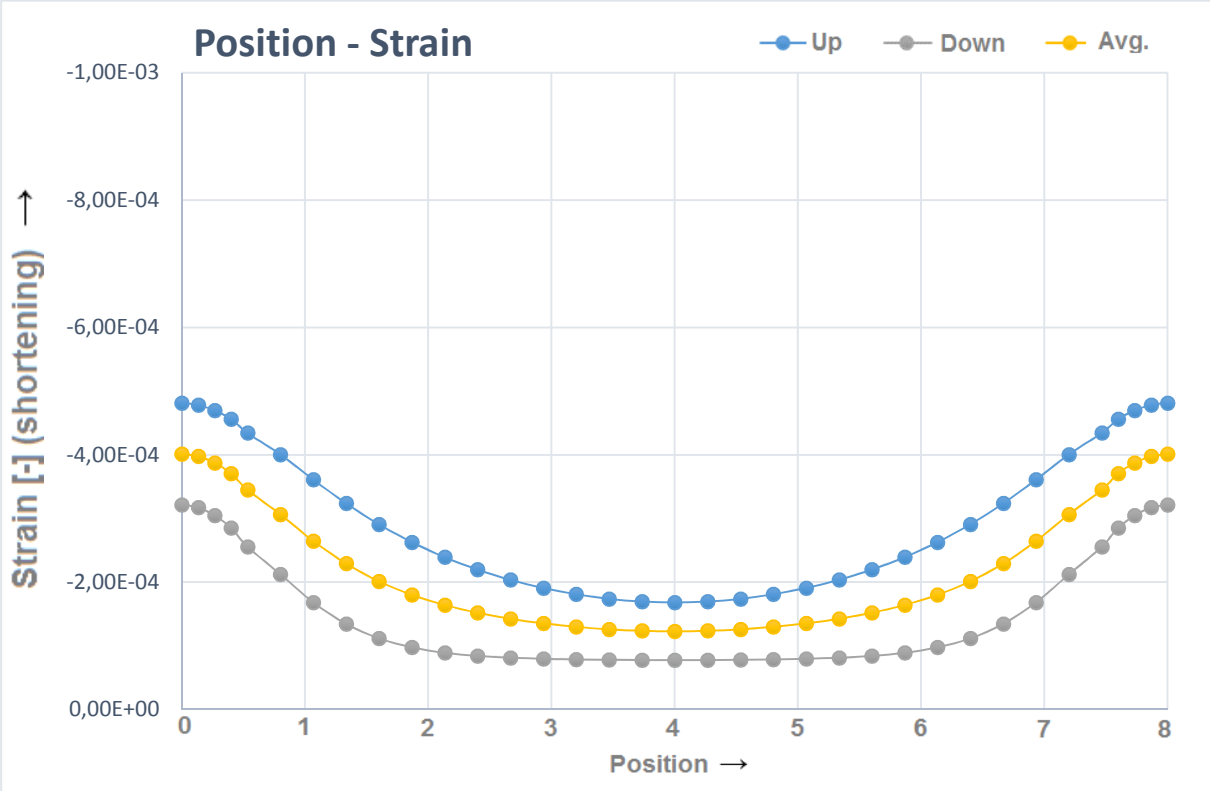

35/1200/L

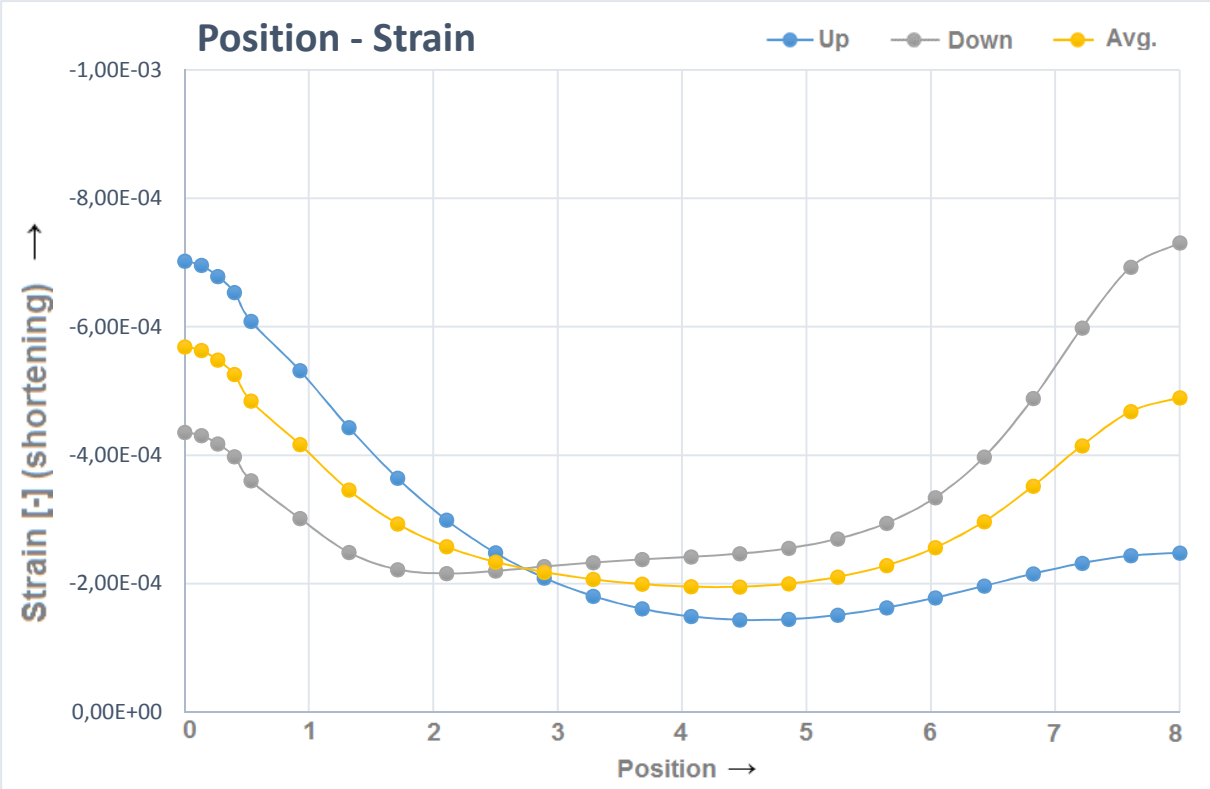

45/600/L

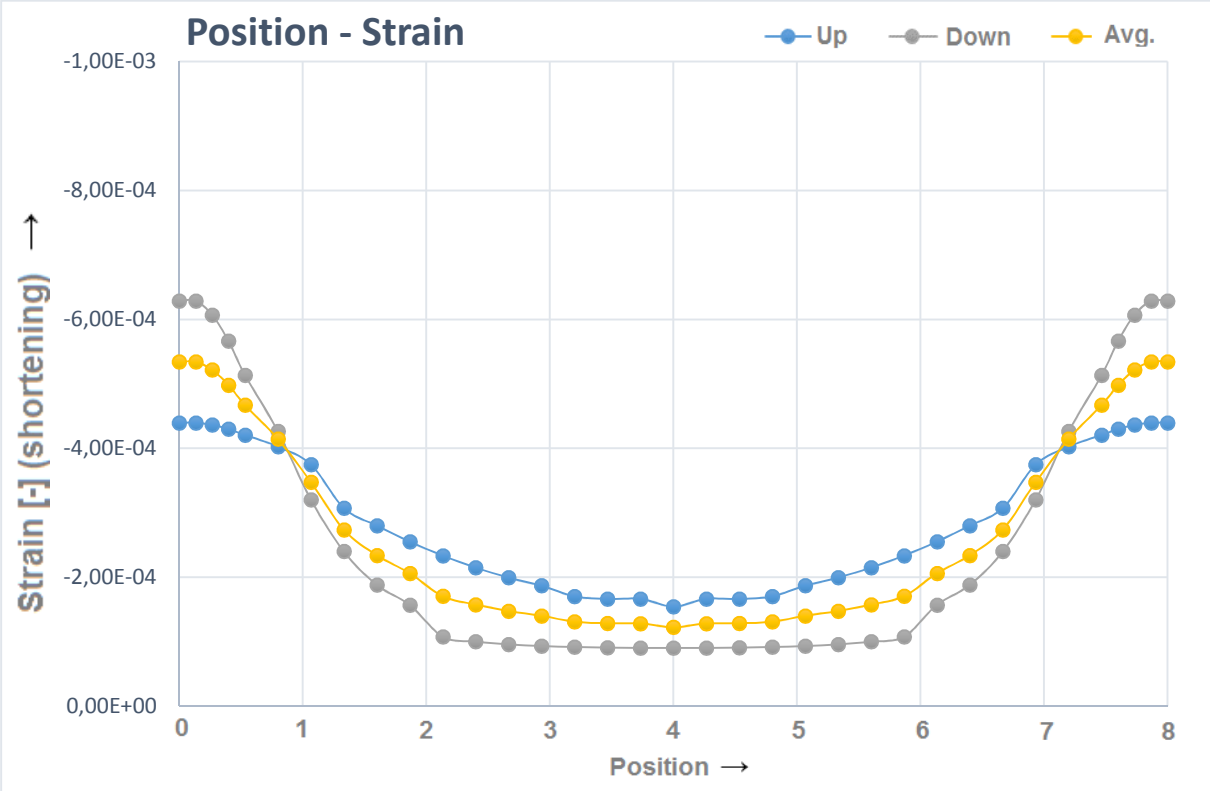

45/1200/L

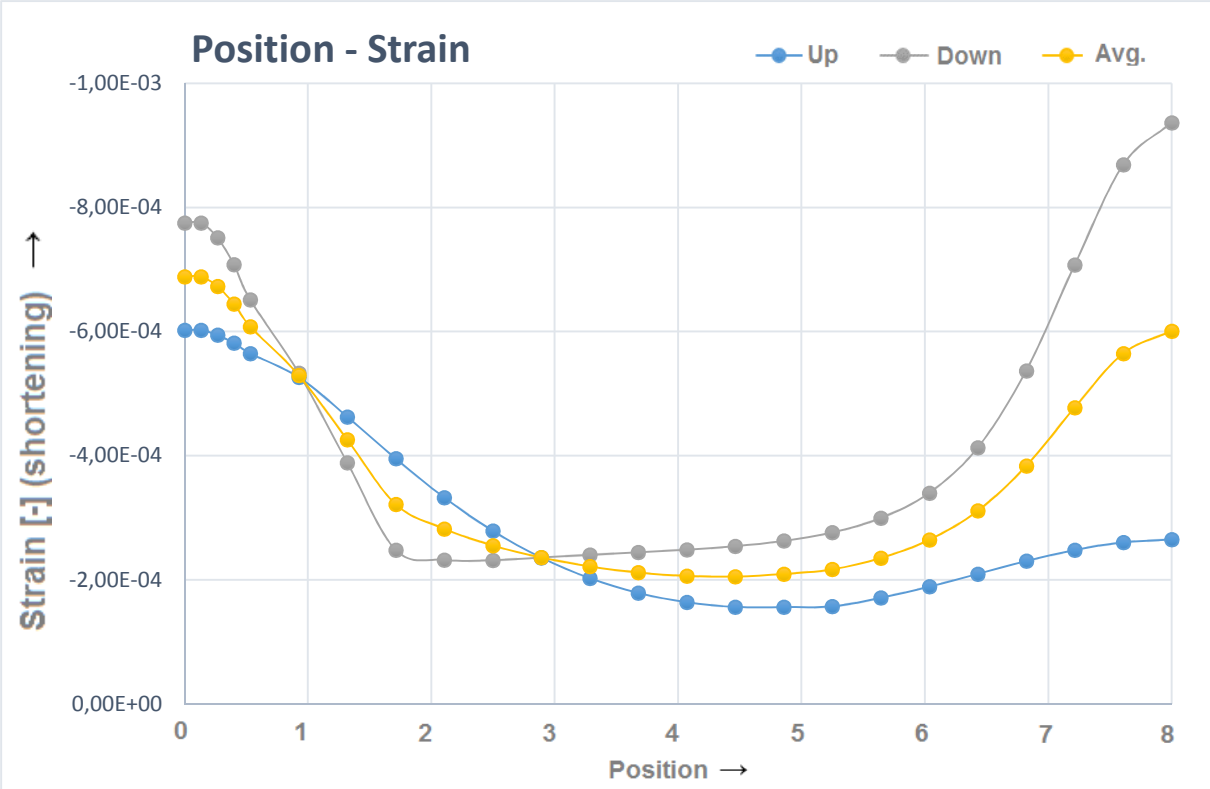

55/600/L

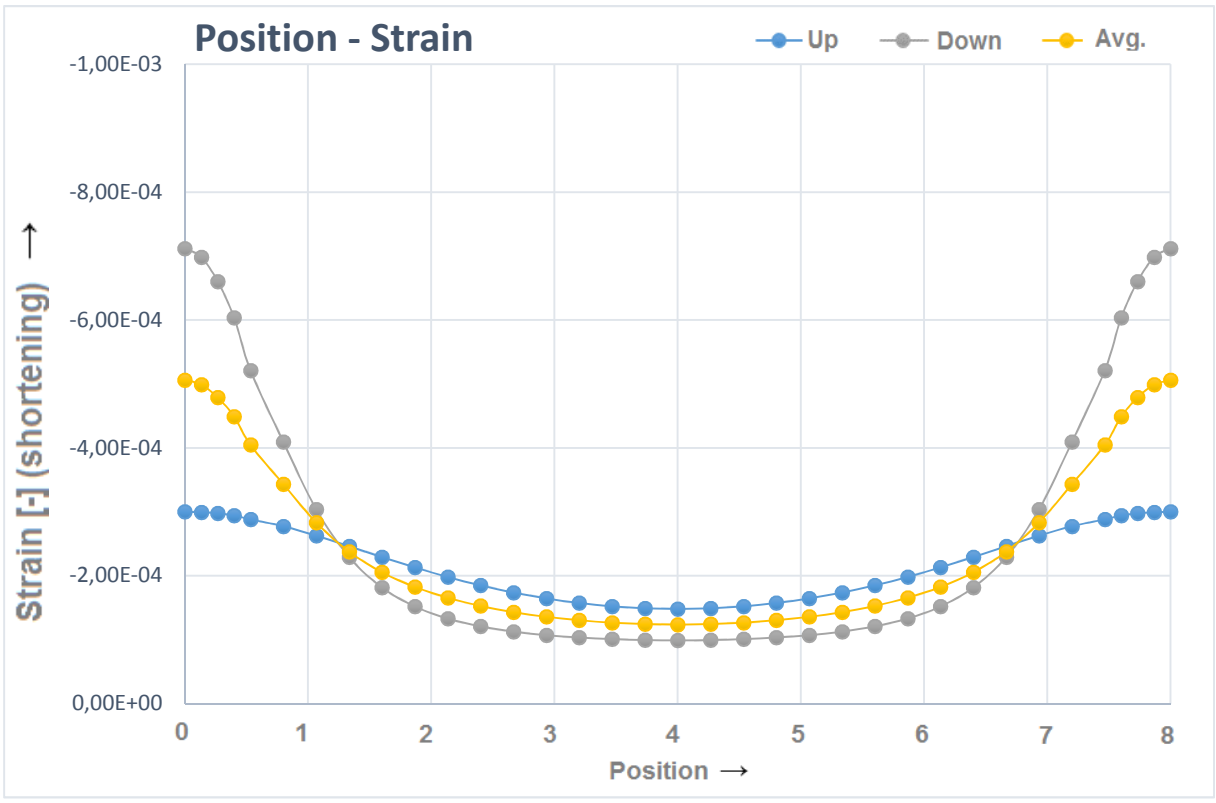

55/1200/L